Iridium-Catalysed Borylation of Heteroaromatic C-H Bonds

WRIGHT, JAY,SAMUEL

Iridium-Catalysed Borylation of Heteroaromatic C-H Bonds

Jay S. Wright

PhD Thesis

Supervisor: Professor Patrick G. Steel

Durham University

Department of Chemistry

2019

Abstract

Organoboron compounds are of great importance to organic, medicinal, and materials chemistry, representing key intermediates for the introduction of a wide variety of functional groups. This is best exemplified by the Suzuki-Miyaura cross-coupling reaction. In recent years, the direct C-H borylation of arenes has become an attractive method for the synthesis of aryl boronate esters. However, this transformation is more challenging for heteroarenes bearing an azinyl nitrogen atom, where the presence of the nitrogen lone pair can inhibit the reaction. This is particularly evident at the proximal C-H bond, where C-H activation often does not occur. Whilst many heteroarenes have been investigated, aminopyrazoles remain underexplored. This nucleus features in an array of bioactive molecules, such as herbicides, anti-cancer, and anti-parastic drugs. This thesis presents simple methods for the selective C-H functionalisation of 3- and 5-aminopyrazoles.

Contents

Abbreviations

(Bpin)$_2$bpy 4,4'-Bis(4,4,5,5-tetramethyl-1,3,2-dioxaborolan-2-yl)-2,2'-bipyridine

ASAP Atmospheric Solids Analysis Probe

ATR Attenuated total reflection

B$_2$pin$_2$ Bis(pinacolato)diboron

Boc tert-Butyloxycarbonyl

bpy 2,2'-Bipyridine

cod 1,5-Cyclooctadiene

coe Cyclooctene

conc. Concentrated

COSY Correlation spectroscopy

DCM Dichloromethane

DG Directing group

DHP 3,4-Dihydropyran

DMAP 4-Dimethylaminopyridine

dmbpy 3,8-Dimethyl-2,2'-bipyridine

DMF Dimethylformamide

DMSO Dimethyl sulphoxide

DoM Directed *ortho* Metalation

dppe 1,2-Bis(diphenylphosphino)ethane

dppf 1,1'- Bis(diphenylphosphanyl)ferrocene

dppp 1,3-Bis(diphenylphosphino)propane

dtbpy 4,4'-Di-tert-butyl-2,2'dipyridyl

dvtms 1,3-Divinyl-1,1,3,3-tetramethyldisiloxane

EI Electron Ionisation

Eg Ethylene Glycol

eq Equivalents

ES Electrospray

GCMS Gas Chromatography–Mass Spectrometry

HBpin Pinacolborane

HIM Hartwig Ishiyama Miyaura

HMBC Heteronuclear multiple-bond correlation spectroscopy

HRMS High-Resolution Mass Spectrometry

HSQC Heteronuclear Single Quantum Coherence Spectroscopy

Ind Indenyl

IR Infrared

LCMS Liquid Chromatography–Mass Spectrometry

LiHMDS Lithium Bis(trimethylsilyl)amide

L-DBTA Dibenzoyl-L-tartaric acid

***m*-Xyl** 1,3-Xylene

MAD Methylaluminumbis(2,6-di-tert-butyl-4-methylphenoxide)

mtbe Methyl Tert-Butyl Ether

Neop Neopentyl

NOESY Nuclear Overhauser Effect Spectroscopy

Phen 1,10-Phenanthroline

PMP *p*-Methoxyphenyl

PMPNCO *p*-Methoxyphenylisocyanate

rt Room Temperature/Ambient Temperature

S_EAr Electrophilic Aromatic Substitution

SEM 2-(Trimethylsilyl)ethoxy]methyl

SM Suzuki-Miyaura

SMAP Silica-supported Silicon-constrained Monodentate Trialkylphosphine

TBAB Tetra-n-butylammonium bromide

TFA Trifluoroacetic Acid

THF Tetrahydfofuran

THP Tetrahydropyranyl

tmphen 3,4,7,8-Tetramethyl-1,10-phenanthroline

TLC Thin Layer Chromatography

TQD Tandem Quadrupole Detector

UV Ultraviolet

XPhos 2-Dicyclohexylphosphino-2′,4′,6′-triisopropylbiphenyl

Declaration and Statement of Copyright

The work described in this thesis was carried out in the Department of Chemistry, Durham University between October 2015 and October 2018. All work is the author's own, unless otherwise stated. This work has not been previously submitted for a degree at this or any other institution.

Acknowledgements

I express my sincere gratitude to my primary research supervisor, Professor Patrick Steel. Paddy, you continuously convinced me that I was capable of achieving feats that I considered out of reach, and you have motivated me to be the best scientist that I can be. I am determined to apply the invaluable lessons you have taught me so that I can remain steadfast and persistent in the laboratory, especially during the inevitable hardships of research. Thank you for offering me the opportunity to study synthesis and catalysis in your group, and for inspiring me to continue my journey into the fascinating world of chemistry. Your contributions to my career journey will not be forgotten.

I also appreciate the time and insights given to me by my secondary research supervisor, Professor Graham Sandford. Graham, you have a talent for remaining down to earth and saying things precisely how they are. I always look forward to chatting with you because I know I will leave your office with resolve, clarity, and a smile on my face. Of all of the advice I have received from you over the years, I especially appreciate everything you have offered to guide my career in the right direction.

My college crest is proudly presented on the covering page of this thesis in order to acknowledge the past and present members of the Grey College Middle Common Room. Over the years, my time at Grey has allowed me to build relationships with some of the most benevolent, fun, and intelligent people that I have had the pleasuring of crossing paths with. You know who you are, and I will miss you all dearly. I am every person I have ever met, so I thank you all for being inspirations and for helping me to become the man I am today. Durham's dance floors will not be the same without us!

The submission of this thesis would not have been possible without the continued support of the past and present PhD, MSci, NatSci. and placement students of CG001. Andrew, your seemingly endless knowledge of C-H borylation is one of the reasons that I am so enthusiastic about the area today. Bex, I thank you for being there for me from beginning to end, and for all of the hilarious memories we've shared. Courtney you always have me in stitches, thank you for always treating CG001 with your delicious food, and for preparing me for my move to your country. Whilst there are far too many more of you to mention in this space, I wish you all good luck in your future endeavors and I hope I am lucky enough to work with you again someday.

I am grateful to all of the Professors and Doctors of Durham's analytical staff for their committed operation of the instrumentation essential for the completion of this project. To Alan Kenwright, Juan Aguilar, Catherine Heffernan, and Raquel Belda, I thank you for running each of my high-field NMR spectra and for helping me to elucidate compound structures. I hope to meet NMR researchers in the future who are as hardworking and friendly as you all are. To Jackie Mosely, Peter Stokes, and David Parker, thank you for providing the means to efficiently collect and interpret MS data. To Dmitry Yufit and Andrei Batsanov, thank you for conducting X-ray analyses of my "crystals of the week" (somehow I don't think I am the only person lucky enough to be commended with that title!).

I owe all of my successes to my family and friends who continue to push me to achieve the things I am most passionate about. Mum, thank you for raising me to value education as much as I do, I don't know of a better life path that that I could be on. Dad, I would not have gotten to the end of this PhD without your support, thank you for keeping me mindful of life's hidden challenges. Sean, thank you for being another extraordinary father figure and setting an impeccable standard to the girls and me over the past decade. To my beautiful three sisters, I feel privileged every day to have siblings who are as hardworking and successful as you all are. Thank you for motivating me to get a little bit better every single day. To my brother Joseph, at the time of writing this section you are five years old. I am convinced you will do great things in your future, and I hope the examples set by the great people around you will help you to go above and beyond us all. To the rest of my family, I thank you for everything you have done for me and I love you very much. I will miss you dearly when I leave for the USA.

Finally, I thank the University of Durham and EPSRC for kindly funding my PhD. Following my time at Birmingham, I knew above anything else that I wanted to study at Durham. I am grateful that I was selected to be a PhD candidate at such a wonderful place.

1 Introduction

1.1 Thesis Overview

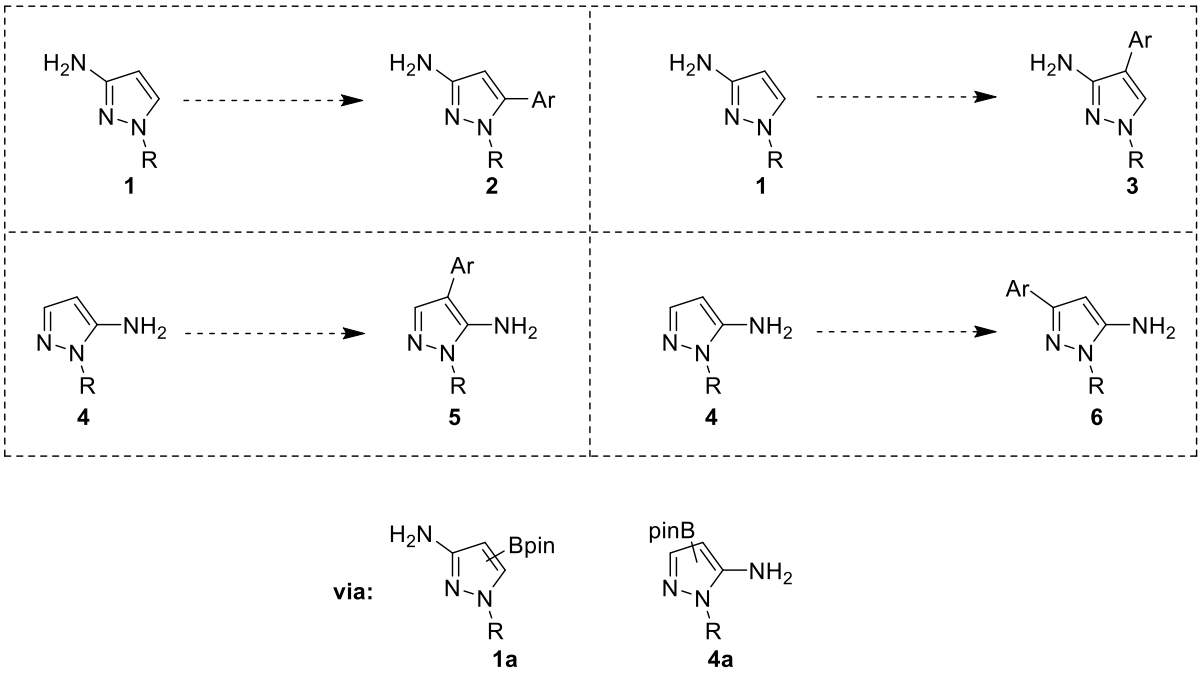

Figure 1: Goal to Regioselectively Functionalise Aminopyrazoles

This thesis discusses new methodology for the regioselective Ir-catalysed C-H borylation of heteroarenes. The focus of this study is the pharmaceutically important aminopyrazole scaffold, with the primary goal to synthesise four arylated aminopyrazole isomers **2**, **3**, **5**, and **6** using Ir C-H borylation and Suzuki Miyaura cross-coupling (Figure 1).

The thesis contains four chapters. Chapter 1 provides an introduction to organoboron compounds and aromatic Ir C-H borylation, with a primary focus on the regiochemistry in heteroaromatic Ir C-H borylation. Chapters 2 and 3 present and discuss the research undertaken. Chapter 4 provides the detailed experimental methods and analytical data to support compound characterisation.

1.2 Introduction to Organoboron Compounds

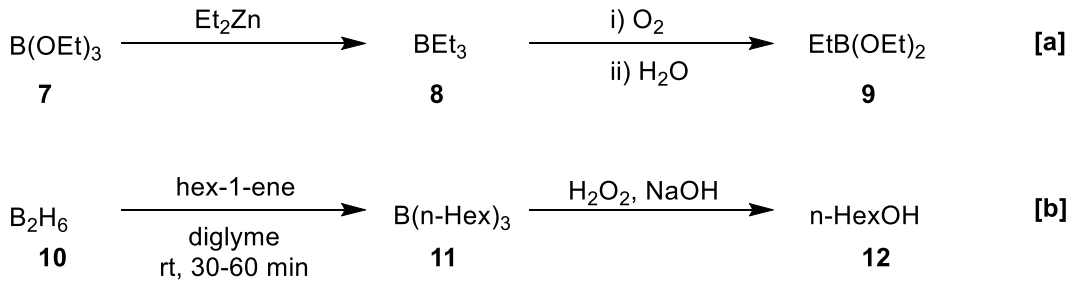

Scheme 1: Early Synthesis and Transformations of Organoboron Compounds

In 1860, the synthesis of triethyl borane **8** and diethyl ethylborate **9** was reported by Frankland and Duppa (Scheme 1a).[1] These were the first recorded compounds to contain a C-B bond, and molecules featuring this linkage are now known as organoboron compounds. Nearly one hundred years later, Brown developed hydroboration of alkenes using diborane **10** for the synthesis of trialkylboranes such as **11**, and discovered that they could be oxidised to alcohols with alkaline peroxide (Scheme 1b).[2] A further twenty years later, Suzuki and Miyaura described that organoboron compounds could be cross-coupled with organohalides to form sp^2-sp^2 C-C bonds with catalytic quantities of Pd (Scheme 2a).[3,4] As of 2014, this is the second most practiced reaction in medicinal and natural product synthesis.[5] Whilst C-B bonds do not appear in nature, their use is emerging slowly in chemical biology and drug discovery.[6,7] For example, Shinkai and co-workers have exploited the Lewis acidity of phenylboronic acid groups in porphyrin-based sugar-sensing agents, such as **13**.[8] Furthermore, the anti-cancer drug Velcade and the antifungal drug Tavaborole both feature a C-B bond (Figure 2).

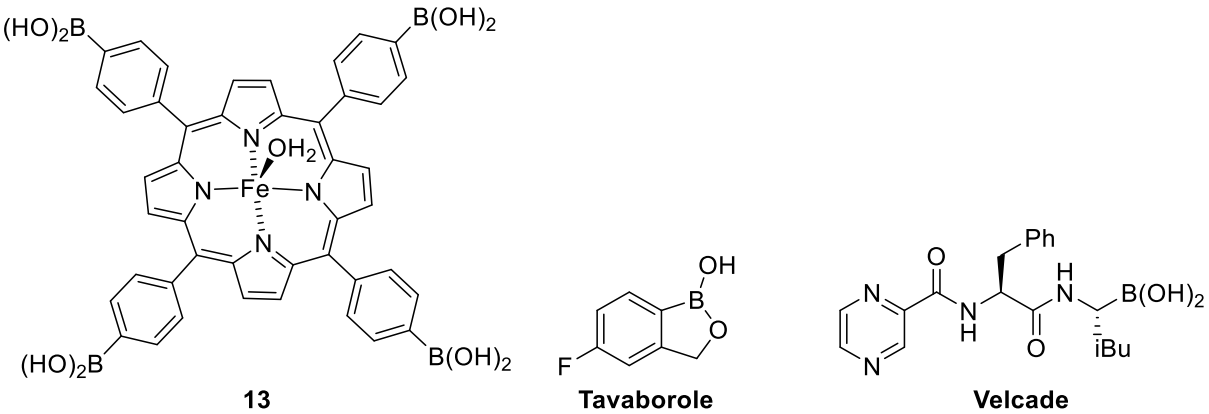

Figure 2: Bioactive Molecules Featuring C-B Bonds

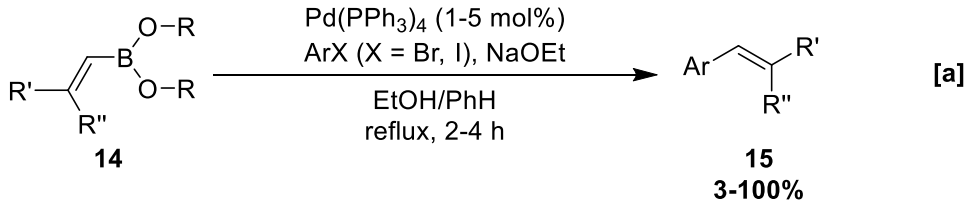

14 **15** **3-100%** **[a]**

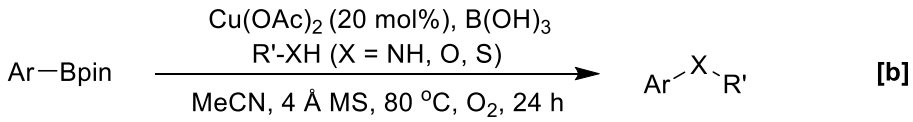

16 **17** **36-94%** **[b]**

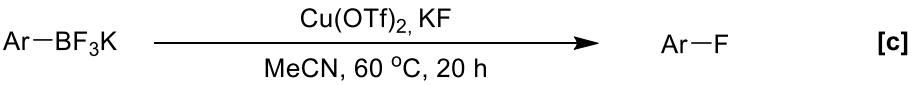

18 **19** **21-71%** **[c]**

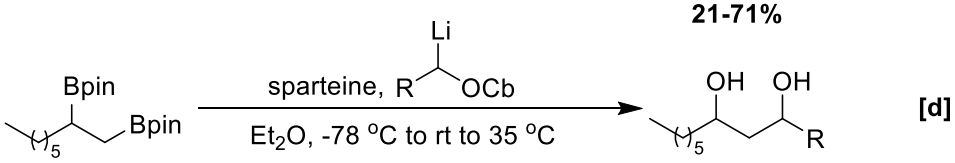

20 **21** >95:5 dr, **43-94%** **[d]**

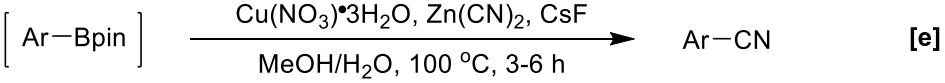

22 **23** **53-70%** **[e]**

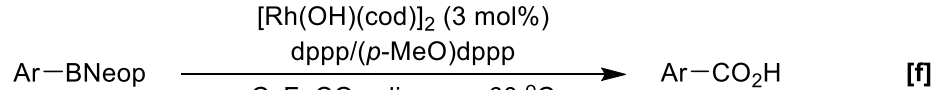

24 **25** **49-95%** **[f]**

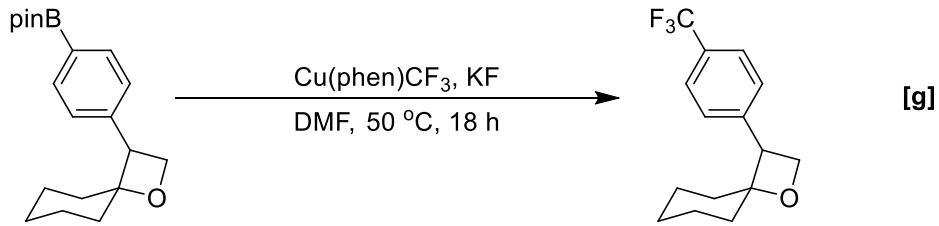

26 **27** **94%** **[g]**

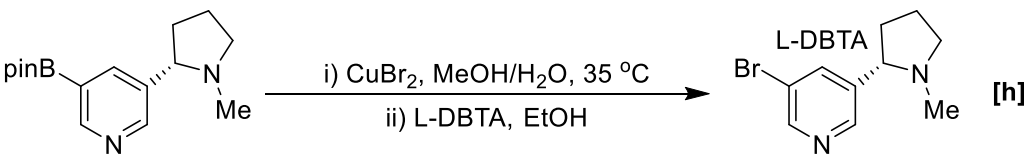

28 **29** **78%** **[h]**

Scheme 2: Selected Transformations of Organoboron Compounds

In the past two decades, further useful transformations of the C-B bond have been developed, which has secured the status of organoboron compounds as important intermediates in synthesis. These include (but are not limited to) amination/etherification/thiolation (Scheme 2b), fluorination (Scheme 2c), homologation/alkylation (Scheme 2d), cyanation (Scheme 2e), and carboxylation (Scheme 2f).[9–13] The utility of these new transformations is illustrated by their widespread usage in drug discovery and process development. For example, trifluoromethylation and bromination of (hetero)aryl boronates have been used for the synthesis of spiro-oxetane drug scaffold **27** and a nicotine hapten precursor **29**, respectively (Scheme 2g, h).[14,15]

A variety of organoboron derivatives, such as boranes, boronic acids, boronic (boronate) esters, borinic acids, borinic esters, boroxines, and trifluoroborates, among others, can be employed for these transformations (Figure 3). Of these derivatives, boronate esters are among the most synthetically useful, owing to their ease of handling, good reactivity, and solubility. Furthermore, these compounds carry advantages over their organometallic analogues, such as organostannane, organozinc, and organocopper reagents, including greater air stability, lower toxicity, and commercial availability.[16,17] Reflecting the abundance of densely functionalised aromatic scaffolds in organic molecules, the development of new methodologies for the formation of aromatic boronate esters is of interest in synthesis. This forms the focus of the following sections in this review. Space precludes a discussion of the borylation of other C-H bonds, such as those within aliphatic, vinylic, allylic, and benzylic systems. However, a number of reviews within this area are available.[18–23]

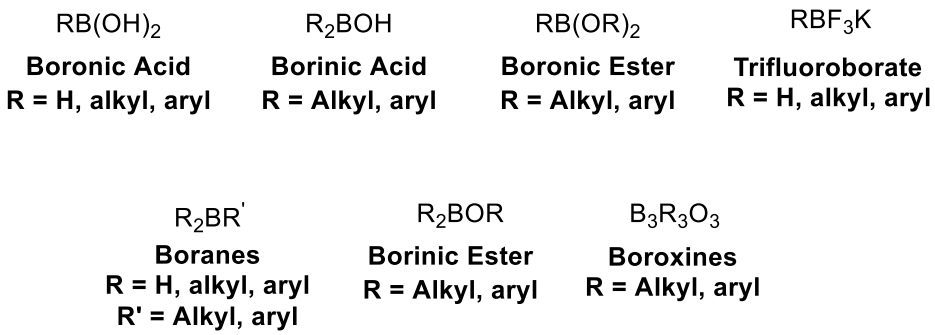

Figure 3: Selected Organoboron Derivatives

1.3 Synthesis of Aromatic Organoboron Compounds

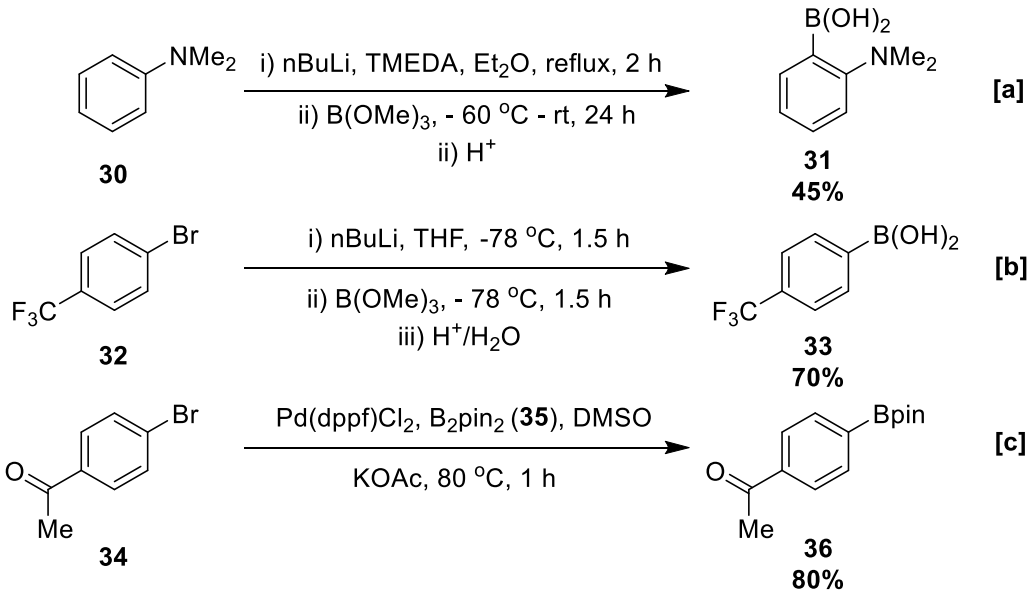

Scheme 3: Selected Syntheses of Organoboron Compounds

Traditionally, the synthesis of aromatic organoboron compounds is accomplished by metalation of a C-H or C-X bond (X = Cl, Br, I) by a representative organometallic reagent, followed by an electrophilic quench with a borate (Scheme 3a, b).[24,25] Whilst this strategy carries advantages, such as low reagent cost and operational simplicity, there are limitations. For instance, in C-H metalation a directing/activating group such as the tertiary amine in **30** can be required to provide C-H acidity and selectivity in the deprotonation step. This is less problematic in metal halogen exchange, which is typically faster than C-H deprotonation. However, pre-functionalisation is required to generate the haloarene precursor. Furthermore, the hard bases required offer poor functional group tolerance (FGT). In this context, transition metal catalysts are attractive because they can offer superior scope, milder reaction conditions, and improved atom economy. For example, in 1995 Miyaura and co-workers described the Pd catalyzed borylation of aryl halides such as aryl ketone **34** using bis(pinacolato)diboron **35** to form the corresponding aryl boronate ester **36** (Scheme 3c).[26] Whilst this approach is amenable to late stage functionalisation, it remains limited by the requirement for a pre-functionalised aromatic halide. A simple approach to borylation involves the direct transformation of C-H to C-B. To a significant extent, catalytic borylation of aromatic C-H bonds has addressed many of the shortcomings of the aforementioned strategies.

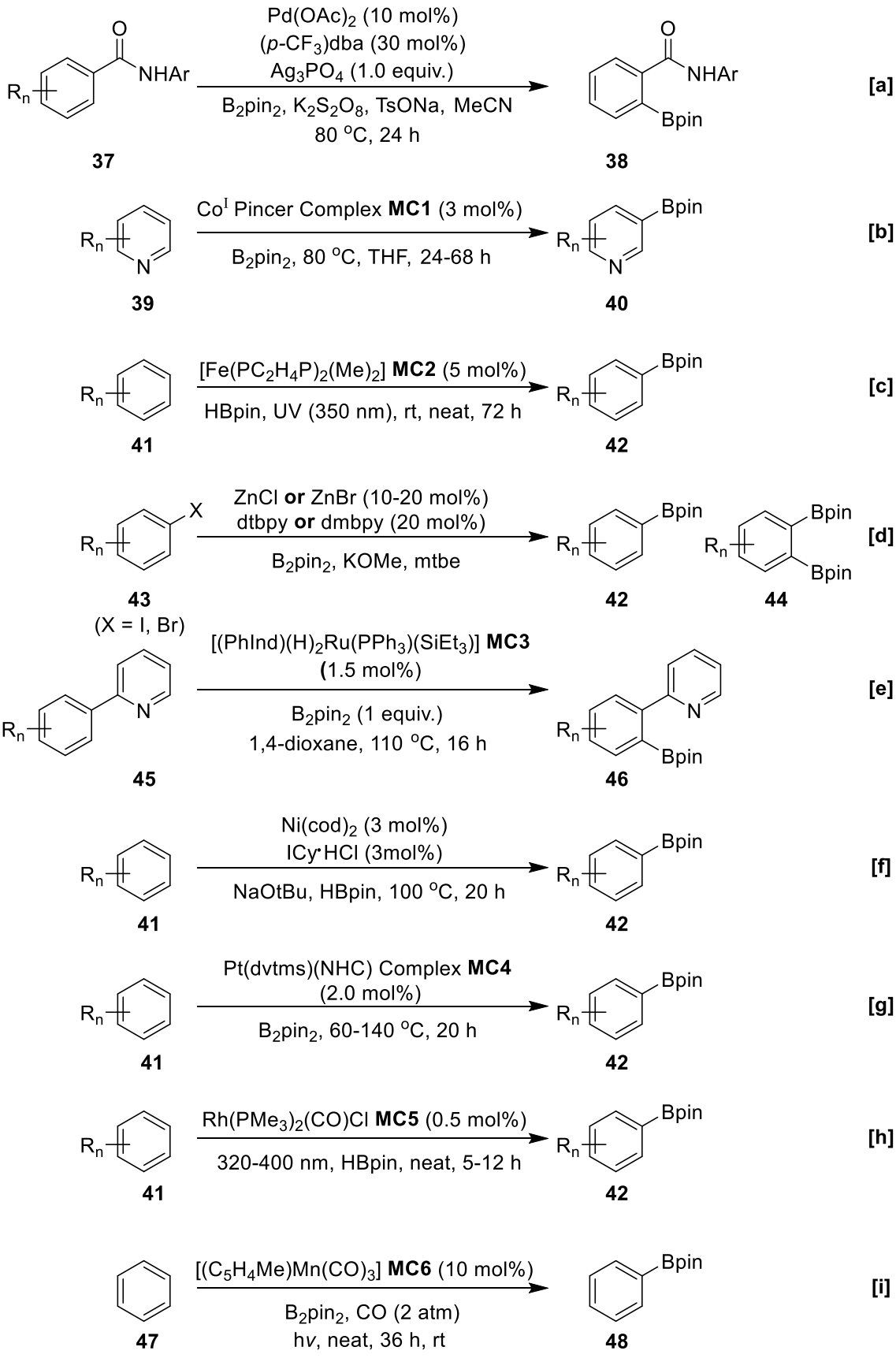

Scheme 4: Transition Metal Catalysed Aromatic C-H Borylations

Transition metals such as Pd, Co, Fe, Zn, Ru, Ni, Pt, Rh, Mn, and Ir have now been shown to catalyse this process (Scheme 4)*.[27–35] However, complexes based on Ir have been particularly effective in constructing C-B bonds. This represents the methodology investigated in this project, and the following section briefly discusses the development of this area.

1.4 Introduction to Ir Catalysed C-H Borylation

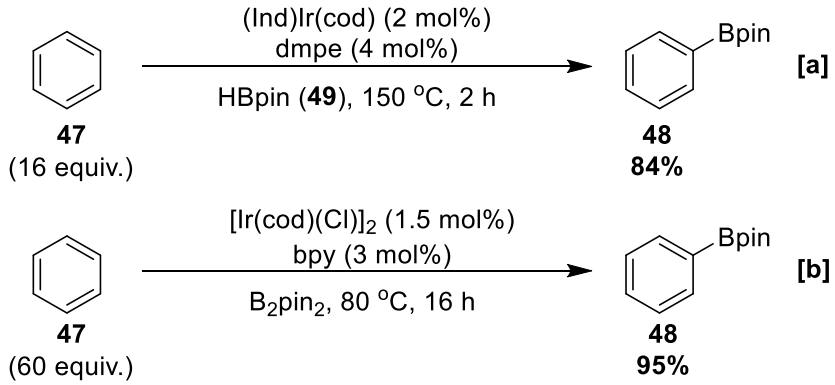

Scheme 5: Initial Reports of Ir-Catalysed C-H Borylation

In 2002, independent publications by Smith *et al.* alongside Hartwig, Ishiyama, Miyaura, *et al.* (HIM) described the catalytic borylation of aryl C-H bonds by Ir^{III} trisboryl complexes (Scheme 5).[36,37] This was built on earlier work using other iridium boryl complexes.[38–40] Smith's system employed (Ind)Ir(cod) as the precatalyst (cod = 1,5-cyclooctadiene, Ind = indenyl), 1,2-bis(dimethylphosphino)ethane (dmpe) as the ligand, and HBpin (**49**) as the boron reagent (Scheme 5a). The HIM system employed $[Ir(cod)Cl]_2$ as the precatalyst, 2,2'-bipyridine (bpy) as the ligand, and B_2pin_2 as the boron reagent (Scheme 5b). Maximum turnover numbers (TON) in the original Smith system were *ca*. 4500, and *ca.* 8000 in the original HIM system. Reflecting this and subsequent developments, most C-H borylations are conducted with $[Ir(cod)(OMe)]_2$ (precatalyst), a ligand derived from bipyridine, and B_2pin_2 or HBpin (boron reagent).[41,42]

1.5 Mechanism

The generally accepted mechanism for this process is given in Scheme 6.[43–47] The reaction involves a catalytic cycle that oscillates between Ir^{III}/Ir^{V} intermediates.

* The structures of these complexes and their associated ligands among others are provided in section 5.3.

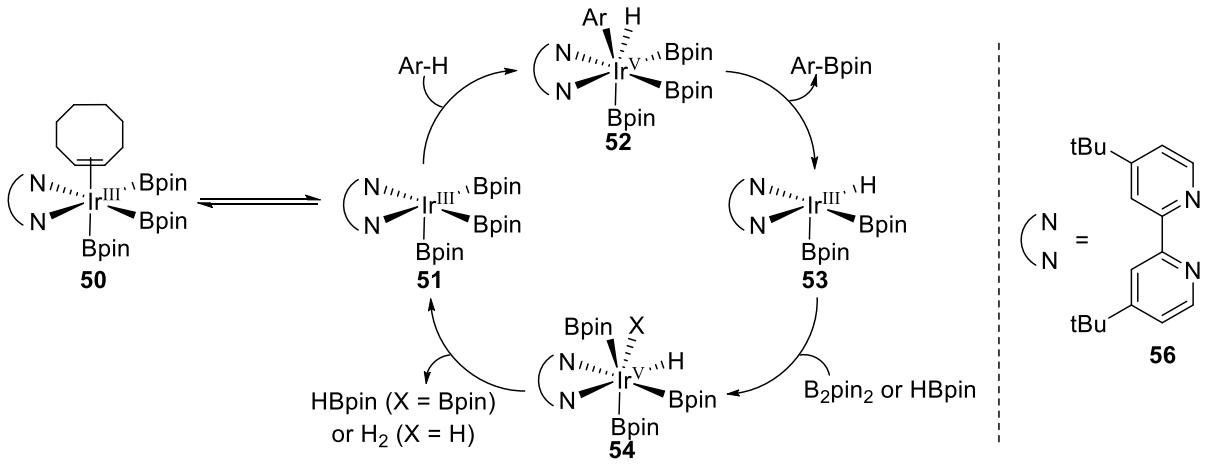

Scheme 6: Catalytic Cycle of the Ir-Catalysed C-H Borylation

Combination of the precatalyst, ligand, boron reagent, and solvent produces the resting state of the catalyst **50**. This is a hexacoordinate Ir^{III} trisboryl complex, bearing two ancillary donor species and a weakly bound cyclooctene (coe) ligand. The production of **50** occurs during an induction period, in which cod is reduced to coe and the boron reagent enables oxidation of the Ir^{I} precatalyst. Following this, coe dissociates to form a pentacoordinate active species **51**, which possesses a vacant coordination site. C-H bond cleavage occurs at **51** via rate limiting oxidative addition to form an Ir^{V} heptacoordinate complex **52**. Reductive elimination of the carbon fragment with a boryl ligand produces an aryl boronate and an Ir^{III} bisboryl hydride **53**. Finally, the cycle is completed via the oxidative addition of B_2pin_2 or HBpin, followed by the reductive elimination of HBpin or H_2, respectively. B_2pin_2 reacts preferentially over HBpin, and therefore the catalysis can be divided into two distinct cycles according to the boron reagent involved.

1.6 Scope and Reactivity

The reaction shows good selectivity for aromatic C-H bonds, with C-Cl, C-Br, and C-I bonds being acceptable. Groups such as nitrile, silyl, ketone, amide, ester, amine, some alcohols, and others are generally well tolerated (*vide infra*). However, nitro, sulphonyl, alkenes, alkynes, and enolisable protons can be problematic. The reaction can be conducted in a variety of solvents, although polar solvents have an inhibitory effect. Of the two most employed ancillary ligands, 3,4,7,8-tetramethyl-1,10-phenanthroline (tmphen, **55**) confers greater reactivity than 4,4′-di-tert-butyl-2,2′-dipyridyl (dtbpy, **56**) at elevated temperature. This is due to tmphen possessing a more constrained geometry, although the effect is less pronounced at room temperature.[41]

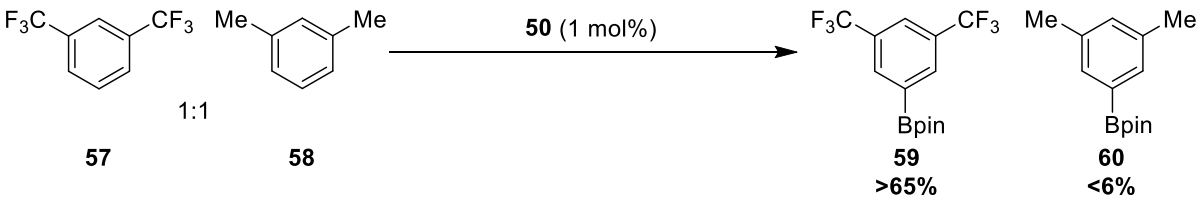

Scheme 7: Competition Experiments Reveal Reactivity in Arenes

Electron-deficient arenes are typically more active than electron-rich arenes, and this has been demonstrated in a competition borylation between a 1:1 mixture of **57** and **58** (Scheme 7).[43] Despite both substrates possessing equally accessible C-H bonds on steric grounds, the GCMS conversion of electron deficient **57** was >65%, compared to the <6% conversion of **58**. The result of this study reflects the activating effect of electron-deficient arenes toward C-H oxidative addition. Most heteroarenes show even greater reactivity and will rapidly borylate under mild conditions. However, there are exceptions to this, and a discussion of the C-H borylation of heteroarenes is provided in section 1.7.3.

1.7 Regiochemistry

In the Ir-catalysed C-H borylation, intrinsic selectivity is substrate dependent, and C-H bonds with distinct steric and/or electronic properties can be cleaved preferentially. In carbocyclic arenes, the regiochemistry is generally governed by steric effects, although electronics can manifest. The selectivity can be altered through modification of the catalyst and/or substrate to produce C-H activation at otherwise less reactive C-H sites. This is referred to as directed borylation and is discussed in section 1.7.2. For simplicity, this section divides the discussion of regiochemistry in carbocyclic arenes by systems which display intrinsic or directed regiocontrol. The regiochemistry observed in heteroarenes is subsequently overviewed. For a given system, a greater manifestation of sterics/electronics is reflected in the distributions of aryl boronate regioisomers.

1.7.1 Intrinsic Selectivity

1.7.1.1 Steric Selectivity

Owing to the crowded nature of the active catalyst **51**, many carbocyclic arenes borylate with steric regiocontrol.[48] In some instances, this provides an orthogonal method to directed *ortho* metalation (DoM) and electrophilic aromatic substitution (S_EAr) strategies.[49]

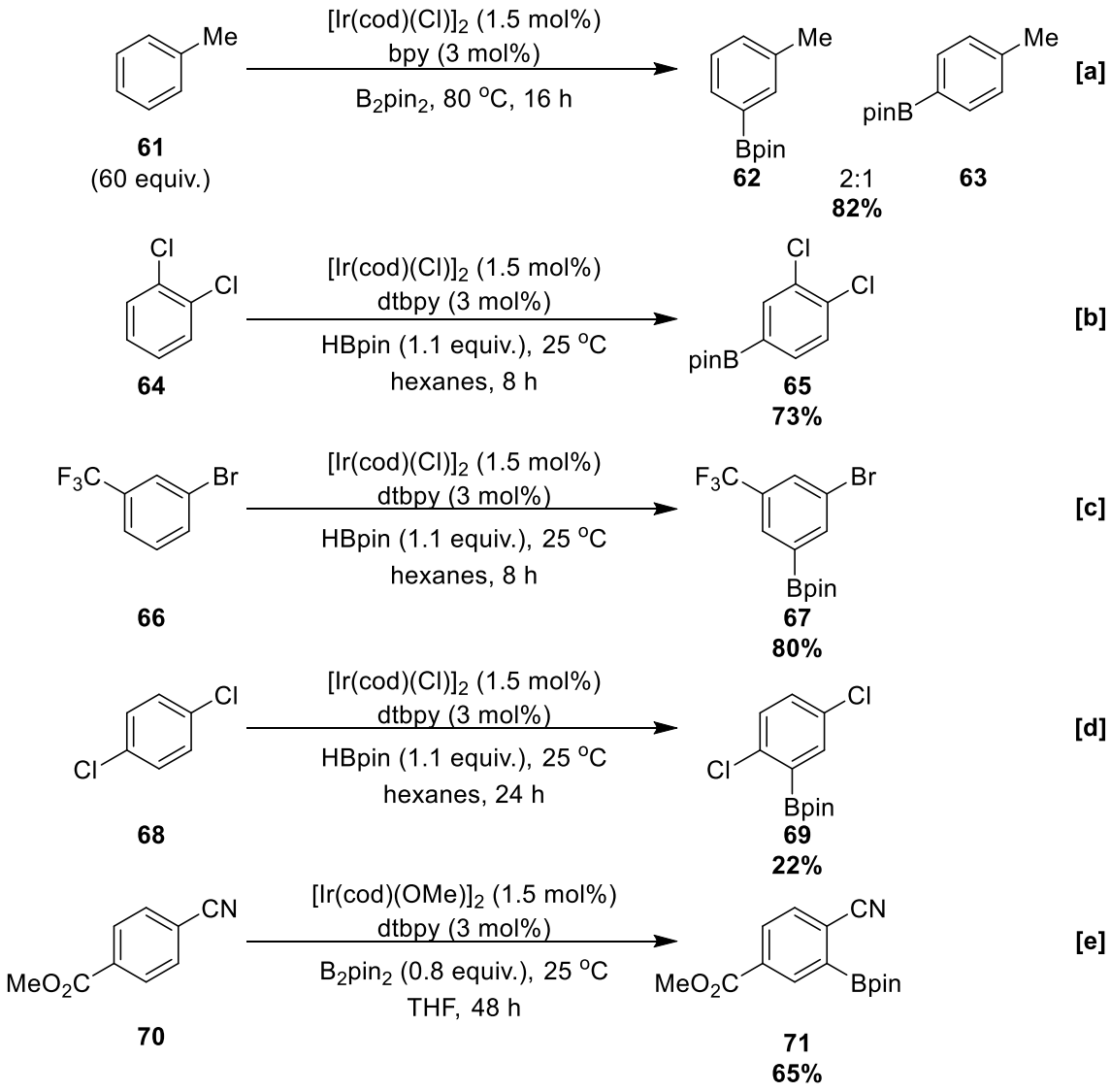

Scheme 8: Sterically Controlled Ir C-H Borylation of Arenes

At elevated temperature, the borylation of mono-substituted arenes such as toluene **61** leads to statistical product outcomes (Scheme 8a). The borylation of symmetrical 1,2- disubstituted arenes and 1,3- disubstituted arenes **64** and **66** proceeds at the uncongested C-H bonds and affords a single product. This is because C-H cleavage *ortho* to substituents which are moderate/large in size is disfavoured (Scheme 8b, 8c). However, if the catalyst is not offered an unhindered C-H site, C-H activation *ortho* to moderately sized substituents can occur, and this is observed in the borylation of 1,4-disubstituted **68** (Scheme 8d). Borylation *ortho* to small substituents (F, CN) is facile, for instance nitrile **70** is selectively borylated at the C-H bond *ortho* to the nitrile group (Scheme 8e).[48,50,51]

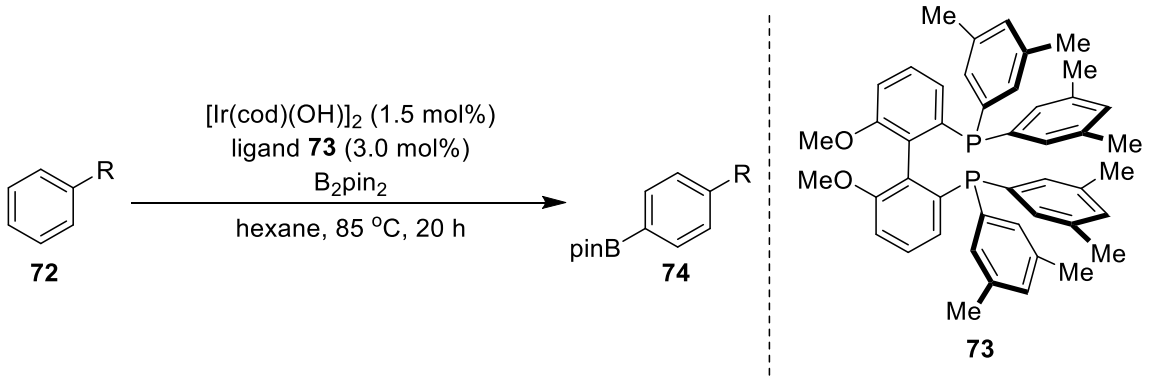

Scheme 9: *para* Selective Borylation using Ligand **73**

Systems have been described which offer improved steric selectivity in substrates with multiple reactive C-H bonds. For instance, *para* selective borylation can be achieved by establishing a more congested environment around the active catalyst. An example of this uses bulky phosphine ligand **73**, which forms an active species which roughly mimics an enzyme active site, sterically inhibiting access of the catalyst to the *ortho* and *meta* C-H bonds (Scheme 9).[52,53] Furthermore, the *para* selective C-H borylation of aromatic esters, amides, and pyridines has been developed using cooperative Ir/Al catalysis.[54] Selectivity is primarily conferred by a bulky Al Lewis acid methylaluminumbis(2,6-di-tert-butyl-4-methylphenoxide) (MAD), which forms an adduct **78** with the substrate.

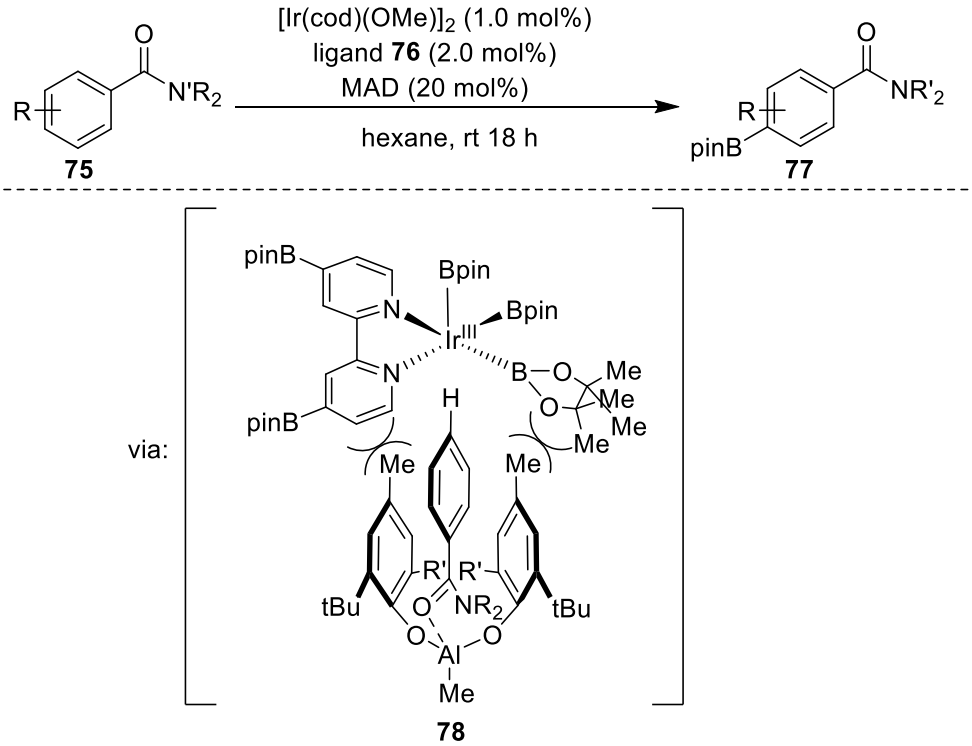

Scheme 10: *para* Selective Borylation with a Bulky Lewis Acid

Selectivity is enhanced with the ligand 4,4'-bis(4,4,5,5-tetramethyl-1,3,2-dioxaborolan-2-yl)-2,2'-bipyridine ($(Bpin)_2bpy$, **76**), owing to the large size of the Bpin substituents. The authors suggested that steric repulsion between the catalyst and the adduct blocks the *ortho* and *meta* positions (Scheme 10). Other systems which offer *ortho*, *meta*, and *para* selectivity have been developed; however the remainder discussed in section 1.7.2 exploit a chelation-controlled directing effect.

1.7.1.2 Electronic Selectivity

Some carbocyclic arenes borylate under electronic control, and this is most evident in reactions that are conducted at ambient temperature. For example, benzodioxole **79** borylates with near complete selectivity for the more hindered *ortho* position, despite the presence of uncongested C-H sites (Scheme 11a). Computational and experimental results conducted by Smith and co-workers indicated that the transition state of C-H cleavage possesses significant proton transfer character, and is facilitated by boryl basicity.[55] This suggested that regioselectivity of this reaction may be controlled to a degree by C-H acidity.

Later, Steel and co-workers reported that monosubstituted and unsymmetrical 1,2-disubstituted arenes undergo borylation with significant electronic selectivity at room temperature.

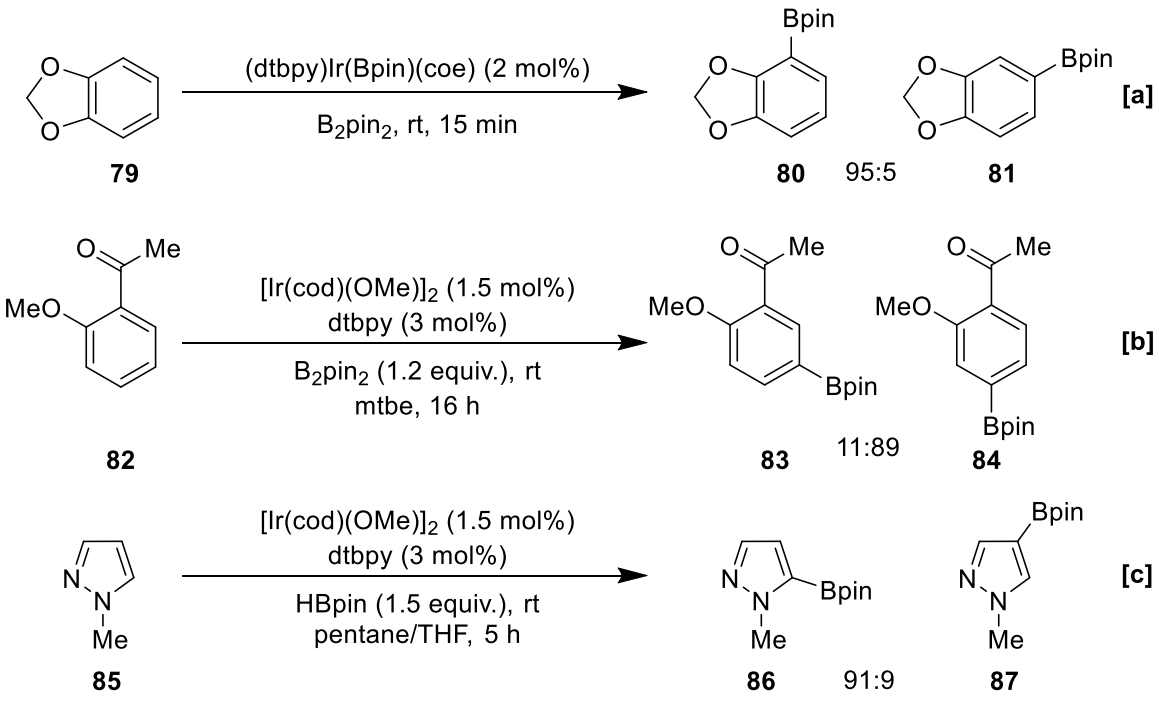

Scheme 11: Electronically Controlled Regiochemistry in Ir C-H Borylation of Aromatics

For example, aryl methoxy ketone **82** shows high selectivity for one C-H site, despite the fact that sterics would afford a statistical (1:1) product distribution (Scheme 11b). This selectivity was eroded at elevated temperature, reverting to normal steric selectivity. This study led to the general observation that π-electron acceptors (-M) favour *para* borylation, and π-donors (+M) (also σ-acceptors) favour *meta* borylation. Therefore, the selectivities offered by ±M substituents are orthogonal to those found in S_EAr. Mirroring Smith's conclusion, C-H acidity values correlated well with site-selectivity.[44] In particular, electronic selectivity manifests frequently in the borylation of heteroaromatic substrates. For instance, the borylation of N-methylpyrazole **85** shows high selectivity for the sterically hindered alpha position (Scheme 11c). Recently, Houk and co-workers used a distortion/interaction analysis to probe the selectivities in the Ir C-H borylation of aromatic C-H bonds. It was shown that regioselectivity is primarily governed by the interaction energy of the substrate and the active species in the transition state. The transition state of C-H oxidative addition was calculated to be late and to possess an Ir-C bond that is largely formed. Therefore, Ir-C bond strengths were shown to correlate well with the activation energy, giving a robust predictor of regiochemistry.[56]

1.7.2 Directed Borylation

Systems which have been designed to alter the intrinsic selectivity of the catalyst show special regiochemistry. Classes of directing systems can be divided into inner-sphere and outer-sphere, and both of these are presented. Systems are discussed according to their relevance to heteroaromatic borylation. For consistency, specific examples in this section relate to carbocyclic arenes, and the presented systems have been chosen according to their relevance to heteroaromatic C-H borylation, which is the primary focus. A full discussion of directed borylation is not presented, although a review has been published by Lassaletta and co-workers.[57]

1.7.2.1 Inner-Sphere Direction

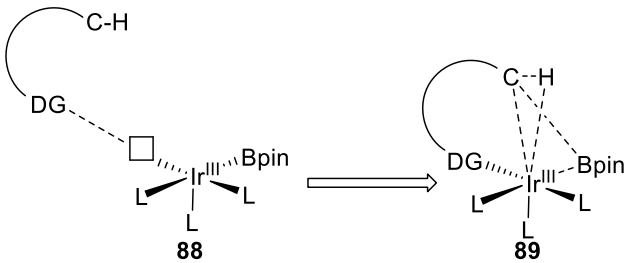

Figure 4: Concept of Inner-Sphere Directed Borylation

Inner-sphere directed borylation refers to a substrate interaction with the Ir metal centre which promotes regioselective borylation, and this tends to promote *ortho* borylation. Reported strategies typically involve the design of a four-coordinate active species with two vacant coordination sites. A basic functionality on the substrate acts a DG (directing group) and ligates at this site, which kinetically facilitates the selective cleavage of a C-H bond (Figure 4). For example, *ortho*-selective borylation is possible with Silica-SMAP (Silica-supported Silicon-constrained Monodentate Trialkylphosphine). This is a phosphine ligand immobilised on a heterogeneous silica-supported surface. The ligand selectively forms a mono-phosphine-ligated active species, permitting substrate coordination. This has been employed extensively in the site-selective borylation of arenes with various coordinating groups, such as aryl esters (Scheme 12), carbamates, ethers, acetals, carbonates, sulphonates, phosphoramides, chlorides, quinolines, and quinoxalines (see sections 1.7.3.2.2 and 1.7.3.4.1).[58–61]

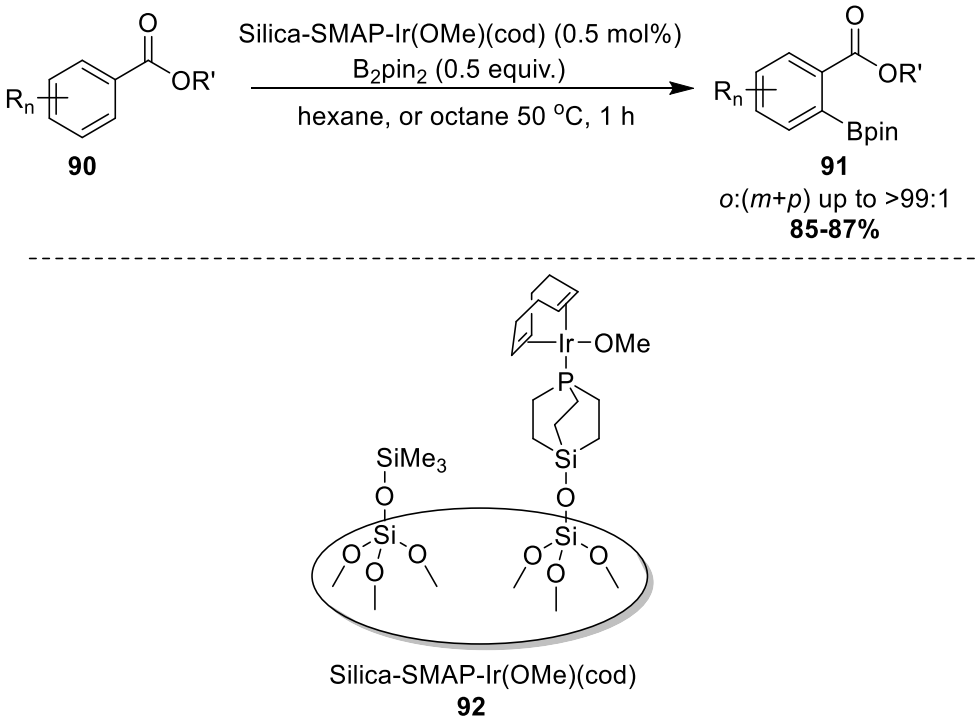

Scheme 12: Silica-SMAP Directed *ortho* Borylation of Aromatic Esters

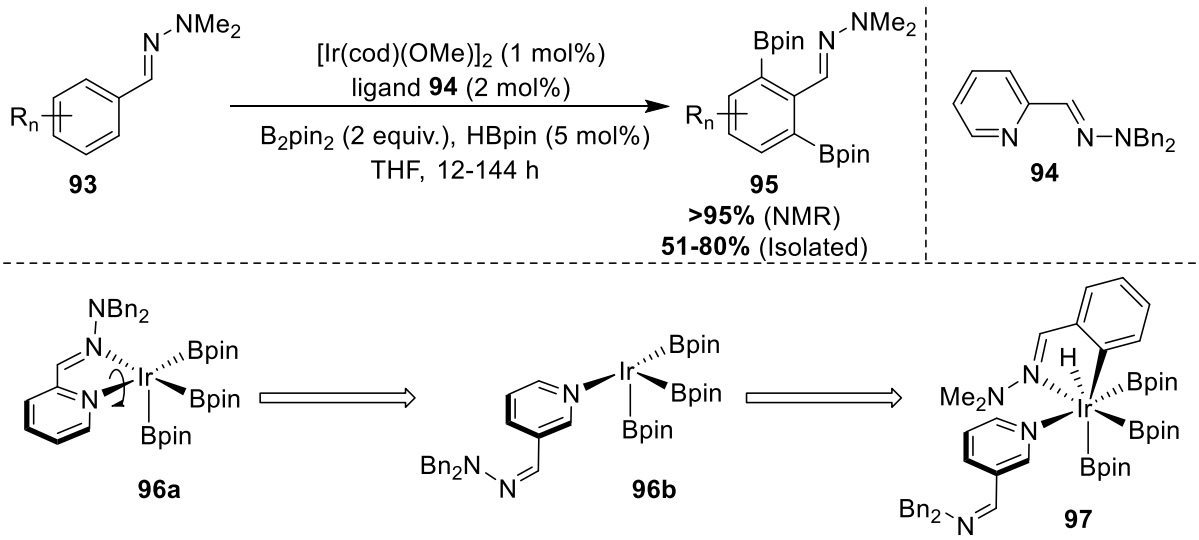

Scheme 13: *Ortho* selective Bisborylation of Aryl Hydrazones with a Hemi-Labile Ligand

Other non-nitrogen based ligands can similarly facilitate *ortho* direction. For instance, the *ortho* selective borylation of heteroaryl esters may be achieved using a labile ligand, such as $AsPh_3$.[62] The development of this system was built on previous work on *ortho* directed C-H borylation using related P and As ligands.[63,64] A communication which describes C-H borylation utilising $AsPh_3$ employs heteroaromatic substrates only, so it is discussed in section 1.7.3.3. Nitrogen-based ligands also feature in inner-sphere direction, and this has been achieved with hemi-labile N,N pyridine-hydrazone ligands such as **94**. Whilst the pyridine moiety remains tightly bound at iridium, the hydrazone portion readily dissociates from the catalyst as shown in **96a** and **96b**, enabling the coordination and subsequent *ortho* (bis)borylation of substrates with a variety of functional groups, including N,N-dimethylhydrazones, quinolines and pyridines (Scheme 13) (see section 1.7.3.2).[65–67]

Ancillary ligands which bind in modes other than dative coordination have also been shown to promote inner-sphere direction. For example, iridium complexes with silyl and phosphorus chelates have been isolated by treating the precatalyst $[Ir(cod)(OMe)]_2$ with ligand **99**, forming **101** (Scheme 14). Presumably, cod dissociates from **101** allowing oxidative addition of B_2pin_2 to form the putative tetravalent active species, which possesses two vacant coordination sites. This enables the *ortho* C-H borylation of arenes with a library of functional groups. These include amides (Scheme 14), ethers, esters, N-alkoxyamides, and quinolines (section 1.7.3.2).[68] Notably, silyl and nitrogen donors can also be used in a similar manner.

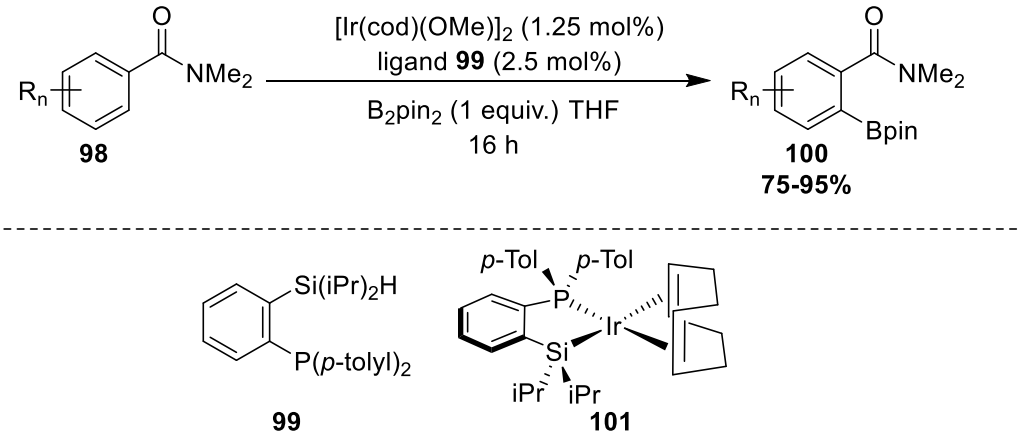

Scheme 14: *ortho*-Selective Borylation of Aryl Amides with Silyl Phosphorus Donors

In a similar fashion, complexes bearing pyridine tethered silyl borane ligands such as **103** have been employed in the *ortho* selective borylation of aromatic esters (Scheme 15). Furthermore, carbamates, acetates, amides, imides, pyridines, amines, oximes, and hydrazones also undergo directed C-H borylation with excellent selectivities.[69] Another strategy for inner-sphere direction involves removal of the ancillary ligand so that a weakly coordinating, monodentate substrate can take its place. For example, cyclic S,S-acetals **107** facilitate the *ortho*-directed borylation of (hetero)arenes with a variety of substitution patterns (Scheme 16). Whilst further mechanistic evidence is required, this is presumably an inner-sphere direction with the substrate binding at S as a labile ligand. **109** was proposed to be an intermediate in the catalytic cycle, rationalising the selectivity.[70]

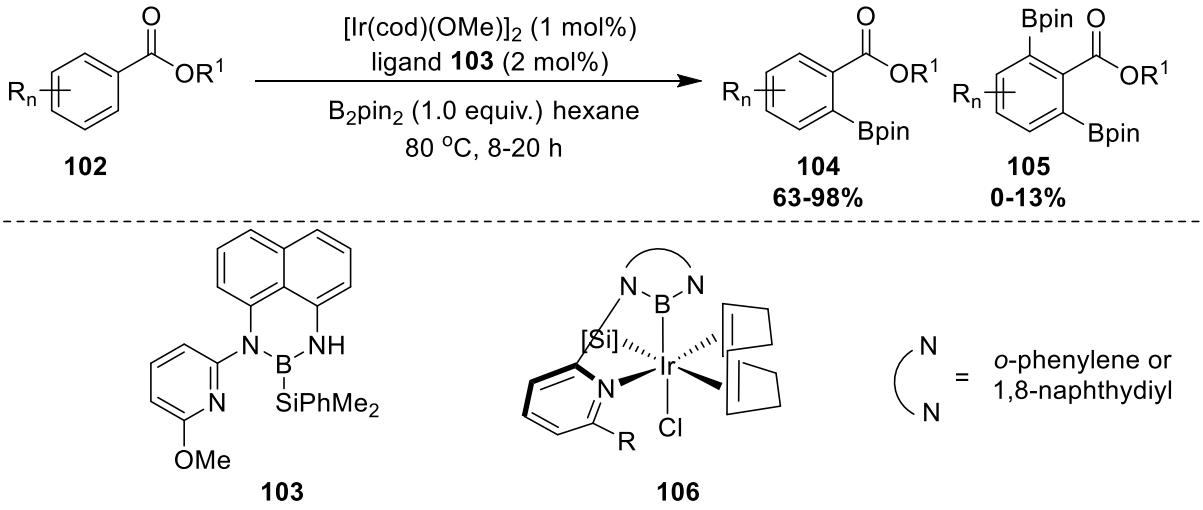

Scheme 15: *Ortho* selective Borylation of Aryl Esters with Nitrogen Boron Donors

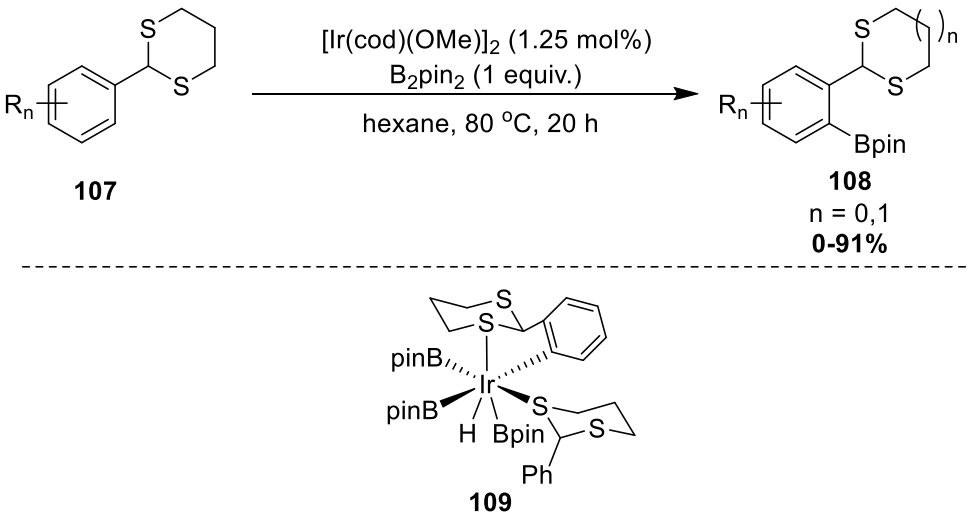

Scheme 16: *Ortho* Selective Borylation of Aryl Dithioacetals

Relay direction is a special sub-class of inner-sphere system which employs substrates with Si-H bonds. A hydrosilyl tether at the substrate **110** (either pre-functionalised or generated *in situ*) adds to the active species, likely by oxidative addition or σ-bond metathesis. Following the expulsion of HBpin, a remote site is rendered kinetically more reactive (Scheme 17). Inner-sphere relay is distinct from the other methods in this section because binding of the directing group with the metal centre does not necessarily require two vacant coordination sites. Substrate scope includes benzylic, phenolic, anilino, N-heterocyclic, and polycyclic aromatic hydrosilanes.[71–73] For example, substituted naphthalenes **113** undergo regioselective *peri* borylation to form **114**.[74,75]

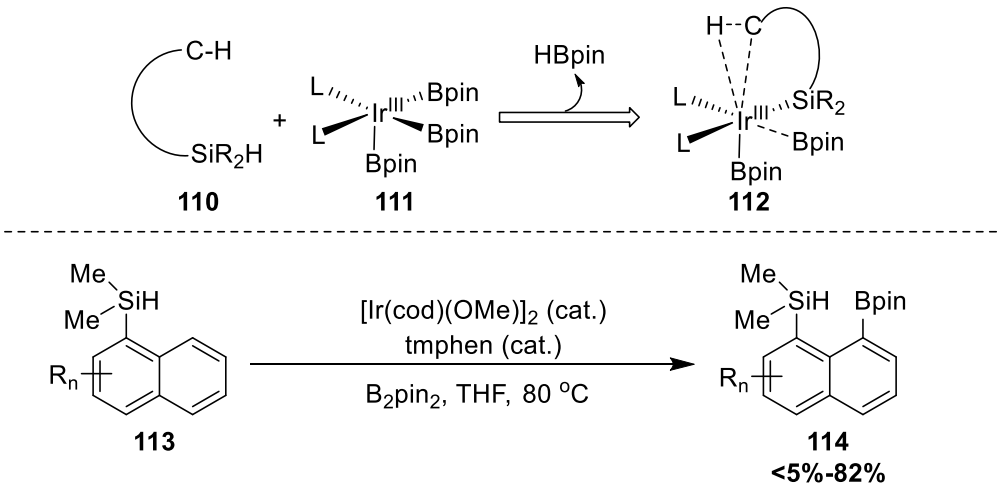

Scheme 17: Concept of Relay Inner-Sphere Directed Borylation (Top), and *peri*-Selective Borylation of Substituted Naphthalenes (Bottom)

1.7.2.2 Outer-Sphere Direction

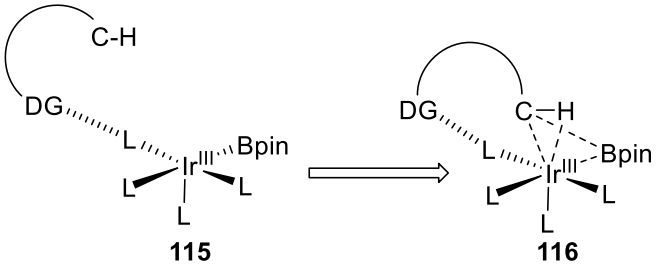

Figure 5: Concept of Outer-Sphere Directed Borylation

Outer-sphere directed borylation refers to a substrate interaction with an ancillary/boryl ligand on the active species which promotes regioselective borylation (Figure 5). This approach tends to promote *ortho* and *meta* borylation. Reported strategies involve the design of substrates and/or ligands that recognise each other via non-covalent interactions, which kinetically facilitates selective C-H cleavage. For example, building on previous work on the *ortho* borylation of NHBoc anilines, the *ortho* borylation of NHBpin anilines **120** has been described (Scheme 18).[76,77] Whilst other N-H bonds undergo borylation via a mechanism that is analogous to the C-H borylation (see section 1.5), anilines spontaneously react with HBpin without catalysis. A calculated transition state **119** indicated that *ortho* selectivity originates from a hydrogen-bond between the *in situ* N-borylated aniline **120** and a boryl ligand on the catalyst (Scheme 18). This approach constitutes a traceless directing group strategy, as the N-B bond is hydrolysed on work-up, reforming the aniline **118**. N-Bpin was shown to be a superior director over NH_2, and N-Boc.

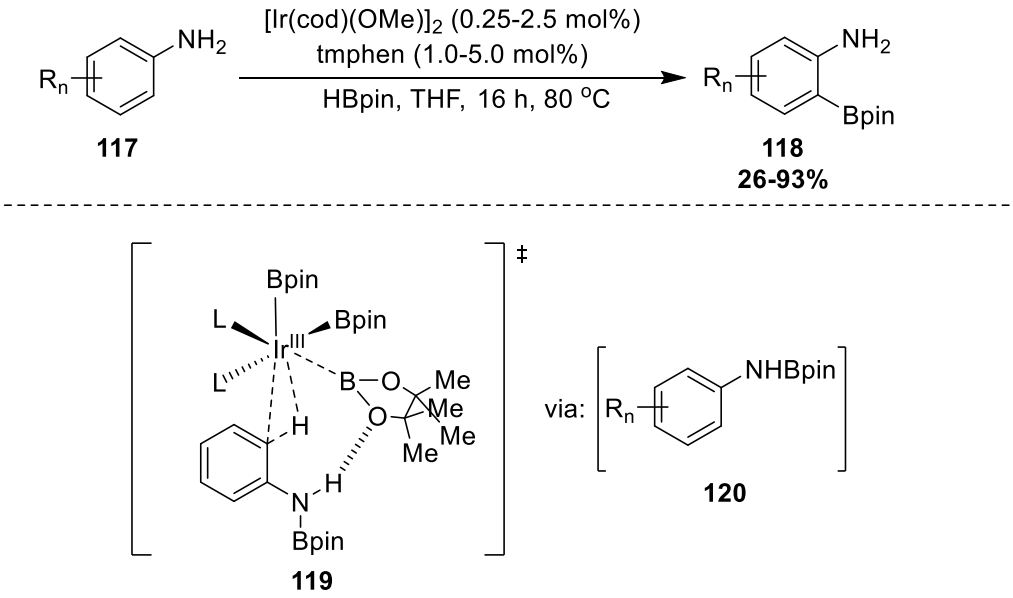

Scheme 18: *Ortho* Selective Borylation of Anilines

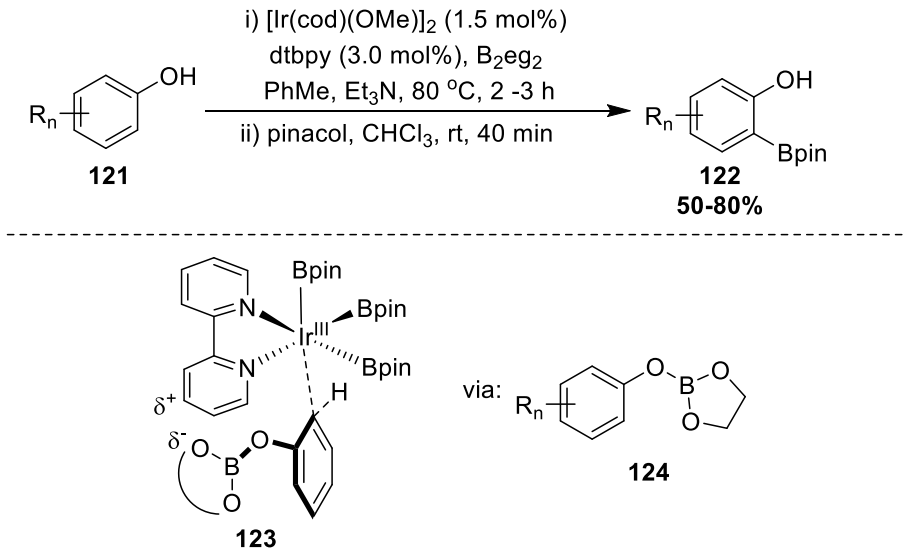

Scheme 19: *Ortho* Borylation of Phenols

However, in the absence of a *para* blocking group regioisomeric mixtures were obtained. It is noteworthy that N-borylation of azoles also led to regioselective borylation, and this is discussed in section 1.7.3.3. Recently, the selectivity of this process was improved significantly by replacing the director NHBpin with the ethylene glycol (eg) ester derivative NHBeg.[78] This likely operates in a similar manner for most substrates; however removal of the *gem* dimethyl groups in Bpin optimises hydrogen-bonding with reduced steric interference. This study was built on previous work involving the *ortho* borylation of phenols **121** with and B_2pin_2 and B_2eg_2, with the latter offering superior selectivity.[79] In a similar fashion, this method relies on the *in situ* borylation of a heteroatom followed by outer-sphere direction. However, the origin of *ortho* selectivity was hypothesised to arise from an unusual electrostatic interaction between the OBeg group and the bpy ligand, rather than from hydrogen-bonding. Substrates without blocking groups bisborylated at the *ortho* positions, and purifications were simplified by isolating boronates as their pinacol esters (Scheme 19).

Outer-sphere direction can also be used to access the *meta* position in aromatic systems. For example, a strategy involving the hydrogen bond recognition between a pendant urea ligand **126** and aromatic amides has been developed which improves *meta* selectivity relative to dtbpy (Scheme 20).[80] Presented evidence suggests that the secondary substrate-ligand interaction places the Ir centre in close proximity to a *meta* C-H bond.

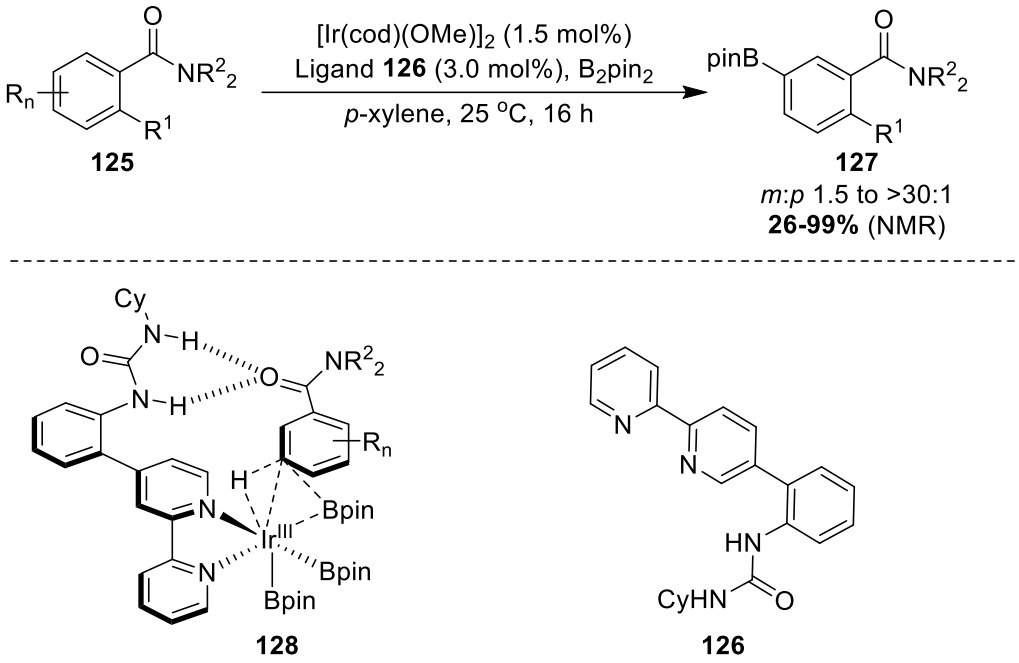

Scheme 20: *meta* Selective Borylation of Aryl Amides

Another example of *meta* selective borylation utilises an ionic sulphonate bipyridine ligand **130** in conjunction with a substrate recognition unit. Substrates bearing ammonium salts in an electrostatic 'ion pairing mode' (Scheme 21a) and amides in a 'hydrogen bond accepting mode' (Scheme 21b) show *meta* selective borylation.[81–84] The latter is an electronically inverted strategy to the *meta* selective C-H borylation described previously using ligand **126**.

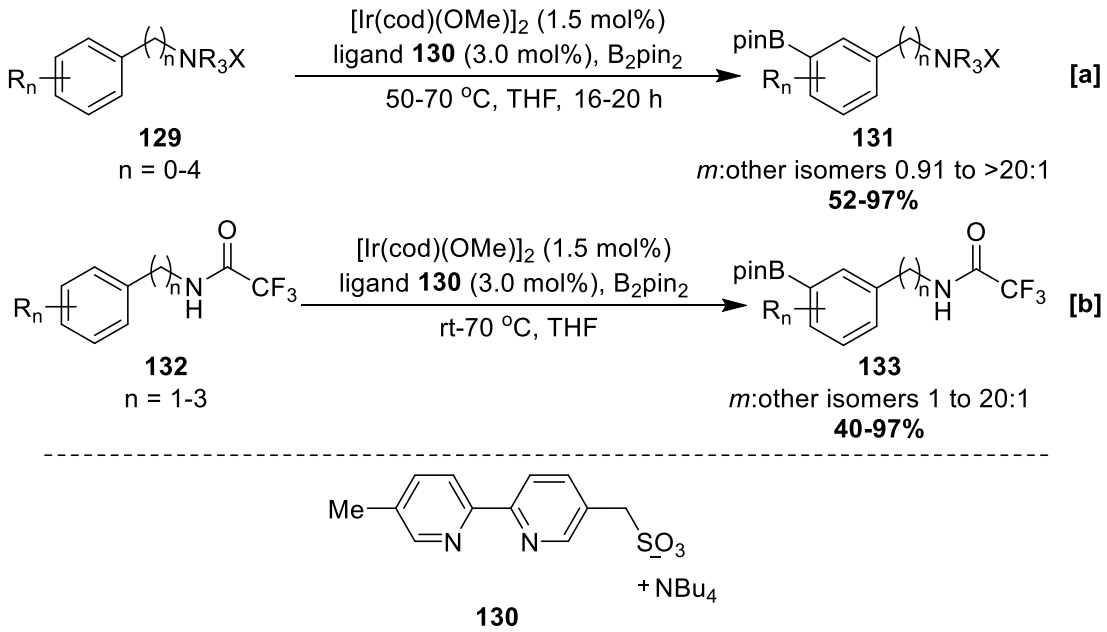

Scheme 21: *meta* Selective Borylation of Aryl Ammonium Salts and Amides

Despite incurring high entropic penalties, arenes bearing recognition units with flexible linkers were tolerated, and up to three (hydrogen bond) or four (ion pair) membered carbon chains displayed largely good to excellent selectivities. Borylations conducted with **130** provided superior *meta* selectivity over dtbpy (ion pair, hydrogen bond) and tmphen (ion pair). Substrate-ligand recognition has also been employed for *para*-selective borylation. One example involves L-shaped bipyridine ligand **135** with a pendant quinolone, which enabled the *para*-selective borylation of aromatic esters.[85] The authors proposed that regiocontrol was established via a non-covalent interaction between the quinolone and the substrate. Selectivity was increased significantly in the presence of KOtBu, and it was suggested that a favourable interaction of K^+ with the substrate promoted the non-covalent interaction (Scheme 22). Despite often presenting a greater challenge, directed systems have also been employed to alter the intrinsic regiochemistry of heteroarenes. In contrast to the sterically governed selectivity observed in carbocyclic systems, heteroarenes show a high degree of intrinsic electronic regiocontrol. Indeed, sterically congested C-H bonds can be activated over unencumbered ones, and the position/nature of constituent heteroatoms can significantly affect regiochemistry. Other reviews of this area are acknowledged, and the next section provides an updated discussion of Ir C-H borylation regiochemistry in heteroarenes.[86,87]

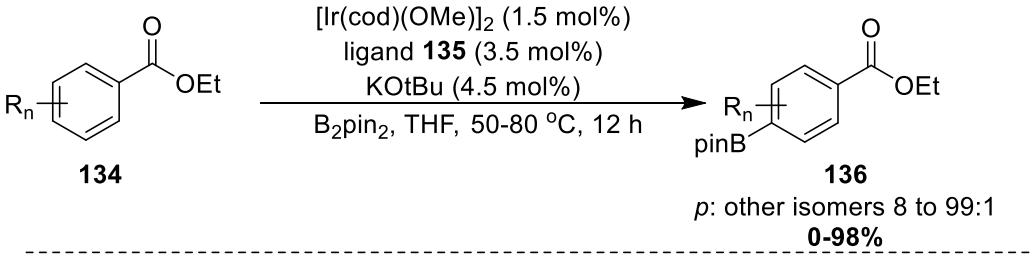

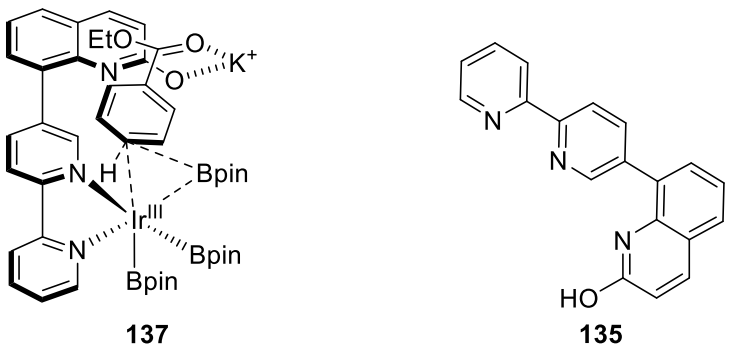

Scheme 22: *para* Selective Borylation of Aryl Esters

1.7.3 Borylation of Heteroarenes

Compounds bearing heteroaromatic scaffolds feature prevalently in pharmaceuticals, bioactive molecules, ligands for metal complexes, natural products, agrochemicals, and functional materials, in addition to others.[88–94] Therefore, atom economical, streamlined syntheses of these molecules are of commercial value. The Ir-catalysed C-H borylation can lend itself well to the late-stage functionalisation of these motifs because the reactivity of heteroarenes is typically high, and proceeds with moderate to excellent regioselectivity. This review outlines the regiochemistry in the Ir C-H borylation of heteroarenes, and substrate classes are divided according to ring type ring size (5/6), and number of heteroatoms (1/2). Heteroarenes that do not fit into these categories are discussed in the miscellaneous section 1.7.3.5.

1.7.3.1 Five-Membered Heteroarenes with One Heteroatom

1.7.3.1.1 Pyrrole, Thiophene and Furan

Pyrroles, thiophenes, and furans generally have high activity and undergo borylation alpha to the heteroatom. Employing $[Ir(cod)(Cl)]_2$, HIM described that even using 10 equivalents of arene in the C-H borylation of the parent heterocycles leads to the formation of a mixture of mono- and bisborylated products (Table 1, Entries 1, 2, 3).[95] Unidentified 3-boryl regioisomers were noted in the borylation of furan alongside **139c** and **140c**. In the borylation of thiophene **138b**, reducing arene equivalents to 2.5 is deleterious to selectivity, whilst increasing the equivalents to 20 improves selectivity but reduces yield (Entries 4, 5). This reduction was attributed to an inhibitory effect of sulphur on the catalyst. Pyrrole and thiophene are exhaustively borylated in the presence of excess B_2pin_2 to afford the corresponding 2,5-diborylated products **140a** and **140b** (Table 1, Entries 6, 7). However, furan affords a mixture 2,5- and 2,4- diborylated products **140c** and **141c**, and this may reflect an enhanced electronic reactivity of the arene (Table 1, Entry 8). It was subsequently shown that all of the parent heterocycles undergo facile and selective bisborylation at room temperature using the related $[Ir(cod)(OMe)]_2$ precatalyst (Table 1, Entries 9-11).[42,48] The corresponding 2-substituted heterocycles also selectively undergo alpha borylation, and this is observed in the borylation of 2-methyl derivatives (Scheme 23a).[96]

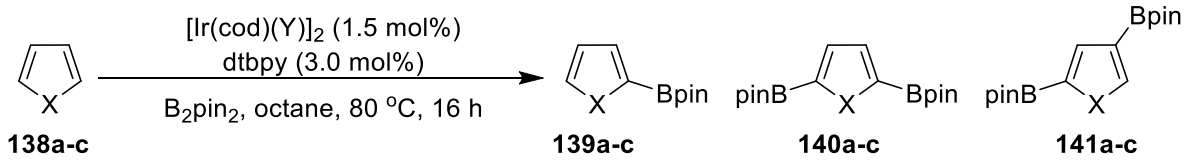

138a-c **139a-c** **140a-c** **141a-c**

Entry	**138**	X (Eq.)	Y	Eq. B_2pin_2	T/ °C	t / h	**139**:**140**:**141**†	Yield /%
1	**a**	NH (10)	Cl	1	80	16	*ca*. 85:15:0	67
2	**b**	S (10)	Cl	1	80	16	*ca*. 85:15:0	83
3	**c**	O (10)	Cl	1	80	16	*ca*. 85:15:0	83*
4	**b**	S (2.5)	Cl	1	80	16	56:44:0	-
5	**b**	S (20)	Cl	1	80	16	93:7:0	69
6	**a**	NH (1)	Cl	1.1	80	16	0:>99:1	80
7	**b**	S (1)	Cl	1.1	80	16	0:>99:1	80
8	**c**	O (1)	Cl	1.1	80	16	0:87:13	71
9	**a**	NH (1)	OMe	1.0	25	0.5	0:100:0	75
10	**b**	S (1)	OMe	1.0	25	0.5	0:100:0	83
11	**c**	O (1)	OMe	1.0	25	1	0:100:0	93

***Isolated alongside unidentified 3-boryl regioisomers
† Isomeric purities were determined with GCMS and NMR

Table 1: C-H Borylation of Pyrrole, Thiophene, and Furan

Other C-substituted pyrroles and furans have been seldom reported. However, some examples are presented in Scheme 23. 3- and 2,3- substituted furans alpha borylate selectively in the presence of an ethyl ester/methyl group in the 3- position. Furthermore, the crude borylation mixtures were amenable to a one-pot Suzuki-Miyaura cross-coupling, affording arylated furans **150a** and **150b** (Scheme 23c, d).[97] In contrast to substituted pyrroles and furans, the borylation of thiophenes with a variety of substitution patterns has been described in some detail.[98,99] As with the other heterocycles, 2- and 2,3- substituted thiophenes undergo alpha borylation selectively.

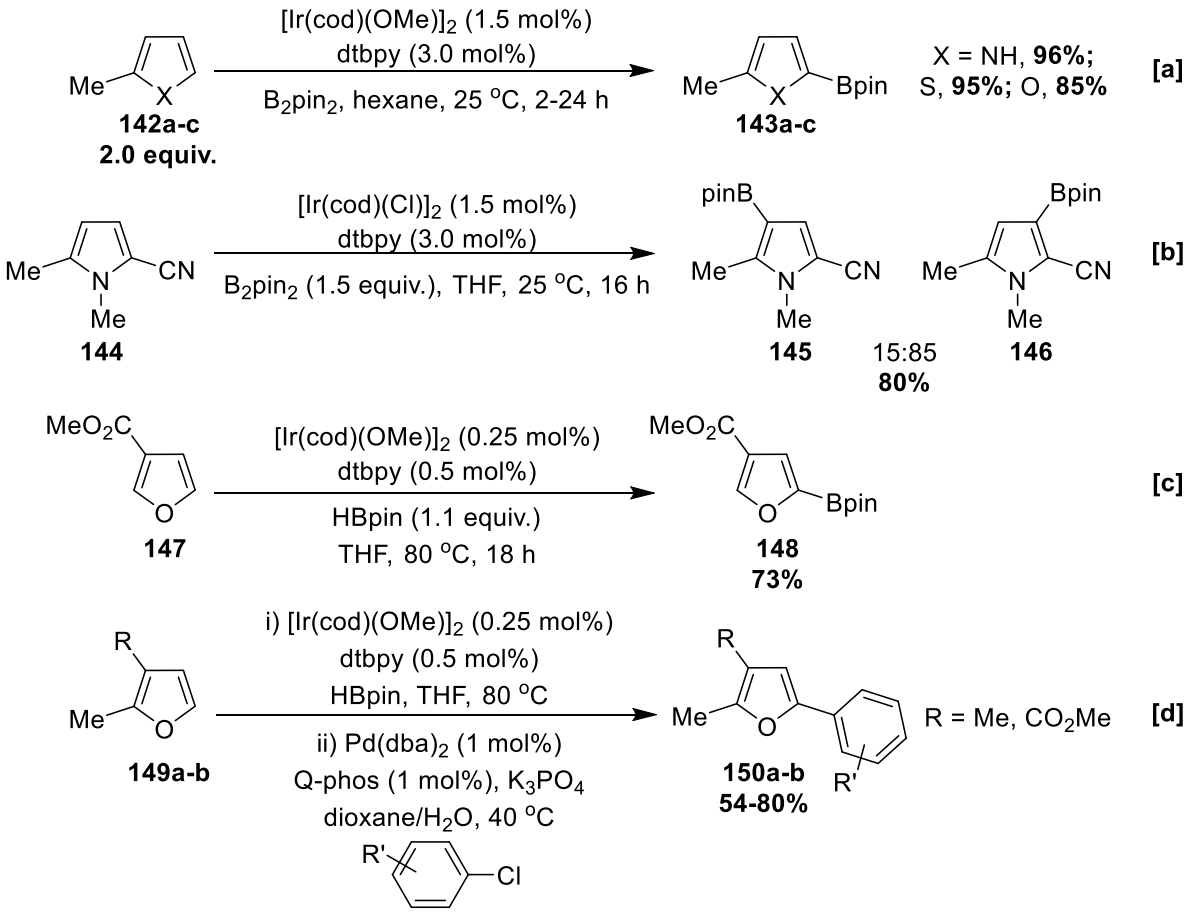

Scheme 23: Selective Borylation of Pyrroles, Thiophenes, and Furans

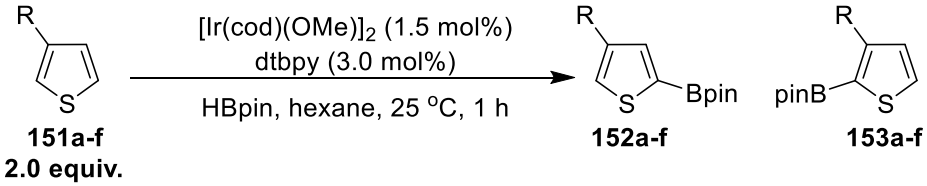

Entry	**151**	R	**152**:**153**	Total Yield /%
1	**a**	CN	1:1.3	54
2	**b**	Cl	3.5:1	66
3	**c**	Br	8.9:1	72
4	**d**	Me	8.9:1	67
5	**e**	*p*-Tol	>32:1	74
6	f	CO_2Me	>99:1	95

Table 2: Borylation of 3-Substituted Thiophenes

In the presence of excess heteroarene, the borylation of 3-substituted thiophenes is generally selective for the uncongested 5- position, reflecting steric control. The borylation of nitrile **151a** is an exception to this rule, because CN has a low steric requirement (Table 2, Entry 1). This regiochemistry may reflect an activating effect of nitrile on the C-2 C-H bond. 3-Substituted thiophenes bearing moderately sized functionalities afford a mixture of 2- and 5-boryl isomers in a ratio which seems to reflect the size of the substituents, although electronics cannot be ruled out (Table 2, Entries 2, 3, 4). The borylation of thiophenes bearing larger 3-substituents, such as *p*-Tol **151e** or CO_2Et **151f** proceeds with higher selectivities based on steric effects (Table 2, Entries 5, 6).

Furthermore, symmetrical and unsymmetrical 2,5-disubstituted thiophenes undergo C-H borylation at the beta positions. Owing to the presence of a sterically encumbering *ortho* substituent, the room temperature borylation of 2,5-disubstituted thiophenes is slower than mono- or unsubstituted derivatives. For example, 2,5-dibromothiophene **154a** borylates at room temperature to afford **155a** (Table 3, Entry 1). Conversely, the corresponding dimethylthiophene **154b** is inactive under the same conditions, presumably owing to the larger size of Me. However, efficient borylation can be achieved under more forcing conditions (Table 3, Entry 2). Unsymmetrically substituted heterocycles borylate with predominantly steric regiocontrol, and the less congested position is borylated selectively (Table 3, Entries 3-6). To date, a 2,5-disubstituted furan has not been investigated, although comparable selectivity is predicted.

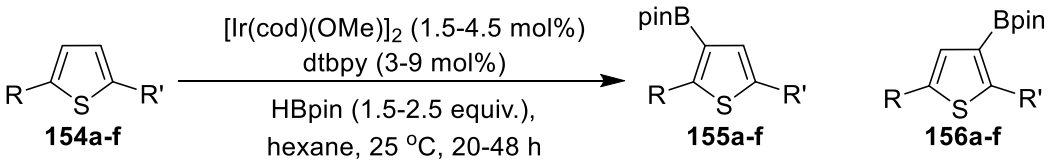

Entry	**154**	R	R'	**155**:**156**	Total Yield /%
1	**a**	Br	Br	-	56
2	**b**	Me	Me	-	97*
3	**c**	Cl	Br	2.0:1	87
4	**d**	Cl	Me	2.3:1	95
5	**e**	Cl	I	5.7:1	89
6	**f**	Cl	TMS	>99:1	93

**Reaction Conditions: 2 mol% Ir/dmpe, 1.5 equiv. HBpin, 150 °C, 16 h*

Table 3: Borylation of 2,5-Disubstituted Thiophenes

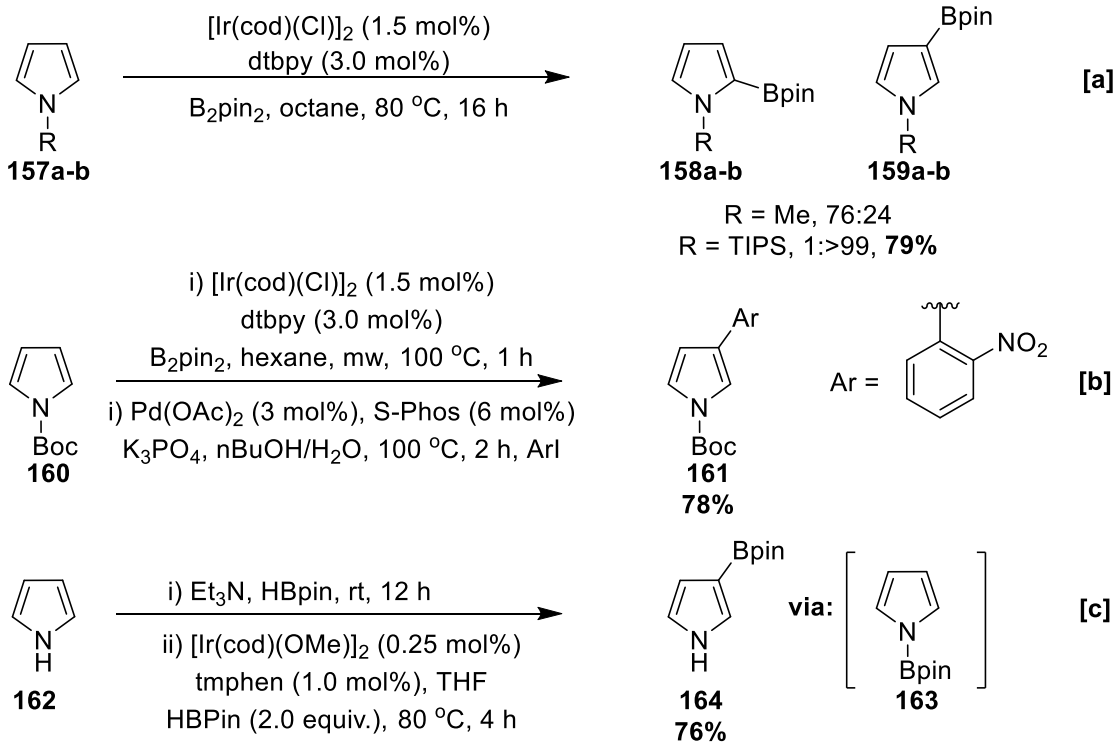

Scheme 24: Borylation of N-Substituted Pyrazole Derivatives

Normal alpha selectivity in pyrroles can be modulated by using N-substituents which have a steric requirement. For instance, N-methyl pyrrole **157a** is reported to borylate at the 2- and 3- positions in a 76:24 ratio (Scheme 24a). Substituents such as TIPS, Boc, and Bpin block alpha borylation, and beta borylated products are afforded exclusively (Scheme 24a-c).[77,95,100–102] Whilst TIPS and Boc are employed as stepwise protecting groups, Bpin may be installed to form **163** and removed analogously to the traceless *ortho* direction of anilines discussed in 1.7.2.2 (Scheme 24c). Pyrrole does not undergo N-H borylation with HBpin or via catalysis, so the NBpin adduct **163** is pre-formed by stirring with base-activated HBpin. Although it is likely that Bpin and TIPS are true steric directors, the degree to which Boc exerts an electronic directing effect is unclear. This is discussed further in chapter 2.

As in other heteroarenes, alternative selectivities in pyrroles, thiophenes, and furans may be obtained via directing effects. This is generally achieved with carbonyl derivatives, except in Li's sulphur directed borylation of S,S-acetal **165** (Scheme 25a).[103] Furthermore, Si, P, N donor ligands and Silica SMAP can override alpha selectivity in favour of *ortho* borylation in pyrrole, thiophene, and furan esters (Scheme 25b, Table 4). It is noted that in the latter system, the directing effect is pronounced enough to facilitate borylation *ortho* to two substituents in the presence of an alpha position (Table 4, Entry 3).[61,68]

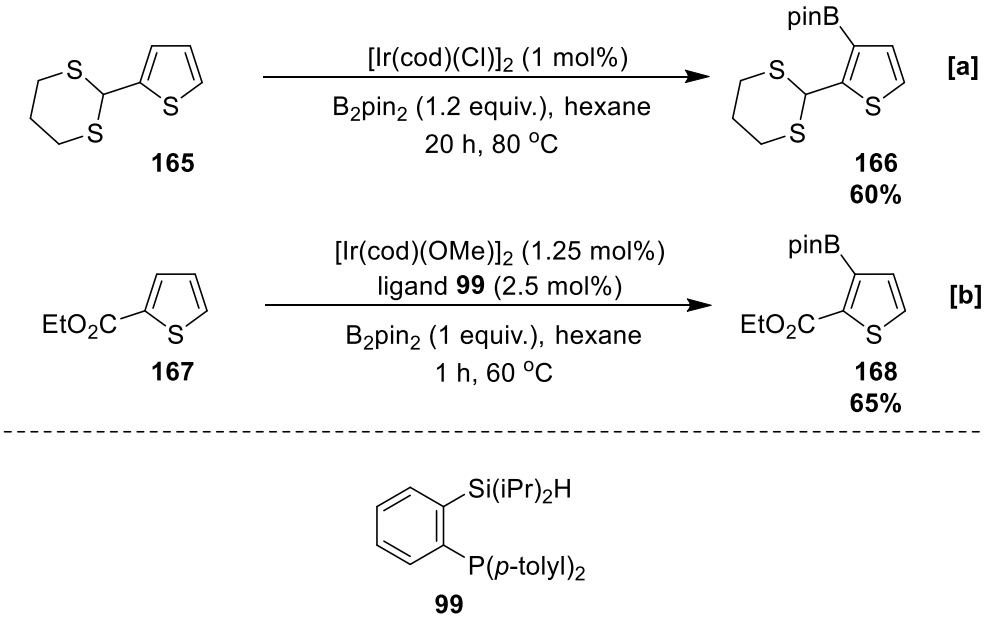

Scheme 25: *Ortho* Selective Borylation of Thiophenes

However, the enhanced C-H acidity in furan ester **169e** led to some alpha selectivity (Table 4, Entry 5). The *ortho* selective borylation of pyrrole, thiophene, and furan derivatives with a large variety of substitution patterns may be achieved using $AsPh_3$, and selected examples are shown in Table 5.[62] This method probably relies on the lability of the ligand to produce an open coordination site and subsequent inner-sphere direction. Control experiments revealed that the use of $AsPh_3$ provides complementary regiochemistry to dtbpy.

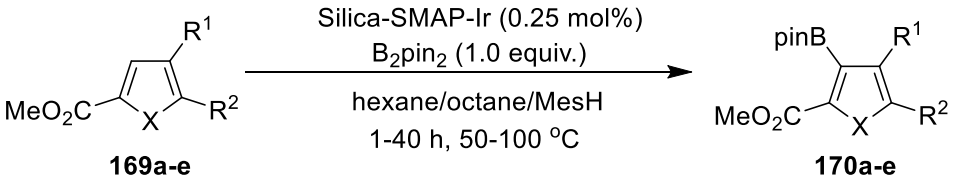

Entry	**169**	X	R^1	R^2	Total Yield /%
1	**a**	S	H	H	74
2	**b**	S	H	Cl	99
3	**c**	S	Me	H	92*
4	**d**	NTIPS	H	H	96
5	**e**	O	H	H	56†

**Obtained alongside 3% 5- isomer*
† Obtained alongside 21% 5- isomer

Table 4: *ortho* Selective Borylation of Pyrrole, Thiophene, and Furan Derivatives with Si-SMAP

In all cases, *ortho* selectivity is >99:1, except for chloride derivatives such as **171d** (Table 5, Entry 4). To account for this, the authors proposed that Cl competes for coordination, enabling *ortho* direction. Evidence for this can be found in related inner-sphere systems, where Cl acts a director.[58]

Selectivities other than *ortho* can be achieved in these heterocycles, although fewer approaches are available for this. For example, hydrogen-bond direction using urea ligand **126** improves the C-4 selectivity in 2-amidopyrrole **174** relative to dtbpy (Scheme 26a).[80] However, it was challenging for this system to overcome the intrinsic selectivities in other heterocycles. Furthermore, C-5 selectivity can be obtained by judicious choice of ligand and additive. For example, ligand **135** non-covalently enhances alpha selectivity in **177** (Scheme 26b), and ligand **76** seems to improve C-5 selectivity in conjunction with the Lewis acid MAD in **179** based on steric effects (Scheme 26c).[54,85]

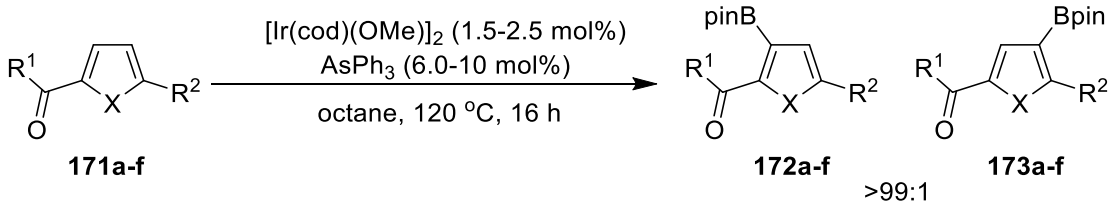

Entry	**171**	X	R^1	R^2	Total Yield /%
1	**a**	O	Me	Me	92
2	**b**	O	Me	OMe	51
3	**c**	S	Et	CF_3	75
4	**d**	S	Et	Cl	46*
5	**e**	NCO_2Et	Et	Me	92
6	**f**	NCO_2Et	OMe	Me	43

Isomer ratio **172:**173** 74:26*

Table 5: *ortho* Selective Borylation of Pyrrole, Thiophene, and Furan Derivatives with $AsPh_3$

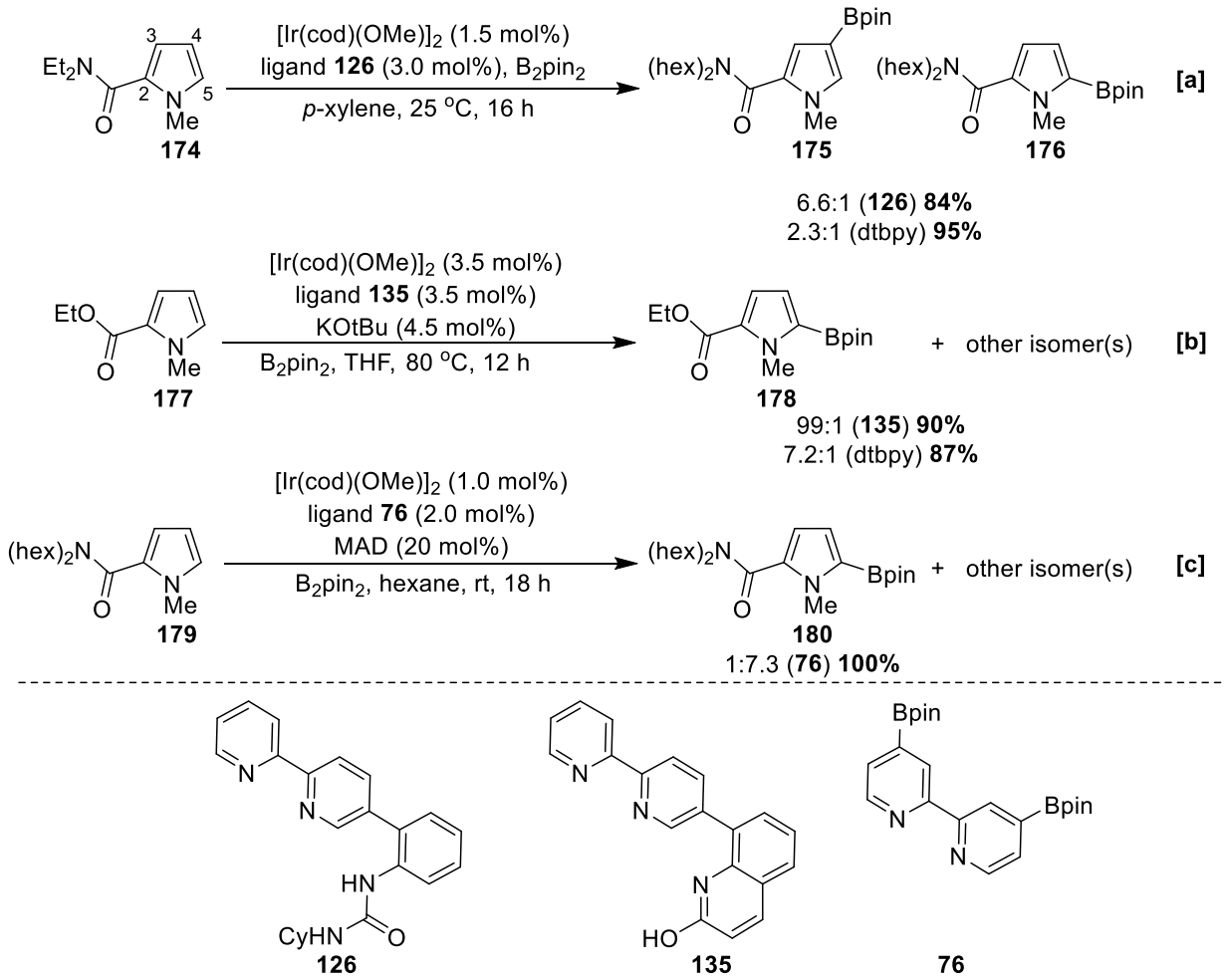

Scheme 26: *meta and para* Selective Borylation of N-Methyl Pyrrole Derivatives

1.7.3.1.2 Indole, Carbazole, Benzothiophene, and Benzofuran

The presence of carbocyclic aryl moeitie(s) in indole, carbazole, benzothiophene, and benzofuran introduces the potentiality for borylation at multiple sites. However, there is a marked preference for borylation at the heterocyclic ring where possible. Like their non-benzofused analogues, indole **181a**, benzothiophene **181b**, and benzofuran **181c** selectively alpha borylate with excess heteroarene (Table 6, Entries 1-8). However, in parallel with furan, benzofuran shows some selectivity for the beta position at elevated temperature (Table 6, Entry 3).[42,48,95] Bisborylation of indole affords the 2,7-disubstituted product **184a**, and Smith has suggested that C-7 selectivity originates from N-chelation to the catalyst, followed by inner/outer-sphere direction.[104]

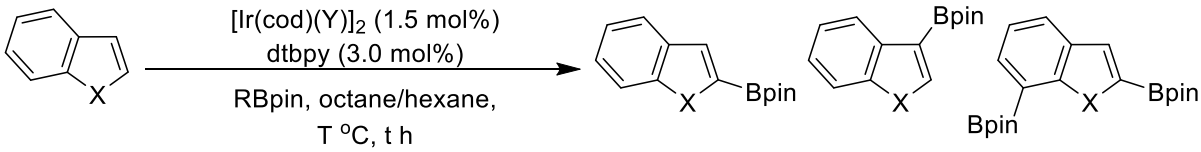

181a-c **182a-c** **183a-c** **184a-c**

Entry	**181**	X (equiv.)	Y	R (eq.)	T/ °C	t / h	**182**:**183**:**184**	Total Yield /%
1	**a**	NH (4)	Cl	Bpin (1)	80	16	>99:1:0	92
2	**b**	S (4)	Cl	Bpin (1)	80	16	>99:1:0	89
3	**c**	O (4)	Cl	Bpin (1)	80	16	>97:3:0	91
6	**a**	NH (2)	OMe	Bpin (1.1)	25	0.5	100:0:0	88
7	**b**	S (2)	OMe	Bpin (1.1)	25	0.5	100:0:0	83
8	**c**	O (2)	OMe	Bpin (1.1)	25	0.5	100:0:0	84
9	**a**	NH (1)	OMe	H (2.2)	25	0.5	0:0:100	90

Table 6: Borylation of Indole, Benzothiophene, and Benzofuran

However, some observations bring this conclusion into question. For instance, *ortho* and *peri* substituents are known to hinder N-chelation in pyridines and quinolines, and why this does not seem to disrupt chelation in indole is unclear (see section 1.7.3.2.1). This is further illustrated in the iterative borylation of carbazole **185**, which is selective for the analogous C-8 position following C-1 despite the high degree of *peri* steric hindrance at N from the boryl group and the carbocycle in the C-1 monoborylated intermediate (Scheme 27a).[105]

Furthermore, the calculated free energies of relative anionic stability in 2-phenylindole **188** indicate that C-7 (-10.96 kcal/mol) should intrinsically be the most reactive C-H site when contrasted to other uncongested C-H sites (0.0-9.4 kcal/mol).[106] Reflecting this, **188** borylates selectively at C-7 and this additionally demonstrates an electronic preference for the heteroaromatic carbocycle over the benzene substituent (Scheme 27b). Moreover, impure 2-borylfuran **190** also displays high selectivity for C-7, and it is probable that this regiochemistry is intrinsic based on the intrinsic *ortho* selectivity observed in the C-H borylation of benzodioxole (27c). Therefore, further studies are required to rule out intrinsic selectivity and support an N-chelation model in the borylation of indole **181a**.

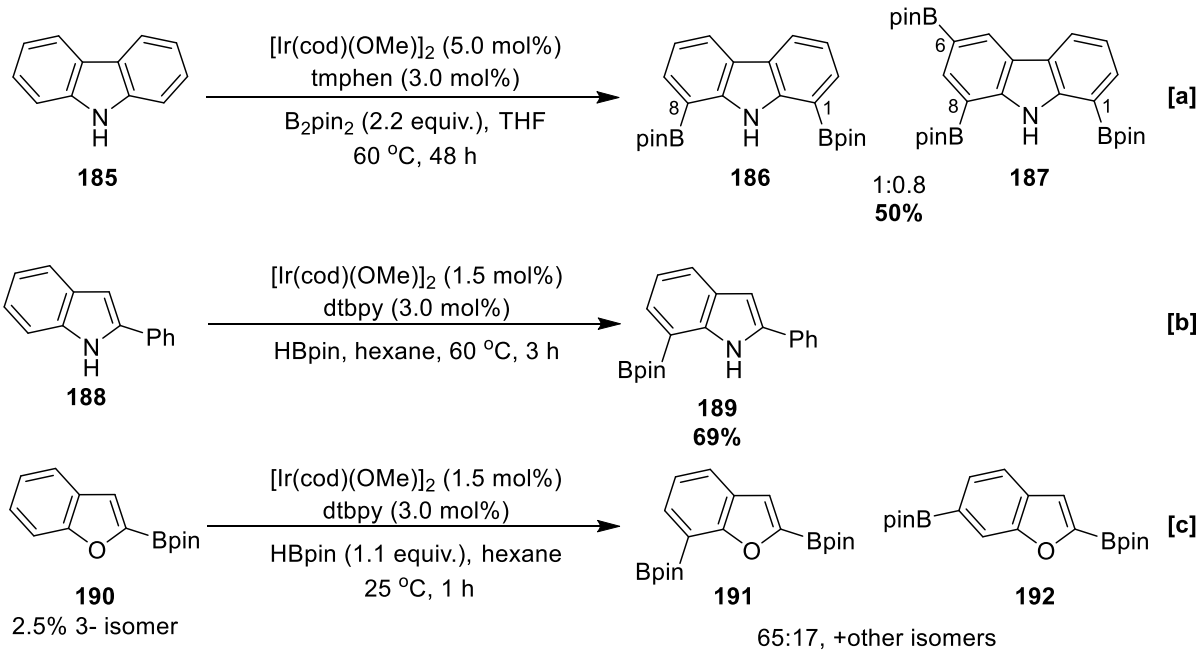

Scheme 27: Borylation of Heteroarenes with a Blocked Alpha Position

Owing to the prevalence of indole in bioactive molecules such as pharmaceutical agents and natural products, the Ir C-H borylation of many substituted indole derivatives has been well documented.[104,105,107–112] Providing that steric congestion is not introduced, other alpha substituted indoles (such as those with C-3, C-4, or C-5 substituents) also borylate at C-7. To date, the intrinsic borylation regiochemistry of substituted benzothiophenes has not been investigated, although C-7 selectivity is predicted in analogy to the borylation of **190**. 3-Alkyl indoles retain selectivity for the 2-position, and therefore borylate with a high degree of electronic control.[113–117] For example, the borylation of **193** efficiently affords the 2-boryl product **194** alongside some of the C-7 bisborylated material **195** (Scheme 28a). Furthermore, iterative borylation of 3-methylindole **196** with 5.0 equivalents of B_2pin_2 leads to a third borylation event at C-5 which is sterically controlled (Scheme 28b). Blocking C-2 and C-7 is possible with an N-TIPS group in **198**, and this leads to non-selective borylation at C-5 and C-6 in 3-substituted indoles. Site-selectivity can be significantly enhanced in systems such as indole **198** by switching the ligand from dtbpy/tmphen to 1,10-phenanthroline (phen), and this is additionally observed in the borylation of carbazole **201** using all three ligands (Scheme 28c, d).

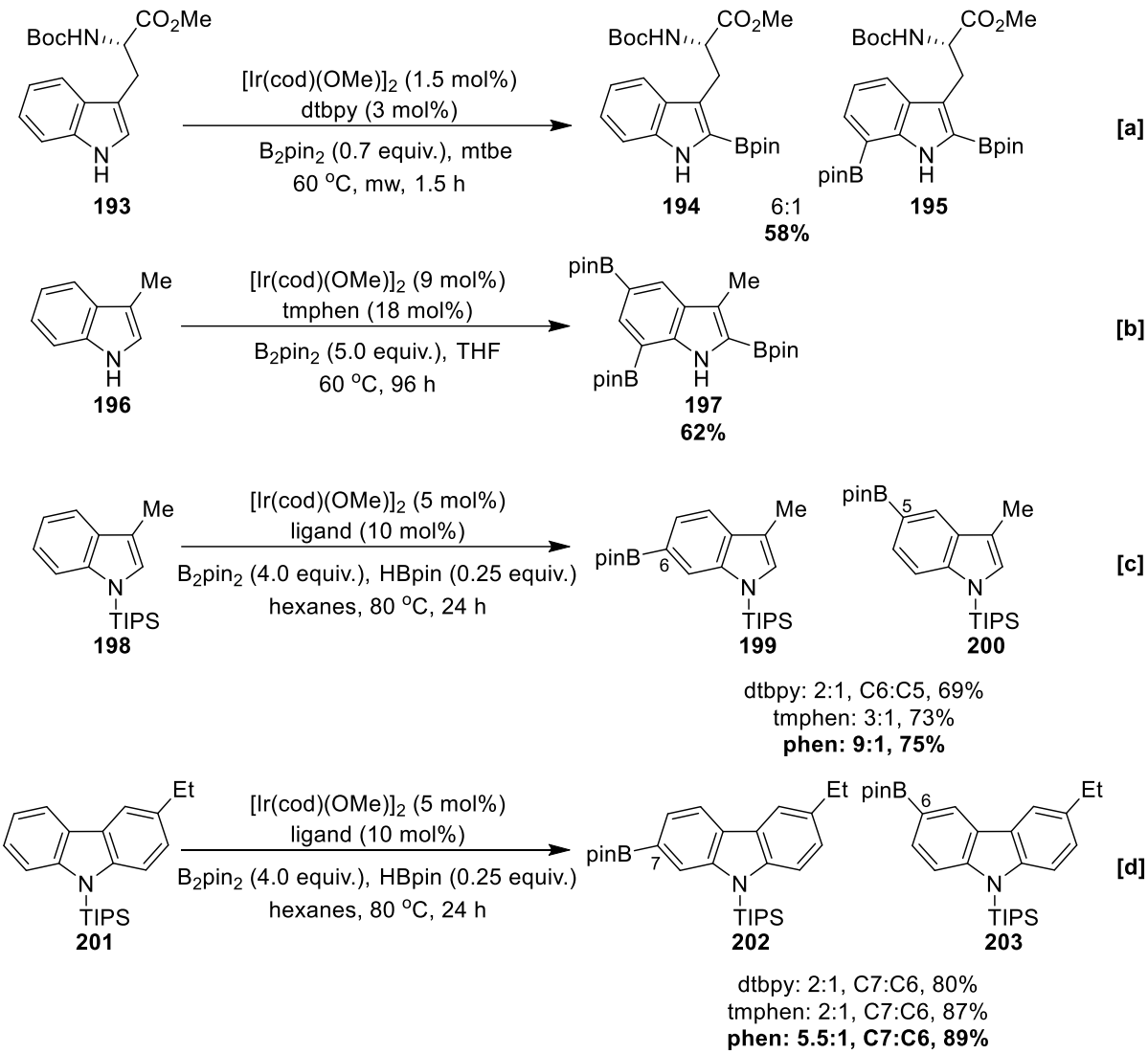

Scheme 28: Borylation of 3- Substituted Indole and Carbazole Derivatives

These substrates possess a structure that is comparable to a 1,2-disubstituted arene, in which intrinsic selectivity can be governed to a high degree by electronic effects, albeit at room temperature. This ligand-mediated selectivity is almost certainly electronically controlled, although further studies are required to determine its origin.[118] Other N-substituents can modify the regiochemistry in indole, and this is observed in the borylation of N-methylindole **204a** which affords a mixture of C-2 and C-3 functionalised products **205a** and **206a** (Table 7, Entries 1, 2).

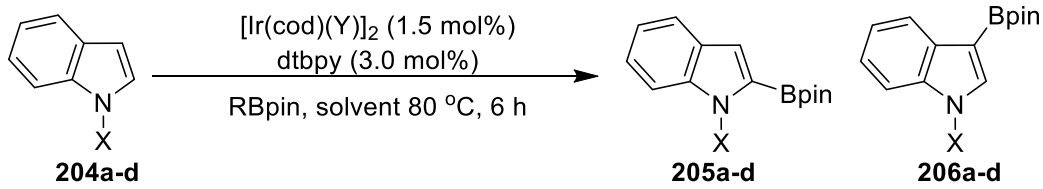

204a-d **205a-d** **206a-d**

Entry	**204**	X (eq.)	Y	R (eq.)	T/ °C	t / h	Solvent	**205**:**206**	Total Yield /%
1	**a**	Me (xs)	Cl	Bpin (1)	80	16	octane	89:11	-
2	**a**	Me (30)	Cl	H (1)	80	6	neat	55:45	81*
3	**b**	TIPS (4)	Cl	Bpin (1)	80	16	octane	0:100	83
4	**c**	Bpin (1.0)	OMe	H (2.0)	80	4	THF	0:100	57†
5	**d**	Boc (1)	OMe	H (2.00)	60	8	hexane	0:100	65

*3.0 mol% bpy as the ligand
† The substrate is indole **181a**, C-H Borylation preceded by N-borylation with HBpin and Et_3N

Table 7: Borylation of N-Substituted Indoles

Independent reports give incongruent selectivities for this process, although this is probably explained by the use of different reaction variables in each system, such as solvent, ligand, and reaction time.[95,111] Like their pyrrole analogues, TIPS indole **204b**, Bpin indole **204c,** and Boc indole **204d** borylate with complete beta selectivity, and **204c** is prepared in a similar manner to NBpin pyrrole **163** (Table 7, Entries 3, 4, 5).[77,95,101,119]

The intrinsic selectivities of indole, benzothiophene, benzofuran, and carbazole derivatives can be altered using directing effects. For example, Li's S directed borylation of 2-substiuted benzothiophene **207** leads to an *ortho* functionalised product **208** (Scheme 29a). Furthermore, N-borylation of indole with B_2eg_2 affords **209**, which undergoes selective borylation at the alpha position to afford **210** (Scheme 29b). This outcome matches intrinsic selectivity, although it is still probably electronically directed because the corresponding NBpin indole **204c** affords the beta product. Using Silica-SMAP, 2-, 3- and N-substituted carbonyl derivatives of these heterocycles undergo *ortho* or *peri* borylation. For example, N-substituted carbazole **211** efficiently borylates at C-1 (Scheme 29c).[61]

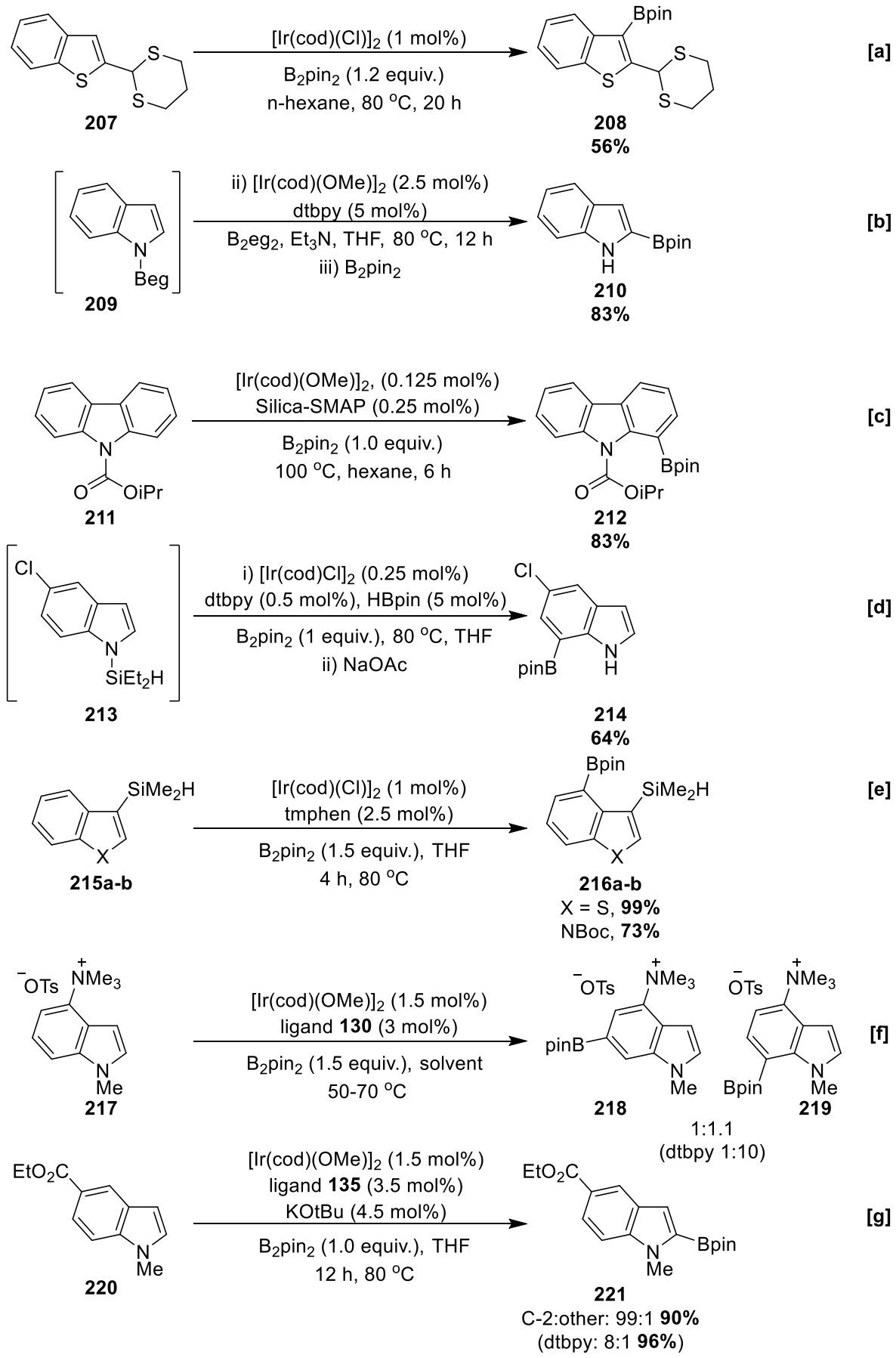

Scheme 29: Directed Borylation of Indole, Benzothiophene, Benzofuran, and Carbazole Derivatives

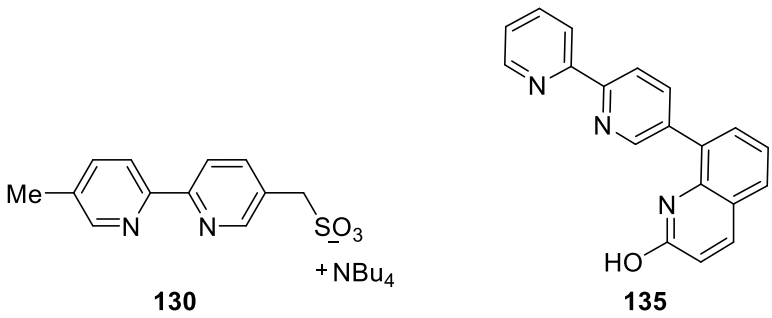

Figure 6: Ligands Used in the Directed Borylation of Indoles

Furthermore, hydrosilyl heteroarenes also undergo selective borylation under relay direction, and the hydrosilyl group can be generated *in situ* or pre-installed. Examples that employ the former strategy include N-hydrosilyl carbazoles, and N-hydrosilyl indoles with substituents at the C-3/C-4/C-5 positions. For example, the borylation of chloroindole **213** is completely C-7 selective despite the presence of an intrinsically reactive heterocyclic ring (Scheme 29d). Furthermore, 3-hydrosilyl indole and benzothiophene **215a** and **215b** undergo *peri*-selective borylation at C-4. Outer-sphere systems can also alter the selectivity in substituted indole derivatives. For instance, ion-pair recognition confers a near tenfold greater *meta* selectivity over dtbpy in ammonium indole **217** using ligand **130** (Scheme 29f). Moreover, borylation with L-shaped ligand **135** leads to essentially complete alpha selectivity in N-methyl indole ester **220**, compared to the 8:1 selectivity using dtbpy (Scheme 29g).[85,120]

1.7.3.2 Six-Membered Heteroarenes with One Heteroatom

This section introduces heteroarenes which contain azinyl (a.k.a. azine, basic) nitrogen atoms. Unlike azole N atoms, borylation is electronically disfavoured alpha to an azinyl N, and this can crudely be likened to the steric inhibitory effect of a substituent. In a given substrate, the degree to which alpha-azinyl borylation occurs is dependent on the electron density at N, and on steric constraints in the rest of the molecule. DFT calculations of the reaction pathway for the C-2 borylation of pyridine show *ca*. 1 kcal/mol higher barrier compared to borylation at the other sites.[121] As this is a relatively small difference, the lack of alpha-azinyl products may also be attributed to the poor stability of 2-azaarylboronates. These are known to decompose via several pathways, including protodeborylation, and this also facilitates secondary decomposition of the catalyst.[122] However, the installation of a boryl group in the alpha-azinyl position may be promoted by stabilising groups, and these are typically electron-withdrawing groups such as other N ring atoms, sulphonyl, trifluoromethyl, and halides.

1.7.3.2.1 – Pyridine

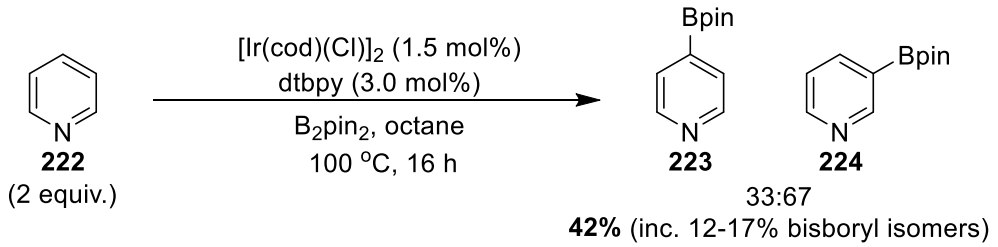

Scheme 30: Ir C-H Borylation of Pyridine

In the seminal report on the Ir C-H borylation of heteroarenes, pyridine **222** stands out as an unusually inactive substrate, requiring increased temperature and affording products in relatively low yield (Scheme 30).[95] A statistical mixture of beta and gamma borylated products was detected, with no evidence of C-2 functionalised products. The poor reactivity of pyridine may be attributed to the rapid decomposition of *in situ* C-2 borylated products, and the reversible deactivation of the active catalyst through substrate ligation. The latter phenomenon has been studied in the C-H borylation of 2,6-lutidine **225**, which normally undergoes facile C-H borylation to form **228**. In this study, the addition of small amounts of 4-tertbutylpyridine **226**, which is essentially inert toward C-H borylation at low temperature, efficiently inhibits the reaction through coordination to the vacant site on the catalyst shown in **227** (Scheme 31).

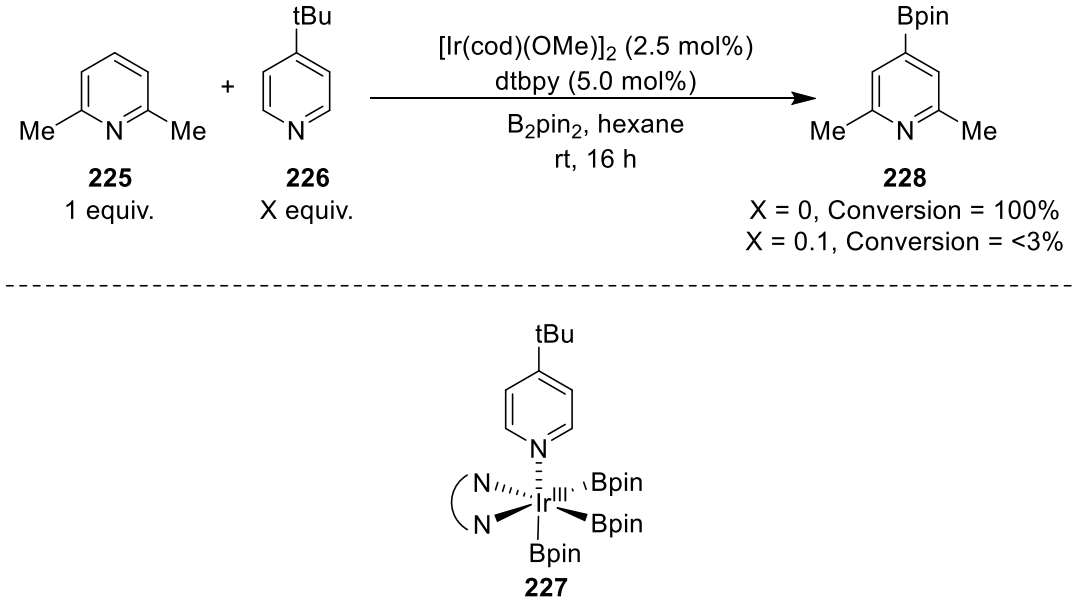

Scheme 31: A Competition Experiment Reveals the Inhibitory Effect of **226**

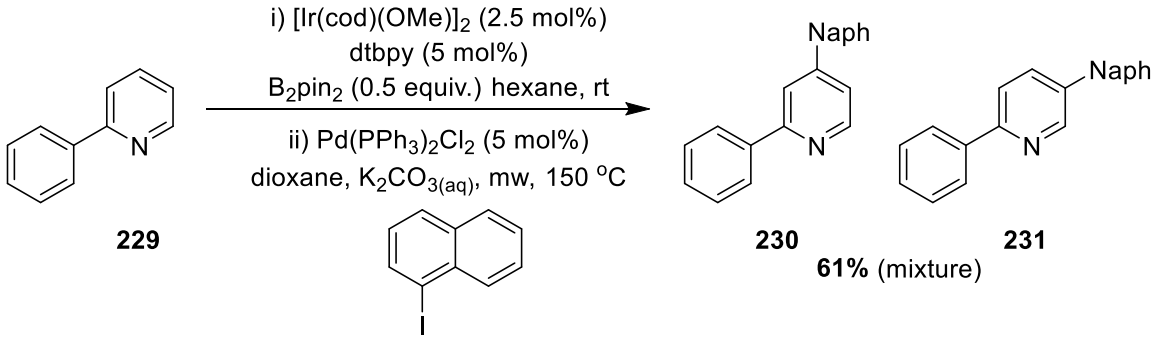

Scheme 32: Ir C-H Borylation of 2-Phenylpyridine

Substrate ligation is most commonly prevented with a 2-substituent. This sterically or electronically prevents substrate coordination, enabling C-H borylation activity. For instance, 2-phenylpyridine **229** borylates at room temperature with complete selectivity for the heteroarene in a 1:1 mixture of C-4 and C-5 isomers (Scheme 32).[123] This regiochemistry was showcased using a one-pot borylation/cross-coupling sequence, affording arylated isomers **230** and **231**. This provides another useful comparison between the reactivity of heteroarenes vs. carbocyclic arenes.

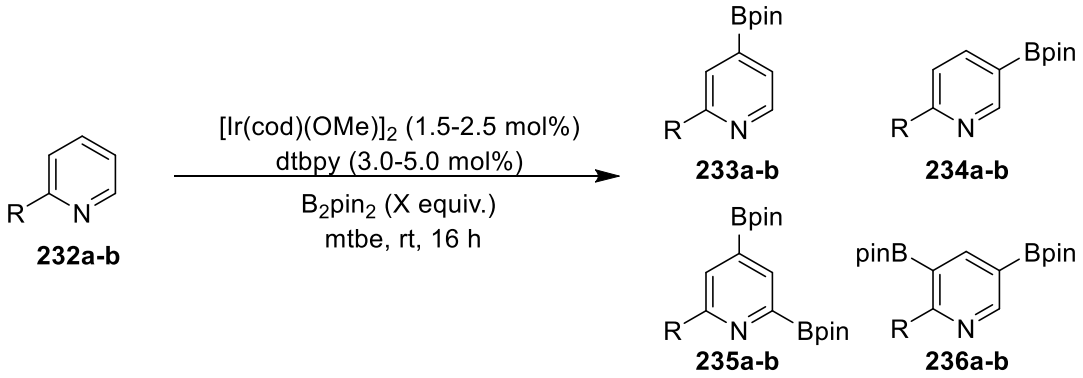

Entry	**232**	R (eq.)	X	**233**:**234**:**235**:**236**	Total Yield /%
1	**a**	OMe	0.5	73:27:0:0	42
2	**a**	OMe	1.2	43:31:17:9	100
3	**b**	F	0.5	57:19:2:5	89*
4	**b**	F	1.2	45:10:15:19	100†

*With 17% 3-borylisomer
†With 11% 3-borylisomer

Table 8: Borylation of 2-Substituted Pyridines

Whilst regiochemistry at the pyridine is approximately statistical, other 2-substituted pyridines borylate with a significant contribution from electronics.[124] For example, in the presence of 0.5 equiv. B_2pin_2, 2-methoxypyridine **232a** and 2-fluoropyridine **232b** show greater selectivity for the 4-position (Table 8). Moving from 0.5 to 1.2 equiv. B_2pin_2, bisborylation occurs with varying selectivities (Entries 3, 4). 2-Fluoropyridine undergoes facile borylation to afford a mixture of isomeric products, including C-6 functionalised **235b**. The capacity for **232a** and **232b** to promote alpha-azinyl regiochemistry is reflected in their reduced basicities relative to pyridine. The products obtained from the borylation of **232b** were also accompanied with 3-substituted isomers, owing to low steric requirement of fluorine.

2,3-Disubstituted pyridines borylate with steric control at C-5. Some electron-deficient systems display a small amount of alpha-azinyl site-selectivity, for example pyridine **237** borylates rapidly to afford 91% isomer **238** alongside 9% C-6 isomer **239** (Scheme 33a). Electron-deficient 2,4-disubstituted pyridines tolerate borylation at C-5 providing that the C-4 substituent has an acceptable steric requirement, and this may be seen in the borylation of 2,4-dichloropyridine **240a** (Scheme 33b)**.** In the C-H borylation of **240b**, the larger size of the trifluoromethyl group switches regiochemistry to C-6 (Scheme 33b). Similarly, providing it is not bound at the catalyst, dtbpy **56** borylates under more forcing conditions at the alpha azinyl positions (Scheme 33c). The regiochemistry was confirmed using a one-pot Suzuki-Miyaura cross-coupling to deliver arylated product **243**. Considering that the related 4-tertbutylpyridine **226** is inactive, the 2-pyridyl unit in **56** likely facilitates the activity of dtbpy, possibly through an electron-withdrawing effect. Replacing tBu with OMe gives the *ortho* functionalised products **245** and **246**, and this reflects the lower steric hindrance of OMe (Scheme 33d). 2,5-Disubstituted pyridines rely on small to moderately sized substituents for activity. For example, the borylation of 2-cyano-5-bromopyridine **247** proceeds efficiently to afford C-3 and C-4 boronates **248** and **249** (Scheme 33e).[50] More congested substrates, such as 2,4-lutidine **250** show poor conversion under comparable conditions, although still afford C-4 boronates selectively (Scheme 33f). Finally, blocked 2,6-disubstituted pyridines generally have good activities and exhibit C-4 selectivity. For example, the borylation of 2,6-dichloropyridine **252** affords C-4 boronate **254** in 93% yield as determined by GCMS with ligand **253** (this is also possible with bipyridine ligand derivatives). (Scheme 33g).[125]

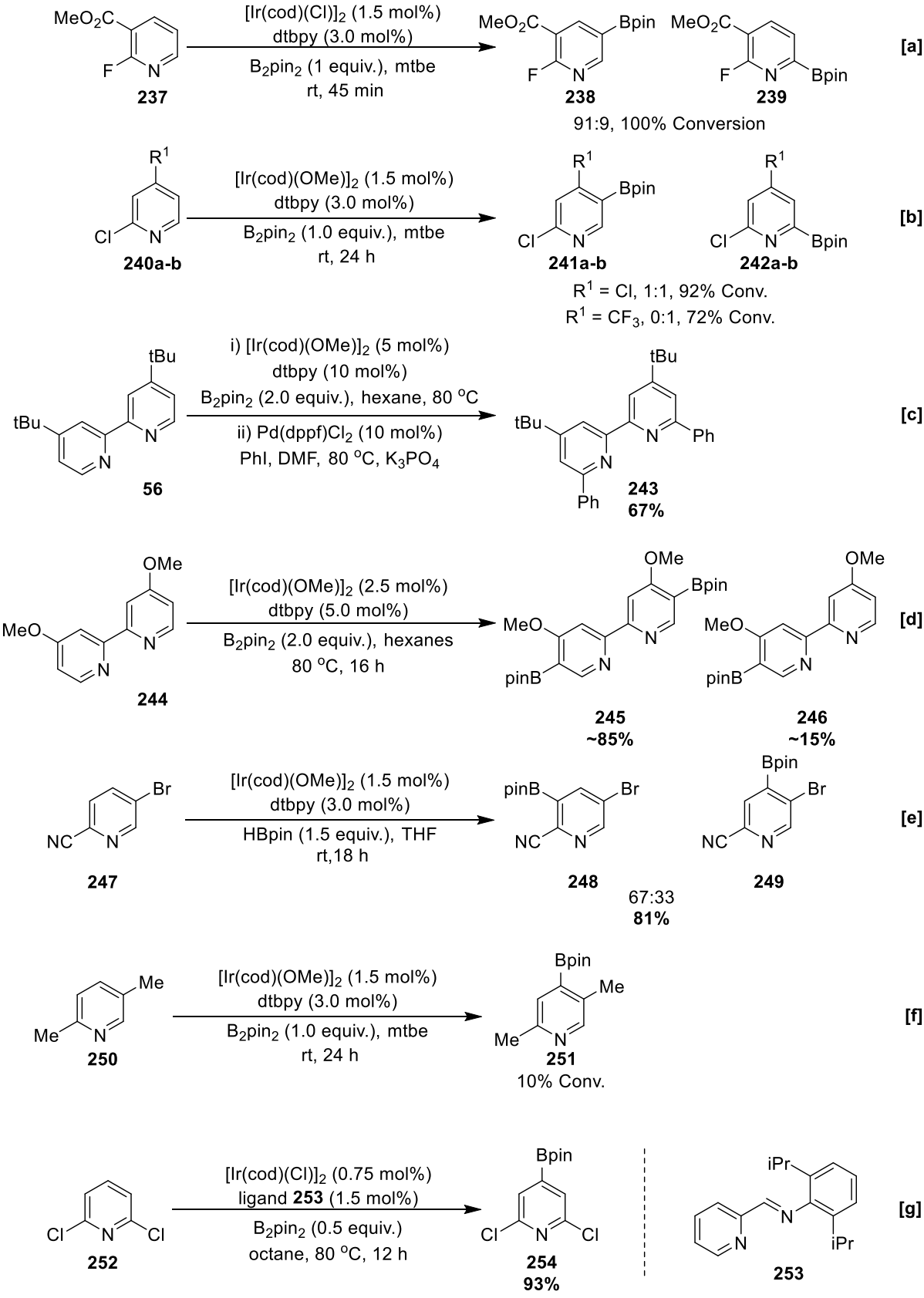

Scheme 33: CHB of Disubstituted Pyridines

Pyridine derivatives can show different site-selectivities in directing systems. For instance, aminopyridines undergo rapid NH borylation to form the corresponding NHBpin adduct. This intermediate facilitates *ortho* selective C-H borylation in 2,4- and 2,5-aminopyridines, and this may be seen in the borylation of **255**, which forms **257** *in situ* (Scheme 34a). It is suggested that HBpin is more efficient for N-H borylation, whilst B_2pin_2 is more efficient for C-H borylation, rationalising the use of both boron reagents in this reaction. In addition, the borylation of 2,5-hydroxypyridine **258** is *ortho* selective following traceless O-borylation with B_2pin_2 to afford **260** (Scheme 34b).[77,78] It is unclear to what extent the regiochemical outcomes of these processes differ from intrinsic regiochemistry. Notably, traceless *ortho* direction is not displayed with 2,6-aminopyridine derivatives, and intrinsic C-4 borylation analogous to the borylation of **252** occurs instead.

Furthermore, 2-substituted pyridines show higher C-4 or C-5 selectivity under outer-sphere directing systems. For example, by employing ionic ligand **130** the C-4 selectivity in pyridine amides and trialkylammoniums is increased, and this may be observed in the borylation of **261**.[82–84] Following C-4 borylation, the powerful electron-withdrawing capacity of trimethylammonium can facilitate borylation at C-6, affording **263**. Analysis of the crude reaction mixture revealed that a small amount of the C-4 borylated product was also generated (Scheme 34c). C-4 selectivity may also be raised with ligand **126**, which facilitates *meta* direction in pyridine amides and esters. For example, in the borylation of amide **264** there is marked increase in C-4 selectivity when compared to dtbpy.[80] Alternatively, C-5 selectivity may be improved in pyridines such as ester **267** with L-shaped ligand **135** and KOtBu (Scheme 34e).

Finally, pyridine derivatives may undergo regioselective borylation via coordination of the azine N in inner-sphere directing systems. Using this approach, the electronic preference for borylation at the pyridine can be overcome in favour of a carbocyclic substituent. For example, hemi-labile ligand **94** efficiently facilitates borylation to the *ortho* position on the phenyl ring in 2-phenylpyridine **229**, producing N-B ylide **269** (Scheme 34f). Similarly, the borylation of **229** using Si, P, and N donor chelates affords **269** (Scheme 34g). N,B bidentate ligand **103** also promotes the selective borylation of **226**, and was additionally shown to promote remote borylation in substrates with a C or O spacer, as seen in **270** (Scheme 34h). The specially engineered ligands involved in the directed borylation of pyridines are provided in Figure 7.

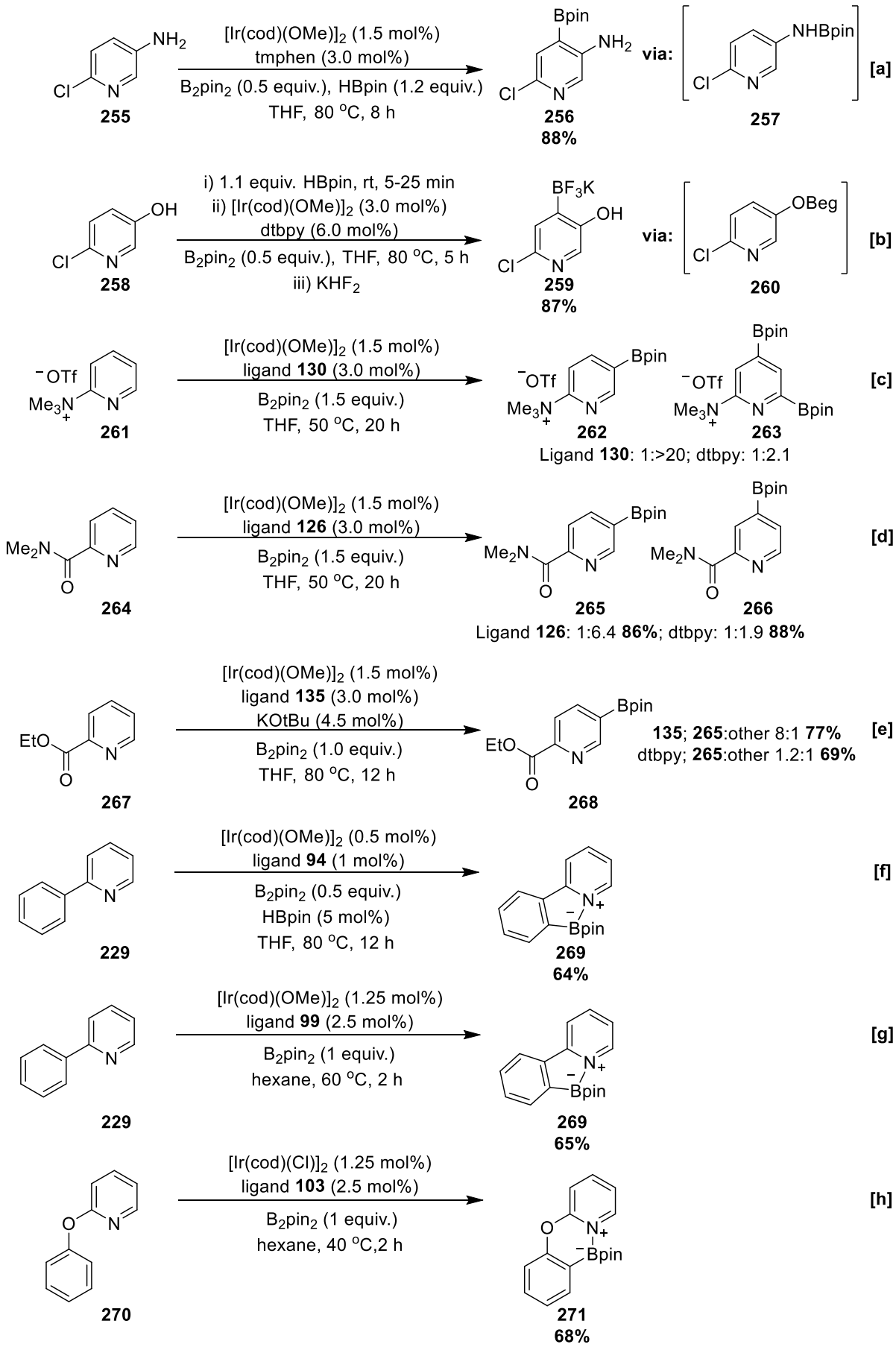

Scheme 34: Directed C-H Borylation of Pyridines

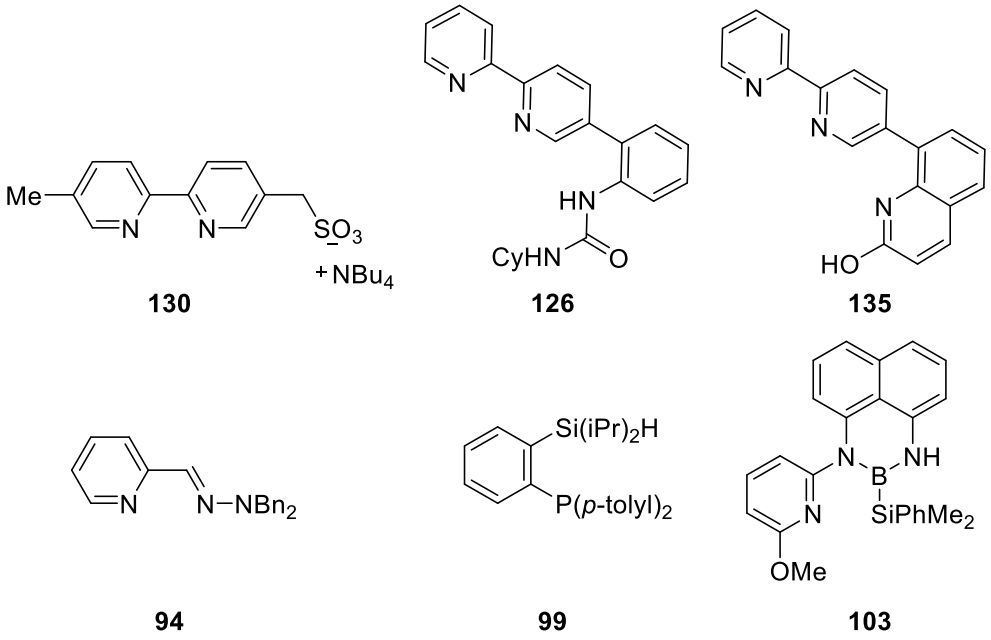

Figure 7: Ligands Used in the Directed Borylation of Pyridines

1.7.3.2.2 – Quinoline and Isoquinoline

Unlike pyridine, quinoline **272** is an active substrate in the C-H borylation because the *peri* C-H bond of the carbocycle blocks inhibitory ligation to the active catalyst.[95] Like other benzofused heteroarenes, quinoline is selectively borylated at the heteroaromatic ring. In the presence of excess heteroarene, C-3 selectivity is observed (Scheme 35a), whilst in the presence of excess boron quinoline bisborylates at C-3 and C6/C7 in a 1:1 ratio (Scheme 35b). Unlike benzofused azoles which show selectivity for C-7, the analogous C-8 position in quinoline is unreactive. A possible explanation for this is that the C-8 position is electronically encumbered by the azinyl N.

Blocking C-3 activation with a C-2 substituent shifts the site-selectivity to C-4 and C-6/C-7, and this occurs in the borylation of 2-methylquinoline **276a** and 2-trifluoromethylquinoline **276b** (Scheme 35c).[44] In the latter substrate an increased selectivity for the carbocycle was observed, suggesting that the electron-withdrawing effect of the trifluoromethyl group is exerting an electronic influence on the selectivity. 2,6-Disubtituted quinolines borylate exclusively at C-4, and this is observed in the borylation of **279** (Scheme 35d). The regiochemical outcome of this reaction suggests that a nitrile group may offer greater steric hindrance than a *peri* C-H bond. Similarly, some 2,7-disubstituted quinolines show selectivity for C-4. For example, 2,7-dimethylquinoline **281a** borylates with near complete C-4 selectivity (Scheme 35e).

Lower selectivity is observed in the C-H borylation of 2-methyl-7-trifluoromethylquinoline **281b**, which affords an isomeric mixture of C-4 and C-5 borylated products (Scheme 35e). This is likely caused by the reduction of C-5 acidity at the carbocycle by the CF_3 group. Indeed, the calculated C-H acidities of C-4 (38.6) and C-5 (39.7) in **281b** show a good correlation with experimental site-selectivity. All C-H sites in 4,7-disubstituted quinolines are encumbered, so successful borylation generally requires forcing conditions and/or small to moderately sized substituents. For example, the borylation of **284a** bearing a chloro group at C-4 is completely selective for C-3 under microwave heating (Scheme 35f).

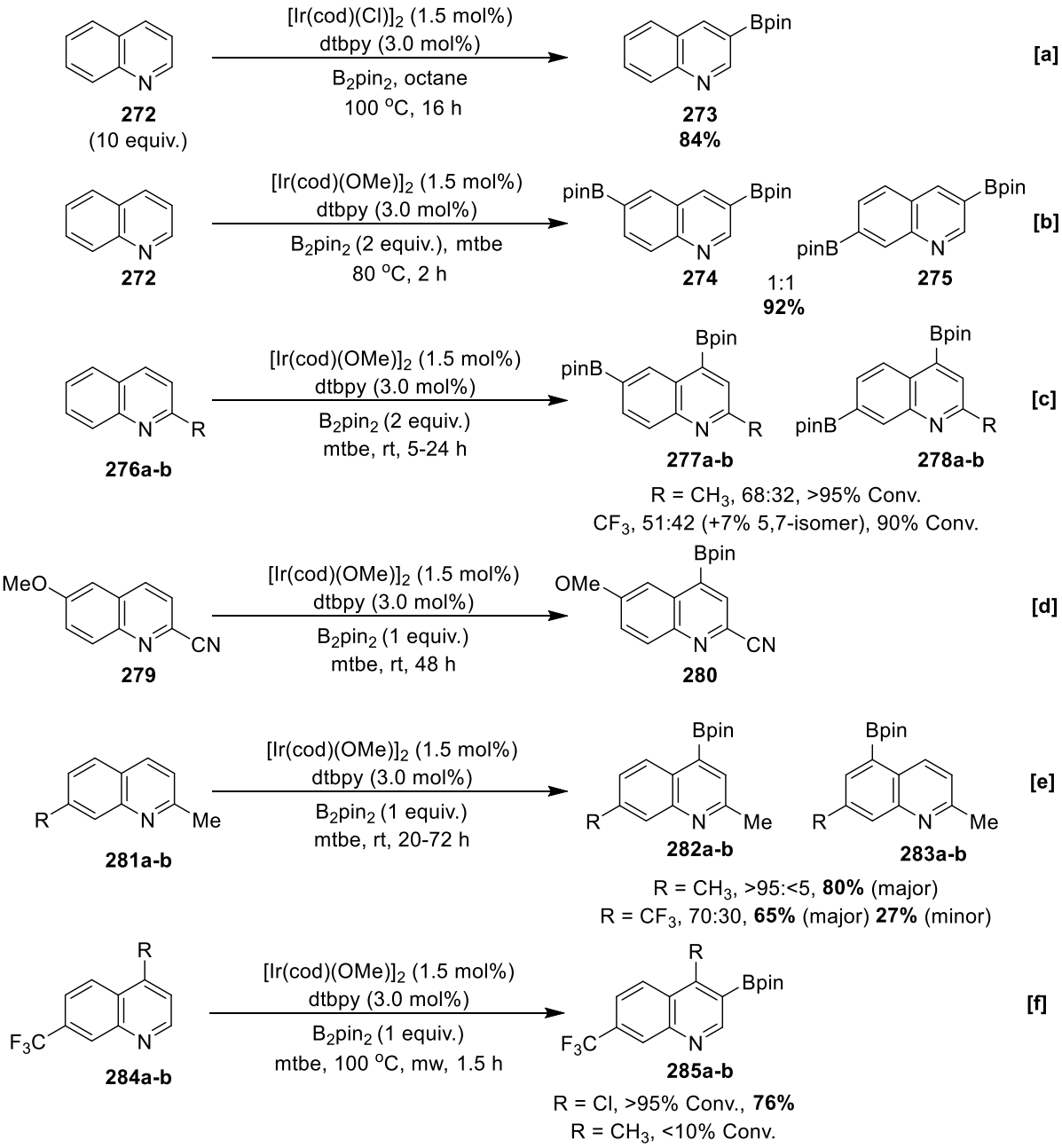

Scheme 35: Ir C-H Borylation of Quinolines

More congested and quinolines give lower conversion under the same conditions, and this is seen in the borylation of **284b** (Scheme 35f).

Silica-SMAP directs borylation to the otherwise unreactive C-8 position in a library of mono-, di-, and trisubstituted quinolines.[60] Remarkably, the system affords C-8 regiochemistry even in congested substrates with a substituent at C-7, and this is observed in the borylation of **286** (Scheme 36a). More recently, aminoquinoline **288** has been shown to undergo *ortho* selective borylation at C-7 via an NHBeg intermediate (Scheme 36b).[78] The intrinsic regiochemistry of isoquinolines has not been investigated, and this is probably due to the fact that they are catalyst inhibitors unless substituted at C-1 or C-3, leaving two remaining C-H sites at the pyridine ring. However, 2-substituted isoquinolines have been regioselectivity functionalised using inner-sphere systems. Similar to 2-arylpyridines, hemi-labile ligands facilitate remote borylation of 2-aryl isoquinolines, and this is observed in the borylation of **291** which is selective for the naphthyl ring (Scheme 36c).[66] Furthermore, relay direction enables the *peri* C-H borylation of hydrosilylated isoquinolines such as **293** (Scheme 36d).[72]

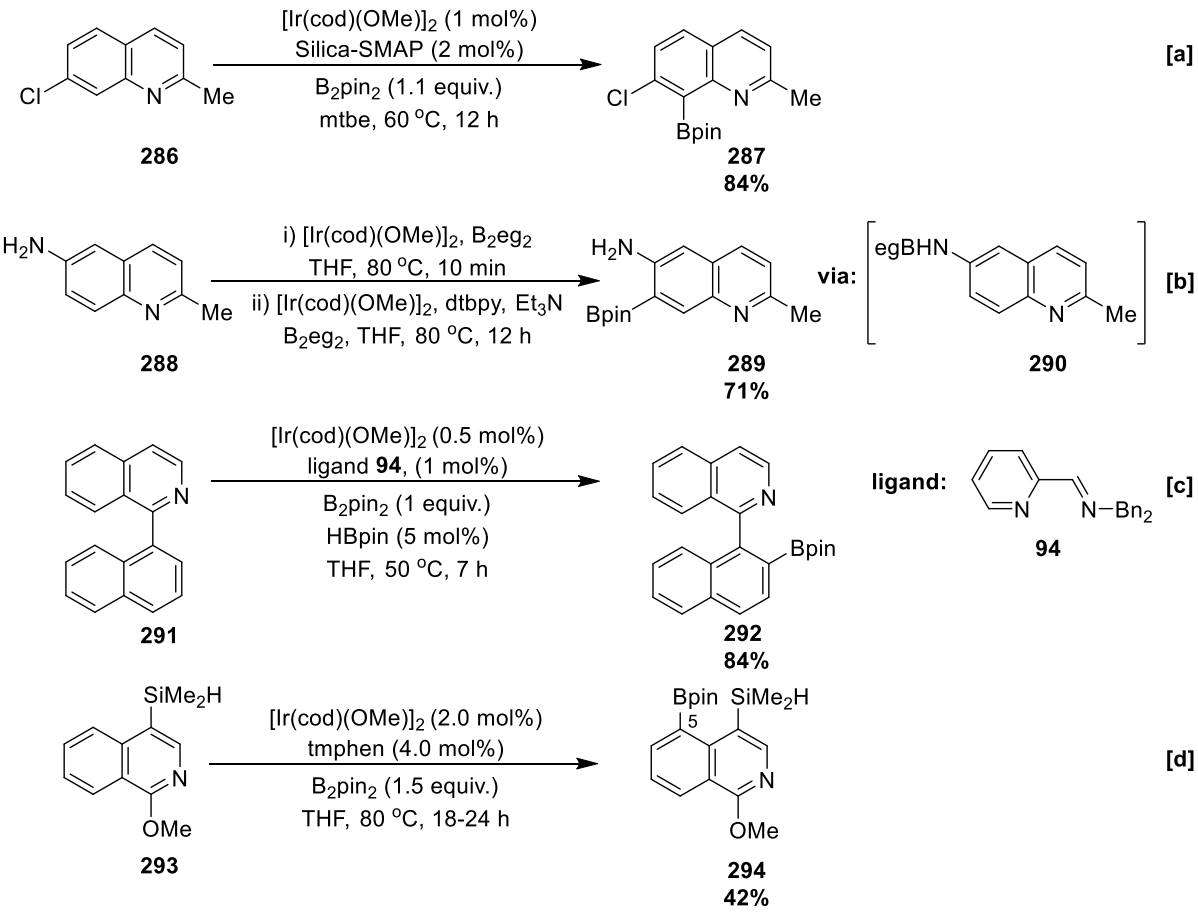

Scheme 36: Directed Borylation of Quinolines

1.7.3.3 Five Membered Rings with Two Heteroatoms

1.7.3.3.1 Pyrazole, Imidazole, and Oxazole

The borylation of imidazole, pyrazole, and oxazole is generally alpha selective to a heteroatom that contributes a lone pair or electrons to the pi system.[126] Free NH imidazole does not borylate, and this could be due to rapid N-borylation to form the corresponding congested N-Bpin adduct. However, N-methylated imidazoles borylate efficiently at C-5, and this is observed in the borylation of **295** in the presence of 1.5 equivalents of HBpin (Scheme 36a). Interestingly, using 2.5 equivalents of HBpin leads to a second borylation event at the *ortho* C-H site on the phenyl ring (Scheme 36b). This could be mediated by an outer-sphere directing effect involving the azinyl N, although the origin of this selectivity awaits further study. Whilst alpha-azinyl regiochemistry is disfavoured, it may be facilitated with an N blocking group such as sulphamoyl, and this is observed in the borylation of **299** (Scheme 36c).[122] Other imidazole C-4 directors such as Boc produce alpha-azinyl functionalised products such as **302** that can be more challenging to isolate (Scheme 36d).

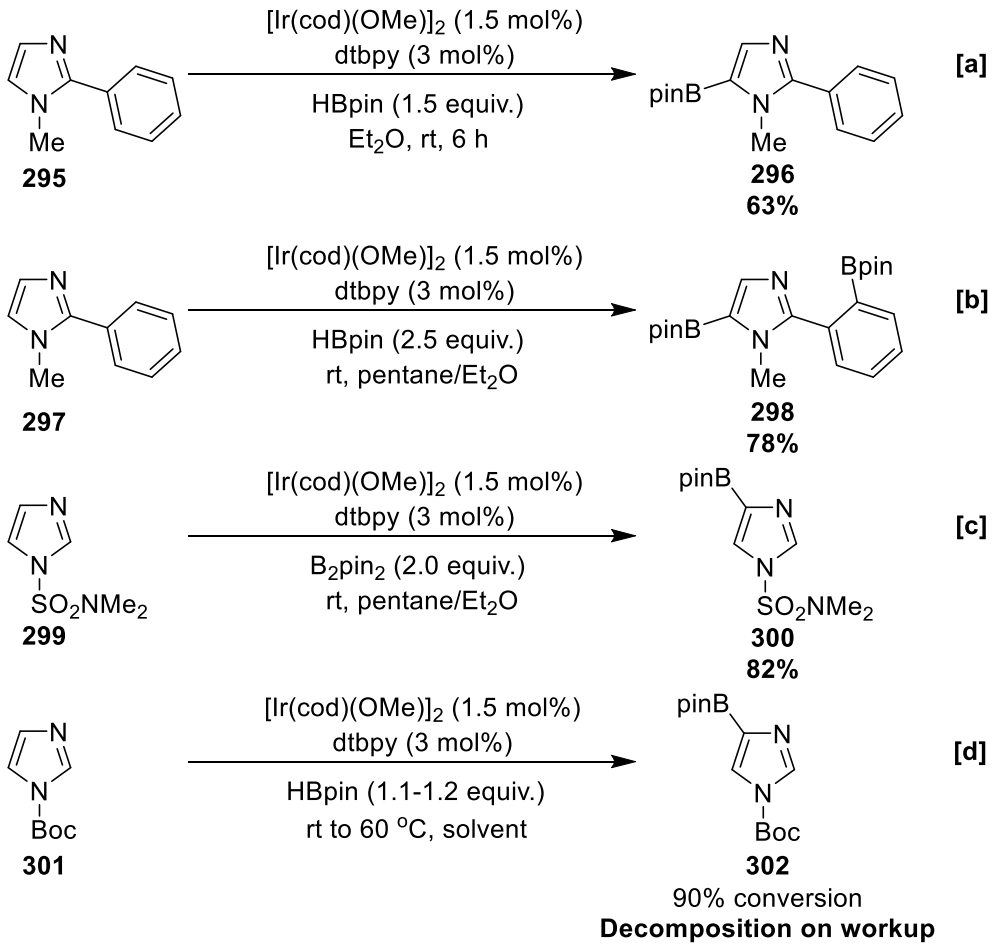

Scheme 36: Borylation of Imidazole Derivatives

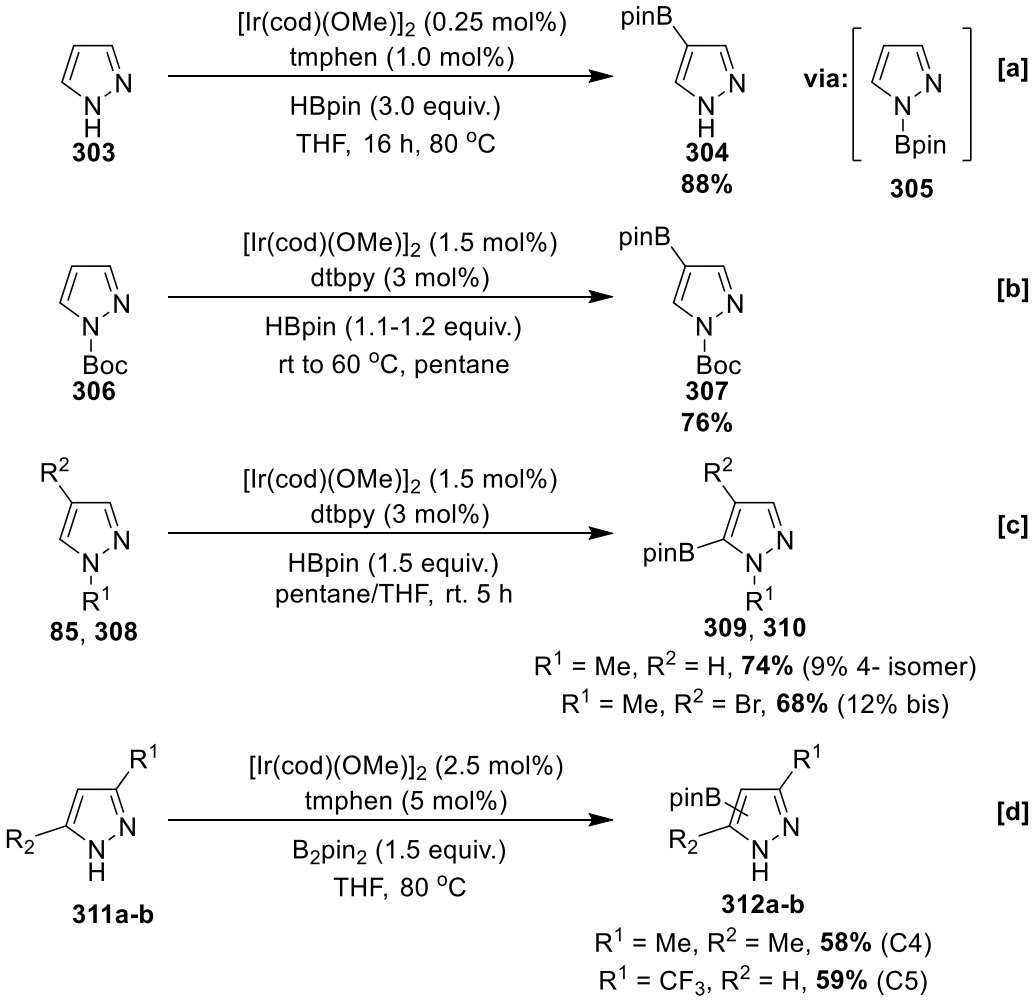

Scheme 37: Borylation of Pyrazole Derivatives

Free NH pyrazole beta borylates owing to the rapid formation of the bulky N-Bpin species **305**, which sterically blocks alpha borylation (Scheme 37a).[77] Unlike indole, this does not require exogenous base, and spontaneous N-H borylation occurs initially through a mechanism that is analogous to the C-H borylation discussed in section 1.5. **303** can also react with HBpin without catalysis to form **305**. Like Bpin, the Boc group of **306** directs beta borylation to produce **307** (Scheme 37b).

In a similar fashion, N-methyl pyrazole derivatives such as **85** and **308** selectively alpha borylate, and **308** surprisingly shows tolerance for C-H borylation at C-5 which possesses two *ortho* substituents (Scheme 37c). This is unprecedented in carbocyclic arenes, and may be possible due to the less congested relationship between substituents in five-membered rings. Substituted 2- and 2,5-subsituted NH pyrazoles such as **311a** borylate with selectivity for C-4, however trifluoromethyl pyrazole **311b** alpha borylates (Scheme 46d).[121] It is unclear why this is the case, although if Bpin is truly a steric director **311b** may not undergo spontaneous N-H borylation.

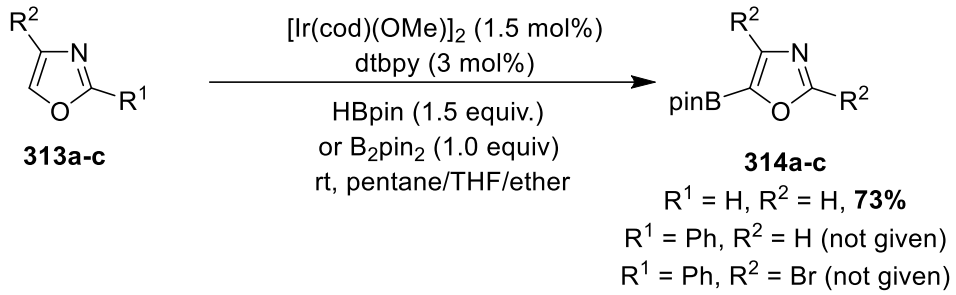

Scheme 38: Borylation of Oxazole and Derivatives

Significantly fewer oxazole derivatives have been reported in the C-H borylation, although some examples are given in Scheme 38. In these substrates, there is a normal preference for borylation at the most acidic site alpha to O.[126] The inner-/outer-sphere borylation of imidazole, pyrazole, or oxazole derivatives has not been investigated.

1.7.3.3.2 Indazole

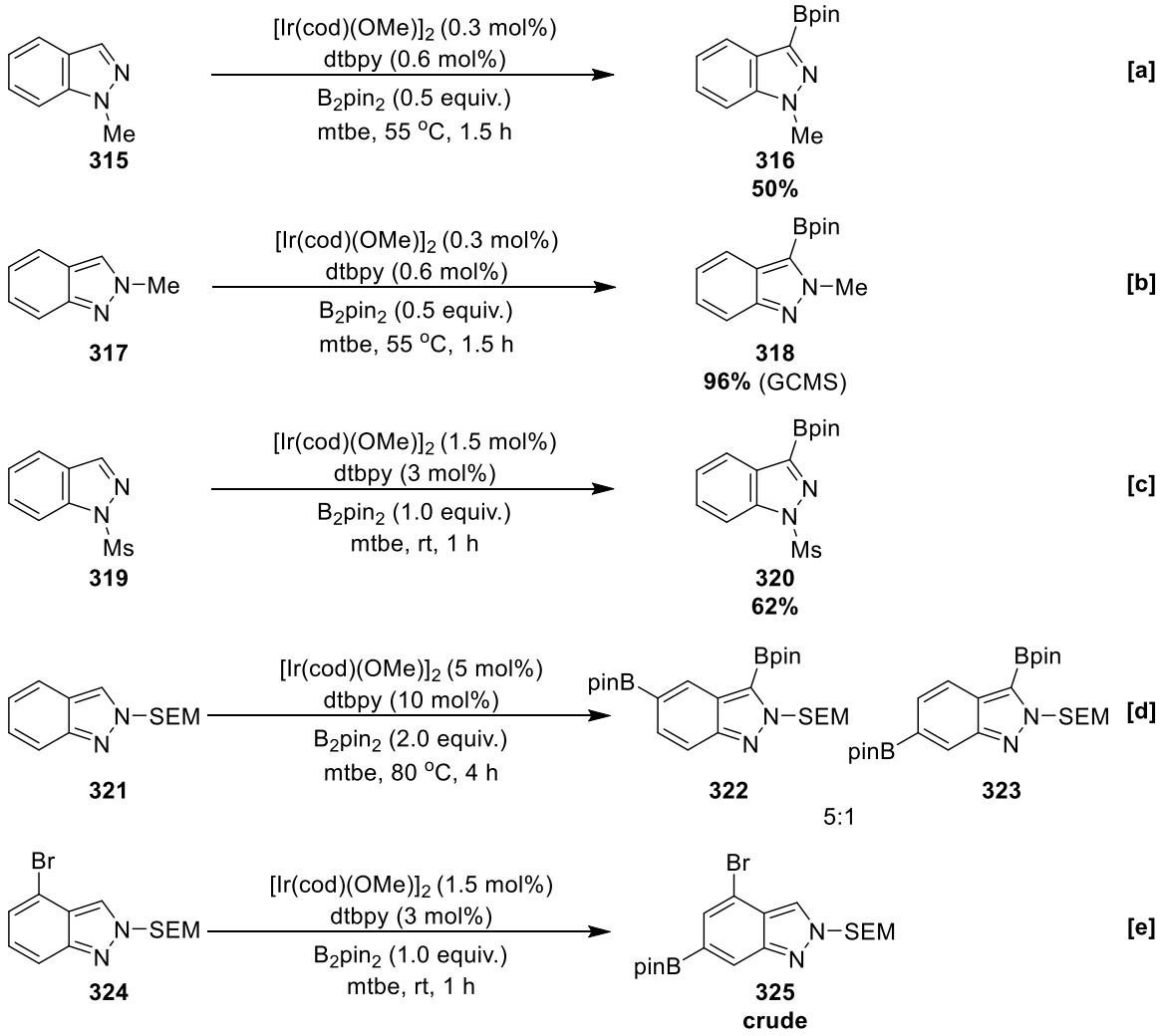

Scheme 39: CHB of Indazoles

Free NH indazole does not borylate, and it has been suggested that this is due to an inhibitory effect of the azinyl N on the catalyst.[127] This is surprising because more basic heteroarenes such as N-methylimidazole have high activity. Furthermore, the related heteroarene pyrazole is active and borylates at C-4 owing to spontaneous N-H borylation. Moreover, the basicity of indazole (p*K*a $[HA]^+$ = 1.25) is comparable to pyrimidine (p*K*a $[HA]^+$ = 1.1), which shows some activity in the C-H borylation (see section 1.7.3.4.1).

If indazole is indeed an inhibitor, it is likely that it does not undergo spontaenous N-H borylation, and this could be due to low Brønsted acidity.[77] In support of this idea, N-substituted indazole derivatives undergo facile borylation, and N-methyl-1H-indazole **315** and N-methyl-2H-indazole **317** show complete selectivity for the heteroaromatic moiety (Scheme 39a, b).[128] Surprisingly, in **315** the steric inhibition of the ring-junction combined with the electronic inhibition of the azinyl N is overridden by this preference. However, when compared to pyridine/quinoline, the inhibitory effect of the azinyl N in **315** is reduced by the electron-withdrawing effect of the azole N.

Moving from N-Me to other substituents, such THP, SEM, or 3,5-dimethylbenzyl does not alter this regiochemistry in 1H and 2H indazoles, although the corresponding C-3 boronates are challenging to purify due to protodeborylation. To mitigate this, the electron-withdrawing effect of the Ms group was employed to stabilise boronate **320**, permitting isolation in 62% yield (Scheme 39c). Furthermore, at elevated temperature in the presence of 2 equiv. of B_2pin_2, N-SEM-2H-indazole **321** iteratively borylates at C-5/C-6 following C-3 in a 5:1 ratio (Scheme 39d). Finally, substitution at C-4 in **324** introduces *peri*-like congestion at C-3, which leads to C-H borylation at C-6 (Scheme 39e).

1.7.3.3.3 Benzoxazole, Benzothiazole, and Benzimidazole

The borylation of benzoxazoles, benzothiazoles, and benzimidazoles requires a substituent at C-2 in order to prevent substrate ligation to the catalyst. In 2-methylbenzoxazole **326**, borylation is selective *ortho* to O (C-7) (Scheme 40a), and other derivatives with substituents at C-4 or C-5 also show this regiochemistry.[121] This is consistent with the *ortho* selectivity observed in benzodioxole **79**, and it has been proposed that C-7 selectivity originates from C-H acidity (see section 1.7.1). 2-Methylbenzothiazole **328** is comparably less active towards C-H borylation and displays poorer intrinsic selectivity (Scheme 40b).

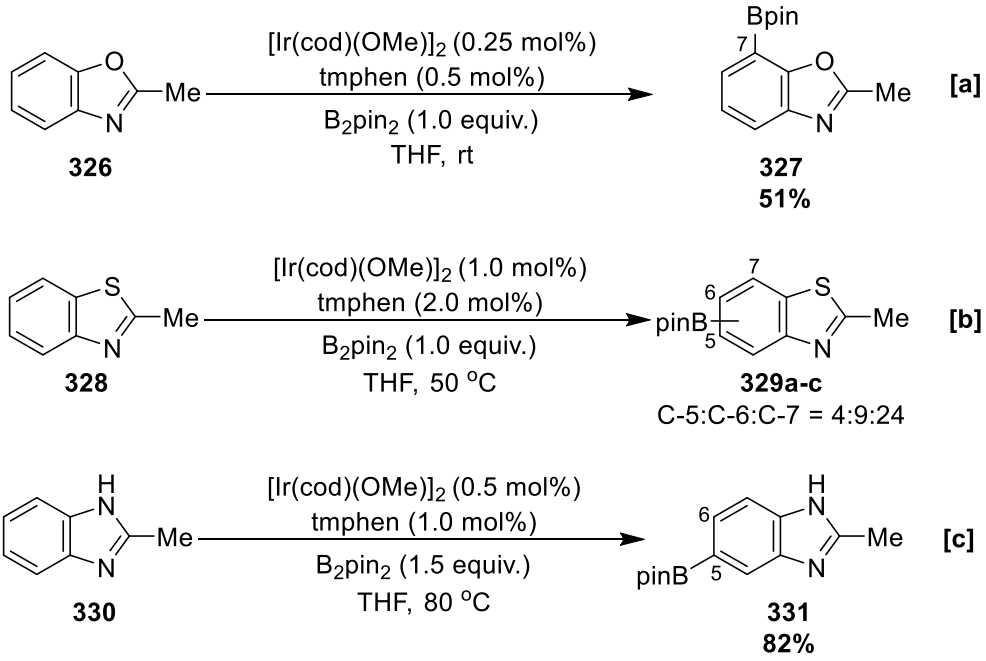

Scheme 40: C-H Borylation of Benzoxazole, Benzothiazole, and Benzimidazole Derivatives

The requirement for elevated temperature and catalyst loadings likely reflects the deactivating effect of sulphur, mirroring the relatively low activity of thiophene (see section 1.7.3.1). In contrast, 2-methylbenzimidazole **330** efficiently undergoes distal borylation at C-5 (alternatively C-6 since tautomerism is rapid), and this regiochemistry is observed in other 2-substituted derivatives (Scheme 40c). The lack of C-4/C-7 selectivity could be attributed to the formation of an N-Bpin adduct, which sterically hinders the *peri* position. This is supported by the requirement for increased equivalents of B_2pin_2 for efficient borylation. Furthermore, the remaining *peri* C-H bond may be inhibited by the azinyl N in analogy to the lack of intrinsic C-8 selectivity in quinoline. Alternatively, the rapid tautomerism in **330** may impart azinyl-character to both ring nitrogen atoms, causing both to electronically inhibit *peri* borylation.

1.7.3.4 Six Membered Rings with Two Heteroatoms

1.7.3.4.1 Diazines

The presence of two N ring atoms renders diazines less Lewis basic then pyridine, permitting greater activity. Indeed, parent pyrimidine **332** borylates at room temperature using tmphen as a ligand, albeit in low NMR yield. In analogy to the C-H borylation of other azinyl systems, the catalyst avoids the alpha-azinyl positions and delivers C-5 functionalised boronate **333** selectively **(**Scheme 41a).

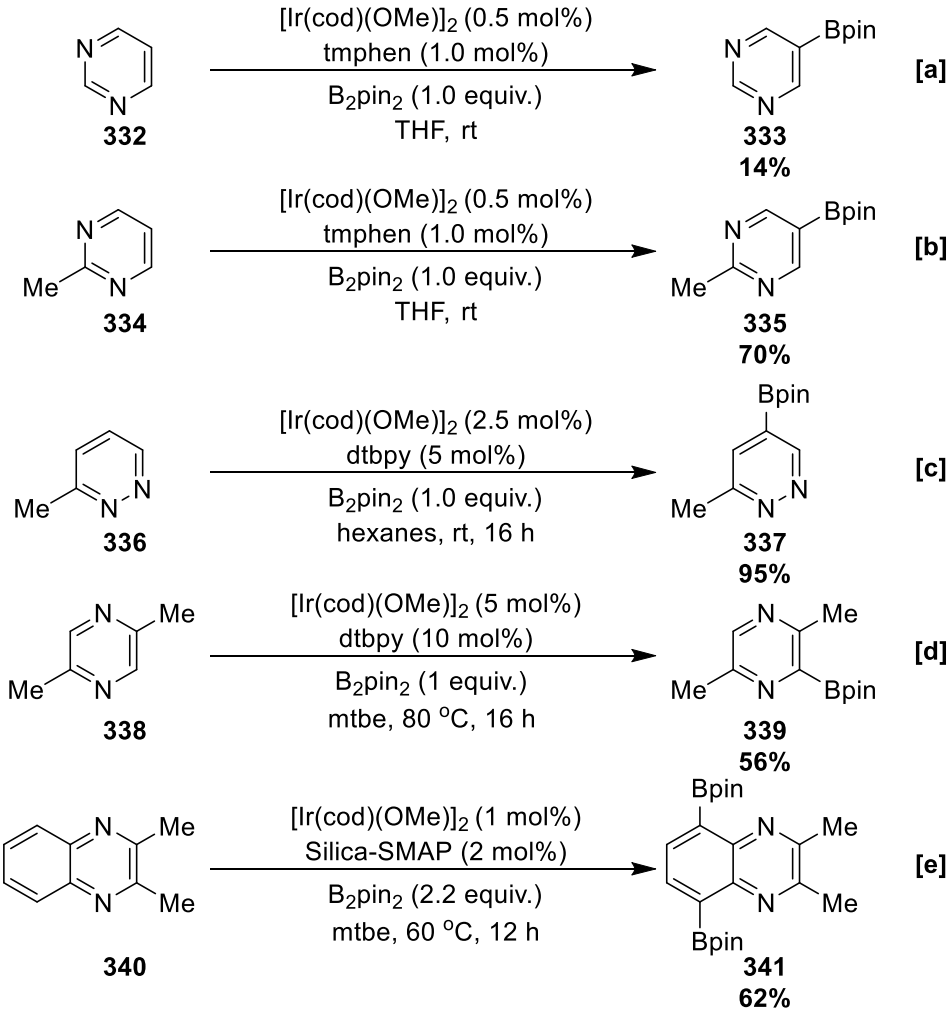

Scheme 41: Borylation of Diazines

Blocking ligation of diazine substrates improves reactivity, and this may be seen in the comparably more efficient borylation of 2-methylpyrimidine **334** (Scheme 41b). Likewise, the borylation of 6-methylpyridazine **336** is efficient and selective for C-4 (Scheme 41c). In contrast to pyridines, substituted pyrazine have been shown to borylate at the alpha-azinyl C-H bond without necessarily requiring electron-withdrawing substituents and this is enabled by the additional ring N atom. For example, pyrazine **338** efficiently borylates in at C-6, despite the presence of an *ortho* azinyl N and methyl group (Scheme 41d). Finally, in parallel with the transformation of quinolines, the borylation of quinoxaline has been reported under the Si-SMAP system, affording bisborylated product **341** via inner-sphere coordination of the azinyl N atoms (Scheme 41e).[60]

1.7.3.4.2 Azaborine and Borazaronaphthalene

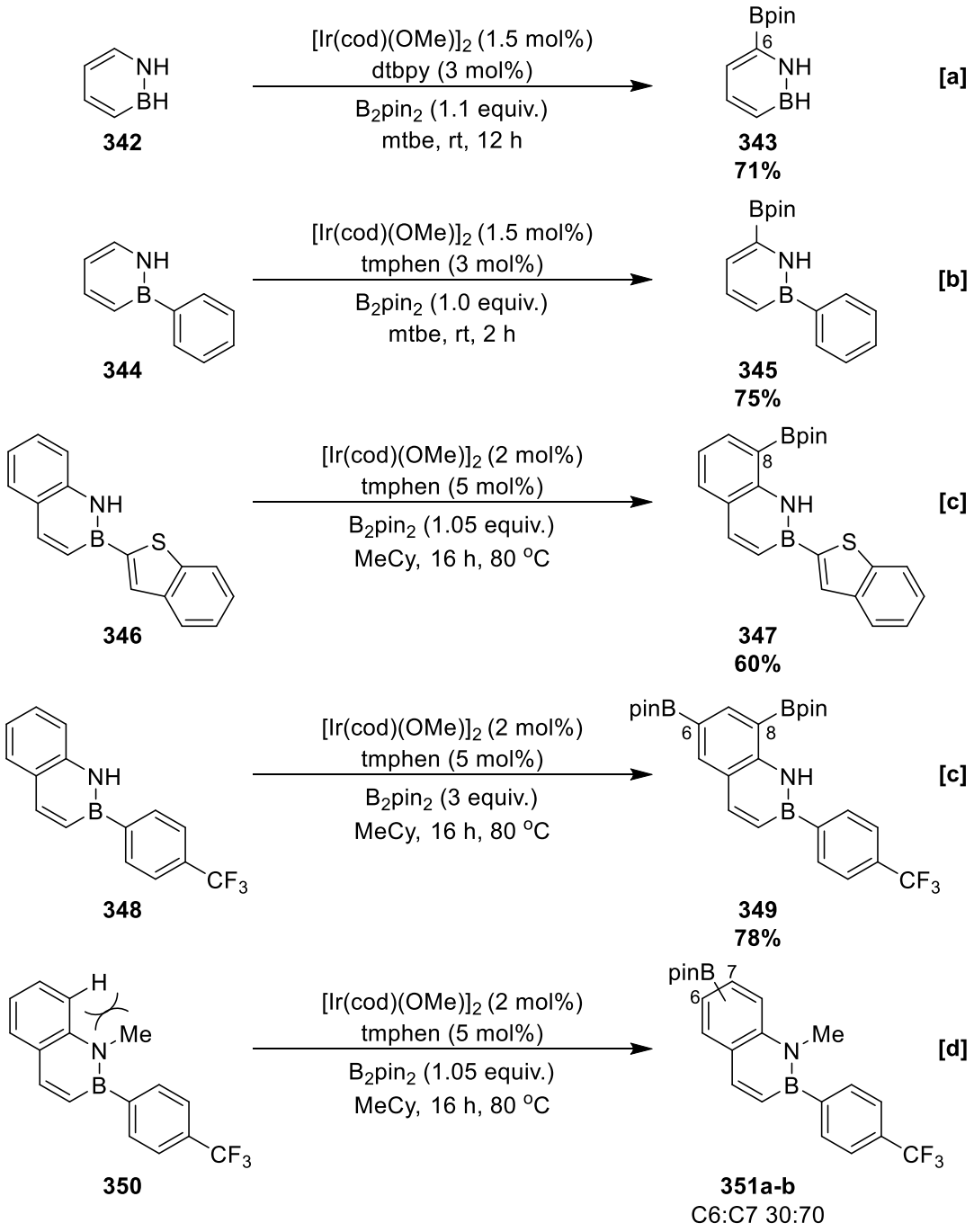

Scheme 42: CHB of Boron Containing Heteroarenes

The Ir C-H borylation is amenable to the functionalisation of boron containing heteroarenes, including azaborine and 2,1-borazaronaphthalene. In analogy to other azoles, azaborine **342** borylates selectively alpha to N at C-6 (Scheme 42a), and this is unaffected by substitution at B.[129] Notably, this selectivity correlates well with calculated gas-phase acidity, rationalising why the introduction of a less C-H acidic phenyl group in **344** is selective for the heterocycle (Scheme 42b).

2,1-Borazaronaphthalenes are benzofused analogues to azaborine, and this motif differs from other benzofused heteroarenes in the C-H borylation as regioselectivity is observed for the carbocyclic ring. For instance, the carbocycle of **346** is more reactive than the azaborine and benzothiophene systems, and undergoes selective borylation at C-8 (Scheme 42c).[106] The use of excess boron leads to bisborylation at C-8 followed by C-6, and this is observed in **348**. To account for C-8 selectivity, it has been suggested that the ring N-H may play a role in an inner/outer-sphere directed process. However, in 2-phenyl-2,1-borazaronaphthalene it has been calculated that C-8 offers the greatest anionic charge stabilisation compared to other uncongested C-H sites, which suggests that the selectivity may be intrinsic in origin. The methylation of the ring N-H to form analogue **350** does erode C-8 borylation selectivity, and this has been offered as evidence for an N-H mediated directing effect. This could alternatively be due to a *peri* steric effect on the C-8 site (Scheme 42d).

1.7.3.5 Miscellaneous

1.7.3.5.1 Azaindole, Azaindazole and Deazapurine

In free NH 4- and 7-azaindole, N-H acidity is elevated by the presence of the azine N, facilitating spontaneous N-H borylation. Consequently, the corresponding N-Bpin adduct blocks C-2, leading to C-3 selective borylation in **352a** and **352b** (Scheme 43a).[77,101,121] The C-H borylation of N-methylazaindazole **354** is C-3 selective and affords **355**. Notably, the sterically hindered pyrazole ring displays greater reactivity than the pyridine ring. (Scheme 43b).

7H-Pyrrolo[2,3-d]pyrimidine (deazapurine) is related to 7-azaindole, except one C-H unit is replaced with an N atom to form a fused pyrimidine. Whilst the C-H borylation activity of deazapurines is variable, some disubstituted deazapurines borylate alpha to the azole N (C-6).[130,131] For example, the borylation of **356** tolerates the steric hindrance of an *ortho* benzyl group, and is selective for the heteroarene (Scheme 43c). The presence and nature of the substituents plays a role in determining activity, for example C-4 substituted free N-H deazapurines such as **358** do not borylate. Spontaneous N-H borylation may account for the lack of C-6 functionalisation, although it is unclear why the phenyl C-H bonds do not undergo C-H borylation (Scheme 43d).

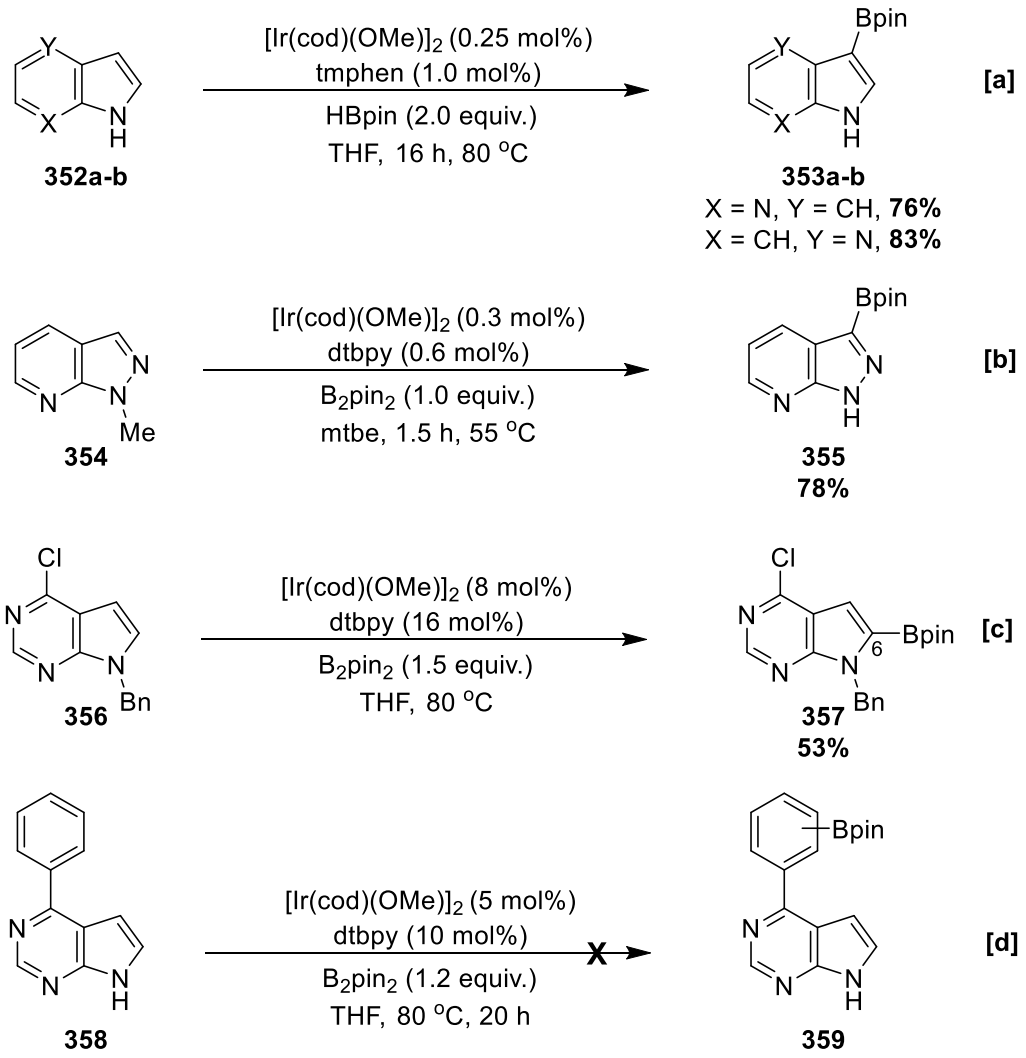

Scheme 43: Borylation of Azaindole and Deazapurine Derivatives

1.7.3.5.2 Porphyrins and Corroles

Porphyrins and corroles are closely related macrocycles consisting of four modified pyrrole units. Therefore, they share aspects of borylation regiochemistry with 2,5-disubstituted pyrroles.[132–136] For example, the borylation of porphyrin **360** is selective for the beta position to N, affording major monoborylated isomer **361** alongside two minor bisborylated isomers **362a** and **362b** in a 1:1 ratio (Scheme 44a). Notably, the borylation also tolerates Ni and Cu coordinated analogues of **360**, affording products with similar selectivities. Judicious *meso* substitution blocks the corresponding *peri* positions, permitting a degree of regiochemical control in iterative borylation reactions.

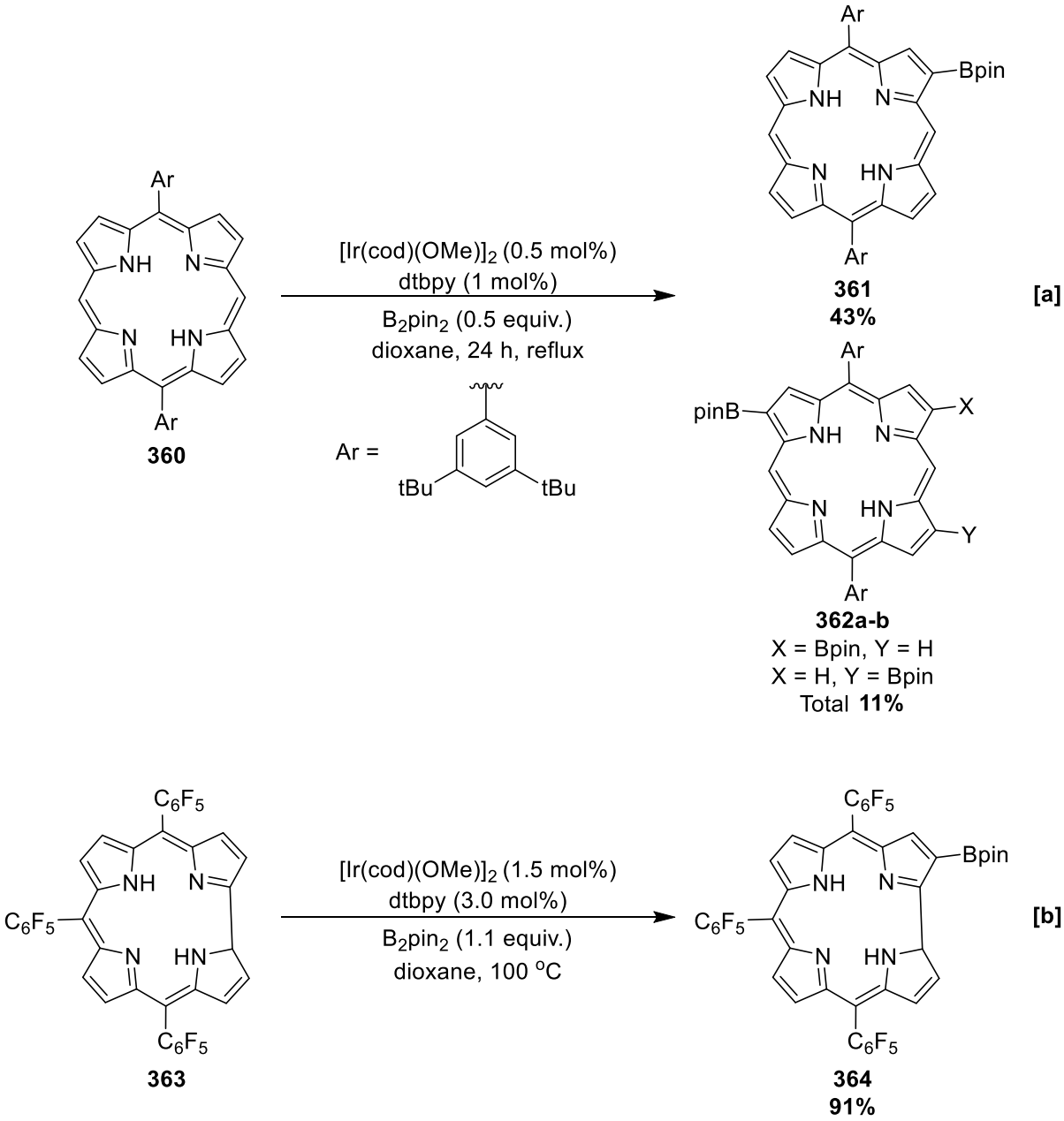

Scheme 44: C-H Borylation of Macrocycles

For instance, one borylation event occurs in the reaction of corrole **363** because the other C-H sites are sterically hindered by the *meso* pentafluorophenyl substituents (Scheme 44b). In porphyrins, substitution with benzene derivatives at all four *meso* positions shuts down reactivity at the macrocycle.

1.8 Summary

Organoboron compounds are versatile intermediates to the synthetic organic chemist. Seventeen years on from its inception, the Ir-catalysed C-H borylation remains a state-of-the-art tool for the regioselective installation of C-B bonds, as it overcomes the limitations of traditional syntheses. The crowded nature of the catalyst permits sterically controlled borylation of carbocyclic C-H bonds, and the least hindered sites are generally the most reactive.

Whilst the site-selectivity observed in the borylation of heteroarenes carries a degree of steric control, a larger contribution from electronic effects is apparent in some systems. This is evident by the observation that more congested C-H bonds can undergo borylation selectively, and this this most prevalent in heteroaromatic substrates. Factors such as Ir-C bond strength, relative anionic stabilisation, and C-H acidity in conjunction with sterics are useful predictors of heteroaromatic site-selectivity. The intrinsic selectivities of aromatics can be altered using directing effects, and a common strategy involves replacing the commonly employed bipyridine-derived ligands with others that facilitate inner-/outer-sphere direction. The reactivity and site-selectivity of other aromatic systems in the Ir C-H borylation will undoubtedly be the subject of future studies.

1.9 References

[1] E. Frankland, B. F. V. Duppa, *Justus Liebigs Ann. Chem.* **1860**, *115*, 319–322.

[2] H. Brown, B. C. Rao, *J. Org. Chem.* **1957**, *22*, 1136–1137.

[3] N. Miyaura, A. Suzuki, *J. Chem. Soc. Chem. Commun.* **1979**, 866-867.

[4] N. Miyaura, K. Yamada, A. Suzuki, *Tetrahedron Lett.* **1979**, *20*, 3437–3440.

[5] D. G. Brown, J. Boström, *J. Med. Chem.* **2016**, *59*, 4443–4458.

[6] D. B. Diaz, A. K. Yudin, *Nat. Chem.* **2017**, *9*, 731–742.

[7] P. Hunter, *EMBO Rep.* **2009**, *10*, 125–128.

[8] M. Takeuchi, I. Tomoyuki, S. Shinkai, *J. Am. Chem. Soc.* **1996**, *118*, 10658–10659.

[9] J. C. Vantourout, H. N. Miras, A. Isidro-Llobet, S. Sproules, A. J. B. Watson, *J. Am. Chem. Soc*

2017, *139*, 4769–4779.

[10] Y. Ye, S. D. Schimler, P. S. Hanley, M. S. Sanford, *J. Am. Chem. Soc.* **2013**, *135*, 16292–16295.

[11] A. Fawcett, D. Nitsch, M. Ali, J. M. Bateman, E. L. Myers, V. K. Aggarwal, *Angew. Chem. Int. Ed.* **2016**, *55*, 14663–14667.

[12] C. W. Liskey, X. Liao, J. F. Hartwig, *J. Am. Chem. Soc.* **2010**, *132*, 11389–11391.

[13] J. Takaya, S. Tadami, K. Ukai, N. Iwasawa, *Org. Lett.* **2008**, *10*, 2697–2700.

[14] S. M. Nicolle, A. Nortcliffe, H. E. Bartrum, W. Lewis, C. J. Hayes, C. J. Moody, *Chem. Eur. J.* **2017**, *23*, 13623–13627.

[15] J. E. Sieser, M. T. Maloney, E. Chisowa, S. Brenek, S. Monfette, J. J. Salisbury, N. Do, R. A. Singer, *Org. Process Res. Dev.* **2018**, *22*, 527–534.

[16] M. A. Soriano-Ursúa, E. D. Farfán-García, Y. López-Cabrera, E. Querejeta, J. G. Trujillo-Ferrara, *Neurotoxicology* **2014**, *40*, 8–15.

[17] R. D. Kimbrough, *Environ. Health Perspect.* **1976**, *14*, 51–56.

[18] I. A. I. Mkhalid, J. H. Barnard, T. B. Marder, J. M. Murphy, J. F. Hartwig, *Chem. Rev.* **2009**, *110*, 890–931.

[19] E. C. Neeve, S. J. Geier, I. A. I. Mkhalid, S. A. Westcott, T. B. Marder, *Chem. Rev.* **2016**, *116*, 9091–9161.

[20] J. W. B. Fyfe, A. J. B. Watson, *Chem* **2017**, *3*, 31–55.

[21] J. F. Hartwig, *Acc. Chem. Res.* **2012**, *45*, 864–873.

[22] J. F. Hartwig, *Chem. Soc. Rev.* **2011**, *40*, 1992–2002.

[23] D. Hemming, R. Fritzemeier, S. A. Westcott, W. L. Santos, P. G. Steel, *Chem. Soc. Rev.* **2018**, *47*, 7477–7494.

[24] G. Wulff, M. Lauer, *J. Organomet. Chem.* **1983**, *256*, 1–9.

[25] J. Morgan, J. T. Pinhey, *J. Chem. Soc. Perkin Trans* **1990**, *1*, 715–720.

[26] T. Ishiyama, M. Murata, N. Miyaura, *J. Org. Chem.* **1995**, *60*, 7508–7510.

[27] H.-X. Dai, J.-Q. Yu, *J. Am. Chem. Soc.* **2012**, *134*, 134–137.

[28] T. Dombray, C. G. Werncke, S. Jiang, M. Grellier, L. Vendier, S. Bontemps, J. B. Sortais, S. Sabo-Etienne, C. Darcel, *J. Am. Chem. Soc.* **2015**, *137*, 4062–4065.

[29] S. K. Bose, A. Deißenberger, A. Eichhorn, P. G. Steel, Z. Lin, T. B. Marder, *Angew. Chem. Int. Ed.* **2015**, *54*, 11843–11847.

[30] J. A. Fernández-Salas, S. Manzini, L. Piola, A. M. Z. Slawin, S. P. Nolan, *Chem. Commun.* **2014**, *2*, 6782–6784.

[31] T. Furukawa, M. Tobisu, N. Chatani, *Chem. Commun.* **2015**, *51*, 6508–6511.

[32] T. Furukawa, M. Tobisu, N. Chatani, *J. Am. Chem. Soc.* **2015**, *137*, 12211–12214.

[33] C. B. Bheeter, A. D. Chowdhury, R. Adam, R. Jackstell, M. Beller, *Org. Biomol. Chem.* **2015**, *13*, 10336–10340.

[34] H. Chen, J. F. Hartwig, *Angew. Chem. Int. Ed.* **1999**, *38*, 3391–3393.

[35] J. V. Obligacion, S. P. Semproni, P. J. Chirik, *J. Am. Chem. Soc.* **2014**, *136*, 4133–4136.

[36] T. Ishiyama, J. Takagi, K. Ishida, N. Miyaura, N. R. Anastasi, J. F. Hartwig, *J. Am. Chem. Soc.* **2002**, *124*, 390–391.

[37] J.-Y. Cho, M. K. Tse, D. Holmes, R. E. Maleczka, M. R. Smith III, *Science,* **2002**, *295*, 305–308.

[38] P. Nguyen, H. P. Blom, S. A. Westcott, N. J. Taylor, T. B. Marder, *J. Am. Chem. Soc.* **1993**, *115*, 9329–9330.

[39] C. N. Iverson, M. R. Smith III, *J. Am. Chem. Soc.* **1999**, *121*, 7696–7697.

[40] K. Kawamura, J. F. Hartwig, *J. Am. Chem. Soc.* **2001**, *123*, 8422–8423.

[41] S. M. Preshlock, B. Ghaffari, P. E. Maligres, S. W. Krska, R. E. Maleczka, M. R. Smith III, *J. Am.*

Chem. Soc. **2013**, *135*, 7572–7582.

[42] T. Ishiyama, J. Takagi, J. F. Hartwig, N. Miyaura, *Angew. Chem., Int. Ed* **2002**, *41*, 3056–3058.

[43] T. M. Boller, J. M. Murphy, M. Hapke, T. Ishiyama, N. Miyaura, J. F. Hartwig, *J. Am. Chem. Soc.* **2005**, *127*, 14263–14278.

[44] H. Tajuddin, P. Harrisson, B. Bitterlich, J. C. Collings, N. Sim, A. S. Batsanov, M. S. Cheung, S. Kawamorita, A. C. Maxwell, L. Shukla, et al., *Chem. Sci.* **2012**, *3*, 3505–3515.

[45] H. Tamura, H. Yamazaki, H. Sato, S. Sakaki, *J. Am. Chem. Soc.* **2003**, *125*, 16114–16126.

[46] C. W. Liskey, C. S. Wei, D. R. Pahls, J. F. Hartwig, *Chem. Commun* **2009**, 5603–5605.

[47] G. A. Chotana, B. A. Vanchura, II, M. K. Tse, R. J. Staples, R. E. Maleczka, Jr, M. R. Smith III, III, *Chem. Commun.* **2009**, 5731-5733.

[48] T. Ishiyama, Y. Nobuta, J. F. Hartwig, N. Miyaura, *Chem. Commun.* **2003**, 2924.

[49] T. E. Hurst, T. K. Macklin, M. Becker, E. Hartmann, W. Kügel, J.-C. Parisienne-La Salle, A. S. Batsanov, T. B. Marder, V. Snieckus, *Chem. A Eur. J.* **2010**, *16*, 8155–8161.

[50] Ghayoor A. Chotana, A. Michael A. Rak, I. Milton R. Smith, *J. Am. Chem. Soc.* **2005**, *127*, 10539–10544.

[51] G. A. Chotana, M. A. Rak, M. R. Smith III, *J. Am. Chem. Soc.* **2005**, *127*, 10539–10544.

[52] B. E. Haines, Y. Saito, Y. Segawa, K. Itami, D. G. Musaev, *ACS Catal.* **2016**, *6*, 7536–7546.

[53] Y. Saito, Y. Segawa, K. Itami, *J. Am. Chem. Soc.* **2015**, *137*, 5193–5198.

[54] L. Yang, K. Semba, Y. Nakao, *Angew. Chem. Int. Ed.* **2017**, *56*, 4853–4857.

[55] B. A. Vanchura, II, S. M. Preshlock, P. C. Roosen, V. A. Kallepalli, R. J. Staples, R. E. Maleczka, Jr., D. A. Singleton, M. R. Smith III, *Chem. Commun.* **2010**, *46*, 7724–7726.

[56] A. G. Green, P. Liu, C. A. Merlic, K. N. Houk, *J. Am. Chem. Soc.* **2014**, *136*, 4575–4583.

[57] A. Ros, J. M. Lassaletta, R. Fernandez, *Chem. Soc. Rev.* **2014**, 3229–3243.

[58] S. Kawamorita, H. Ohmiya, K. Hara, A. Fukuoka, M. Sawamura, *J. Am. Chem. Soc.* **2009**, *131*, 5058–5059.

[59] Y. Kenji, K. Soichiro, O. Hirohisa, S. Masaya, *Org. Lett.* **2010**, *12*, 3978–3981.

[60] S. Konishi, S. Kawamorita, T. Iwai, P. G. Steel, T. B. Marder, M. Sawamura, *Chem. Asian J.* **2014**, *9*, 434–438.

[61] S. Kawamorita, H. Ohmiya, M. Sawamura, *J. Org. Chem.* **2010**, *75*, 3855–3858.

[62] I. Sasaki, J. Taguchi, S. Hiraki, H. Ito, T. Ishiyama, *Chem. A Eur. J.* **2015**, 9236–9241.

[63] T. Ishiyama, H. Isou, T. Kikuchi, N. Miyaura, *Chem. Commun.* **2010**, *46*, 159–161.

[64] H. Itoh, T. Kikuchi, T. Ishiyama, N. Miyaura, *Chem. Lett.* **2011**, *40*, 1007–1008.

[65] A. Ros, R. López-Rodríguez, B. Estepa, E. Álvarez, R. Fernández, J. M. Lassaletta, *J. Am. Chem. Soc.* **2012**, *134*, 4573–4576.

[66] A. Ros, B. Estepa, R. López-Rodríguez, E. Álvarez, R. Fernández, J. M. Lassaletta, *Angew. Chem. Int. Ed.* **2011**, *50*, 11724–11728.

[67] R. López-Rodríguez, A. Ros, R. Fernández, J. M. Lassaletta, *J. Org. Chem.* **2012**, *77*, 9915–9920.

[68] B. Ghaffari, S. M. Preshlock, D. L. Plattner, R. J. Staples, P. E. Maligres, S. W. Krska, R. E. Maleczka, M. R. Smith III, *J. Am. Chem. Soc.* **2014**, *136*, 14345–14348.

[69] G. Wang, L. Liu, H. Wang, Y.-S. Ding, J. Zhou, S. Mao, P. Li, *J. Am. Chem. Soc* **2017**, *139*, 91-94.

[70] L. Liu, G. Wang, J. Jiao, P. Li, *Org. Lett* **2017**, *19*, 6132–6135.

[71] D. W. Robbins, T. A. Boebel, J. F. Hartwig, *J. Am. Chem. Soc.* **2010**, *132*, 4068–4069.

[72] B. Su, J. F. Hartwig, *Angew. Chem. Int. Ed.* **2018**, *57*, 10163–10167.

[73] T. A. Boebel, J. F. Hartwig, *J. Am. Chem. Soc.* **2008**, *130*, 7534–7535.

[74] Y. Sumida, R. Harada, T. Sumida, D. Hashizume, T. Hosoya, *Chem. Lett.* **2018**, *47*, 1251–1254.

[75] Y. Sumida, R. Harada, T. Kato-Sumida, K. Johmoto, H. Uekusa, T. Hosoya, *Org. Lett.* **2014**, *16*, 6240–6243.

[76] P. C. Roosen, V. A. Kallepalli, B. Chattopadhyay, D. A. Singleton, R. E. Maleczka, M. R. Smith III, *J. Am. Chem. Soc.* **2012**, *134*, 11350–11353.

[77] S. M. Preshlock, D. L. Plattner, P. E. Maligres, S. W. Krska, R. E. Maleczka, M. R. Smith III *Angew. Chem. Int. Ed.* **2013**, *52*, 12915–12919.

[78] M. R. Smith III, R. Bisht, C. Haldar, G. Pandey, J. E. Dannatt, B. Ghaffari, R. E. Maleczka, B. Chattopadhyay, *ACS Catal.* **2018**, *8*, 6216–6223.

[79] B. Chattopadhyay, J. E. Dannatt, I. L. Andujar-De Sanctis, K. A. Gore, R. E. Maleczka, D. A. Singleton, M. R. Smith III, *J. Am. Chem. Soc.* **2017**, *139*, 7864-7871.

[80] Y. Kuninobu, H. Ida, M. Nishi, M. Kanai, *Nat. Chem.* **2015**, *7*, 712–717.

[81] M. Mihai, R. Phipps, *Synlett* **2017**, *28*, 1011–1017.

[82] H. J. Davis, M. T. Mihai, R. J. Phipps, *J. Am. Chem. Soc.* **2016**, *138*, 12759–12762.

[83] H. J. Davis, G. R. Genov, R. J. Phipps, *Angew. Chem. Int. Ed.* **2017**, *56*, 13351–13355.

[84] M. T. Mihai, H. J. Davis, G. R. Genov, R. J. Phipps, *ACS Catal.* **2018**, *8*, 3764–3769.

[85] M. E. Hoque, R. Bisht, C. Haldar, B. Chattopadhyay, *J. Am. Chem. Soc.* **2017**, *139*, 7745–7748.

[86] J. F. Hartwig, *Chem. Soc. Rev.* **2011**, *40*, 1992-2002.

[87] N. Primas, A. Bouillon, S. Rault, *Tetrahedron* **2010**, *66*, 8121–8136.

[88] R. A. Ward, J. G. Kettle, *J. Med. Chem.* **2011**, *54*, 4670–4677.

[89] E. Vitaku, D. T. Smith, J. T. Njardarson, *J. Med. Chem.* **2014**, *57*, 10257–10274.

[90] A. R. D. Taylor, M. Maccoss, A. D. G. Lawson, *J. Med. Chem.* **2014**, *57*, 5845–5859.

[91] W. Pitt, D. M. Parry, B. G. Perry, C. R. Groom, *J. Med. Chem.* **2009**, 2952–2963.

[92] D. J. Newman, G. M. Cragg, *J. Nat. Prod.* **2016**, *79*, 629–661.

[93] P. Jeschke, *Pest Manag. Sci.* **2016**, *72*, 210–225.

[94] K. Murakami, S. Yamada, T. Kaneda, K. Itami, *Chem. Rev.* **2017**, *117*, 9302–9332.

[95] J. Takagi, K. Sato, J. F. Hartwig, T. Ishiyama, N. Miyaura, *Tetrahedron Lett.* **2002**, *43*, 5649–5651.

[96] T. Ishiyama, J. Takagi, Y. Yonekawa, J. F. Hartwig, N. Miyaura, *Adv. Synth. Catal.* **2003**, *345*, 1103–1106.

[97] D. W. Robbins, J. F. Hartwig, *Org Lett*. **2012**, *14*, 4266-4269.

[98] G. A. Chotana, V. A. Kallepalli, R. E. Maleczka, M. R. Smith III, *Tetrahedron* **2008**, *64*, 6103–6114.

[99] V. A. Kallepalli, L. Sanchez, H. Li, N. J. Gesmundo, C. L. Turton, R. E. Maleczka, M. R. Smith III, *Heterocycles* **2010**, *80*, 1429–1448.

[100] E. M. Beck, R. Hatley, M. J. Gaunt, *Angew. Chem. Int. Ed.* **2008**, *47*, 3004–3007.

[101] V. A. Kallepalli, F. Shi, S. Paul, E. N. Onyeozili, R. E. Maleczka, M. R. Smith III, *J. Org. Chem.* **2009**, *74*, 9199–9201.

[102] P. Harrisson, J. Morris, T. B. Marder, P. G. Steel, *Org. Lett.* **2009**, *11*, 3586–3589.

[103] L. Liu, G. Wang, J. Jiao, P. Li, *Org. Lett.* **2017**, *19*, 6132–6135.

[104] S. Paul, G. A. Chotana, D. Holmes, R. C. Reichle, R. E. Maleczka, M. R. Smith III, *J. Am. Chem. Soc.* **2006**, *128*, 15552–15553.

[105] J. Liyu, J. Sperry, *Tetrahedron Lett.* **2017**, *58*, 1699–1701.

[106] G. H. M. Davies, M. Jouffroy, F. Sherafat, B. Saeednia, C. Howshall, G. A. Molander, *J. Org. Chem.* **2017**, *82*, 8072–8084.

[107] V. A. Kallepalli, K. A. Gore, F. Shi, L. Sanchez, G. A. Chotana, S. L. Miller, R. E. Maleczka, M. R. Smith III, *J. Org. Chem.* **2015**, *80*, 8341–8353.

[108] G. R. Humphrey, J. T. Kuethe, *Chem. Rev.* **2006**, *106*, 2875–2911.

[109] F. Batool, S. Parveen, A. H. Emwas, S. Sioud, X. Gao, M. A. Munawar, G. A. Chotana, *Org. Lett.* **2015**, *17*, 4256–4259.

[110] A. S. Eastabrook, C. Wang, E. K. Davison, J. Sperry, *J. Org. Chem.* **2015**, *80*, 1006–1017.

[111] W. F. Lo, H. M. Kaiser, A. Spannenberg, M. Beller, M. K. Tse, *Tetrahedron Lett.* **2007**, *48*, 371–375.

[112] F. Shen, S. Tyagarajan, D. Perera, S. W. Krska, P. E. Maligres, M. R. Smith III, R. E. Maleczka, *Org. Lett* **2016**, *18*, 1554-1557.

[113] F. M. Meyer, S. Liras, A. Guzman-Perez, C. Perreault, J. Bian, K. James, *Org. Lett.* **2010**, *12*, 3870–3873.

[114] R. P. Loach, O. S. Fenton, K. Amaike, D. S. Siegel, E. Ozkal, M. Movassaghi, *J. Org. Chem.* **2014**, *79*, 11254–11263.

[115] J. A. Homer, J. Sperry, *Tetrahedron Lett.* **2014**, *55*, 5798–5800.

[116] A. S. Eastabrook, J. Sperry, *Aust. J. Chem.* **2015**, *68*, 1810–1814.

[117] A. S. Eastabrook, J. Sperry, *Synth.* **2017**, *49*, 4731–4737.

[118] Y. Feng, D. Holte, J. Zoller, S. Umemiya, L. R. Simke, P. S. Baran, *J. Am. Chem. Soc.* **2015**, *137*, 10160–10163.

[119] C. C. C. J. Seechurn, V. Sivakumar, D. Satoskar, T. J. Colacot, *Organometallics* **2014**, *33*, 3514–3522.

[120] H. J. Davis, M. T. Mihai, R. J. Phipps, *J. Am. Chem. Soc.* **2016**, *138*, 12759–12762.

[121] M. A. Larsen, J. F. Hartwig, *J. Am. Chem. Soc.* **2014**, *136*, 4287–4299.

[122] P. A. Cox, A. G. Leach, A. D. Campbell, G. C. Lloyd-Jones, *J. Am. Chem. Soc.* **2016**, *138*, 9145-9157.

[123] I. A. I. Mkhalid, D. N. Coventry, D. Albesa-Jove, A. S. Batsanov, J. A. K. Howard, R. N. Perutz,

T. B. Marder, *Angew. Chem. Int. Ed.* **2006**, *45*, 489–491.

[124] S. A. Sadler, H. Tajuddin, I. A. I. Mkhalid, A. S. Batsanov, D. Albesa-Jove, M. S. Cheung, A. C. Maxwell, L. Shukla, B. Roberts, D. C. Blakemore, Z. Lin, T. B. Marder, P. G. Steel, *Org. Biomol. Chem.* **2014**, *12*, 7318–7327.

[125] T. Tagata, M. Nishida, *Adv. Synth. Catal.* **2004**, *346*, 1655–1660.

[126] M. R. Smith III, R. E. Maleczka, Jr, A. K. Venkata, E. Onyeozili, *Process for Producing Oxazole, Imidazole, Pyrazole Boryl Compounds*, US PAT, **2008**, 0091027.

[127] S. A. Sadler, A. C. Hones, B. Roberts, D. Blakemore, T. B. Marder, P. G. Steel, *J. Org. Chem.* **2015**, *80*, 5308–5314.

[128] B. A. Egan, P. M. Burton, *RSC Adv.* **2014**, *4*, 27726-27729.

[129] A. W. Baggett, M. Vasiliu, B. Li, D. A. Dixon, S. Y. Liu, *J. Am. Chem. Soc.* **2015**, *137*, 5536–5541.

[130] M. Klečka, R. Pohl, B. Klepetářová, M. Hocek, *Org. Biomol. Chem.* **2009**, *7*, 866.

[131] M. Klečka, L. P. Slavětínská, M. Hocek, *European J. Org. Chem.* **2015**, 7943–7961.

[132] H. Hata, S. Yamaguchi, G. Mori, S. Nakazono, T. Katoh, K. Takatsu, S. Hiroto, H. Shinokubo, A. Osuka, *Chem. Asian J.* **2007**, *2*, 849–859.

[133] H. Hata, H. Shinokubo, A. Osuka, *J. Am. Chem. Soc.* **2005**, *127*, 8264–8265.

[134] S. Hiroto, I. Hisaki, H. Shinokubo, A. Osuka, *Angew. Chem. Int. Ed.* **2005**, *44*, 6763–6766.

[135] J. Chen, N. Aratani, H. Shinokubo, A. Osuka, *Chem. Asian J.* **2009**, *4*, 1126–1133.

[136] G. Mori, H. Shinokubo, A. Osuka, *Tetrahedron Lett.* **2008**, *49*, 2170–2172.

2 Previous Work and Aims

2.1 Previous Work

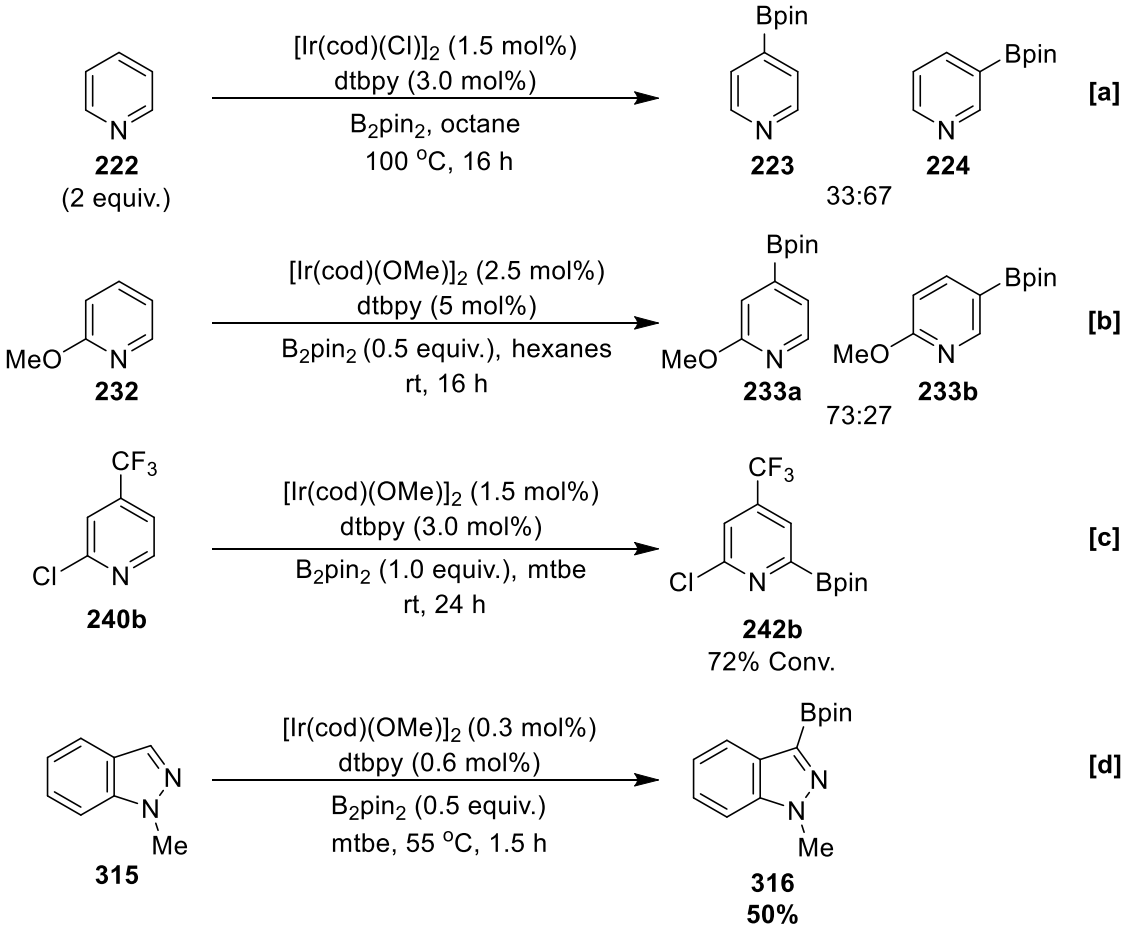

Scheme 1: Ir C-H Borylation of Nitrogen-Containing Heteroarenes

Previous work in the group has investigated the reactivity and site-selectivity in the Ir C-H borylation of heteroarenes containing azinyl N atoms, such as pyridine, quinoline, and indazole. Takagi described that the borylation of pyridine requires elevated temperature, and affords an approximately statistical ratio of C-3 and C-4 boronates (Scheme 1a).[1] Our group and others have shown with competition experiments that the poor reactivity of pyridine may be attributed to N-coordination to the active catalyst, impeding reactivity (see section 1.7.3.2.1).[2,3] However, this coordination can be blocked by a C-2 substituent, enabling the facile C-H borylation of pyridines such as 2-methoxypyridine **232** (Scheme 1b). Further studies by Sadler, Tajuddin, and others attribute the lack of C-2 functionalised boronates in the C-H borylation of pyridine to dipolar repulsion in the transition state, and to the rapid decomposition of the corresponding alpha-azinyl boronate via protodeborylation pathways.

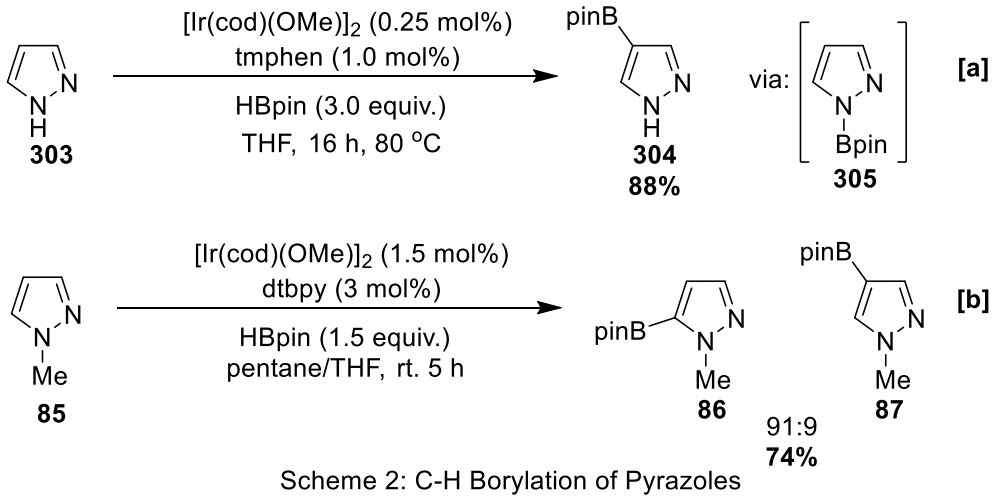

Scheme 2: C-H Borylation of Pyrazoles

However, reducing the electron density at N promotes alpha-azinyl selectivity, and this may be achieved by the introduction of electron-withdrawing substituents. For example, the C-H borylation of electron-deficient pyridine **240b** is C-6 selective due to the combined electron-withdrawing effects of the Cl and CF_3 groups (Scheme 1c). Furthermore, other ring N atoms also facilitate alpha-azinyl regiochemistry, and this is observed in the C-3 selective C-H borylation of indazole **315** (Scheme 1d).[4,5] In this example, the use of 0.5 equiv. of B_2pin_2 is possible since the catalyst may also turnover HBpin. The related heteroarene pyrazole does not show alpha-azinyl regiochemistry due to the presence of other unencumbered C-H sites with relatively high C-H acidity. Instead, pyrazole first undergoes rapid N-H borylation to form NBpin adduct **305**, which sterically directs borylation to C-4 (Scheme 2a).[77] Reducing the steric demand of the N-substituent shifts selectivity to the electronically activated C-5 site, and this is observed in the borylation of N-methylpyrazole **85** (Scheme 2b). Pyrazole is a ubiquitous scaffold in bioactive molecules, agrochemicals, natural products, and few reports have studied pyrazole substrates in the Ir C-H borylation. Therefore, we sought to develop this area by investigating the borylation reactivity and site-selectivity of pyrazole derivatives.

2.2 Aims

As discussed in the previous section, past studies in the group concerning the Ir C-H borylation of azinyl heterocycles led to our interest in the pyrazole scaffold. As part of an ongoing collaboration with Pfizer laboratories, we were interested to investigate how an amino substituent in 3- and 5-aminopyrazoles would affect reactivity and/or site-selectivity in the Ir C-H borylation.

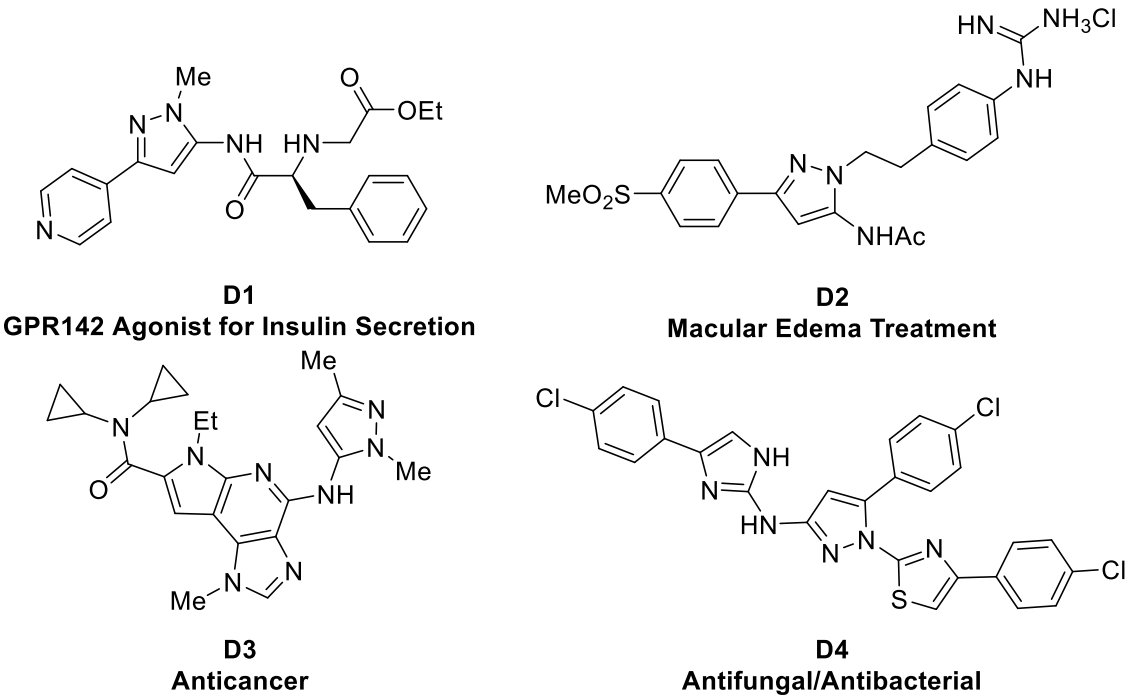

Figure 1: Drug Molecules Containing a 3- or 5-Aminopyrazole Core

Aminopyrazoles are considered to be privileged structures in chemical biology, and 3- and 5-aminopyrazole motifs are particularly important scaffolds in a variety of drug molecules, such as **D1-D4** (Figure 1).[7-12] Traditionally, the synthesis of 3- and 5-aminopyrazoles is achieved *de novo* via the condensation of a hydrazine with a 1,3-dielectrophile (generally a conjugated nitrile). For example, **D1** precursor **D1c** was synthesised by treating α-cyanoketone **D1a** with methylhydrazine under acidic conditions, which concurrently afforded isomer **D1b** (Scheme 3a).[9] Similarly, **D2** precursor **D2c** was synthesised *de novo* ring α-cyanoketone **D2a** and hydrazine, followed by acylation and N-alkylation (Scheme 3b).[10] The alkylation step also led to the formation of isomer **D2b** in significant quantity.

These approaches carry some drawbacks, such as use of N-substituted hydrazines which can lead to the formation of intractable pyrazole regioisomers. When using the parent hydrazine, subsequent N-functionalisation can raise the same issue. To an extent, this issue can be mitigated by reaction optimisation, although this is a laborious and costly endeavor. Furthermore, the range of functionalities that may be introduced prior to the formation of the pyrazole core is limited by the conditions of the ring assembly, introducing complexity into synthetic routes. Therefore, we aimed to develop an Ir C-H borylation/Suzuki-Miyaura cross-coupling methodology for the late-stage, regioselective introduction of aryl groups into aminopyrazole scaffolds.

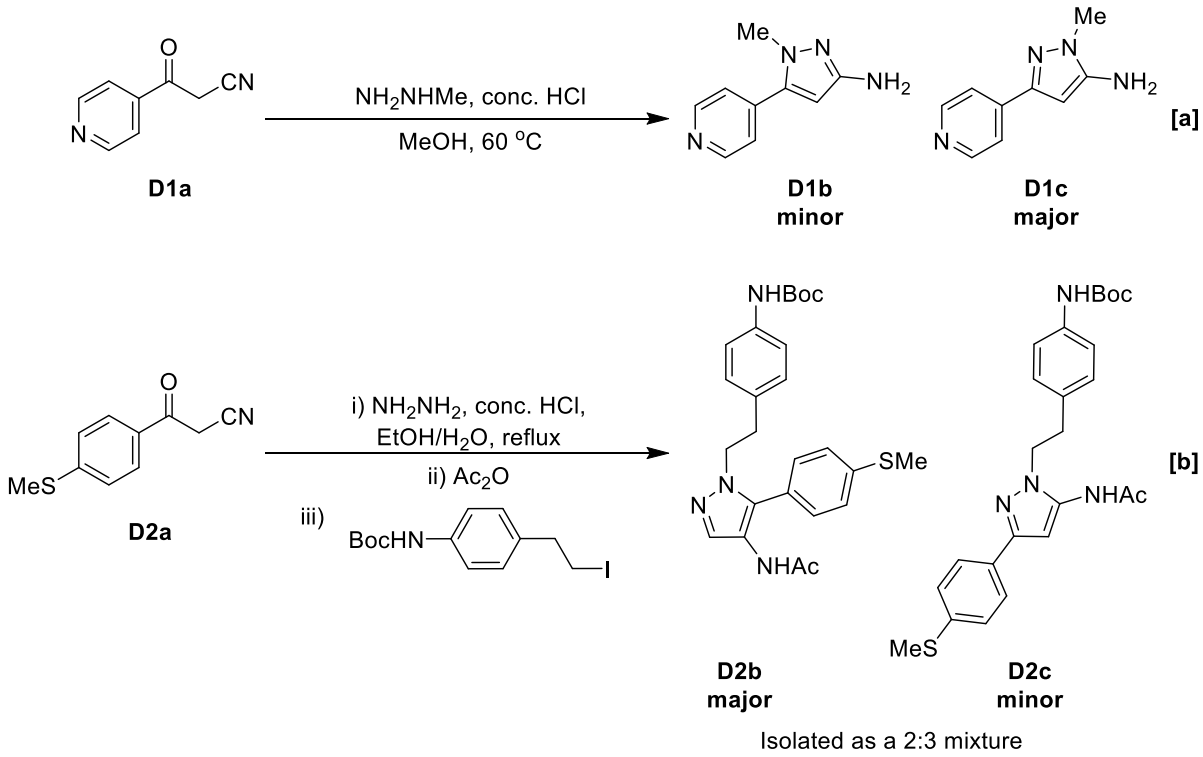

Scheme 3: *De Novo* Assembly of Aminopyrazoles

Taking inspiration from previous work, we set targets to (a) determine the intrinsic Ir C-H borylation regiochemistry in 3- and 5- aminopyrazoles, (b) develop processes that deliver the C-B bond regioselectively (c) provide complementary selectivity to the regiodselectivity obtained in (b). In order to showcase the utility of this approach, we decided to employ Suzuki-Miyaura cross-coupling in order to obtain all isomers in their arylated forms, and Figure 2 presents this. This project was conducted in collaboration with Andrew Hones (Durham), Alpay Dermenci, David Blakemore, and Andrew Flick (Pfizer, CT, acknowledgement also given to the C-H borylation and Suzuki-Miyaura team there).

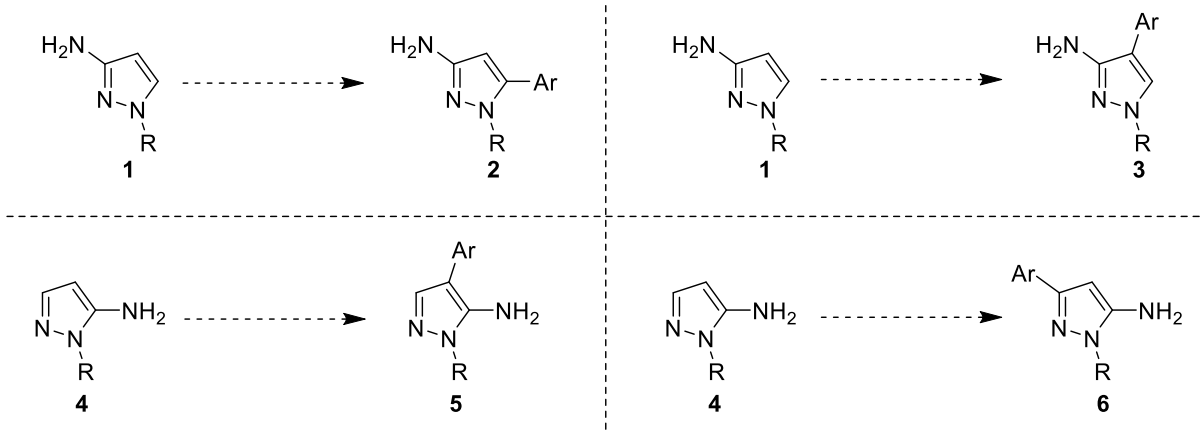

Figure 2: Goal to Regioselectively Functionalise Aminopyrazoles

2.3 References

[1] J. Takagi, K. Sato, J. F. Hartwig, T. Ishiyama, N. Miyaura, *Tetrahedron Lett.* **2002**, *43*, 5649–5651.

[2] M. A. Larsen, J. F. Hartwig, *J. Am. Chem. Soc.* **2014**, *136*, 4287–4299.

[3] S. A. Sadler, H. Tajuddin, I. A. I. Mkhalid, A. S. Batsanov, D. Albesa-Jove, M. S. Cheung, A. C. Maxwell, L. Shukla, B. Roberts, D. C. Blakemore, Z. Lin, T. B. Marder, P. G. Steel, *Org. Biomol. Chem.* **2014**, *12*, 7318–7327.

[4] S. A. Sadler, A. C. Hones, B. Roberts, D. Blakemore, T. B. Marder, P. G. Steel, *J. Org. Chem.* **2015**, *80*, 5308–5314.

[5] B. A. Egan, P. M. Burton, *RSC Adv.* **2014**, *4*, 27726-27729.

[6] S. M. Preshlock, B. Ghaffari, P. E. Maligres, S. W. Krska, R. E. Maleczka, M. R. Smith III, *J. Am. Chem. Soc.* **2013**, *135*, 7572–7582

[7] G. M. Nitulescu, G. Nedelcu, A. Buzescu, O. T. Olaru, *Bulg. Chem. Commun.* **2016**, *48*, 55–60.

[8] M. Marinozzi, A. Carotti, G. Marcelli, *Mini-Reviews Med. Chem.* **2015**, *15*, 272–299.

[9] M. Yu, M. Lizarzaburu, A. Motani, Z. Fu, X. Du, J. (Jim) Liu, X. Jiao, S. Lai, P. Fan, A. Fu, et al., *ACS Med. Chem. Lett.* **2013**, *4*, 829–834.

[10] T. Inoue, M. Morita, T. Tojo, A. Nagashima, A. Moritomo, K. Imai, H. Miyake, *Bioorg. Med. Chem.* **2013**, *21*, 2478–2494.

[11] H. Wan, G. M. Schroeder, A. C. Hart, J. Inghrim, J. Grebinski, J. S. Tokarski, M. V. Lorenzi, D. You, T. Mcdevitt, B. Penhallow, et al., *ACS Med. Chem. Lett.* **2015**, *6*, 850–855.

[12] T. Bhanu Prakash, G. Dinneswara Reddy, A. Padmaja, V. Padmavathi, *Eur. J. Med. Chem.* **2014**, *82*, 347–354.

3 Results and Discussion

As discussed in section 2.2 the goal of this study was to develop new methodologies for the regioselective elaboration of 3- and 5-aminopyrazoles using Ir C-H borylation and Suzuki-Miyaura cross-coupling. The first aim was to establish the intrinsic C-H borylation selectivity in these heterocycles. Following this, this intrinsic selectivity would be reversed in order to synthesise a total of four arylated aminopyrazole isomers **2**, **3**, **5**, and **6** (Figure 1).

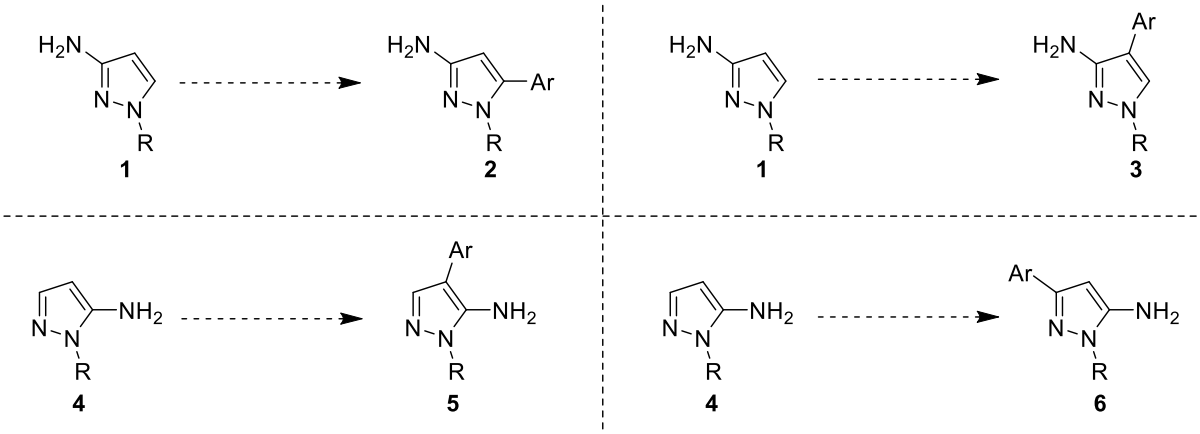

Figure 1: Goal to Regioselectively Functionalise Aminopyrazoles

3.1 Intrinsic Selectivities

3.1.1 3(5)-Aminopyrazole

Initially, the Ir C-H borylation of the parent scaffold 3(5)-aminopyrazole **369** was investigated. It was suggested that this substrate may not be active, because the 5-tautomer **369b** contains an unencumbered basic azinyl N, which carries the potential to coordinate to the catalyst and inhibit C-H activation (Figure 2).[1] This is in analogy to the C-H borylation of free N-H indazole, which is likely to be inactive for similar reasons (see section 1.7.3.3.2).[2]

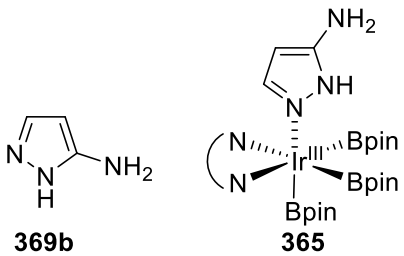

Figure 2: Hypothesis of Catalyst Deactivation by 5-Aminopyrazole **369b**

On the other hand, N-H borylation precedes C-H borylation in pyrazole **303**, forming the N-Bpin adduct **305** which undergoes C-H borylation at C-3 due to steric effects (Scheme 1a). Furthermore, primary aromatic amines such as **366** can undergo N-H borylation to form NHBpin adduct **368**, and this enables outer-sphere *ortho* selective C-H borylation to form **367** (Scheme 1b).[3,4] Therefore, it was hypothesised that these phenomena could jointly facilitate the C-H borylation of **369** at C-3 and afford **370** (Scheme 1c).

To test this idea, a set of standard borylation reactions were conducted using $[Ir(cod)(OMe)]_2$, tmphen, and boron reagents. The catalyst mixture was combined with the substrate, and each reaction was monitored using ^{1}H NMR spectroscopy with 1,3,5-trimethoxybenzene as an internal standard. Conducting the reaction with B_2pin_2 at 80 ºC led to quantitative substrate recovery (Table 1, Entries 1 and 2). In both cases, the dark shade of the catalyst turned to a light red colour over the course of the reaction, and this commonly suggests catalyst decomposition. Switching the boron reagent to HBpin led to decomposition of the substrate to unknown materials, and this was evident from the crude ^{1}H NMR spectrum (Table 1, Entry 3). Recently, addition of the substrate to the catalyst at elevated temperature has been described by Hartwig for the N-H/C-H borylation of heteroarenes such 7-azaindole.

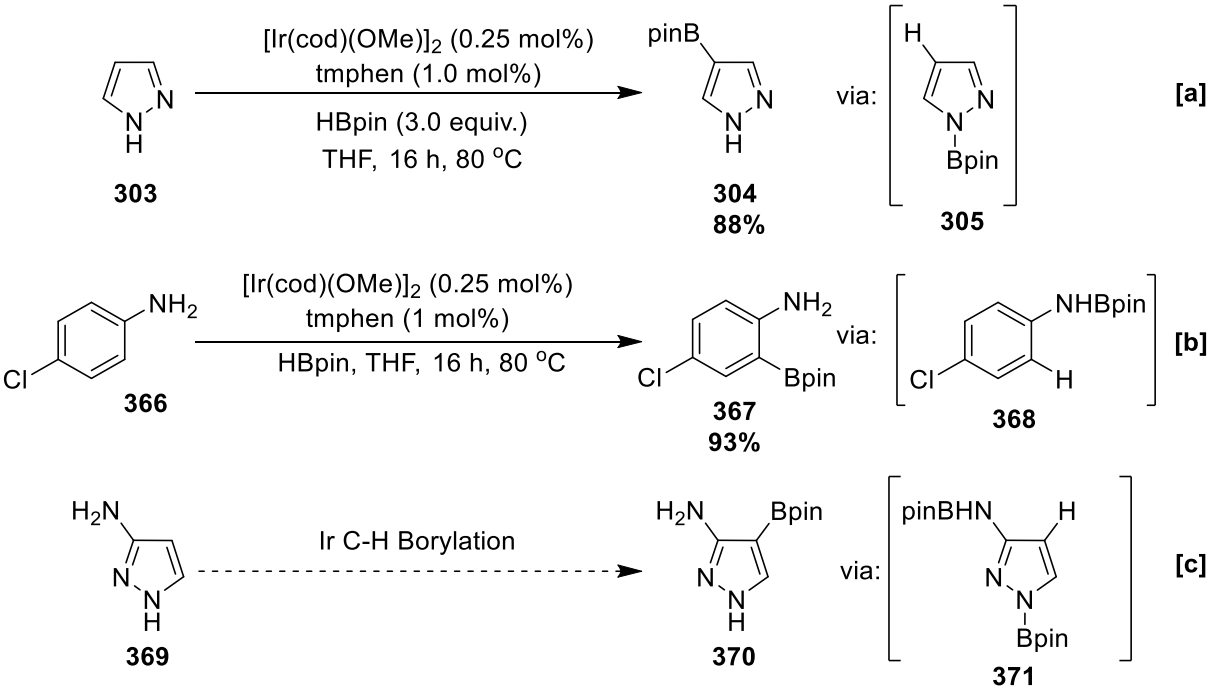

Scheme 1: N-Bpin Mediated Borylation of Aromatics

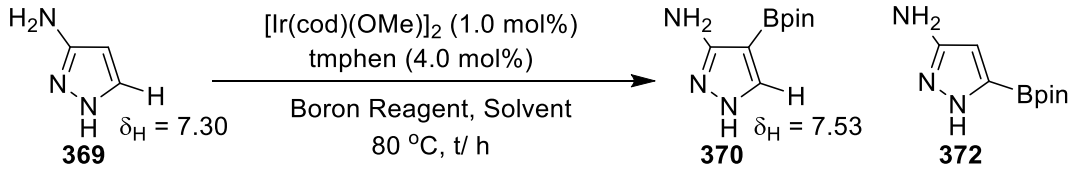

Entry	Boron Reagent (eq.)	Solvent	t/ h	NMR Yield **370** /%	NMR Yield **372** /%
1	B_2pin_2 (2.2)	THF	1	-	-
2	B_2pin_2 (2.2)	THF	16	-	-
3	HBpin (4)	2-MeTHF	1	-	-
4	HBpin (3)	2-MeTHF	1	10*	0

*Following addition of the substrate to the catalyst the temperature was decreased from 80 °C to rt.

Table 1: C-H Borylation Screen of **369**

Whilst the reasons for this are not obvious, addition of **369** to a solution of the catalyst and HBpin at 80 °C led to rapid gas evolution, which was presumed to be H_2 and was tentatively attributed to N-H borylation (Table 1, Entry 4).[4] The reaction temperature was subsequently reduced, and after 1 h a 10% NMR yield of **370** was evident in the crude ^{1}H NMR spectrum by a singlet at 7.53 ppm displaced downfield from the C-5 proton in **369**, consistent with the deshielding effect (ca. 0.1-0.5 ppm) that Bpin substituents exert on *ortho* protons. Evidence of this product could also be found in the EI and ESI mass spectra, with peaks at m/z = 209.2 and 210.2 m/z attributed to the $[M]^+$ and $[M+H]^+$ molecular ions, respectively. This could suggest that the addition of the substrate to the pre-heated catalyst permitted rapid N-H borylation at one or more of the N-H bonds and facilitated C-H borylation at C-4. Whilst the C-H borylation of **369** was possible, approximately 50% of the substrate had decomposed into unknown side-products after 1 h. Attempts to isolate the small quantity of **370** produced using SiO_2 gel chromatography were unsuccessful, and this was attributed to the affinity of the N-H bonds for the chromatographic media. In order to rectify this, attention was turned to N-substituted pyrazoles.

3.1.2 N-Methyl-3-Aminopyrazole

Five-membered azoles such as pyrrole, imidazole, and pyrazole generally display alpha C-H borylation selectivity in the absence of a sterically large N-blocking group (such as Bpin, TIPS, etc.) (see section 1.7.3.1). On this basis, the C-H borylation of N-methyl-3-aminopyrazole **373** was predicted to be C-5 selective.

As expected, **373** C-H borylated efficiently at C-5 affording boronate **374** in quantitative NMR yield after 1 h at 80 °C. Regiochemistry was assigned based on the presence of a boron-shifted singlet at 5.98 ppm in the crude ^{1}H NMR spectrum, attributed to the C-4 hydrogen.* One-pot borylation/Suzuki-Miyaura (SM) cross-coupling enabled the isolation of arylated adduct **375**, albeit in low yield (Scheme 2).† ^{13}C NMR analysis of purified **375** displayed a characteristic signal at 94.3 ppm, which was attributed to C-4. Furthermore, this signal displayed a ^{1}J interaction in the 2D ^{1}H-^{13}C HSQC spectrum with the C-4 hydrogen found at 5.76 ppm in the ^{1}H NMR spectrum, supporting C-5 site-selectivity. The inefficiency of this process was attributed to protodeborylation during the arylation and to contamination by other pinacol derivatives, which jointly led to intractable product mixtures.

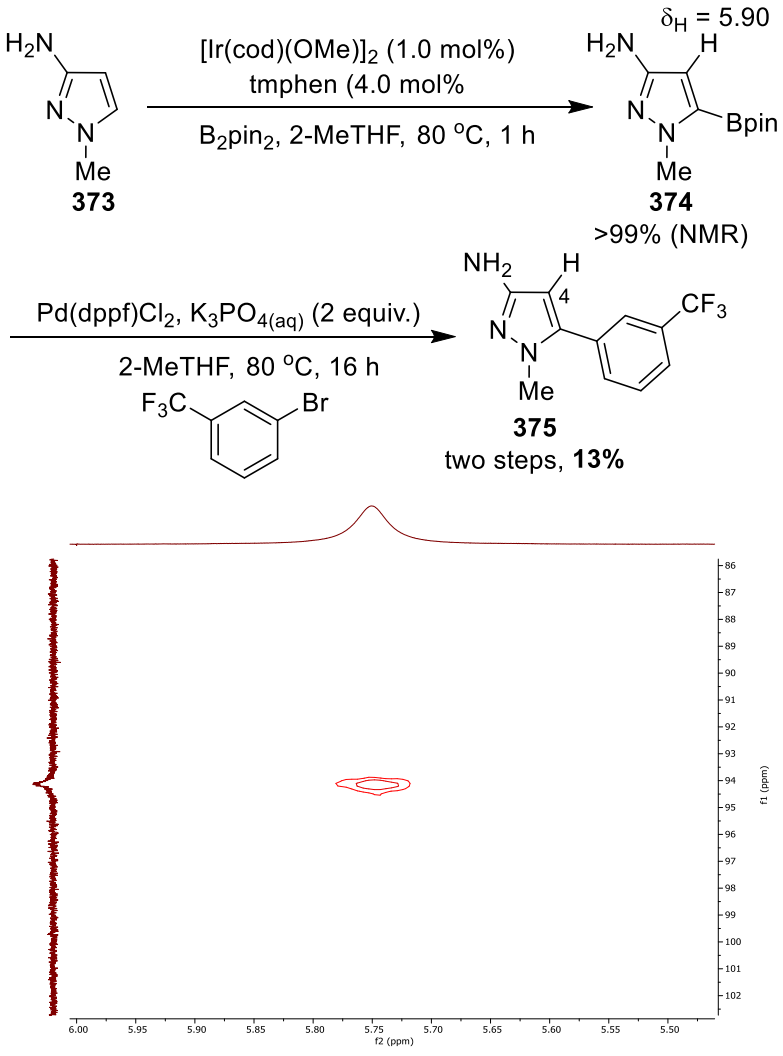

Scheme 2: Regioselective C-H Borylation and Arylation of **373** (Top) and ^{1}H-^{13}C HSQC between C-4 and H-4 in **375** (Bottom)

* Boronate ester was also isolated in 51% yield under modified conditions by collaborator Alpay Dermenci

† The 6-quinolyl adduct was obtained using 6-bromoquinoline by Alpay Dermenci in 81% isolated yield under identical coupling conditions.

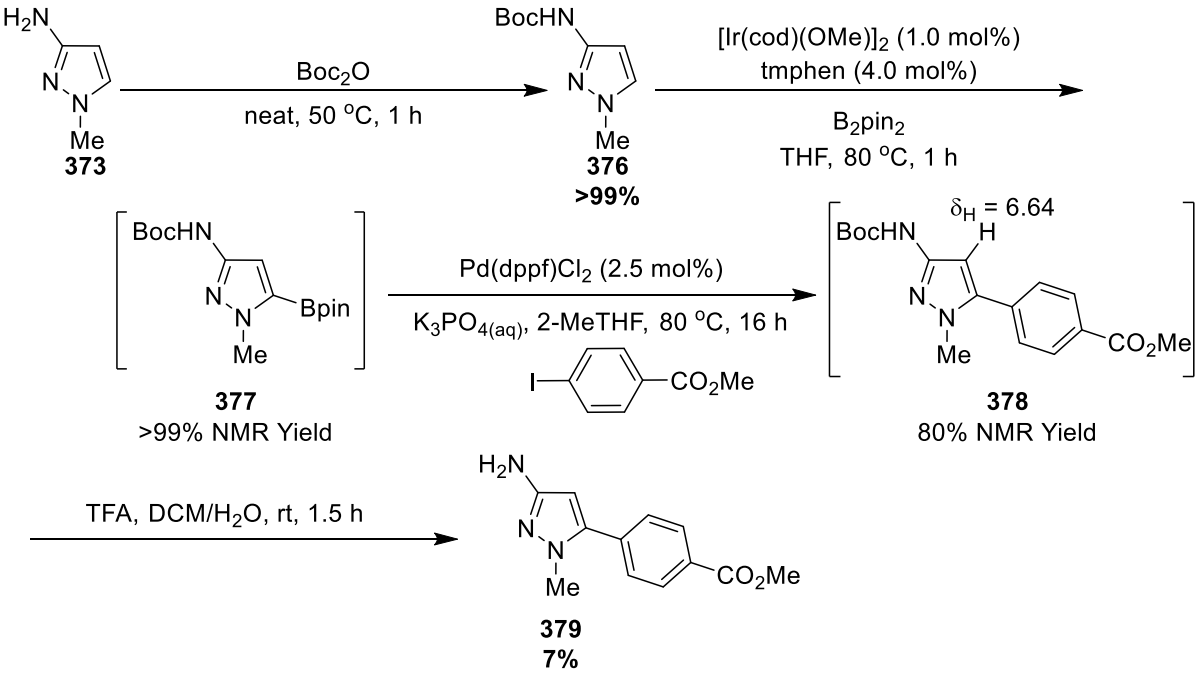

Scheme 3: Synthesis, Borylation, Arylation, and Deprotection of **376**

The goal of future studies is to determine the origin of protodeborylation. In particular, this process may be catalysed by Pd, so a control experiment on **374** which includes the reagents in the arylation except Pd could probe this. The event of inseperable contaminants was attributed to the interaction of the free amine with pinacolatoboryl contaminants (e.g HOBpin), so protection as the corresponding Boc carbamate **376** was undertaken in an attempt to simplify purification. Neat Boc protection of **373** was achieved in quantitative yield with Boc_2O at 50 °C. Subsequent C-H borylation of Boc carbamate **376** then efficiently delivered the C-5 functionalised boronate **377**, and this was evident by the presence of a boron-shifted singlet in the crude ^1H NMR spectrum (Scheme 3). Unfortunately, attempts at chromatographic purification of **377** again led to decomposition. To address this problem, Suzuki-Miyaura cross-coupling of the crude borylation reaction mixture was undertaken, affording **378** in excellent NMR yield, as evident by the presence of a single pyrazole C-H signal at 6.64 ppm attributed to C-4. Attempted purification of **378** was challenged by the presence of pinacol derivatives (such as pinacol, HOBpin, pinBOBpin), so the crude material was globally deprotected with TFA. Whilst this permitted the isolation of **379**, this was accompanied by significant decomposition, lowering the overall efficiency of the sequence. The generation of **379** was evident by a signal in EI GCMS spectrum with a m/z = 231.1 corresponding to the $[M]^+$ molecular ion. ^{13}C NMR analysis of purified **379** displayed a characteristic signal at 98.5 ppm, which was attributed to C-4.

Furthermore, this signal displayed a ^{1}J interaction in the 2D ^{1}H-^{13}C HSQC spectrum with the C-4 hydrogen found at 6.87 ppm in the ^{1}H NMR spectrum, supporting C-5 site-selectivity. In addition, the presence of a primary amine in **379** was evident from two bands at 3385 and 3278 cm^{-1} displayed in the infrared spectrum. Whilst the cross-coupling process requires further optimisation, this small study established that N-methyl-3-aminopyrazoles are active substrates in the Ir C-H borylation, affording the corresponding C-5 boronates selectively and in excellent NMR yield. Focus then moved to the corresponding C-5 regioisomer, N-methyl-5-aminopyrazole **380**.

3.1.3 N-Methyl-5-Aminopyrazole

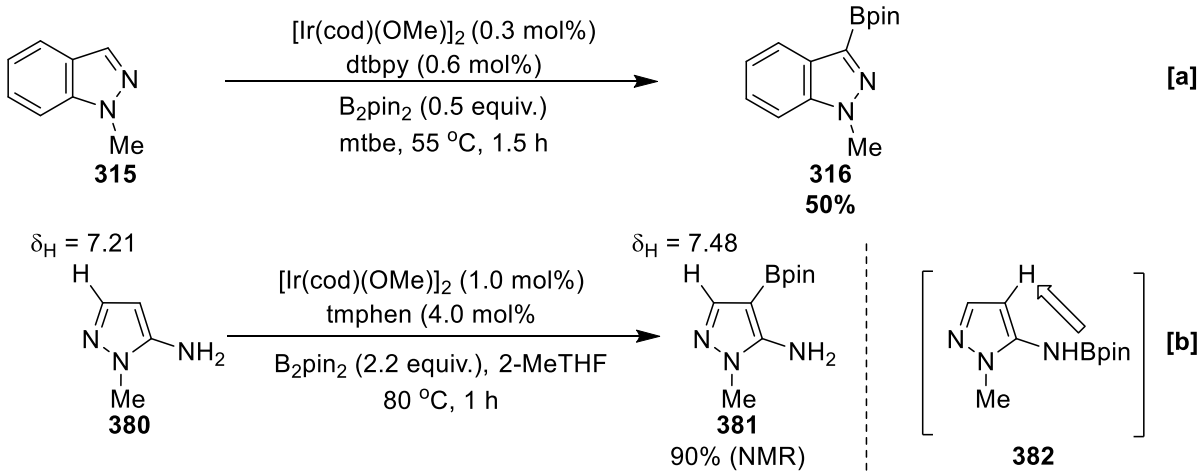

Scheme 4: Regioselective C-H Borylation of Azoles

The borylation selectivity of **380** was difficult to predict because related systems give orthogonal selectivities. For example, N-methyl-1H-indazole **315** shows selectivity for C-3 (Scheme 4a), whilst NHBpin may act as an *ortho* (C-4) director in the event of N-H borylation (section 1.7.2). However, the borylation of **380** efficiently delivered C-3 boronate **381** with complete selectivity, suggesting that site-selectivity may be governed either by the *ortho* directed borylation of the corresponding NHBpin adduct **382**, the electronic preference to avoid the alpha-azinyl position, or a combination of both effects (Scheme 4b). At this time, the *in situ* formation of **382** from **380** was not investigated, although the N-H borylation of related aminopyrazoles was later explored. A control experiment involving C-3 methylated **381** could be used to more conveniently to determine if N-H borylation of these systems is possible. A boron-shifted singlet at 7.48 ppm in the crude ^{1}H NMR spectrum, and a signal in the EI mass spectrum with m/z = 223.2 attributed to the $[M]^{+}$ molecular ion supported the assignment of **381**. However, attempts to isolate or cross-couple **381** caused decomposition to unknown materials, so **380** was protected as a Boc carbamate **383** in order to promote the cross-coupling step (Scheme 5).

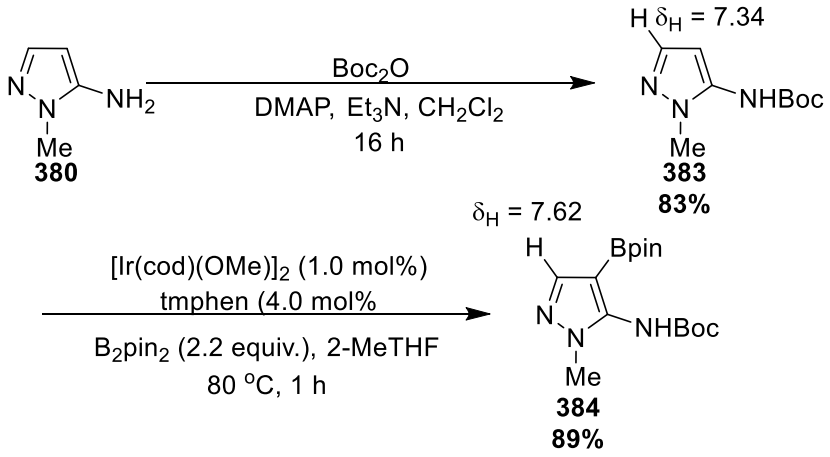

Scheme 5: Synthesis and C-H Borylation of Protected Pyrazole **383**

It was hypothesised that **383** would display the same C-4 borylation regiochemistry as **380** because NHBoc acts as an *ortho* director in a similar fashion to NHBpin. Pleasingly, the synthesis and borylation of **383** was efficient and ultimately led to the isolation of boronate **384** in high yield. This was evident from the ^{1}H NMR spectrum, which displayed a boron-shifted singlet at 7.62 ppm attributed to the C-3 hydrogen. Furthermore, crude boronate **384** could be arylated under a one-pot borylation/cross-coupling protocol (Scheme 6).* Despite an extended reaction time, the cross-coupling reaction did not proceed to completion, and *ca.* 30% of **384** was recovered. The ^{1}H NMR spectrum of **385** contained a pyrazole C-H singlet at 7.67 ppm, which is characteristically high due to the electron-withdrawing effect of the alpha azinyl N. These studies established the excellent Ir C-H borylation regioselectivity and reactivity of N-methyl-3-aminopyrazole **373** and N-methyl-5-aminopyrazole **380** and their Boc-protected derivatives, and our next focus was to achieve complementary selectivities in these systems.

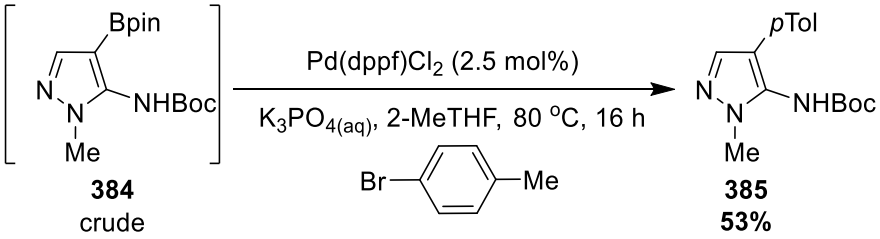

Scheme 6: Suzuki-Miyaura Cross-Coupling of Crude Boronate **384**

* 6-Bromoquinoline and 3-bromopyridine were also reported by Alpay Dermenci to couple under the same conditions in 73% and 63% yield, respectively

3.2 Orthogonal Selectivities

3.2.1 N-H Borylation

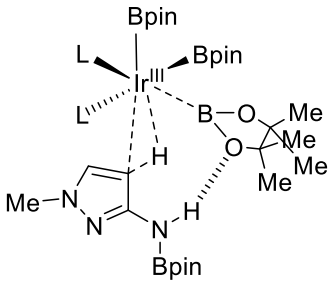

386

Figure 3: NHBpin Directed C-H Borylation

An understanding of the intrinsic C-5 borylation regiochemistry in N-methyl-5-aminopyrazole **373** was first required in order to develop a method with complementary site-selectivity. It was hypothesised that **373** does not display C-4 selectivity because the primary amine does not undergo N-borylation to afford a corresponding NHBpin adduct required for directed *ortho* C-H borylation (Figure 3). From the initial C-H borylation of **373** a signal at 27.6 ppm in the ^{11}B NMR was attributed to the NHBpin adduct, and this shift is characteristic in systems containing N-B bonds.[5,6] Furthermore, two signals at 1.32 and 1.33 ppm in the in the crude ^{1}H NMR spectrum were assigned as the C-5 Bpin and NHBpin CH_3 signals in **387**, respectively. However, a disparity in their relative integrations was measured, and it was hypothesised that N-B hydrolysis upon exposure of the reaction to adventitious moisture could account for this.

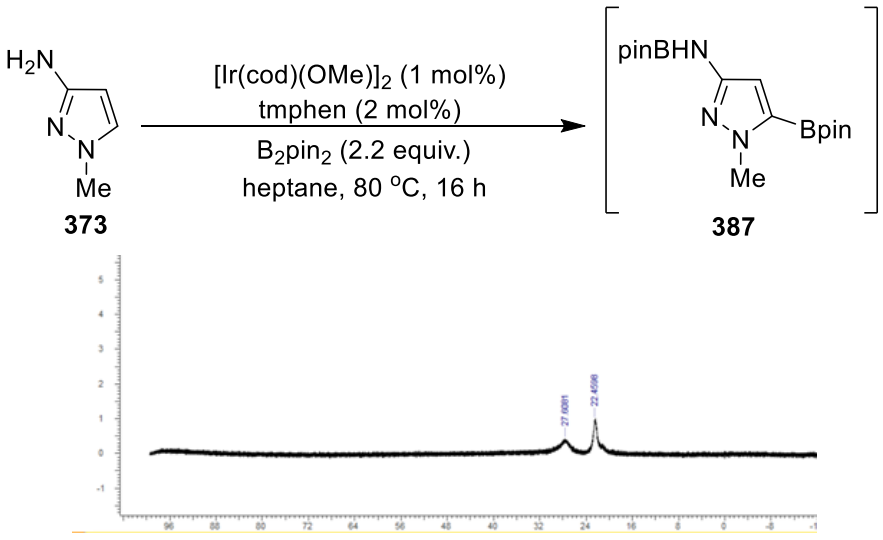

373 **387**

Scheme 7: N-H and C-H Borylation in **373** (Top) and ^{11}B NMR of the Crude Reaction Mixture (Bottom)

To test this, the reaction was conducted in heptane whilst minimising air exposure during analysis and this revealed that **387** forms quantitatively (Scheme 7). This was evident by the presence of characteristic signals at 27.6 and 22.5 ppm in the ^{11}B NMR spectrum, corresponding to boron nuclei in the N-B and C-B bonds, respectively. Stirring crude **387** in MeOH led to the disappearance of the signal at 27.6 ppm only, and this is indicative of N-B methanolysis.* These experiments indicate that the primary amine in **373** does undergo N-H borylation at some stage of the reaction but does not facilitate directed C-H borylation to C-4.

3.2.2 Urea-Directed Borylation

3.2.2.1 Aminopyrazole Ureas

The next study aimed to understand why the N-borylation of **373** does not enable *ortho* borylation at C-4. Comparing the rotamers associated with the (C-3)-N bond rotation in the NHBpin adduct **388a** suggested that coulombic repulsion between the boryl O and the azinyl N leads to the significant population of conformer **388b**, which may prevent directed borylation and sterically block the C-4 C-H bond (Scheme 8a).

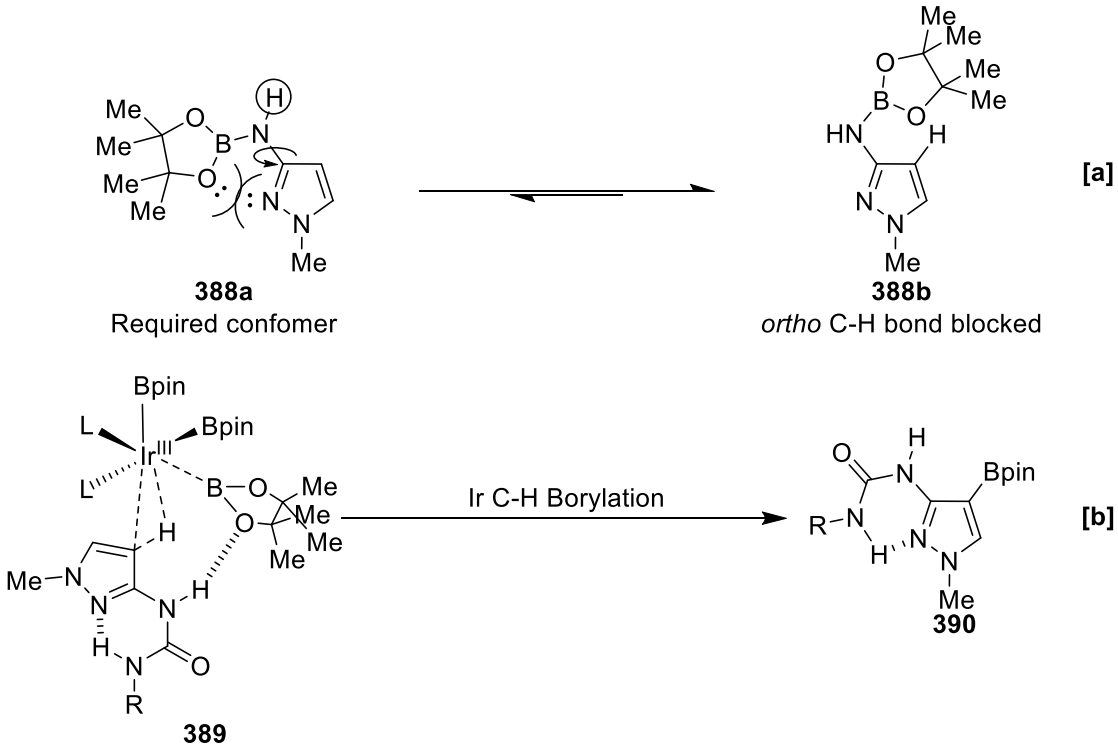

Scheme 8: Postulated Rotamers of **388** and a Urea Model to Access C-4

* Experiment performed and data collected by Alpay Dermenci (Pfizer)

In order to overcome this effect, a model involving a urea **389** was suggested. In this model, a remote portion of the directing group could favourably hydrogen bond with the azinyl N, rather than repel it (Scheme 8b). Consequently, the fixed orientation of the urea would provide the N-H bond necessary for hydrogen-bond mediated *ortho* directed C-H activation. To test this hypothesis, urea **391** was synthesised by stirring **373** with 4-methoxyphenylisocyanate (PMPNCO) in MeCN for 16 h (Scheme 9). Formation of the urea was evident from the IR spectrum, which displayed an absorption at 1674 cm^{-1} attributed a urea carbonyl stretching frequency. Furthermore, a peak at m/z = 247.1183 was found in the ASAP mass spectrum, and this was attributed to the $[M+H]^+$ molecular ion. With urea **391** successfully synthesised, focus turned to the C-H borylation reaction. Using HBpin and tmphen the C-H borylation of **391** showed reactivity at C-4, and this was confirmed via isolation and characterisation of C-4 boronate **392** following standard workup and chromatography (Scheme 9). A through-space interaction of the C-5 hydrogen with the N-CH_3 hydrogens was observed in the 2D ^1H-^1H NOESY spectrum, and indicated that the C-5 C-H bond remained intact. Furthermore, the presence of a boron-shifted singlet at 7.53 ppm in the ^1H NMR spectrum provided additional evidence for C-4 selectivity. Subsequently, **392** was arylated using Suzuki-Miyaura cross-coupling with 2-chloropyridine, affording **394** in modest yield (Scheme 10). X-ray analysis of **394** provided good evidence for key intramolecular N-H hydrogen bond between the pyrazole and the urea, suggesting that C-4 selectivity may originate from a directing-effect.*

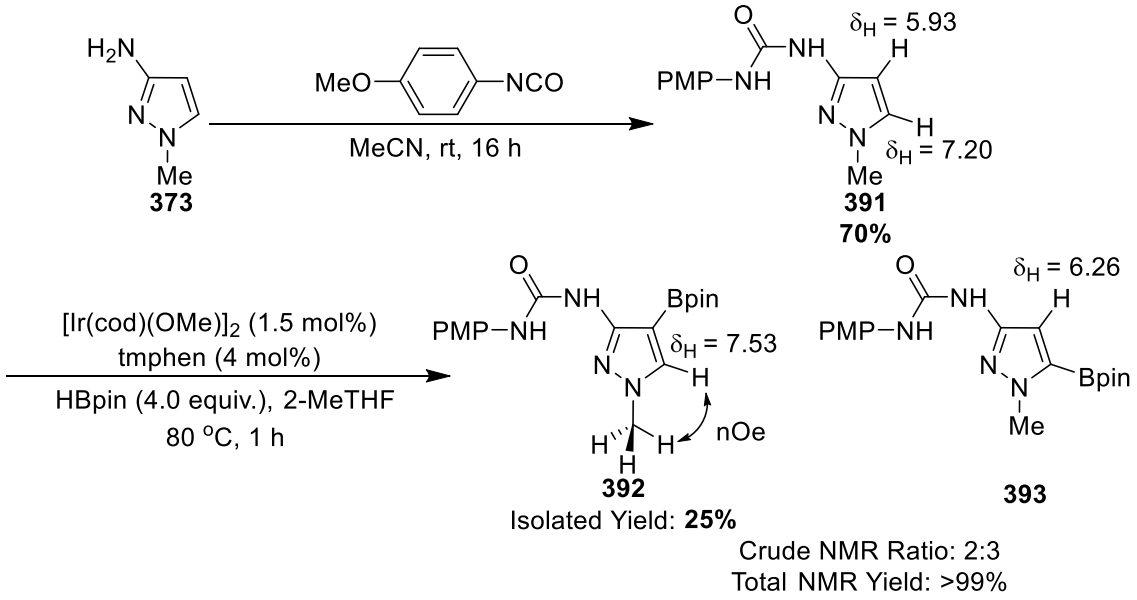

Scheme 9: Synthesis and C-H Borylation of Pyrazole Urea **391**

* Experiment performed by Alpay Dermenci

The low yield of **392** was a concern, and a more detailed analysis of the crude ^{1}H NMR spectrum revealed that the formation of **392** was accompanied by C-5 boronate **393** in a 2:3 ratio **392**:**393**. The generation of **393** was evident from a boron-shifted singlet found at 6.26 ppm in the crude ^{1}H NMR spectrum, and by the presence of two signals with similar m/z patterns displayed in the HPLC spectrum.* Furthermore, despite the complete conversion of parent urea **391** measured by ^{1}H NMR, purification of the reaction mixture led to substrate recovery. Therefore, it was reasoned that **393** had undergone protodeborylation during SiO_2 gel chromatography. Following this discovery, the next goal was to gain a further understanding of the observed C-4 site-selectivity. It was posited that if *ortho* C-H borylation relies on an intramolecular hydrogen-bond network, then substitution of the urea nitrogens should diminish it.

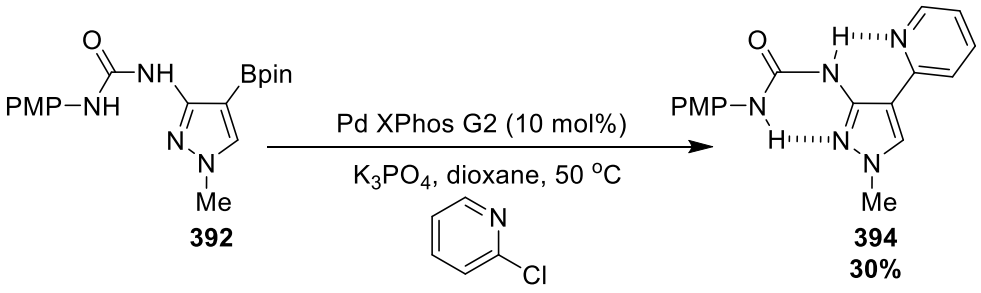

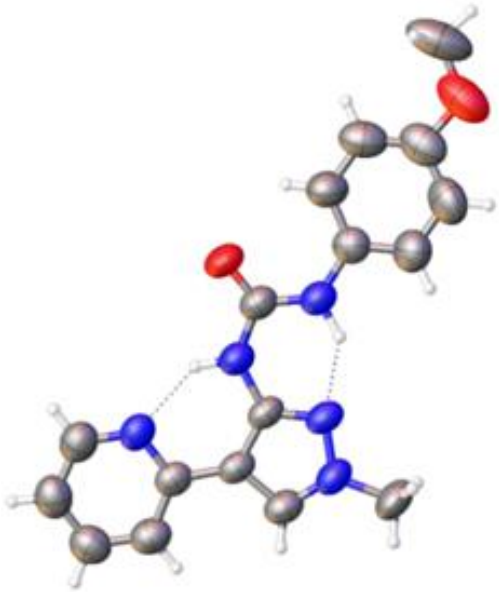

394

Scheme 10: Suzuki-Miyaura Cross-Coupling of **392**

* HPLC analysis conducted by Alpay Dermenci

To test this, each N-H bond in parent urea **391** was selectively methylated (Scheme 11). On the basis that each N-H bond in **391** may possess distinct acidities, a selective alkylation with LiHMDS (1.20 equiv.) and MeI (1.00 equiv.) was conducted (Scheme 11a). Pleasingly, this furnished N-alkylated urea **395** as indicated by the appearance of an additional CH_3 signal at 3.34 ppm in the ^1H NMR spectrum, for a total of three CH_3 signals. Furthermore, a through-space interaction of the C-4 hydrogen with the urea N-CH_3 hydrogens was observed in the 2D ^1H-^1H NOESY spectrum, confirming the selectivity of this process (Figure 4). It was noted during SiO_2 gel purification of the crude reaction mixture that the isolation of **395** was accompanied by *ca.* 10% bismethylated urea **396**. Therefore, a modified alkylation procedure was conducted using LiHMDS (2.40 equiv.) and MeI (10.0 equiv.), which generated bismethylated urea **396** in good yield (Scheme 11b). Evidence for the methylation of both N-H bonds was found in the ^1H NMR spectrum, which displayed two new CH_3 signals at 3.18 and 3.05 ppm, for a total of four CH_3 signals.

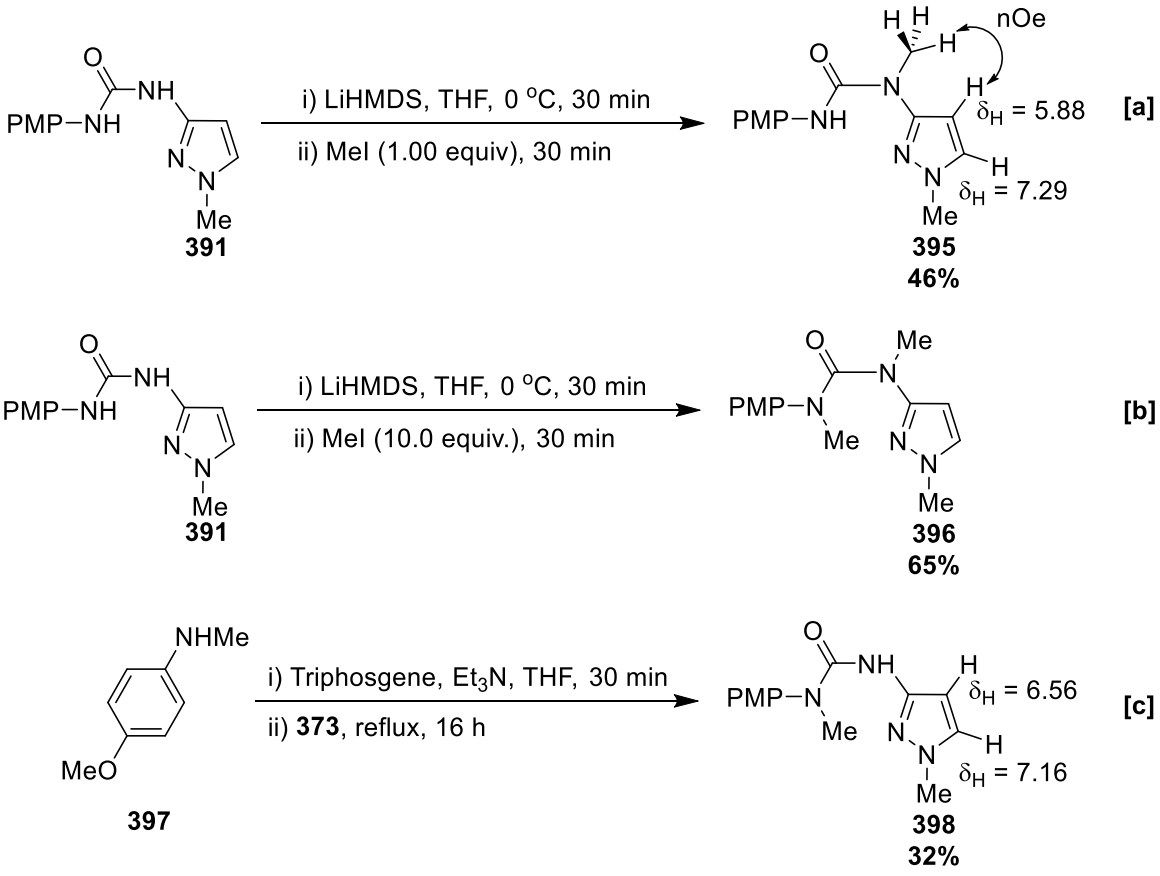

Scheme 11: Synthesis of Control Ureas

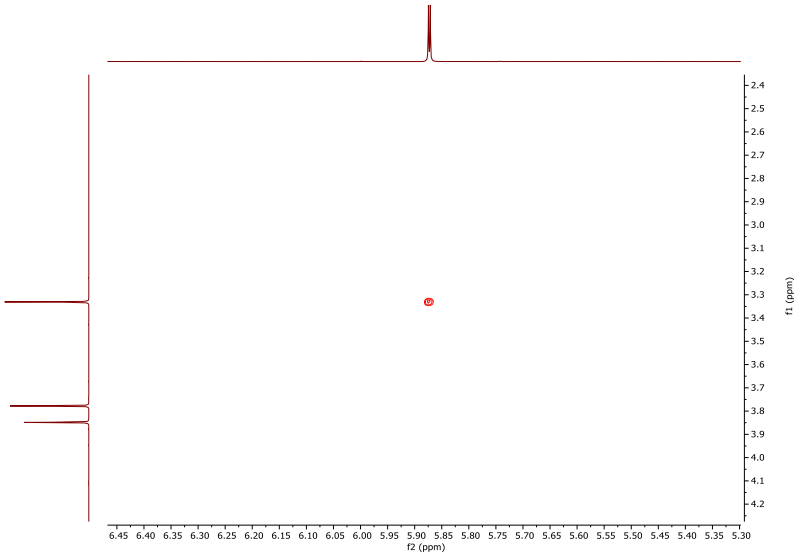

Figure 4: Key nOe Interaction in **395**

The synthesis of the final control urea **398** presented a greater challenge because it could not easily be obtained from **391**. In order to overcome this, urea **398** was assembled by treating anisidine **397** with triphosgene, generating the corresponding carbamoyl chloride *in situ*. The reaction mixture was then combined with N-methyl-3-aminopyrazole **373**, affording **398** in acceptable yield (Scheme 11c). Evidence for the generation of a monomethylated urea was found in the ^{1}H NMR spectrum, which displayed a signal at 3.27 ppm attributed to the N-CH_3 protons for a total of three CH_3 signals. Furthermore, the ^{1}H and ^{13}C NMR spectra of **395** and **398** resemble each other but possess different shifts, and this provided good evidence that both monomethylated isomers were synthesised successfully.

The next goal was the investigation of the site-selectivity of each control urea in the C-H borylation. In contrast to the parent urea **391**, the reaction of mono-methylated isomers **395** and **398** displayed complete C-5 selectivity, providing good evidence that the borylation regiochemistry of **391** is governed to some extent by an *ortho* directing-effect (Table 2, Entries 1, 2). The borylation regiochemistry of **395** and **398** was evident from the crude borylation ^{1}H NMR spectra, which displayed boron shifted singlets at 6.31 and 7.01 ppm, respectively. In order to obtain more evidence for C-5 selectivity, one-pot Suzuki-Miyaura cross-couplings of boronates **395a** and **398a** was conducted with methyl 4-iodobenzoate, and this led to the isolation of arylated isomers **395b** and **398b**. Evidence for C-5 selectivity in the arylation of **395a** was evident in the ^{1}H NMR spectrum, which displayed a singlet at 6.03 ppm attributed to the C-4 hydrogen.

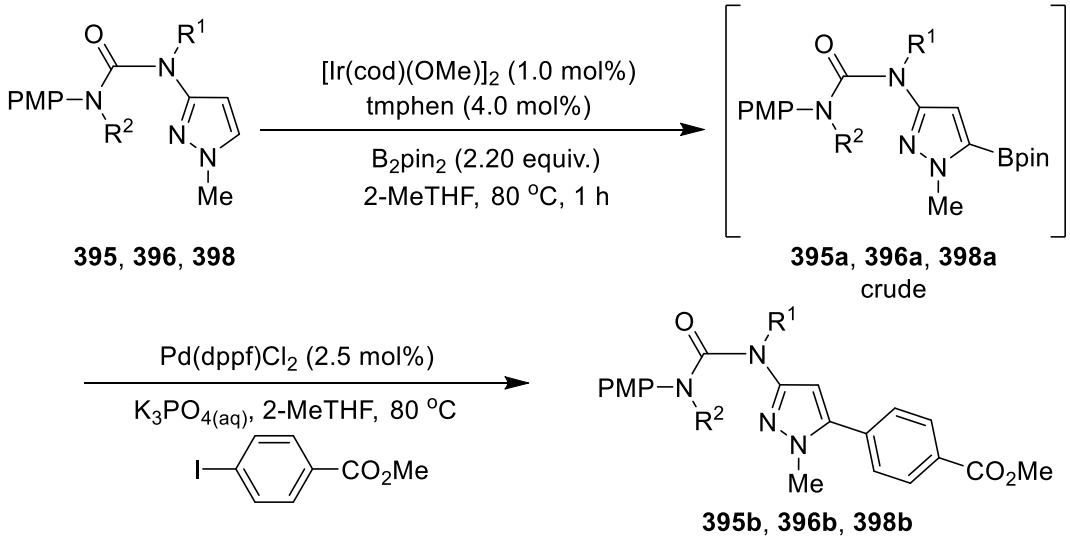

395, **396**, **398**

395a, **396a**, **398a**
crude

395b, **396b**, **398b**

Entry	R^1	R^2	Boronate NMR Yield /%	SM Isolated Yield /%
1 (**395**)	Me	H	>99	37
2 (**398**)	H	Me	>99	35
3 (**396**)	Me	Me	n.r.	-

Table 2: Control Experiments with Methylated Ureas

Furthermore, a ^1J through-bond coupling of this signal with the characteristic C-4 carbon signal at 95.8 ppm in the ^{13}C NMR spectrum was displayed in the 2D HSQC ^{1}H-^{13}C spectrum. Similarly, the C-4 proton in **398b** was displayed as a singlet at 6.77 ppm in the ^{1}H NMR spectrum, and exhibited a ^1J through-bond coupling with the characteristic C-4 carbon at 97.0 ppm in the ^{13}C NMR spectrum (Figure 5). Despite multiple reaction attempts, the borylation of bismethylated urea **396** led to quantitative substrate recovery, even with prolonged reaction times (Table 2, Entry 3). One explanation for this is that the urea group aligns over the pyrazole ring and sterically blocks access of the catalyst to the C-H sites. Indeed, this conformation is predicted to be favoured in the ground state by DFT calculations, and it is speculated that this is promoted by pi-stacking interactions between the two aromatic rings (Figure 6).* The outcome of these control experiments demonstrate that the N-H bonds in **391** are essential for *ortho* C-H borylation, lending credence to the idea that C-4 site-selectivity is facilitated by a hydrogen-bonding network. Encouraged by these results, we sought to improve the C-4 selectivity of the directed borylation by varying different reaction parameters. It has been observed in our laboratory that different boron reagents can confer modified C-H borylation selectivities in some fluorinated systems.[7]

* Performed by Boye Zhu

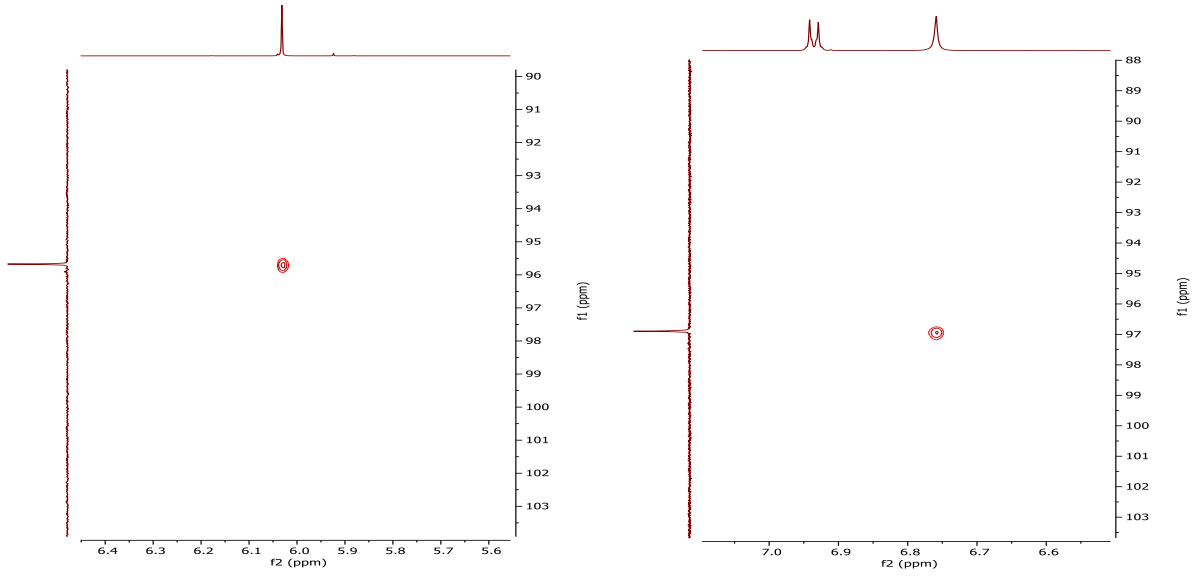

Figure 5: Key ^{1}H-^{13}C HSQC Interactions in **395b** (Left) and **398b** (Right)

Therefore, HBpin was replaced with B_2pin_2, and this led to no change in selectivity at 80 °C and room temperature (Table 3, Entries 2 and 3). The replacement of HBpin with HBcat led to complete decomposition to unknown materials at room and elevated temperature (Table 3, Entries 4 and 5). An explanation for this could be the elevated Lewis-acidity of catecholatoboryl derivatives, which may promote side-reactions. Baran has described that different bipyridine-derived ligands can alter intrinsic selectivities in the C-H borylation of indoles and carbazoles such as **198** (Scheme 12). Indole substrates were judiciously substituted with steric blocking groups at N-1 and C-3 in order to investigate the selectivity between the C-5 and C-6 sites. Therefore, different ligands were screened to mediate electron density at the catalyst and promote C-4 selectivity. Whilst this was successful in improving regioselectivity, an increased quantity of undesired isomer for **393** was observed with electron-rich/electron-neutral bipyridines (Table 3, Entries 9-11), and an electron-deficient monodentate phosphine (Table 3, Entry 12).

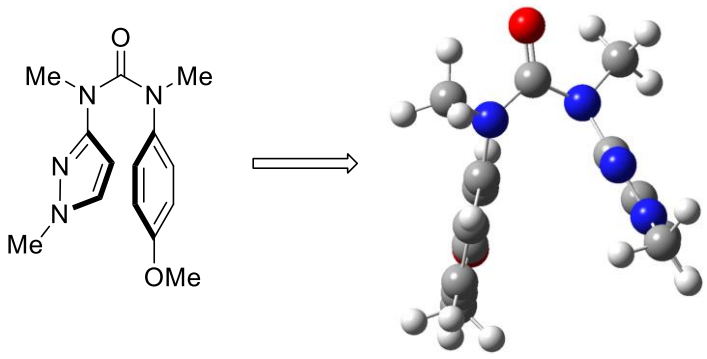

Figure 6: Steric Congestion at the Pyrazole C-H Bonds of **396**

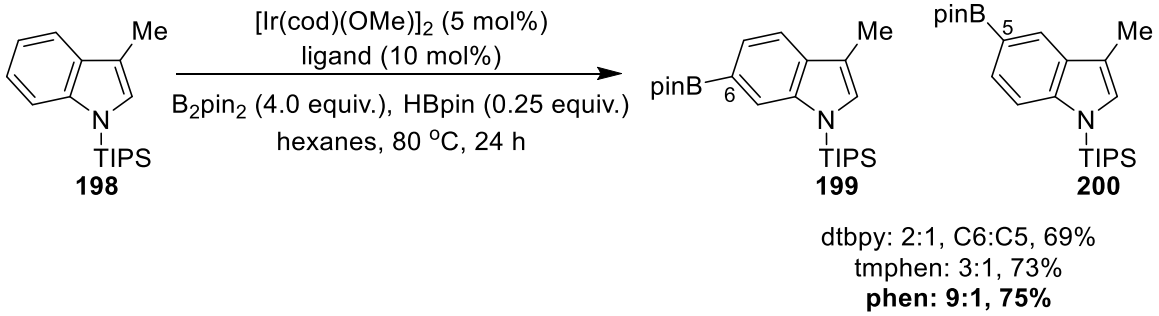

Scheme 12: Ligand-Controlled Regioselective C-H Borylation of Indole **198**

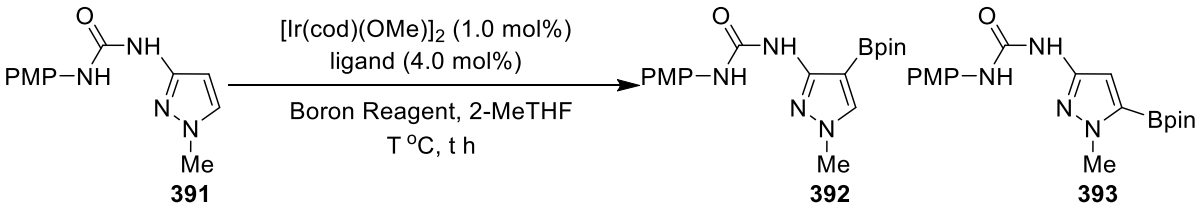

Entry	Ligand	Boron Reagent (eq)	T / °C	t / h	NMR Yield /%	**392**:**393**
1	tmphen	HBpin (4)	80	1	>99	40:60
2	tmphen	B_2pin_2 (2)	80	1	90	40:60
3	tmphen	B_2pin_2 (2)	rt	18	90	40:60
4	tmphen	HBcat (4)	80	1	-	-
5	tmphen	HBcat (4)	rt	1	-	-
9	bpy	B_2pin_2 (2.2)	80	5 min	>99	35:65
10	dtbpy	B_2pin_2 (2.2)	80	5 min	>99	30:70
11	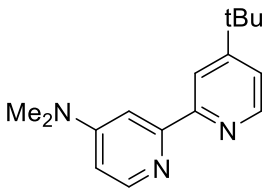	B_2pin_2 (2.2)	80	0.25	>99	25:75
12*	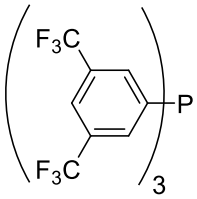	B_2pin_2 (2.2)	120	1	70	15:85

* 3 mol% ligand used

Table 3: Modification of Different Variables in the C-H Borylation of Urea **391**

One possible explanation for this is that the modification of the ligand ultimately alters the electron-density at the boryl ligands, and this may disrupt the putative hydrogen-bond network. However, further studies are required to determine the origin of ligand-controlled intrinsic C-H selectivity differences. This study demonstrated that altering reaction variables in the C-H borylation of **391** including temperature, ligand, and boron reagent does not improve C-4 selectivity. Following this, it was hypothesised that increased steric congestion at C-5 may improve C-4 selectivity as the catalyst is sensitive to steric effects. The bulky 3,5-dimethylbenzyl (Xyl(Me)$_2$) group was selected in order to investigate this. Notably, Sadler previously described that the Ir C-H borylation of indazole **399** exhibits good tolerance towards this group, and this provided good precedent for this selection.[2] This group was chosen over the simpler benzyl group as the methyl groups were designed to prevent unwanted C-H borylation events and to increase steric bulk. Therefore, attention was given to the synthesis of urea **401** and how the 3,5-dimethylbenzyl group may affect the C-H borylation selectivity.

It was predicted that direct alkylation of 3(5)-aminopyrazole **369** would be non-selective, so an alternative approach was developed. A retrosynthetic analysis on urea **401** revealed novel nitropyrazole **403** as the first target (Scheme 14a). Precedent for this was obtained from a report from Chroder, who described the N-1 selective benzylation of 3(5)-nitropyrazole with NaH (Scheme 14b). On this basis, a modified procedure which employed lower temperature was developed based on this which afforded **403** with complete isomeric purity in good yield (Scheme 14c). N-1 selectivity was evident by a through-space interaction of the C-5 hydrogen with the benzylic methylene hydrogens in the 2D ^{1}H-^{1}H NOESY spectrum. To prevent competitive hydrogenolysis of the 3,5-dimethylbenzyl group, the reduction of **403** was performed with Fe over the more standard Pd/H_2 system, which afforded primary amine **402** in good yield. With **402** in hand the C-H borylation was investigated using HBpin and tmphen.

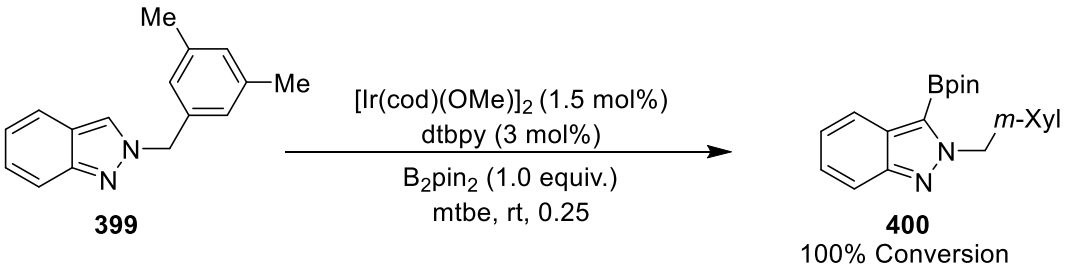

Scheme 13: C-H Borylation of THP and 3,5-Dimethylbenzyl Indazole **399**

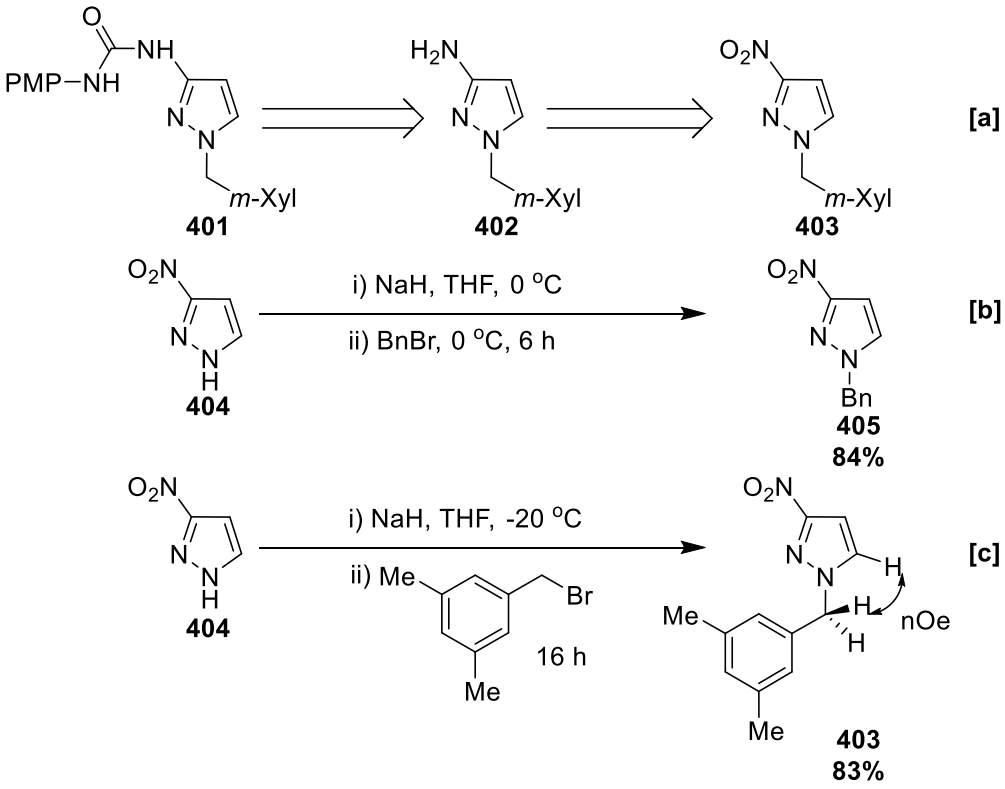

Scheme 14: Selective Alkylations with NaH

This afforded two distinct C-5 borylated products, which was evident by the presence of two shifted singlets at 6.03 and 6.49 ppm with equal intensity in the crude ^{1}H NMR spectrum (Scheme 15). The latter signal was assigned as N-borylated adduct **407**, and this is supported by the presence of an additional Bpin CH_3 signal at 1.30 ppm in the ^{1}H NMR spectrum, and by the presence of a signal at 28.2 ppm in the ^{11}B NMR spectrum attributed to the N-Bpin group.

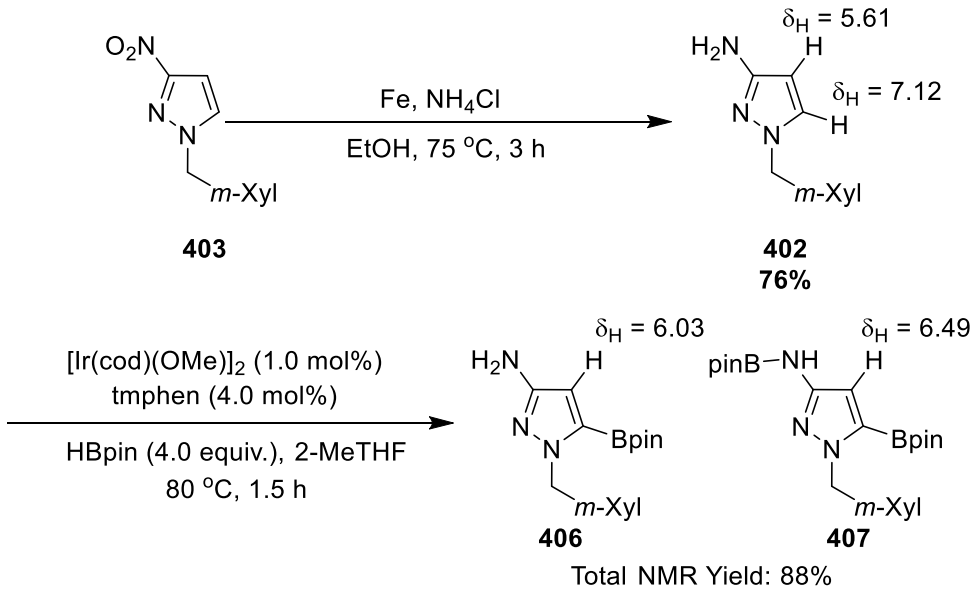

Scheme 15: Synthesis and C-H Borylation of Dimethylbenzyl Pyrazole **402**

A peak in the ESI LCMS spectrum with m/z = 202.1 attributed to the $[M+H]^+$ ion provided good evidence for the successful reduction of **403**. C-4 selectivity was ruled out by the absence of boron-shifted C-5 hydrogen, which would otherwise appear shifted ~0.1-0.5 ppm downfield from 7.12 ppm. Furthermore, one peak with m/z = 327.3 corresponding to the $[M]^+$ ion was displayed in the crude EI GCMS spectrum, supporting the production of a single isomer since the N-B bond in **407** likely cleaved during EI analysis.[8] Unfortunately, multiple attempts to isolate the product of this reaction and arylate the crude reaction mixture led to protodeborylation. Therefore, our attention turned to the synthesis of urea derivative **401**, which was performed analogously to the synthesis of parent urea **391** and was obtained in excellent yield. With the urea in hand, the next focus became the C-H borylation of **401**. Unfortunately, this gave similar selectivity to the parent urea **391** at 80 °C (Table 4, Entry 1). Performing the reaction at room temperature led to higher selectivity for undesired isomer **409**, although C-4 selectivity was raised somewhat at 100 °C (Table 4 Entries 2, 3). From this study, it was concluded that C-4 selectivity is not improved with steric hindrance introduced by N-substitution with a 3,5-dimethylbenzyl group in **401** or **402**.

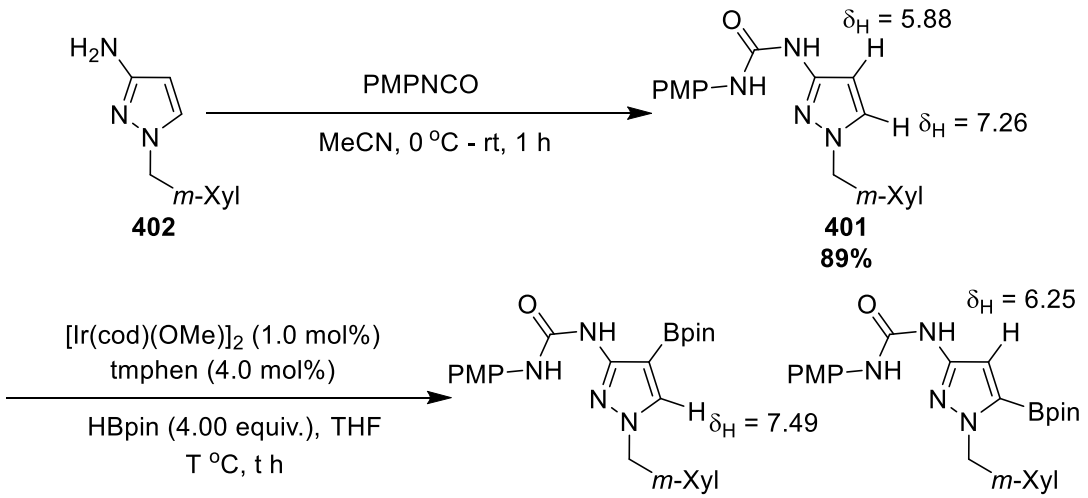

Entry	T /°C	t/ h	NMR Yield	**408**:**409**
1	80	1	80	60:40
2	rt	16	>99	30:70
3*	100	1	90	50:50

*2-MeTHF used as a solvent

Table 4: Synthesis and C-H Borylation of **401**

Following this study, it was hypothesised that removal of the benzylic methylene spacer in **401** may incur increased steric congestion at C-5 and therefore improve the regioselectivity in the urea-directed C-H borylation. In order to test this, *p*-methoxyphenyl pyrazole **410** was synthesised following a modified Ullmann coupling originally developed by Prestat from 3(5)-aminopyrazole.[9] Subsequently, **410** was treated with PMPNCO under standard urea-formation conditions, affording **411** in acceptable yield following recrystallisation from THF. The successful synthesis of **411** was evident from the purified ^{1}H NMR spectrum, which displayed two sets of two PMP doublets at 7.50, 7.44, 6.99, and 6.89 ppm. Furthermore, two pyrazole C-H signals were displayed at 7.70 and 5.55 ppm in the ^{1}H NMR spectrum. Unlike the previously investigated pyrazole ureas, **411** displayed no conversion in the C-H borylation at room temperature, whilst repeated attempts at elevated temperature led to decomposition to unknown materials (Scheme 16). Therefore, it was suggested that substitution at the azole N with a six-membered ring was deleterious to C-H borylation activity. In conjunction with efforts to improve C-4 selectivity in the urea-directed C-H borylation, this was tested by switching PMP for tetrahydropyran (THP). A retrosynthetic analysis led to the identification of THP nitropyrazole **413** as the first target required to achieve this. **413** had previously been reported in a patent by Agostino, and attempts to reproduce this procedure led to the formation of regioisomers **413** and **414** (Scheme 17).[10] The generation of two isomers was evident from the crude ^{1}H NMR spectrum, which displayed two sets of pyrazole signals at 7.68/6.88 ppm (**413**) and 7.64/6.85 ppm (**414**). Furthermore, two peaks with m/z = 197.1 attributed to the $[M]^+$ ions were displayed in the EI GCMS spectrum.

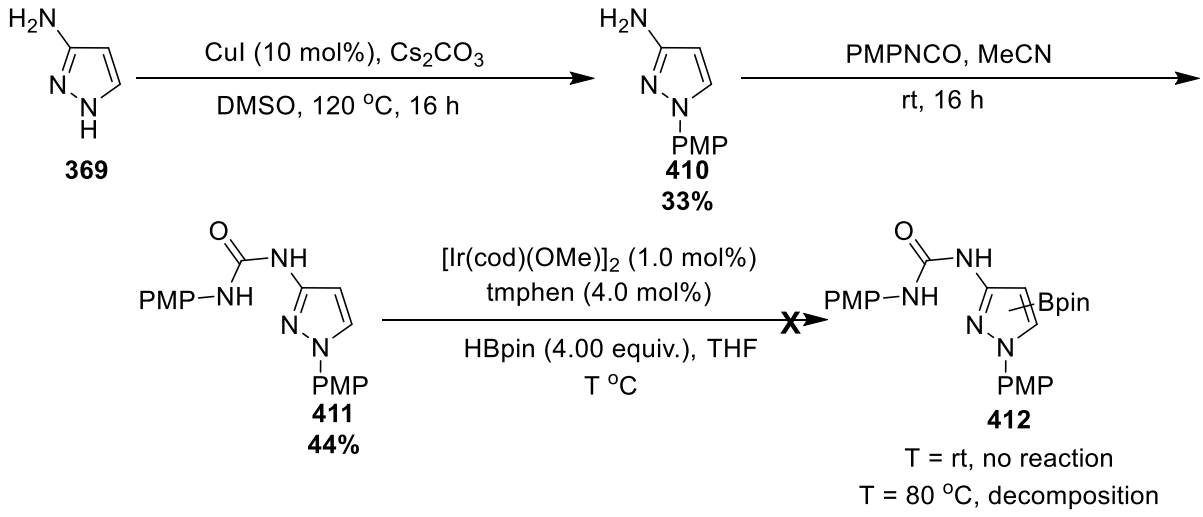

Scheme 16: Synthesis and C-H Borylation of PMP Urea **411**

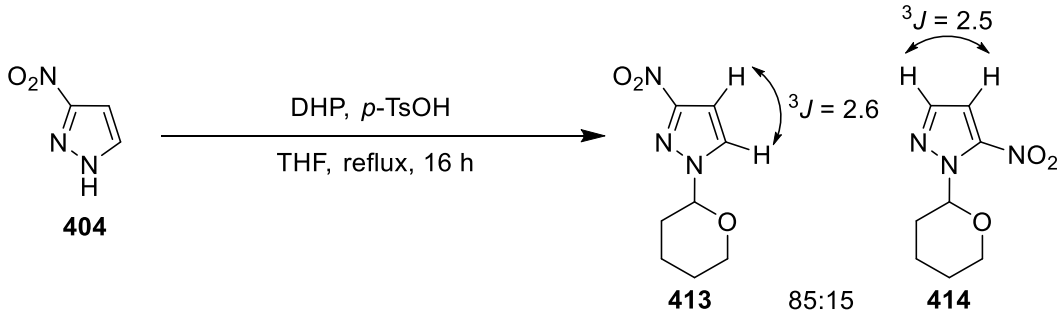

Scheme 17: THP Protection of **404**

Generally, 3- and 5-substituted pyrazoles may be distinguished based on the magnitude of the ^3J coupling between C-4 and C-5 protons in the 3-substituted isomer, which is larger than the ^3J coupling between the C-3 and C-4 protons in the corresponding 5-substituted isomer. Accordingly, the pyrazole C-H ^3J coupling was measured at 2.6 Hz in **413** and 2.5 Hz in **414**, although the associated error of these measurements rendered assignments somewhat dubious. Unfortunately, further characterisation was not possible as the crude mixture was challenging to separate, so focus was given to developing a more selective protection. Slade had previously described the regioselective THP protection of indazoles, and this system furnished N-1 protected indazoles such as **416** selectively (Scheme 18a).[11] This was suggested to operate through the room temperature equilibration of the N-1 and N-2 isomers via indazolium **417** promoted by the strong acid *p*-TsOH. These conditions were adopted in order to improve the selectivity in the THP protection of 3(5)-nitropyrazole **404**, and this pleasingly furnished **413** with complete selectivity and excellent yield (Scheme 18b).

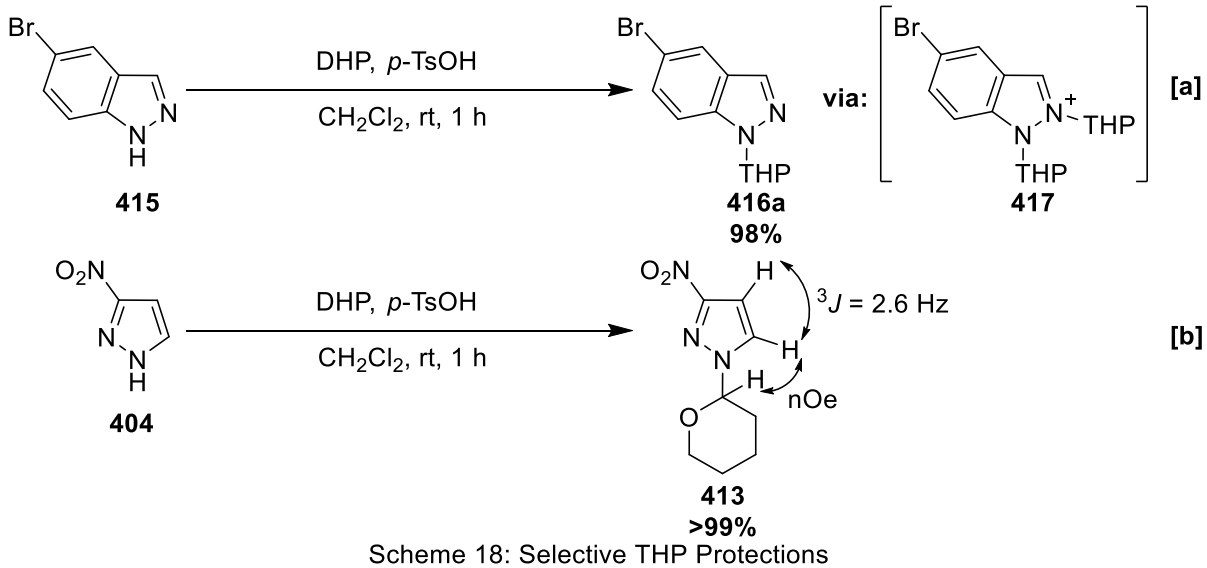

Scheme 18: Selective THP Protections

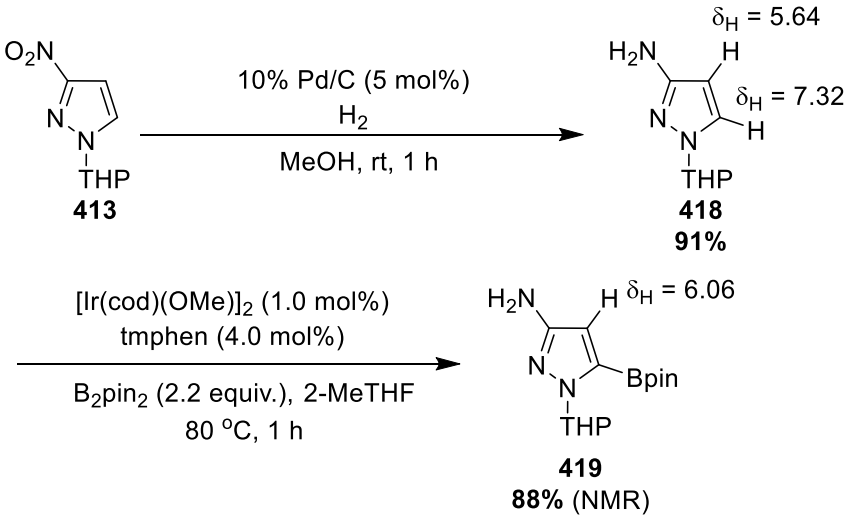

Scheme 19: Synthesis and C-H Borylation of THP Aminopyrazole **418**

A through-space interaction of the C-5 hydrogen with the pyranyl methine C-H was observed in the 2D ^{1}H-^{1}H NOESY spectrum, which supported the assignment of **413**. The reduction of **413** via Pd-catalysed hydrogenation afforded aminopyrazole **418**, which was subsequently C-H borylated to afford **419** with complete C-5 selectivity in excellent NMR yield (Scheme 19). This was evident by the presence of a boron-shifted singlet in the ^{1}H NMR spectrum at 6.06 ppm, and indicated that the additional congestion at C-5 incurred by THP does not alter the C-H borylation selectivity in the primary amine. Unfortunately, attempts to chromatographically purify and cross-couple **419** led to protodeborylation, so focus was turned to the synthesis and C-H borylation of THP urea **420**. In order to achieve this, **418** was treated with PMPNCO in MeCN to in analogy to the synthesis of parent urea **391** (Scheme 20).* The subsequent C-H borylation of **420** under standard conditions led to slightly improved selectivity for C-4 boronate **421** and conducting the reaction at room temperature provided the same selectivity with lower conversion. This selectivity was evident by the presence of two boron-shifted singlets at 7.77 and 6.31 ppm in the crude ^{1}H NMR spectrum attributed to **421** and **422**, respectively. This suggested that the THP group may assist C-4 selectivity in the urea-directed C-H borylation of **420** on steric grounds. Chromatographic separation of the two isomers led to the isolation of C-4 boronate **421** in a higher yield than parent urea C-4 boronate **392**, and this may have been facilitated by the increased C-4 selectivity. A through-space interaction between the C-5 hydrogen and pyranyl methine hydrogen observed in the ^{1}H-^{1}H 2D NOESY spectrum provided good evidence for C-4 selectivity.

* ^{1}H NMR shifts quoted in $CDCl_3$, compound reported in d^6-DMSO.

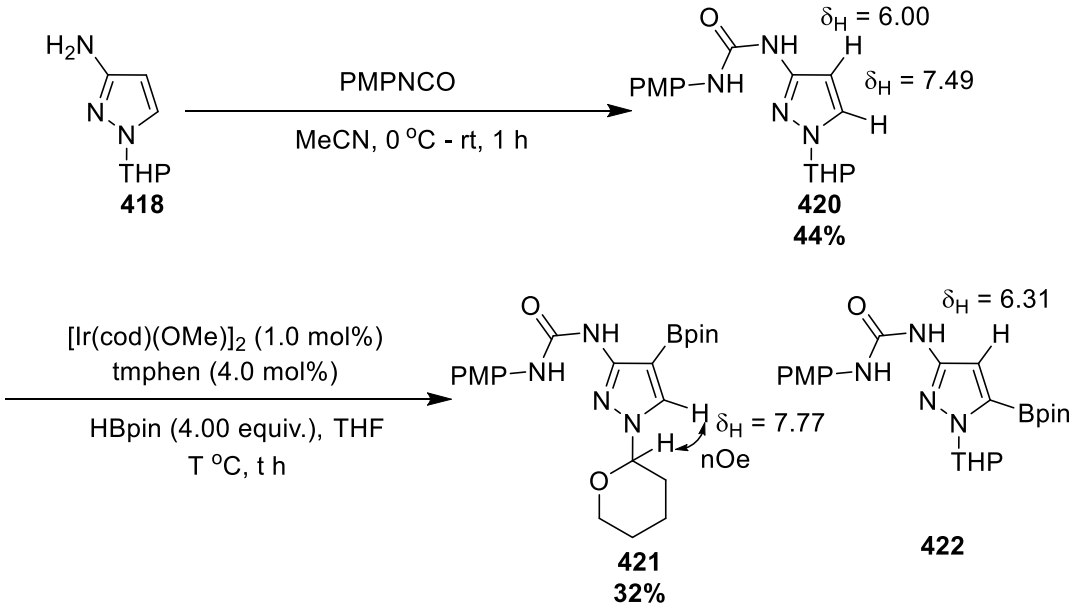

T = 80, t = 1; 1:1 Ratio; 90% NMR Yield; **32%** Isolated Yield **422**
T = rt, t = 16; 1:1 Ratio; 50% NMR Yield

Scheme 20: Synthesis and C-H Borylation of THP Urea **421**

Despite the complete conversion deduced using ^{1}H NMR spectroscopy monitoring experiments, a considerable quantity of the starting heteroarene could also be recovered after chromatography, suggesting that **422** protodeborylates on SiO_2 gel. This instability was consistent with the observation that multiple attempts to arylate **421** under Suzuki-Miyaura cross-coupling led to complex, intractable mixtures typically accompanied by significant degrees of protodeborylation. However, C-5 arylated urea **423** could be obtained following one-pot Suzuki-Miyaura cross-coupling of the crude mixture of boronates using 6-bromoquinoline (Scheme 21). Whilst the THP group offered a small increase in C-4 selectivity, this study demonstrated that the regiochemistry in the urea-directed C-H borylation of aminopyrazole ureas was challenging to modulate using steric effects. It was speculated that the directing effect was not pronounced enough to overcome the intrinsic electronic selectivity for the most acidic C-5 C-H site, even in the presence of bulky substituents at the azole N.

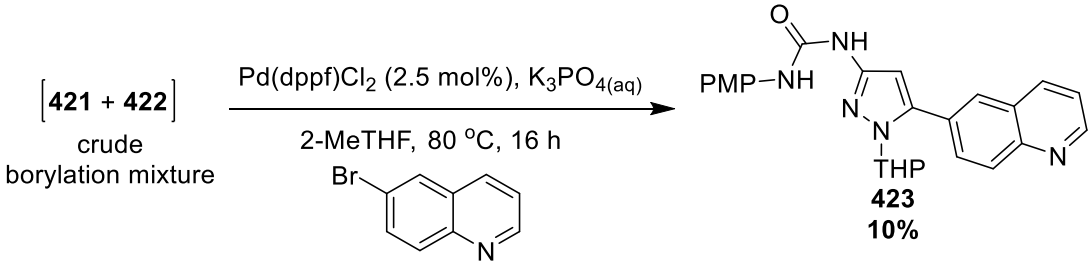

Scheme 21: Suzuki-Miyaura Cross-Coupling of Crude Boronates **421** and **422**

Based on the C-4 selectivity observed in three different pyrazole ureas, it was hypothesised that the urea directing effect may also manifest in other heteroarenes.

3.2.2.2 Other Heterocyclic Ureas

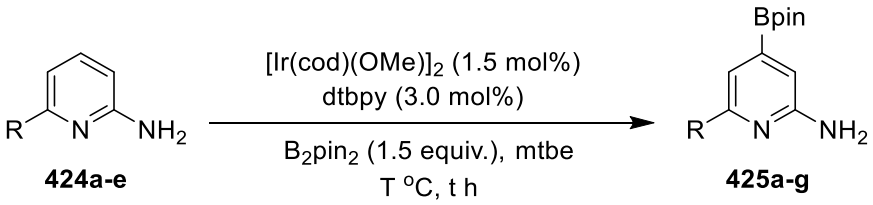

Entry	424	R	R^1	T / °C	t/ h	Conversion /%	Isolated Yield /%
1	**a**	CF_3	H	80	1	>99	18*
2	**a**	CF_3	H	rt	16	>99	72
3	**b**	F	H	80	1	>99	-†
4	**b**	F	H	rt	22	>99	59‡
5	**c**	Cl	H	80	1	>99	52
6	**c**	Cl	H	rt	16	>99	-
7	**d**	OMe	H	80	4.5	95	-
8	**e**	Me	H	80	1	>99	-
9	**e**	Me	H	rt	16	24	-

*Crude mixture obtained as a 87:13 mixture of C-4:unknown boronates.
† Crude ratio of C3:C4 isomers 7:13
‡ Isolated as a mixture of C3:C4 isomers in a 6:5 ratio

Table 5: Borylation of Aminopyridines

To test this, the borylation of various heteroaromatic amines was undertaken in order to first determine their intrinsic selectivities for reference. Our focus began with pyridines owing to the group's ongoing interest in this important scaffold. Previously, it has been reported by Sadler and others that the borylation of 2,6-disubstituted pyridines is selective for C-4.[3,12] Consistent with this observation, all of the studied 2,6-aminopyridines **424** displayed selectivity for C-4 in the C-H borylation with dtbpy and B_2pin_2 (Table 5, Entries 1-9). However, the borylation of trifluoromethylpyridine **424a** led to the formation of an unknown C-H borylated isomer. It was speculated that this could be C-5 isomer **425b** afforded via *ortho* direction of the *in situ* NHBpin adduct **426** (Scheme 22). This assignment is supported by the fact that C-H borylation *ortho* to a CF_3 group is unprecedented due to steric effects.

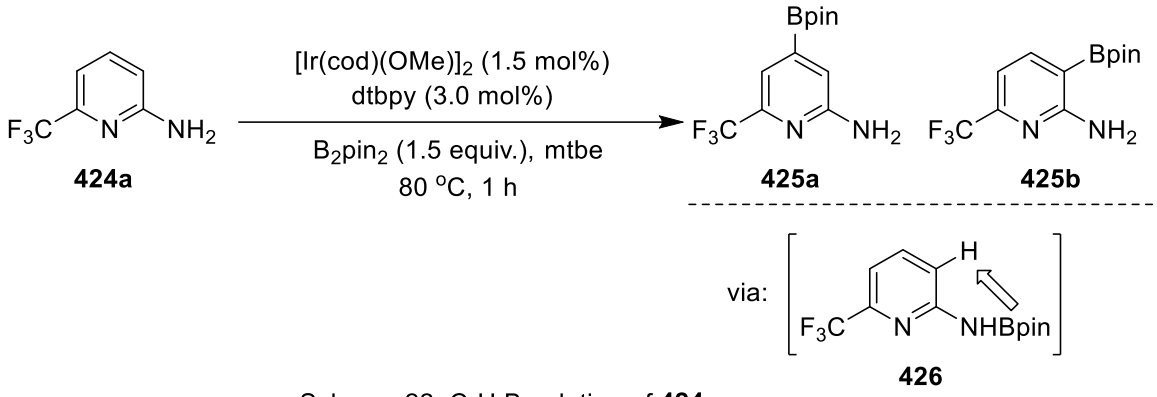

Scheme 22: C-H Borylation of **424a**

Furthermore, 2-fluoro-6-aminopyridine **424b** additionally displayed C-3 selectivity as expected owing to the small size of F, affording a mixture of isomeric boronates **426c** and **426d** (Table 5, Entries 3, 4). Moreover, elevated temperature was required for the efficient borylation of methoxypyridine **424d**, and this is consistent with the higher barrier associated with the C-H activation of electron-rich aromatics (Table 5, Entry 7). Where possible, boronates **425** were isolated via binary solvent recrystallisation according to a modified procedure by Smith, although purification was sometimes challenging due to protodeborylation. Concurrently, the C-H borylation of 2,5-aminopyridines was explored. The heterocycles **427** investigated in this study showed no activity in the C-H borylation even under forcing conditions, and this was attributed to steric effects (Scheme 23).* Having successfully established the C-H borylation selectivities and activities in aminopyridines, the next focus became synthesis and C-H borylation of aminopyridyl ureas. It was speculated that the urea-directed C-H borylation may be more selective in pyridines as the beta and gamma C-H pK_a values are generally more comparable than the alpha and beta C-H pK_a values in pyrazoles.[13,14] Pyridyl ureas were synthesised under standard conditions by the reaction of an aminopyridine with an aromatic isocyanate in MeCN (Table 6).

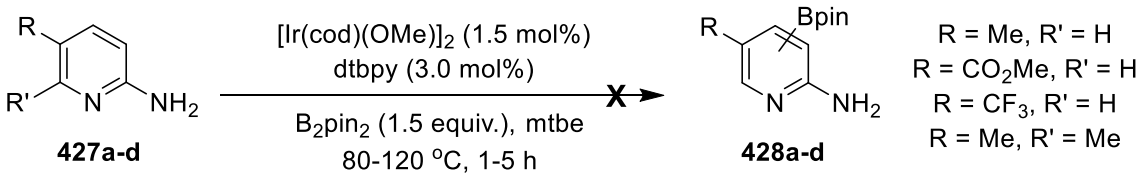

Scheme 23: C-H Borylation of 2,5-Substituted Aminopyridines

* The C-H Borylation of other aminopyridines was performed by Andrew Hones

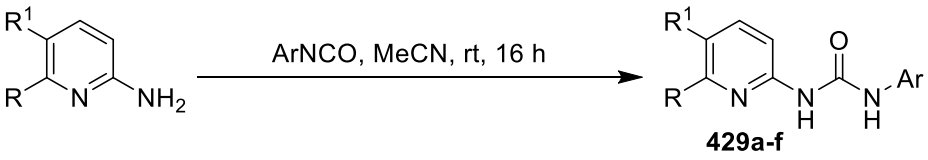

429a-f

Entry	Substrate	R	R^1	Ar	Isolated Yield /%
1	**424c**	Cl	H	Ph	65
2	**424e**	Me	H	Ph	93
3	**424f**	Et	H	Ph	96
4	**424e**	Me	H	PMP	99
5	**427a**	H	Me	PMP	91
6	**427d**	Me	Me	PMP	81

Table 6: Synthesis of Pyridyl Ureas

Typically, the low solubility of the products permitted isolation by filtration with Et_2O, in acceptable purity.* Following this, the C-H borylation of the ureas was explored, and conversions were measured via ^{1}H NMR spectroscopy with 1,3,5-trimethoxybenzene as an internal standard (Table 7). All of the investigated 2,6-pyridylureas exhibited C-4 borylation selectivity like their aminopyridine analogues, and did not display *ortho* directed regiochemistry. Changing the nature of the urea aryl group did not affect this result (Table 7, Entries 1-11). The generally poor solubility of the pyridyl ureas necessitated more polar solvents (2-MeTHF, THF) over methyl tert-butyl ether (mtbe) in the majority of reactions. In analogy to their aminopyridine analogues, 5-substituted pyridyl ureas were inactive and eventually decomposed over prolonged reaction periods (Table 7, Entries 12-16). Attempts to purify the aryl boronates with chromatography and/or recrystallisation led to protodeborylation. This outcome was also observed after attempts to derivatise the boronate esters with Suzuki-Miyaura cross-coupling. Notably, after 6 hours at room temperature the conversion of **429e** was 60% and the reaction produced a colour change from a homogenous dark solution to a heterogeneous orange solution (Table 7, Entry 13). This was accompanied by the appearance of a new set of proton signals in the crude ^{1}H NMR spectrum. These proton signals possessed identical splitting patterns and integrations to the substrate shifted downfield *ca.* 0.2 ppm, except for the absence of one N-H signal.

* The synthesis of and C-H borylation of other ureas was performed by Andrew Hones

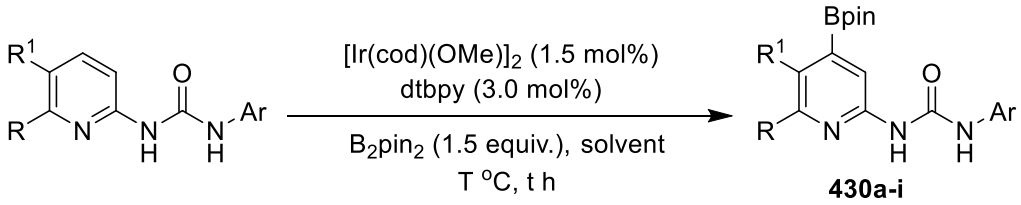

430a-i

Entry	Substrate	R	R^1	Ar	Solvent	T / °C	t/ h	Conversion /%
1	**429a**	Cl	H	Ph	2-MeTHF	80	3	50
2	**429b**	Me	H	Ph	2-MeTHF	40	23	40
3	**429b**	Me	H	Ph	THF	30	16	0
4	**429b**	Me	H	Ph	2-MeTHF	40	18	40*
5	**429b**	Me	H	Ph	mtbe	80	1	100
6	**429d**	Me	H	PMP	2-MeTHF	80	2	60†
7	**429d**	Me	H	PMP	2-MeTHF	40	16	10†
8	**429d**	Me	H	PMP	mtbe	80	2	60‡
9	**429g**	Me	H	*p*-CF_3Ph	2-MeTHF	60	1	72§
10	**429c**	Et	H	Ph	2-MeTHF	40	2	10
11	**429c**	Et	H	Ph	2-MeTHF	80	16	75
12	**429e**	H	Me	PMP	mtbe	80	0.5	0§
13	**429e**	H	Me	PMP	2-MeTHF	rt	6	60§∩
14	**429h**	H	CO_2Me	Ph	2-MeTHF	80	1	0§
15	**429f**	Me	Me	PMP	2-MeTHF	80	2	0§
16	**429f**	Me	Me	PMP	2-MeTHF	120	3	0§

*3 equiv. HBpin was used instead of B_2pin_2
† Reaction conditions: $[Ir(cod)(OMe)]_2$ (1.0 mol%), tmphen (4.0 mol%), HBPin (3.0 equiv.)
‡ Isolated C-4 boronate ester in 8% yield
§ Prolonged reaction periods led to decomposition
∩ Converted into an adduct with no evidence of C-H borylation

Table 7: Borylation of Pyridyl Ureas

Therefore, a C-H borylated product was ruled out. Concurrently, a new up-field shifted signal appeared at 6.02 ppm in the ^{11}B NMR spectrum, and this indicative of four-coordinate boron. Furthermore, leaving this reaction mixture to stand for 16 h d^6-DMSO led to a decrease in the concentration of this species and to an increase in the concentration of the substrate, suggesting that the unknown compound can revert into **429e**.

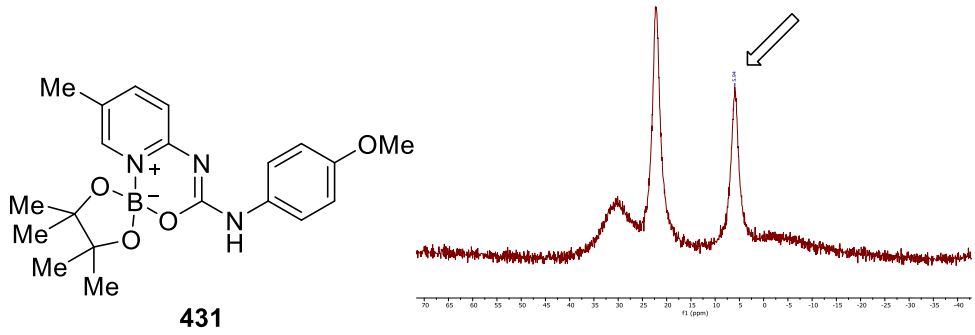

Figure 7: Proposed Structure for a Boryl Adduct **431** (Left) and Crude ^{11}B NMR Showing a New Signal Shifted Upfield (Right)

Therefore, the identity of this species was tentatively assigned as **431**, containing a pseudo-aromatic six-membered N-B-O ring system (Figure 7). Attempts to gain further evidence for this (EI/ESI MS, purification and isolation) were unsuccessful, and this likely reflects the propensity of **431** to deborylate. The formation of putative adduct **431** may suggest that the N-H bonds in pyridyl ureas can undergo borylation, which would disrupt an intramolecular hydrogen-bonding network. This may explain the lack of *ortho* directed borylation in these systems, although further evidence of N-H borylation in other ureas could not be obtained. This study established that aminopyridyl ureas undergo regioselective C-H borylation at C-4. However, *ortho* selective C-H borylation to the urea group was not observed via the urea directing effect developed for pyrazole ureas. It was also suggested that the larger bond angles in six-membered heterocycles may kinetically disfavour directed C-H borylation.

Therefore, it was hypothesised that the urea directing effect may manifest in other heteroaryl ureas which possess substituents that are closer together in space.* To test this, the synthesis of aminoisoxazole and aminoindazole ureas **433** was conducted, and this was achieved in analogy to the synthesis of the previously presented heteroaryl ureas from the corresponding heterocyclic amines (Table 8). With ureas **433** in hand, the C-H borylation was subsequently investigated. Isoxazole ureas **433a** and **433b** displayed no activity under the reaction conditions using dtbpy and tmphen, and the reaction of **433b** led to discolouration of the catalyst solution (Scheme 24a, b). This was surprising as related five-membered heteroarenes such as oxazole undergo facile C-H borylation with alpha selectivity.

* The synthesis and C-H borylation of other heteroaryl ureas was performed by Andrew Hones

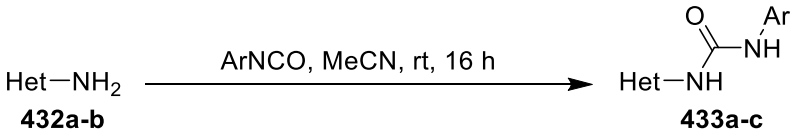

432a-b **433a-c**

Entry	**432**	Het-NH_2	Ar	Isolated Yield /%
1	**a**	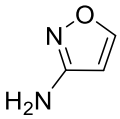	Ph	>99%
2	**a**	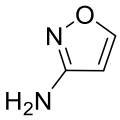	PMP	95
3	**b**	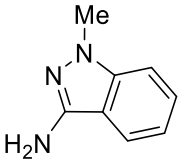	Ph	95

Table 8: Synthesis of Other Heteroaromatic Ureas

This led to the conclusion that isoxazole ureas **433a** and **433b** may be catalyst inhibitors, although the mechanism of this inhibition remains unclear. Following this result, it was hypothesised that the urea-directing effect may enable *peri*–selective C-H borylation, since mutually *peri* substituents are closer in space than *ortho* ones.[15] Previous work on the C-H borylation of indazoles led to the investigation of indazole urea **433c** in the C-H borylation (Scheme 24c). This produced a complex mixture by ^{1}H NMR spectroscopy, which seemed to consist of the substrate, two monoborylated isomers in a 4:1 ratio, and some trace bisborylation. However, the unambiguous regiochemistry of this process was challenging to determine. The aim of future studies is to determine the regiochemistry of this process. Finally, the C-H borylation of quinolin-2-one **435** was investigated. Whilst **435** contains a lactam and not a urea, it was hypothesised that it may undergo *peri*-selective C-H borylation at C-8 since it possesses a structure that is comparable to the hydrogen-bond network in the parent pyrazole urea **391**. Whilst complete conversion was recorded by ^{1}H NMR monitoring after 3 h, **435** had decomposed during the C-H borylation at 80 ^{o}C into unknown materials (Scheme 24e). Attempts to lower the reaction temperature did not lead to C-H borylation, and **435** was recovered after an extended period.

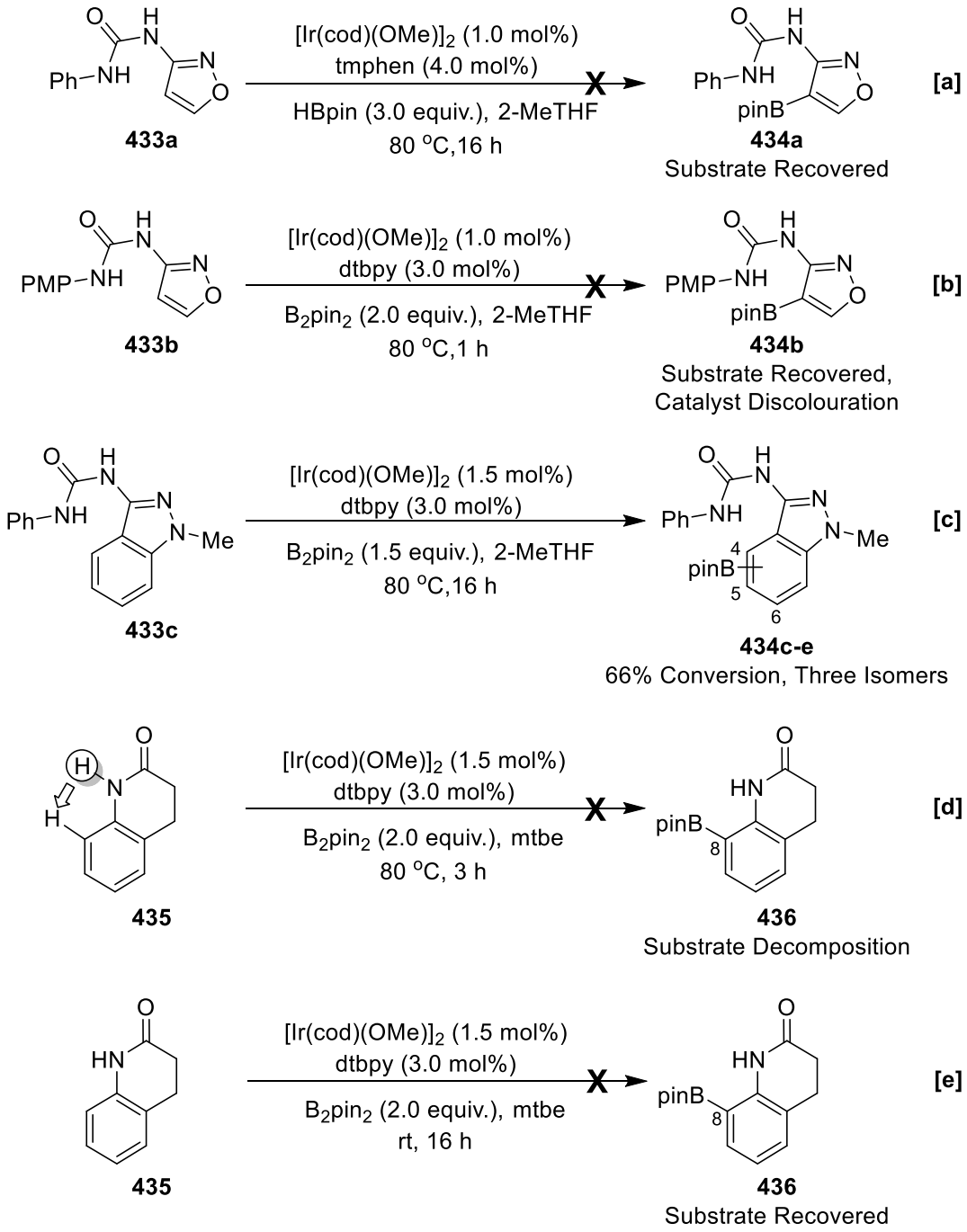

Scheme 24: Directed Borylation Screen in Other Systems

The results from the study into urea-directed C-H borylation suggested that whilst the directing effect manifests in pyrazole ureas, it does not extend in a general fashion to other (hetero)arenes. Further evidence is required to understand these observations, although a possibility for the lack of direction is deleterious borylation at the urea N-H bonds, disrupting the intramolecular hydrogen-bonding network. Given these challenges, other methods were explored in order to reliably afford orthogonal C-H borylation regiochemistry in N-substituted aminopyrazoles with improved selectivities.

3.2.3 Protecting Group Switch

As discussed in the previous section, the directed C-H borylation of aminopyrazole ureas was found to give modest C-4 selectivity, and did not extend in a general fashion to other heteroarenes. At this stage, we had reversed the intrinsic regiochemistry of N-methyl-5-aminopyrazole **373** (intrinsic C-5 borylation selectivity) to a degree using the parent urea **391**. However, the developed method was complicated by the concurrent generation of C-4 and C-5 regioisomeric boronates. Therefore, the next goal was to develop a more efficient method that would provide complementary C-H functionalisation selectivities in **373** and N-methyl-5-aminopyrazole **380** (intrinsic C-4 borylation selectivity).

One related method for altering regiochemistry in pyrazoles had been described by Sames. This involved the use of a labile N-substituent which is cleaved upon quaternisation of the azinyl N with an alkylating reagent. For example, the Pd C-H arylation of SEM pyrazole **437** was intrinsically selective for C-5, affording pyrazole **438**. On treatment of **438** with strong alkylating agent followed by SEM deprotection, the net C-3 functionalised **440** was isolated (Scheme 25). It was hypothesised that this protecting group switch process could be adopted in order to achieve complementary selectivities in N-SEM aminopyrazoles by a C-H borylation/arylation/alkylation/deprotection sequence. The goal was to apply this method to aminopyrazoles for the efficient synthesis of the remaining two targets of this project, **444** and **448** (Scheme 26a, b).

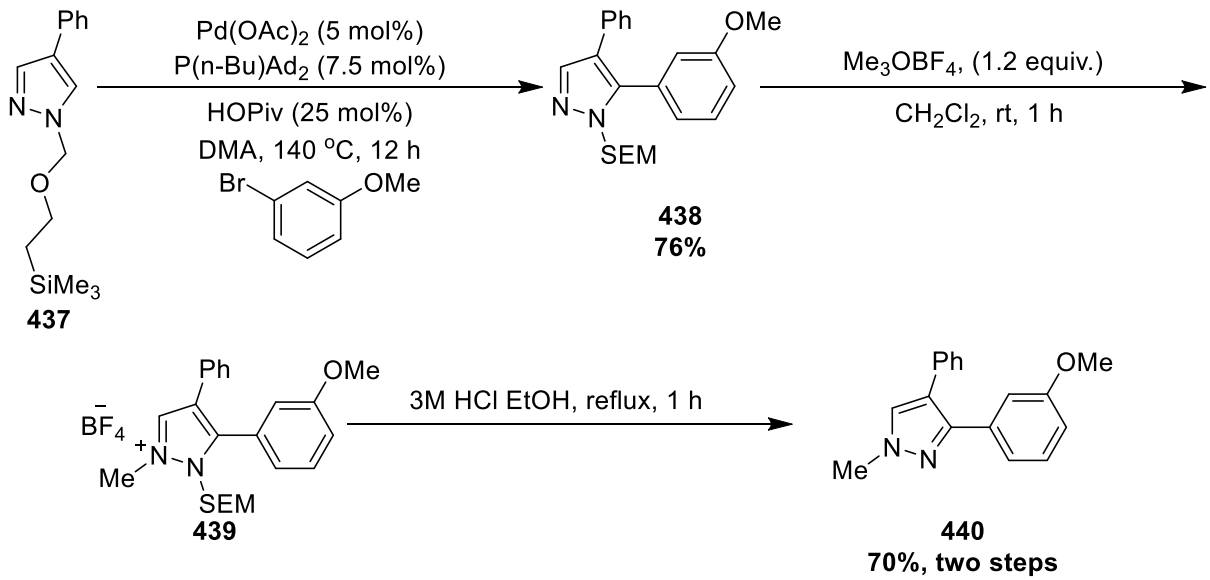

Scheme 25: Pd-Catalysed Arylation and Switch of N-SEM Pyrazole **438**

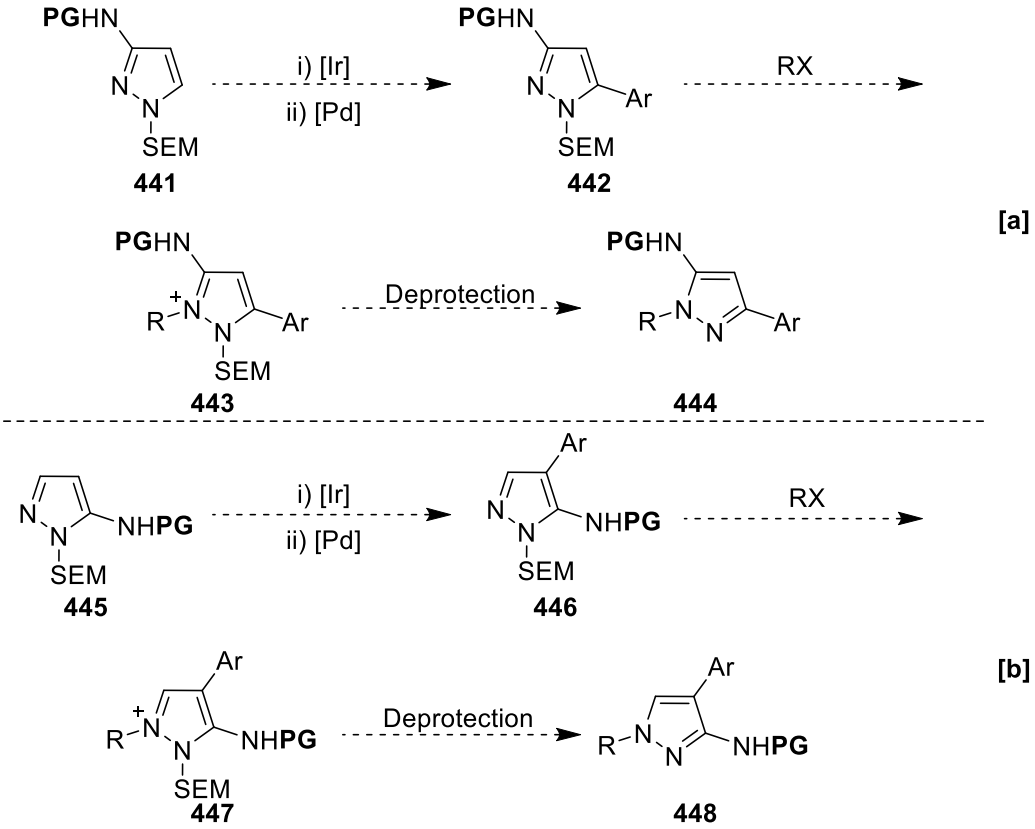

Scheme 26: Hypotheses for a Selectivity Switch in Aminopyrazoles

3.2.3.1 3-Aminopyrazoles

To test this, the synthesis of N-SEM-3-aminopyrazole **450** was first investigated. The synthesis of nitropyrazole precursor **449** had previously been reported by Spring.[16] Following this reported procedure enabled the synthesis of **449** from 3(5)-nitropyrazole **404** to be achieved in excellent yield. (Scheme 27). Subsequent Pd-catalysed hydrogenolysis led to the isolation of aminopyrazole **450** again in excellent yield. The structure of this compound was unambiguously confirmed by a single crystal from X-ray analysis (Figure 8). Having completed the synthesis of target **450**, focus turned to the C-H borylation reaction. Using B_2pin_2 and tmphen, this led to the isolation of C-5 boronate **451** as expected, and this was evident by the presence of a boron-shifted singlet in the ^{1}H NMR spectrum at 6.09 ppm attributed to the C-4 hydrogen. Furthermore, this signal displays a HSQC interaction with a characteristic C-4 carbon signal at 103.9 ppm, supporting C-5 site-selectivity. Whilst the borylation of **450** was efficient, the modest yield was attributed to slow protodeborylation during chromatographic purification.

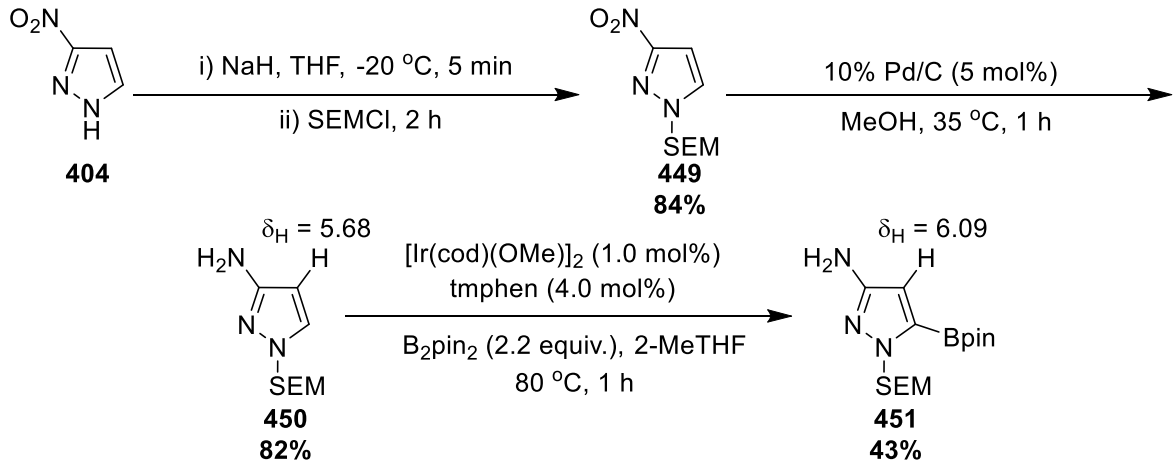

Scheme 27: Synthesis and C-H Borylation of SEM Pyrazole **450**

Multiple attempts to cross-couple boronate **451** with Suzuki-Miyaura arylation led to intractable product mixtures containing protodeborylated **450** and contaminant pinacol and pinacolatoboryl derivatives (such as HOBpin). It was hypothesised that these contaminants could not be separated because they remained coordinated to the primary amine. Owing to the high oxophilicity of boron, it was suggested that competitive coordination from an alcoholic solvent may simplify purification. Therefore, the crude product mixtures were stirred in MeOH/H_2O for extended periods. Whilst this method led to a significant reduction in the quantities of contaminants following chromatographic purification, complete separation of the arylated aminopyrazole products remained challenging. In order to overcome this challenge, **450** was protected as the corresponding Boc carbamate **452** in 63% yield under similar conditions to previously presented neat Boc protections. As expected, the C-H borylation of **452** was selective for C-5, and this was evident by the appearance of a boron-shifted singlet at 7.01 ppm in the crude ^{1}H NMR spectrum.

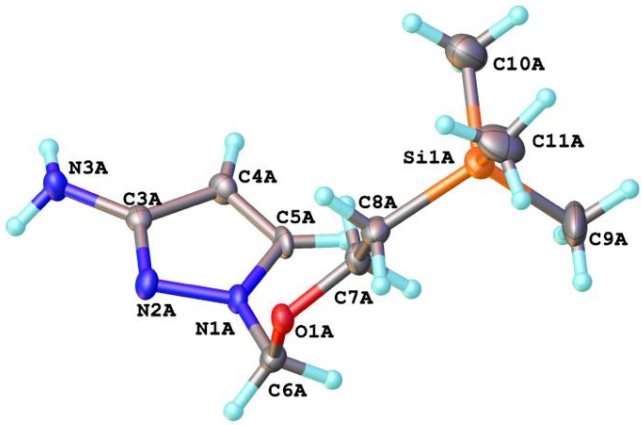

Figure 8: Crystal Structure of **450**

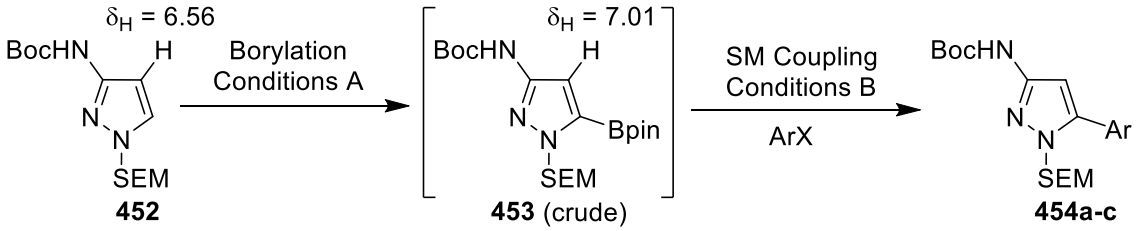

Entry	ArX	SM t / h	SM Isolated Yield /%
1	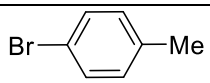	3	56
2	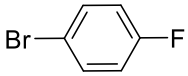	16	47
3	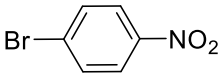	16	39

Borylation Conditions A: $[Ir(cod)(OMe)]_2$ (1.0 mol%), tmphen (4.0 mol%), B_2pin_2 (2.00 equiv.), 2-MeTHF, 80 °C, 1 h
SM Coupling Conditions B: $Pd(dppf)Cl_2$, $K_3PO_{4(aq)}$ (2.00 equiv., 3M), 2-MeTHF, 80 °C

Table 9: One-Pot Borylation/Arylation of SEM Pyrazole **452**

One-pot Suzuki-Miyaura cross-coupling of the crude boronate **453** pleasingly led to product mixtures that were amenable to purification with SiO_2 gel chromatography, and this enabled the isolation of arylated adducts **454a-c** in moderate to good yields (Table 9, Entries 1-3). With the arylated adducts in hand, the next goal became to test a protecting group switch sequence by first quaternising the azinyl N of **454a** using Me_3OBF_4 (Scheme 28a). In refluxing CH_2Cl_2, this pleasingly furnished pyrazolium salt **455**, and this was evident from the ^1H NMR spectrum which displayed a signal at 3.96 ppm attributed to the NCH_3 hydrogens. However, further data on **455** could not be obtained owing to decomposition during solvent removal under vacuum.

In order to understand the reasons for this, the quaternisation was repeated on the less precious aminopyrazole **453**. Using the same conditions, pyrazolium salt **456** was afforded in quantitative mass balance with complete substrate conversion (Scheme 28b). This was apparent from the crude ^1H NMR spectrum, which contained a new signal at 3.96 ppm corresponding to the N-CH_3 hydrogens. Further evidence of this product could be found in the ESI mass spectrum, with a peak at m/z = 328.2 attributed to the pyrazolium cation. Similar to **455**, **456** was found to possess low thermal stability and complete decomposition to unknown materials was observed on concentration.

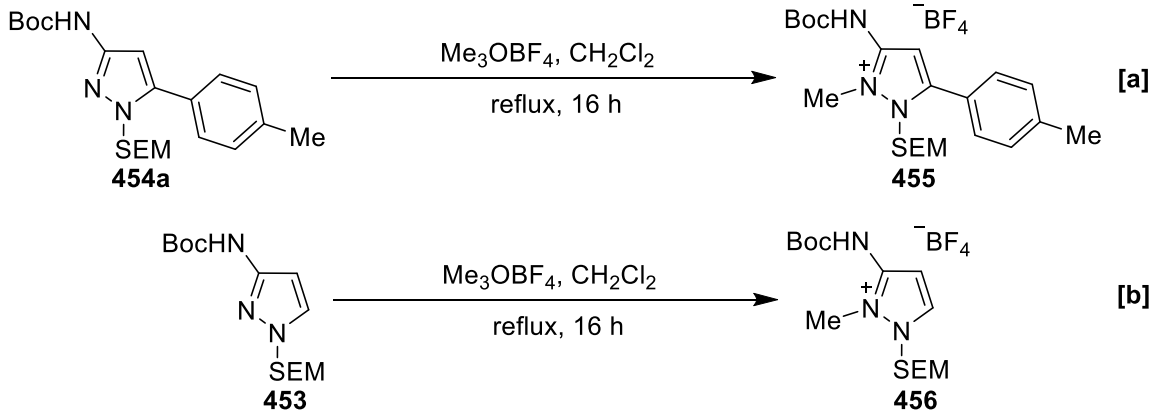

Scheme 28: Quaternisation Experiments of Aminopyrazoles

Attempts to undertake the deprotection of **456** *in situ* using a variety of deprotection conditions including HCl, TFA, TBAF, $MgBr_2$ /$MeNO_2$, NaOH, and triethylamine trihydrofluoride (TREATHF), all led to rapid (<5 min) decomposition of the substrate (Scheme 29a). The reasons for this could not be elucidated but it was subsequently speculated that the decomposition of **456** may be attributed to the collapse of the Boc protecting group to afford **457** (Scheme 29b). It was speculated that **457** may decompose by pathways such as polymerisation. To test this, the Boc group was replaced with the more robust acetyl protecting group. This was achieved by treating **451** with neat Ac_2O, affording acetamide **458** in high yield. The next focus became the quaternisation of **458**, which was conducted under standard conditions using Me_3OBF_4 affording pyrazolium salt **459** in 79% mass balance following removal of the volatiles (Scheme 30). This was evident from the crude ^1H NMR spectrum, which contained a new signal at 4.01 ppm corresponding to the N-CH_3 protons.

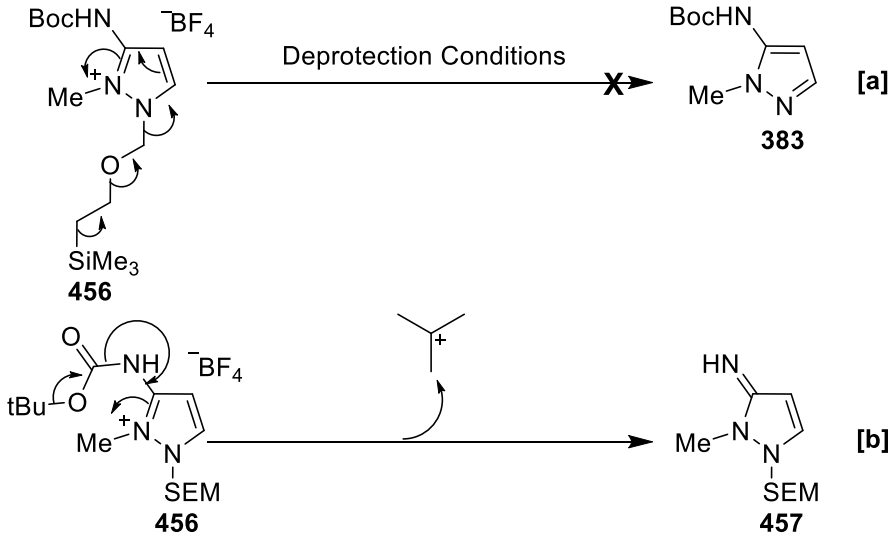

Scheme 29: Reactions of Pyrazolium Salt **456**

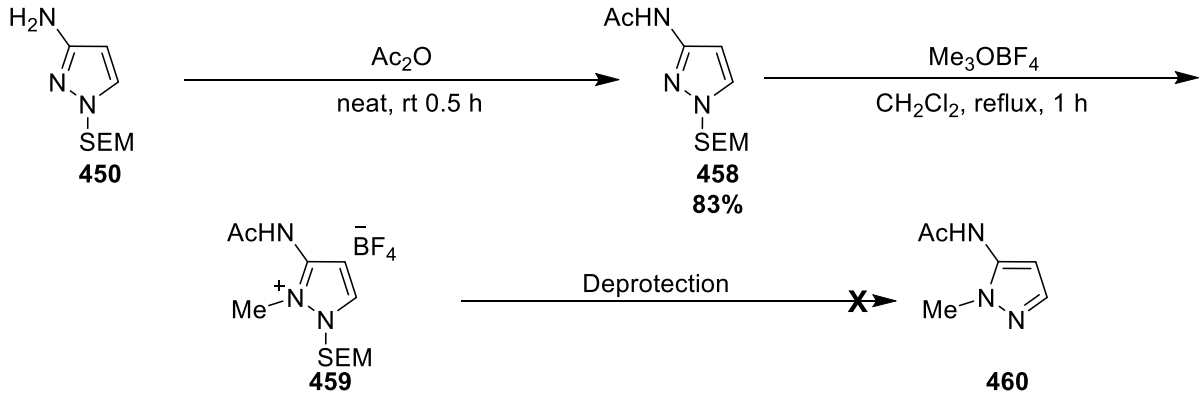

Scheme 30: Synthesis and Protecting Group Switch of Acetamide **458**

Further evidence of this product was found in the ESI mass spectrum, with a peak at m/z = 270.2 attributed to the pyrazolium cation. Unfortunately, attempts to deprotect **459** with HCl and TBAF also led to decomposition. Whilst aminopyrazolium salts **455**, **458** and **459** could efficiently synthesised, this study led to the conclusion that they possessed an intrinsic sensitivity toward deprotection and prolonged storage.

However, other pyrazolium salts do not possess this sensitivity. For instance, Begtrup described the synthesis of pyrazolium tosylate **462** via the alkylation of chloropyrazole **461** with MeOTs (Scheme 31a). In contrast to the poor stability of aminopyrazolium salts, **462** was subsequently used in a nucleophilic displacement reaction, affording **463**.[17] Based on this precedent, the quaternisation of **452** with other alkylating reagents was investigated in order to improve the stability of the corresponding pyrazolium salt (Scheme 31b). Unfortunately, attempts to alkylate **452** with MeOTs and $(Me)_2SO_4$ also led to decomposition, and MeI and EtI did not react even under forcing conditions.

Since the stability of **464** bearing different counterions could not readily be assessed, focus was turned to other possible variables responsible for the decomposition of aminopyrazolium salts. It was hypothesised that SEM removal may also be challenging for aminopyrazoles **452** and **458**. In order to test this, the SEM deprotection of each pyrazole with standard reagents including HCl, TBAF, TFA, TREATHF, and CsF was conducted, with all leading to substrate decomposition (Scheme 32a). In order to rule out other sources of error, the SEM deprotection of an isomeric mixture of phenylpyrazoles **465a** and **465b** previously reported in a related procedure by Rault was successfully reproduced (Scheme 32b).[18] At this time, it was noted that Grainger had also met difficulty with SEM deprotection during the final step in the total synthesis of kottamide E.[19]

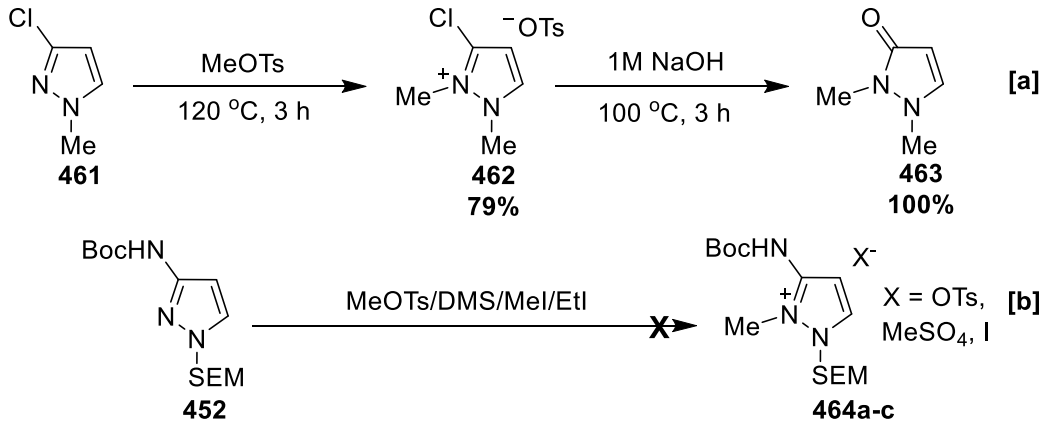

Scheme 31: Quaternisation of Pyrazoles with Other Alkylating Reagents

Consistent with attempts to deprotect **451** and **457**, a range of conditions led to the fragmentation of the target **468** to unknown by-products (Scheme 32c). It is noteworthy is that all of the SEM-protected substrates which decompose during deprotection contain N-H bond(s). Therefore, it was speculated that the sensitivity of each substrate toward deprotection reflected an unknown instability associated with this functional group.

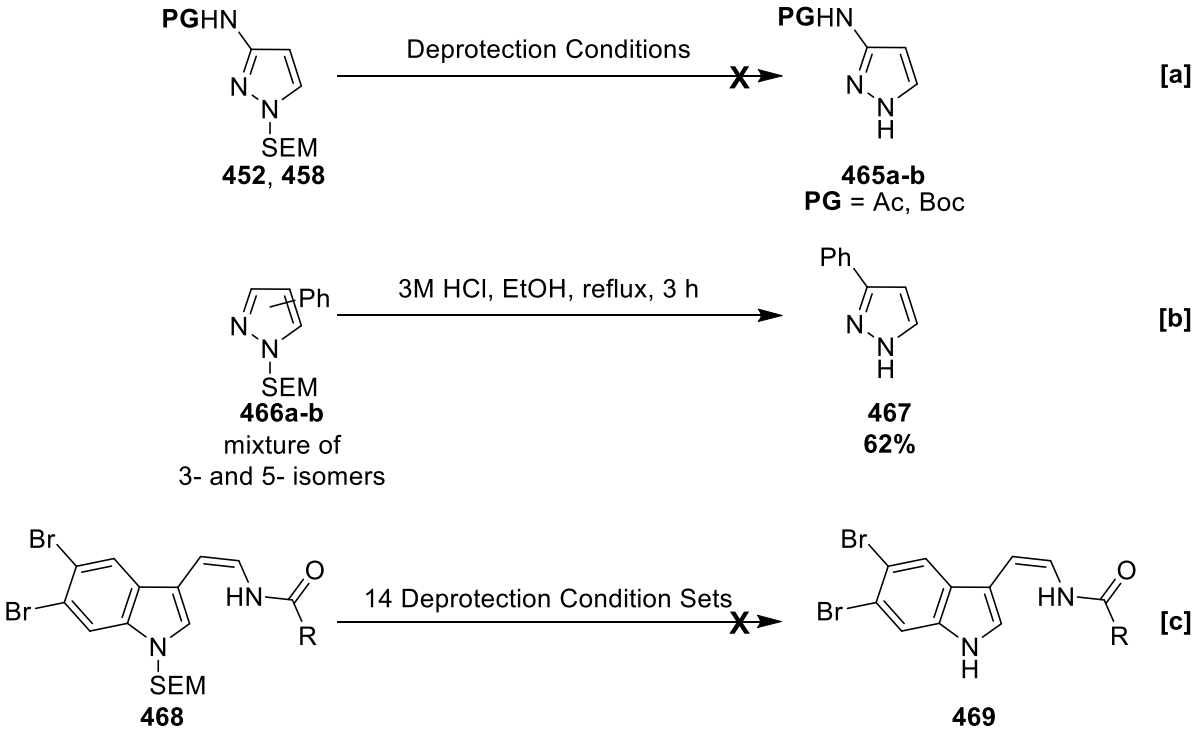

Scheme 32: Attempts at SEM Deprotection in Different Systems

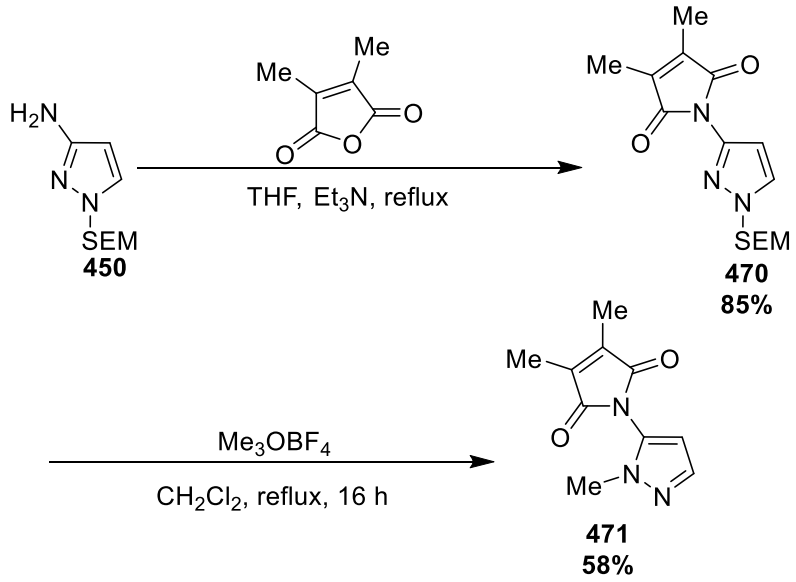

Scheme 33: Successful Protecting Group Switch of Maleimide **470**

Consequently, it was suggested that double-protection of the primary amine in **450** may facilitate the intended protecting group switch process. To test this, **450** was treated with 2,3-dimethylmaleic anhydride in basic refluxing THF, which furnished doubly-protected maleimide **470** in high yield. Two bands at 1729 and 1705 cm^{1} attributed to the symmetric and asymmetric stretches of the imide were displayed in the IR spectrum, and provided good evidence for the successful protection. The same protection could be performed “on water”, affording **470** in 95% yield. With **470** in hand the quaternisation was subsequently attempted under standard conditions with Me_3OBF_4. However, the product of this reaction was not a pyrazolium salt as expected, and this was evident from the absence of signals in the crude ^{19}F and ^{11}B NMR spectra. Following chromatographic purification, switched product **471** was isolated in moderate yield (Scheme 33). This was evident from the ^{1}H NMR spectrum, in which a single CH_3 signal at 3.71 ppm could be observed. Furthermore, there were no signals originating from a SEM group. Evidence for the presence of a maleimide was displayed in the IR spectrum as two bands at 1731 and 1708 cm^{-1}, which were attributed to the symmetric and asymmetric C=O stretches. Furthermore, the identity of **471** was confirmed via an independent synthesis via the direct “on water” protection of **380**. Pleasingly, the data obtained for both compounds from each experiment was identical (Scheme 34). Since an intermediate pyrazolium salt was not observed following prompt analysis, it was speculated that the SEM group may collapse during the reaction or upon exposure to adventitious moisture. From this study, it was concluded that it was the presence of N-H bonds that had impeded the protecting group switch, and double protection overcame this challenge.

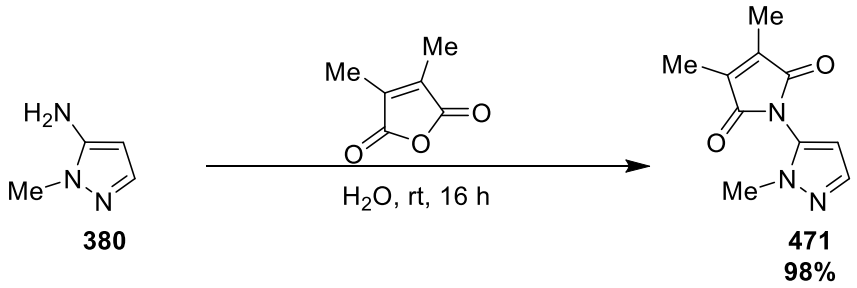

Scheme 34: Independent Synthesis of Imide **471**

Having successfully conducted a protecting group switch which employed a maleimide group as a suitable amine protector, it was necessary to test this group in a C-H borylation sequence. Therefore, attention was subsequently turned to the C-H borylation of maleimide protected aminopyrazole **470**. Under standard conditions, this afforded exclusively C-5 borylated products in excellent NMR yield (Scheme 35). However, a significant amount of reduction at the maleimide during the reaction led to a complex and intractable product mixture. The generation of the three boronates was evident by the presence of three sets of signals corresponding to analogous protons environments in each product found in the crude ^{1}H NMR spectrum. In particular, the presence of three overlapping boron-shifted singlets at 6.77 and 6.78 ppm indicated C-5 selectivity, and new characteristic multiplets at 2.52-2.62 and 3.05-3.04 were assigned as the imide C-H protons. Furthermore, three peaks were displayed in the crude EI GCMS chromatogram, each with m/z = 376.2, 376.2, and 374.2, respectively. Accordingly, these masses were attributed to the $[M]^{+}$ ions of the boronates **472**, **473a**, and **473b**. An attempt to cross-couple this mixture with 4-bromotoluene also led to a complex product mixture.

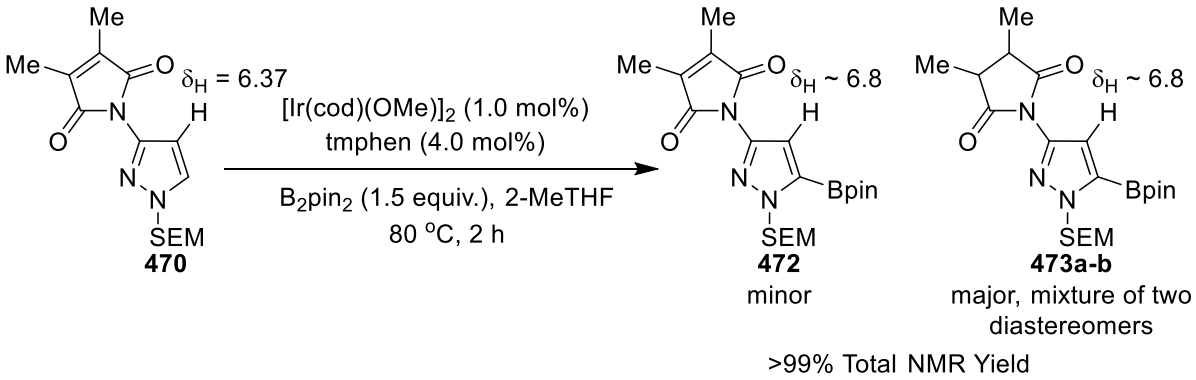

Scheme 35: C-H Borylation of **470**

Whilst the maleimide protecting group had facilitated the protecting group switch, it was not tolerated in the C-H borylation. In order to overcome this challenge, an alternative protecting group was considered. It was hypothesised that a succinimide protecting group would be inert in the C-H borylation whilst providing the required double-protection of the primary amine. As 2,3-dimethylsuccinic anhydride was not commercially available, succinic anhydride was initially selected. To test a protection with this reagent, **450** was treated with succinic anhydride in basic refluxing THF. This led to rapid precipitation of a white solid after 5 min, so the reaction was left for 1 h before removal of the volatiles. Subsequent purification led to the isolation of the linear gamma-amidocarboxylate **474**, in contrast to the facile formation of the corresponding maleimide previously observed under the same conditions (Scheme 36a). This was evident by the presence of a broad O-H stretch at 3296 cm^{-1} in the infrared spectrum. This difference in reactivity was attributed to a larger entropic penalty for cyclisation in **474** owing to the greater conformational freedom of the saturated γ-amidocarboxylate chain. A screen of protection conditions on the less precious N-methyl-5-aminopyrazole including the use of solvents such as PhMe and DMF was undertaken. However, despite the use of catalysts including DMAP and elevated temperatures, this similarly led to the isolation of **474**. It was found that cyclisation of **475** could be facilitated by transforming the carboxyl group into an acid chloride using oxalyl dichloride catalysed by DMF, although this process was accompanied by significant decomposition. Recrystallisation of the crude reaction mixture from EtOH furnished **476**, albeit in low yield (Scheme 36b).

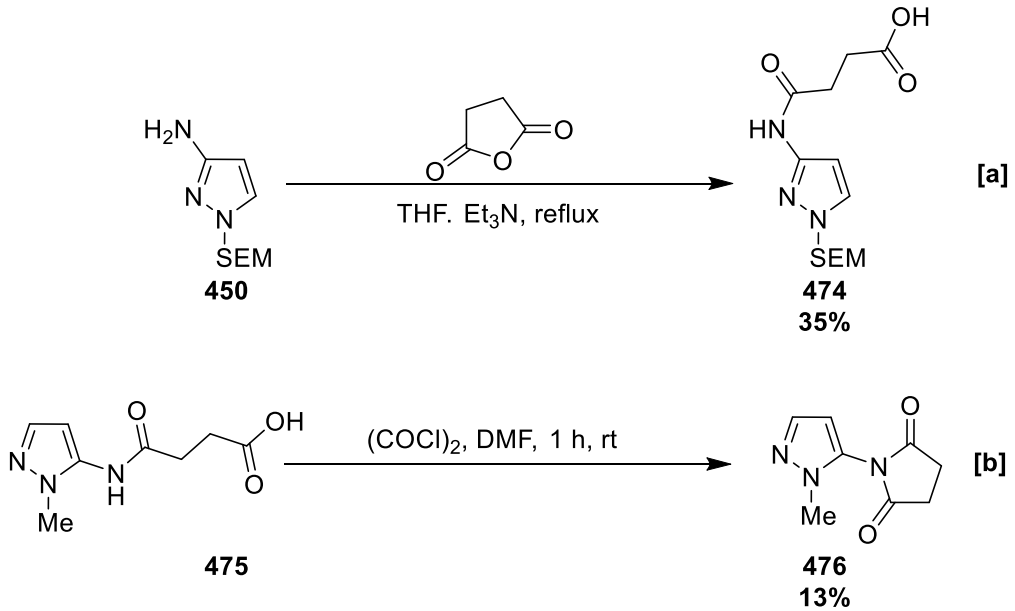

Scheme 36: Installation of a Succinimide Protecting Group

A modified cyclisation was subsequently performed on **474**, which initially formed succinimide **477**. This was evident by the presence of a characteristic succinimide methylene signal at 2.02 ppm in the crude ^{1}H NMR spectrum. Following chromatographic purification **474** was recovered, suggesting that **477** ring-opened during the isolation attempt, and this was unchanged by switching SiO_2 gel for Al_2O_3 gel. This generated concern that **477** may similarly decompose during the Suzuki-Miyaura cross-coupling via base-mediated hydrolysis, so it was subsequently abandoned. This study demonstrated that protection with succinic anhydride was not appropriate for the intended borylation/arylation/switch sequence, so an alternative method was pursued.

Previously, it was established that the C-H borylation tolerates primary amines, so it was hypothesised that the borylation reaction could precede protection. To test this, a one-pot borylation/arylation/protection sequence was conducted. First, **450** was C-H borylated as previously described, and subsequently the crude boronate **451** was arylated using Suzuki-Miyaura cross-coupling with 4-bromotoluene. Following complete conversion of the substrate by TLC analysis, the crude arylated amine **478** was treated with 2,3-dimethylmaleic anhydride, which afforded arylated maleimide **479** in excellent yield over three steps following purification with SiO_2 gel chromatography. The successful cross-coupling was evident from the ^{1}H NMR spectrum, which displayed a singlet at 2.40 ppm attributed to the tolyl CH_3 hydrogens. Furthermore, successful protection was evident from the IR spectrum, which displayed two bands at 1728 and 1713 cm^{1} attributed to the asymmetric and symmetric stretches of the imide. Having successfully circumvented the issue of maleimide reduction during the C-H borylation, attention was subsequently turned to a protecting group switch. Pleasingly, treatment of **479** with Me_3OBF_4 under standard quaternisation conditions afforded the corresponding switched C-3 arylated 5-aminopyrazole **480** in good yield. This was evident by the presence of a singlet at 3.75 ppm in the ^{1}H NMR spectrum, attributed to the NCH_3 hydrogens.

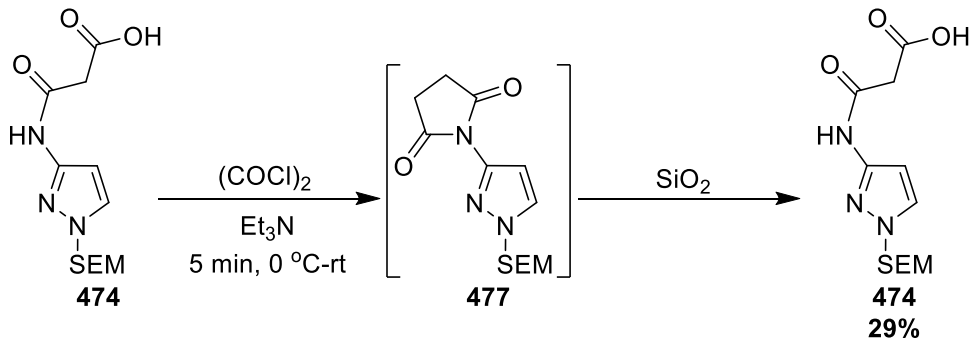

Scheme 37: Cyclisation of Amic Acid **481**

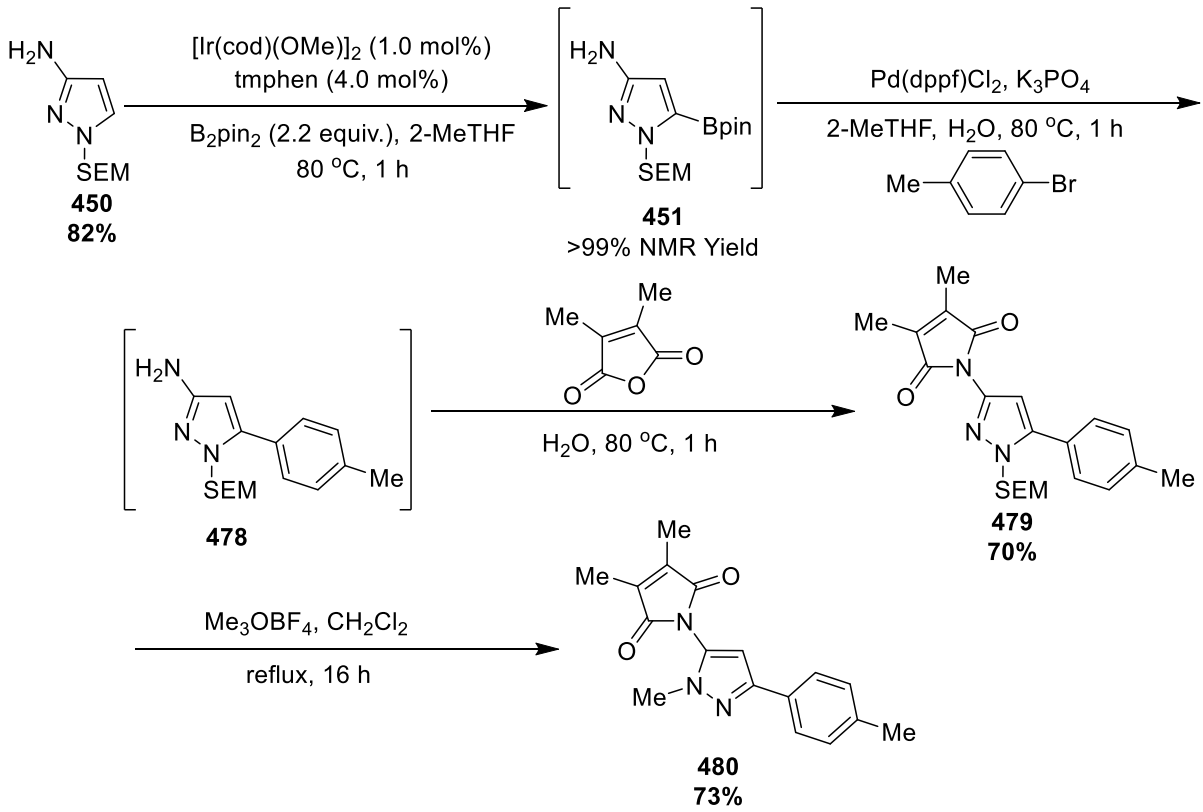

Scheme 38: A Successful C-H Borylation/Arylation/PGS Sequence

As previously described, the C-H borylation of other N-substituted 5-aminopyrazoles was C-4 selective, so the net functionalisation at C-3 was a pleasing result. From this study, it was demonstrated that the developed protecting group switch developed could be efficiently extended to arylated aminopyrazole **479**. Amine double-protection had facilitated a successful borylation/arylation/protection/switch sequence in SEM protected aminopyrazoles. Building on this development, it was hypothesised that groups other than SEM may be suitable for this process, and this was desirable owing to the high cost of SEMCl ($4.60/ mmol, TCI). To test this, our attention first turned to THP-protected aminopyrazole **418**, which was previously synthesised during the study on urea-directed C-H borylation (see section 3.2.2.1) (Scheme 38). Notably, DHP is >hundredfold cheaper ($0.04/ mmol, TCI) than SEMCl.

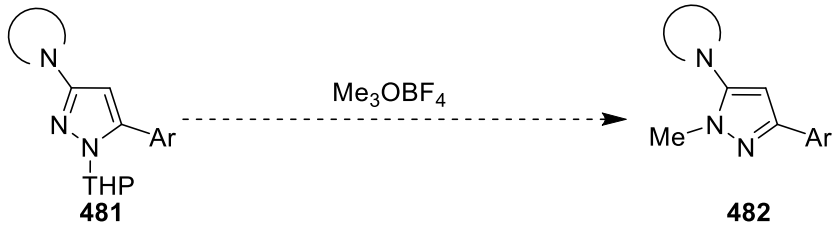

Scheme 39: Hypothesis for the Transposition of a THP Pyrazole

It was previously established that **418** displayed C-5 selectivity in the C-H borylation, and that attempts to arylate the corresponding C-5 THP boronate **419** was challenging. It was suggested that prior protection of the amine may facilitate the Suzuki-Miyaura reaction. Previous studies had shown that succinimide and 2,3-dimethylmaleimide were unsuitable protecting groups, so the installation of a more robust imide was investigated. It was hypothesised that the ring-opening observed in succinimide **477** could be prevented by ring-substitution, as predicted by the Thorpe-Ingold effect (Scheme 40a). To test this, the protection of **418** as the corresponding 2,2-dimethylsuccinimide was investigated. Initial attempts to protect **418** using 2,2-dimethylsuccinic anhydride in basic refluxing THF did not give efficient conversion. However, the use of higher temperatures (refluxing DMF) afforded **485** in high yield (Scheme 40b). A through-space interaction of the pyranyl methine hydrogen with the pyrazole C-5 hydrogen was observed in the 2D ^{1}H-^{1}H NOESY spectrum, and this provided good evidence that no isomerisation had taken place during the reaction. Furthermore, the formation of **485** was evident from ESI LCMS, which displayed a peak with m/z = 278.7 corresponding to the $[M+H]^{+}$ molecular ion. Alternatively, **485** could be synthesised via the selective protection of **369** using 2,2-dimethylsuccinic anhydride in refluxing DMF.

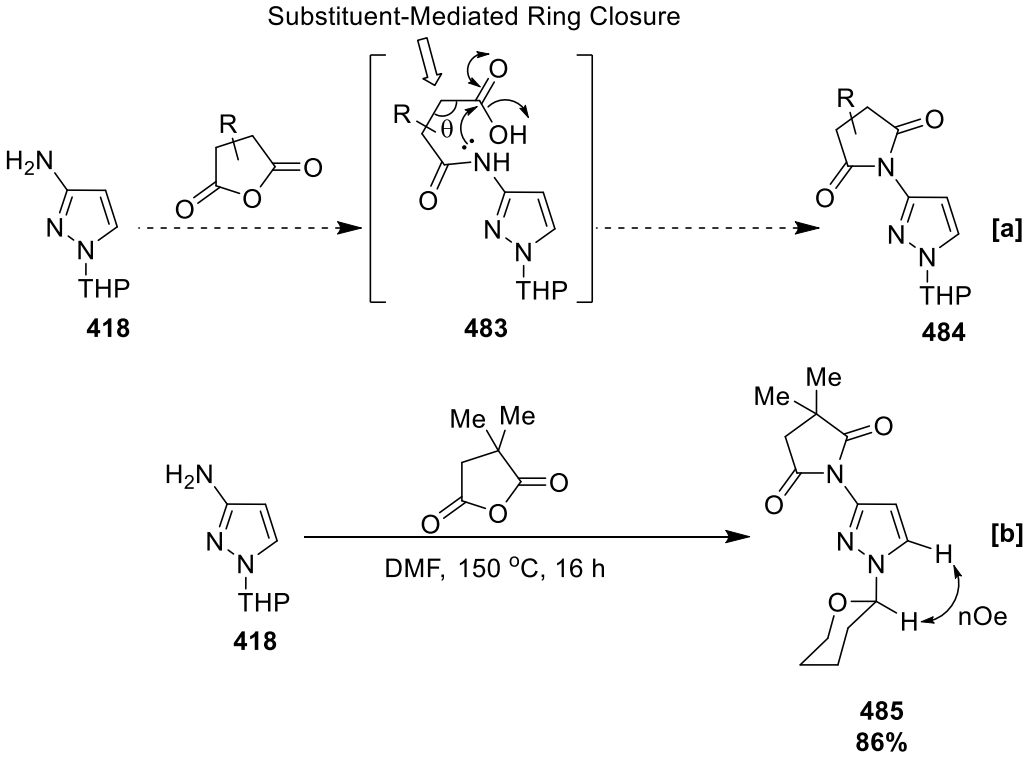

Scheme 40: Installation of a Robust Succinimide Protecting Group

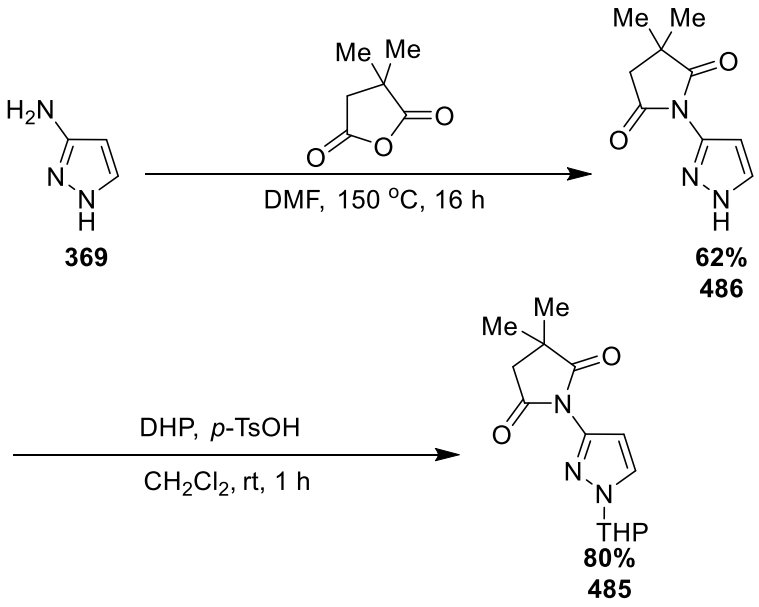

Scheme 41: Improved Synthesis of **485**

The corresponding succinimide **486** was subsequently protected with DHP and *p*-TsOH in CH_2Cl_2, affording **485** in high yield (Scheme 41). The data obtained for the products of both methods was identical. In both cases. Noteworthy is that **485** was purified with SiO_2 gel chromatography, which led to ring opening of the unsubstituted succinimide ring in pyrazole succinimide **477**. This supports the claim that the *gem*-dimethyl substituents kinetically stabilise the imide in **485** toward ring-opening.

With **485** successfully synthesised, attention was turned to the C-H borylation reaction and whether the imide would remain inert. Pleasingly, **485** underwent C-5 functionalisation under standard borylation conditions with 96% selectivity in 86% NMR yield (against 1,3,5-trimethoxybenzene as an internal standard), and this was evident by the presence of a boron-shifted singlet at 6.68 ppm in the crude ^{1}H NMR spectrum. Attempts to chromatographically purify **487** led to protodeborylation, so the crude boronate was arylated with Suzuki-Miyaura cross-coupling (Table 10). Whilst the efficiency of this process was hampered by protodeborylation, the isolation of C-5 arylated adducts **488** was possible. With the arylated adducts **488** in hand, focus was turned to the protecting group switch of a THP-protected aminopyrazole. To test this, the tolyl derivative **488a** was treated with Me_3OBF_4 under standard quaternisation conditions (Scheme 42). Pleasingly, this furnished switch C-5 aminopyrazole **489** in acceptable yield, which was evident by a through-space interaction of the C-4 hydrogen with the tolyl hydrogens in the 2D ^{1}H-^{1}H NOESY spectrum.

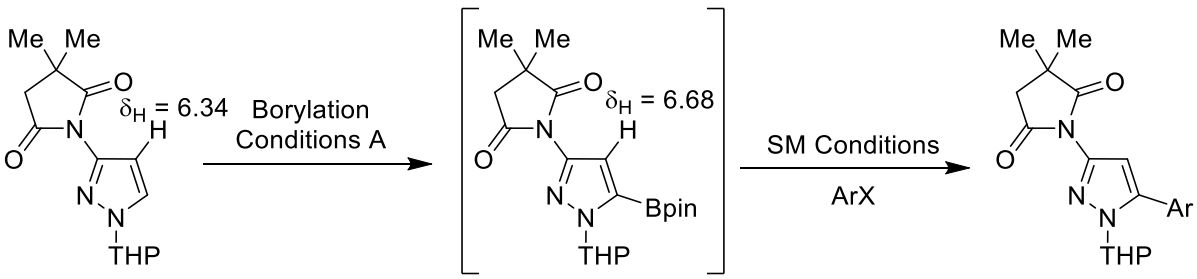

485 **487** **488a-c**

86% NMR Yield

Entry	ArX	SM Isolated Yield /%
1	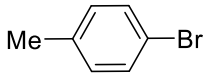	11*
2	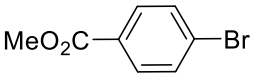	18†
3	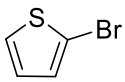	16‡

Borylation Conditions A: $[Ir(cod)(OMe)]_2$ (1.0 mol%), tmphen (4.0 mol%), B_2pin_2 (1.00 equiv.), 2-MeTHF, 80 °C, 2 h
**SM Conditions: $Pd(dppf)Cl_2$, $K_3PO_{4(aq)}$, 2-MeTHF, 80 °C, 2 h, product obtained in 85% isomeric purity.*
† SM Conditions: $Pd(dba)_2$, PCy_3HBF_4, , K_3PO_4, dioxane, 80 °C, 16 h
‡SM Conditions: $Pd(dppf)Cl_2(CH_2Cl_2$ Complex), KOCHO, K_3PO_4, dioxane, 80 °C, 16 h

Table 10: One-Pot Borylation/Arylation of **485**

Whilst the Suzuki-Miyaura cross-coupling would require further optimisation, this study demonstrated that the SEM protecting group switch of aminopyrazoles could also extend to a significantly cheaper THP-protected aminopyrazole. Furthermore, 2,2-dimethylsuccinimide was shown to be a more robust protecting group than the corresponding unsubstituted succinimide due to the Thorpe-Ingold effect. Based on this result, it was subsequently hypothesised that a carbonyl may also be used as an alternative to SEM in a switch process. Notably, N-carbonyl imidazoles such as **490** undergo a related switching process following quaternisation, lending credence to this idea (Scheme 43a).

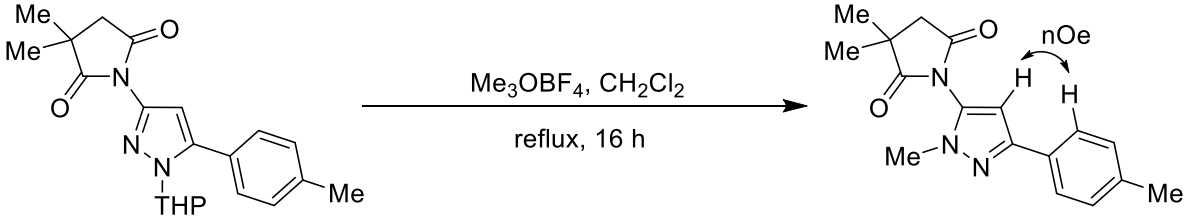

488a **489**
52%

Scheme 42: THP Protecting Group Switch

Attracted by the low cost of Boc_2O ($0.16/ mmol, TCI), Boc was chosen as a potential transposition group. Notably, Boc has been used to direct beta C-H borylation in 3-substituted N-Boc pyrazoles such as **493a** (containing ca. 10% 5-methyl isomer **493b**), so it was predicted that Boc may also facilitate C-H borylation selectivity at C-4 rather than C-5 (Scheme 43b).[8] To test this, the synthesis of Boc pyrazole **496** was investigated. This commenced by treating 3(5)-nitropyrazole **405** with LiHMDS followed by Boc_2O. The serendipitous use of LiHMDS over NaH led to the production of **495** alongside the corresponding Boc protected 5-nitropyrazole isomer in 95:5 ratio (Scheme 44). Accordingly, the major isomer with pyrazole C-H coupling constant 2.9 Hz was assigned to be **495**, whilst the minor isomer with pyrazole C-H coupling constant 2.5 Hz was assigned to be the corresponding N-Boc-5-nitropyrazole. This is discussed in greater detail in section 3.2.3.3. Chromatographic purification followed by recrystallisation enabled the isolation of **496** in modest yield which was analysed by single crystal X-ray diffraction, confirming its structure. Standard Pd-catalysed hydrogenation of **495** afforded amine **496** in good yield, and this was evident from the presence of two bands at 3460 and 3316 cm^{-1} in the infrared spectrum. With the target amine **496** in hand, the C-H borylation was subsequently investigated. Using tmphen and B_2pin_2, this led to formation of C-4 functionalised boronate **497** in excellent NMR yield. This regiochemistry was evident from the crude ^1H NMR spectrum, which displayed a boron-shifted singlet at 8.08 ppm.

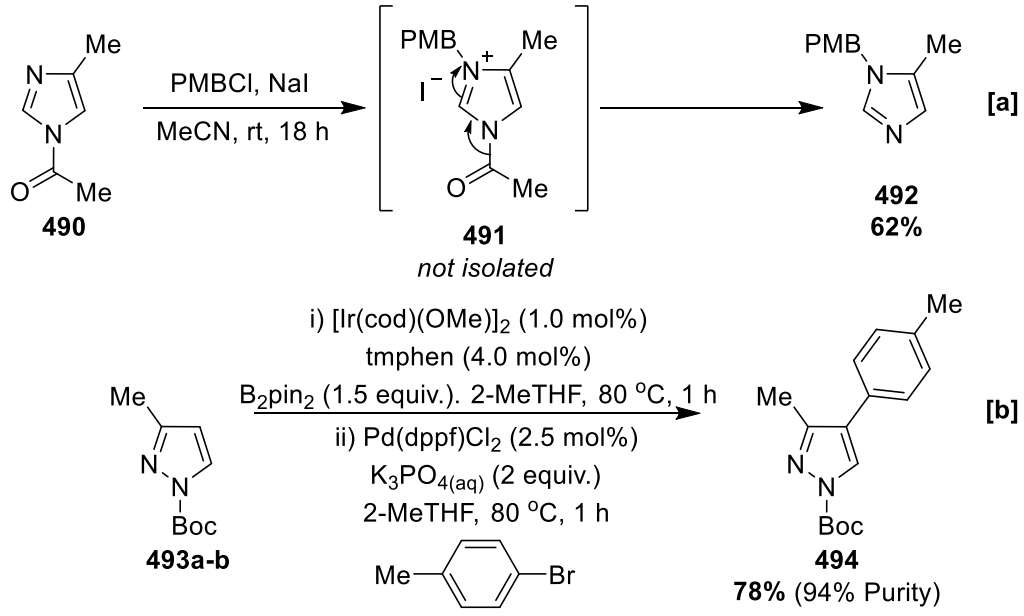

Scheme 43: Reactions of Acylated Azoles

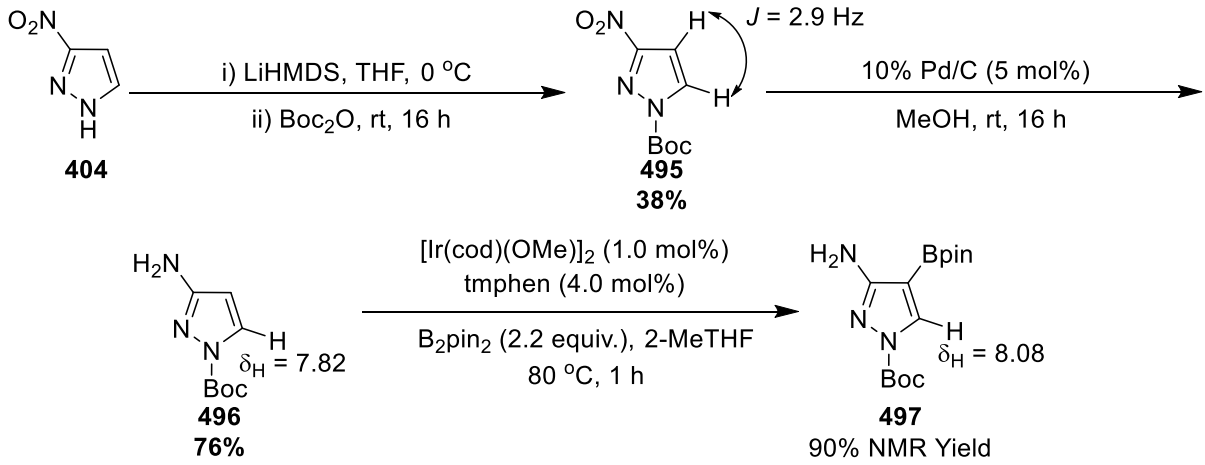

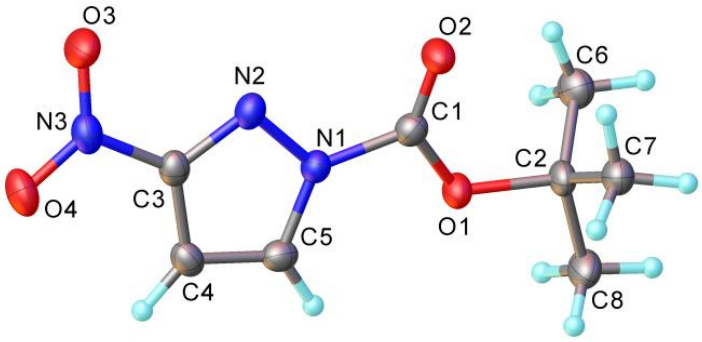

495

Scheme 44: Synthesis and C-H Borylation of Boc Pyrazole **495**

Attempts to protect and arylate crude boronate **497** led to substrate decomposition, so the route was redesigned to include the installation of a 2,2-dimethylsuccinimide protecting group prior to the C-H borylation and arylation reactions. It was hypothesised that the high steric requirement of 2,2-dimethylmaleimide may alter the C-4 C-H borylation selectivity. In order to investigate this, 3-succinimidepyrazole **486** was treated with Boc_2O and DMAP in MeCN. After 1 h, the presence of the 3- and 5-substituted Boc protected isomers in a 9:1 ratio was evident from the crude ^1H NMR. This isomer assignment was made based on the pyrazole C-H ^3J coupling constants, which were measured to be 2.8 Hz in the major isomer **498**, and 2.3 Hz in the minor isomer **499**. The selectivity of this process was increased to >99:1 by leaving the reaction for 16 hours, suggesting that the reaction conditions may promote equilibration between the two isomers (Scheme 45a). Next the C-H borylation of **500** under standard conditions was investigated. Surprisingly, C-4 functionalised boronate **501** was afforded with 95% selectivity in 90% NMR yield and could be isolated in 76% yield (Scheme 45b).

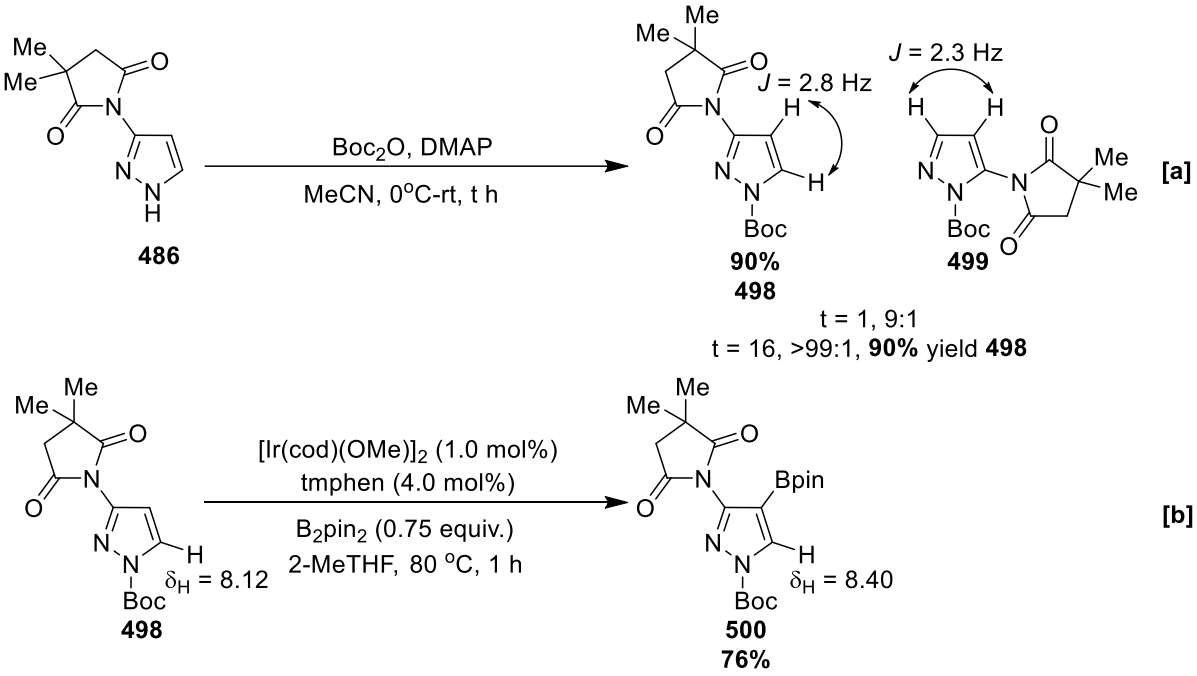

Scheme 45: Synthesis and C-H Borylation of Boc Pyrazole **498**

The regiochemistry was evident by a boron-shifted singlet at 8.40 ppm in the purified ^{1}H NMR spectrum. Furthermore, no C-4 carbon signal at *ca.* 100 ppm was observed in the ^{13}C NMR spectrum, which is consistent with the peak-broadening effect of boryl substituents on carbon atoms.

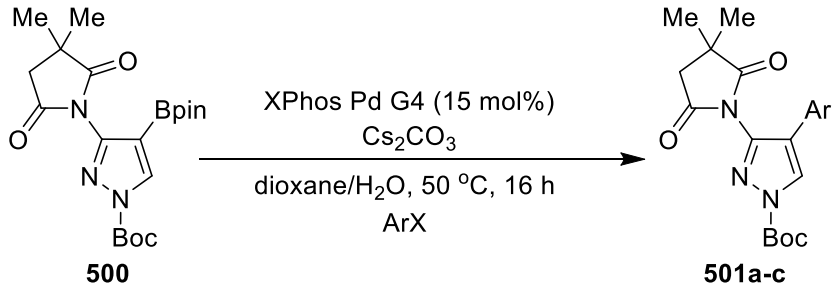

Entry	ArX	SM Isolated Yield /%
1	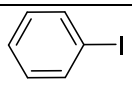	49
2	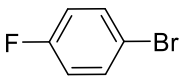	66
3	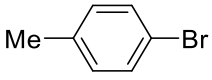	35

Table 11: Suzuki-Miyaura Arylation of **500**

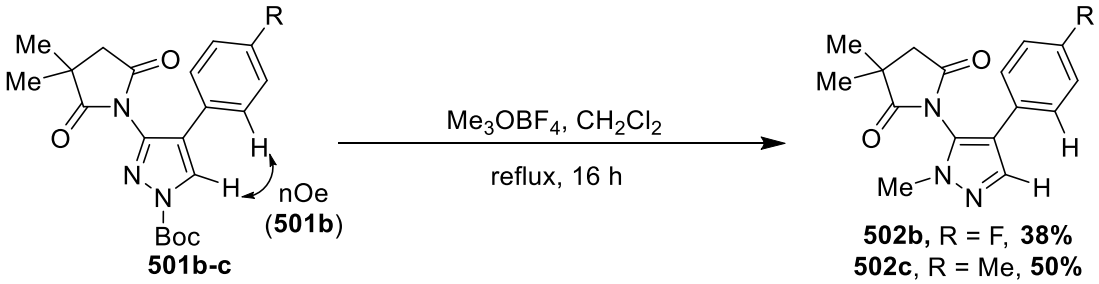

Scheme 46: PGS of Boc Pyrazoles **501**

Our next focus became to arylate the purified boronate **500** with Suzuki-Miyaura cross-coupling, and this pleasingly afforded arylated adducts **501a-c** in moderate yields (Table 11). This was evident in the synthesis of **501b** by an nOe interaction between C-5 and the *ortho* aryl C-H. One-pot borylation/arylation produced the arylated adducts in lower yields. Having successfully arylated the C-4 position in **498**, the protecting group switch of **501b** and **501c** was subsequently investigated under standard alkylation conditions using Me_3OBF_4 (Scheme 46). Pleasingly, this led to the formation of switched aminopyrazoles **502a** and **502b**, and this was evident by the appearance of a signal at 3.73 and 3.71 ppm in each ^1H NMR spectrum attributed to the NCH_3 hydrogens, respectively. It was surprising that the seemingly high steric requirement of the succinimide in **498** did not alter the C-4 C-H borylation selectivity conferred by Boc. This led to a small study which sought to understand the origin of this C-H borylation beta direction to form **500**. DFT calculations predicted that the succinimide ring in **498** twists out of planarity with the pyrazole ring, reducing the steric congestion at C-4 incurred by the succinimide (Figure 9). Furthermore, it was hypothesised that the tBu group in **498** may block C-5 and deliver C-4 selectivity on steric grounds. To test this, replacement of the tBu with OMe and Me was conducted via the synthesis of **503** and **505**, respectively (Scheme 47).

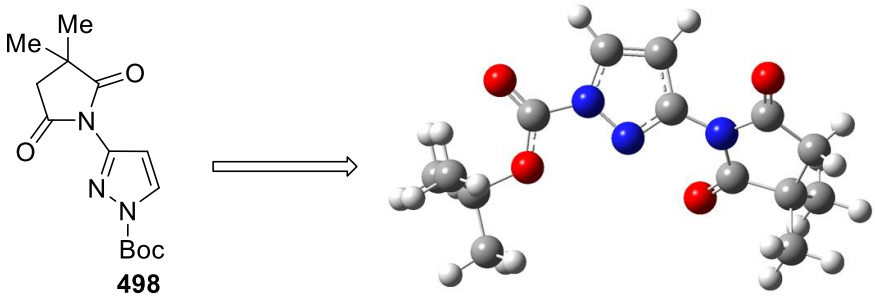

Figure 9: Calculated Ground State DFT Representation of **498**

This was performed using similar procedures to the synthesis of Boc analogue **498**. In each acylation reaction, the concurrent formation of the corresponding 5-aminopyrazole isomer was evident in crude ^{1}H NMR spectra, which permitted the structural assignment of **503** and **505** based on pyrazole C-H ^{3}J coupling constants. However, both major isomers could be obtained as single components following chromatography. Following the synthesis of these two control aminopyrazoles, the C-H borylation reactions were investigated. In the C-H borylation of these two compounds, some evidence of C-4 selectivity was displayed by appropriately boron-shifted singlets in the crude ^{1}H NMR spectra (Scheme 48). However, the poor (<10% conversion) borylation activity of both pyrazoles necessitate further investigation, which was not possible in the timeframe of this project.

This study demonstrated that alongside THP and SEM, Boc may also be employed as a protector for the protecting group switch of aminopyrazoles. Unlike the former two groups, Boc directs borylation to C-4, despite the presence of a bulky succinimide. This provided an alternative route for the synthesis of C-4 arylated 5-aminopyrazoles **502** (see section 3.1.2). Provisional control experiments provided some evidence to suggest that this selectivity may be electronic in origin, although this requires further study.

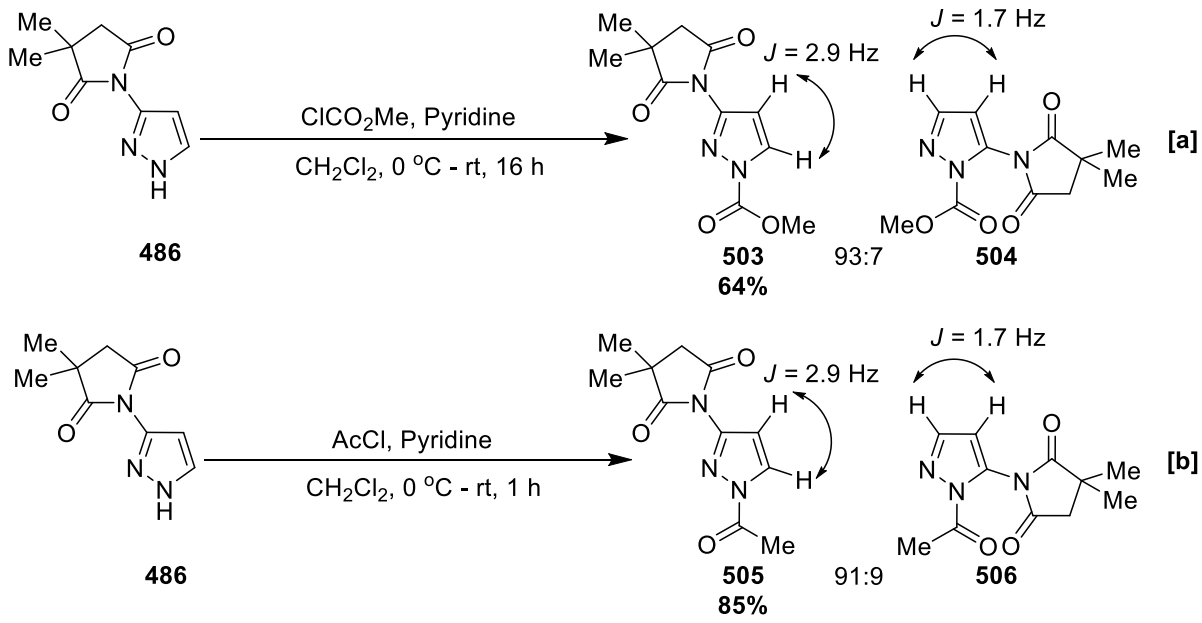

Scheme 47: Synthesis of N-Carbonyl Aminopyrazole Controls

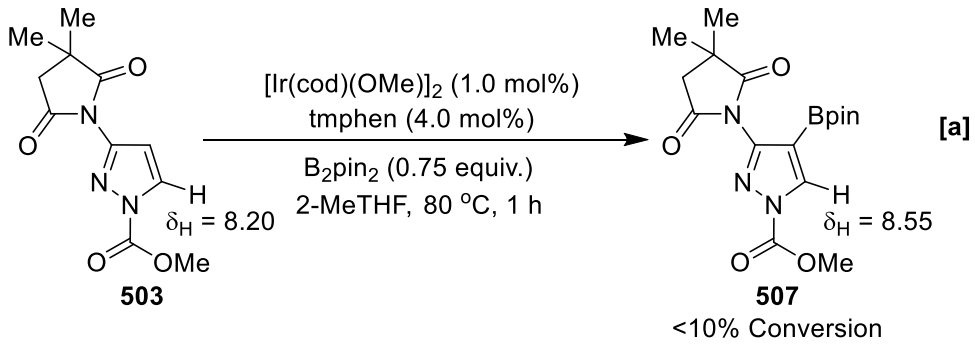

Scheme 48: Control C-H Borylations

3.2.3.2.1.1 Other Studies

Concurrent with the successful approach described above, other avenues were pursued in an effort to facilitate a protecting group switch of 3-aminopyrazolium salts. It was hypothesised that previously synthesised nitropyrazole **449** could act as a suitable amine surrogate and facilitate a SEM switch (Scheme 49a).

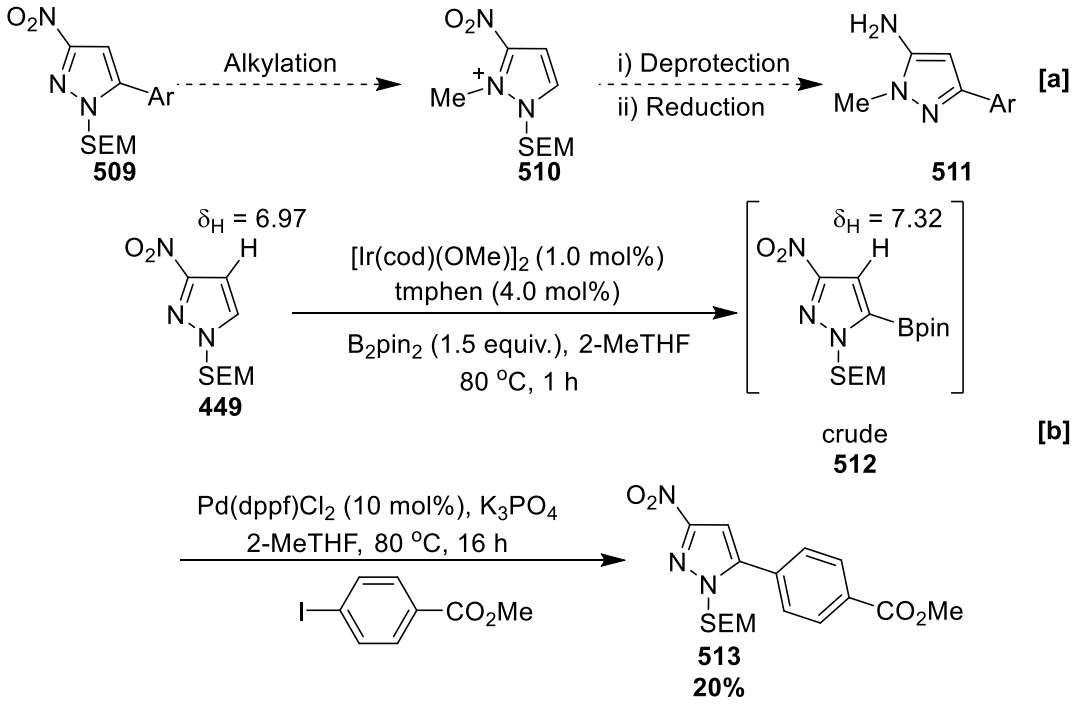

Scheme 49: A "Nitro" Strategy for a Protecting Group Switch

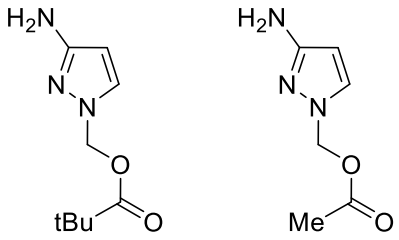

514 **515**

Figure 10: Aminopyrazoles with other Azole N-Protecting Groups

However, NO_2 is commonly considered to be too oxidising to be tolerated in the C-H borylation, so the substrate activity was initially investigated. Surprisingly, **449** underwent rapid (<5 min) borylation under standard conditions, forming C-5 boronate **512** exclusively. This was apparent from the crude ^{1}H NMR spectrum, which displayed a boron-shifted singlet at 7.32 ppm attributed to the C-4 hydrogen. Subsequent Suzuki-Miyaura cross-coupling of the crude reaction mixture under standard conditions with methyl 4-iodobenzoate led to complete protodeborylation. Through experimentation, it was discovered that a rapid deborylation event occurred upon addition of H_2O, so it was excluded from the reaction. In conjunction with raising the Pd loading, arylated nitropyrazole **513** could be isolated, albeit in low yield (Scheme 49b). This was evident from the ^{1}H NMR spectrum, which displayed a singlet at 3.96 ppm attributed to the OCH_3 hydrogens. The inefficiency of this process was attributed also to protodeborylation, suggesting that this process may also be promoted by one of the other reagents. Whilst further optimisation of this sequence may have provided a solution, the maleimide approach described in section 3.2.3.1 proved more novel and this “nitro” strategy was not pursued further. Furthermore, preliminary investigations into the protecting group switch of aminopyrazoles with other azole protecting groups such as methyl pivalate **514** and methyl acetate **515** were halted in the interest of time so that attention could be focused on synthesising the final target isomer of this project via 5-aminopyrazoles (Figure 10).

3.2.3.2 5-Aminopyrazoles

As discussed in section 3.2.3.1, appropriately protected 3-aminopyrazoles undergo efficient C-H borylation with excellent selectivities. The pyrazole boronates may be arylated with Suzuki-Miyaura cross-coupling and subsequently quaternised/deprotected *in situ*, affording switched aminopyrazole products. Our next focus became to apply this method to 5-aminopyrazoles in order to synthesise target isomer **519** with a greater efficiency than offered by the urea-directed process (Scheme 50).

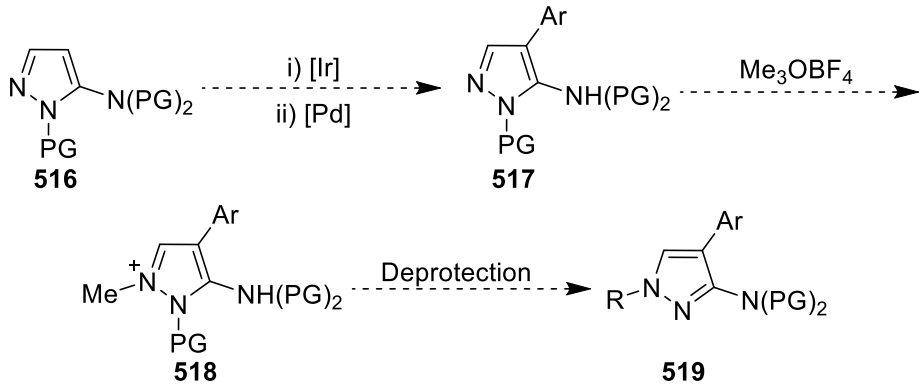

Scheme 50: Hypothesis for the Synthesis of Target **519**

However, this presents a greater challenge because the N-functionalisation of 3(5)-substituted pyrazoles generally carries greater selectivity for the less hindered 3-substituted isomer (Scheme 51a). Furthermore, some 5-aminopyrazoles such as **523** are known to thermally isomerise into the corresponding 3-aminopyrazole isomer **524** (Scheme 51b).[20] Aware of these potential challenges, the initial goal was to synthesise N-SEM-5-aminopyrazole **526** in order to ultimately conduct a SEM switch. At the time, nitropyrazole **525** was a novel compound so a new synthesis of this precursor was required. Previously, it was noted that the use of LiHMDS in the acylation of 3(5)-nitropyrazole **404** gave a mixture of 3- and 5-subsitituted isomers. Therefore, **404** was treated with LiHMDS followed by SEMCl in THF, and this pleasingly furnished a mixture of two 3- and 5-substituted isomers **525** and **450** (Scheme 52a). These were distinguished based on the relative magnitudes of the ^{3}J pyrazole C-H coupling constants. By performing the reaction at room temperature, higher selectivity for the desired isomer was obtained, and chromatographic separation led to the isolation of **525** in acceptable yield.

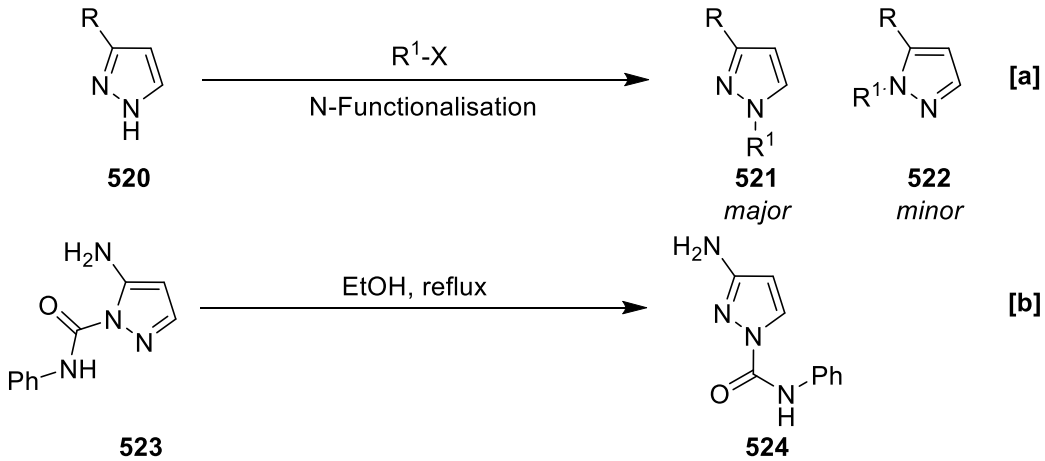

Scheme 51: Challenges Associated with 5-Substituted Pyrazoles

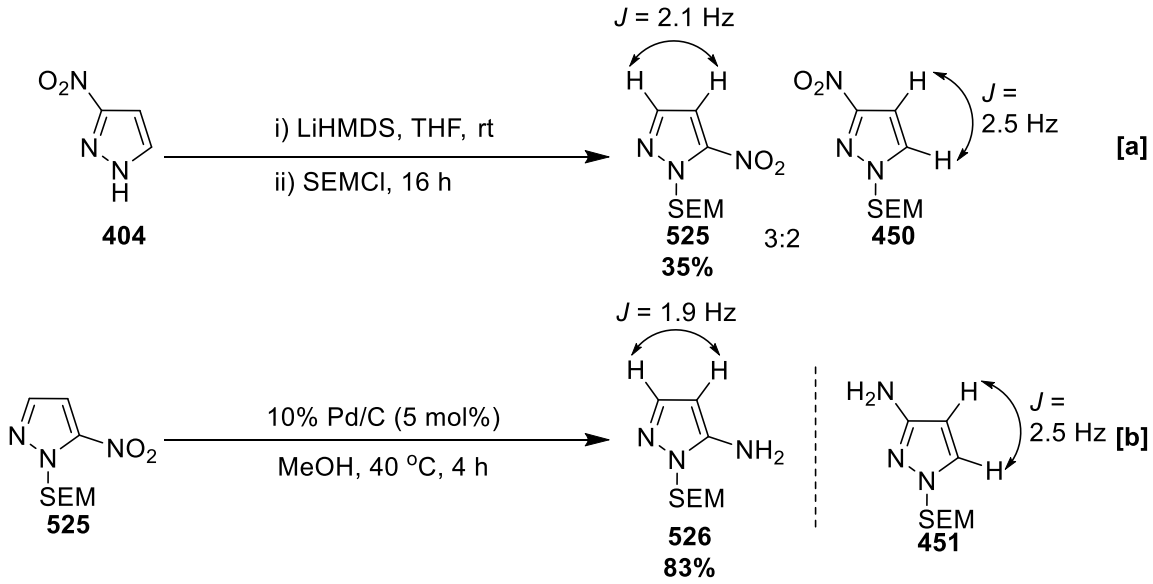

Scheme 52: Synthesis of 5-Aminopyrazole **526**

Subsequently, **525** was reduced to 5-aminopyrazole **526** in high yield with Pd-catalysed hydrogenation (Scheme 52b). The structural assignment of **526** was supported by the distinct ^{1}H NMR shifts and coupling constants from the corresponding 3-aminopyrazole isomer **450**. In particular, the ^{3}J pyrazole C-H coupling constant was measured in **526** to be 0.6 Hz lower than in **450**. With the 5-aminopyrazole **526** in hand, focus turned to the C-H borylation.

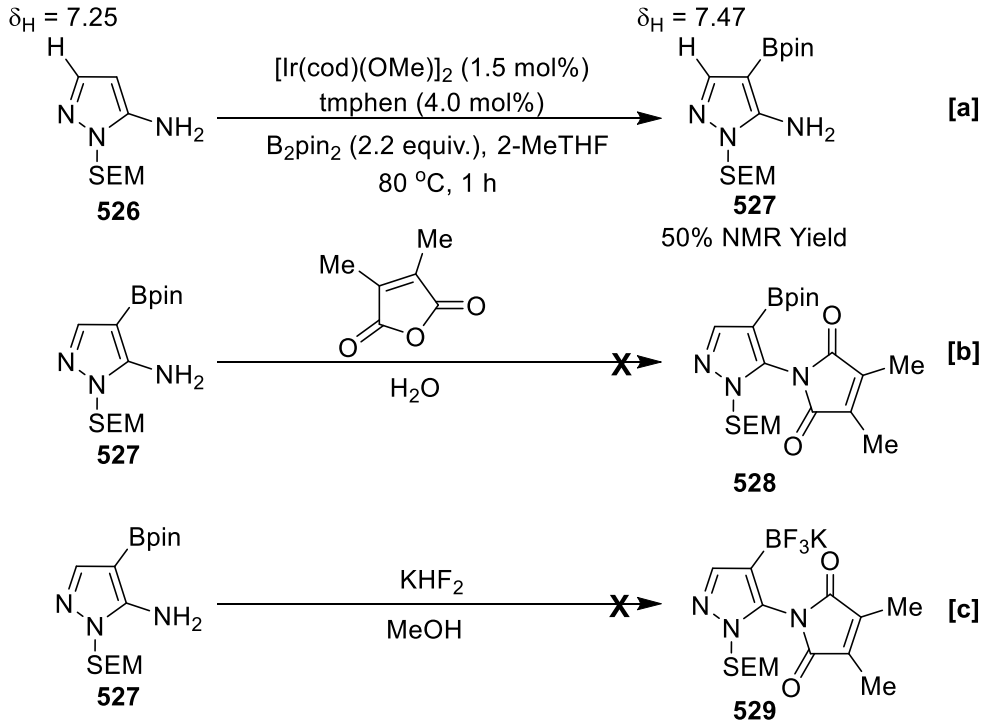

Scheme 53: Synthesis and Derivatisations of **527**

Initial experiments afforded C-4 functionalised boronate **527** in 50% NMR yield, and this was evident by the appearance of a boron-shifted singlet at 7.47 ppm in the crude ^{1}H NMR spectrum (Scheme 53a). The fate of the rest of the material was not clear, and isomerisation was not observed. Numerous attempts to chromatographically isolate and arylate boronate **527** led to decomposition and protodeborylation, so various protection experiments were conducted in order to resolve this. Attempts to install 2,3-dimethylmaleimide led to no conversion at low temperature, whilst elevated temperature led to protodeborylation (Scheme 53b). It was suggested that the congested environment of the primary amine was responsible for this, so crude boronate **527** was treated with KHF_2 in order to covert the Bpin group to the smaller and typically more stable BF_3K group (Scheme 53c). Unfortunately, this also led to protodeborylation, and **529** was not detected. Since protection of the crude boronate proved difficult, the next focus became to protect **526** prior to the C-H borylation. However, it was suggested that the imide protecting groups previously employed in the 3-aminopyrazole series may alter the C-4 C-H borylation selectivity obtained for **526** on steric grounds. In order to prevent this issue, mono-protection was initially attempted with the goal to protect a second time following the arylation reaction and prior to the protecting group switch. Initial protection experiments focused on synthesis of Boc carbamate **530**. Unfortunately, repeated attempts at the Boc-protection of **526** under a variety of protocols did not proceed, and the use of elevated temperatures led to decomposition into unknown materials. However, it was found that by treating **526** with Boc_2O, DMAP, and Et_3N in CH_2Cl_2 for an extended period followed by chromatography over base-treated SiO_2 gel afforded **530** with 37% crude mass recovery.

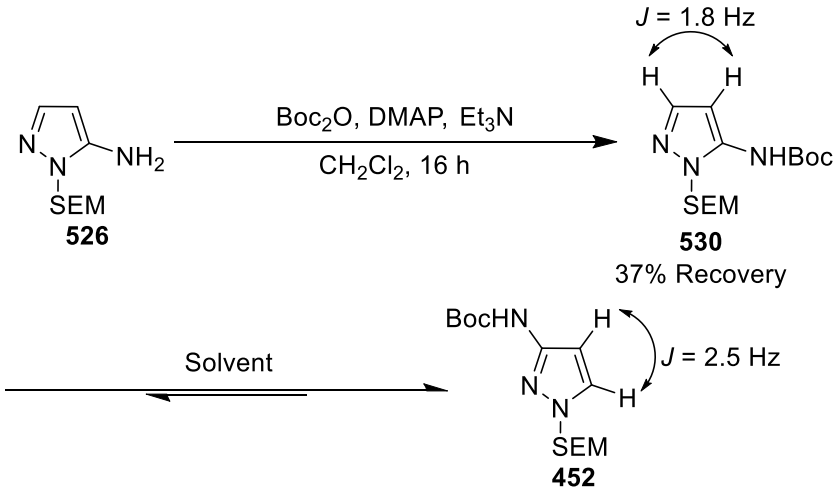

Scheme 54: Synthesis and Isomerisation of **530**

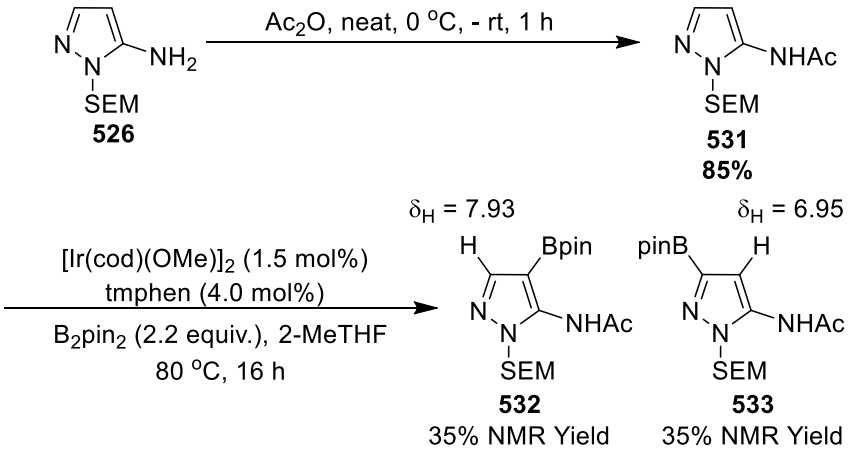

Scheme 55: Synthesis and C-H Borylation of **531**

This was evident from differences in the ^{1}H and ^{13}C NMR data between **530** and previously synthesised **452**. Further attempts to manipulate **530** including dissolution in organic solvent led to isomerisation affording **452**, precluding an investigation into the C-H borylation. Based on these observations, further attempts to synthesise and isolate **530** were halted so that the protection of aminopyrazole **526** as other carbonyl derivatives could be investigated. It was hypothesised that the protection of **526** as acetamide **531** may be more facile, owing to the greater reactivity of reagents used for acetylation (Ac_2O, AcCl) when compared to Boc_2O. To test this, **526** was treated with neat Ac_2O dropwise at reduced temperature. After 1 h, the substrate had been consumed by TLC analysis, and **531** was isolated following purification (Scheme 55). This was performed using base-treated SiO_2 gel in order to prevent decomposition. In contrast to carbamate **530**, no isomerisation of acetamide **531** was observed even after refluxing for prolonged periods in 2-MeTHF. With the successfully protected 5-aminopyrazole in hand, attention was turned to the C-H borylation reaction. Under standard conditions, the borylation of **531** was relatively sluggish, and produced two boronates **532** and **533** in a total NMR yield of 70% (Scheme 55). This was evident from the crude ^{1}H NMR spectrum, which displayed two boron-shifted singlets at 7.93 ppm and 6.95 ppm. Furthermore, two peaks were displayed in the EI GCMS chromatogram, and both possessed m/z = 381.2 attributed to the $[M]^{+}$ ions of the products. Unfortunately, further characterisation was precluded by decomposition into unknown species during chromatographic purification and Suzuki-Miyaura cross-coupling.

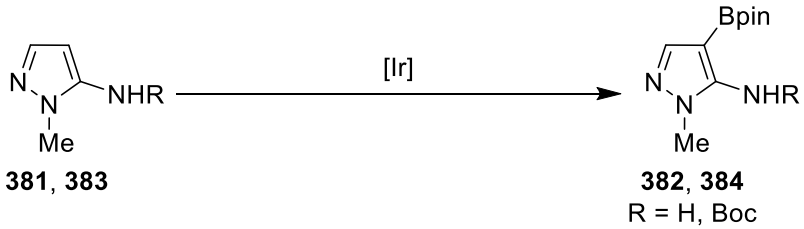

381, **383** **382**, **384**
R = H, Boc

Scheme 56: C-4 Selective C-H Borylation of **381** and **383**

The non-selective C-H borylation of acetamide **531** suggested that C-4 selectivity observed in **381** and **383** may be controlled by an *ortho* directing effect (Scheme 56). Given the challenges that were encountered using SEM as an azole protecting group, focus was turned to the installation of a more robust alternative. Owing to previous success with Boc as an azole N protecting group, the synthesis of Boc-protected aminopyrazole **534** was subsequently investigated. (Scheme 57).

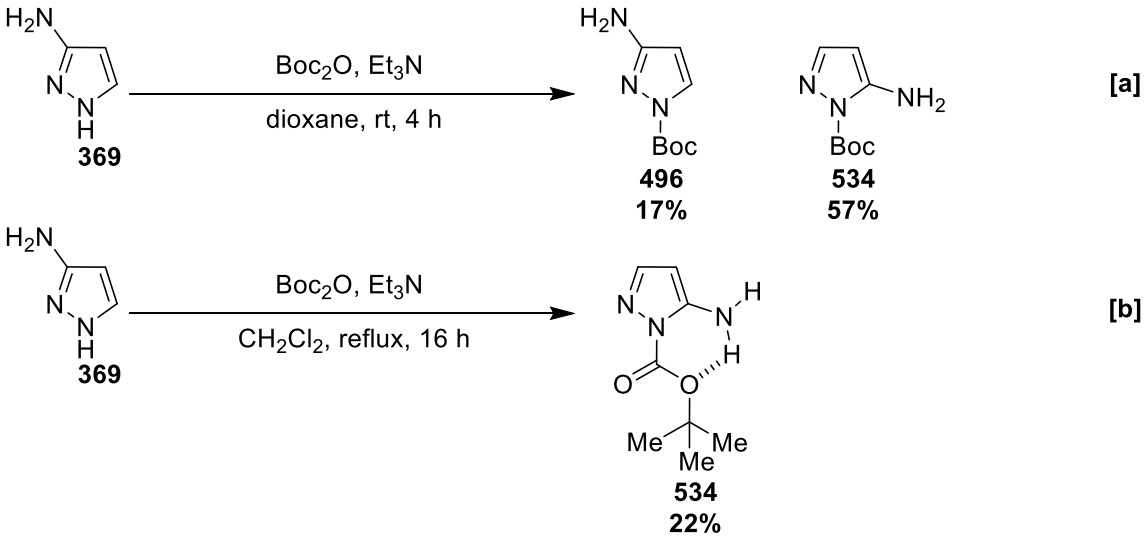

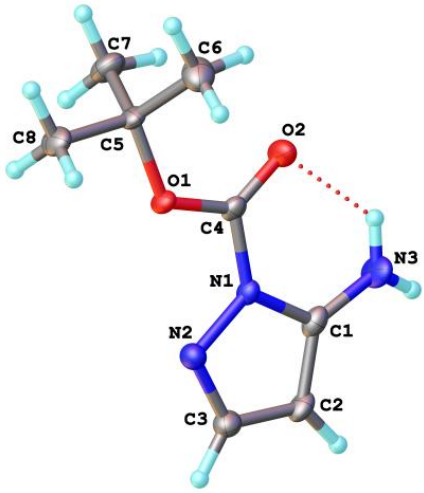

534

Scheme 57: Synthesis and X-ray Structure of **534**

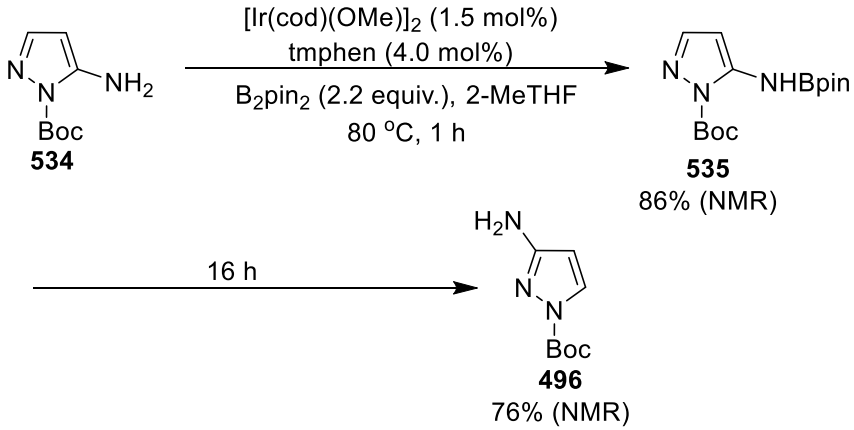

Scheme 58: C-H Borylation of **534**

The synthesis of **534** had previously been reported in a patent by Berthel in good yield alongside a minor quantity of regioisomer N-Boc-3-aminopyrazole **496** (Scheme 57a). Under modified conditions, **534** was produced in 75% isomeric purity alongside 3-substituted isomer **496**, although difficulties during chromatographic separation led to a low isolated yield. Confirmation that the desired regioisomer had been formed was obtained by single crystal X-ray analysis, which unambiguously confirmed the structure of **534**. Interestingly, this indicated a hydrogen-bond between the amine N-H and the carbonyl C=O. Having the synthesised the target aminopyrazole, the next focus became the C-H borylation reaction. Using tmphen and B_2pin_2, two pyrazole doublets and a Bpin CH_3 singlet were observed after 1 h at 7.38, 5.39, and 1.26 ppm in the crude ^1H spectrum, respectively. This was accompanied by the appearance of a signal at 28.2 ppm in the ^{11}B NMR spectrum, and these data suggest that **534** had undergone N-H borylation and not C-H borylation after 1 h. After a further 15 h the volatiles were removed, and ^1H NMR analysis displayed two new doublets at 5.80 and 7.82 ppm with each possessing J = 2.9 Hz coupling constants. These signals are consistent with N-Boc-3-aminopyrazole **496**, so it was concluded that extended reaction times led to isomerisation (Scheme 58).

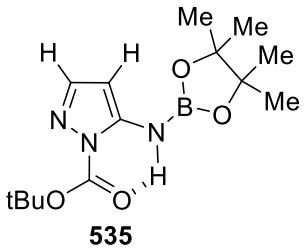

535

Figure 11: Steric Congestion at C-4 Incurred by the Boryl Group

As previously discussed, Boc-protected 3-aminopyrazole **496** is an active substrate and undergoes C-4 selective C-H borylation, so the catalyst must have been rendered inactive at some stage of the reaction. To account for the inactivity of **534**, it was hypothesised that the intramolecular hydrogen-bond may similarly feature in N-borylated adduct **535**. This would position the boryl group in high proximity with the C-4 C-H bond, blocking access of the catalyst (Figure 11). This hypothesis may also be used to explain the poor selectivity obtained in the C-H borylation of acetamide **531**. The lack of C-3 C-H borylation in **534** was attributed to the inhibitory effect of the azinyl N. It was hypothesised that protection of **534** may facilitate C-H borylation activity. However, attempted protections of the amine using either Boc_2O or Ac_2O in the presence of a base were not successful even with elevated temperature, returning the substrate. The use of acyl transfer catalysts such as DMAP and more reactive acylation reagents such as AcCl was also unsuccessful, leading to substrate isomerisation followed by decomposition. Whilst the reasons for the relatively low reactivity of **534** toward protection are unclear, the electron-withdrawing effect of the Boc group may lower the nucleophilicity of the amine.

These challenges led to the investigation of a suitable alternative azole N protector. Owing to the previous success with the developed THP-switch, THP was subsequently selected as the next azole protecting group to be investigated. Therefore, the next target became THP 5-aminopyrazole **537**. Slade has developed the kinetically controlled THP protection of indazoles such as **415** catalysed by PPTS (Scheme 59a).

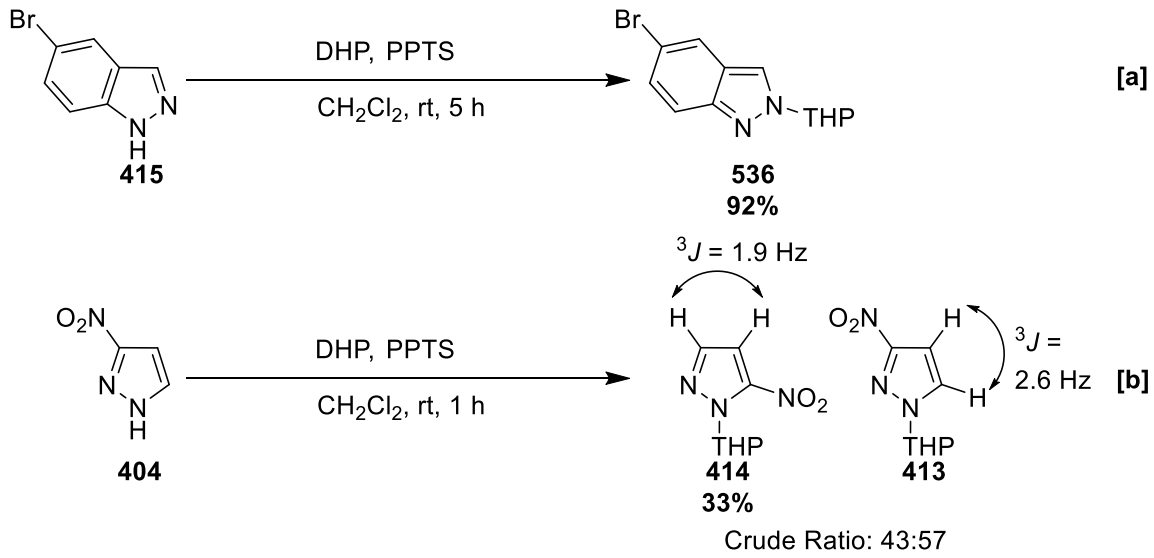

Scheme 59: THP Protection with PPTS

The N-2 selectively functionalised product **536** cannot isomerise under the reaction conditions, which would otherwise be possible with *p*-TsOH (see section 2.2.2). To test the kinetic preference of **404** toward THP protection these conditions were adopted, and this pleasingly afforded THP-protected 5-nitropyrazole **414** alongside 3-substituted isomer **413** in a 43:57 ratio with 80% substrate conversion (Scheme 59b). Chromatographic separation of these isomers led to the isolation of **414** in acceptable yield, and this was evident from the pyrazole C-H ^{3}J coupling constant which was measured to be 0.7 Hz lower than the corresponding coupling in 3-substituted isomer **413**. Subsequently, the reduction of **414** was conducted under Pd/C standard conditions to afford aminopyrazole **537**. Unfortunately, the purification of **537** from a small amount of unidentified contaminants proved challenging and this was attributed to the interaction of the primary amine with the chromatographic media. In order to overcome this challenge, **537** was protected by treating the crude reaction mixture with Ac_2O and Et_3N, which permitted the chromatographic isolation of the acetamide **538** with base-treated SiO_2 gel (Scheme 60). This was evident from an absorption in the infrared spectrum at 1668 cm^{-1}, which was attributed to the amide C=O stretch.

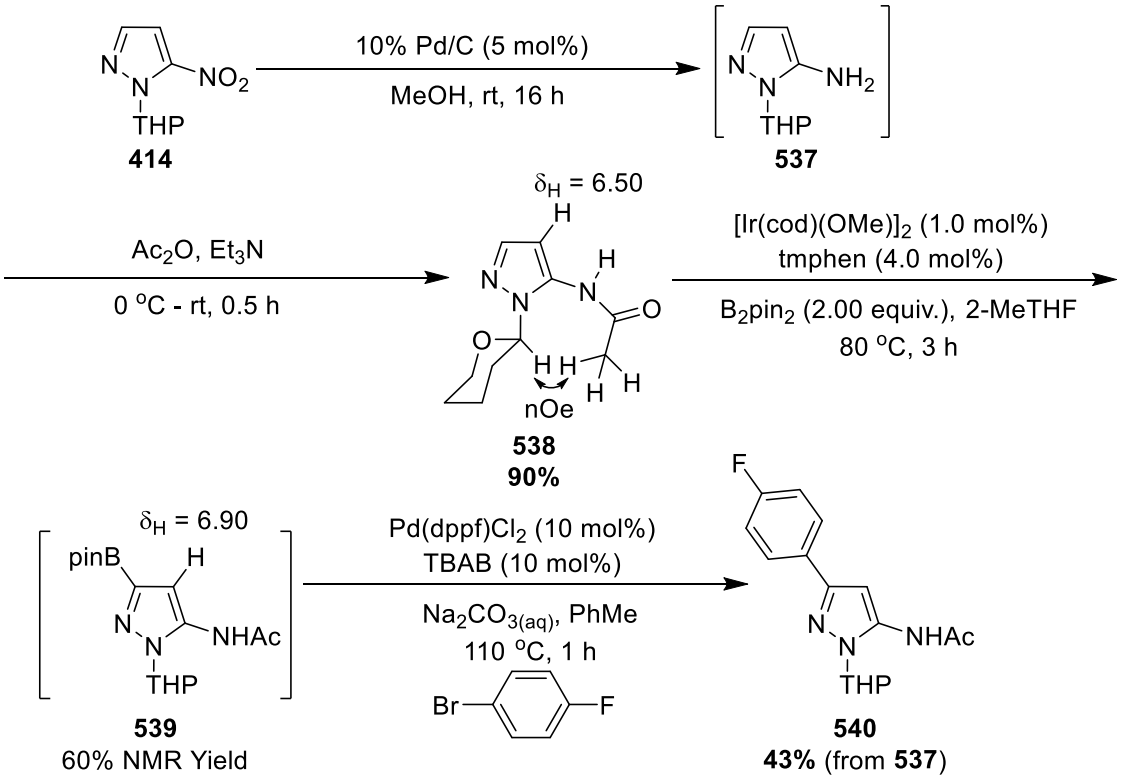

Scheme 60: Synthesis, C-H Borylation and Arylation of **538**

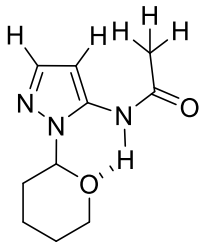

538

Figure 12: Steric Congestion at C-4 Incurred by the Acetamide

Furthermore, the structure of **538** was evident by an nOe correlation of the acetamide CH_3 hydrogens with the pyranyl methine hydrogen in the 2D ^{1}H-^{1}H NOESY spectrum. With the successfully protected pyrazole in hand, the C-H borylation of acetamide **538** became the next focus. This led to exclusive C-H borylation at C-3 alpha to the azinyl N, and this was evident from the crude ^{1}H NMR spectrum which displayed a boron shifted singlet at 6.90 ppm. This process was comparably slower than other C-H borylation reactions of aminopyrazoles, and this likely reflects the inhibitory effect of the azinyl N on the reaction rate. Whilst boronate **539** was not isolated, one-pot Suzuki-Miyaura cross-coupling led to the isolation of arylated adduct **540**. This was evident from the presence of a signal at 95.2 ppm in the ^{13}C NMR attributed to the C-4 carbon. Furthermore, this signal displayed a ^{1}J interaction in the 2D ^{1}H-^{13}C HSQC spectrum with the C-4 hydrogen displayed at 6.88 ppm in the ^{1}H NMR spectrum. In addition, a peak with m/z = 304.1 was found in the ESI LCMS spectrum, which was attributed to the $[M+H]^{+}$ ion. The observation of complete C-3 selectivity in the C-H borylation of **538** was unusual, because previously studied 5-aminopyrazoles displayed reactivity at the *ortho* C-4 site. Based on the intramolecular hydrogen-bond discovered in Boc aminopyrazole **534**, it was suggested that an analogous interaction may position the acetamide over the C-4 C-H bond and sterically block borylation at this site (Figure 12).

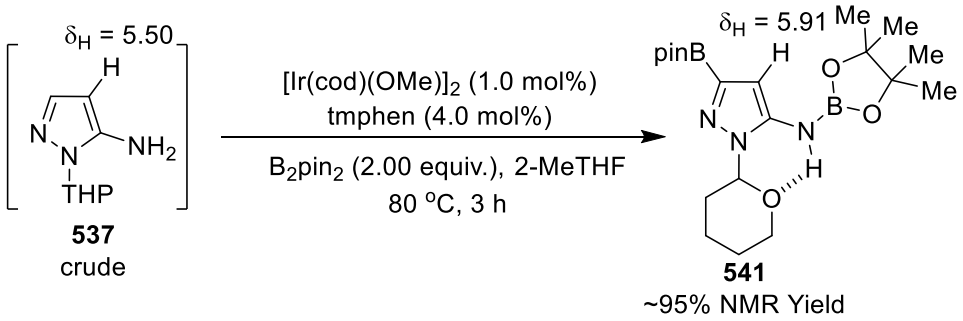

537
crude

541
~95% NMR Yield

Scheme 61: C-H Borylation of Crude Aminopyrazole **537**

However, the nOe interaction observed in **538** between the acetamide and the THP group suggests that the C-3 C-H borylation selectivity may not originate from another effect. To gain a further understanding of this regiochemistry, the C-H borylation of crude amine **537** was investigated (Scheme 61). Monitoring experiments with EI GCMS after 1 h displayed peaks with m/z = 167.1 and 293.2 attributed to the $[M]^+$ ions of the substrate and a monoborylated product, respectively. After 3 h, the ^{1}H NMR spectrum displayed a single boron-shifted singlet at 5.91 ppm with no evidence of **537** or isomerisation into a 3-aminopyrazole derivative. Evidence for N-H borylation and C-H borylation to form **541** was displayed as two singlets at 1.26 and 1.30 ppm in the crude ^{1}H NMR spectrum, attributed to the NBpin and CBpin CH_3 hydrogens. Attempts to protect **541** with Boc_2O/Ac_2O and/or arylate the crude reaction mixture led to intractable mixtures of the desired products with protodeborylated **537**.

In contrast to the C-4 *ortho* selectivity observed in other 5-aminopyrazoles, this study demonstrated that C-3 selectivity could be realised in the C-H borylation of **537** and **538**. Whilst the origin of the selectivity is unclear, it was tentatively suggested that this manifested due to the steric congestion at the C-4 site caused by the amine protecting group. To better understand the role of sterics in conferring C-3 selectivity, the introduction of the 2,2-dimethylsuccinimide group was investigated. Whilst this group cannot hydrogen-bond to the O atom on the THP group, it was hypothesised that it would confer C-3 selectivity owing its large steric requirement.

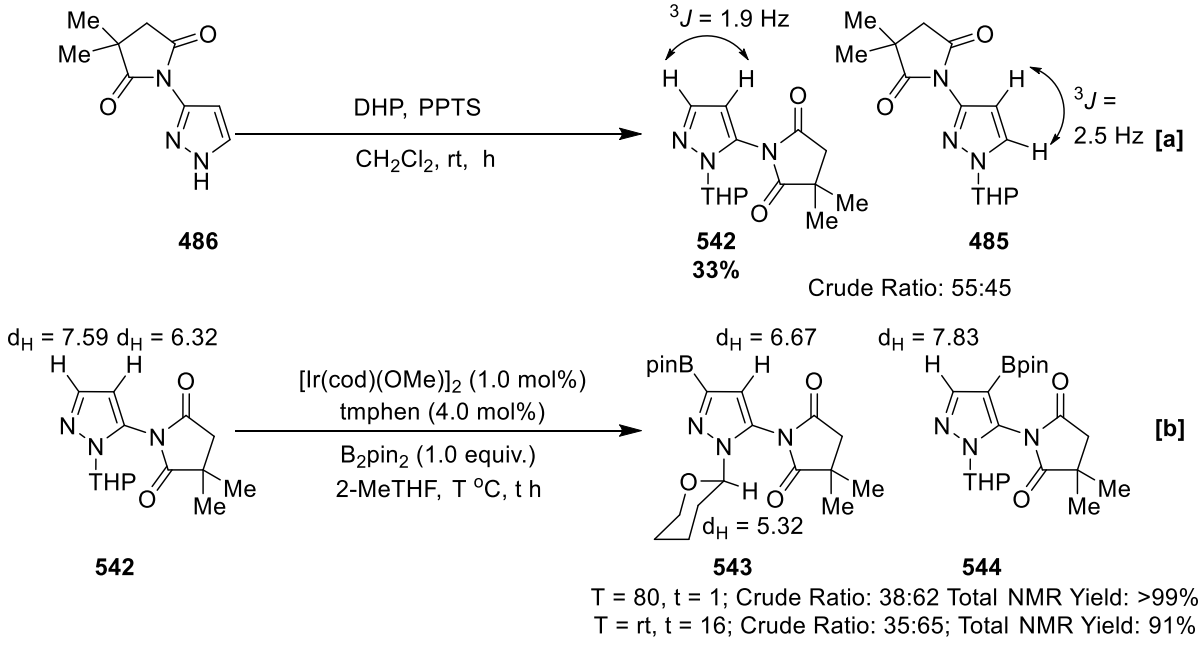

Scheme 62: Synthesis and C-H Borylation of 5-Imido Pyarazole **542**

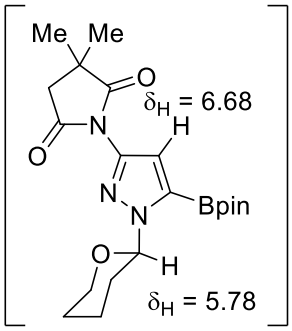

Figure 13: 3-Imidoboronate **487**

To test this, **542** was initially synthesised by treating succinimide **486** with DHP and PPTS. This also led to the formation of previously synthesised 3-substituted isomer **485**, and the two isomers were chromatographically separated to afford the desired 5-aminopyrazole **542** in acceptable yield (Scheme 62a). **542** was distinguished from **485** via differences in ^{1}H and coupling constants of the pyrazole C-H signals. In particular, the major isomer with pyrazole C-H ^3J = 1.9 Hz was attributed to **542**, whilst the minor isomer with pyrazole C-H ^3J = 2.5 Hz was attributed to **485**. With the successfully synthesised imide **542** in hand, attention turned to the C-H borylation reaction. At 80 °C, this proceeded with complete conversion after 0.5 h as measured by GCMS monitoring experiments (Scheme 62b). Crude ^{1}H NMR analysis after 1 h displayed two boron-shifted signals at 6.67 and 7.83 ppm, which were attributed to C-3 and C-4 boronates **543** and **544**. Isomerisation of **542** and **543** was ruled out by the comparison of the crude ^{1}H NMR spectra with 3-imidoboronate **487** (Figure 13). In particular, the pyranyl methine signal in 5-imidopyrazole boronate **543** was displayed at 5.32 ppm, whilst the corresponding signal appeared at 5.78 ppm in **487**. Further evidence for the generation of two isomeric boronates was found in the crude EI GCMS spectrum, which displayed two signals with m/z = 403.2 attributed to the $[M]^+$ molecular ions of two monoborylated products. Unfortunately, attempts to isolate these isomers following Suzuki-Miyaura cross-coupling led to complex product mixtures containing protodeborylated substrate **542** alongside the corresponding arylated derivatives. Nevertheless, this study demonstrated that the nature of the amine protecting group can influence C-H borylation selectivity in THP protected pyrazoles. It was suggested that the imide and the pyrazole rings in **542** may share an orthogonal relationship in order to reduce unfavourable steric interactions with the *ortho* THP substituent.

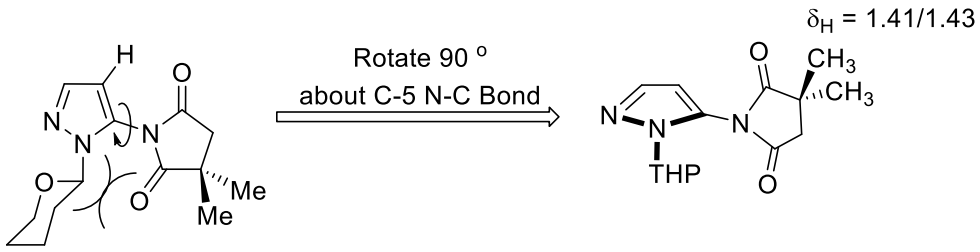

Coplanar Relationship: Steric Congestion at C-4 and THP Group

Orthogonal Relationship: Steric Congestion Relieved, Rotation Restricted at the C-5 C-N Bond

Figure 14: Rotamers of **542**

This could relieve steric congestion at C-4, explaining why there is a degree of C-H borylation selectivity at this site (Figure 14). Evidence for restricted rotation about the C-5 N-C bond could be found in the ^{1}H NMR spectrum, which displayed splitting of the succinimide *gem*-dimethyl groups into two signals at 1.41 and 1.43 ppm. This does not occur in the ^{1}H NMR spectrum of the corresponding 3-imidoisomer **485**, which displayed a single CH_3 signal at 1.39 ppm (*vide supra*).

Collectively, the evidence gathered from the C-H borylation of studied 5-aminopyrazoles suggested C-4 may be sterically congested by the amino protecting group. It was tentatively suggested that an intramolecular hydrogen-bond between the amine and the azole protecting group may create "*peri*-like" steric hindrance by forcing the amine protecting group (PG) into the plane of the C-4 C-H bond, inhibiting the approach trajectory of the catalyst (Figure 15). However, the role of other effects such as outer-sphere direction was not ruled out. On this basis, it was hypothesised that an azole protecting group without an alpha heteroatom would overcome this challenge, since it would be unable to hydrogen bond to the amino substituent.

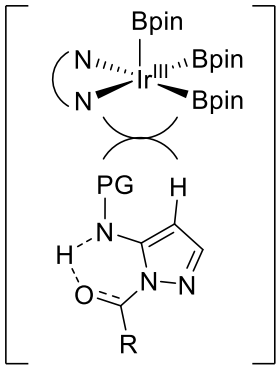

545

Figure 15: Model for the Lack of C-4 Selectivity in Studied 5-Aminopyrazoles

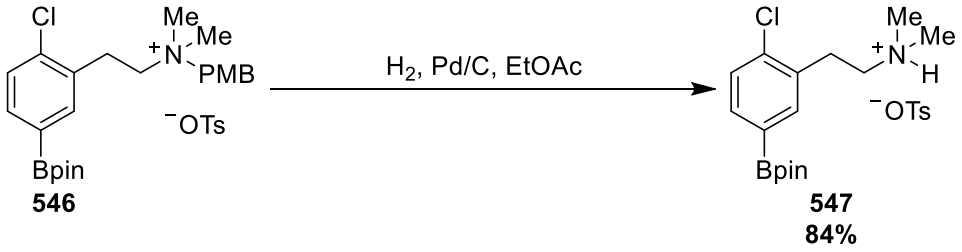

Scheme 63: Hydrogenolysis of Quaternary PMB Ammonium Salt **546**

In order to investigate this, *p*-methoxybenzyl (PMB) protected 5-aminopyrazole **548** was initially selected due to previous success with benzyl-derived protecting groups. Since PMB does not possess a readily cleavable hemiaminal/carbonyl group, it was a concern that it may not collapse upon quaternisation of the azinyl N. However, Phipps has recently described the Pd-catalysed hydrogenolysis of PMB protected quaternary ammonium salts, which provided a good contingency in the event of difficulties with PMB removal (Scheme 63). Studies commenced with the C-H borylation of **548**, which was fully consumed under the reaction conditions after 3 h (Scheme 64). This was clear from EI and GCMS monitoring experiments. Over the course of the reaction, a peak with m/z = 329.2 could be observed, which was attributed to a monoborylated adduct of **548**.

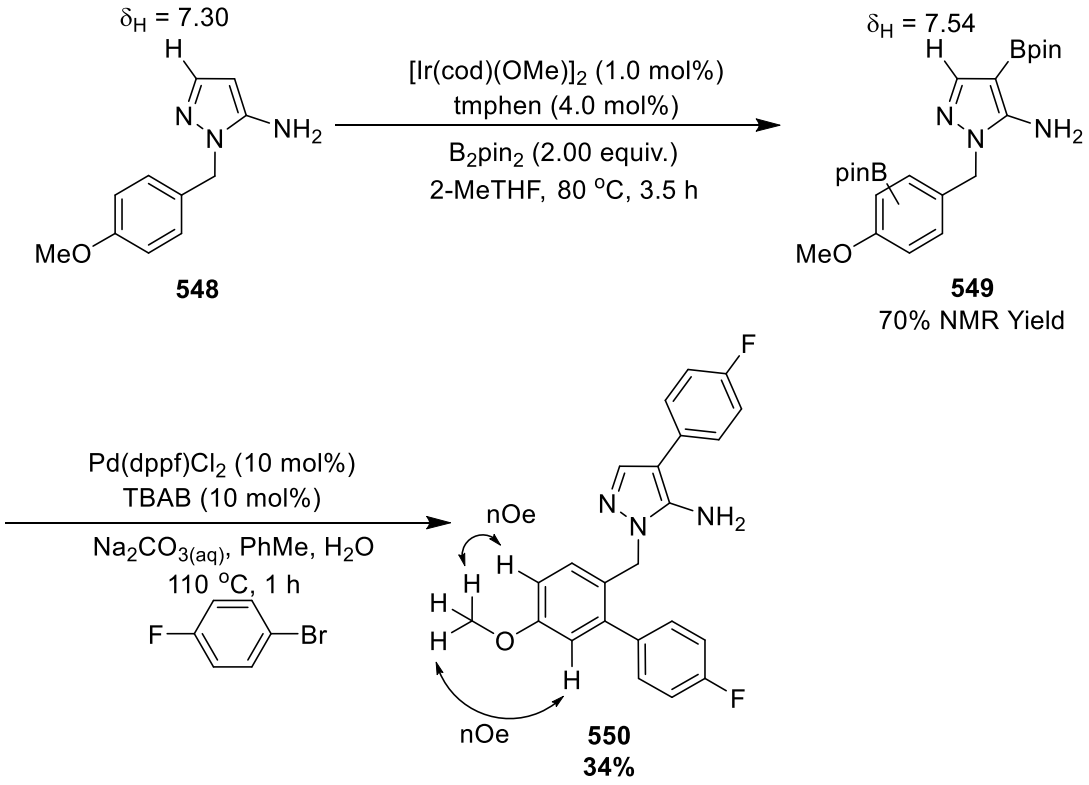

Scheme 64: C-H Borylation and Arylation of **548**

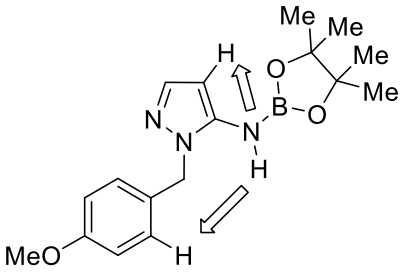

551

Figure 16: NHBpin-Mediated *ortho* and Remote C-H Borylation

However, a crude ^{1}H NMR spectrum recorded at t = 3.5 h displayed signals corresponding to a doubly C-H borylated species **549** with C-4 selectivity at the azole and unknown selectivity at the PMB ring. This was evident by the presence of a boron-shifted ^{1}H singlet at 7.54 ppm, and by the total integrals of the remaining aromatic signals summing to three. Attempts to purify and protect bisboronate **549** were unsuccessful, so Suzuki-Miyaura cross-coupling was attempted. Pleasingly, the use of TBAB with Pd(dppf)Cl_2 led to the isolation of bisarylated pyrazole **550** functionalised *ortho* to the benzylic methylene group at the PMB ring (Scheme 64). The product of a bisarylated pyrazole was evident by a signal with m/z = 392.2 found in the ESI LCMS spectrum attributed to the $[M+H]^+$ ion. Furthermore, the regiochemistry at the PMB group was evident by two through-space interactions of the OCH_3 groups with the *ortho* PMB hydrogens displayed in the 2D ^{1}H-^{1}H NOESY spectrum. One explanation for selectivity at a typically less reactive carbocyclic ring is an outer-sphere directing effect involving the NHBpin adduct **551**, which may serve to direct *ortho* borylation to C-4 on the pyrazole and remote C-H borylation to the PMB group (Figure 16). Evidence for the N-H borylation of **548** was found in the crude ^{11}B NMR spectrum, which displayed a characteristic signal at 27.5 ppm. However, this would occur with a high entropic penalty.

3.3 Conclusions and Future Work

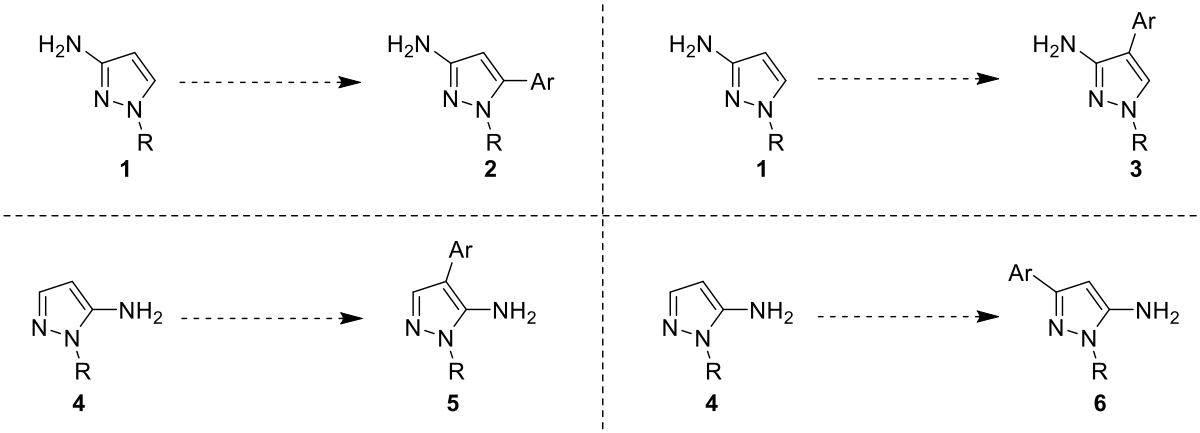

Figure 17: Goal to Regioselectively Functionalise Aminopyrazoles

This project developed strategies for the synthesis of four arylated aminopyrazole isomers **2**, **3**, **5**, and **6** (Figure 17). These strategies incorporated iridium-catalysed C-H borylation, Suzuki-Miyaura cross-coupling, and a protecting group switch.

3.3.1 3-Aminopyrazoles

Initially, it was shown that 3(5)aminopyrazole **369** was inactive in the C-H borylation. By introducing the substrate to the catalyst mixture at elevated temperature, low C-H borylation activity was achieved, although attempts to purify C-5 boronate **370** were unsuccessful (Scheme 65a). In contrast, the N-substituted-3-aminopyrazoles studied (that were not ureas) exhibited high activity and intrinsic C-H borylation site-selectivity for the C-H bond alpha to the azole N (C-5), and this is consistent with the observation that aromatic C-H bonds with low pK_a values are preferentially activated. This selectivity was not altered by increasing the steric bulk of the azole N substituent from Me to 3,5-dimethylbenzyl or THP (Scheme 65b). An exception to this rule was demonstrated following the substitution of a carbonyl group at the azole N. This led to a complete reversal in C-H borylation regioselectivity and afforded C-4 functionalised boronates, even in the C-H borylation of Boc protected pyrazole **498** with a bulky imide substituent at *ortho* position (C-3) (Scheme 65c). It was calculated that the imide in **498** twists out the plane of the pyrazole ring, reducing steric congestion at C-4. Future studies should aim to elucidate the role of the N-Boc group in conferring C-4 C-H borylation selectivity. Whilst the C-H borylation efficiencies were typically excellent, the subsequent arylation using Suzuki-Miyaura cross-coupling often led to protodeborylation which complicated purifications.

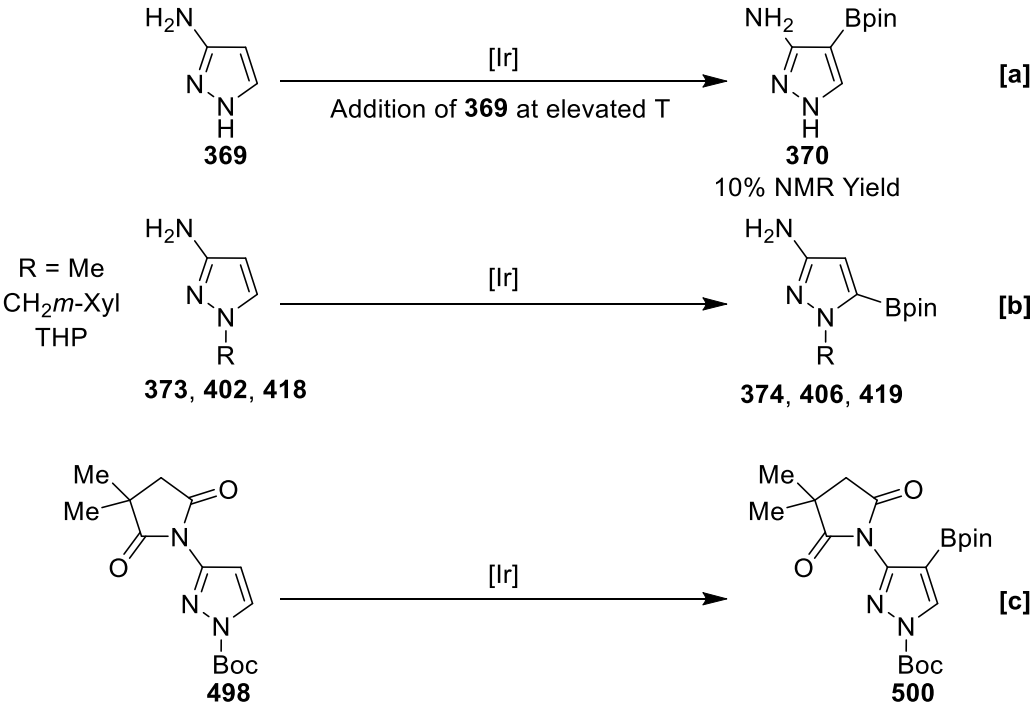

Scheme 65: Intrinsic C-H Borylation Selectivities of 3-Aminopyrazole Derivatives

Therefore, future studies should aim to improve the efficiency of these processes by identifying systems that can create the desired C-C bond at a faster rate than protodeborylation.

The N-H borylation of N-methyl-3-aminopyrazole **373** was shown to occur during the C-H borylation reaction. Despite the capability of NHBpin to act as an *ortho* C-H borylation director in other systems, no *ortho* (C-4) selectivity was observed.

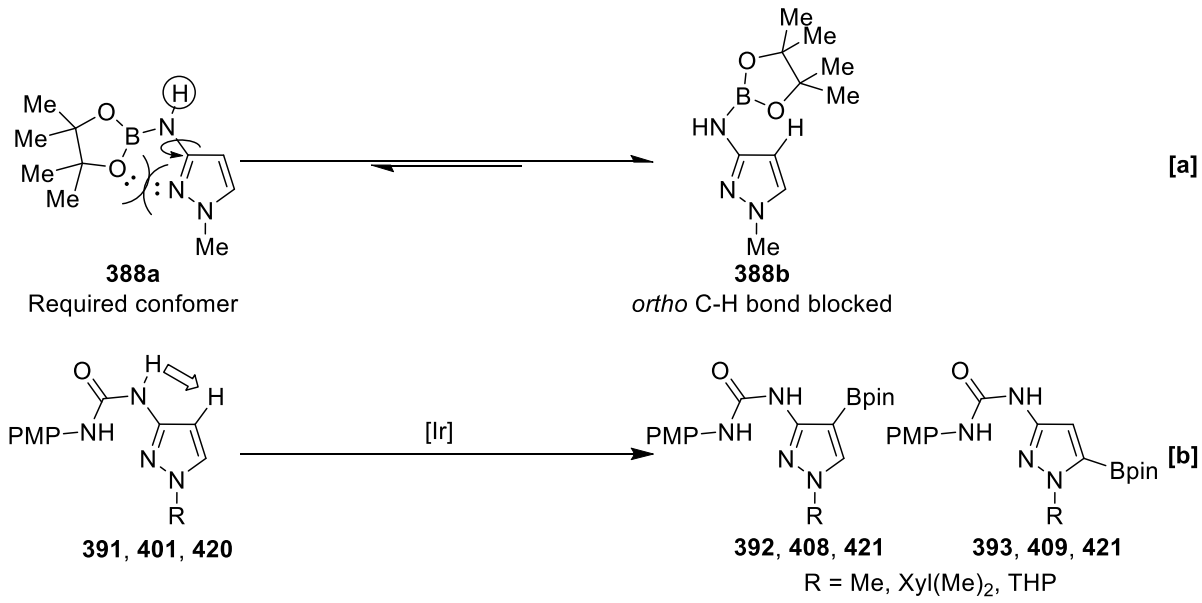

Scheme 66: Study on the C-4 Selective C-H Borylation of 3-Aminopyrazoles

It was speculated that unfavourable lone-pair repulsion between the azinyl N and the O of the N-boryl group disfavoured the rotamer **388a** required for directed borylation and favoured rotamer **388b** with a congested C-4 site (Scheme 66a). To overcome this, a urea model was developed in which an intramolecular hydrogen-bond would conformationally lock the N-H bond required for *ortho* directed C-H borylation. Pleasingly, the C-H borylation of 3-aminopyrazole ureas delivered C-4 boronates, albeit with modest selectivity alongside the corresponding C-5 boronate (Scheme 66b). This directing effect was proposed to operate via an outer-sphere hydrogen-bonding system with the boryl ligands of the catalyst. Different variables were investigated in order to improve the selectivity of this process. However, selectivities that surpassed a 1:1 ratio of the two isomeric boronate products could not be achieved. Furthermore, this directing effect did not extend to other heterocycles, including pyridine, isoxazole, indazole, and quinolin-2-one. Future work should seek to enhance the C-4 selectivity of this directing effect in pyrazole ureas by varying further reaction parameters, such as solvent, ancillary/reactive ligands, and substitution at the urea carbocycle.

3-Aminopyrazoles with labile protecting groups at the azole N including SEM, THP and Boc could be employed in a protecting group switch. This ultimately transposed the azole substituent and provided access to arylated aminopyrazoles which would otherwise be challenging to access directly using C-H borylation followed by Suzuki-Miyaura cross-coupling. Treatment of an arylated aminopyrazole such as **502b** with Me_3OBF_4 led to a quaternisation/deprotection cascade, which furnished switched pyrazole **503b** (Scheme 67). It was established that the presence of N-H bonds retarded the removal of the azole protecting group in SEM aminopyrazoles, and this could be circumvented via double protection of the amino substituent with a maleimide or a substituted succininimide. It is not clear why the presence of N-H bonds was deleterious to the protecting group switch, and elucidating this should be a goal of future studies.

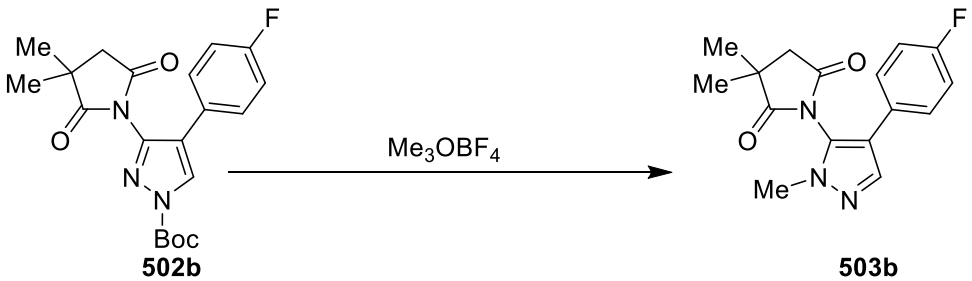

502b **503b**

Scheme 67: Protecting Group Switch of **502b**

3.3.2 5-Aminopyrazoles

The regioselectivity exhibited in the C-H borylation of N-substituted-5-aminopyrazoles was comparably more challenging to control. However, the substitution of a hydrocarbon-based group (Me, PMB) at the azole N led to high C-4 selectivity at the pyrazole ring. Additionally, the C-H borylation of PMB pyrazole **548** led to a second borylation event at a sterically congested position on the methoxybenzyl ring (Scheme 68a). Future studies should establish the role of NHBpin and NHBoc in affording these selectivities. A way to test if NHBoc and/or NHBpin act as directors would be to investigate the C-H borylation of acetamide **552** and the subsequent regiochemical outcome (Scheme 68b). This would constitute an effective control experiment because acetamides are not known to act as outer-sphere directors in the C-H borylation.

Applying the switch methodology developed in 3-aminopyrazoles to 5-aminopyrazoles bearing azole protecting groups such as SEM, THP, and Boc presented challenges which lowered the C-H borylation efficiency and selectivity in some instances. One explanation offered to explain this was a hydrogen-bond interaction between the azole protecting group and the amino-substituent, which led to increased steric congestion between C-4 and the amine protecting group. Evidence for this intramolecular hydrogen-bond was obtained from an X-ray analysis of 5-aminopyrazole **534** (Figure 18).

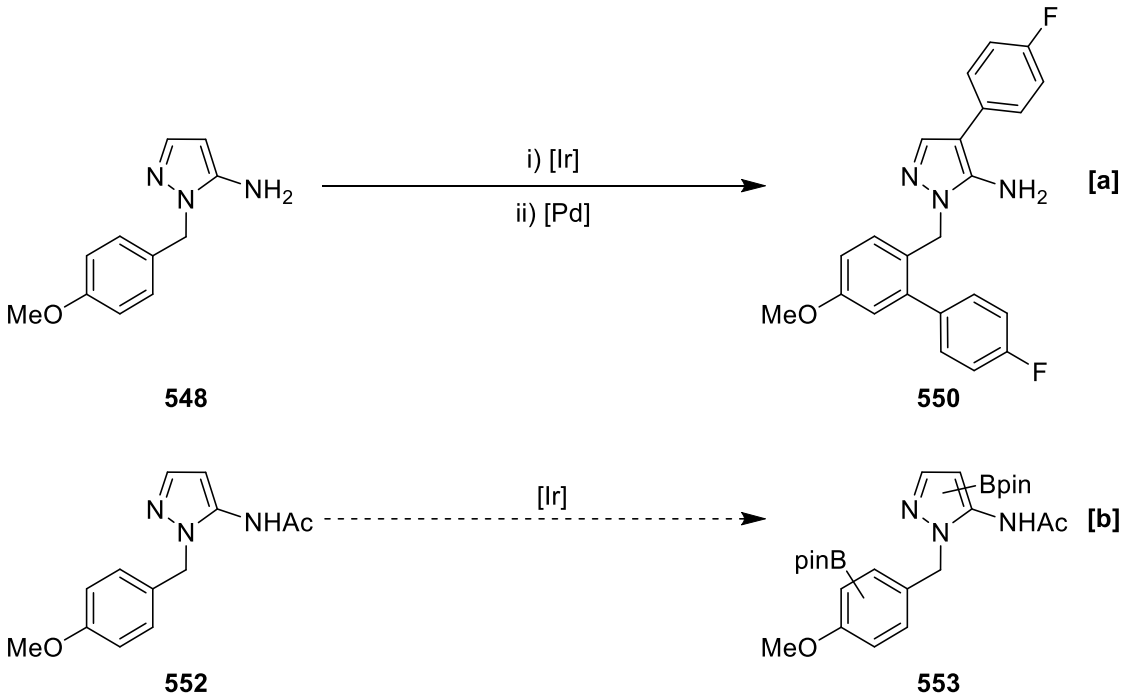

548 **550** **552** **553**

Scheme 68: C-H Borylation of PMB-Protected 5-Aminopyrazoles

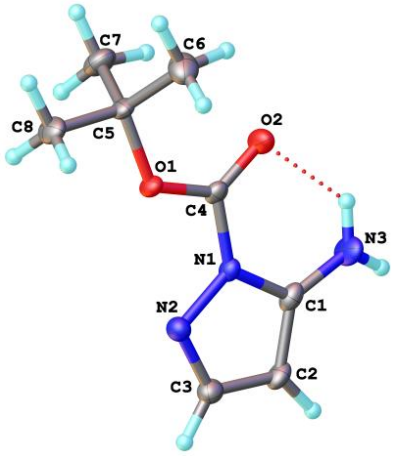

Figure 18: X-Ray Structure of **534**

Whilst this could explain the C-5 selective C-H borylation acetamide **538**, further studies are required to establish the origin of this regiochemistry (Scheme 69a). Future studies should complete the investigation into suitable azole protecting groups for 5-aminopyrazoles in order to improve the C-H borylation efficiency/selectivity and subsequently facilitate a protecting group switch. This could be achieved by investigating the C-H borylation of trimethylbenzyl pyrazole **554**. Whilst PMB pyrazole **548** C-H borylates at the PMB ring, the corresponding sites in **554** are blocked by methyl substituents, so it is predicted that C-4 borylation at the pyrazole ring would occur exclusively. The development of a Suzuki-Miyaura arylation on the corresponding C-4 aryl boronate followed by a protecting group switch would furnish desired isomer **558** (Scheme 69b).

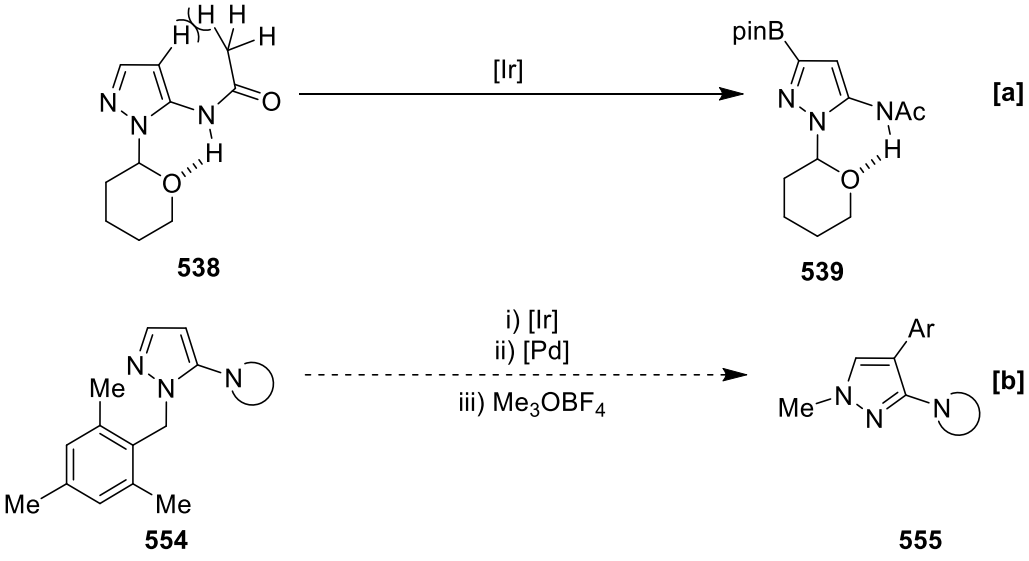

Scheme 69: C-H Borylation of 5-Aminopyrazoles

3.4 References

[1] J. Catalán, M. Menéndez, J. Laynez, R. M. Claramunt, M. Bruix, J. D. Mendoza, J. Elguero, *J. Heterocycl. Chem.* **1985**, *22*, 997–1000.

[2] S. A. Sadler, A. C. Hones, B. Roberts, D. Blakemore, T. B. Marder, P. G. Steel, *J. Org. Chem.* **2015**, *80*, 5308–5314.

[3] S. M. Preshlock, D. L. Plattner, P. E. Maligres, S. W. Krska, R. E. Maleczka, M. R. Smith III, *Angew. Chem*. *Int. Ed.* **2013**, *52*, 12915–12919.

[4] M. A. Larsen, J. F. Hartwig, *J. Am. Chem. Soc.* **2014**, *136*, 4287–4299.

[5] C. R. K. Jayasundara, D. Sabasovs, R. J. Staples, J. Oppenheimer, M. R. Smith III, R. E. Maleczka, *Organometallics* **2018**, *37*, 1567–1574.

[6] E. A. Romero, J. L. Peltier, R. Jazzar, G. Bertrand, *Chem. Commun.* **2016**, *52*, 10563–10565.

[7] M. Ding, P. G. Steel, *Unpublished Results*, **2019**.

[8] V. A. Kallepalli, F. Shi, S. Paul, E. N. Onyeozili, R. E. Maleczka, M. R. Smith III, *J. Org. Chem.* **2009**, *74*, 9199–9201.

[9] A. Beyer, T. Castanheiro, P. Busca, G. Prestat, *ChemCatChem* **2015**, *7*, 2433–2436.

[10] L. A. D'Agostino, R. T. T. Sjin, D. Niu, J. J. Mcdonad, Z. Zhu, H. Liu, H. Mazdiyansi, R. C. Petter, J. Singh, M. Barrague, et al., *Heteroaryl Compounds and Uses Thereof*, US Pat, **2014**, 144737.

[11] D. J. Slade, N. F. Pelz, W. Bodnar, J. W. Lampe, P. S. Watson, *J. Org. Chem* **2009**, *74*, 6331–6334.

[12] S. A. Sadler, H. Tajuddin, I. A. I. Mkhalid, A. S. Batsanov, D. Albesa-Jove, M. S. Cheung, A. C. Maxwell, L. Shukla, B. Roberts, D. C. Blakemore, Z. Lin, T. B. Marder, P. G. Steel, *Org. Biomol. Chem.* **2014**, *12*, 7318–7327.

[13] K. Shen, Y. Fu, J.-N. Li, L. Liu, Q.-X. Guo, *Tetrahedron* **2007**, *63*, 1568–1576.

[14] F. Chevallier, Y. S. Halauko, C. Pecceu, I. F. Nassar, T. U. Dam, T. Roisnel, V. E. Matulis, O.

A. Ivashkevich, F. Mongin, *Org. Biomol. Chem.* **2011**, *9*, 4671.

[15] V. Balasubramaniyan, *Chem. Rev.* **1966**, *66*, 567–641.

[16] D. G. Twigg, N. Kondo, S. L. Mitchell, W. R. J. D. Galloway, H. F. Sore, A. Madin, D. R. Spring, *Angew. Chem. Int. Ed.* **2016**, *55*, 12479–12483.

[17] U. C. Pande, H. Egsgaard, E. Larsen Mikael Begbrup, *Org. Mass Spectrom.* **1981**, *16*, 377–380.

[18] A.-L. Gérard, A. Bouillon, C. Mahatsekake, V. Collot, S. Rault, *Tetrahedron Lett.* **2006**, *47*, 4665–4669.

[19] T. B. Parsons, N. Spencer, C. W. Tsang, R. S. Grainger, *Chem. Commun.* **2013**, *49*, 2296-2298.

[20] H. Graubaum, *J. Prakt. Chem.* **1993**, *335*, 585–588.

4 Experimental

4.1 Chemical Synthesis

4.1.1 General Notes

Chemicals: [Ir(cod)OMe]$_2$ was synthesised as previously described from $IrCl_3 \bullet 3H_2O$, obtained from Precious Metals Online.[1] All other chemicals were purchased from commercial suppliers and were used without further purification unless otherwise stated.

Dry Solvents: Tetrahydrofuran (THF), 2-methyltetrahydrofuran (2-MeTHF), and methyl-tert-butyl-ether (mtbe) were purchased anhydrous from Fisher. All other dry reaction solvents were dried using an Innovative Technology Solvent Purification System and stored under argon.

Column chromatography: Flash column chromatography was performed on a CombiFlash® System from Teledyne Isco equipped with an UV-light detector using prepacked silica RediSep Rf cartridges with the stated solvent gradient. Crude mixtures to be purified were dry loaded onto silica prior to loading on the column.

ESI LC-MS: Purity of all final compounds was checked by LC-MS. LC-MS analyses were conducted on a TQD mass spectrometer (Waters Ltd, UK), which was equipped with an Acquity UPLC, using an Acquity UPLC BEH C18 (2.1 mm × 50 mm, 1.7 µm) column, and an electrospray ion source. Absorbance data were acquired from 210 to 400 nm using an Acquity photodiode array detector.

EI GC-MS: GC-MS analyses were performed on a Shimadzu QP2010-Ultra using electron ionization (EI). The mass spectrometer was equipped with either an Rxi-5Sil MS column (0.15 µm × 10 m × 0.15 mm) for non-polar compounds or an Rxi-17Sil MS column (0.15 µm × 10 m × 0.15 mm) for polar compounds.

ASAP: ASAP measurements were performed on a LCT Premier XE mass spectrometer and ASAP ion source.

HRMS: HRMS measurements were carried out on a QToF Premier mass spectrometer (Waters Ltd, UK) with an electrospray ion source or a LCT Premier XE mass spectrometer with an ASAP ion source.

IR spectroscopy: Infrared (IR) spectra were recorded on a Perkin-Elmer RX I FT-IR spectrometer via use of a Pike ATR accessory in the range of 3500 – 600 cm^{-1}. Assigned peaks are reported in wavenumbers (cm^{-1}).

Melting points: Melting points were measured in open capillary tubes using a Thermo Scientific™ Melting Point Apparatus and are uncorrected.

Microwave: Microwave reactions were performed in septum-containing, crimp capped sealed vials in an EmrysTM Optimizer microwave unit from Personal Chemistry. The reported times include hold times.

NMR Spectroscopy: NMR-spectra were recorded in $CDCl_3$, d^6-DMSO, or CD_3OD solutions on a Bruker Advance-400 (^1H, ^{13}C, ^{19}F, DEPT, COSY), Varian Inova-600 (^{1} H, ^{13}C, ^{19}F, HSQC, HMBC, COSY, NOESY) or Varian VNMRS-700 (^1H, ^{13}C, ^{19}F, HSQC, HMBC, COSY, NOESY) spectrometer, using the solvent peaks ($CDCl_3$: δ = 7.26 ppm (^1H), δ = 77.16 ppm (^{13}C), d^6-DMSO: δ = 2.50 ppm (^1H), δ = 39.52 ppm (^{13}C) CD_3OD: δ = 3.31 ppm (^1H), δ = 49.00 ppm (^{13}C) as reference. For some spectra tetramethylsilane (TMS) was used as an internal standard. ^{13}C spectra were run in proton decoupled mode. Chemical shift values (δ) are reported in parts per million (ppm) and coupling constants (*J*) are given in Hertz (Hz). The multiplicity is indicated by singlet (s), doublet (d), triplet (t), quartet (q), multiplet (m), broad (br) or a combination thereof. Assignment of spectra was carried out using 2D HSQC, HMBC, COSY and NOESY techniques.

TLC: TLC analyses were performed on pre-coated aluminum-backed plates (Silica gel 60 F254, Merck). Signals were visualized with UV-light (254 nm and 365 nm) or by staining where necessary.

4.2 Synthetic Procedures

4.2.1 C-H Borylation and Suzuki-Miyaura Cross-Coupling of Aminopyrazole Derivatives

General Procedure A for the Ir-catalysed Borylation of Aminopyrazole Derivatives: An oven-dried Schlenk tube was charged with $[Ir(cod)(OMe)]_2$ (1.0 mol%), tmphen (4.0 mol%) and B_2pin_2 (2.20 equiv), sealed and subject to three N_2 purge/refill cycles. Anhydrous, Ar degassed 2-MeTHF was added in the specified molarity, and the dark active catalyst solution was transferred to a sealed vial containing the substrate (1.00 equiv.). The reaction mixture was stirred at 80 ^oC for 1 h, followed by complete removal of the volatiles. The crude pyrazole boronic ester was then either purified, or cross-coupled directly. Where necessary, 1,3,5-trimethoxybenzene was added in order to assess the NMR yield. In most ^{13}C spectra, no signal is observed for boron-bound carbon atoms. This is due to line broadening caused by ^{10}B and ^{11}B quadrupolar nuclei.

General Procedure B for the Suzuki Reaction of Aminopyrazoles with Aryl Halides: To an oven-dried vial was added $Pd(dppf)Cl_2$ (2.5 mol%) and K_3PO_4 (2.00 equiv.). The vial was subjected to three N_2 purge/refill cycles. Aryl halide (1.10 equiv.) followed by a solution of crude pyrazole boronate ester in degassed 2-MeTHF (synthesised according to General Procedure A, see the borylation procedure for molarity) were added. The resulting solution was cooled to 0 ^oC and degassed H_2O (1.50 M) was added dropwise. The reaction mixture was stirred at 80 ^oC for the allotted time before removal of the volatiles and subsequent chromatographic purification.

General Procedure C for the Suzuki Reaction of Aminopyrazoles with Aryl Halides: To an oven-dried Schlenk tube was added XPhos Pd G4 (15 mol%) and Cs_2CO_3 (2 equiv.). The tube was subjected to three N_2 purge/refill cycles, before addition of aryl halide (1.1 equiv.) followed by a solution of pyrazole boronate ester in degassed 1,4-dioxane (0.16 M). H_2O (2 M) was added and the mixture was stirred at 50 ^oC for 16 h. The cooled reaction was diluted with EtOAc (5 mL) and H_2O (5 mL) and the aqueous phase was extracted with EtOAc (3 x 5 mL).

The combined organic fractions were dried over $MgSO_4$, filtered, and evaporated before chromatographic purification.

1-Methyl-5-[3'-(trifluoromethyl)phenyl]-1H-pyrazol-3-amine (**375**)

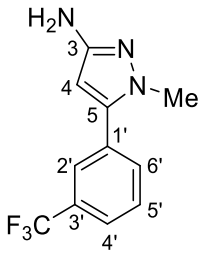

Synthesised from 1-methyl-1H-pyrazol-3-amine **373** (194 mg, 2.00 mmol, 0.5 M, 1.00 equiv.) according to General Procedure A followed by General Procedure B in a one-pot borylation/cross-coupling procedure using 1-bromo-3-(trifluoromethyl)benzene. After 16 h, the reaction was filtered over Celite® with EtOAc (10 mL) and diluted with H_2O (5 mL). The aqueous layer was extracted with EtOAc (3 x 5 mL), and the combined organic fractions were dried over $MgSO_4$, filtered, and evaporated. SiO_2 gel column chromatography (0 → 100 % EtOAc in hexanes) afforded the arylated pyrazole as a yellow oil (60 mg, 0.25 mmol, 13%); ν_{max} (ATR) 3327 (NH_2), 3213 (NH_2), 2940, 1617, 1554, 1510, 1328, 1281, 1225, 1166, 1120, 1074 cm^{-1}; δ_H (700 MHz, $CDCl_3$) 7.64-7.32 (2H, m, 2'-H, 4'-H), 7.58-7.56 (2H, m, 5'-H, 6'-H), 5.76 (1H, s, 4-H), 3.69 (3H, s, CH_3), 3.34 (2H, s br, NH_2); δ_C (176 MHz, $CDCl_3$) 132.0 (C-5'), 131.7 (C-1'), 131.3 (q, *J* = 33 Hz, C-3'), 129.3 (C-6'), 125.6 (C-2'), 125.2 (q, *J* = 4 Hz, C-4'), 123.9 (q, *J* = 272 Hz, CF_3), 94.3 (C-4), 37.04 (CH_3); HRMS (ESI) *m/z* found $[M+H]^+$ 242.0920, $C_{11}H_{11}N_3F_3$ requires *M*, 242.0905. The quaternary C-3 and C-5 signals are weak and as a result are not observed.

Methyl 4-(3'-amino-1'-methyl-1H-pyrazol-5'-yl)benzoate (**379**)

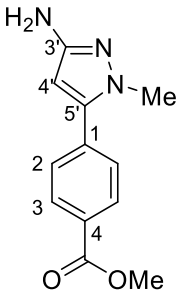

Synthesised from tert-butyl N-(1-methyl-1H-pyrazol-3-yl)carbamate **377** (197 mg, 1.00 mmol, 0.50 M, 1.00 equiv.) according to General Procedure A using 2.00 equiv. B_2pin_2 followed by General Procedure B in a one-pot borylation/cross-coupling procedure using methyl 4-iodobenzoate. After 16 h, the volatiles were moved and the residue was dissolved in CH_2Cl_2 (2.6 mL) before the addition of water (0.05 mL) and TFA (1.3 mL) dropwise. After stirring for 3 h, the volatiles were removed and CH_2Cl_2 (5 mL) and saturated $NaHCO_{3(aq)}$ (5 mL) were added. The aqueous layer was extracted with CH_2Cl_2 (3 x 5 mL), and the combined organic fractions were dried over $MgSO_4$, filtered, and evaporated. SiO_2 gel column chromatography (0 → 100% EtOAc in hexanes) afforded the arylated aminopyrazole as a yellow oil (5 mg, 0.02 mmol, 7%); ν_{max} (ATR) 3385 (NH_2), 3278 (NH_2), 2966, 1727 (C=O), 1585, 1502, 1441, 1286, 1217, 1187, 1157 cm^{-1}; δ_H (700 MHz, $CDCl_3$) 8.57 (1H, s br, NH), 8.15 (2H, d, *J* = 8.6 Hz, 2-H), 7.53 (2H, d, *J* = 8.6 Hz, 3-H), 6.87 (1H, s, 4'-H), 3.96 (3H, s, OCH_3), 3.84 (3H, s, 1'-CH_3); δ_C (176 MHz, $CDCl_3$) 166.5 (C=O), 144.2 (C-5'), 143.6 (C-3'), 134.1 (C-1), 130.7 (C-4), 130.2 (C-2), 128.8 (C-3), 98.5 (C-4'), 52.5 (OCH_3), 37.8 (1'-CH_3); *m/z* (ESI) $[M+H]^+$ found 232.2.

Tert-butyl N-[1-methyl-4-(4,4,5,5-tetramethyl-1,3,2-dioxaborolan-2-yl)-1H-pyrazol-5-yl]carbamate (**384**)

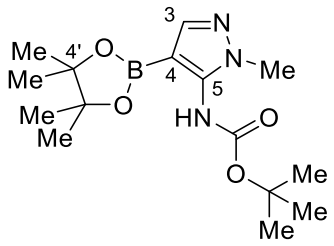

Synthesised from tert-butyl N-(1-methyl-1H-pyrazol-5-yl)carbamate **383** (197 mg, 1.00 mmol, 0.50 M, 1.00 equiv.) according to General Procedure A. SiO_2 gel flash chromatography (40 → 60 % Et_2O in CH_2Cl_2) afforded the borylated pyrazole as a colourless oil (288 mg, 0.89 mmol, 89%); ν_{max} (ATR) 3260 (NH) 2984, 1728 (C=O), 1578, 1503, 1477, 1459, 1395, 1374, 1252, 1144 cm^{-1}; δ_H (700 MHz, $CDCl_3$) 7.62 (1H, s, 3-H), 6.70 (1H, s br, NH), 3.76 (3H, s, 1-CH_3), 1.49 (9H, s, $C(CH_3)_3$), 1.28 (12H, s, 4'-CH_3); δ_C (176 MHz, $CDCl_3$) 153.5 (C=O), 143.9 (C-3), 143.2 (C-5), 83.4 (C-4'), 81.5 ($C(CH_3)_3$), 36.4 (1-CH_3), 28.3 ($C(CH_3)_3$), 25.0 (4'-CH_3); HRMS (ESI) *m/z* found $[M+H]^+$ 323.2137, $C_{15}H_{27}BN_3O_4$ requires *M*, 323.2131.

Tert-butyl N-[1-methyl-4-(4'-methylphenyl)-1H-pyrazol-5-yl]carbamate (**385**)

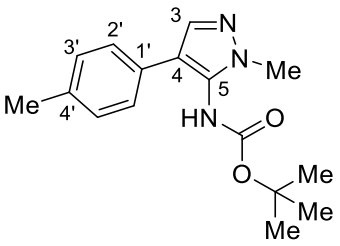

Synthesised from tert-butyl N-(1-methyl-1H-pyrazol-5-yl)carbamate **383** (60 mg, 0.30 mmol, 0.50 M, 1.00 equiv.) according to General Procedure A followed by General Procedure B in a one-pot borylation/cross-coupling procedure using 1-bromo-4-methylbenzene. After 16 h, the volatiles were removed and SiO_2 gel column chromatography (5 → 15 % acetone in PhMe) afforded the cross-coupled pyrazole as an off yellow solid (46 mg, 0.16 mmol, 53%); mp: 154-155 ^oC; ν_{max} (ATR) 2954, 1728 (C=O), 1560, 1408, 1371, 1308, 1248, 1171, 1074 cm^{-1}; δ_H (700 MHz, CD_3OD) 7.67 (1H, s, 3-H), 7.39 (2H, d, *J* = 8.2 Hz, 2'-H), 7.20 (2H, d, *J* = 8.2 Hz, 3'-H) 3.75 (3H, s, NCH_3), 2.35 (3H, s, 4'-CH_3), 1.53 (9H, s, $C(CH_3)_3$); δ_C (176 MHz, CD_3OD) 156.4 (C=O), 137.5 (C-3), 137.4 (C-4'), 133.8 (C-5), 130.4 (C-1'), 130.3 (C-3'), 127.5 (C-2'), 118.6 (C-4), 82.1 (*C*$(CH_3)_3$), 35.5 (1-CH_3), 28.5 (C(*C*$H_3)_3$), 21.2 (4'-CH_3); HRMS (ESI) *m/z* found $[M+H]^+$ 278.1715, $C_{16}H_{22}N_3O_2$ requires *M*, 278.1712.

1-(4'-methoxyphenyl)-3-[1''-methyl-4''-(4''',4''',5''',5'''-tetramethyl-1''',3''',2'''-dioxaborolan-2-yl)-1H-pyrazol-3''-yl]urea (**392**)

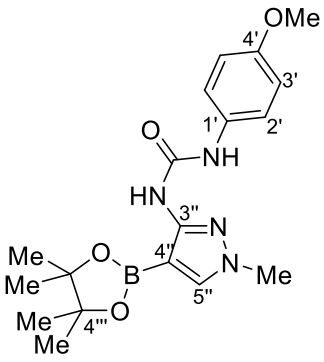

Synthesised from 1-(4-methoxyphenyl)-3-(1-methyl-1H-pyrazol-3-yl)urea **391** (246 mg, 1.00 mmol, 0.5 M, 1.00 equiv.) according to General Procedure A using HBpin (0.53 mL, 4.00 mmol, 4.00 equiv.) in place of B_2pin_2. SiO_2 gel column chromatography (30 → 60% EtOAc in hexanes) afforded the borylated pyrazole as a white solid (94 mg, 0.25 mmol, 25%); mp: 161-162 ^oC; ν_{max} (ATR) 3403 (NH), 2981, 1687

(C=O), 1624, 1573, 1509, 1319, 1263, 1235, 1144, 1103, 1032 cm^{-1}; δ_H (700 MHz, $CDCl_3$) 10.16 (1H, s br, NH), 7.51 (1H, s br, NH), 7.47-7.46 (3H, m, 2'-H, 5''-H), 6.88 (2H, d, *J* = 9.0 Hz, 3'-H), 3.81 (3H, s, 1''-CH_3), 3.79 (OCH_3), 1.31 (12H, s, 4'''-CH_3); δ_C (176 MHz, $CDCl_3$) 155.9 (C-4'), 154.6 (C-3''), 152.7 (C=O), 137.4 (C-5''), 132.1 (C-1'), 122.1 (C-2'), 114.2 (C-3'), 83.9 (C-4'''), 55.6 (OCH_3), 38.9 (1''-CH_3), 24.9 (4'''-CH_3); HRMS (ESI) *m/z* found $[M+H]^+$ 372.2085, $C_{18}H_{26}N_4O_4{}^{10}B$ requires *M*, 372.2083.

Methyl 4-(3-{[(4-methoxyphenyl)carbamoyl](methyl)amino}-1-methyl-1H-pyrazol-5-yl)benzoate (**395b**)

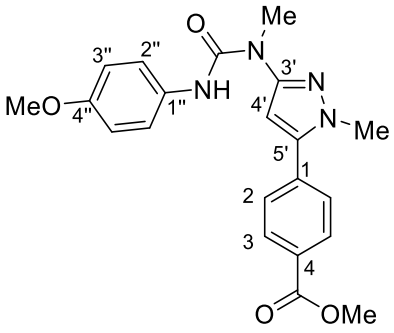

Synthesised from 1-(4-methoxyphenyl)-3-methyl-3-(1-methyl-1H-pyrazol-3-yl)urea **395** (132 mg, 0.50 mmol, 0.20 M, 1.00 equiv) according to General Procedure A followed by General Procedure B in a one-pot procedure using methyl 4-iodobenzoate. After 1 h, the volatiles were removed and SiO_2 gel column chromatography (15 → 30 % EtOAc in PhMe) afforded the arylated pyrazole urea as an off white solid (72 mg, 0.19mmol, 37%) Product contains *ca.* 4% of substrate **392**; mp: 149-150 °C; ν_{max} (ATR) 2981, 1741 (C=O), 1667 (C=O), 1609, 1562, 1551, 1509, 1478, 1281, 1235, 1109, 1023 cm^{-1}; δ_H (600 MHz, $CDCl_3$) 10.56 (1H, s br, NH), 8.15 (2H, d, *J* = 8.5 Hz, 3-H), 7.53 (2H, d, *J* = 8.5 Hz, 2-H), 7.45 (2H, d, *J* = 8.9 Hz, 2''-H), 6.87 (2H, d, *J* = 8.9 Hz, 3''-H), 6.03 (1H, s, 4'-H), 3.96 (3H, s, CH_3O_2C), 3.86 (3H, s, CH_3N-5'), 3.79 (3H, s, CH_3O-4''), 3.37 (CH_3N-3'); δ_C (151 MHz, $CDCl_3$) 166.5 (CO_2), 155.8 (C-4''), 153.4 (NCO), 151.7 (C-3'), 143.8 (C-5'), 134.1 (C-1), 132.6 (C-1''), 130.7 (C-4), 130.2 (C-3), 128.7 (C-2), 122.0 (C-2''), 114.2 (C-3''), 95.8 (C-4'), 55.6 (CH_3O-4''), 52.5 (CH_3O_2C), 37.7 (5'-NCH_3), 33.3 (3'-NCH_3); HRMS (ESI) m/z found $[M+H]^+$ 395.1725, $C_{21}H_{23}N_4O_4$ requires *M*, 395.1719.

Methyl 4-(3-{[(4-methoxyphenyl)(methyl)carbamoyl]amino}-1-methyl-1H-pyrazol-5-yl)benzoate (**398b**)

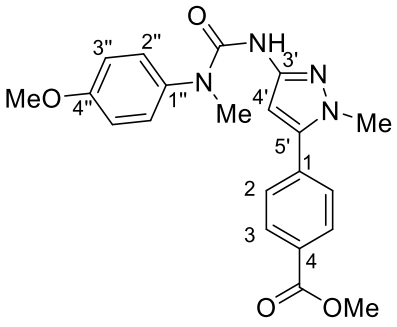

Synthesised from 1-(4-methoxyphenyl)-1-methyl-3-(1-methyl-1H-pyrazol-3-yl)urea **398** (274 mg, 1.00 mmol, 0.20 M, 1.00 equiv) according to General Procedure A followed by General Procedure B in a one-pot procedure using methyl 4-iodobenzoate. After 3 h, the volatiles were removed and basic Al_2O_3 gel column chromatography (20 → 30 % EtOAc in PhMe) afforded the arylated pyrazole urea as an off white solid (138 mg, 0.35 mmol, 35%); mp: 130 °C (decomposes); ν_{max} (ATR) 2947, 1738 (C=O), 1676 (C=O), 1558, 1510, 1469, 1274, 1246, 1103, cm^{-1}; δ_H (700 MHz, $CDCl_3$,) 8.09 (2H, d, *J* = 8.6 Hz, 3-H), 7.49 (2H, d, *J* = 8.6 Hz, 2-H), 7.22 (2H, d, *J* = 8.7 Hz, 2''-H), 6.95 (2H, d, *J* = 8.7 Hz, 3''-H), 6.77 (2H, s br, NH, 4'-H), 3.92 (3H, s, CH_3O_2C) 3.83 (s, 4''-OCH_3, 3 H), 3.70 (3H, s, 1'-CH_3), 3.28 (3H, s, 1''-NCH_3); δ_C (176 MHz, $CDCl_3$) 166.6 (CO_2), 159.3 (C-4''), 154.2 (NCO), 147.5 (C-3'), 143.5 (C-5'), 135.0 (C-1''), 134.8 (C-4) 130.1 (C-1), 130.0 (C-3), 129.0 (C-2''), 128.6 (C-2), 115.7 (C-3''), 97.0 (C-4'), 55.7 (4''-OCH_3), 52.4 (CH_3O_2C), 37.6 (1''-NCH_3), 37.2 (5'-NCH_3); HRMS (ASAP) *m/z* found $[M+H]^+$ 395.1705, $C_{21}H_{23}N_4O_4$ requires *M*, 395.1719.

1-(4'-methoxyphenyl)-3-[1''-(oxan-2'''-yl)-4-(4'''',4'''',5'''',5''''-tetramethyl-1'''',3'''',2''''-dioxaborolan-2''''-yl)-1H-pyrazol-3''-yl]urea (**421**)

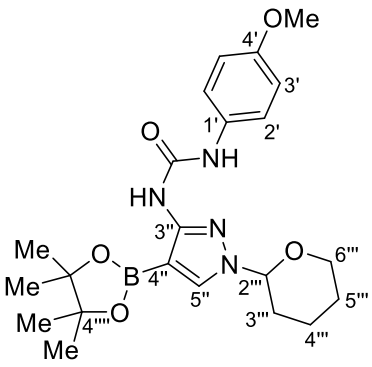

Synthesised from 1-(4-methoxyphenyl)-3-[1-(oxan-2-yl)-1H-pyrazol-3-yl]urea **420** (20 mg, 0.06 mmol, 0.20 M, 1.00 equiv.) according to General Procedure A using HBpin (4.00 equiv.) instead of B_2pin_2. SiO_2 gel column chromatography (20 → 50% EtOAc in PhMe) afforded the boronate ester as a colourless oil (9 mg, 0.02 mmol, 32%); δ_H (600 MHz, $CDCl_3$) 10.18 (1H, s br, NH) 7.77 (1H, s, 5''-H), 7.53 (1H, s br, NH) 7.46 (2H, d, *J* = 9.1 Hz, 2'-H) , 6.88 (2H, d, *J* = 9.1 Hz, 3'-H) 5.29-5.27 (1H, dd, *J* = 8.8, 2.8 Hz, 2'''-H), 4.06-4.02 (1H, m, 6'''-H), 3.80 (3H, s, OCH_3), 3.71-3.67 (1H, m, 6'''-H), 2.15-2.03 (3H, m, 3'''-H, 4'''-H) 1.73-1.62 (3H, m, 4'''-H, 5'''-H), 1.31 (12H, s, 4''''-CH_3); δ_C (151 MHz, $CDCl_3$) 155.9 (C-4'), 154.2 (C-3''), 152.6 (C=O), 135.8 (C-5''), 132.1 (C-1'), 122.1 (C-2'), 114.3 (C-3'), 87.2 (C-2'''), 84.0 (C-4''''), 67.6 (C-6'''), 55.7 (OCH_3), 30.2 (C-3'''), 25.1 (C-5'''), 24.9 (4''''-CH_3), 24.9 (4''''-CH_3), 22.3 (C-4'''); HRMS (ESI) *m/z* found $[M]^+$ 442.2507, $C_{22}H_{32}BN_4O_5$ requires *M*, 442.2502.

1-(4'-methoxyphenyl)-3-[1''-(oxan-2'''-yl)-5-(quinolin-6''''-yl)-1H-pyrazol-3''-yl]urea (**423**)

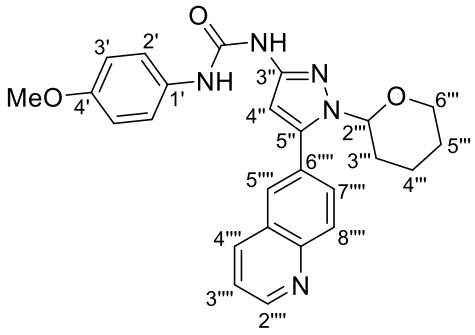

Synthesised from 1-(4-methoxyphenyl)-3-[1-(oxan-2-yl)-1H-pyrazol-3-yl]urea **420** (50 mg, 0.16 mmol, 1.00 equiv.) according to General Procedure A followed by General Procedure B in a one-pot borylation/cross-coupling procedure using 6-bromoquinoline. After 16 h, removal of the volatiles followed by SiO_2 gel flash chromatography (0 → 20% EtOAc in CH_2Cl_2) afforded the arylated aminopyrazole urea as a white solid (7 mg, 0.02 mmol, 10%); mp: 166-168 °C; ν_{max} (ATR) 3277 (NH), 2946, 1687 (C=O), 1607, 1564, 1510, 1314, 1244, 1181, 1038 cm^{-1}; δ_H (700 MHz, $CDCl_3$) 9.01 (1H, d, *J* = 4.0 Hz, 2''''-H) 8.24-8.23 (2H, m, 4''''-H, 8''''-H), 8.04 (1H, d, *J* = 1.6 Hz, 5''''-H) 7.89 (1H, dd, *J* = 8.6, 1.6 Hz, 7''''-H), 7.51 (1H, dd, *J* = 8.2, 4.0 Hz, 3''''-H) 7.44 (2H, d, 8.7 Hz, 2'-H), 6.90 (2H, d, *J* = 8.7 Hz, 3'-H), 6.27 (1H, s, 4''-H), 5.18 (1H, dd, *J* = 10.1, 2.0 Hz, 2'''-H), 4.16 (1H, d, *J* = 11.7 Hz, 6'''-H), 3.80 (3H, s, OCH_3), 3.61 (1H, t, *J* = 11.7 Hz, 6'''-H), 2.52-2.47 (1H, m, 3'''-H), 2.08-2.06 (1H, m, 4'''-H), 1.93 (1H, d, *J* = 13.1 Hz, 4'''-H), 1.74 (1H, m, 5'''-H), 1.60-1.53 (2H, m, 4'''-H, 5'''-H); δ_C (176 MHz, $CDCl_3$) 156.3 (C-4'), 153.2 (C=O), 151.4 (C-2''''), 148.6 (C-3''), 148.0 (C-8_a''''), 144.9 (5''-H), 136.9 (C-

4’’’’), 131.7 (C-1’), 130.2 (C-7’’’’), 130.1 (C-8’’’’), 128.6 (C-5’’’’), 128.3 (4’’’’-*C*-5’’’’), 128.0 (C-6’’’’), 122.5 (C-2’), 122.1 (C-3’’’’), 114.4 (C-4_a’’’) 96.8 (C-4’’), 84.5 (C-2’’’), 68.0 (C6’’’), 55.7 (OCH_3), 30.0 (C-3’’’), 24.9 (C-5’’’), 23.1 (C-4’’’); HRMS (ASAP) *m/z* found $[M]^+$ 443.1930, $C_{25}H_{25}N_5O_3$ requires *M*, 443.1957.

5-(4’,4’,5’,5’-tetramethyl-1,3,2-dioxaborolan-2-yl)-1-{[2’’-(trimethylsilyl)ethoxy]methyl}-1H-pyrazol-3-amine (**451**)

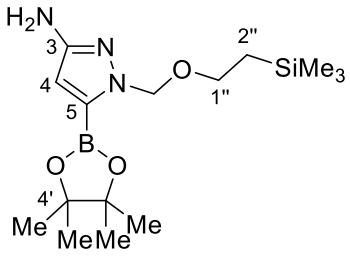

Synthesised from tert-butyl N-(1-{[2-(trimethylsilyl)ethoxy]methyl}-1H-pyrazol-3-yl)carbamate **450** (426 mg, 2.00 mmol, 0.50 M, 1.00 equiv.) according to General Procedure A. SiO_2 gel column chromatography (0 → 100 % EtOAc in Hexanes) afforded the borylated pyrazole as a colourless oil (292 mg, 0.86 mmol, 43%); ν_{max} (ATR) 3342 (NH_2), 3268 (NH_2), 2978, 1618, 1485, 1296, 1248, 1143, 1088, 1066 cm^{-1}; δ_H (700 MHz, $CDCl_3$) 6.09 (1H, s, 4-H), 5.47 (2H, s, OCH_2), 3.79 (2H, s br, NH_2), 3.54-3.51 (2H, m, 1’’-H), 1.31 (12H, s, 4’-CH_3), 0.90-0.87 (2H, m, 2’’-H), -0.05 (9H, s, $SiCH_3$); δ_C (176 MHz, $CDCl_3$) 154.6 (C-3), 104.1 (C-4), 84.4 (C-4’), 79.0 (OCH_2), 66.0 (C-1’’), 24.9 (4’-CH_3), 18.0 (C-2’’), -1.3 ($SiCH_3$); δ_B (128 MHz, $CDCl_3$) 27.5; HRMS (ESI) *m/z* found $[M+H]^+$ 339.2281, $C_{15}H_{30}BN_3O_3Si$ requires *M*, 339.2264.

Tert-butyl N-[5-(4’-methylphenyl)-1-{[2’’-(trimethylsilyl)ethoxy]methyl}-1H-pyrazol-3-yl]carbamate (**454a**)

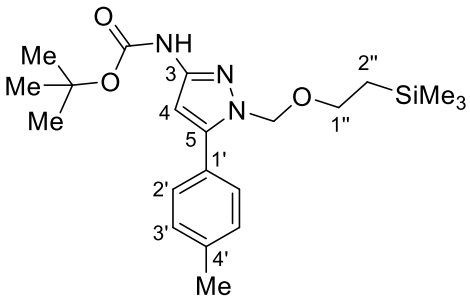

Synthesised from tert-butyl N-(1-{[2-(trimethylsilyl)ethoxy]methyl}-1H-pyrazol-3-yl)carbamate **452** (157 mg, 0.50 mmol, 1.00 M, 1.00 equiv) according to General Procedure A followed by General Procedure

B in a one-pot borylation/cross-coupling procedure using 1-bromo-4-methylbenzene. After 3 h, the volatiles were removed and SiO_2 gel flash chromatography (5 → 15 % EtOAc in hexanes) afforded the cross-coupled pyrazole as an oily orange solid (113 mg, 0.28 mmol, 56%); ν_{max} (ATR) 3225 (NH), 2948, 1718 (C=O), 1587, 1543, 1483, 1367, 1260, 1242, 1153, 1079, 1025 cm^{-1}; δ_H ($CDCl_3$, 700 MHz) 7.82 (1H, s br, NH), 7.52 (2H, d, *J* = 8.0 Hz, 2'-H), 7.24 (2H, d, *J* = 8.0 Hz, 3'-H) 6.69 (1H, s br, 4-H), 5.32 (2H, s, NCH_2), 3.69-3.67 (2H, m, 2'-H), 2.39 (3H, s, 4'-CH_3) 1.51 (9H, s, CCH_3), 0.93-0.91 (2H, m, 2''-H), -0.04 (9H, s, $SiCH_3$); δ_C (176 MHz, $CDCl_3$) 152.9 (C=O), 147.5 (C-3), 145.7 (C-5), 138.8 (C-4'), 129.5 (C-3'), 128.9 (C-2'), 127.4 (C-1'), 97.2 (C-4), 80.7 ($OCCH_3$) 77.5 (OCH_2), 66.7 (C-1''), 28.5 ($OCCH_3$), 21.4 (4'-CH_3), 18.1 (C-2''), -1.3 ($SiCH_3$); δ_{Si} (139 MHz, $CDCl_3$) -0.10; HRMS (ASAP) *m/z* found $[M+H]^+$ 404.2361, $C_{21}H_{34}N_3O_3Si$ requires *M*, 404.2374.

Tert-butyl N-[5-(4'-fluorophenyl)-1-{[2''-(trimethylsilyl)ethoxy]methyl}-1H-pyrazol-3-yl]carbamate (**454b**)

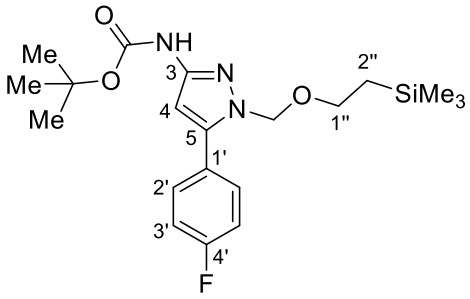

Synthesised from tert-butyl N-(1-{[2-(trimethylsilyl)ethoxy]methyl}-1H-pyrazol-3-yl)carbamate **452** (313 mg, 1.00 mmol, 1.00 M, 1.00 equiv) according to General Procedure A followed by General Procedure B in a one-pot procedure using 1-bromo-4-fluorobenzene. After 16 h, the volatiles were removed and SiO_2 gel flash chromatography (0 → 20 % EtOAc in hexanes) afforded the arylated pyrazole as a white solid (191 mg, 0.47 mmol, 47%); mp: 129-130 °C; ν_{max} (ATR) 3254 (NH), 2960, 1718 (C=O), 1608, 1564, 1511, 1234, 1154 cm^{-1}; δ_H ($CDCl_3$, 700 MHz) 7.94 (1H, s br, NH), 7.62-7.61 (2H, m, 2'-H), 7.13 (2H, t, *J* = 8.5 Hz, 3'-H), 6.71 (1H, s br, 4-H), 5.31 (2H, s, NCH_2), 3.72-3.69 (2H, m, 2''-H), 1.53 (9H, s, CCH_3), 0.94-0.91 (2H, m, 1''-H), -0.04 (9H, s, $SiCH_3$); δ_C (151 MHz, $CDCl_3$) 163.2 (d, *J* = 250 Hz, C-4'), 152.9 (C=O), 147.5 (C-3), 144.5 (C-5), 130.9 (d, *J* = 8 Hz, C-2'), 126.3 (d, *J* = 3 Hz, C-1'), 115.9 (d, *J* = 22 Hz, C-3'), 97.6 (C-4), 80.9 (CCH_3), 77.5 (OCH_2), 66.8 (C-1''), 28.5 (CCH_3), 18.1 (C-2''), -1.3 ($SiCH_3$); δ_F (376 MHz, $CDCl_3$) -112.8; HRMS (ASAP) m/z found $[M+H]^+$ 408.2119, $C_{20}H_{31}FN_3O_3Si$ requires *M*, 408.2119.

Tert-butyl N-[5-(4'-nitrophenyl)-1-{[2''-(trimethylsilyl)ethoxy]methyl}-1H-pyrazol-3-yl]carbamate (**454c**)

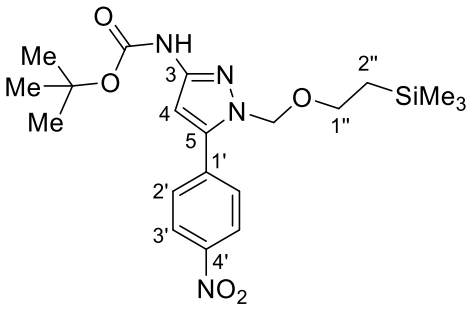

Synthesised from tert-butyl N-(1-{[2-(trimethylsilyl)ethoxy]methyl}-1H-pyrazol-3-yl)carbamate **452** (313 mg, 1.00 mmol, 1.00 M, 1.00 equiv) according to General Procedure A followed by General Procedure B in a one-pot borylation/cross-coupling procedure using 1-bromo-4-nitrobenzene. After 16 h, the volatiles were removed and SiO_2 gel column chromatography (0 → 10 % Et_2O in PhMe) afforded the cross-coupled pyrazole as a bright yellow solid (169 mg, 0.39 mmol, 39%); mp: 139-141 ^oC; ν_{max} (ATR) 3254 (NH) 2960, 1722 (C=O), 1613, 1566, 1514, 1478, 1343, 1238, 1156, 1112 cm^{-1}; δ_H ($CDCl_3$, 700 MHz) 8.29 (2H, d, *J* = 8.7 Hz, 3'-H), 7.89 (1H, s br, NH), 7.87 (2H, d, *J* = 8.7 Hz, 2'-H), 6.88 (1H, s, 4-H), 5.36 (2H, s, OCH_2), 3.76-3.74 (2H, m, 2''-H), 1.53 (9H, s, CCH_3), 0.96-0.94 (2H, m, 1''-H), -0.03 (9H, s, $SiCH_3$); δ_C (176 MHz, $CDCl_3$) 152.8 (C=O), 147.9 (C-4'), 147.7 (C-3), 143.0 (C-5), 136.2 (C-1'), 129.6 (C-2'), 124.2 (C-3'), 98.8 (C-4), 81.2 ($OCCH_3$), 77.9 (NCH_2), 67.1 (C-1''), 28.5 ($OCCH_3$), 18.1 (C-2''), -1.3 ($SiCH_3$); HRMS (ESI) *m/z* found $[M+H]^+$ 435.2065, $C_{20}H_{31}N_4O_5Si$ requires *M*, 435.2064.

3,4-dimethyl-1-[5'-(4''-methylphenyl)-1'-{[2'''-(trimethylsilyl)ethoxy]methyl}-1H-pyrazol-3'-yl]-2,5-dihydro-1H-pyrrole-2,5-dione (**479**)

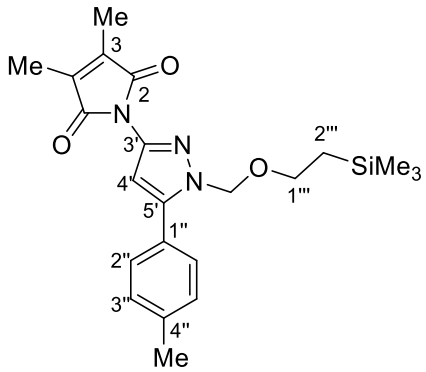

Synthesised from 1-{[2-(trimethylsilyl)ethoxy]methyl}-1H-pyrazol-3-amine **450** (213 mg, 1.00 mmol, 0.50 M, 1.00 equiv) according to General Procedure A followed by General Procedure B in a one-pot borylation/cross-coupling procedure using 1-bromo-4-methylbenzene. After 16 h, the volatiles were removed and the crude arylated aminopyrazole **485** was suspended in H_2O (5 mL). Dimethyl-2,5-dihydrofuran-2,5-dione (304 mg, 1.00 mmol, 1.00 equiv) was added and the reaction was stirred at 80 ^oC for 1 h, cooled, and diluted with CH_2Cl_2 (10 mL). The aqueous layer was extracted with CH_2Cl_2 (3 x 5 mL), and the combined organic fractions were dried over $MgSO_4$, filtered, an evaporated. SiO_2 gel column chromatography (60 → 100% CH_2Cl_2 in hexanes) followed by recrystallisation from hexanes afforded the corresponding arylated pyrazole as a white solid (289 mg, 0.70 mmol, 70%); mp: 81-83 ^oC (hexanes); ν_{max} (ATR) 2957, 1728 (C=O), 1713 (C=O), 1516, 1487, 1346, 1250, 1087, cm^{-1}; δ_H (600 MHz, $CDCl_3$) 7.53 (2H, d, *J* = 8.0 Hz, 2''-H) 7.26-7.25 (2H, m, 3''-H), 6.40 (1H, s, 4'-H), 5.41 (2H, s, OCH_2), 3.79- 3.76 (2H, m, 1'''-H), 2.40 (3H, s, 4''-CH_3) 2.05 (6H, s, 3-CH_3), 0.95-0.92 (2H, m, 2'''-H), -0.01 (9H, s, $SiCH_3$); δ_C (151 MHz, $CDCl_3$) 170.3 (C-2), 146.1 (C-5'), 140.2 (C-3'), 139.1 (C-4''), 138.1 (C-3), 129.6 (C-3''), 129.1 (C-2''), 126.8 (C-1''), 103.1 (C-4'), 78.3 (OCH_2), 67.2 (C-1'''), 21.4 (4''-CH_3), 18.1 (C-2'''), 9.1 (3-CH_3), -1.3 ($SiCH_3$); HRMS (ESI) *m/z* found $[M+H]^+$ 412.2048, $C_{22}H_{30}N_3O_3Si$ requires *M*, 412.2056.

3,3-dimethyl-1-[5'-(4''-methylphenyl)-1'-(oxan-2''-yl)-1H-pyrazol-3'-yl]pyrrolidine-2,5-dione (**488a**)

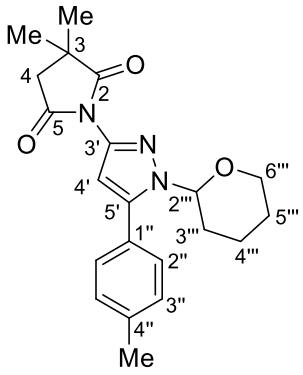

Synthesised from 3,3-dimethyl-1-[1-(oxan-2-yl)-1H-pyrazol-3-yl]pyrrolidine-2,5-dione **485** (146 mg, 0.36 mmol, 1.00 equiv.) according to General Procedure A followed by General Procedure B in a one-pot borylation/cross-coupling procedure using 4-methylbromobenzene. After 2 h, the volatiles were removed and SiO_2 gel column chromatography (20 → 50% acetone in hexanes) afforded the arylated

aminopyrazole as a colourless oil (product contains 15% constitutional isomer 3,3-dimethyl-1-[4-(4-methylphenyl)-1-(oxan-2-yl)-1H-pyrazol-3-yl]pyrrolidine-2,5-dione **499ai**) (14 mg, 0.04 mmol, 11%); ν_{max} (ATR) 2933, 1789 (C=O), 1722 (C=O), 1509, 1477, 1209, 1152, 1084, 1042 cm^{-1}; δ_H (700 MHz, $CDCl_3$) 7.43 (2H, d, *J* = 8.0 Hz, 2''-H) 7.27-7.26 (2H, m, 3''-H), 6.34 (1H, s, 4'-H), 5.22 (1H, dd, *J* = 10.1, 2.5 Hz, 2'''-H) 4.13, 4.13-4.10 (1H, m, 6'''-H), 3.59-3.55 (1H, td, *J* = 11.6, 2.4 Hz, 6'''-H) 2.71 (2H, m, 4-H) 2.54-2.48 (1H, m, 3'''-H) 2.42 (3H, s, 4''-CH_3), 2.05-2.02 (1H, m, 4'''-H) 1.87-1.84 (1H, m, 3'''-H) 1.77-1.70 (1H, m, 5'''-H), 1.55-1.51 (2H, m, 4'''-H, 5'''-H), 1.43 (3H, s, 3-CH_3), 1.41 (3H, s, 3-CH_3); δ_C (176 MHz, $CDCl_3$) 181.5 (C-2), 174.2 (C-5), 145.8 (C-5'), 140.5 (C-3'), 139.2 (C-4''), 129.5 (C-3''), 129.2 (C-2''), 126.9 (C-1''), 103.2 (C-4'), 84.6 (C-2'''), 67.8 (C-6'''), 44.0 (C-4), 40.4 (C-3), 29.8 (C-3'''), 26.0 (3-CH_3), 25.9 (3-CH_3), 24.9 (C-5'''), 22.9 (C-4'''), 21.5 (4''-CH_3); HRMS (ESI) m/z found $[M+H]^+$ 368.1959, $C_{21}H_{26}N_3O_3$ requires *M*, 368.1974.

Methyl 4-[3'-(3'',3''-dimethyl-2'',5''-dioxopyrrolidin-1''-yl)-1'-(oxan-2'''-yl)-1H-pyrazol-5'-yl]benzoate (**488b**)

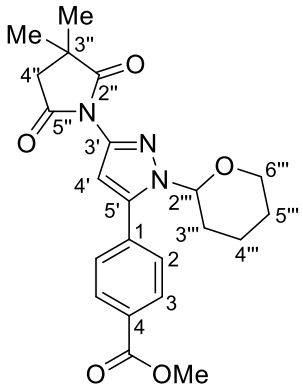

Synthesised from 3,3-dimethyl-1-[1-(oxan-2-yl)-1H-pyrazol-3-yl]pyrrolidine-2,5-dione **485** (50 mg, 0.18 mmol, 1.00 equiv.) in a one-pot procedure according to General Procedure A followed by Suzuki-Miyaura according to a modified procedure of Mclaughlin *et al.*[2]. To an oven-dried vial was added $Pd(dba)_2$ (2 mg, 2.5 mol%), PCy_3HBF_4 (2 mg, 4 mol%), K_3PO_4 (115 mg, 0.54 mmol, 3.00 equiv.), and methyl 4-bromobenzoate (39 mg, 0.18 mmol, 1.00 equiv.). The vial was sealed and subjected to three N_2 purge/refill cycles. A solution of crude pyrazole boronate ester in degassed dioxane (0.54 mL) was added, and the reaction mixture was stirred at 80 °C for 16 h, before filtration over Celite® with EtOAc (5 mL). SiO_2 gel column chromatography (0 → 40% EtOAc in PhMe (1% Et_3N)) afforded the arylated aminopyrazole as a colourless oil (13 mg, 0.03 mmol, 18%); ν_{max} (ATR) 2950, 1791 (C=O), 1724 (C=O),

1617, 1557, 1507, 1481, 1444, 1338, 1284, 1111, 1048 cm^{-1}; δ_H (700 MHz, $CDCl_3$) 8.13 (2H, d, *J* = 8.6 Hz, 3-H) 7.64 (2H, d, *J* = 8.6 Hz, 2-H), 6.45 (1H, s, 4'-H), 5.20 (1H, dd, *J* = 10.0 Hz, 2.6 Hz, 2'''-H), 4.14-4.11 (1H, m, 6'''-H), 3.95 (3H, s, OCH_3) 3.57 (1H, td, *J* = 11.6, 2.3 Hz, 6'''-H), 2.72 (2H, d, *J* = 1.5 Hz, 4''-H) 2.54-2.48 (1H, m, 3'''-H) 2.07-2.04 (1H, m, 4'''-H), 1.89-1.86 (1H, m, 3'''-H), 1.76-1.70 (1H, m, 5'''-H), 1.57-1.51 (2H, m, 4'''-H, 5'''-H), 1.43 (3H, s, 3''-CH_3), 1.42 (3H, s, 3''-CH_3); δ_C (176 MHz, $CDCl_3$) 181.5 (C-2''), 174.1 (C-5''), 166.7 (C=O), 144.6 (C-5'), 140.6 (C-3'), 134.1 (C-1), 130.7 (C-4), 130.1 (C-3), 129.2 (C-2), 104.0 (C-4'), 85.0 (C-2'''), 67.8 (C-6'''), 52.5 (OCH_3), 44.0 (C-4''), 40.5 (C-3''), 29.7 (C-3'''), 25.9 (3''-CH_3), 25.87 (3''-CH_3), 24.8 (C-5'''), 22.8 (C-4'''); HRMS (ESI) *m/z* found $[M+H]^+$ 412.1880, $C_{22}H_{26}N_3O_5$ requires *M*, 412.1872.

3,3-Dimethyl-1-[1'-(oxan-2''-yl)-5'-(thiophen-2'''-yl)-1H-pyrazol-3'-yl]pyrrolidine-2,5-dione (**488c**)

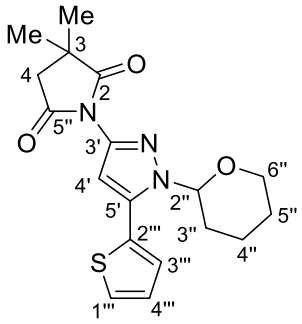

Synthesised from 3,3-dimethyl-1-[1-(oxan-2-yl)-1H-pyrazol-3-yl]pyrrolidine-2,5-dione **485** (50 mg, 0.18 mmol, 1.00 equiv.) in a one-pot procedure according to General Procedure A followed by Suzuki-Miyaura cross-coupling according to a modified procedure of Clapham *et al*.[3]. To an oven-dried vial was added $Pd(dppf)Cl_2•CH_2Cl_2$ (13 mg, 10 mol%), K_3PO_4 (102 mg, 0.48 mmol, 3.00 equiv.), and KOCHO (7 mg, 0.08 mmol, 0.50 equiv.). The vial was sealed and subject to three N_2 purge/refill cycles. The crude boronate ester (1.1 equiv.) in degassed dioxane (1.1 mL) followed by 2-bromothiophene (0.02 mL, 0.16 mmol, 1.00 equiv.) were added and the reaction was stirred at 80 °C for 16 h. Filtration over Celite® with EtOAc (10 mL) followed by SiO_2 gel column chromatography (0 → 40% EtOAc in PhMe) afforded the heteroarylated aminopyrazole as a colourless oil (9 mg, 0.03 mmol 16%); ν_{max} (ATR) 2967, 1788 (C=O), 1726 (C=O), 1518, 1481, 1457, 1321, 1234, 1208, 1154, 1088, 1038 cm^{-1}; δ_H (700 MHz, $CDCl_3$) 7.45 (1H, dd, *J* = 5.1, 1.1 Hz, 1'''-H) 7.31 (1H, dd, *J* = 3.5, 1.1 Hz, 3'''-H) 7.14-7.12 (1H, m, 4'''-H), 6.46 (1H, s, 4''-H), 5.38 (1H, dd, *J* = 9.8, 2.5 Hz, 2''-H) 4.12-4.08 (1H, m, 6''-H), 3.65 (1H, td, *J* = 11.4, 2.7 Hz, 6''-H), 2.71 (2H, d, *J* = 1.5 Hz, 4-H), 2.54-2.48 (1H, m, 3''-H) 2.11-2.08 (1H,

m, 4''-H), 1.96-1.94 (1H, m, 3''-H), 1.75-1.72 (1H, m, 5''-H) 1.63-1.55 (2H, m, 5''-H, 4''-H) 1.43 (3H, s, 3-CH_3), 1.42 (3H, s, 2-CH_3); δ_C (176 MHz, $CDCl_3$) 181.5 (C-2), 174.1 (C-5), 140.3 (C-3'), 138.8 (C-5'), 129.9 (C-2'''), 128.6 (C-3'''), 127.83 (C-1'''), 127.81 (C-4'''), 104.4 (C-4'), 84.8 (C-2''), 67.5 (C-6''), 44.0 (C-4), 40.5 (C-3), 29.3 (C-3''), 26.0 (3-CH_3), 25.9 (3-CH_3), 24.9 (C-5''), 22.8 (C-4''); HRMS (ESI) *m/z* found $[M+H]^+$ 360.1374, $C_{18}H_{22}N_3O_3S$ requires *M*, 360.1382.

Tert-butyl 3-methyl-4-(4'-methylphenyl)-1H-pyrazole-1-carboxylate (**494**)

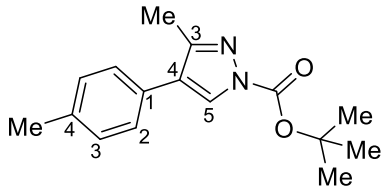

Synthesised from a 9:1 mixture of tert-butyl 3-methyl-1H-pyrazole-1-carboxylate and tert-butyl 5-methyl-1H-pyrazole-1-carboxylate **493a** and **493b** (182 mg, 1.00 mmol, 1.00 M, 1.00 equiv) according to General Procedure A using 1.50 equiv. B_2pin_2 followed by General Procedure B in a one-pot borylation/cross-coupling procedure using 4-bromotoluene. After 1 h, the volatiles were removed and SiO_2 gel flash chromatography (10 → 20 % EtOAc in hexanes) afforded the cross-coupled pyrazole as a yellow/orange oil (272 mg, 78%). Product contains *ca.* 6% of isomer tert-butyl 5-methyl-4-(4-methylphenyl)-1H-pyrazole-1-carboxylate **494b**; δ_H (600 MHz, $CDCl_3$) 8.05 (1H, s, 5-H), 7.30 (2H, d, *J* = 7.9 Hz, 2'-H), 7.21 (2H, d, *J* = 7.9 Hz, 3'-H), 2.43 (3H, s, 3-CH_3), 2.38 (3H, s, 4'-CH_3), 1.66 (9H, s, $OCCH_3$); δ_C (151 MHz, $CDCl_3$) 151.7 (C-3), 147.8 (C=O), 137.2 (C-4'), 129.5 (C-3'), 129.0 (C-1'), 128.3 (C-5), 127.8 (C-2'), 124.7 (C-4), 85.1 ($OCCH_3$) 28.1 ($OCCH_3$), 21.3 (4'-CH_3), 13.8 (3-CH_3); HRMS (ESI) *m/z* found $[M+H]^+$ 273.1630, $C_{16}H_{21}N_2O_2$ requires *M*, 273.1603.

tert-butyl 3-(3',3'-dimethyl-2',5'-dioxopyrrolidin-1'-yl)-4-(4'',4'',5'',5''-tetramethyl-1'',3'',2''-dioxaborolan-2''-yl)-1H-pyrazole-1-carboxylate (**500**)

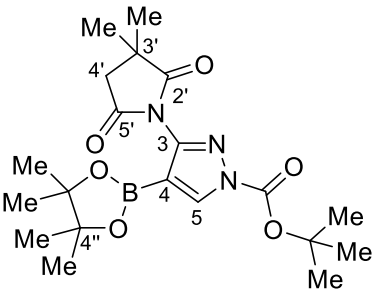

Synthesised from tert-butyl 3-(3,3-dimethyl-2,5-dioxopyrrolidin-1-yl)-1H-pyrazole-1-carboxylate **498** (35 mg, 0.12 mmol, 1.00 equiv.) according to General Procedure A using 1.00 equiv. B_2pin_2. SiO_2 gel column chromatography (0 → 100% EtOAc in hexanes) afforded the the borylated pyrazole as a white solid (38 mg, 0.10 mmol, 76%); mp: 158-159 °C; ν_{max} (ATR) 2984, 1781 (C=O), 1764 (C=O), 1731 (C=O), 1574, 1498, 1377, 1314, 1231, 1148, 1088 cm^{-1}; δ_H (700 MHz, $CDCl_3$) 8.40 (1H, s, 5-H), 2.69 (2H, s, 4'-H), 1.62 (9H, s, $C(CH_3)_3$), 1.43 (6H, s, 3'-CH_3), 1.25 (12H, s, 4''-CH_3); δ_C (176 MHz, $CDCl_3$) 181.3 (C-2'), 174.5 (C-5'), 149.0 (C-3), 146.5 (C=O), 139.4 (C-5), 86.5 ($C(CH_3)_3$), 84.1 (C-4'), 44.3 (C-4'), 40.6 (C-3'), 28.0 ($C(CH_3)_3$), 25.7 (3'-CH_3), 24.9 (4''-CH_3); HRMS (ESI) *m/z* found $[M]^+$ 419.2326, $C_{20}H_{30}BN_3O_6$ requires *M*, 419.2342.

Tert-butyl 3-(3',3'-dimethyl-2',5'-dioxopyrrolidin-1'-yl)-4''-phenyl-1H-pyrazole-1-carboxylate (**501a**)

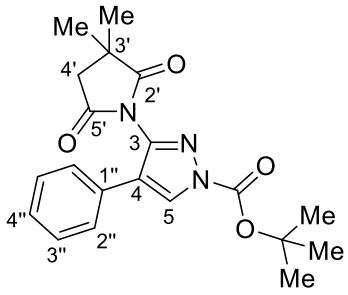

Synthesised from tert-butyl 3-(3,3-dimethyl-2',5'-dioxopyrrolidin-1'-yl)-4-(4,4,5,5-tetramethyl-1,3,2-dioxaborolan-2-yl)-1H-pyrazole-1-carboxylate **500** (30 mg, 0.07 mmol, 1.00 equiv.) according to General Procedure C with iodobenzene. SiO_2 gel column chromatography (20 → 40 % EtOAc in hexanes) afforded the arylated aminopyrazole as a colourless oil (13 mg, 0.04 mmol, 49%); ν_{max} (ATR) 2981, 1781 (C=O), 1760 (C=O), 1727 (C=O), 1507, 1483, 1450, 1402, 1372, 1308, 1292, 1251, 1235, 1215, 1150 cm^{-1}; δ_H (600 MHz, $CDCl_3$) 8.22 (1H, s, 5-H), 7.37-7.31 (3H, m, Ph H) 7.28-7.26 (2H, m, Ph H), 2.67 (2H, s, 4'-H), 1.66 (9H, s, $C(CH_3)_3$), 1.33 (6H, s, 3'-CH_3); δ_C (151 MHz, $CDCl_3$) 181.7 (C-2'), 174.5 (C-5'), 146.8 (CO_2), 142.4 (C-3), 130.0 (C-5), 129.5 (C-1''), 129.0 (Ph C), 128.4 (Ph C), 127.9 (Ph C), 123.4 (C-4), 86.7 ($C(CH_3)_3$), 44.2 (C-4'), 40.9 (C-3'), 28.1 ($C(CH_3)_3$), 25.7 (3'-CH_3); HRMS (ESI) *m/z* found $[M+H]^+$ 370.1779, $C_{20}H_{24}N_3O_4$ requires *M*, 370.1767.

Tert-butyl 3-(3',3'-dimethyl-2',5'-dioxopyrrolidin-1'-yl)-4-(4''-fluorophenyl)-1H-pyrazole-1-carboxylate (**501b**)

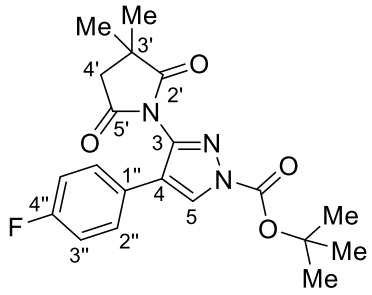

Synthesised from tert-butyl 3-(3,3'-dimethyl-2',5'-dioxopyrrolidin-1'-yl)-4-(4,4,5,5-tetramethyl-1,3,2-dioxaborolan-2-yl)-1H-pyrazole-1-carboxylate **500** (62 mg, 0.15 mmol, 1.00 equiv.) according to General Procedure C with 1-bromo-4-fluorobenzene. SiO_2 gel column chromatography (20 → 40 % EtOAc in hexanes) afforded the arylated aminopyrazole as a white solid (38 mg, 0.10 mmol, 66%); mp: 148-150 ^oC; ν_{max} (ATR) 2984, 1779 (C=O), 1761 (C=O), 1726 (C=O), 1579, 1514, 1488, 1420, 1396, 1371, 1306, 1291, 1252, 1230, 1149, cm^{-1}; δ_H (600 MHz, $CDCl_3$) 8.19 (1H, s, 5-H), 7.25-7.22 (2H, m, 2''-H), 7.04 (2H, t, *J* = 8.7 Hz, 3''-H) 2.67 (2H, s, 4'-H), 1.65 (9H, s, $C(CH_3)_3$), 1.32 (6H, s, 3'-CH_3); δ_C (151 MHz, $CDCl_3$) 181.7 (C-2'), 174.4 (C-5'), 162.8 (d, *J* = 248 Hz, C-4'') 146.7 (CO_2), 142.3 (C-5), 130.0 (C-5), 129.8 (d, *J* = 8 Hz, C-2'') 125.5 (d, *J* = 3 Hz, C-1'') 122.4 (C-4), 116.0 (d, *J* = 22 Hz, 3''-H), 86.7 ($C(CH_3)_3$), 44.1 (C-4'), 40.9 (C-3'), 28.0 ($C(CH_3)_3$), 25.6 (3'-CH_3); HRMS (ESI) *m/z* found $[M+H]^+$ 388.1671, $C_{20}H_{23}N_3O_4F$ requires *M*, 388.1673.

Tert-butyl 3-(3',3'-dimethyl-2',5'-dioxopyrrolidin-1'-yl)-4-(4''-methylphenyl)-1H-pyrazole-1-carboxylate (**501c**)

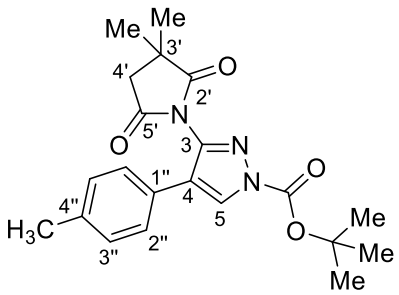

Synthesised from tert-butyl 3-(3,3-dimethyl-2,5-dioxopyrrolidin-1-yl)-4-(4,4,5,5-tetramethyl-1,3,2-dioxaborolan-2-yl)-1H-pyrazole-1-carboxylate **500** (62 mg, 0.15 mmol, 1.00 equiv.) according to

General Procedure C with 1-bromo-4-methylbenzene. SiO_2 gel column chromatography (25 → 35 % EtOAc in hexanes) afforded the arylated aminopyrazole as a colourless oil (20 mg, 0.05 mmol, 35%); ν_{max} (ATR) 2981, 1779 (C=O), 1758 (C=O), 1727 (C=O), 1587, 1518, 1488, 1399, 1371, 1306, 1293, 1253, 1235, 1212, 1150 cm^{-1}; δ_H (600 MHz, $CDCl_3$) 8.19 (1H, s, 5-H), 7.15 (4H, s, 2''-H, 3''-H) 2.67 (2H, s, 4'-H), 2.34 (3H, s, 4''-CH_3), 1.65 (9H, s, $C(CH_3)_3$), 1.34 (6H, s, 3'-CH_3); δ_C (151 MHz, $CDCl_3$) 181.7 (C-2'), 174.5 (C-5'), 146.8 (CO_2), 142.4 (C-3), 138.2 (C-4''), 129.8 (C-5), 129.7 (C-2''), 127.6 (C-3''), 126.5 (C-1''), 123.3 (C-4), 44.2 (C-4'), 40.9 (C-3'), 28.0 ($C(CH_3)_3$), 25.7 (3'-CH_3), 21.3 (4''-CH_3); HRMS (ESI) *m/z* found $[M+H]^+$ 384.1923, $C_{21}H_{26}N_3O_4$ requires *M*, 384.1923.

Methyl 4-(3'-nitro-1'-{[2''-(trimethylsilyl)ethoxy]methyl}-1H-pyrazol-5'-yl)benzoate (**513**)

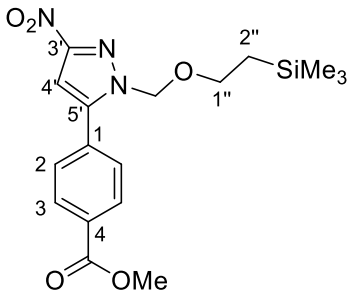

Synthesised from 3-nitro-1-{[2-(trimethylsilyl)ethoxy]methyl}-1H-pyrazole **449** (61 mg, 0.25 mmol, 0.50 M, 1.00 equiv) according to General Procedure A using 1.50 equiv. B_2pin_2. The crude pyrazole boronate ester was cross-coupled according to the following procedure. To an oven-dried vial was added $Pd(dppf)Cl_2$ (18 mg, 10 mol%) and K_3PO_4 (106 mg, 0.50 mmol, 2.00 equiv.). The vial was subjected to three N_2 purge/refill cycles. Methyl 4-iodobenzoate (72 mg, 0.28 mmol, 1.10 equiv.) followed by a solution of crude pyrazole boronate ester in degassed 2-MeTHF (0.5 mL) were added. The reaction mixture was stirred at 80 °C for 16 h before removal of the volatiles. SiO_2 gel column chromatography (5 → 20 % EtOAc in Hexanes) afforded the corresponding arylated pyrazole as a colourless oil (19 mg, 0.05 mmol, 20%); ν_{max} (ATR) 2971, 1739 (C=O), 1608, 1510, 1447, 1343, 1235, 1154, cm^{-1}; δ_H (600 MHz, $CDCl_3$) 8.17 (2H, d, *J* = 8.4 Hz, 3-H), 7.76 (2H, d, *J* = 8.4 Hz, 2-H), 7.08 (1H, s, 4'-H), 5.49 (2H, s, OCH_2), 3.96 (3H, s, OCH_3), 3.84-3.81 (2H, m, 2''-H), 0.98-0.95 (2H, m, 1''-H), -0.01 (9H, s, $SiCH_3$); δ_C (151 MHz, $CDCl_3$) 166.3 (C=O), 155.6 (C-3'), 146.5 (C-5'), 132.2 (C-1), 131.6 (C-4), 130.4 (C-3), 129.1 (C-2), 103.3 (C-4'), 79.7 (OCH_2), 68.2 (C-2''), 52.6 (OCH_3), 18.1 (C-1''), -1.3 ($SiCH_3$); HRMS (ASAP) *m/z* found $[M-H]^+$ 376.1327, $C_{17}H_{22}N_3O_5Si$ requires *M*, 376.1329.

N-[3-(4'-fluorophenyl)-1-(oxan-2''-yl)-1H-pyrazol-5-yl]acetamide (**540**)

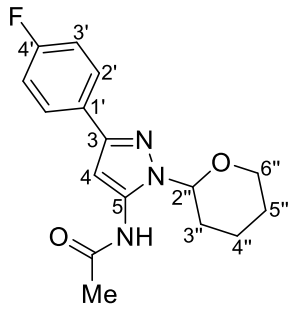

Synthesised from N-[1-(oxan-2-yl)-1H-pyrazol-5-yl]acetamide **538** (77 mg, 0.37 mmol, 1.00 equiv.) in a one-pot procedure according to General Procedure A with modifications. The borylation was stirred for 3 h. Suzuki-Miyaura cross-coupling according to a modified procedure of Chai *et al.* of the crude pyrazole boronate ester was performed as follows.[4] To an oven-dried vial was added Pd(dppf)Cl_2 (16 mg, 10 mol%) and tetrabutylammonium bromide (7 mg, 0.02 mmol, 0.10 equiv. The vial was sealed and subject to three N_2 purge/refill cycles. The crude boronate ester (1.0 equiv.) in degassed PhMe (1.1 mL) followed by 1-bromo-4-fluorobenzene (0.02 mL, 0.22 mmol, 1.00 equiv.) were added and the mixture was cooled to 0 °C. 2M Na_2CO_3 (0.22 mL, 0.44 mmol, 2.00 equiv.) was added and the reaction was stirred at 110 °C for 1 h. EtOAc (5 mL) and H_2O (5 mL) were added the aqueous layer was extracted with EtOAc (3 x 5mL). The combined organic layers were dried over $MgSO_4$, filtered, and evaporated. SiO_2 gel column chromatography (0 → 100% iPrOH in hexanes (1%Et_3N)) afforded the arylated aminopyrazole as a white solid (48 mg, 0.16 mmol 43%); mp: 150-151 °C; ν_{max} (ATR) 3275 (NH), 2943, 1674 (C=O), 1608, 1551, 1523, 1442, 1334, 1252, 1206, 1155, 1082, 1040 cm^{-1}; δ_H (600 MHz, $CDCl_3$) 8.45 (1H, s br, NH), 7.77-7.75 (2H, m, 2'-H), 7.05 (2H, t, *J* = 8.7 Hz, 3'-H) 6.88 (1H, s, 4-H), 5.52 (1H, dd, *J* = 7.5, 2.9 Hz, 2''-H), 4.00-3.97 (1H, m, 6''-H), 3.74-3.70 (1H, m, 6''-H), 2.31-2.25 (1H, m, 3''-H), 2.20 (3H, s, CH_3) 2.14-2.08 (2H, m, 3''-H, 4''-H), 1.75-1.63 (3H, m, 4''-H, 5''-H); δ_C (151 MHz, $CDCl_3$) 166.6 (C=O), 162.7 (d, *J* = 246 Hz, C-4'), 149.5 (C-3), 138.2 (C-5), 129.8 (d, *J* = 3 Hz, C-4') 127.4 (d, *J* = 8 Hz, C-2'), 115.5 (d, *J* = 21 Hz, C-3') 95.2 (C-4), 86.9 (C-2''), 66.8 (C-6''), 29.2 (C-3''), 25.2 (C-5''), 24.2 (CH_3), 21.2 (C-4''); HRMS (ESI) *m/z* found $[M+H]^+$ 304.1478, $C_{16}H_{19}N_3O_2F$ requires *M*, 304.1461.

1-({4''-fluoro-5'-methoxy-[1',1''-biphenyl]-2'-yl}methyl)-4-(4'''-fluorophenyl)-1H-pyrazol-5-amine

(**550**)

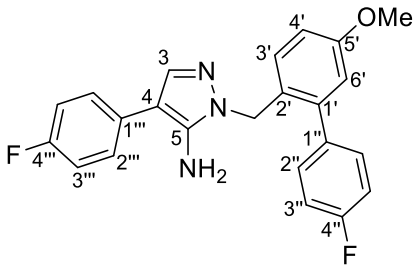

Synthesised from 1-[(4-methoxyphenyl)methyl]-1H-pyrazol-5-amine **548** (102 mg, 0.50 mmol, 1.00 equiv.) in a one-pot procedure according to General Procedure A with modifications. The borylation was left for 3.5 h. Suzuki-Miyaura cross-coupling of half of the material was conducted as follows.[162] To an oven-dried vial was added Pd(dppf)Cl_2 (25 mg, 10 mol%) and tetrabutylammonium bromide (8 mg, 0.03 mmol, 0.10 equiv). The vial was sealed and subject to three N_2 purge/refill cycles. The crude boronate ester (1.0 equiv.) in degassed PhMe (1.3 mL) followed by 1-bromo-4-fluorobenzene (0.03 mL, 0.25 mmol, 1.00 equiv.) were added and the mixture was cooled to 0 °C. 2M Na_2CO_3 (0.25 mL, 0.50 mmol, 2.00 equiv.) was added and the reaction as stirred at 110 °C for 1 h. The reaction was filtered over Celite® before removal of the volatiles. SiO_2 gel column chromatography (0 → 100% EtOAc in hexanes) afforded the arylated aminopyrazole as a colourless oil; ν_{max} (ATR) 3431 (NH_2), 3325 (NH_2), 2964, 1607, 1574, 1494, 1373, 1297, 1220, 1158, 1094, 1034 cm^{-1}; δ_H (700 MHz, $CDCl_3$) 7.43 (1H, s, 3-H), 7.31-7.29 (2H, m, 2''-H), 7.28- 7.26 (2H, m, 2'''-H), 7.14 (2H, t, *J* = 8.9 Hz, 3''-H), 7.11 (1H, d, *J* = 8.6 Hz, 3'-H), 7.06 (2H, t, *J* = 8.8 Hz, 3'''-H) 6.89 (1H, dd, *J* = 2.7, 8.6 Hz, 4'-H) 6.79, (1H, d, *J* = 2.7 Hz, 6'-H) 5.07 (2H, s, NCH_2), 3.80 (3H, s, OCH_3); δ_C (176 MHz, $CDCl_3$) 162.5 (d, *J* = 247 Hz, 4''-H), 161.2 (d, *J* = 245 Hz, 4'''-H) 159.1 (C-5'), 141.5 (C-1'), 140.9 (C-5), 137.5 (C-3), 136.4 (d, *J* = 3 Hz, C-1''), 130.8 (d, *J* = 8 Hz, C-2''), 129.8 (C-4'), 129.7 (d, *J* = 3 Hz C-1''') 128.1 (d, *J* = 8 Hz, C-2'''), 125.9 (C-3'), 116.0 (d, *J* = 21 Hz, C-3''), 115.9 (C-2'), 115.8 (d, *J* = 21 Hz, C-3'''), 113.9 (C-3''), 106.1 (C-4), 55.5 (OCH_3), 49.2 (NCH_2); HRMS (ESI) *m/z* found $[M+H]^+$ 392.1585, $C_{23}H_{20}N_3OF_2$ requires *M*, 392.1574.

4.2.2 Synthesis of Pyrazole Derivatives

Tert-butyl N-(1-methyl-1H-pyrazol-3-yl)carbamate (**376**)[5]

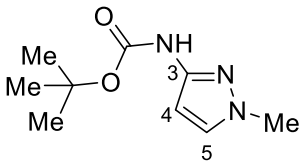

1-Methyl-1H-pyrazol-3-amine **373** (0.16 mL, 2.00 mmol, 1.00 equiv.) and Boc_2O (480 mg, 2.20 mmol, 1.10 equiv.) were stirred at 50 °C for 5 min. The resulting precipitate was dissolved in CH_2Cl_2 (15 mL) and washed with H_2O (2 x 10 mL), saturated $NaHCO_{3(aq)}$ (10 mL) and brine (10 mL). The organic layer was dried over $MgSO_4$, filtered, and evaporated. Recrystallisation from iPrOH afforded the Boc pyrazole as a white solid (351 mg, 1.78 mmol, 89%); mp: 112-113 °C; ν_{max} (ATR) 3187 (NH), 2983, 1743 (C=O), 1553, 1370, 1286, 1147 cm^{-1}; δ_H (700 MHz, $CDCl_3$) 8.29-8.46 (1H, m br, NH), 7.19 (1H, s, 5-H), 6.45 (1H, s, 4-H), 3.80 (3H, s, 1-CH_3) 1.50 (9H, s, CCH_3); δ_C (176 MHz, $CDCl_3$) 153.0 (C-3), 148.0 (C=O), 130.8 (C-5), 96.0 (C-4), 80.3 (*C*CH_3), 38.8 (CH_3N), 28.5 (C*C*H_3); *m/z* (ESI) $[M+H]^+$ 198.1. Data for **376** was consistent with a previous report.

Tert-butyl N-methyl-N-(1-methyl-1H-pyrazol-3-yl)carbamate (**376b**)

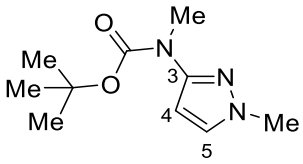

At 0 °C under N_2, a solution of tert-butyl N-(1-methyl-1H-pyrazol-3-yl)carbamate **376** (280 mg, 1.36 mmol, 1.0 equiv.) in anhydrous THF (2 mL) was treated dropwise with 1M LiHMDS in THF (2.15 mL, 2.15 mmol, 1.50 equiv.). After stirring for 30 min, MeI (0.45 mL, 7.2 mmol, 5.00 equiv.) was added and the mixture was warmed to rt. After stirring for 30 min, the reaction was poured into saturated NH_4Cl (10 mL) and the crude mixture was concentrated to ca. half volume. H_2O (20 mL) was added and aqueous phase was extracted with EtOAc (3 x 30 mL). The combined organic fractions were dried over $MgSO_4$, filtered and evaporated. SiO_2 gel column chromatography (30% → 40% EtOAc in hexanes) afforded the methylated pyrazole as a colourless oil (342 mg, 0.73 mmol, 54%); ν_{max} (ATR) 2981, 1700 (C=O), 1535, 1495, 1387, 1253, 1148 cm^{-1}; δ_H (600 MHz, $CDCl_3$) 7.16 (1H, d, *J* = 2.1 Hz, 5-H) 6.33

(1H, s br, 4-H), 3.74 (3H, s, 1-CH_3), 3.28 (3H, s, 3-NCH_3), 1.47 (9H, s, CCH_3); δ_C (151 MHz, $CDCl_3$) 153.7 (C=O), 151.1 (C-3), 130.5 (C-5), 98.8 (C-4), 80.6 (*C*CH_3), 38.8 (1-CH_3), 34.3 (3-NCH_3), 28.4 (C*C*H_3); HRMS (ASAP) *m/z* found $[M+H]^+$ 212.1405, $C_{10}H_{18}N_3O_2$ requires *M*, 212.1399.

tert-butyl N-(1'-methyl-1H-pyrazol-5'-yl)carbamate (**383**)

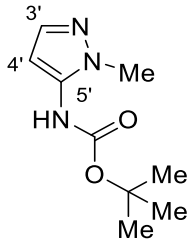

At 0 °C, a solution of 1-methyl-1H-pyrazol-5-amine **380** (1.94 g, 20.0 mmol, 1 equiv.), trimethylamine (4.20 mL, 30.0 mmol, 1.50 equiv.), and DMAP (244 mg, 2.00 mmol, 0.10 equiv.) in CH_2Cl_2 (20 mL) was charged portionwise with Boc_2O (4.80 g, 22.0 mmol, 1.10 equiv.). The reaction was stirred for 16 h before addition of saturated saturated $NaHCO_{3(aq)}$ (10 mL). The organic layer was washed with saturated $NaHCO_{3(aq)}$ (3 x 20 mL) and the combined aqueous fractions were back-extracted with CH_2Cl_2 (3 x 20 mL). The combined organic fractions were dried over $MgSO_4$, filtered, and evaporated. Recrystallisation from tert-butyl methyl ether afforded the Boc pyrazole as a white solid (3.26 g, 16.5 mmol, 83%); mp: 93-94 °C (mtbe); ν_{max} (ATR) 3182 (NH), 2977, 1733 (C=O), 1573, 1395, 1367, 1274, 1249, 1160, 1002 cm^{-1}; δ_H (700 MHz, $CDCl_3$) 7.34 (1H, d, *J* = 2.0 Hz, 3'-H), 6.87 (1H, s br, NH), 6.09 (1H, s br, 4'-H), 3.70 (3H, s, 1'-CH_3), 1.47 (9H, s, CCH_3); δ_C (176 MHz, $CDCl_3$) 153.0 (C=O), 138.2 (C-3'), 136.2 (C-5'), 99.4 (C-4'), 81.6 (*C*CH_3), 35.4 (1'-CH_3), 28.3 (C*C*H_3); HRMS (ESI) *m/z* found $[M+H]^+$ 198.1243, $C_9H_{16}N_3O_2$ requires *M*, 198.1243.

1-[(3',5'-dimethylphenyl)methyl]-1H-pyrazol-3-amine (**402**)

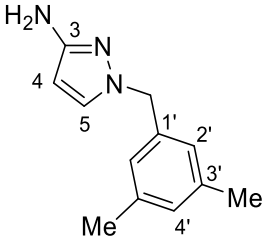

To a solution of 1-[(3,5-dimethylphenyl)methyl]-3-nitro-1H-pyrazole **403** (384 mg, 1.66 mmol, 1.00 equiv.) in EtOH (17 mL) and NH_4Cl (2.3 mL) was added Fe (1.39 g, 24.9 mmol, 15 equiv.). The reaction

was refluxed for 3 h, cooled, and filtered over Celite®. Removal of the volatiles followed by filtration over SiO_2 with CH_2Cl_2 (50 mL) afforded the aminopyrazole as a white solid (254 mg, 1.26 mmol, 76%); mp: 91-92 ^oC; δ_H (700 MHz, $CDCl_3$) 7.13 (1H, d, *J* = 2.3 Hz, 5-H) 6.91 (1H, s br, 4'-H), 6.82 (2H, s br, 2'-H), 5.61 (1H, d, *J* = 2.3 Hz 4-H), 5.01 (2H, s, CH_2), 3.44 (2H, s br, NH_2), 2.28 (6H, s, CH_3); δ_C (176 MHz, $CDCl_3$) 154.6 (C-3), 138.4 (C-3'), 136.9 (C-1'), 130.9 (C-5), 129.6 (C-4'), 125.5 (C-2'), 93.3 (C-4), 55.6 (CH_2), 21.4 (CH_3); HRMS (ESI) *m/z* found $[M+H]^+$ 202.1344, $C_{12}H_{16}N_3$ requires *M*, 202.1344.

1-[(3',5'-dimethylphenyl)methyl]-3-nitro-1H-pyrazole (**403**)

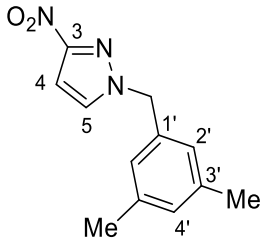

To a solution of 3-nitro-1H-pyrazole **404** (565 g, 5.00 mmol, 1.00 equiv.) in THF (5 mL) under N_2 at - 20 ^oC was added portionwise 60% NaH dispersion in mineral oil (220 mg, 5.50 mmol, 1.1 equiv.). The reaction was allowed to stir for 30 min before the addition of 1-(bromomethyl)-3,5-dimethylbenzene (1.10 g, 5.50 mmol, 1.10 equiv.). The cooling bath was removed and after 2 h, the reaction was quenched with NH_4Cl (10 mL) and approximately one third of the volatiles were removed. EtOAc (20 mL) and H_2O (10 mL) were added and the aqueous layer was extracted with EtOAc (3 x 10 mL). The combined organic layers were dried over $MgSO_4$, filtered and evaporated. Recrystallisation of the residue from tert-butyl methyl ether afforded the benzylated pyrazole as a white solid (2.03 g, 4.2 mmol, 84%); mp: 91-92 ^oC; ν_{max} (ATR) 2923, 1611, 1544, 1505, 1382, 1303, 1193, 1055, cm^{-1}; δ_H (700 MHz, $CDCl_3$) 7.39 (1H, d, *J* = 2.6 Hz, 5-H) 6.99 (1H, s br, 4'-H), 6.90 (2H, s br, 2'-H), 6.88 (1H, d, *J* = 2.6 Hz, 3-H), 5.28 (2H, s, CH_2), 2.30 (6H, s, CH_3); δ_C (176 MHz, $CDCl_3$) 155.8 (C-3), 139.0 (C-3'), 134.0 (C-1'), 131.8 (C-5), 130.7 (C-4'), 126.2 (C-2'), 103.4 (C-4), 57.8 (CH_2), 21.3 (CH_3); HRMS (ESI) *m/z* found $[M+H]^+$ 232.1075, $C_{12}H_{14}N_3O_2$ requires *M*, 232.1086.

1-(4-methoxyphenyl)-1H-pyrazol-3-amine (**410**) [6]

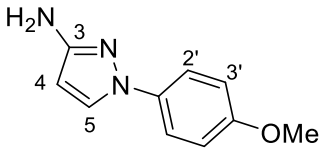

A flame-dried vial was charged with 1H-pyrazol-3-amine **369** (416 mg, 5.00 mmol, 1.00 equiv.), Cu_2O (72 mg, 0.50 mmol, 10 mol%), and KOH (561 mg, 10.0 mmol, 2.00 equiv.). The vial was sealed and purged/refilled x3 with N_2, followed by addition of 1-iodo-4-methoxybenzene (1.76 g, 7.50 mmol, 1.50 equiv.) and DMSO (10 mL). The reaction was stirred at 120 °C for 16 h, cooled, and diluted with EtOAc (20 mL) and H_2O (50 mL). The organic phase was washed with H_2O (3 x 40 mL) and brine (40 mL), and the organic phase was dried over $MgSO_4$, filtered, and evaporated. SiO_2 gel column chromatography (65 → 75% EtOAc in hexanes) afforded the aminopyrazoles as a brown solid (316 mg, 1.67 mmol, 33%); mp: 146-150 °C; δ_H (600 MHz, DMSO) 7.99 (1H, d, *J* = 2.1 Hz, 5-H) 7.55 (2H, d, *J* = 8.8 Hz, 2'-H) 6.96 (2H, d, *J* = 8.8 Hz, 3'-H) 5.67 (1H, d, *J* = 2.1 Hz, 4-H) 4.92 (2H, s br, NH_2), 3.75 (CH_3); δ_C (151 MHz, DMSO) 157.1, 156.5, 134.3, 127.9, 118.3, 114.8, 95.8, 55.8; *m/z* (EI) $[M]^+$ 189.1, 174.1, 77.1. Data for **410** was consistent with a previous report.

3-nitro-1-(oxan-2'-yl)-1H-pyrazole (**413**)[7]

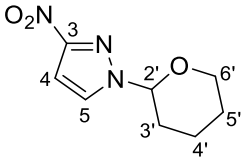

To a solution of 3-nitro-1H-pyrazole **404** (117 mg, 1.04 mmol, 1.00 equiv.) and 3,4-dihydro-2H-pyran (0.28 mL, 3.10 mmol, 3.00 equiv.) in CH_2Cl_2 (8.5 mL) was added *p*-TsOH (20 mg, 0.10 mmol, 10 mol%). The reaction was stirred for 1 h, poured into saturated $NaHCO_{3(aq)}$ (10 mL), and the aqueous layer was extracted with CH_2Cl_2 (3 x 5 mL). SiO_2 gel column chromatography (0 → 100% EtOAc in hexanes) afforded the THP pyrazole as a colourless oil; (203 mg, 1.03 mmol, 99%); ν_{max} (ATR) 2946, 1541, 1510, 1457, 1381, 1314, 1184, 1084, cm^{-1}; δ_H (600 MHz, $CDCl_3$) 7.70 (1H, d, *J* = 2.6 Hz, 5-H), 6.92 (1H, d, *J* = 2.6 Hz, 4-H), 5.44 (1H, dd, *J* = 9.0, 2.8 Hz, 2'-H), 4.06-4.03 (1H, m, 6'-H) 3.72-3.68 (1H, m, 6'-H), 2.17-2.13 (1H, m, 3'-H), 2.05-1.98 (2H, m, 4'-H, 3'-H), 1.73-1.60 (3H, m, 4'-H, 5'-H); δ_C (151 MHz,

$CDCl_3$) 155.8 (C-3), 130.2 (C-5), 103.0 (C-4), 88.8 (C-2'), 67.9 (C-6'), 30.7 (C-3'), 24.8 (C-5'), 21.7 (C-4'). *m/z* (ESI) $[M]^+$ 197.3. Data for **415** was consistent with a previous report.

5-nitro-1-(oxan-2'-yl)-1H-pyrazole (**414**)

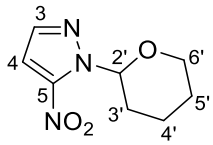

To a solution of 3-nitro-1H-pyrazole **404** (500 mg, 4.42 mmol, 1.00 equiv.) and 3,4-dihydro-2H-pyran (1.20 mL, 13.3 mmol, 3.00 equiv.) in CH_2Cl_2 (36 mL) was added PPTS (111 mg, 0.44 mmol, 10 mol%). The reaction was stirred for 16 h, poured into saturated $NaHCO_{3(aq)}$ (15 mL), and the aqueous layer was extracted with CH_2Cl_2 (3 x 15 mL). SiO_2 gel column chromatography (0 → 50% EtOAc in hexanes) afforded the THP pyrazole as a crude colourless oil, (1.47 g, 1.47 mmol, 33%); ν_{max} (ATR) 2950, 1552, 1511, 1442, 1351, 1242, 1209, 1182, 1130, 1089, 1047 cm^{-1}; δ_H (600 MHz, $CDCl_3$) 7.56 (1H, d, *J* = 1.9 Hz, 3-H), 7.07 (1H, d, *J* = 1.9 Hz, 4-H), 6.17 (1H, dd, *J* = 9.5, 2.6 Hz, 2'-H), 3.98 (1H, d, *J* = 11.6 Hz, 2'-H), 3.72 (1H, td, *J* = 11.6 Hz, 2.6 Hz, 6'-H), 2.43-2.37 (1H, m, 3'-H), 2.13-2.10 (1H, m, 4'-H), 2.05-2.03 (1H, m, 3'-H), 1.76-1.59 (3H, m, 4'-H, 5'-H); δ_C (151 MHz, $CDCl_3$) 146.1 (C-5), 138.4 (C-3), 107.7 (C-4), 85.9 (C-2'), 68.0 (C-6'), 29.0 (C-3'), 24.9 (C-5'), 22.4 (C-4'); HRMS (ASAP) *m/z* found $[M]^+$ 197.0793, $C_8H_{11}N_3O_3$ requires *M*, 197.0800. **416** was found to isomerise slowly in untreated $CDCl_3$ catalysed by the presence of trace HCl.

1-(oxan-2'-yl)-1H-pyrazol-3-amine (**418**)

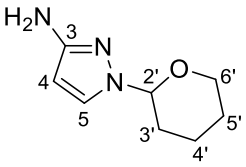

Under N_2, a solution of 3-nitro-1-(oxan-2-yl)-1H-pyrazole **413** (167 mg, 0.85 mmol, 1.00 equiv.) in EtOAc (1 mL) was charged with 10% dry Pd/C (45 mg, 5 mol%) followed by MeOH (5 mL). The reaction was allowed to stir under H_2 for 1 h at rt. The reaction mixture was filtered over Celite® and the volatiles were removed. Filtration through a SiO_2 plug with EtOAc (1% Et_3N) (50 mL) afforded the aminopyrazole as an orange oil (129 mg, 0.77 mmol, 91%); ν_{max} (ATR) 3426 (NH_2), 3340 (NH_2), 2950, 1621, 1554,

1498, 1438, 1388, 1208, 1084, 1041 cm^{-1}; δ_H (600 MHz, $CDCl_3$) 7.32 (1H, d, *J* = 2.5 Hz, H-5) 5.64 (1H, d, *J* = 2.5 Hz, H-4), 5.10 (1H, dd, *J* = 10.3, 2.4 Hz, 2'-H), 4.06-4.03 (1H, m, 6'-H), 3.66-3.62 (1H, m, 6'-H), 3.54 (2H, s br, NH_2), 2.11-2.05 (1H, m, 3'-H), 2.02-1.94 (2H, m, 3'-H, 5'-H), 1.69-1.60 (2H, m, 5'-H, 4'-H), 1.57-1.52 (1H, m, 5'-H); δ_C (151 MHz, $CDCl_3$) 154.8 (C-3), 129.3 (C-5), 94.2 (C-4), 87.2 (C-2'), 67.9 (C-6'), 30.2 (C-3'), 25.1 (C-5'), 22.9 (C-4'); HRMS (ESI) *m/z* found $[M+H]^+$ 168.1153, $C_8H_{14}N_3O$ requires *M*, 168.1137.

3-Nitro-1-{[2'-(trimethylsilyl)ethoxy]methyl}-1H-pyrazole (**449**)[8]

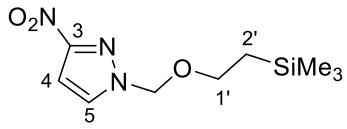

Method A: To a solution of 3-nitro-1H-pyrazole **404** (1.13 g, 10.0 mmol, 1.00 equiv.) in THF (20 mL) under N_2 at - 20 °C was added portionwise 60% NaH dispersion in mineral oil (440 mg, 11.0 mmol, 1.10 equiv.). The reaction was allowed to stir for 5 min before the addition of SEMCl (1.93 mL, 11.0 mmol, 1.10 equiv.). The cooling bath was removed and after 2 h, the reaction was quenched with NH_4Cl (20 mL) and *ca.* one third of the volatiles were removed. EtOAc (30 mL) and H_2O (20 mL) were added and the aqueous layer was extracted with EtOAc (3 x 20 mL). The combined organic layers were dried over $MgSO_4$, filtered and evaporated. SiO_2 gel column chromatography (10 → 40% Et_2O in hexanes) afforded the SEM pyrazole as a white solid (2.03 g, 8.40 mmol, 84%). Alternatively, the crude solid could be recrystallised from hexanes to afford lustrous white crystals in identical yield.

Method B: To a solution of 3-nitro-1H-pyrazole (1.13 g, 10.0 mmol, 1.00 equiv.) in THF (20 mL) under N_2 at rt was rapidly added LiHMDS in THF (11 mL, 11 mmol, 1.0 M, 1.1 equiv.). SEMCl (1.93 mL, 11.0 mmol, 1.10 equiv.) was added immediately thereafter and the solution was allowed to stir for 16 h. The reaction was quenched with NH_4Cl (20 mL) and *ca.* one third of the volatiles were removed. EtOAc (30 mL) and H_2O (20 mL) were added and the aqueous layer was extracted with EtOAc (3 x 20 mL). The combined organic layers were dried over $MgSO_4$, filtered and evaporated. SiO_2 gel column chromatography (5 → 20% EtOAc in hexanes) afforded the protected pyrazole as a white solid (550 mg, 2.13 mmol, 23%); mp: 60–62 °C (hexanes); ν_{max} (ATR) 2925, 1545, 1503, 1374, 1296, 1247, 1176,

1093, cm^{-1}; δ_H (700 MHz, $CDCl_3$) 7.66 (1H, d, *J* = 2.5 Hz, 5-H) 6.97 (1H, d, *J* = 2.5 Hz, 4-H), 5.49, (2H, s, NCH_2) 3.61-3.59 (2H, m, 1'-H), 0.92-0.90 (2H, m, 2'-H), -0.03 (9H, s, $SiCH_3$); δ_C (176 MHz, $CDCl_3$) 156.1 (C-4), 131.8 (C-5), 103.9 (C-4), 81.9 (NCH_2), 68.0 (C-1'), 17.9 (C-2'), -1.3 ($SiCH_3$); *m/z* (EI) [M – C_2H_5]$^+$ 214.1, 188.0, 170.1. Data for **449** was consistent with a previous report.

1-{[2'-(trimethylsilyl)ethoxy]methyl}-1H-pyrazol-3-amine (**450**)[9]

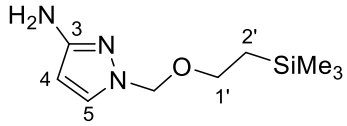

Under N_2, a solution of 3-nitro-1-{[2-(trimethylsilyl)ethoxy]methyl}-1H-pyrazole **457** (2.03 g, 8.40 mmol, 1.00 equiv.) in EtOAc (10 mL) was charged with 10% dry Pd/C (445 mg, 5 mol%) followed by MeOH (40 mL). The reaction was allowed to stir under H_2 for 1 h at 35 °C. The reaction mixture was filtered over Celite® and the volatiles were removed. SiO_2 gel column chromatography (0 → 100% Et_2O in hexanes) afforded the aminopyrazole as a white solid (1.47 g, 6.89 mmol, 82%); mp: 62-64 °C; ν_{max} (ATR) 3330 (NH_2), 3261 (NH_2), 2952, 1616, 1551, 1250, 1086 cm^{-1}; δ_H (700 MHz, $CDCl_3$) 7.28, (1H, d, *J* = 2.5 Hz, 5-H) 5.68 (1H, d, *J* = 2.5 Hz, 4-H), 5.20 (2H, s, NCH_2), 3.76 (2H, s br, NH_2), 3.55-3.52 (2H, m, 1'-H), 0.90-0.88 (2H, m, 2'-H), -0.03 (9H, s, $SiCH_3$); δ_C (176 MHz, $CDCl_3$) 155.2 (C-3), 131.9 (C-5), 95.3 (C-4), 80.2 (NCH_2), 67.0 (C-1'), 18.4 (C-2'), -0.9 ($SiCH_3$); *m/z* (EI) [M]$^+$ 213.2, 140.2, 96.1. Alternatively, the crude solid can be recrystallised from hexanes to afford lustrous, white crystals in identical yield. Data for **450** was consistent with a previous report.

Tert-butyl N-(1-{[2'-(trimethylsilyl)ethoxy]methyl}-1H-pyrazol-3-yl)carbamate (**452**)

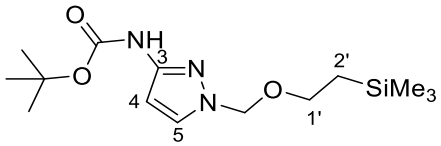

1-{[2'-(trimethylsilyl)ethoxy]methyl}-1H-pyrazol-3-amine **450** (213 mg, 1.00 mmol, 1.00 equiv.) and Boc_2O (240 mg, 1.10 mmol, 1.10 equiv.), were stirred neat at 50 °C for 3 h. The cooled reaction was dissolved in CH_2Cl_2 (10 mL), washed with saturated $NaHCO_{3(aq)}$ (3 x 5 mL). The aqueous layer was extracted with CH_2Cl_2 (3 x 5 mL), and the combined organic fractions were dried over $MgSO_4$, filtered and evaporated. SiO_2 gel column chromatography (20 → 30% EtOAc in hexanes) afforded the Boc

pyrazole as a colourless oil (197 mg, 0.63 mmol, 63%); ν_{max} (ATR) 3195 (NH), 2954, 1727 (C=O), 1583, 1356, 1246, 1163, 1092 cm^{-1}; δ_H (400 MHz, $CDCl_3$) 7.49 (1H, s br, NH), 7.40 (1H, d, *J* = 2.5 Hz, 5-H), 6.56 (1H, s br, 4-H), 5.29 (2H, s, NCH_2), 3.54-3.50 (2H, m, 1'-H), 1.50 (9H, s, CCH_3), 0.91-0.87 (2H, m, 2'-H) 0.05 (9H, s, $SiCH_3$); δ_C (176 MHz, $CDCl_3$) 152.8 (C=O), 148.3 (C-3), 130.8 (C-5), 97.35 (C-4), 80.8 (CCH_3) 80.0 (NCH_2), 66.7 (C-1'), 28.5 (CCH_3), 17.9 (C-2'), -1.3 ($SiCH_3$); HRMS (ASAP) $[M+H]^+$ *m/z* found 314.1909, $C_{14}H_{28}N_3O_3Si$ requires *M*, 314.1900.

N-(1-{[2'-(trimethylsilyl)ethoxy]methyl}-1H-pyrazol-3-yl)acetamide (**458**)

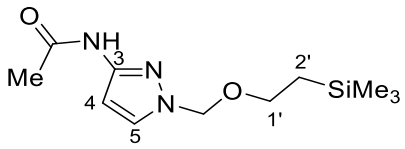

1-{[2-(trimethylsilyl)ethoxy]methyl}-1H-pyrazol-3-amine **450** (213 mg, 1.00 mmol, 1.00 equiv.) and Ac_2O (0.11 mL, 1.10 mmol, 1.10 equiv.) were stirred neat for 0.5 h. The reaction mixture was diluted in EtOAc (20 mL), washed with saturated $NaHCO_{3(aq)}$ (10 mL), H_2O (10 mL) and brine (10 mL). The organic layer was dried over $MgSO_4$, filtered, and evaporated. Filtration through an SiO_2 plug CH_2Cl_2 (3 x 20 mL) afforded the acetylated pyrazole as a colourless oil (212 mg, 0.83 mmol, 83%); ν_{max} (ATR) 3241 (NH), 2952, 1673 (C=O), 1580, 1539, 1425, 1372, 1250, 1208, 1094 cm^{-1}; δ_H (700 MHz, $CDCl_3$) 8.19 (1H, s br, NH), 7.44 (1H, d *J* = 2.6 Hz, 5-H), 6.77 (1H, d, *J* = 2.6 Hz, 4-H), 5.28 (2H, s, NCH_2), 3.53-3.50 (2H, m, 1'-H), 2.15 (3H, s, Ac CH_3), 0.90-0.88 (2H, m, 2'-H), -0.03 (9H, s, $SiCH_3$); δ_C (176 MHz, $CDCl_3$) 167.8 (C=O), 147.7 (C-3), 131.0 (C-5), 98.9 (C-4), 80.1 (NCH_2), 66.9 (C-1'), 24.0 (CH_3CO), 17.9 (C-2'), -1.3 ($SiCH_3$); HRMS (ESI) *m/z* found $[M+H]^+$ 256.1496, $C_{11}H_{22}N_3O_2Si$ requires *M*, 212.1481.

3-phenyl-1-{[2'-(trimethylsilyl)ethoxy]methyl}-1H-pyrazole (**466a**)[10]

5-phenyl-1-{[2-(trimethylsilyl)ethoxy]methyl}-1H-pyrazole (**466b**)

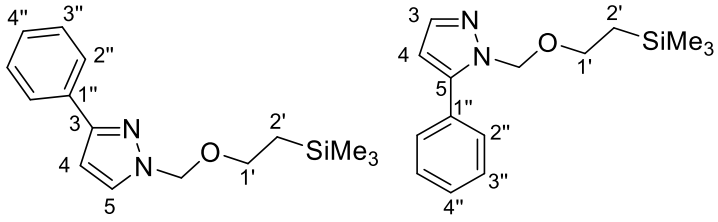

At 0 °C under N_2, 60% NaH dispersion in mineral oil (110 mg, 2.80 mmol, 1.10 equiv.) was added to a solution of 3-phenyl-1H-pyrazole (360 mg, 2.50 mmol, 1.00 equiv.) in THF (7.5 mL). After 5 min, SEMCl

(0.88 ml, 5.00 mmol, 2.00 equiv.) was added before removal of the cooling bath. After 0.5 h, the reaction was quenched with NH_4Cl (10 mL) and the reaction was concentrated to ca. half volume. H_2O (10 mL) was added and the aqueous layer was extracted with EtOAc (3 x 20 mL). The organic layer was dried over $MgSO_4$, filtered, and the volatiles were removed to obtain the crude alkylated pyrazole. NMR analysis indicated a 3:2 isomeric ratio **466a**:**466b**. SiO_2 gel column chromatography (5 → 15% EtOAc in hexanes) afforded the SEM pyrazole as a colourless oil (25 mg, 0.09 mmol, 4%); δ_H (700 MHz, $CDCl_3$) 7.83 (2H, d, *J* = 7.6 Hz, 2''-H), 7.59 (1H, d, *J* = 2.3 Hz, 5-H), 7.40 (2H, t, *J* = 7.6 Hz, 3''-H), 7.31 (1H, t, *J* = 7.6 Hz, 4''-H), 6.63 (1H, d, *J* = 2.3 Hz, 4-H), 5.47 (2H, s, NCH_2), 3.63 (2H, m, 1'-H), 0.93 (2H, m, 2'-H), -0.02 (9H, s, $SiCH_3$); δ_C (176 MHz, $CDCl_3$) 152.2, 133.5, 130.9, 128.7, 127.9, 125.9, 104.2, 80.4, 66.8, 17.9, -1.3; *m/z* (ESI) $[M+H]^+$ 275.2, 216.1, 158.1. Data for **466a** was consistent with a previous report.

3-phenyl-1H-pyrazole (**467**)[11]

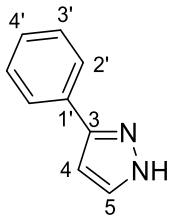

Method A: To a solution of (2E)-3-amino-1-phenylprop-2-en-1-one (350 mg, 2.00 mmol, 1.00 equiv.) in EtOH (4 mL) was added 50% hydrazine hydrate (0.18 mL, 3.8 mmol, 1.90 equiv.). The reaction was refluxed for 2 h, before removal of the volatiles. SiO_2 gel column chromatography (30% EtOAc in hexanes) afforded the phenyl pyrazole as a brown solid (285 mg, 1.98 mmol, 99%).

Method B: To a crude mixture of 3-phenyl-1-{[2-(trimethylsilyl)ethoxy]methyl}-1H-pyrazole (**466a**) and 5-phenyl-1-{[2-(trimethylsilyl)ethoxy]methyl}-1H-pyrazole (**466b**) (25 mg, 0.09 mmol, 1 equiv.) in EtOH (4 mL) was added 3M HCl (1 mL). The resulting solution was refluxed for 3 h, and the reaction was neutralized with saturated $NaHCO_{3(aq)}$ (10 mL). Approximately one third of the volatiles were removed, and saturated $NaHCO_{3(aq)}$ (10 mL) followed by EtOAc (20 mL) were added. The organic layer was washed with saturated $NaHCO_{3(aq)}$ (3 x 10 mL) and the aqueous layer was back-extracted with EtOAc (3 x 10 mL). The combined organic fractions were dried over $MgSO_4$, filtered, and evaporated. SiO_2 gel

column chromatography (0 → 20% EtOAc in hexanes) afforded the phenyl pyrazole as a brown solid (8 mg, 62%) mp: 76-77 °C; δ_H (700 MHz, $CDCl_3$) 7.76 (2H, d, *J* = 7.7 Hz, 2'-H), 7.62 (1H, s br, 5-H), 7.42 (2H, t, *J* = 7.7 Hz, 3'-H), 7.34 (1H, t, *J* = 7.7 Hz, 4'-H), 6.62 (1H, s br, 4-H); δ_C (176 MHz, $CDCl_3$) 132.2, 128.9, 128.2, 125.9, 102.9; *m/z* (ESI) $[M+H+MeCN]^+$ 186.3, 145.3. Data for **467** was consistent with a previous report.

3,4-dimethyl-1-(1'-{[2''-(trimethylsilyl)ethoxy]methyl}-1H-pyrazol-3'-yl)-2,5-dihydro-1H-pyrrole-2,5-dione (**470**)

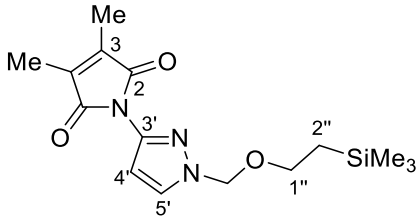

To a solution of 1-{[2'-(trimethylsilyl)ethoxy]methyl}-1H-pyrazol-3-amine **450** (126 mg, 1.00 mmol, 1.00 equiv.) in water (5 mL) was added dimethyl-2,5-dihydrofuran-2,5-dione (126 mg, 1.00 mmol, 1.00 eq). The reaction was stirred at 80 °C for 1 h, cooled, and diluted with CH_2Cl_2 (5 mL). The aqueous layer was extracted with CH_2Cl_2 (3 x 10 mL), dried over $MgSO_4$, and evaporated. SiO_2 gel column chromatography (40 → 60 → 100% CH_2Cl_2 in hexanes) afforded the maleimide as a white solid (306 mg, 0.95 mmol, 95%); mp: 81-83 °C (hexanes); ν_{max} (ATR) 2953, 1729 (C=O), 1705 (C=O), 1525, 1497, 1425, 1349, 1249, 1211, 1095 cm^{-1}; δ_H (700 MHz, $CDCl_3$) 7.59 (1H, d, *J* = 2.5 Hz, 5'-H), 6.37 (1H, d, *J* = 2.5 Hz, 4'-H), 5.41 (2H, s, NCH_2), 3.60-3.57 (2H, m, 1''-H), 2.02 (6H, s, 3-CH_3), 0.90-0.88 (2H, m, 2''-H), -0.04 ($SiCH_3$); δ_C (176 MHz, $CDCl_3$) 170.1 (C=O), 140.9 (C-3'), 138.0 (C-3), 130.7 (C-5'), 103.6 (C-4'), 80.8 (NCH_2), 67.1 (C-1''), 17.9 (C-2''), 9.0 (3-CH_3), -1.3 ($SiCH_3$); HRMS (ASAP) *m/z* found $[M+H]^+$ 322.1588, $C_{15}H_{24}N_3O_3$ requires *M*, 322.1587.

3,4-dimethyl-1-(1-methyl-1H-pyrazol-5-yl)-2,5-dihydro-1H-pyrrole-2,5-dione (**471**)

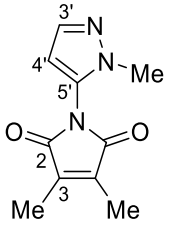

To a solution of 1-methyl-1H-pyrazol-5-amine **380** (194 mg, 2.00 mmol, 1.00 eq) in H_2O (10 mL) was added dimethyl-2,5-dihydrofuran-2,5-dione (252 mg, 2.00 mmol, 1.00 eq.). The reaction was stirred at rt for 16 h, cooled, and diluted with CH_2Cl_2 (10 mL). The organic layer was washed with saturated $NaHCO_{3(aq)}$ (10 mL), dried over $MgSO_4$, and filtered over a SiO_2 plug with CH_2Cl_2 (20 mL). Removal of the volatiles afforded the maleimide as a white solid (401 mg, 1.95 mmol, 98%); mp: 136-137 ^oC; ν_{max} (ATR) 2960, 1731 (C=O), 1708 (C=O), 1554, 1421, 1388, 1311, 1278, 1078 cm^{-1}; δ_H (700 MHz, $CDCl_3$) 7.54 (1H, d, *J* = 2.0 Hz, 3'-H), 6.19 (1H, d, *J* = 2.0 Hz, 4'-H), 3.71 (3H, s, 1'-CH_3), 2.08 (6H, s, 3-CH_3); δ_C (176 MHz, $CDCl_3$) 169.8 (C=O), 138.9 (C-3), 138.8 (C-3'), 129.8 (C-5'), 104.2 (C-4'), 36.4 (1'-CH_3), 9.2 (3-CH_3); HRMS (ESI) *m/z* found $[M+H]^+$ 206.0943, $C_{10}H_{11}N_3O_2$ requires *M*, 206.0930.

3,4-dimethyl-1-(1'-methyl-1H-pyrazol-3'-yl)-2,5-dihydro-1H-pyrrole-2,5-dione (**471b**)

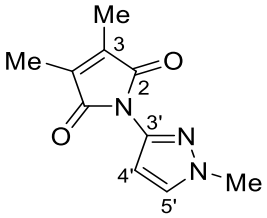

To a solution of 1-methyl-1H-pyrazol-3-amine **373** (0.43 mL, 5.00 mmol, 1.00 eq) in H_2O (5 mL) was added dimethyl-2,5-dihydrofuran-2,5-dione (631 mg, 5.00 mmol, 1.00 eq). The reaction was refluxed for 1 h, cooled, and diluted with CH_2Cl_2 (15 mL). The organic layer was washed with saturated $NaHCO_{3(aq)}$ (10 mL), dried over $MgSO_4$, and filtered over a SiO_2 plug with CH_2Cl_2 (50 mL). Removal of the volatiles afforded the maleimide as a white solid (984 mg, 4.80 mmol, 96%); mp = 146-148 ^oC; ν_{max} (ATR) 2925, 1759 (C=O), 1722 (C=O), 1505, 1435, 1414, 1386, 1343, 1302, 1224, 1090 cm^{-1}; δ_H (700 MHz, $CDCl_3$) 7.37 (1H, d, *J* = 2.4 Hz, 5'-H), 6.26 (1H, d, *J* = 2.4 Hz, 4'-H), 3.90 (3H, s, CH_3N), 2.02 (6H, s, 3'-CH_3); δ_C (176 MHz, $CDCl_3$) 170.4 (C=O), 140.2 (C-3'), 137.9 (C-3), 131.4 (C-5'), 102.5 (C-4'), 39.6 (1'-CH_3), 9.0 (3-CH_3); HRMS (ESI) *m/z* found $[M+H]^+$ 206.0936, $C_{10}H_{11}N_3O_2$ requires *M*, 206.0930.

3-[(1'-{[2''-(trimethylsilyl)ethoxy]methyl}-1H-pyrazol-3-yl)carbamoyl]propanoic acid (**474**)

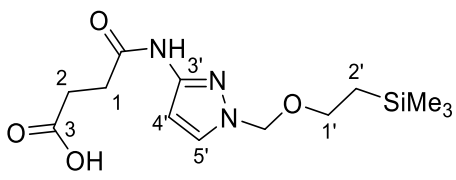

To a solution of 1-{[2'-(trimethylsilyl)ethoxy]methyl}-1H-pyrazol-3-amine **450** (213 mg, 1.00 mmol, 1.00 equiv.) and Et_3N (0.28 mL, 2.00 mmol, 2.00 equiv.) in THF (2 mL) was added succinic anhydride (220 mg, 2.20 mmol, 2.20 equiv.). The reaction was refluxed for 1 h, cooled, and diluted with EtOAc (10 mL) and H_2O (10 mL). The aqueous layer was extracted with EtOAc (3 x 10 mL), dried over $MgSO_4$, filtered and evaporated. Purification via SiO_2 gel column chromatography (0 → 10%, 10 → 100% Et_2O in PhMe (2% Et_3N)) afforded the amic acid as a white solid (112 mg, 0.35 mmol, 35%); mp: 80-83 °C; ν_{max} (ATR) 3296 (OH), 3249 (NH), 2953, 1708 (C=O), 1697 (C=O), 1614, 1584, 1502, 1428, 1403, 1378, 1342, 1246, 1209, 1169, 1013 cm^{-1}; δ_H (700 MHz, $CDCl_3$) 10.41 (1H, s br, NH), 7.44 (1H, d, *J* = 1.7 Hz, 5'-H), 6.85 (1H, d, 1.7 Hz, 4'-H), 5.26 (2H, s, NCH_2), 3.52-3.50 (2H, m, 1'-H), 2.83-2.77 (4H, m, 1-H, 2-H), 0.91-0.88 (2H, m, 2'-H), -0.02 (9H, s, $SiCH_3$); δ_C (176 MHz, $CDCl_3$) 177.3 (C-3), 170.0 (1-CO), 148.6 (C-3'), 131.4 (C-5'), 98.9 (C-4'), 79.8 (NCH_2), 67.2 (C-1'), 31.3 (C-1), 29.3 (C-2), 17.8 (C-2'), -1.3 ($SiCH_3$); HRMS (ESI) *m/z* found $[M+H]^+$ 314.1534 $C_{13}H_{24}N_3O_4Si$ requires *M*, 314.1536.

3-[(1-methyl-1H-pyrazol-5-yl)carbamoyl]propanoic acid (**475**)

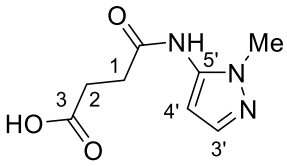

To a solution of 1-methyl-1H-pyrazol-5-amine **380** (485 mg, 5.00 mmol, 5.00 equiv.) in PhMe (5 mL) was added succinic anhydride (505 mg 1.05 mmol, 1.05 equiv.). The reaction was refluxed for 1h, cooled, and diluted with H_2O (10 mL). The aqueous layer was extracted with EtOAc (3 x 10 mL), dried over $MgSO_4$, filtered and evaporated. Recrystallisation from EtOH afforded the amic acid as a white solid (486 mg, 2.47 mmol, 49%); mp: 155-156 °C; ν_{max} (ATR) 3274 (OH), 3149 (NH), 2495, 1702 (C=O), 1671 (C=O), 1545, 1428, 1399, 1321, 1291, 1179, 1071 cm^{-1}; δ_H (600 MHz, DMSO) 12.14 (1H, s br, OH), 9.93 (1H, s br, NH), 7.30 (1H, d, *J* = 1.7 Hz, 3'-H), 6.14 (1H, d, *J* = 1.7 Hz, 4'-H) 3.63 (3H, s, CH_3), 2.60-2.58 (2H, m, CH_2), 2.53-2.51 (2H, m, CH_2); δ_C (151 MHz, DMSO) 173.7 (C=O), 170.2 (C=O), 137.3 (C-5'), 136.4 (C-3'), 98.6 (C-4'), 35.5 (CH_3), 30.1 (CH_2), 28.7 (CH_2); HRMS (ASAP) *m/z* found $[M+H]^+$ 198.0843 $C_8H_{12}N_3O_3$ requires *M*, 198.0879.

1-(1'-methyl-1H-pyrazol-3'-yl)pyrrolidine-2,5-dione (**476**)

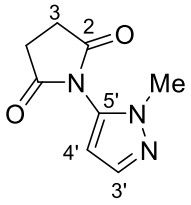

Oxalyl dichloride (1 mL), followed by DMF (0.1 mL) were added to 3-[(1-methyl-1H-pyrazol-5-yl)carbamoyl]propanoic acid **475** (197 mg, 1.00 mmol, 1.00 equiv.) and stirred for 1 h. The volatiles were removed and the residue was recrystallised from EtOH to afford the succinimide as a yellow solid (23 mg, 0.13 mmol, 13%); mp: 197-198 ^{o}C; ν_{max} (ATR) 2946, 1777 (C=O), 1714 (C=O), 1554, 1488, 1427, 1397, 1381, 1301, 1302, 1184, 1161, 1054 cm^{-1}; δ_H (600 MHz, DMSO) 7.49, (1H, d, *J* = 2.0 Hz, 3'-H) 6.20 (1H, d, *J* = 2.0 Hz, 4'-H), 3.60 (3H, s, 1'-H), 2.82 (4H, s, 3-H) δ_C (151 MHz, DMSO) 176.6 (C=O), 138.5 (C-3'), 131.0 (C-5'), 104.4 (C-4'), 36.2 (CH_3), 29.2 (C-3); HRMS (ESI) *m/z* found $[M+H]^+$ 180.0774, $C_8H_{10}N_3O_2$ requires *M*, 180.0773.

3,3-dimethyl-1-[1'-(oxan-2''-yl)-1H-pyrazol-3'-yl]pyrrolidine-2,5-dione (**485**)

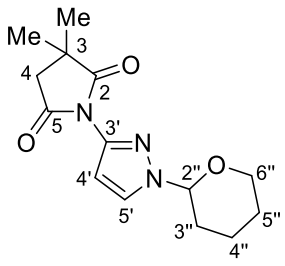

Method A: To a solution of 1-(oxan-2-yl)-1H-pyrazol-3-amine **418** (42 mg, 0.25 mmol, 1.00 equiv.) in DMF (1.3 mL) was added 3,3-dimethyloxolane-2,5-dione (35 mg, 0.28 mmol, 1.1 equiv.). The reaction was refluxed overnight, cooled, and diluted with EtOAc (10 mL) and H_2O (10 mL). The organic phase was washed with H_2O (4 x 10 mL), dried over $MgSO_4$, filtered, and evaporated. SiO_2 gel column chromatography (0 → 100% acetone in hexanes) afforded the maleimide as an orange oil (60 mg, 0.22 mmol, 86%).

Method B: To a solution of 3,3-dimethyl-1-(1H-pyrazol-3-yl)pyrrolidine-2,5-dione **486** (21 mg, 0.19 mmol, 1.00 equiv.) and 3,4-dihydro-2H-pyran (0.03 mL, 0.33 mmol, 3.00 equiv.) in CH_2Cl_2 (0.89 mL) was added *p*-TsOH (2.1 mg, 0.01 mmol, 10 mol%). The reaction was stirred for 1 h, poured into

saturated $NaHCO_{3(aq)}$ (10 mL), and the organic layer was collected. The aqueous layer was extracted with CH_2Cl_2 (3 x 5 mL). SiO_2 gel column chromatography (0 → 100% acetone in hexanes) afforded the THP pyrazole as an orange oil; (24 mg, 0.09 mmol, 80%); ν_{max} (ATR) 2934, 1790 (C=O), 1715 (C=O), 1519, 1492, 1425, 1376, 1335, 1233, 1203, 1146, 1084, 1042 cm^{-1}; δ_H (700 MHz, $CDCl_3$) 7.65 (1H, d, *J* = 2.6 Hz, 5'-H) 6.34 (1H, d, *J* = 2.6 Hz, 4'-H), 5.40 (1H, dd, *J* = 9.3, 2.7 Hz, 2''-H) , 4.04-4.01 (1H, m, 6''-H) 3.66 (1H, td, *J* = 11.2, 2.8 Hz, 6''-H), 2.68 (2H, s, 4-H), 2.10-1.95 (3H, m, 3''-H, 4''-H), 1.69-1.61 (2H, m, 5''-H, 4''-H), 1.60-1.55 (1H, m, 5''-H), 1.39 (6H, s, CH_3); δ_C (176 MHz, $CDCl_3$) 181.4 (C-2), 174.1 (C-5), 140.6 (C-3'), 128.7 (C-5'), 103.1 (C-4'), 88.0 (C-2''), 67.7 (C-6''), 43.9 (C-4), 40.3 (C-3), 30.6 (C-3''), 25.8 (CH_3), 24.9 (C-5''), 22.2 (C-4''); HRMS (ESI) *m/z* found $[M+H]^+$ 278.1524, $C_{14}H_{20}N_3O_3$ requires *M*, 278.1505.

3,3-dimethyl-1-(1H-pyrazol-3'-yl)pyrrolidine-2,5-dione (**486**)

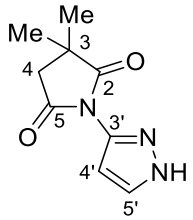

To a solution of 1H-pyrazol-3-amine **369** (83 mg, 1.00 mmol, 1.00 equiv.) in DMF (5 mL) was added 3,3-dimethyloxolane-2,5-dione (141 mg, 1.10 mmol, 1.10 equiv.). The reaction was stirred at 150 °C for 16 h, cooled, and diluted with PhMe (30 mL). The volatiles were azeotropically removed, and SiO_2 gel column chromatography (70 → 100% EtOAc in hexanes (1% Et_3N)) afforded the succinimide as a white solid (120 mg, 0.62 mmol, 62%); mp: 145-148 °C; ν_{max} (ATR) 3300 (NH), 2981, 1791 (C=O), 1711 (C=O), 1531, 1347, 1264, 1208, 1145, 1091 cm^{-1}; δ_H (700 MHz, $CDCl_3$) 12.22 (1H, s br, NH), 7.65 (1H, d, *J* = 2.4 Hz, 5'-H), 6.45 (1H, d, *J* = 2.4 Hz, 5'-H), 2.71 (2H, s, 4-H), 1.39 (6H, s, CH_3); δ_C (176 MHz, $CDCl_3$) 181.6 (C-2), 174.2 (C-5), 140.6 (C-3'), 131.0 (C-5'), 100.9 (C-4'), 43.8 (C-4), 40.3 (C-3) 25.8 (CH_3); HRMS (ESI) *m/z* found $[M+H]^+$ 194.0938, $C_9H_{12}N_3O_2$ requires *M*, 194.0930.

Tert-butyl 3-methyl-1H-pyrazole-1-carboxylate (493a)[12]

Tert-butyl 5-methyl-1H-pyrazole-1-carboxylate (493b)

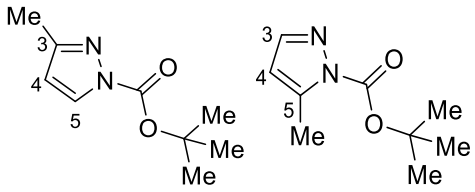

At 0 °C under N_2, Boc_2O (2.62 g, 12.0 mmol, 1.20 equiv.) followed by DMAP (122 mg, 1.00 mmol, 0.10 equiv.) were added to a solution of 3-methyl-1H-pyrazole (820 mg, 10.0 mmol, 1.00 equiv.) in MeCN (10 mL). The reaction was warmed to rt, stirred for 2 h, and diluted with EtOAc (30 mL). The organic phase was washed with 1M HCl (10 mL), saturated $NaHCO_{3(aq)}$ (10 mL), and brine (10 mL). The aqueous fractions were back-extracted with EtOAc (3 x 20 mL) and the combined organic fractions were dried over $MgSO_4$, filtered, and evaporated. SiO_2 gel column chromatography (60 → 100% CH_2Cl_2 in hexanes) afforded the Boc pyrazoles **493a** and **493b** in a 9:1 ratio as a colourless oil; ν_{max} (ATR) 2984, 1714 (C=O), 1553, 1412, 1351, 1204, 1147 cm^{-1}; *m/z* (ESI) $[M+H]^+$ 182.1; δ_H **493a** (700 MHz, $CDCl_3$) 7.95 (1H, d, *J* = 2.7 Hz, 5-H), 6.16 (1H, s, 4-H), 2.32 (3H, s, 3-CH_3), 1.62 (9H, s, CCH_3); δ_C **493a** (176 MHz, $CDCl_3$) 153.9 (C=O), 147.8 (C-3), 131.4 (C-5), 109.3 (C-4), 85.1 (*C*CH_3), 28.1 (C*C*H_3), 14.1 (3-CH_3); δ_H **493b** (700 MHz, $CDCl_3$) 7.54 (1H, s, 3'-H), 6.10 (1H, s, 4'-H), 2.52 (3H, s, 5'-CH_3), 1.64 (9H, s, CCH_3); δ_C **493b** (176 MHz, $CDCl_3$) 153.8 (C=O) 143.7 (C-3'), 142.5 (C-5'), 109.7 (C-4'), 85.0 (*C*CH_3), 29.80 (C*C*H_3) 14.55 (5-CH_3); Data for **493a** was consistent with a previous report.

tert-butyl 3-nitro-1H-pyrazole-1-carboxylate (**495**)

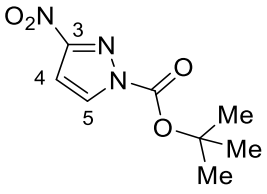

At 0 °C under N_2, a solution of 3-nitro-1H-pyrazole **404** (565 mg, 5.00 mmol, 1.00 equiv.) in THF (5.00 mL) was treated with 1M LiHMDS in THF (5.50 mL, 5.50 mmol, 1.10 equiv.) and stirred for 0.5 h. Boc_2O was added and the reaction was allowed to warm to rt and stirred for 1 h. The reaction was quenched

with NH_4Cl (10 mL) and diluted with EtOAc (10 mL). The organic layer was washed with saturated $NaHCO_{3(aq)}$ (2 x 10 mL), and the combined aqueous layers were back-extracted with EtOAc (3 x 5 mL). The combined organic fractions were dried over $MgSO_4$, filtered, and evaporated. SiO_2 gel column chromatography (5% Et_2O in PhMe) followed by recrystallisation from iPrOH afforded the Boc pyrazole as a white solid (400 mg, 1.88 mmol, 38%); mp: 104-105 ^oC (iPrOH); ν_{max} (ATR) 2997, 1774 (C=O), 1551, 1521, 1401, 1430, 1374, 1321, 1291, 1054 cm^{-1}; δ_H (600 MHz, $CDCl_3$) 8.18 (1H, d, *J* = 2.9 Hz, H-5), 6.98 (1H, d, *J* = 2.9 Hz, H-4) 1.68 (9H, s, CH_3); δ_C (151 MHz, $CDCl_3$) 158.1 (C=O), 146.2 (C-3), 133.3 (C-5), 104.4 (C-4), 88.5 (O*C*CH_3), 27.9 (CH_3); HRMS (ESI) *m/z* found $[M-H]^-$ 212.0671, $C_8H_{10}N_3O_4$ requires *M*, 212.0671.

tert-butyl 3-amino-1H-pyrazole-1-carboxylate (**496**) [13]

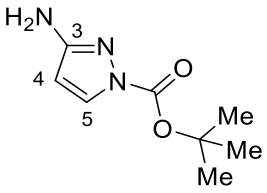

Under N_2, a solution of tert-butyl 3-nitro-1H-pyrazole-1-carboxylate **495** (350 mg, 1.64 mmol, 1.00 equiv.) in EtOAc (2 mL) was charged with 10% dry Pd/C (87 mg, 5 mol%) followed by MeOH (10 mL). The reaction was allowed to stir under H_2 for 4 h at rt. The reaction mixture was cooled and filtered over Celite®, followed by removal of the volatiles. SiO_2 gel column chromatography (0 → 100% acetone in hexanes) afforded the aminopyrazole as a white solid (227 mg, 1.24 mmol, 76%); mp: 107-109 ^oC; ν_{max} (ATR) 3460 (NH_2), 3316 (NH_2), 2990, 1734 (C=O), 1624, 1584, 1488, 1388, 1308, 1244, 1141 cm^{-1} δ_H (700 MHz, $CDCl_3$) 7.82, (1H, s br, 5-H) 5.81 (1H, d, *J* = 2.9 Hz) , 5.80, 3.89 (2H, s br, NH_2), 1.60 (9H, s, CH_3); δ_C (176 MHz, $CDCl_3$) 157.3 (C-3), 147.8 (C=O), 132.1 (C-5), 99.2 (C-4), 84.3 (*C*CH_3), 28.0 (CH_3); *m/z* (ESI) $[M-H]^-$ 182.1. Data for **495** was consistent with a previous report.

Tert-butyl 3-(3',3'-dimethyl-2',5'-dioxopyrrolidin-1-yl)-1H-pyrazole-1-carboxylate (**498**)

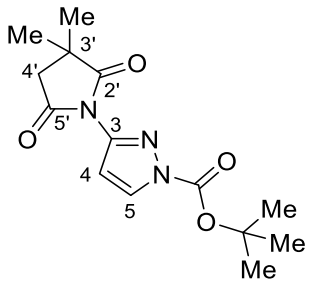

At 0 °C under N_2, Boc_2O (408 mg, 1.83 mmol, 1.20 equiv.) followed by DMAP (19 mg, 0.16 mmol, 0.10 equiv.) were added to a solution of 3,3-dimethyl-1-(1H-pyrazol-3'-yl)pyrrolidine-2,5-dione **486** (300 mg, 1.55 mmol, 1.00 equiv.) in MeCN (1.6 mL). The reaction was warmed to rt, stirred for 16 h, and diluted with EtOAc (5 mL). The organic phase was washed with 1M HCl (5 mL), saturated $NaHCO_{3(aq)}$ (5 mL) and brine (5 mL). The aqueous fractions were back-extracted with EtOAc (3 x 5 mL) and the combined organic fractions were dried over $MgSO_4$, filtered, and evaporated. SiO_2 gel column chromatography (20 → 35% acetone in hexanes) afforded the Boc pyrazole as a white solid (411 mg, 1.40 mmol, 90%); ν_{max} (ATR) 2981, 1791 (C=O), 1758 (C=O), 1720 (C=O), 1542, 1480, 1412, 1366, 1305, 1236, 1147, 1058, cm^{-1}; δ_H (700 MHz, $CDCl_3$) 8.12 (1H, d, *J* = 2.8 Hz, 5-H), 6.48 (1H, d, *J* = 2.8 Hz, 4-H), 2.70 (2H, s, 4'-H), 1.63 (9H, s, OCH_3), 1.40 (6H, s, 3'-CH_3); δ_C (176 MHz, $CDCl_3$) 181.0 (C-2'), 173.6 (C-5'), 146.9 (CO_2), 144.6 (C-3), 132.1 (C-5), 106.0 (C-4), 86.4 (O*C*CH_3), 44.0 (C-4'), 40.5 (C-3'), 27.9 (OC*C*H_3), 25.8 (3'-CH_3); HRMS (ESI) *m/z* found $[M+H]^+$ 294.1464, $C_{14}H_{20}N_3O_4$ requires *M*, 294.1454.

Methyl 3-(3',3'-dimethyl-2',5'-dioxopyrrolidin-1'-yl)-1H-pyrazole-1-carboxylate (**503**)

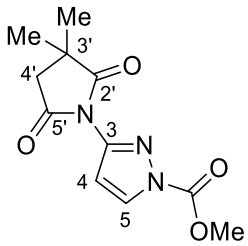

At 0 °C under N_2, methyl chlorofomate (0.05 mL, 0.62 mmol, 1.20 equiv.) was added to a solution of 3,3-dimethyl-1-(1H-pyrazol-3'-yl)pyrrolidine-2,5-dione **486** (300 mg, 1.55 mmol, 1.00 equiv.) and pyridine (0.05 mL, 0.62 mmol, 1.20 equiv.) in CH_2Cl_2 (0.5 mL). The reaction was warmed to rt, stirred for 16 h, and diluted with CH_2Cl_2 (5 mL). The organic phase was washed with 1M HCl (5 mL), saturated

$NaHCO_{3(aq)}$ (5 mL) and brine (5 mL). The aqueous fractions were back-extracted with CH_2Cl_2 (3 x 5 mL) and the combined organic fractions were dried over $MgSO_4$, filtered, and evaporated. SiO_2 gel column chromatography (0 → 100% EtOAc in hexanes) afforded the acylated pyrazole as a white solid (83 mg, 0.44 mmol, 64%); mp: 131-132 °C; ν_{max} (ATR) 2976, 1785 (C=O), 1720 (C=O), 1541, 1481, 1444, 1373, 1305, 1282, 1232, 1141 cm^{-1}; δ_H (700 MHz, $CDCl_3$) 8.20 (1H, d, *J* = 2.9 Hz, 5-H) 6.55 (1H, d, *J* = 2.9 Hz, 4-H), 4.05 (3H, s, OCH_3), 2.70 (2H, s, 4'-H), 1.39 (6H, s, 3'-CH_3); δ_C (176 MHz, $CDCl_3$) 180.7 (C-2'), 173.3 (C-4'), 149.4 (CO_2), 145.2 (C-3), 132.4 (C-5), 106.5 (C-4), 55.4 (OCH_3), 43.9 (C-4'), 40.5 (C-3'), 25.8 (3'-CH_3); HRMS (ESI) *m/z* found $[M+H]^+$ 252.0989, $C_{11}H_{14}N_3O_4$ requires *M*, 252.0984.

1-(1-acetyl-1H-pyrazol-3-yl)-3,3-dimethylpyrrolidine-2,5-dione (**505**)

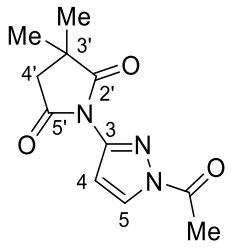

At 0 °C under N_2, acetyl chloride (0.04 mL, 0.62 mmol, 1.20 equiv.) was added to a solution of 3,3-dimethyl-1-(1H-pyrazol-3'-yl)pyrrolidine-2,5-dione **486** (300 mg, 1.55 mmol, 1.00 equiv.) and pyridine (0.05 mL, 0.62 mmol, 1.20 equiv.) in CH_2Cl_2 (0.5 mL). The reaction was warmed to rt, stirred for 1 h, and diluted with CH_2Cl_2 (5 mL). The organic phase was washed with 1M HCl (5 mL), saturated $NaHCO_{3(aq)}$ (5 mL) and brine (5 mL). The aqueous fractions were back-extracted with CH_2Cl_2 (3 x 5 mL) and the combined organic fractions were dried over $MgSO_4$, filtered, and evaporated. SiO_2 gel column chromatography (0 → 100% acetone in hexanes) afforded the acetyl pyrazole as a white solid (103 mg, 0.44 mmol, 85%); mp: 97- 98°C; ν_{max} (ATR) 2976, 1797 (C=O), 1720 (C=O), 1544, 1476, 1411, 1371, 1353, 1269, 1223, 1147, 1042 cm^{-1}; δ_H (700 MHz, $CDCl_3$) 8.29 (1H, d, *J* = 2.9 Hz, 5-H), 6.57 (1H, d, *J* = 2.9 Hz, 4-H), 2.74 (2H, s, 4'-H), 2.70 (3H, s, Ac CH_3), 1.43 (6H, s, 3'-CH_3); δ_H (176 MHz, $CDCl_3$) 181.0 (C-2'), 173.5 (C-5'), 169.1 (Ac C=O), 144.7 (C-3), 129.4 (C-5), 106.9 (C-4), 43.9 (C-4'), 40.6 (C-3'), 25.8 (3'-CH_3), 21.7 (Ac CH_3); HRMS (ESI) *m/z* found $[M+H]^+$ 236.1059, $C_{11}H_{14}N_3O_3$ requires *M*, 236.1035.

(3'-Amino-1H-pyrazol-1-yl)methyl 2,2-dimethylpropanoate (**514**)

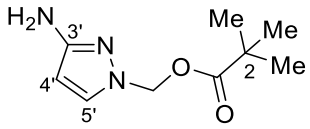

Under N_2, a solution of (3-nitro-1H-pyrazol-1-yl)methyl 2,2-dimethylpropanoate **514b** (2.17 g, 9.56 mmol, 1.00 equiv.) in EtOAc (10 mL) was charged with 10% dry Pd/C (507 mg, 5 mol%), NH_4OCOH (6.0 g, 96 mmol, 10 equiv.) followed by MeOH (30 mL). The reaction was allowed to stir under N_2 for 0.5 h at 40 °C. The reaction mixture was filtered over Celite® with Et_2O (100 mL) and the volatiles were removed. Purification with SiO_2 column chromatography (0 → 100% EtOAc in hexanes) afforded the aminopyrazole as a yellow oil (0.80g, 4.01 mmol, 42%); ν_{max} (ATR) 3446 (NH_2), 3346 (NH_2), 2981, 1731 (C=O), 1621, 1560, 1488, 1438, 1281, 1131, 1031 cm^{-1} δ_H (700 MHz, $CDCl_3$) 7.34 (1H, s br, 5'-H), 5.77 (NCH_2), 5.63 (1H, s br, 4'-H) 3.59 (2H, s br, NH_2), 1.13 (9H, s, CH_3); δ_C (176 MHz, $CDCl_3$) 178.2 (C=O), 155.5 (C-3'), 133.0 (C-5'), 95.5 (C-4'), 72.1 (OCH_2), 38.8 (C-2), 26.9 (CH_3); HRMS (ESI) *m/z* found $[M+H]^+$ 198.1252, $C_9H_{16}N_3O_2$ requires *M*, 198.1243.

(3'-Nitro-1H-pyrazol-1-yl)methyl 2,2-dimethylpropanoate (**514b**)

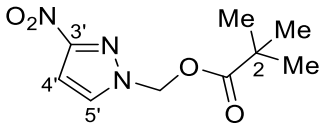

At -20 °C under N_2, a solution of 3-nitro-1H-pyrazole **405** (1.13 g, 10.0 mmol, 1.00 equiv.) in THF (20 mL) was treated with 60% NaH dispersion in mineral oil (440 mg, 11.0 mmol, 1.10 equiv.) portionwise. After stirring at 0 °C for 30 min, chloromethyl 2,2-dimethylpropanoate (2.90 mL, 20.0 mmol, 2.00 equiv.) was added and the reaction was allowed to warm to rt over 30 min. The reaction was reverse quenched with NH_4Cl (10 mL) and ca. one third of the volatiles were removed. EtOAc (30 mL) was added and the aqueous layer was extracted with EtOAc (3 x 20 mL) and dried over $MgSO_4$, filtered, and evaporated. Filtration over an SiO_2 plug with Et_2O (50 mL) afforded the pivalate as a colourless oil (2.21 g, 9.74 mmol, 97%); ν_{max} (ATR) 2981, 1744 (C=O), 1554, 1518, 1383, 1115, 1038 cm^{-1}; δ_H (600 MHz, $CDCl_3$) 7.75 (1H, d, *J* = 2.7 Hz, 5'-H), 6.91 (1H, d, *J* = 2.7 Hz), 6.04 (2H, s, NCH_2), 1.17 (CH_3); δ_C (151 MHz, $CDCl_3$) 177.9 (C=O), 156.7 (C-3'), 134.2 (C-5'), 103.6 (C-4'), 72.8 (NCH_2), 38.8 (C-2), 26.8 (CH_3); HRMS (ESI) *m/z* found $[M+H]^+$ 228.0984, $C_9H_{14}N_3O_4$ requires *M*, 228.0984.

(3-Amino-1H-pyrazol-1-yl)methyl acetate (**515**)

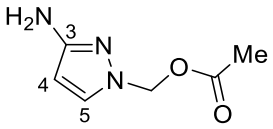

Under N_2, a solution of (3-nitro-1H-pyrazol-1-yl)methyl acetate **515b** (47.0 mg, 0.25 mmol, 1.00 equiv.) in EtOAc (0.5 mL) was charged with 10% dry Pd/C (13.0 mg, 5 mol%) followed by MeOH (1 mL). The reaction was allowed to stir under H_2 for 1 h at 35 °C. The reaction mixture was filtered over Celite® and the volatiles were removed. SiO_2 gel column chromatography (50% EtOAc in hexanes) afforded the aminopyrazole as an off-white solid (16 mg, 0.10 mmol, 41%); mp: 115-116 °C; ν_{max} (ATR) 3418 (NH_2), 3308 (NH_2), 2975, 1712 (C=O), 1633, 1567, 1484, 1428, 1369, 1334, 1276, 1250, 1227, 1205, 1129, 1029 cm^{-1}; δ_H (700 MHz, $CDCl_3$) 7.37 (1H, d, *J* = 2.4 Hz, 5-H), 5.79 (2H, s, NCH_2) 5.66 (1H, d, *J* = 2.4 Hz, 4-H), 3.73 (2H, s br, NH_2), 2.06 (3H, s, CH_3); δ_C (176 MHz, $CDCl_3$) 170.7 (C=O), 156.0 (C-3), 133.3 (C-5), 95.7 (C-4), 72.3 (NCH_2), 21.0 (CH_3); HRMS (ESI) *m/z* found $[M+Na]^+$ 178.0594, $C_6H_9N_3O_2Na$ requires *M*, 178.0592.

(3-Nitro-1H-pyrazol-1-yl)methyl acetate (**515b**)

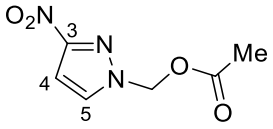

At 0 °C under N_2, a solution of 3-nitro-1H-pyrazole **404** (219 mg, 1.94 mmol, 1.00 equiv.) in THF (4 mL) was treated with 60% NaH dispersion in mineral oil (85 mg, 2.13 mmol, 1.1 equiv.) portionwise. After stirring at 0 °C for 5 min, bromomethylacetate (0.38 mL, 3.87 mmol, 2.00 equiv.) was added and the reaction was allowed to warm to rt over 10 min. The reaction was reverse quenched with NH_4Cl (10 mL) and ca. one third of the volatiles were removed. EtOAc (10 mL) was added and the aqueous layer was extracted with EtOAc (3 x 5 mL), dried over $MgSO_4$, filtered, and evaporated. SiO_2 gel column chromatography (40 → 60% EtOAc in hexanes) afforded the pyrazole acetate as a white solid (244 mg, 1.32 mmol, 68%); mp: 82-84 °C; ν_{max} (ATR) 2984, 1738 (C=O), 1552, 1507, 1463, 1370, 1310, 1236, 1222, 1070, 1033, cm^{-1}; δ_H (700 MHz, $CDCl_3$) 7.77 (1H, d, *J* = 2.7 Hz, 5-H), 6.91 (1H, d, *J* = 2.7 Hz, 4-H) 6.03 (2H, s, NCH_2), 2.12 (3H, s, CH_3); δ_C (176 MHz, $CDCl_3$) 170.3 (C=O), 157.0 (C-3), 134.6 (C-5),

103.8 (C-4), 72.8 (NCH_2), 20.7 (CH_3); HRMS (ASAP) *m/z* found $[M+H]^+$ 186.0521, $C_6H_8N_3O_4$ requires *M*, 186.0515.

[3-(3,4-Dimethyl-2,5-dioxo-2,5-dihydro-1H-pyrrol-1-yl)-1H-pyrazol-1'-yl]methyl 2,2-dimethylpropanoate (**515c**)

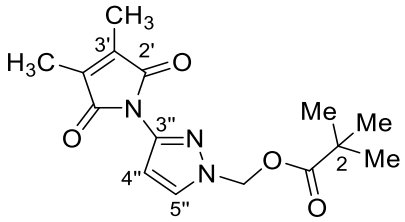

To a solution of (3'-amino-1H-pyrazol-1-yl)methyl 2,2-dimethylpropanoate **515** (394 mg, 2.00 mmol, 1.00 equiv.) and Et_3N (0.28 mL, 2.00 mmol, 2.00 equiv.) in THF (4 mL) was added dimethyl-2,5-dihydrofuran-2,5-dione (277 mg, 2.20 mmol, 1.10 equiv.). The reaction was refluxed for 2 h, cooled, followed by removal of the volatiles. CH_2Cl_2 (10 mL) and saturated $NaHCO_{3(aq)}$ (10 mL) were added and the aqueous layer was extracted with CH_2Cl_2 (3 x 10 mL). The organic fractions were dried over $MgSO_4$, filtered, and evaporated. SiO_2 gel column chromatography (0 → 100% EtOAc in hexanes) afforded the maleimide as a white solid (263 mg, 0.86 mmol, 43%); mp: 101-103 ^oC; ν_{max} (ATR) 2984, 1738 (C=O), 1724 (C=O), 1708 (C=O), 1531, 1498, 1430, 1355, 1281, 1124, 1095 cm^{-1}; δ_H (700 MHz, $CDCl_3$) 7.66 (1H, d, *J* = 2.6 Hz, 5''-H), 6.37 (1H, d, *J* = 2.6 Hz, 4''-H), 5.99 (2H, s, NCH_2), 2.02 (6H, s, 3'-CH_3), 1.16 (9H, s, 2-CH_3); δ_C (176 MHz, $CDCl_3$) 178.1 (CO_2), 169.8 (C-2'), 142.0 (C-3''), 138.0 (C-3'), 132.6 (C-5''), 103.2 (C-4''), 72.5 (NCH_2), 38.8 (C-2), 26.8 (2-CH_3), 8.9 (3'-CH_3); HRMS (ESI) *m/z* found $[M+H]^+$ 306.1464, $C_{15}H_{20}N_3O_4$ requires *M*, 306.1454.

(3-acetamido-1H-pyrazol-1-yl)methyl acetate (**515d**)

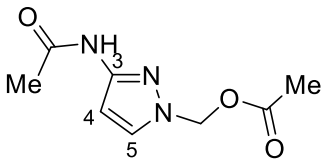

(3-amino-1H-pyrazol-1-yl)methyl acetate (34 mg, 0.22 mmol, 1.00 equiv.) and Ac_2O (25 mg, 0.24 mmol, 1.10 equiv.) were stirred neat for 0.5 h. SiO_2 gel column chromatography (0 → 100% EtOAc in hexanes) afforded the acetylated pyrazole as a colourless oil (42 mg, 0.21 mmol, 98%); δ_H (700 MHz, $CDCl_3$)

8.22 (1H, s br, NH), 7.53 (1H, d, *J* = 2.5 Hz, 5-H), 6.78 (1H, d, *J* = 2.5 Hz, 4-H) 5.87 (2H, s, NCH_2), 2.15 (3H, s, NAc CH_3), 2.07 (3H, s, OAc CH_3); δ_C (176 MHz, $CDCl_3$) 170.4 (CO_2), 167.9 (CONH), 148.8 (C-3), 132.8 (C-5), 99.7 (C-4), 72.1 (NCH_2), 24.0 (NAc CH_3), 20.9 (OAc CH_3); HRMS (ESI) *m/z* found $[M+H]^+$ 198.0882, $C_8H_{12}N_3O_3$ requires *M*, 198.0879.

5-nitro-1-{[2-(trimethylsilyl)ethoxy]methyl}-1H-pyrazole (**525**)

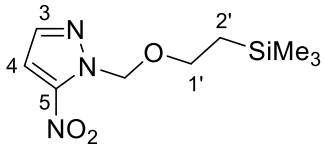

To a solution of 3-nitro-1H-pyrazole **404** (1.13 g, 10.0 mmol, 1.00 equiv.) in THF (20 mL) under N_2 at 0 °C was rapidly added LiHMDS in THF (11 mL, 11 mmol, 1.0 M, 1.1 equiv.). After 5 min, SEMCl (1.93 mL, 11.0 mmol, 1.10 equiv.) was added and the reaction was allowed to warm to rt. After 3 h, the reaction was quenched with NH_4Cl (20 mL) and *ca.* one third of the volatiles were removed. EtOAc (30 mL) and H_2O (20 mL) were added and the aqueous layer was extracted with EtOAc (3 x 20 mL). The combined organic layers were dried over $MgSO_4$, filtered and evaporated. SiO_2 chromatography (5 → 20% EtOAc in hexanes) afforded the SEM pyrazole as a colourless oil (846 mg, 3.50 mmol, 35%); ν_{max} (ATR) 2952, 1549, 1510, 1460, 1350, 1250, 1094 cm^{-1}; δ_H (700 MHz, $CDCl_3$) 7.57 (1H, d, *J* = 2.1 Hz, 3-H), 7.11 (1H, d, *J* = 2.1 Hz, 4-H), 5.88 (2H, s, NCH_2), 3.61-3.58 (2H, m, 1'-H), 0.90-0.88 (2H, m, 2'-H), -0.04 (9H, s, $SiCH_3$); δ_C (176 MHz, $CDCl_3$) 146.0 (C-5), 138.6 (C-3), 107.8 (C-4), 80.7 (NCH_2), 67.6 (C-1'), 17.9 (C-2'), -1.4 ($SiCH_3$); HRMS (ASAP) $[M]^+$ *m/z* found 243.1040, $C_9H_{17}N_3O_3Si$, requires *M*, 243.1039.

5-Amino-1-{[2-(trimethylsilyl)ethoxy]methyl}-1H-pyrazole (**526**)

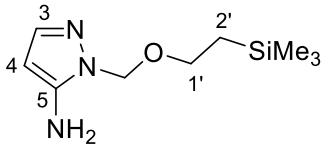

Under N_2, a solution of 5-nitro-1-{[2-(trimethylsilyl)ethoxy]methyl}-1H-pyrazole **531** (772 mg, 3.10 mmol, 1.00 equiv.) in EtOAc (2 mL) was charged with 10% dry Pd/C (164 mg, 5 mol%) followed by MeOH (15 mL). The reaction was allowed to stir under H_2 for 4 h at 40 °C. The reaction mixture was filtered over Celite® and the volatiles were removed. SiO_2 gel column chromatography (0 → 100% EtOAc in

hexanes) afforded the aminopyrazole as an off-white solid (560 mg, 83%); mp: 60–62 °C; ν_{max} (ATR) 3321 (NH_2), 3259 (NH_2), 2957, 1626, 1526, 1511, 1417, 1250, 1072 cm^{-1}; δ_H (700 MHz, $CDCl_3$) 7.25 (1H, d, *J* = 1.9 Hz, 3-H), 5.51 (1H, d, *J* = 1.9 Hz, 4-H), 5.34 (2H, s, NCH_2), 3.94 (2H, s br, NH_2), 3.55-3.53 (2H, m, 1'-H), 0.89-0.87 (2H, m, 2'-H), -0.04 (9H, s, $SiCH_3$); δ_C (176 MHz, $CDCl_3$); 145.7 (C-5), 139.0 (C-3), 91.1 (C-4), 77.2 (NCH_2), 66.2 (C-1'), 17.9 (C-2'), -1.3 ($SiCH_3$); HRMS (ASAP) $[M+H]^+$ *m/z* found 214.1365, $C_9H_{20}N_3OSi$ requires *M*, 214.1376.

Tert-butyl N-[(tert-butoxy)carbonyl]-N-(1-{[2'-(trimethylsilyl)ethoxy]methyl}-1H-pyrazol-5-yl)carbamate (**526b**)

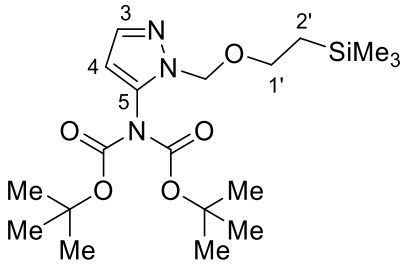

At 0 °C under N_2, a solution of 5-amino-1-{[2-(trimethylsilyl)ethoxy]methyl}-1H-pyrazole **532** (107 mg, 0.50 mmol, 1.00 equiv.) in THF (0.75 mL) was treated with 1M LDA in THF (0.50 mL, 1.00 mmol, 2.00 equiv.) and stirred for 0.5 h. Boc_2O was added and the reaction was allowed to warm to rt and stirred for 1 h. The reaction was quenched with NH_4Cl (10 mL) and diluted with EtOAc (10 mL). The organic layer was washed with saturated $NaHCO_{3(aq)}$ (2 x 10 mL), and the combined aqueous layers were back-extracted with EtOAc (3 x 5 mL). The combined organic fractions were dried over $MgSO_4$, filtered, and evaporated. SiO_2 gel column chromatography (0 → 100% EtOAc in hexanes) afforded the bisBoc pyrazole as a yellow solid (124 mg, 0.30 mmol, 60%); mp: 61-62 °C; ν_{max} (ATR) 2987, 1804 (C=O), 1764 (C=O), 1564, 1474, 1368, 1278, 1251, 1151, 1095 cm^{-1}; δ_H (700 MHz, $CDCl_3$) 7.49 (2H, d, *J* = 1.9 Hz, 3-H), 6.15 (2H, d, *J* = 1.9 Hz, 4-H), 5.30 (2H, s, NCH_2), 3.56-3.53 (2H, m, 1'-H), 1.42 (18H, s, CCH_3), 0.90 (2H, m, 2'-H), -0.03 (9H, s, $SiCH_3$); δ_C (176 MHz, $CDCl_3$) 150.1 (C=O), 138.8 (C-3), 136.7 (C-5), 104.6 (C-4), 76.9 (NCH_2), 83.7 (CCH_3), 66.6 (C-1'), 27.8 (CCH_3), 17.7 (C-2'), -1.5 ($SiCH_3$); HRMS (ESI) *m/z* found $[M+H]^+$ 414.2418, $C_{19}H_{36}N_3O_5Si$ requires *M*, 414.2424.

N-(1-{[2'-(trimethylsilyl)ethoxy]methyl}-1H-pyrazol-5-yl)acetamide (**531**)

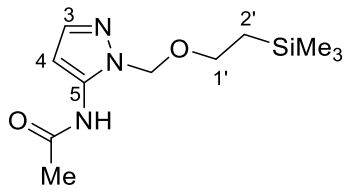

1-{[2-(trimethylsilyl)ethoxy]methyl}-1H-pyrazol-5-amine **526** (80 mg, 0.38 mmol, 1.00 equiv.) and Ac_2O (0.04 mL, 0.41 mmol, 1.10 equiv.) were stirred neat for 0.5 h. The reaction mixture was diluted in EtOAc (5 mL), washed with saturated $NaHCO_{3(aq)}$ (5 mL), H_2O (5 mL) and brine (5 mL). The organic layer was dried over $MgSO_4$, filtered, and evaporated. SiO_2 gel (pre-treated with Et_3N) column chromatography (0% → 100% EtOAc in hexanes (1% Et_3N)) afforded the acylated pyrazole as a white solid (99 mg, 0.32 mmol, 84%); mp: 68-70 ^oC; ν_{max} (ATR) 3288 (NH), 2954, 1678 (C=O), 1572, 1549, 1406, 1380, 1309, 1270, 1248, 1089 cm^{-1}; δ_H (700 MHz, CD_3OD) 7.48 (1H, d, *J* = 1.9 Hz, 3-H) 6.42 (1H, d, *J* = 1.9 Hz, 4-H) 5.44 (2H, s, NCH_2), 3.56-3.53 (2H, m, 1'-H), 2.18 (3H, s, Ac CH_3), 0.89-0.87 (2H, m, 2'-H), -0.01 (9H, s, $SiCH_3$); δ_C (176 MHz, CD_3OD) 171.4 (C=O), 140.3 (C-5), 138.5 (C-3), 101.2 (C-4), 77.9 (NCH_2), 67.5 (C-1'), 23.0 (Ac CH_3), 18.6 (C-2'), -1.4 ($SiCH_3$); HRMS (ESI) *m/z* found $[M+H]^+$ 256.1496, $C_{11}H_{22}N_3O_2Si$ requires *M*, 212.1481.

tert-butyl 5-amino-1H-pyrazole-1-carboxylate (**534**)

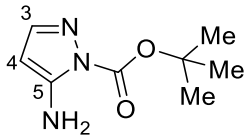

To a solution of 1H-pyrazol-3-amine **369** (500 mg, 6.02 mmol, 1.00 equiv.) and triethylamine (0.92 mL, 6.62 mmol, 1.10 equiv.) in CH_2Cl_2 (6 mL) was charged portionwise with Boc_2O (1.44 g, 6.62 mmol, 1.10 equiv.). The reaction was refluxed for 16 h before addition of saturated $NaHCO_{3(aq)}$ (10 mL). The organic layer was washed with saturated $NaHCO_{3(aq)}$ (3 x 10 mL) and the combined aqueous fractions were back-extracted with CH_2Cl_2 (3 x 10 mL). The combined organic fractions were dried over $MgSO_4$, filtered, and evaporated. SiO_2 gel column chromatography (45 → 55% EtOAc in hexanes (1% Et_3N)) afforded the Boc pyrazole as a white solid (243 mg, 1.33 mmol, 22%); ν_{max} (ATR) 3480 (NH_2), 3373 (NH_2), 2934, 1737 (C=O), 1609, 1479, 1454, 1372, 1332, 1207, 1151, 1126, 1068 cm^{-1}; δ_H (700 MHz, CD_3OD) 7.36 (1H, d, *J* = 1.9 Hz, 3-H) 5.41 (1H, d, *J* = 1.9 Hz, 4-H) 1.64 (9H, s, CH_3); δ_C (176 MHz,

CD_3OD) 153.0 (C-5), 151.5 (C=O), 144.8 (C-3), 88.8 (C-4), 86.4 (O*C*CH_3), 28.2 (OC*C*H_3); HRMS (ESI) *m/z* found $[M+H]^+$ 184.1096, $C_{10}H_{14}N_3O_2$ requires *M*, 184.1086.

N-[1-(oxan-2'-yl)-1H-pyrazol-5-yl]acetamide (**538**)

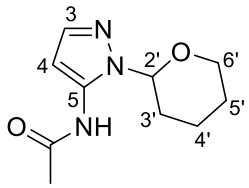

Crude 1-(oxan-2-yl)-1H-pyrazol-5-amine **537** (107 mg, 0.64 mmol, 1.00 equiv.), Et_3N (0.10 mL, 0.70 mmol, 1.10 equiv.), and Ac_2O (0.06 mL, 0.67 mmol, 1.05 equiv.) were stirred neat for 0.5 h. The reaction mixture was diluted in EtOAc (5 mL), washed with saturated $NaHCO_{3(aq)}$ (2 mL), H_2O (2 mL) and brine (2 mL). The organic layer was dried over $MgSO_4$, filtered, and evaporated. SiO_2 gel column chromatography (0 → 100% EtOAc in hexanes (1% Et_3N)) afforded the acetylated pyrazole as a colourless oil (120 mg, 0.58 mmol, 90%); ν_{max} (ATR) 3280 (NH), 2963, 1675 (C=O), 1546, 1456, 1374, 1251, 1205, 1181, 1082, 1040 cm^{-1}; δ_H (600 MHz, $CDCl_3$) 8.45 (1H, s br, NH), 7.39 (1H, s, 3-H), 6.50 (1H, s, 4-H), 5.42-5.40 (1H, m, 2'-H), 3.92-3.89 (1H, m, 6'-H), 3.68-3.64 (1H, m, 6'-H), 2.23-2.19 (1H, m, 3'-H), 2.14 (3H, s, CH_3), 2.06-2.01 (2H, m, 3'-H, 4'-H), 1.69-1.60 (3H, m, 4'-H, 5'-H); δ_C (151 MHz, $CDCl_3$) 166.9 (C=O), 139.0 (C-3), 137.0 (C-5), 98.3 (C-4), 86.1 (C-2'), 66.7 (C-6'), 29.0 (C-3'), 25.1 (C-5'), 24.0 (CH_3), 21.3 (C-4'); HRMS (ESI) *m/z* found $[M+H]^+$ 210.1240, $C_{10}H_{16}N_3O_2$ requires *M*, 210.1243. **547** was found to decompose on SiO_2 gel unless pre-treated with Et_3N.

3,3-dimethyl-1-[1-(oxan-2''-yl)-1H-pyrazol-5'-yl]pyrrolidine-2,5-dione (**542**)

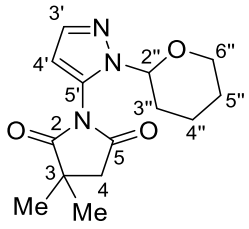

To a solution of 3,3-dimethyl-1-(1H-pyrazol-3-yl)pyrrolidine-2,5-dione **486** (100 mg, 0.52 mmol, 1.00 equiv.) and 3,4-dihydro-2H-pyran (0.14 mL, 1.55 mmol, 3.00 equiv.) in CH_2Cl_2 (4.2 mL) was added PPTS (13.1 mg, 0.05 mmol, 10 mol%). The reaction was stirred for 0.5 h, poured into saturated $NaHCO_{3(aq)}$ (5 mL), and the aqueous layer was extracted with CH_2Cl_2 (3 x 5 mL). SiO_2 gel column

chromatography (15 → 25% acetone in hexanes) afforded the THP pyrazole as a white solid; (77 mg, 0.28 mmol, 54%); mp: 93-94 °C; ν_{max} (ATR) 2950, 1794 (C=O), 1720 (C=O), 1568, 1468, 1407, 1291, 1210, 1142, 1083 cm^{-1}; δ_H (700 MHz, $CDCl_3$) 7.59 (1H, d, *J* = 1.9 Hz, 3'-H), 6.32 (1H, d, *J* = 1.9 Hz, 4'-H) 5.36-5.35 (1H, m, 2''-H), 3.64-3.61 (1H, m, 6''-H), 3.49-3.46 (1H, m, 6''-H), 2.71 (2H, s, 4-H), 2.46-2.41 (1H, m, 3''-H), 2.08-2.00 (2H, m, 3''-H, 4''-H) 1.67-1.63 (1H, m, 4''-H) 1.60-1.53 (2H, m, 5''-H), 1.43 (3H, s, CH_3), 1.41 (3H, s, CH_3); δ_C (176 MHz, $CDCl_3$) 181.2 (C-2), 173.8 (C-5), 138.7 (C-3'), 130.3 (C-5'), 106.2 (C-4'), 85.2 (C-2''), 65.3 (C-6''), 43.9 (C-4), 40.7 (C-3), 28.1 (C-3''), 25.7 (CH_3), 25.6 (CH_3), 24.9 (C-5''), 20.6 (C-4''); HRMS (ESI) *m/z* found $[M+H]^+$ 278.1524, $C_{14}H_{20}N_3O_3$ requires *M*, 278.1505.

Chloromethyl 5-amino-1H-pyrazole-1-carboxylate (**556**)

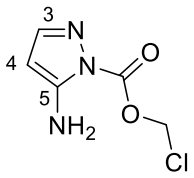

Under N_2 at 0 °C, a solution chloromethyl chloroformate (0.09 mL, 1.00 mmol, 1.00 equiv.) in CH_2Cl_2 (2.5 mL) was treated with a solution of 1H-pyrazol-3-amine **369** (83 mg, 1.0 mmol, 1.0 equiv.) and Et_3N (0.14 mL, 1.00 mmol, 1.00 equiv.) in CH_2Cl_2 (2.5 mL) dropwise over 5 min. The reaction was warmed to rt and stirred for 1.5 h before addition of H_2O (5 mL). The aqueous layer was extracted with CH_2Cl_2 (3 x 5 mL), dried over $MgSO_4$, filtered, and evaporated. Purification with SiO_2 gel column chromatography (0 → 100% EtOAc in hexanes (1% Et_3N)) afforded the acylated pyrazole as a white solid (62 mg, 0.35 mmol, 35%); mp: 133-135 °C; ν_{max} (ATR) 3472 (NH_2), 3300 (NH_2), 2975, 1756 (C=O), 1622, 1578, 1494, 1452, 1393, 1241, 1154, 1095 cm^{-1}; δ_H (700 MHz, DMSO) 7.42 (1H, d, *J* = 1.8 Hz, 3-H), 6.51 (2H, s br, NH_2), 6.11 (2H, s, CH_2), 5.34, (1H, d, *J* = 1.8 Hz, 4-H); δ_C (176 MHz, DMSO) 152.1 (C-5), 149.8 (C=O), 145.7 (C-3), 87.7 (C-4), 72.2 (CH_2); HRMS (ESI) *m/z* found $[M+H]^+$ 176.0217, $C_5H_7N_3O_2{}^{35}Cl$ requires *M*, 176.0227.

Chloromethyl 3-amino-1H-pyrazole-1-carboxylate (**557**)

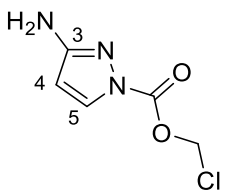

Under N_2 at 0 °C, a solution chloromethyl chloroformate (1.80 mL, 20.0 mmol, 1.00 equiv.) in CH_2Cl_2 (50 mL) was treated with a solution of 1H-pyrazol-3-amine **369** (1.66 g, 20.0 mmol, 1.0 equiv.) and Et_3N (2.80 mL, 20.0 mmol, 1.00 equiv.) in CH_2Cl_2 (50 mL) dropwise over 1 h. The reaction was warmed to rt and stirred for 1 h before addition of H_2O (50 mL). The aqueous layer was extracted with CH_2Cl_2 (3 x 25 mL), dried over $MgSO_4$, filtered, and evaporated. Purification with SiO_2 gel column chromatography (0 → 100% EtOAc in hexanes (1% Et_3N)) afforded the acylated pyrazole as a white solid (600 mg, 3.42 mmol, 17%); mp: 141-143 °C (MeCN); ν_{max} (ATR) 3466 (NH_2), 3297 (NH_2), 2995, 1751 (C=O), 1619, 1573, 1492, 1449, 1387, 1348, 1312, 1240, 1150, 1094 cm^{-1}; δ_H (700 MHz, DMSO) 7.96 (1H d, *J* = 2.8 Hz, 5-H), 6.04 (2H, s, CH_2), 5.91 (1H, d, *J* = 2.8 Hz, 4-H), 5.67 (2H, s br, NH_2); δ_C (176 MHz, DMSO) 160.0 (C-3), 132.8 (C-5), 102.6 (C-4), 72.4 (CH_2). HRMS (ESI) *m/z* found $[M+H]^+$ 176.0231, $C_5H_7N_3O_2{}^{35}Cl$ requires *M*, 176.0227.

1-[2-(trimethylsilyl)ethyl]-1H-pyrazole (**558**)

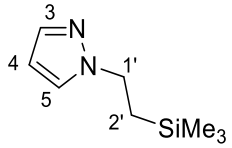

Under N_2 at 0 °C, a solution of 2-(trimethylsilyl)ethan-1-ol (0.72 g, 5.00 mmol, 1.00 equiv.) in THF (5 mL) was treated with 60% NaH dispersion in mineral oil (220 mg, 5.50 mmol, 1.10 equiv.) portionwise. After stirring for 0.5 h, MsCl was added dropwise (0.39 mL, 5.00 mmol, 1.00 equiv.) and the reaction was warmed to rt. After 2 h, the reaction was cooled to 0 °C and 1M sodium 1H-pyrazol-1-ide in THF (5.00 mL, 5.00 mmol, 5.00 equiv.) was added dropwise. After warming to rt, the reaction was stirred for 16 h and quenched with NH_4Cl (10 mL). The aqueous layer was extracted with Et_2O (3 x 10 mL), and the combined organic fractions were dried over $MgSO_4$ and filtered. Removal of the volatiles at 0 °C followed by SiO_2 gel column chromatography (0 → 50% EtOAc in hexanes) afforded the pyrazole as a colourless oil (110 mg, 0.65 mmol, 13%); ν_{max} (ATR) 2957, 1510, 1397, 1494, 1258, 1091, cm^{-1}; δ_H (700 MHz, $CDCl_3$) 7.48, (1H, d, *J* = 1.5 Hz, 3-H) 7.39 (1H, d, *J* = 2.2 Hz 5-H), 6.22 (1H, t, *J* = 2.0 Hz, 4-H), 4.18-4.16 (2H, m, 1'-H), 1.23-1.20 (2H, m, 2'-H, 2'-H), 0.03 (9H, s, $SiCH_3$); δ_C (176 MHz, $CDCl_3$) 138.8 (C-3), 127.8 (C-5), 105.1 (C-4), 48.5 (C-1'), 18.66 (C-2') , -1.86 ($SiCH_3$); HRMS (ESI) *m/z* found $[M+H]^+$ 169.1147, $C_8H_{16}N_2Si$ requires *M*, 169.1161.

(9H-Fluoren-9'-yl)methyl 3-amino-1H-pyrazole-1-carboxylate (**559**)

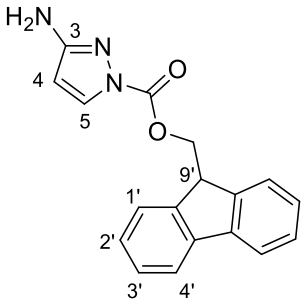

Under N_2 at 0 °C, a solution of FmocCl (4.37 g, 16.9 mmol, 1.00 equiv) in CH_2Cl_2 (40 mL) was treated with a solution of 1H-pyrazol-3-amine **369** (1.40 g, 16.9 mmol, 1.00 equiv.) and Et_3N (2.40 mL, 16.9 mmol, 1.00 equiv.) in CH_2Cl_2 (40 mL) dropwise over 10 min. The reaction was warmed to rt and stirred for 2 h before addition of NH_4Cl (50 mL). The aqueous layer was extracted with CH_2Cl_2 (3 x 25 mL), dried over $MgSO_4$, filtered, and evaporated. Crude NMR analysis indicated a 3:2 isomeric ratio of products. SiO_2 gel column chromatography (0 → 100% EtOAc in hexanes) afforded the acylated pyrazole as a white solid (1.51 g, 4.95 mmol, 29%); mp: 138 °C (iPrOH); ν_{max} (ATR) 3467 (NH_2), 3293 (NH_2), 2970, 1724 (C=O), 1624, 1576, 1435, 1405, 1372, 1295, 1244, 1143, 1041 cm^{-1}; δ_H (700 MHz, DMSO) 7.89 (2H, d, *J* = 7.7 Hz, 4'-H), 7.81 (1H, s br, 5-H), 7.71 (2H, d, *J* = 7.7 Hz, 1'-H), 7.41 (2H, t, *J* = 7.4 Hz, 3'-H) 7.32 (2H, td, *J* = 7.5, 1.1 Hz, 2'-H), 5.85 (1H, d, *J* = 3.0 Hz) 5.55 (2H, s br, NH_2), 4.59 (2H, d, *J* = 7.1 Hz, CH_2), 4.38 (1H, t, *J* = 7.1 Hz, 9'-H); δ_C (176 MHz, DMSO) 159.5 (C-3), 149.3 (C=O), 143.8 (9'-*C*), 141.2 (4'-*C*), 132.2 (C-5), 128.3 (C-3'), 127.7 (C-2'), 125.6 (C-1'), 120.7 (C-4'), 101.4 (C-4), 68.5 (CH_2), 46.7 (C-9'); HRMS (ESI) *m/z* found $[M+H]^+$ 306.1247, $C_{18}H_{16}N_3O_2$ requires *M*, 306.1243.

(9H-fluoren-9'-yl)methyl 3-{[(chloromethoxy)carbonyl]amino}-1H-pyrazole-1-carboxylate (**560**)

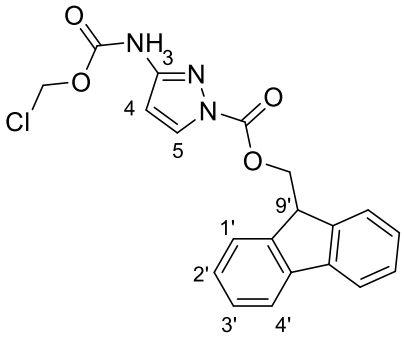

Under N_2 at 0 °C, a solution of (9H-Fluoren-9-yl)methyl 3-amino-1H-pyrazole-1-carboxylate **559** (960 mg, 3.14 mmol, 1.00 equiv) in CH_2Cl_2 (9.5 mL) was treated with chloromethyl chloroformate (0.28 mL, 3.14 mmol, 1.00 equiv.) and Et_3N (0.44 mL, 3.14 mmol, 1.00 equiv.) dropwise simultaneously. The reaction was warmed to rt and stirred for 1 h before addition of NH_4Cl (10 mL). The aqueous layer was extracted with CH_2Cl_2 (3 x 10 mL), dried over $MgSO_4$, filtered, and evaporated. SiO_2 gel column chromatography (0 → 100% EtOAc in hexanes) afforded the acylated pyrazole as a white solid (650 mg, 1.63 mmol, 52%); mp: 177-178 °C; ν_{max} 3248 (NH), 2975, 1763 (C=O), 1734 (C=O), 1603, 1448, 1383, 1364, 1315, 1223, 1207, 1157, 1097, 1004 cm^{-1}; δ_H (700 MHz, CD_2Cl_2) 8.21 (1H, s br, NH), 8.03 (1H, d, *J* = 2.7 Hz, 5-H) 7.81 (2H, d, *J* = 7.5 Hz, 4'-H) 7.67 (2H, dd, *J* = 7.5, 0.8 Hz, 1'-H), 7.43 (2H, d, 3'-H) 7.32 (2H, td, *J* = 7.5, 0.8 Hz, 2'-H), 6.86 (1H, s br, 4-H), 5.82 (2H, s, CH_2Cl), 4.71 (2H, d, *J* = 7.3 Hz, 9'-CH_2), 4.40 (1H, t, *J* = 7.3 Hz, 9'-H); δ_C (176 MHz, CD_2Cl_2) 151.4 (NC=O), 151.2 (C-3), 149.4 (CO_2), 143.6 (C-1_a'), 141.9 (C-4_a'), 132.7 (C-5), 128.6 (C-3'), 127.8 (C-2'), 125.6 (C-1'), 120.7 (C-4'), 102.2 (C-4), 71.2 (CH_2Cl), 70.3 (9'-CH_2), 47.2 (C-9'); HRMS (ESI) *m/z* found $[M+H]^+$ 398.0919, $C_{20}H_{17}N_3O_4{}^{35}Cl$ requires *M*, 398.0908.

3,4-dimethyl-1-(1H-pyrazol-3'-yl)-2,5-dihydro-1H-pyrrole-2,5-dione (**561**)

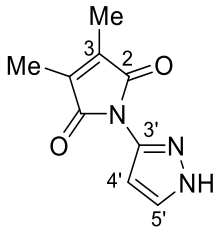

To a suspension of 1H-pyrazol-3-amine **369** (2.00 g, 24.1 mmol, 1.00 equiv.) in H_2O (120 mL) was added dimethyl-2,5-dihydrofuran-2,5-dione (3.34 g, 26.5 mmol, 1.10 equiv.). The inhomogeneous reaction was stirred at rt for 3 h, diluted with EtOAc (50 mL), and the aqueous fractions were extracted with EtOAc (3 x30 mL). The combined organic fractions were dried over $MgSO_4$, filtered, and evaporated. The obtained maleimide was obtained as a yellow solid which was used without further purification (4.40 g, 23.0 mmol, 96%); mp: 153-154 °C; ν_{max} (ATR) 3256 (NH), 2919, 1735 (C=O), 1704 (C=O), 1611, 1542, 1497, 1433, 1347, 1283, 1202, 1081 cm^{-1} δ_H (700 MHz, $CDCl_3$) 12.29 (1H, s br, NH), 7.67 (1H, d, *J* = 2.4 Hz, 5'-H), 6.42 (1H, d, *J* = 2.4 Hz, 4'-H), 2.03 (6H, s, CH_3); δ_C (176 MHz, $CDCl_3$) 170.1 (C=O), 140.6, (C-3'), 138.0 (C-2), 130.9 (C-5'), 99.8 (C-4'), 8.98 (CH_3); HRMS (ESI) *m/z* found $[M+H]^+$ 192.0759, $C_9H_{10}N_3O_2$ requires *M*, 192.0773.

1-{1'-[(3'',5''-dimethylphenyl)methyl]-1H-pyrazol-3'-yl}-3,3-dimethylpyrrolidine-2,5-dione (**562**)

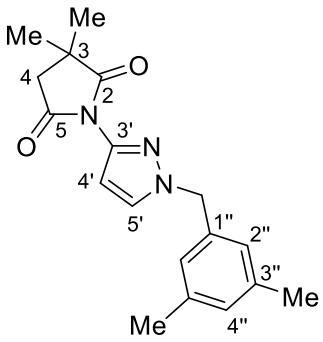

To a solution of 1-[(3,5-dimethylphenyl)methyl]-1H-pyrazol-3-amine **402** (49 mg, 0.24 mmol, 1.00 equiv.) and Et_3N (0.03 mL, 0.24 mmol, 1.00 equiv.) in PhMe (2.5 mL) was added 3,3-dimethyloxolane-2,5-dione (37 mg, 0.29 mmol, 1.10 equiv.). The reaction was refluxed for 16 h, cooled, and diluted with EtOAc (5 mL) and H_2O (5 mL). The aqueous phase was extracted with EtOAc (3 x 5 mL), and the combined organic fractions were dried over $MgSO_4$, filtered, and evaporated. SiO_2 gel column chromatography (0 → 100% EtOAc in hexanes) afforded the succinimide as a white solid (39 mg, 0.13 mmol, 51%); mp: 121-122 ^oC; ν_{max} (ATR) 2987, 1798 (C=O), 1724 (C=O), 1604, 1521, 1501, 1418, 1344, 1234, 1211, 1148 cm^{-1}; δ_H (700 MHz, $CDCl_3$) δ 7.33 (1H, d, *J* = 2.4 Hz, 5'-H) 6.94 (1H, s br, 4''-H), 6.86 (1H, s br, 2'-H), 6.30 (1H, d, *J* = 2.4 Hz, 4'-H), 5.24 (2H, s, 1''-CH_2), 2.70 (2H, s, 4-H), 2.28 (6H, s, 3''-CH_3), 1.41 (6H, s, 3-CH_3); δ_C (176 MHz, $CDCl_3$) 181.7 (C-2), 174.4 (C-5), 140.4 (C-3'), 138.6 (C-3''), 135.3 (C-1''), 130.7 (C-5'), 130.1 (C-4''), 126.1 (C-2''), 103.1 (C-4'), 56.7 (1''-CH_2), 43.9 (C-4), 40.3 (C-3), 25.9 (3-CH_3), 21.3 (3''-CH_3); HRMS (ESI) *m/z* found $[M+H]^+$ 312.1714, $C_{16}H_{22}N_3O_2$ requires *M*, 312.1712.

3,3-dimethyl-1-(1'-{[2''-(trimethylsilyl)ethoxy]methyl}-1H-pyrazol-3'-yl)pyrrolidine-2,5-dione (**563**)

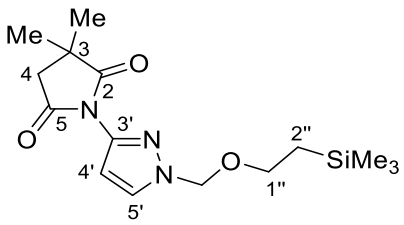

To a solution of 1-{[2-(trimethylsilyl)ethoxy]methyl}-1H-pyrazol-3-amine **450** (107 mg, 0.50 mmol, 1.00 equiv.) and Et_3N (0.07 mL, 0.05 mmol, 1.00 equiv.) in PhMe (5 mL) was added 3,3-dimethyloxolane-

2,5-dione (77 mg, 0.60 mmol, 1.20 equiv.). The reaction was stirred at 100 °C for 1 h, cooled, and diluted with EtOAc (5 mL) and H_2O (5 mL). The aqueous phase was extracted with EtOAc (3 x 5 mL), and the combined organic fractions were dried over $MgSO_4$, filtered, and evaporated. SiO_2 gel column chromatography (0 → 100% EtOAc in hexanes) afforded the succinimide as a colourless oil (73 mg, 0.23 mmol, 45%); ν_{max} (ATR) 2957, 1794 (C=O), 1720 (C=O), 1524, 1498, 1424, 1350, 1255, 1208, 1195, 1148, 1098 cm^{-1}; δ_H (700 MHz, $CDCl_3$) 7.63 (1H, d, *J* = 2.5 Hz, 5'-H) 6.40 (1H, d, *J* = 2.5 Hz, 4'-H) 5.44 (2H, s, OCH_2) , 3.60-3.58 (2H, m, 1''-H), 2.71 (2H, s, 4-H), 1.42 (6H, s, CH_3), 0.91-0.89 (2H, m, 2''-H), -0.02 (9H, s, $SiCH_3$); δ_C (176 MHz, $CDCl_3$) 181.5 (C-2), 174.2 (C-5), 141.0 (C-3'), 130.9 (C-5'), 104.2 (C-4'), 80.9 (CH_2), 67.2 (C-1''), 44.0 (C-4), 40.4 (C-3), 25.9 (3-CH_3), 17.9 (C-2''), -1.3 ($SiCH_3$); HRMS (ESI) *m/z* found $[M+H]^+$ 324.1749, $C_{15}H_{26}N_3O_3Si$ requires *M*, 312.1743.

N-[1-(oxan-2'-yl)-1H-pyrazol-3-yl]acetamide (**564**)

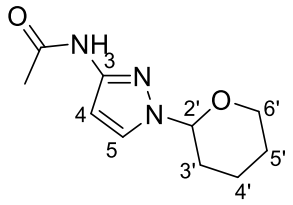

1-(oxan-2-yl)-1H-pyrazol-3-amine **418** (107 mg, 0.64 mmol, 1.00 equiv.), Et_3N (0.10 mL, 0.70 mmol, 1.10 equiv.), and Ac_2O (0.06 mL, 0.67 mmol, 1.05 equiv.) were stirred neat for 0.5 h. The reaction mixture was diluted in EtOAc (5 mL), washed with saturated $NaHCO_{3(aq)}$ (2 mL), H_2O (2 mL) and brine (2 mL). The organic layer was dried over $MgSO_4$, filtered, and evaporated. SiO_2 gel column chromatography (50 → 100% EtOAc in hexanes (1% Et_3N)) afforded the acetylated pyrazole as a colourless oil (90 mg, 0.43 mmol, 67%); ν_{max} (ATR) 3290 (NH) 2944, 1668 (C=O), 1574, 1487, 1428, 1376, 1250, 1202, 1083, 1000 cm^{-1}; δ_H (600 MHz, $CDCl_3$) 8.21 (1H, s br, NH), 7.47 (1H, d, *J* = 2.1 Hz, 5-H), 6.73 (1H, d, *J* = 2.1 Hz, 4-H), 5.20 (1H, dd, *J* = 9.7, 2.1 Hz, 2'-H) 4.03 (1H, d, *J* = 11.6 Hz, 6'-H), 3.65 (1H, td, *J* = 11.6, 2.3 Hz, 6'-H) 2.11 (3H, s, CH_3), 2.08-1.93 (3H, m, 3'-H, 4'-H), 1.67-1.64 (2H, m, 5'-H, 4'-H) 1.61-1.56 (1H, m, 5'-H); δ_C (151 MHz, $CDCl_3$) 167.8 (C=O), 147.6 (C-3), 128.9 (C-5), 98.3 (C-4), 87.4 (C-2'), 67.9 (C-6'), 30.3 (C-3'), 25.0 (C-5'), 23.9 (CH_3), 22.6 (C-4'); HRMS (ESI) *m/z* found $[M+H]^+$ 210.1245, $C_{10}H_{16}N_3O_2$ requires *M*, 210.1243

Tert-butyl N-{1-[(4'-methoxyphenyl)methyl]-1H-pyrazol-5-yl}carbamate (**565**)

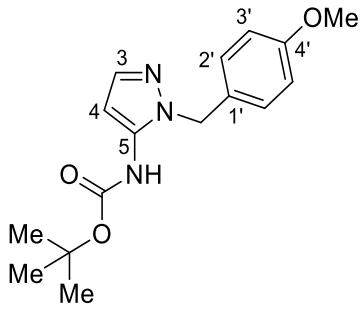

1-[(4-methoxyphenyl)methyl]-1H-pyrazol-5-amine **548** (300 mg, 1.48 mmol, 1.00 equiv.) and Boc_2O (1.61 g, 7.38 mmol, 5.00 equiv.), were stirred neat at 50 °C for 16 h. The reaction was dissolved in CH_2Cl_2 (20 mL) and washed with $NaHCO_3$ (3 x 5 mL). The aqueous layer was extracted with CH_2Cl_2 (3 x 10 mL), and the combined organic fractions were dried over $MgSO_4$, filtered and evaporated. SiO_2 gel column chromatography (0 → 100% EtOAc in hexanes) afforded the Boc pyrazole as a white solid (350 mg, 1.15 mmol, 78%); mp: 81-83 °C; ν_{max} (ATR) 3196 (NH), 2977, 1722 (C=O), 1613, 1565, 1513, 1457, 1367, 1304, 1243, 1156, 1117, 1033 cm^{-1}; δ_H (600 MHz, $CDCl_3$) 7.43 (1H, s, 3-H), 7.09 (2H, d, *J* = 8.5 Hz, 2'-H), 6.84 (2H, d, *J* = 8.5 Hz, 3'-H), 6.26 (1H, s br, NH), 6.19 (1H, s br, 4-H), 5.17 (2H, s, CH_2), 3.77 (3H, s, OCH_3), 1.46 (9H, s, CCH_3); δ_C (151 MHz, $CDCl_3$) 159.4 (4'-H), 152.6 (C=O), 138.8 (C-3), 135.9 (C-5), 128.6 (C-2'), 128.3 (C-1'), 114.4 (C-3'), 99.8 (C-4), 81.7 (CCH_3), 55.4 (OCH_3), 52.0 (CH_2), 28.3 (CCH_3); HRMS (ESI) *m/z* found $[M+H]^+$ 304.1668 $C_{16}H_{22}N_3O_3$ requires *M*, 304.1661.

3,4-Dimethyl-1-{1'-[(2'',4'',6''-trimethylphenyl)methyl]-1H-pyrazol-3'-yl}-2,5-dihydro-1H-pyrrole-2,5-dione (**566**)

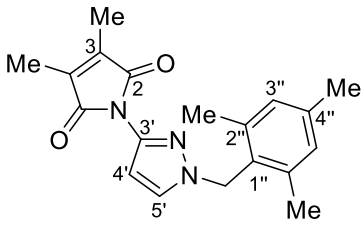

Under N_2, a suspension of 3,4-dimethyl-1-(1H-pyrazol-3-yl)-2,5-dihydro-1H-pyrrole-2,5-dione **561** (500 mg, 2.61 mmol, 1.00 equiv.) and Cs_2CO_3 (1.28 g, 3.92 mmol, 1.50 mmol) in MeCN (20 mL) was treated with 2-(chloromethyl)-1,3,5-trimethylbenzene (529 mg, 3.14 mmol, 1.20 equiv.). The reaction was refluxed for 16 h, cooled, and poured into H_2O (20 mL). The aqueous phase was extracted with EtOAc

(3 x 10 mL), and the combined organic fractions were dried over $MgSO_4$, filtered, and evaporated. SiO_2 gel column chromatography (20 → 50% EtOAc in hexanes) afforded the benzylated pyrazole as a white solid (196 mg, 0.61 mmol, 23%); mp: 164-165 °C; ν_{max} (ATR) 2923, 1728 (C=O), 1705 (C=O), 1521, 1500, 1424, 1386, 1343, 1206, 1092, 1058 cm^{-1}; δ_H (700 MHz, $CDCl_3$) 6.96 (1H, d, *J* = 2.4 Hz, 5'-H), 6.91 (2H, s, 3''-H), 6.21 (1H, d, *J* = 2.4 Hz, 4'-H) 5.34 (2H, s, CH_2), 2.29 (3H, s, 4''-CH_3), 2.28 (6H, s, 2''-CH_3), 2.03 (6H, s, 3-CH_3); δ_C (176 MHz, $CDCl_3$) 170.4 (C=O), 140.2 (C-3'), 138.7 (C-4''), 138.4 (C-1''), 137.9 (C-3), 129.5 (C-3''), 129.0 (C-5'), 128.1 (C-2''), 101.8 (C-4'), 50.6 (CH_2), 21.1 (4''-CH_3), 19.8 (2''-CH_3), 9.0 (3-CH_3); HRMS (ESI) *m/z* found $[M+H]^+$ 324.1731, $C_{19}H_{22}N_3O_2$ requires *M*, 324.1712.

3,4-Dimethyl-1-{1'-[(2'',4'',6''-trimethylphenyl)methyl]-1H-pyrazol-5'-yl}-2,5-dihydro-1H-pyrrole-2,5-dione (**567**)

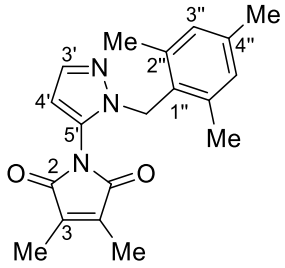

Synthesised alongside 3,4-dimethyl-1-{1-[(2,4,6-trimethylphenyl)methyl]-1H-pyrazol-3-yl}-2,5-dihydro-1H-pyrrole-2,5-dione **561** using an identical procedure for the synthesis of **564** (*vide supra*). Obtained as a white solid (229 mg, 0.71 mmol, 27%); mp: 98-99 °C; ν_{max} (ATR) 2927, 1739 (C=O), 1715 (C=O), 1563, 1481, 1463, 1388, 1343, 1295, 1084, 1037 cm^{-1}; δ_H (700 MHz, $CDCl_3$) 7.55 (1H, d, *J* = 1.9 Hz, 3'-H), 6.78 (2H, s, 3''-H), 6.19 (1H, d, *J* = 1.9 Hz, 4'-H), 5.24 (2H, s, CH_2), 2.22 (3H, s, 4''-CH_3), 2.10 (6H, s, 2''-CH_3), 1.93 (6H, s, 3-CH_3); δ_C (176 MHz, $CDCl_3$) 169.4 (C=O), 138.7 (C-3'), 138.3 (C-3), 138.0 (C-1''), 137.7 (C-4''), 129.5 (C-3''), 129.3 (C-5'), 127.9 (C-2''), 105.3 (C-4'), 49.0 (CH_2), 21.0 (4''-CH_3), 19.8 (2''-CH_3), 8.9 (3-CH_3); HRMS (ESI) *m/z* found $[M+H]^+$ 324.1731, $C_{19}H_{22}N_3O_2$ requires *M*, 324.1712.

4.2.3 Synthesis of Heterocyclic Ureas

General Procedure E for the Synthesis of Heteroaryl Ureas: To a solution of an aminoheterocycle (5.00 mmol, 1.00 equiv.) in anhydrous MeCN (15 mL) was added an isocyanate (10.0 mmol, 2.00 equiv.). After stirring the reaction for 16 h, the volatiles were removed and the resulting solid was

suspended in Et_2O (20 mL) and filtered. After washing with Et_2O (3 x 10 mL), the urea product was purified by SiO_2 gel chromatography or recrystallisation where necessary.

1-(4'-Methoxyphenyl)-3-(1''-methyl-1H-pyrazol-3''-yl)urea (**391**)

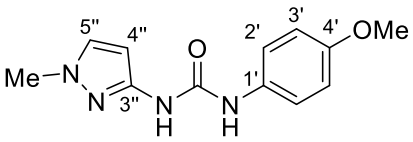

To a solution of 1-methyl-1H-pyrazol-3-amine **373** (0.40 ml, 5.00 mmol, 2.00 equiv.) in MeCN (15 mL) was added 1-isocyanato-4-methoxybenzene (0.32 mL, 2.50 mmol, 1.00 equiv.). After stirring at rt for 16 h, the volatiles were removed and purification by SiO_2 gel column chromatography (1:1 Hexanes:EtOAc) afforded the pyrazole urea as a yellow solid (425 mg, 1.75 mmol, 70%); mp: 124-125 ^oC; ν_{max} (ATR) 3333 (NH), 2984, 1674 (C=O), 1539, 1510, 1417, 1353, 1292, 1169, 1029 cm^{-1}; δ_H (600 MHz, $CDCl_3$) 9.58 (1H, s br, NH), 8.51 (1H, s br, NH) 7.42 (2H, d, *J* = 8.9 Hz, 2'-H) 7.20 (1H, d, *J* = 2.2 Hz, 5''-H), 6.86 (2H, d, *J* = 8.9 Hz, 3'-H), 5.93 (1H, s br, 4''-H), 3.80 (3H, s, 1''-CH_3), 3.79 (3H, s, OCH_3); δ_C (151 MHz, $CDCl_3$) 156.0 (C-4'), 153.8 (C=O), 148.7 (C-3''), 131.9 (C-1'), 131.1 (C-5''), 122.3 (C-2'), 114.2 (C-3'), 94.5 (C-4''), 55.6 (OCH_3), 38.9 (1''-CH_3); HRMS (ASAP) *m/z* found $[M+H]^+$ 247.1183 $C_{12}H_{15}N_4O_2$ requires *M*, 247.1195.

1-(4'-Methoxyphenyl)-3-methyl-3-(1''-methyl-1H-pyrrol-3''-yl)urea (**395**)

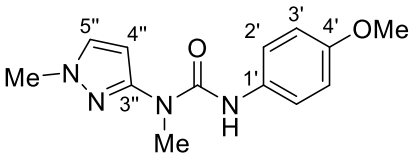

At 0 ^oC under N_2, a solution of lithium bis(trimethylsilyl)amide in THF (6 mL, 6.0 mmol, 1.2 equiv.) was added dropwise at 0 ^oC to a solution of 1-(4-methoxyphenyl)-3-(1-methyl-1H-pyrazol-3-yl)urea **391** (1.23 g, 5.00 mmol, 1.00 equiv.) in anhydrous THF (15 mL). The ice bath was removed and the resulting mixture was stirred at rt for 30 min before the addition of methyl iodide (0.65 mL, 5.00 mmol, 1.00 equiv.). The resulting solution was stirred for 30 min, quenched with NH_4Cl (10 mL) and approximately one third of the volatiles were removed. EtOAc (35 mL) and H_2O (25 mL) were added and the solution

was extracted with EtOAc (3 x 20 mL). The combined organic fractions were dried over $MgSO_4$, filtered and evaporated. SiO_2 gel column chromatography (50 → 60% EtOAc in hexanes) afforded the methylated urea as a white solid; (600 mg, 2.30 mmol, 46%); mp = 99 - 100 °C; ν_{max} (ATR) 3254 (NH), 2950, 1658 (C=O), 1510, 1498, 1412, 1348, 1243, 1148, 1030 cm^{-1}; δ_H (700 MHz, $CDCl_3$) 10.50 (1H, br s, NH); 7.43 (2H, d, *J* = 8.5 Hz, 2'-H), 7.29 (1H, s br, 5''-H), 6.85 (2H, d, *J* = 8.5 Hz, 3'-H) 5.88 (1H, s br, 4''-H), 3.85 (3H, s, 1''-CH_3), 3.78 (3H, s, OCH_3) 3.34 (3H, s, 3-CH_3); δ_C (176 MHz, $CDCl_3$) 155.7 (C-4'), 153.5 (C=O), 152.5 (C-3''), 132.7 (C-1'), 131.1 (C-5''), 122.0 (C-4''), 114.1 (C-3'), 95.0 (C-4''), 55.6 (O CH_3), 39.2 (1''-CH_3), 33.3 (3-CH_3); HRMS (ASAP) *m/z* found $[M+H]^+$ 261.1351, $C_{13}H_{17}N_4O_2$ requires *M*, 261.1352.

1-(4'-Methoxyphenyl)-1,3-dimethyl-3-(1''-methyl-1H-pyrrol-3''-yl)urea (**396**)

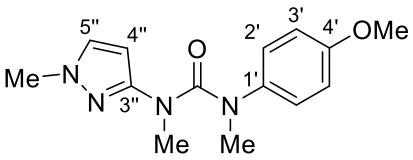

At 0 °C under N_2, a solution of lithium bis(trimethylsilyl)amide in THF (4.80 mL, 4.80 mmol, 2.40 equiv.) was added dropwise to a solution of 1-(4-methoxyphenyl)-3-(1-methyl-1H-pyrazol-3-yl)urea **391** (492 mg, 4.80 mmol, 1.00 equiv.) in THF (3.5 mL). The ice bath was removed and the resulting mixture was stirred at rt for 30 min before the addition of methyl iodide (1.25 mL, 20.0 mmol, 10.0 equiv.). The resulting solution was stirred for 30 min, quenched with NH_4Cl (10 mL) and approximately one third of the volatiles were removed. EtOAc (35 mL) and H_2O (25 mL) were added and the solution was extracted with EtOAc (3 x 20 mL). The combined organic fractions were dried over $MgSO_4$, filtered and evaporated. SiO_2 gel column chromatography (EtOAc) afforded the bismethylated urea as a yellow oil (359 mg, 3.12 mmol, 65%); ν_{max} (ATR) 2930, 1652 (C=O), 1510, 1412, 1358, 1148, 1243, 1028 cm^{-1}; δ_H (700 MHz, $CDCl_3$) 7.00 (1H, s br, 5''-H), 6.88 (2H, d, *J* = 8.9 Hz, Ph H), 6.70 (2H, d, *J* = 8.9 Hz, Ph H), 5.91 (1H, s br, 4''-H), 3.72 (3H, s, OCH_3), 3.64 (3H, s, 1''-CH_3), 3.18 (3H, s, 1-CH_3), 3.05 (3H, s, 3-CH_3); δ_C (176 MHz, $CDCl_3$) 160.4 (C=O), 157.0 (C-4'), 152.5 (C-3''), 138.8 (C-1'), 130.4 (C-5'') 126.7 (Ar CH), 114.1 (Ar CH), 99.8 (C-4''), 55.5 (OCH_3), 40.0 (1-CH_3), 38.9 (1''-CH_3), 37.8 (3-CH_3); HRMS (ASAP) *m/z* found $[M+H]^+$ 275.1510, $C_{14}H_{19}N_4O_2$ requires *M*, 275.1508 m/z.

1-(4'-methoxyphenyl)-1-methyl-3-(1''-methyl-1H-pyrazol-3''-yl)urea (**398**)

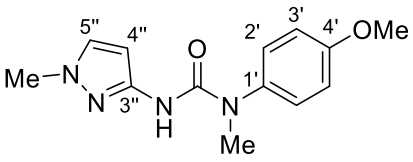

To a solution of 4-methoxy-N-methylaniline **397** (685 mg, 5.00 mmol, 1.00 equiv.) and Et_3N (2.10 mL, 15.0 mmol, 3.00 equiv.) in THF (65 mL) under N_2 was added triphosgene (743 mg, 2.5 mmol, 0.5 equiv.) in one portion. After allowing the mixture to stir for 30 min at rt, 1-methyl-1H-pyrazol-3-amine **373** (0.21 mL, 2.40 mmol, 3.00 equiv.) was added. The resulting solution was stirred at reflux for 16 h before cooling and addition of NH_4Cl (100 mL). EtOAc (100 mL) was added and the aqueous layer was extracted with EtOAc (3 x 50 mL). The organics were dried over $MgSO_4$, filtered, and evaporated. SiO_2 gel column chromatography (step gradient, 30 → 45%, 90 → 100% EtOAc in hexanes) afforded the methylated urea as a white solid (416 mg, 1.32 mmol, 32%); mp = 117-120 °C; ν_{max} (ATR) 3236 (NH), 2940, 1658 (C=O), 1549, 1498, 1352, 1246, 1149, 1029 cm^{-1}; δ_H (700 MHz, $CDCl_3$) 7.20 (2H, d, *J* = 8.4 Hz, 2'-H), 7.16 (1H, s br, 5''-H), 6.93 (2H, d, *J* = 8.4 Hz, 3'-H), 6.73 (1H, s br, NH), 6.56 (1H, s br, 4''-H), 3.81 (3H, s, OCH_3), 3.68 (3H, s, 1''-CH_3), 3.27 (3H, s, 1-CH_3); δ_C (176 MHz, $CDCl_3$) 159.3 (C-4'), 154.3 (C=O), 148.3 (C-3''), 135.1 (C-1'), 131.0 (C-5''), 129.0 (C-2'), 115.7 (C-3'), 96.1 (C-4''), 55.7 (OCH_3), 38.6, (1''-CH_3), 37.5 (1-CH_3); HRMS (ASAP) *m/z* found $[M+H]^+$ 261.1332, $C_{13}H_{16}N_4O_2$ requires *M*, 261.1327; Anal. Calc. for $C_{13}H_{16}N_4O_2$: C 59.99, H 6.20, N 21.52, found C 59.42, H 6.19, N 21.51.

3-{1'-[(3'',5''-dimethylphenyl)methyl]-1H-pyrazol-3'-yl}-1-(4'''-methoxyphenyl)urea (**401**)

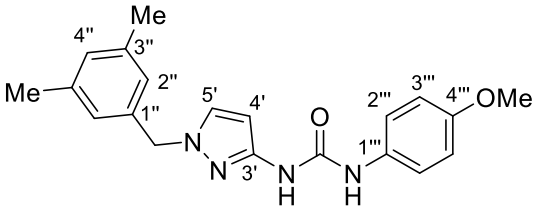

Synthesised according to General Procedure E from 1-[(3,5-dimethylphenyl)methyl]-1H-pyrazol-3-amine **403** (254 mg, 1.26 mmol, 1.00 equiv.) and 1-isocyanato-4-methoxybenzene (0.33 mL, 2.52 mmol, 2.00 equiv.). Obtained as a white solid (395 mg, 1.13 mmol, 89%); mp = 173 °C; ν_{max} (ATR) 3340 (NH), 2964, 1653 (C=O), 1468, 1377, 1305, 1161, 1128 cm^{-1}; δ_H (700 MHz, $CDCl_3$) 7.34 (2H, d, *J* = 8.7 Hz, 2'''-H), 7.26 (1H, s br, 5'-H), 6.97 (1H, s, 4''-H), 6.87 (2H, s, 2''-H), 6.85 (2H, d, *J* = 8.7 Hz, 3'''-H) , 5.88 (1H, s br, 4'-H), 5.11 (2H, s, CH_2), 3.79 (3H, s, OCH_3), 2.30 (6H, s, 3''-CH_3); δ_C (176 MHz, $CDCl_3$)

156.1 (C-4’’’), 153.1 (C=O), 148.5 (C-3’), 138.7 (C-3’’), 135.8 (C-1’’), 130.7 (C-5’), 130.1 (C-4’’), 125.9 (C-2’’), 122.3 (C-2’’’), 114.3 (C-3’’’), 94.6 (C-4’), 56.1 (CH_2), 55.7 (OCH_3), 21.4 (3’’-CH_3); HRMS (ESI) *m/z* found $[M+H]^+$ 351.1839, $C_{20}H_{23}N_4O_2$ requires *M*, 351.1821 m/z.

1-(4’-methoxyphenyl)-3’’-[1-(oxan-2’’’-yl)-1H-pyrazol-3’’-yl]urea (**420**)

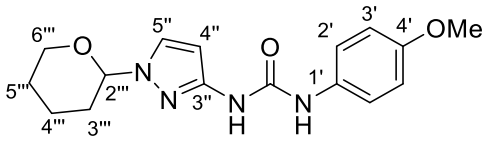

Synthesised according to General Procedure E from 1-(oxan-2-yl)-1H-pyrazol-3-amine **418** (334 mg, 2.00 mmol, 1.00 equiv.) and 1-isocyanato-4-methoxybenzene (0.52 mL, 4.00 mmol, 2.00 equiv.). Obtained as a white solid (275 mg, 0.87 mmol, 44%); mp = 161-162 ^oC; ν_{max} (ATR) 3373 (NH), 2954, 1691 (C=O), 1584, 1554, 1415, 1244, 1198, 1062 cm^{-1}; δ_H (700 MHz, DMSO) 8.92 (1H, s br, NH), 8.84 (1H, s br, NH), 7.72 (1H, d, *J* = 2.5 Hz, 5’’-H), 7.35 (2H, d, *J* = 9.1 Hz, 2’-H), 6.87 (2H, d, *J* = 9.1 Hz, 3’-H), 6.27 (1H, s, 4’’-H), 5.26, (1H, dd, *J* = 10.0, 2.4 Hz, 2’’’-H) 3.91-3.90 (1H, m, 6’’’-H), 3.71 (3H, s, OCH_3) 3.61-3.58 (1H, m, 6’’’-H), 2.07-2.02 (1H, m, 3’’’-H) 1.94-1.92 (1H, m, 4’’’-H), 1.89-1.87 (1H, m, 3’’’-H), 1.66-1.62 (1H, m, 4’’’-H), 1.53-1.50 (2H, m, 5’’’-H); δ_C (176 MHz, DMSO) 154.5 (C-4’), 152.1 (C=O), 147.9 (C-3’’), 132.5 (C-1’), 129.7 (C-5’’), 120.0 (C-2’), 114.0 (C-3’), 95.8 (C-4’’), 86.3 (C-2’’’), 66.7 (C-6’’’), 55.2 (OCH_3), 29.5 (C-3’’’), 24.6 (C-5’’’), 22.1 (C-4’’’); HRMS (ESI) *m/z* found $[M+H]^+$ 317.1621, $C_{16}H_{21}N_4O_3$ requires *M*, 317.1614.

3-(6’-Chloropyridin-2’-yl)-1-phenylurea (**429a**)

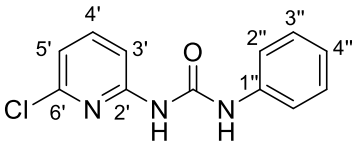

Synthesised according to General Procedure E from 6-chloropyridin-2-amine **424c** (643 mg, 5.00 mmol, 1.00 equiv.) and isocyanatobenzene (1.09 mL, 10.0 mmol, 2.00 equiv.). Obtained as a white solid and used without further purification (805 mg, 3.25 mmol, 65%); mp: 193-194 ^oC; ν_{max} (ATR) 3371 (NH), 2964, 1687 (C=O), 1561, 1498, 1450, 1394, 1304, 1253, 1162, 1022 cm^{-1}; δ_H (600 MHz, DMSO) 9.54 (1H, s br, NH), 9.33 (1H, s br, NH), 7.79 (1H, t, *J* = 7.5 Hz, 4’-H), 7.76 (1H, d, *J* = 7.8 Hz, 3’-H), 7.46 (2H, d, *J* = 7.8 Hz, 2’’-H), 7.31 (2H, t, *J* = 7.8 Hz, 3’’-H) 7.10 (1H, d, *J* = 7.5 Hz, 5’-H), 7.02 (1H, t, *J* =

7.5 Hz, 4''-H); δ_C (151 MHz, DMSO) 152.8 (C-2'), 151.6 (C=O), 147.5 (C-6'), 141.6 (C-4'), 138.8 (C-1''), 128.9 (C-3''), 122.6 (C-4''), 118.6 (C-2''), 117.2 (C-5'), 110.3 (C-3'); HRMS (ASAP) *m/z* found $[M+H]^+$ 248.0589 $C_{12}H_{11}{}^{35}ClN_3O$ requires *M*, 248.0591.

3-(6'-Methylpyridin-2'-yl)-1-phenylurea (**429b**)

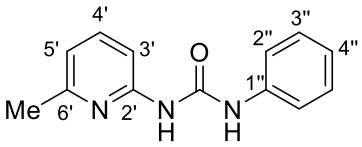

Synthesised according to General Procedure E from 6-methylpyridin-2-amine **424e** (541 mg, 5.00 mmol, 1.00 equiv.) and isocyanatobenzene (1.09 mL, 10.0 mmol, 2.00 equiv.). Obtained as a white solid and used without further purification (1.05 g, 4.65 mmol, 93%); mp: 183-184 °C; ν_{max} (ATR) 3373 (NH), 2984, 1687 (C=O), 1592, 1562, 1445, 1315, 1273, 1159 cm^{-1}; δ_H (700 MHz, DMSO) 10.89 (1H, s br, NH), 9.47 (1H, s br, NH), 7.63 (1H, t, *J* = 8.0 Hz, 4'-H), 7.52 (2H, d, *J* = 7.6 Hz, 2''-H), 7.31 (2H, t, *J* = 7.6 Hz, 3''-H), 7.20 (1H, d, *J* = 8.0 Hz, 3'-H), 7.02 (1H, t, *J* = 7.6 Hz, 4''-H), 6.87 (1H, d, *J* = 8.0 Hz, 5'-H), 2.45 (3H, s, CH_3); δ_C (176 MHz, DMSO) 155.3 (C-6'), 152.3 (C-2'), 152.2 (C=O), 139.1 (C-1''), 138.9 (C-4'), 128.9 (C-3''), 122.4 (C-4''), 118.6 (C-2''), 116.5 (C-5'), 108.7 (C-3') 23.6 (CH_3); HRMS (ASAP) *m/z* found $[M+H]^+$ 228.1140 $C_{13}H_{14}N_3O$ requires *M*, 228.1137.

3-(6-Ethylpyridin-2-yl)-1-phenylurea (**429c**)

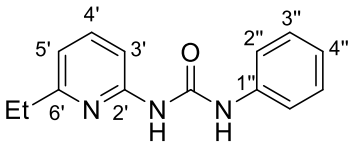

Synthesised according to General Procedure E from 6-ethylpyridin-2-amine **424f** (610 mg, 5.00 mmol, 1.00 equiv.) and isocyanatobenzene (1.09 mL, 10.0 mmol, 2.00 equiv.). Recrystallisation from EtOAc afforded the urea as a white crystalline solid (1.16 g, 4.80 mmol, 96%); mp: 179-181 °C; ν_{max} (ATR) 3373 (NH), 2977, 1686 (C=O), 1594, 1559, 1499, 1446, 1316, 1275, 1179, 1162, 1030 cm^{-1}; δ_H (600 MHz, DMSO) 11.00 (1H, s br, NH), 9.50 (1H, s br, NH), 7.65 (1H, t, *J* = 8.0 Hz, 4'-H), 7.51 (2H, d, *J* = 7.8 Hz, 2''-H), 7.32 (2H, t, *J* = 7.8 Hz, 3''-H) 7.18 (1H, d, *J* = 8.0 Hz, 3'-H), 7.02 (1H, t, *J* = 7.8 Hz, 4''-H), 6.89 (1H, d, *J* = 8.0 Hz, 5'-H) 2.75 (2H, q, *J* = 7.6 Hz, CH_2), 1.27 (3H, t, *J* = 7.6 Hz, CH_3); δ_C (151 MHz, DMSO) 160.1 (C-6'), 152.4 (C-2'), 152.2 (C=O), 139.0 (C-1''), 139.0 (C-4'), 128.9 (C-3''), 122.5

(C-4''), 118.7 (C-2''), 115.3 (C-5'), 109.0 (C-3'), 30.1 (CH_2), 13.5 (CH_3); *m/z* (ASAP) $[M+H]^+$ 242.1; CHN calculated for $C_{14}H_{15}N_3O$: C 69.49%, H 6.27%, N 17.43%, found: 69.69%, H 6.27%, N 17.41%;

1-(4'-Methoxyphenyl)-3-(6''-methylpyridin-2''-yl)urea (**429d**)

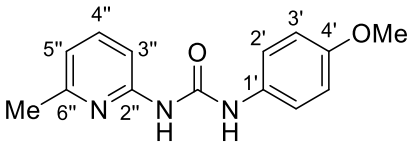

Synthesised according to General Procedure E from 6-methylpyridin-2-amine **425e** (541 mg, 5.00 mmol, 1.00 equiv.) and 1-isocyanato-4-methoxybenzene (1.30 mL, 10.0 mmol, 2.00 equiv.). Obtained as a white solid and used without further purification (1.28 g, 4.95 mmol, 99%); mp: 189-190 °C; ν_{max} (ATR) 3359 (NH), 2981, 2843, 1685 (C=O), 1588, 1505, 1456, 1297, 1225, 1108, 1035 cm^{-1}; δ_H (600 MHz, DMSO) 10.73 (1H, s br, NH), 9.39 (1H, s br, NH), 7.61 (1H, t, *J* = 8.0 Hz, 4''-H), 7.42 (2H, d, *J* = 8.0 Hz, 2'-H), 7.16 (1H, d, *J* = 9.0 Hz, 3''-H), 6.90 (2H, d, *J* = 9.0 Hz, 3'-H), 6.85 (1H, d, *J* = 9.0 Hz, 5''-H), 3.72 (3H, s, CH_3O), 2.44 (3H, s, 6''-CH_3); δ_C (151 MHz, DMSO) 155.2 (C-6''), 154.8 (C-4'), 152.5 (C-2''), 152.3 (C=O), 138.8 (C-4''), 132.1 (C-1'), 120.3 (C-2'), 116.3 (C-5''), 114.1 (C-3'), 108.6 (C-3''), 55.2 (OCH_3), 23.6 (6''-CH_3); HRMS (ASAP) *m/z* found $[M+H]^+$ 258.1250, $C_{14}H_{16}N_3O_2$ requires *M*, 258.1243; CHN calculated for $C_{14}H_{15}N_3O_2$: C 65.35%, H 5.88%, N 16.33%, found: 65.06%, H 5.78%, N 16.27%.

1-(4'-Methoxyphenyl)-3-(5''-methylpyridin-2''-yl)urea (**429e**)

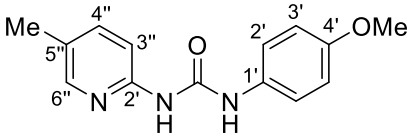

To a solution of 5-methylpyridin-2-amine **427a** (1.08 g, 10.0 mmol, 2.00 equiv.) in MeCN (20 mL) was added 1-isocyanato-4-methoxybenzene (0.65 mL, 5.00 mmol, 1.00 equiv.). After stirring at rt for 16 h, the volatiles were removed before filtration in Et_2O (3 x 10 mL). The pyridyl urea was obtained as a white solid and used without further purification (1.17 g, 4.55 mmol, 91%); mp: 153-154 °C; ν_{max} (ATR) 3360 (NH), 2987, 1683 (C=O), 1593, 1559, 1491, 1375, 1316, 1299, 1234, 1170, 1026 cm^{-1}; δ_H (600 MHz, DMSO) 10.32 (1H, s br, NH), 9.25 (1H, s br, NH), 8.09 (1H, s, 6''-H), 7.56 (1H, d, *J* = 8.3 Hz, 4''-H) 7.41 (2H, d, *J* = 8.0 Hz, 2'-H), 7.36 (1H, d, *J* = 8.3 Hz, 3''-H), 6.88 (2H, d, *J* = 8.0 Hz, 3'-H), 3.72 (3H,

s, OCH_3), 2.22 (3H, s, 5''-CH_3); δ_C (151 MHz, DMSO) 154.8 (C-4'), 152.3 (C=O), 150.9 (C-2''), 146.3 (C-6''), 139.1 (C-4''), 132.1 (C-1'), 126.0 (C-5''), 120.5 (C-2'), 114.0 (C-3'), 111.4 (C-3''), 55.2 (OCH_3), 17.1 (5''-CH_3); HRMS (ASAP) *m/z* found $[M+H]^+$ 258.1226, $C_{14}H_{16}N_3O_2$ requires *M*, 258.1243; CHN calculated for $C_{14}H_{15}N_3O_2$: C 65.35%, H 5.88%, N 16.33%, found: 65.23%, H 5.86%, N 16.24%.

3-(5',6'-Dimethylpyridin-2'-yl)-1-(4''-methoxyphenyl)urea (**429f**)

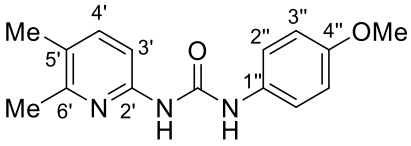

To a solution of 5,6-dimethylpyridin-2-amine **427d** (793 mg, 6.50 mmol, 2.00 equiv.) in MeCN (10 mL) was added 1-isocyanato-4-methoxybenzene (0.42 mL, 3.25 mmol, 1.00 equiv.). After stirring at rt for 16 h, the volatiles were removed before filtration in Et_2O (3 x 10 mL). The pyridyl urea was obtained as a white solid and used without further purification (1.10 g, 4.06 mmol, 81%); mp: 194-195 °C; ν_{max} (ATR) 3357 (NH), 2987, 1680 (C=O), 1598, 1566, 1512, 1466, 1397, 1323, 1228, 1159 cm^{-1}; δ_H (700 MHz, DMSO) 10.76 (1H, s br, NH), 9.28 (1H, s br, NH), 7.44 (1H, d, *J* = 8.3 Hz, 4'-H), 7.42 (2H, d, *J* = 9.0 Hz, 2''-H), 7.10 (1H, d, *J* = 8.3 Hz, 3'-H), 6.89 (2H, d, *J* = 9.0 Hz, 3''-H), 3.72 (3H, s, OCH_3), 2.39 (3H, s, 5'-CH_3), 2.16 (3H, s, 6'-CH_3); δ_C (176 MHz, DMSO) 154.7 (C-4''), 153.2 (C-6'), 152.4 (C=O), 150.4 (C-2'), 139.7 (C-4'), 132.3 (C-1''), 123.9 (C-5'), 120.2 (C-2''), 114.1 (C-3''), 108.9 (C-3'), 55.2 (OCH_3), 21.9 (6'-CH_3), 17.6 (5'-CH_3); *m/z* (ASAP) $[M+H]^+$ 272.1; CHN calculated for $C_{15}H_{17}N_3O_2$: C 66.40%, H 6.32%, N 15.49%, found: 66.51%, H 6.38%, N 15.55%.

3-(1',2'-Oxazol-3'-yl)-1-phenylurea (**433a**)

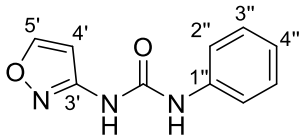

Synthesised according to General Procedure E from 1,2-oxazol-3-amine **432a** (0.38 mL, 5.00 mmol, 1.00 equiv.) and isocyanatobenzene (1.09 mL, 10.0 mmol, 2.00 equiv.). Obtained as a white solid and used without further purification (1.01 g, 4.95 mmol, 99%); mp: 187-189 °C; ν_{max} (ATR) 3279 (NH), 1673 (C=O), 1599, 1565, 1534, 1495, 1444, 1315, 1283, 1230, 1131, 1027 cm^{-1}; δ_H (600 MHz, DMSO) 9.57 (1H, s br, NH), 8.81 (1H, s br, NH), 8.74 (1H, d, *J* = 1.6 Hz, 5'-H), 7.45 (2H, d, *J* = 7.4 Hz, 2''-H), 7.30

(2H, t, *J* = 7.4 Hz, 3''-H), 7.02 (1H, t, *J* = 7.4 Hz, 4''-H), 6.84 (1H, d, *J* = 1.6 Hz, 4'-H); δ_C (151 MHz, DMSO) 159.8 (C-5') 158.1 (C-3'), 151.3 (C=O), 138.8 (C-1''), 128.9 (C-3''), 122.6 (C-4''), 118.5 (C-2''), 98.3 (C-4'); HRMS (ASAP) *m/z* found $[M+H]^+$ 204.0770, $C_{10}H_{10}N_3O_2$ requires *M*, 204.0773; CHN calculated for $C_{10}H_9N_3O_2$: C 59.11%, H 4.46%, N 20.68%, found: C 59.06%, H 4.47%, N 20.86%.

1-(4'-Methoxyphenyl)-3-(1'',2''-oxazol-3''-yl)urea (**433b**)

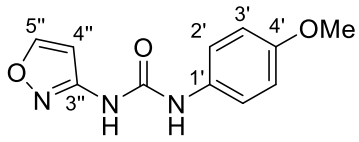

Synthesised according to General Procedure E from 1,2-oxazol-3-amine **432** (0.38 mL, 5.00 mmol, 1.00 equiv.) and 1-isocyanato-4-methoxybenzene (1.30 mL, 10.0 mmol, 2.00 equiv.). Obtained as a white solid following an additional filtration with MeOH (10 mL) (1.26 g, 4.75 mmol, 95%); mp: 198-199 ^oC; ν_{max} (ATR) 3398 (NH), 1675 (C=O), 1607, 1560, 1508, 1233, 1026 cm^{-1}; δ_H (700 MHz, DMSO) 9.50 (1H, s br, NH), 8.72 (1H, d, *J* = 1.6 Hz, 5''-H), 8.64 (1H, s br, NH), 7.35 (2H, d, *J* = 9.0 Hz, 2'-H), 6.88 (2H, d, *J* = 9.0 Hz, 3'-H), 6.82 (1H, d, *J* = 1.6 Hz, 4''-H), 3.72 (3H, s, CH_3); δ_C (176 MHz, DMSO) 159.7 (C-5''), 158.2 (C-3''), 155.0 (C-4'), 151.5 (C=O), 131.8 (C-1'), 120.5 (C-2'), 114.0 (C-3'), 98.3 (C-4''), 55.2 (CH_3); HRMS (ASAP) *m/z* found $[M+H]^+$ 234.0879, $C_{11}H_{12}N_3O_3$ requires *M*, 234.0879.

3-(1'-Methyl-1H-indazol-3'-yl)-1-phenylurea (**433c**)

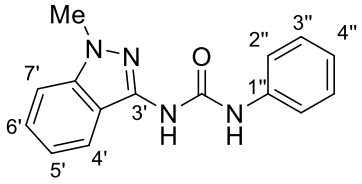

Synthesised according to General Procedure E from 1-methyl-1H-indazol-3-amine **432b** (735 mg, 5 mmol, 1 equiv.) and isocyanatobenzene (1.09 mL, 10.0 mmol, 2.00 equiv.). Obtained as a white solid and used without further purification (1.26 g, 4.75 mmol, 95%); mp: 219-220 ^oC; ν_{max} (ATR) 3340 (NH), 2979, 1664 (C=O), 1598, 1495, 1449, 1343, 1326, 1235, 1159 cm^{-1}; δ_H (700 MHz, DMSO) 9.80 (1H, s br, NH), 9.56 (1H, s br, NH), 8.00 (1H, d, *J* = 8.0 Hz, 4'-H), 7.56 (2H, d, *J* = 7.5 Hz, 2''-H), 7.53 (1H, d, *J* = 8.0 Hz, 7'-H), 7.41 (1H, t, *J* = 8.0 Hz, 6'-H), 7.32 (2H, t, *J* = 7.5 Hz, 3''-H), 7.08 (1H, t, *J* = 8.0 Hz, 5'-H), 7.02 (1H, t, *J* = 7.5 Hz, 4''-H), 3.97 (3H, s, CH_3); δ_C (176 MHz, DMSO) 152.3 (C=O), 140.5 (1'-*C*-

7'), 140.3 (C-3'), 139.3 (C-1''), 128.8 (C-3''), 127.1 (C-6'), 122.4 (C-4''), 121.4 (C-4'), 119.3 (C-5'), 118.8 (C-2''), 114.8 (3'-*C*-4'), 109.3 (C-7'), 35.0 (CH_3); HRMS (ASAP) *m/z* found $[M]^+$ 266.1251, $C_{15}H_{14}N_4O$ requires *M*, 266.1246.

4.2.4 Borylation of Aminopyridyl Derivatives

General Procedure A – C-H Borylation of Pyridyl Derivatives: An oven-dried Schlenk tube was charged with $[Ir(cod)(OMe)]_2$ (10 mg, 1.5 mol%), dtbpy (8 mg, 3.0 mol%), and B_2pin_2 (381 mg, 1.50 mmol, 1.50 equiv.), sealed and subject to three N_2 purge/refill cycles. Anhydrous, Ar degassed mtbe was added (molarity *vide infra*), and the dark active catalyst solution was transferred to a sealed vial containing the pyridyl substrate (1.00 equiv.). The reaction mixture was stirred at for the allotted time at the allotted temperature, followed by complete removal of the volatiles and subsequent purification.

4-(4',4',5',5'-Tetramethyl-1',3',2'-dioxaborolan-2'-yl)-6-(trifluoromethyl)pyridin-2-amine (**425a**)[14]

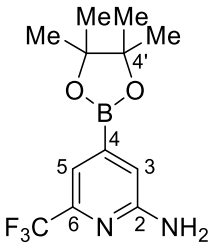

Synthesised according to General Procedure A from 2-amino-6-trifluoromethylpyridine **424a** (162 mg, 1.00 mmol, 1.0 M, 1.00 equiv.). After 16 h at rt, the reaction was cooled and diluted with EtOAc (10 mL) before filtration over SiO_2. Removal of the volatiles followed by recrystallisation from $MeOH/H_2O$ afforded the borylated pyridine as an off-white solid (207 mg, 0.72 mmol, 72%); ν_{max} (ATR) 3333, 3218, 1639, 1438, 1316, 1275, 1191, 1139 cm^{-1}; δ_H (700 MHz; $CDCl_3$) 7.33 (1H, s, 5-H), 7.03 (1H, s, 3-H), 4.70 (2H, s br, NH_2), 1.34 (12H, s, CH_3); δ_C (176 MHz, $CDCl_3$) 158.1 (C-2), 146.0 (q, *J* = 34 Hz, C-6), 121.9 (q, *J* = 277 Hz, CF_3), 117.9 (C-3), 114.7 (q, *J* = 3.1 Hz, C-5), 84.9 (C-4'), 25.0 (CH_3); δ_F (376 MHz, $CDCl_3$) -68.3; δ_B (128 MHz, $CDCl_3$) 30.0; HRMS (ASAP) m/z found $[M+H]^+$ 288.1390, $C_{12}H_{16}BF_3N_2O_2$ requires 288.1372. Data for **430a** was consistent with a previous report.

6-Fluoro-4-(4,4,5,5-tetramethyl-1,3,2-dioxaborolan-2-yl)pyridin-2-amine (**425b**)

6-Fluoro-5-(4,4,5,5-tetramethyl-1,3,2-dioxaborolan-2-yl)pyridin-2-amine (**425c**)[15]

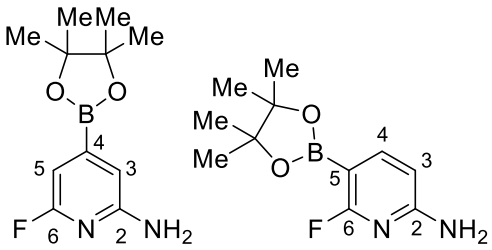

Synthesised as a 6:5 ratio **425b:425c** mixture of regioisomers according to General Procedure A from 2-amino-6-fluoropyridine **424b** (112 mg, 1.00 mmol, 1.0 M, 1.00 equiv.). After 22 h at rt, the reaction was cooled and diluted with EtOAc (10 mL) before filtration over SiO_2. Removal of the volatiles followed by recrystallisation from MeOH/H_2O afforded the two borylated pyridines as an off-white solid (160 mg, 0.67 mmol, 67%); ν_{max} (ATR) 3325, 3185, 2980, 1627, 1545, 1436, 1384, 1358, 1212, 1143 cm^{-1}; δ_H **425b** (700 MHz, $CDCl_3$) 6.69 (1H, d, *J* = 2.6 Hz, 5-H), 6.55 (1H, d, *J* = 2.6 Hz, 3-H), 4.75 (2H, s br, NH_2), 1.33 (12H, s, CH_3); δ_H **425c** (700 MHz, $CDCl_3$) 7.86 (1H, t, *J* = 7.9 Hz, 4'-H), 6.30, (1H, dd, *J* = 7.9, 2.7 Hz, 3'-H), 4.49 (2H, s br, NH_2), 1.33 (12H, s, CH_3); δ_C **425b** (128 MHz, $CDCl_3$) 163.3 (d, *J* = 239 Hz, C-6), 157.5 (d, *J* = 16 Hz, C-2), 110.3 (d, *J* = 4 Hz, C-5), 101.8 (d, *J* = 34 Hz, C-3), 84.7 (OC), 24.9 (CH_3); δ_C **430c** (128 MHz, $CDCl_3$) 167.6 (d, *J* = 243 Hz C-6'), 160.1 (d, *J* = 17 Hz, C-2'), 104.4 (d, *J* = 4 Hz, C-3'), 149.3 (d, *J* = 9.0 Hz, C-4'), 83.8 (OC), 25.0 (CH_3); δ_F **425b** (376 MHz, $CDCl_3$) -71.88; δ_F **425c** (376 MHz, $CDCl_3$) -59.09; HRMS (ASAP) m/z found $[M+H]^+$ 238.1380, $C_{11}H_{16}BFN_2O$ requires 2238.1403; Data for **425c** was consistent with a previous report.

6-Chloro-4-(4,4,5,5-tetramethyl-1,3,2-dioxaborolan-2-yl)pyridin-2-amine (**425d**)[14]

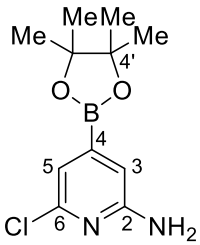

Synthesised according to General Procedure A from 2-amino-6-chloropyridine **424c** (129 mg, 1.00 mmol, 1.0 M, 1.00 equiv.). After 1 h at 80 °C, the reaction was cooled and diluted with EtOAc (10 mL) before filtration over SiO_2. Removal of the volatiles followed by recrystallisation from MeOH/H_2O

afforded the borylated pyridine as an off-white solid (133 mg, 0.52 mmol, 52%); ν_{max} (ATR) 3335, 3193, 2980, 1630, 1536, 1435, 1350, 1142 cm^{-1}; δ_H (700 MHz, $CDCl_3$) 6.99 (1H, s, 5-H), 6.75 (1H, s, 3-H), 4.50 (2H, s br, NH_2), 1.33 (12H, s, CH_3); δ_C (176 MHz, $CDCl_3$) 158.2 (C-2), 149.5 (C-6), 118.0 (C-3), 112.2 (C-5), 84.8 (C-4'), 25.0 (CH_3); δ_B (128 MHz, $CDCl_3$) 29.9; HRMS (ASAP) m/z found $[M+H]^+$ 254.1111, $C_{11}H_{16}BClN_2O_2$ requires 254.1108. Data for this compound was consistent with reported literature.

1-(4'-Methoxyphenyl)-3-[6-methyl-4-(4,4,5,5-tetramethyl-1,3,2-dioxaborolan-2-yl)pyridin-2-yl]urea (**430c**)

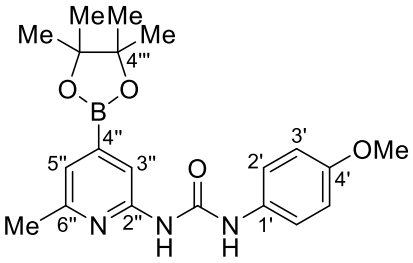

Synthesised according to General Procedure A from 1-(4-methoxyphenyl)-3-(6-methylpyridin-2-yl)urea **429e** (257 mg, 1.00 mmol, 0.2 M, 1.00 equiv.). After 2 h at 80 °C, the reaction was cooled and the volatiles were removed. Recrystallisation from EtOAc afforded the borylated urea as an oily white solid (30 mg, 0.08 mmol, 8%); δ_H (600 MHz, DMSO) 10.53 (1H, s br, NH), 9.36 (1H s br, NH), 7.51 (1H, s, 3''-H), 7.42 (2H, d, *J* = 9.2 Hz, 2'-H), 7.04 (1H, s, H-5''), 6.89 (2H, d, *J* = 9.2 Hz, 3'-H), 3.73 (3H, s, OCH_3), 2.45 (3H, s, 6''-CH_3), 1.31 (12H, s, 4'''-CH_3); δ_C (151 MHz, DMSO) 154.9 (C-6'') 154.8 (C-4'), 152.2 (C-2''), 152.2 (C=O), 139.3 (C-4''), 132.1 (C-1'), 120.8 (C-5''), 120.3 (C-2'), 114.1 (C-3'), 113.7 (C-3''), 84.3 (C-4'''), 55.2 (OCH_3), 24.6 (4'''-CH_3), 23.4 (6''-CH_3); HRMS (ASAP) m/z found $[M+H]^+$ 383.2103, $C_{20}H_{26}BN_3O$ requires 383.2131.

4.2.5 Protecting Group Switch of Aminopyrazole Derivatives

General Procedure F for the Alkylation Switch of Aminopyrazoles: To a solution of Me_3OBF_4 (1.00 equiv.) suspended in CH_2Cl_2 (0.6 M) was added a pyrazole (1.00 equiv) in CH_2Cl_2 (0.6M). After refluxing for the allotted time, the volatiles were removed and the resulting solid was chromatographically purified.

3,4-dimethyl-1-[1'-methyl-3'-(4''-methylphenyl)-1H-pyrazol-5'-yl]-2,5-dihydro-1H-pyrrole-2,5-dione (**480**)

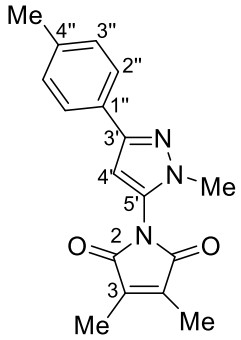

Synthesised from 3,4-dimethyl-1-[5-(4-methylphenyl)-1-{[2-(trimethylsilyl)ethoxy]methyl}-1H-pyrazol-3-yl]-2,5-dihydro-1H-pyrrole-2,5-dione **479** (70 mg, 0.17 mmol, 1.00 equiv.) according to General Procedure F. After 5 h, the volatiles were removed and SiO_2 gel chromatography (10 → 20% EtOAc in PhMe) afforded the switched pyrazole as a white solid (37 mg, 0.13 mmol, 73%); 112-114 °C; ν_{max} (ATR) 2950, 1783 (C=O), 1711 (C=O), 1558, 1531, 1365, 1348, 1083 cm^{-1}; δ_H (600 MHz, $CDCl_3$) 7.66 (2H, d, *J* = 8.1 Hz, 2''-H), 7.19 (2H d, *J* = 8.1 Hz, 3''-H), 6.46 (1H, s, 4'-H), 3.75 (3H, s, NCH_3), 2.36 (6H, s, 3-CH_3), 2.08 (3H, s, 4''-CH_3); δ_C (151 MHz, $CDCl_3$) 169.7 (C-2), 150.6 (C-3'), 138.9 (C-3), 137.8 (C-4''), 130.8 (C-5'), 130.2 (C-1''), 129.4 (C-3''), 125.5 (C-2''), 101.1 (C-4'), 36.5 (NCH_3), 21.4 (4''-CH_3), 9.2 (3-CH_3); HRMS (ESI) *m/z* found $[M+H]^+$ 296.1402, $C_{17}H_{18}N_3O_2$ requires *M*, 296.1399.

3,3-dimethyl-1-[1'-methyl-3'-(4''-methylphenyl)-1H-pyrazol-5'-yl]pyrrolidine-2,5-dione (**489**)

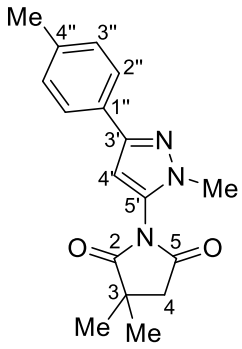

Synthesised from 3,3-dimethyl-1-[5-(4-methylphenyl)-1-(oxan-2-yl)-1H-pyrazol-3-yl]pyrrolidine-2,5-dione **488a** (12 mg, 0.03 mmol, 1.00 equiv.) according to General Procedure F. After 16 h, the volatiles were removed and SiO_2 gel chromatography (15 → 25% EtOAc in PhMe) afforded the switched pyrazole as a colourless oil (5 mg, 0.02 mmol, 52%); ν_{max} (ATR) 2930, 1794 (C=O), 1728 (C=O), 1559, 1534,

1362, 1347, 1297, 1211 1136 cm^{-1}; δ_H (700 MHz, $CDCl_3$) 7.65 (2H, d, *J* = 8.1 Hz, 2''-H), 7.20 (2H, d, *J* = 8.1 Hz, 3''-H), 6.52 (1H, s, 4'-H), 3.72 (3H, s, NCH_3), 2.80 (2H, s, 4-H), 2.36 (3H, s, 4''-CH_3), 1.48 (6H, s, 3-CH_3); δ_C (176 MHz, $CDCl_3$) 181.1 (C-2), 173.5 (C-5), 150.8 (C-3'), 137.8 (C-4''), 130.8 (C-5'), 130.3 (C-1''), 129.4 (C-3''), 125.5 (C-2''), 101.3 (C-4'), 44.0 (C-4), 40.9, (C-3), 36.4 (NCH_3), 25.9 (3-CH_3), 21.4 (4''-CH_3); HRMS (ESI) *m/z* found $[M+H]^+$ 298.1566, $C_{17}H_{20}N_3O_2$ requires *M*, 298.1566.

1-[4'-(4''-fluorophenyl)-1'-methyl-1H-pyrazol-5'-yl]-3,3-dimethylpyrrolidine-2,5-dione (**502b**)

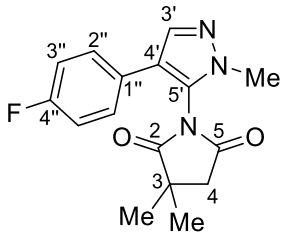

Synthesised from tert-butyl 3-(3,3-dimethyl-2,5-dioxopyrrolidin-1-yl)-4-(4-fluorophenyl)-1H-pyrazole-1-carboxylate **501b** (35 mg, 0.09 mmol, 1.00 equiv.) according to General Procedure F. After 16 h, the volatiles were removed and SiO_2 gel chromatography (0 → 50% EtOAc in PhMe) afforded the switched pyrazole as a colourless oil (10 mg, 0.03 mmol, 37%); ν_{max} (ATR) 2969, 1793 (C=O), 1725 (C=O), 1582, 1511, 1429, 1343, 1230, 1179, 1140 cm^{-1}; δ_H (700 MHz, $CDCl_3$) 7.67 (1H, s, 3'-H), 7.21-7.19 (2H, m, 2''-H), 7.03 (2H, t, *J* = 8.7 Hz, 3''-H), 3.71 (3H, s, NCH_3), 2.79-2.70 (2H, m, 4-H) 1.46 (3H, s, 3-CH_3), 1.34 (3H, s, 3-CH_3); δ_C (176 MHz, $CDCl_3$) 181.4 (C-2), 173.8 (C-5), 162.3 (d, *J* = 247 Hz, C-4''), 137.8 (C-3'), 129.2 (d, *J* = 8 Hz, C-2''), 127.4 (d, *J* = 3 Hz, C-1'') 126.7 (C-5'), 119.8 (C-4'), 115.9 (d, *J* = 22 Hz, C-3''), 44.0 (C-4), 41.0 (C-3), 36.1 (1'-CH_3), 25.9 (3-CH_3), 25.7 (3-CH_3); HRMS (ESI) *m/z* found $[M+H]^+$ 302.1316, $C_{16}H_{17}N_3O_2F$ requires *M*, 302.1305.

3,3-dimethyl-1-[1'-methyl-4'-(4''-methylphenyl)-1H-pyrazol-5'-yl]pyrrolidine-2,5-dione (**502c**)

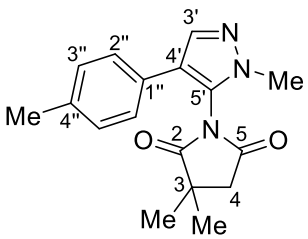

Synthesised from tert-butyl 3-(3,3-dimethyl-2,5-dioxopyrrolidin-1-yl)-4-(4-methylphenyl)-1H-pyrazole-1-carboxylate **501c** (18 mg, 0.05 mmol, 1.00 equiv.) according to General Procedure F. After 16 h, the

volatiles were removed and SiO_2 gel column chromatography (0 → 50% EtOAc in PhMe) afforded the switched pyrazole as a colourless oil (7 mg, 0.02 mmol, 50%); ν_{max} (ATR) 2927, 1799 (C=O), 1726 (C=O), 1586, 1514, 1397, 1344, 1347, 1232, 1205, 1140 cm^{-1}; δ_H (700 MHz, $CDCl_3$) 7.69 (1H, s, 3'-H), 7.15-7.12 (4H, m, 2''-H, 3''-H), 3.71 (3H, s, 1'-CH_3), 2.75 (2H, q, J = 18.4 Hz, 4-H), 2.33 (3H, s, 4''-CH_3), 1.46 (3H, s, 3-CH_3), 1.36 (3H, s, 3-CH_3); δ_C (176 MHz, $CDCl_3$) 181.4 (C-2), 173.8 (C-5), 137.9 (C-3'), 137.2 (C-4''), 129.6 (C-2''), 128.4 (C-1''), 127.1 (C-3''), 126.5 (C-5'), 120.5 (C-4'), 44.0 (C-4), 41.0 (C-3), 36.0 (NCH_3), 25.9 (3-CH_3), 25.8 (3-CH_3), 21.3 (4''-CH_3); HRMS (ESI) *m/z* found $[M+H]^+$ 298.1570, $C_{17}H_{20}N_3O_2$ requires *M*, 298.1556

4.3 X-ray Crystallography Data*

3-Nitro-1-{[2'-(trimethylsilyl)ethoxy]methyl}-1H-pyrazole (**450**)

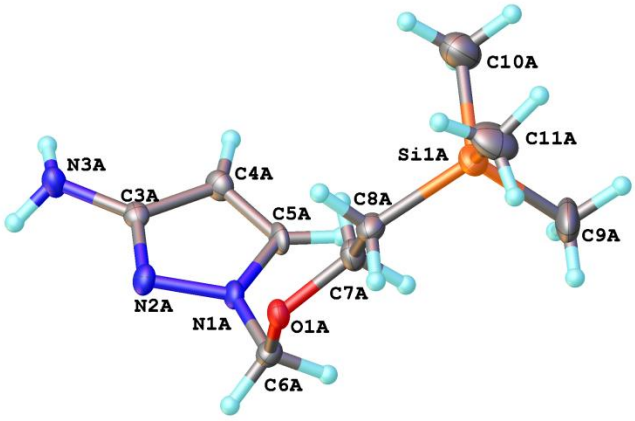

Single crystals of $C_9H_{19}N_3OSi$ (FW 213.36) were obtained via recrystallisation from iPrOH. A suitable crystal was selected and analysed on a Bruker D8Venture diffractometer (IμS microfocus sources, focusing mirrors, CMOS Photo100 detector) using MoKα (λ = 0.71073 Å) radiation, equipped with Crysostream (Oxford Cryosystems) open-flow nitrogen cryostats. The temperature was maintained at 120 K during data collection. Using Olex2 the structure was solved with the ShelXS structure solution program using Intrinsic Phasing and refined with the ShelXL refinement package using Least Squares minimisation.

* Analyses performed by Dr Dmitry Yufit and Dr Andrei Batsanov

Crystallographic Data: plate, colourless, 0.36 × 0.18 × 0.05 mm^3, triclinic P-1, a = 7.7755(19) Å, b = 7.7755(19) Å, c = 7.7755(19) Å, α = 93.324(9)°, β = 102.300(9)°, γ = 91.292(9)°, V = 1267.1(5) $Å^3$, Z = 4, ρ_{calc} = 1.118 g cm^{-3}, T = 120 K, μ(MoKα) = 0.163 mm^{-1}, 20779 reflections measured (4.246° ≤ 2θ ≤ 54.998°), 5719 unique (R_{int} = 0.0738, R_{sigma} = 0.0934) which were used in all calculations. The final R_1 was 0.0980 (I > 2σ(I)) and wR_2 was 0.3477 (all data).

Tert-butyl 3-nitro-1H-pyrazole-1-carboxylate (**495**)

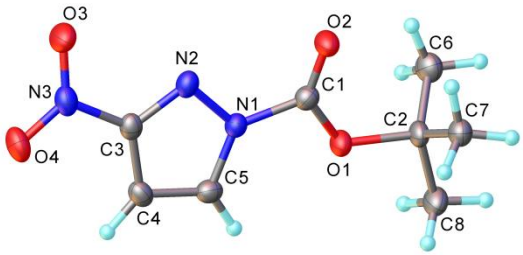

Single crystals of $C_8H_{11}N_3O_4$ (FW 213.19) were obtained via recrystallisation from iPrOH. A suitable crystal was selected and analysed on a Bruker D8Venture diffractometer (IμS microfocus sources, focusing mirrors, CMOS Photo100 detector) using MoKα (λ = 0.71073 Å) radiation, equipped with Crysostream (Oxford Cryosystems) open-flow nitrogen cryostats. The temperature was maintained at 120 K during data collection. Using Olex2[16] the structure was solved with the ShelXT[17] structure solution program using Intrinsic Phasing and refined with the ShelXL[18] refinement package using Least Squares minimisation.

Crystallographic Data: plate, colourless, 0.337 × 0.266 × 0.102 mm^3, monoclinic $P2_1/c$, a = 5.8959(5) Å, b = 26.572(2) Å, c = 6.4821(6) Å, α = 90.0000°, β = 101.672(4)°, γ = 90.0000°, V = 994.53(15) $Å^3$, Z = 1, ρ_{calc} = 1.424 g cm^{-3}, T = 120 K, μ(MoKα) = 0.116 mm^{-1}, 3363 reflections measured (6.132° ≤ 2θ ≤ 50.082°), 3363 unique (R_{int} = n/a, R_{sigma} = 0.0473) which were used in all calculations. The final R_1 was 0.0423 (I>2σ(I)) and wR_2 was 0.1037 (all data)

Tert-butyl 5-amino-1H-pyrazole-1-carboxylate (**534**)

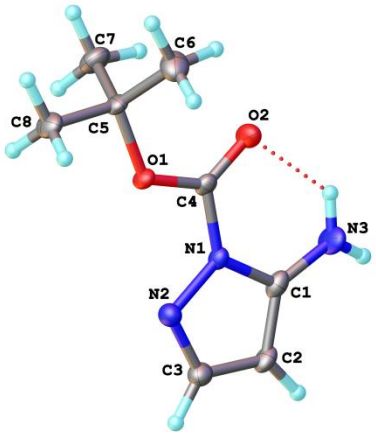

Single crystals of $C_8H_{13}N_3O_2$ (FW 183.21) were obtained via recrystallisation from iPrOH. A suitable crystal was selected and analysed on a Bruker D8Venture diffractometer (IμS microfocus sources, focusing mirrors, CMOS Photo100 detector) using MoKα (λ = 0.71073 Å) radiation, equipped with Crysostream (Oxford Cryosystems) open-flow nitrogen cryostats. The temperature was maintained at 120 K during data collection. Using Olex2 the structure was solved with the ShelXS[19] structure solution program using Intrinsic Phasing and refined with the ShelXL refinement package using Least Squares minimisation.

Crystallographic Data: irregular, colourless, 0.29 × 0.17 × 0.04 mm^3, monoclinic $P2_1/c$, a = 9.9588(6) Å, b = 9.9588(6) Å, c = 12.2360(7) Å, α = 90.0000°, β = 108.404(3)°, γ = 90.0000°, V = 967.48(10) $Å^3$, Z = 4, ρ_{calc} = 1.258 g cm^{-3}, T = 120 K, μ(MoKα) = 0.093 mm^{-1}, 2318 reflections measured (6.002° ≤ 2θ ≤ 55.986°), 2318 unique (R_{int} = 0.0660, R_{sigma} = 0.0395) which were used in all calculations. The final R_1 was 0.0492 (I > 2σ(I)) and wR_2 was 0.1249 (all data).

4.4 References

[1] R. Uson, L. A. Oro, J. A. Cabeza, H. E. Bryndza, M. P. Stepro, John Wiley & Sons, Ltd, **2007**, pp. 126–130.

[2] M. McLaughlin, K. Marcantonio, G. Y. Chen, I. W. Davies, *J. Org. Chem.* **2008**, *73*, 4309–4312.

[3] K. M. Clapham, A. S. Batsanov, M. R. Bryce, B. Tarbit, *Org. Biomol. Chem.* **2009**, *7*, 2155.

[4] M. Chai, Wenying; Letavic, Michael, A.; Ly, Kiev, S.; Pippel, Daniel, J.; Rudolph, Dale, A.; Sappey, Kathleen, C.; Savall, Brad, M.; Shah, Chandravadan, R.; Shireman, Brock, T.; Soyode-Johnson, Akinola; Stocking, Emily, M.; Swanson, Devin, *Janssen Pharmaceutica NV US Pat*, **2011**, 50198.

[5] J. Yuntao; Bridges, Alexander, *CS Therapeutics Inc US Pat*, **2015**, 50989.

[6] A. Beyer, T. Castanheiro, P. Busca, G. Prestat, *ChemCatChem* **2015**, *7*, 2433–2436.

[7] S. Sanfoi; D'Agostino, Laura Akullian; Sjin, Robert Tjin Tham; NIU, Deqiang; Mcdonald, Joseph John; Zhu, Zhendong; Liu, Haibo; Mazdiyansi, Hormoz; Petter, Russell C.; Singh, Juswinder; Barrague, Matthieu; Gross, Alexandre; Munson, Mark; Harvey, Darren; Schlo, *Celgene Avilomics Research Inc. US Pat*, **2014**, 144737.

[8] D. G. Twigg, N. Kondo, S. L. Mitchell, W. R. J. D. Galloway, H. F. Sore, A. Madin, D. R. Spring, *Angew. Chem. Int. Ed.* **2016**, *55*, 12479–12483.

[9] P. Robert, A., Jr.; Artis, Dean, Richard; Ye, Xiaocong, Michael; Aubele, Danielle, L.; Truong, Anh, P.; Bowers, Simeon; Hom, Roy, K.; Zhu, Yong-Liang; Neitz, R., Jeffrey; Sealy, Jennifer; Adler, Marc; Beroza, Paul; Anderson, John, *Elan Pharmaceuticals US Pat*, **2011**, 26914.

[10] R. Goikhman, T. L. Jacques, D. Sames, *J. Am. Chem. Soc.* **2009**, *131*, 3042–3048.

[11] A.-K. Pleier, H. Glas, M. Grosche, P. Sirsch, W. R. Thiel, *Synthesis Stuttgart* **2001**, 55–62.

[12] C. K. Son, Jong Chan; Kim, Bong Jin; Kim, Jae Hak; Lee, Ill Young; Yun, Chang Soo; Lee, Sang Ho; Lee, *Korea Research Institute of Chemical Technology KR Pat*, **2014**, 249162.

[13] T. K. Weber, Olivia D. Shangfi, Michael B. Grice, Cheryl A. Jones, *Abide Theraputics Inc. US*

Pat, **2017**, 87854.

[14] S. M. Preshlock, D. L. Plattner, P. E. Maligres, S. W. Krska, R. E. Maleczka, M. R. Smith III, *Angew. Chem*. *Int. Ed.* **2013**, *52*, 12915–12919.

[15] J. J. Zhao, Q. Wang, *Dana-Farber Cancer Institute Inc.*, **2012**, 109423.

[16] O. V. Dolomanov, L. J. Bourhis, R. J. Gildea, J. A. K. Howard, H. Puschmann, IUCr, *J. Appl. Crystallogr.* **2009**, *42*, 339–341.

[17] G. M. Sheldrick, IUCr, *Acta Crystallogr. Sect. A Found. Adv.* **2015**, *71*, 3–8.

[18] G. M. Sheldrick, IUCr, *Acta Crystallogr. Sect. C Struct. Chem.* **2015**, *71*, 3–8.

[19] G. M. Sheldrick, IUCr, *Acta Crystallogr. Sect. A Found. Crystallogr.* **2008**, *64*, 112–122.

5 Appendix

5.1 NMR Spectra

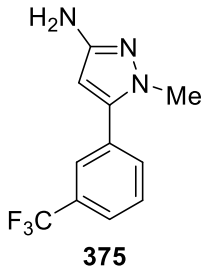

375

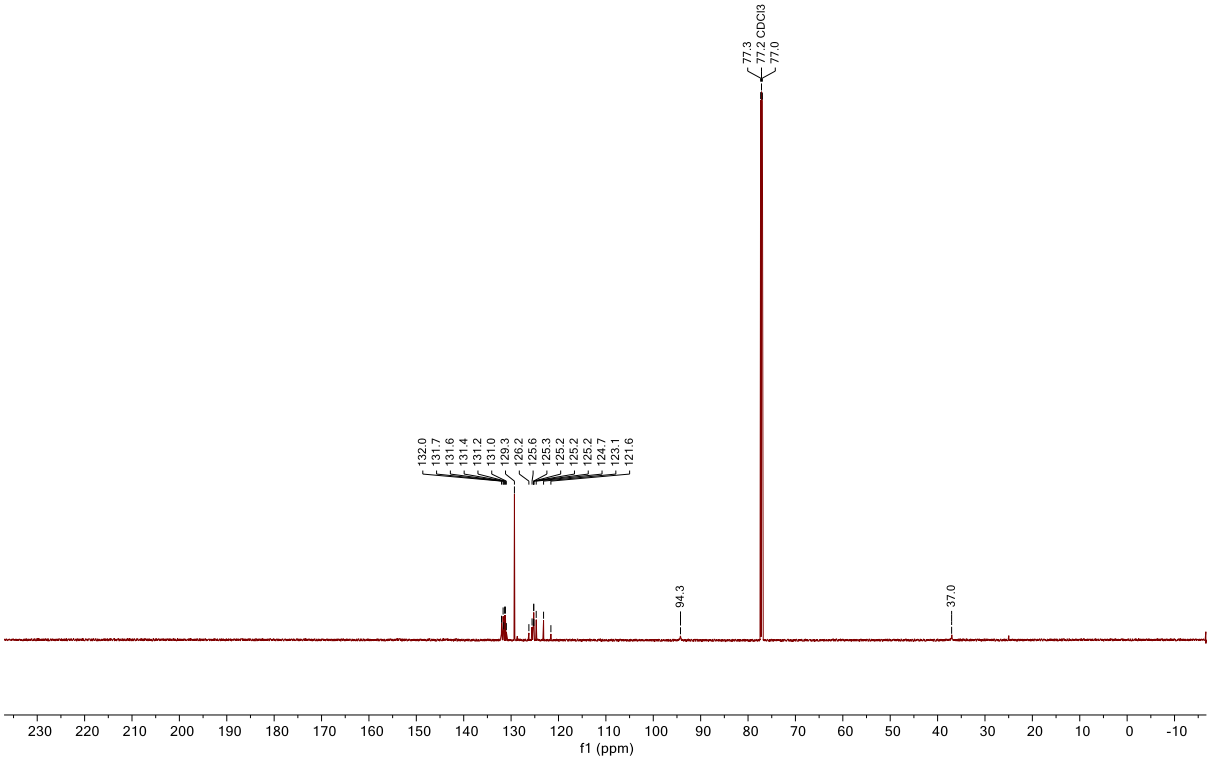

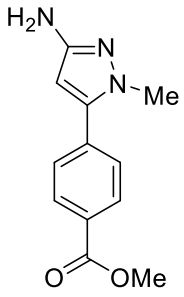
H2N
N
N
Me
O
OMe

379

7.53
7.52
7.26 CDCl3
3.96
3.84
6.87
8.15
8.14
8.57
1.00
2.04
2.06
1.05
2.95
2.99
13 12 11 10 9 8 7 6 5 4 3 2 1 0 -1
f1 (ppm)

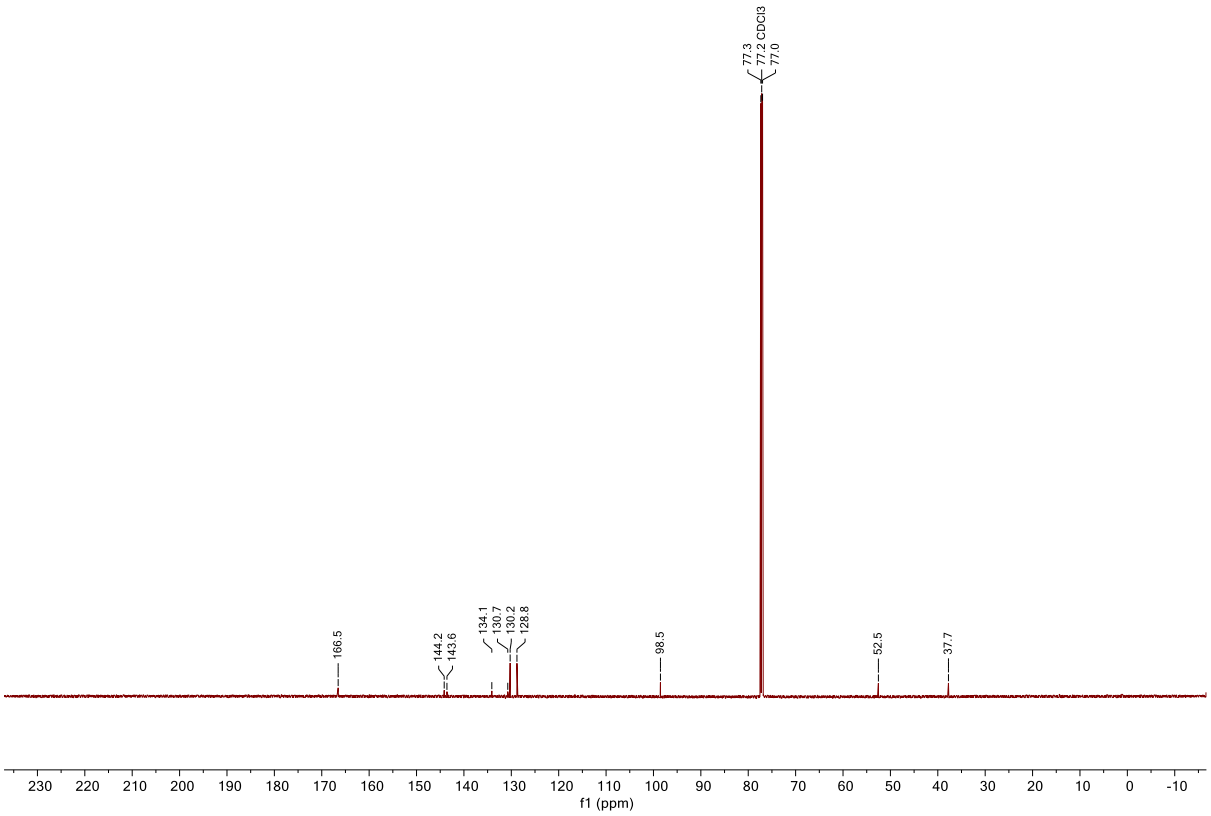
77.3
77.2 CDCl3
77.0
166.5
144.2
143.6
134.1
130.7
130.2
128.8
98.5
52.5
37.7
230 220 210 200 190 180 170 160 150 140 130 120 110 100 90 80 70 60 50 40 30 20 10 0 -10
f1 (ppm)

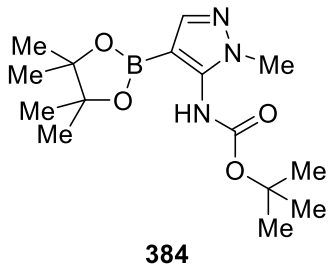
Me
Me
Me
Me
O
B
O
N
N
Me
HN
O
O
Me
Me
Me

384

1.49
1.28
3.76
7.62
7.26 CDCl3
6.70
1.00
1.03
2.95
9.23
11.85
13 12 11 10 9 8 7 6 5 4 3 2 1 0 -1
f1 (ppm)

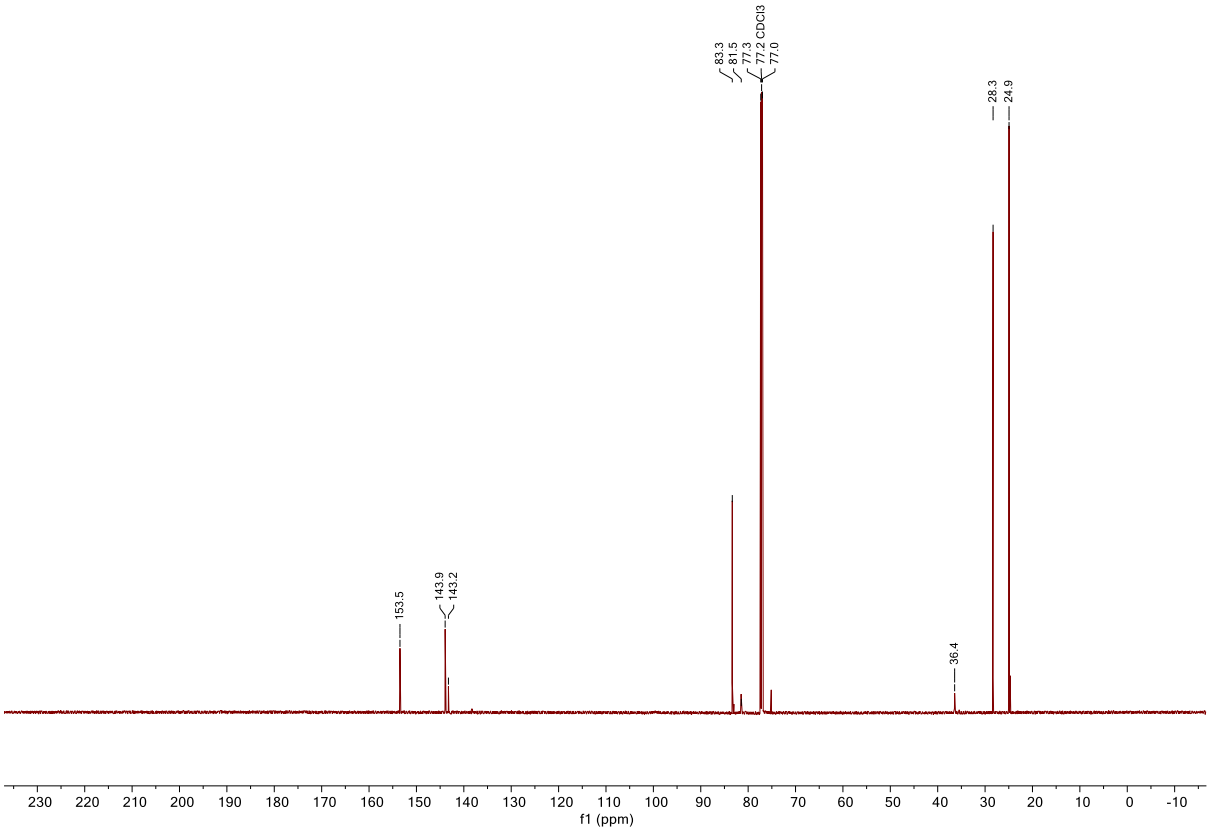
83.3
81.5
77.3
77.2 CDCl3
77.0
28.3
24.9
153.5
143.9
143.2
36.4
230 220 210 200 190 180 170 160 150 140 130 120 110 100 90 80 70 60 50 40 30 20 10 0 -10
f1 (ppm)

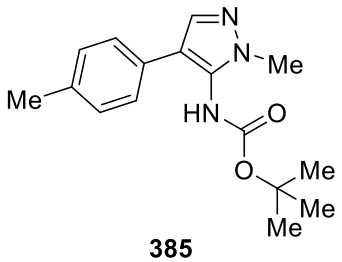
N
N
Me
Me
HN
O
O
Me
Me
Me

385

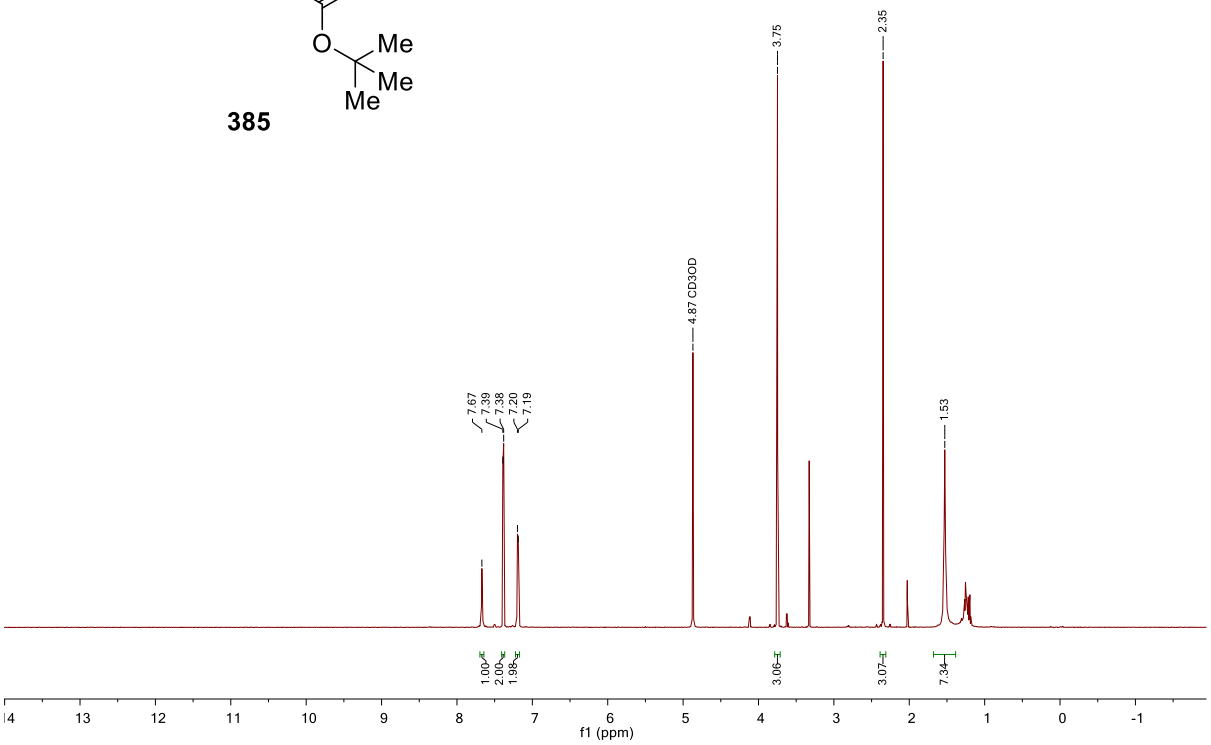
7.67
7.39
7.38
7.20
7.19
4.87 CD3OD
3.75
2.35
1.53
1.00
2.00
1.98
3.06
3.07
7.34
f1 (ppm)

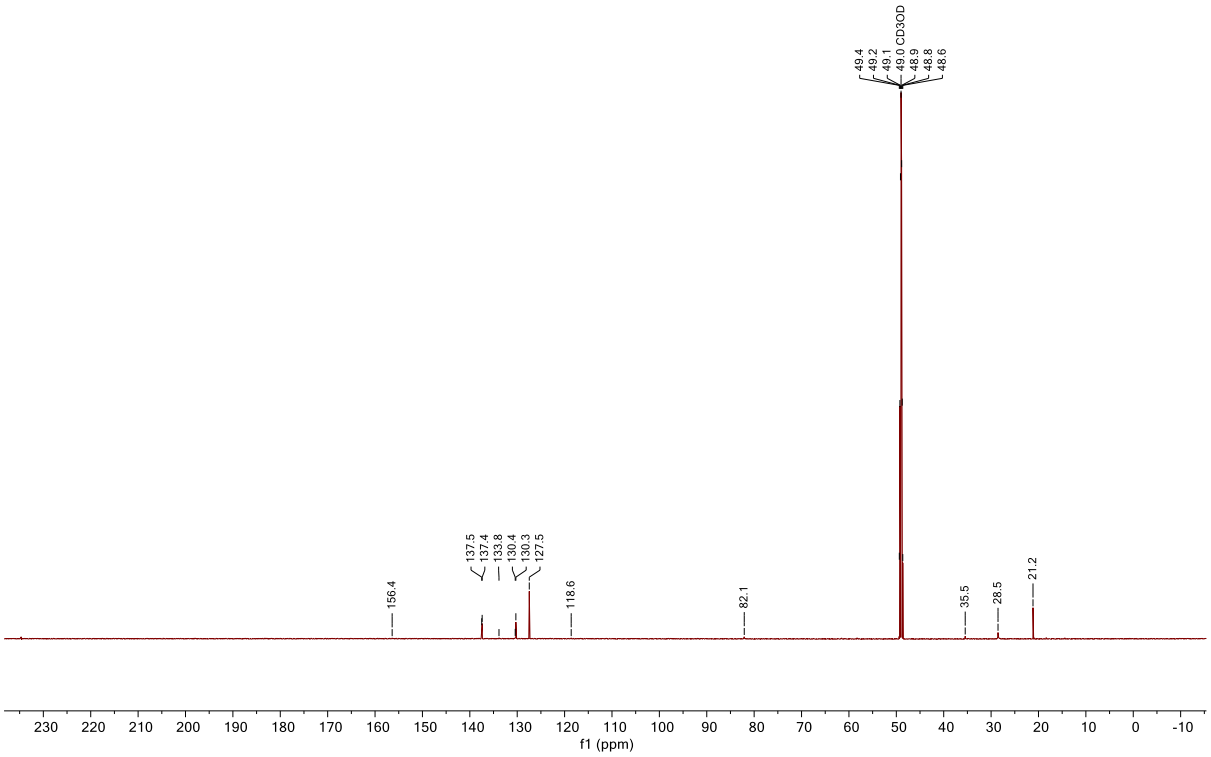
49.4
49.2
49.1
49.0 CD3OD
48.9
48.8
48.6
156.4
137.5
137.4
133.8
130.4
130.3
127.5
118.6
82.1
35.5
28.5
21.2
f1 (ppm)

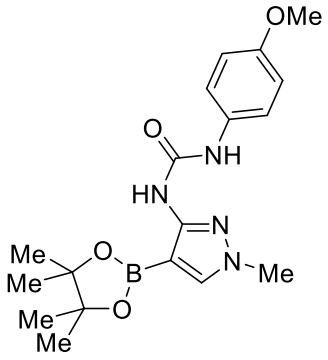
OMe
O
NH
HN
N
N
Me
Me
O
B
O
Me
Me
Me

392

10.16
7.51
7.47
7.46
7.26 CDCl3
6.88
6.87
3.81
3.79
1.31
1.01
1.00
3.06
2.04
3.00
3.00
11.94
f1 (ppm)

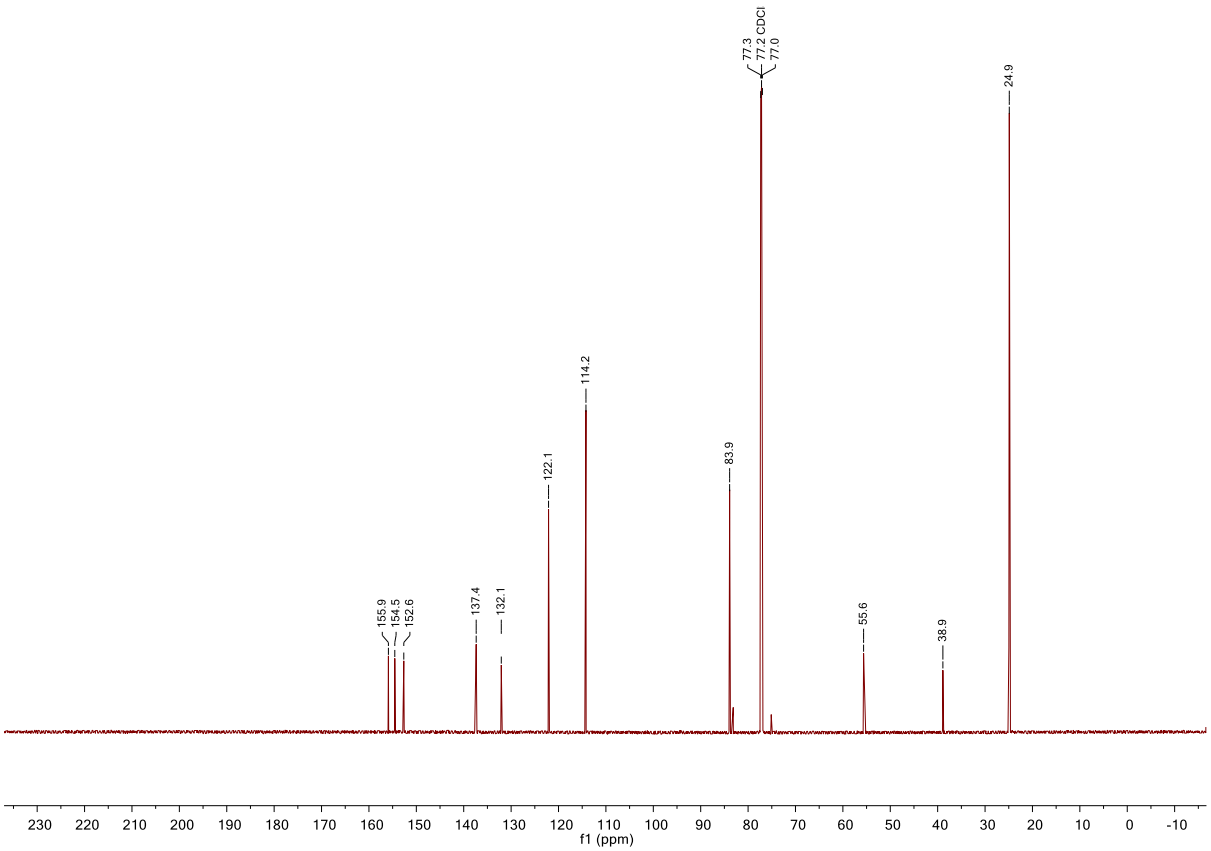
155.9
154.5
152.6
137.4
132.1
122.1
114.2
83.9
77.3
77.2 CDCl
77.0
55.6
38.9
24.9
f1 (ppm)

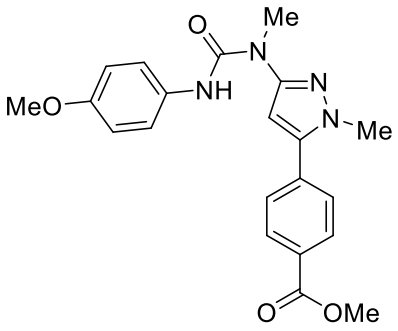
O
Me
N
NH
N
N
Me
MeO
O
OMe

395b

3.92
3.83
3.70
3.28
8.10
8.08
7.49
7.48
7.26 CDCl3
7.23
7.21
6.95
6.94
6.77
1.99
2.07
1.98
2.02
1.99
3.12
3.14
3.02
3.00
13 12 11 10 9 8 7 6 5 4 3 2 1 0 -1
f1 (ppm)

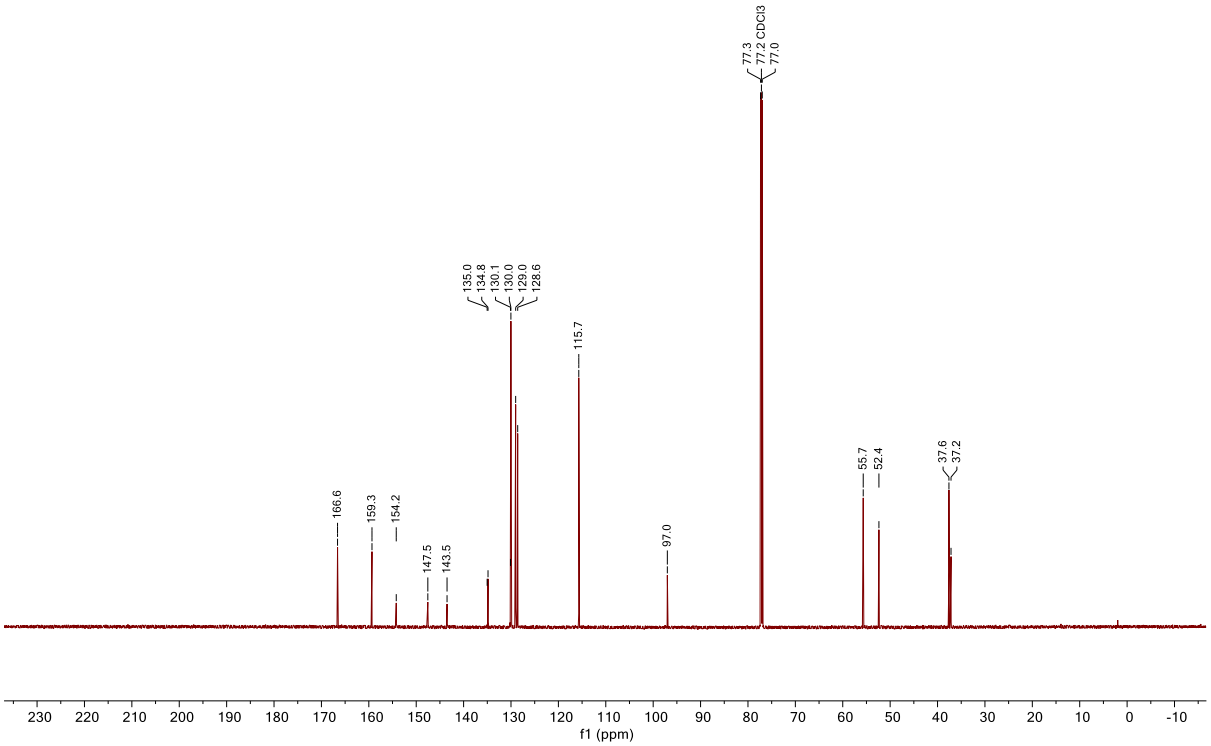
77.3
77.2 CDCl3
77.0
135.0
134.8
130.1
130.0
129.0
128.6
115.7
166.6
159.3
154.2
147.5
143.5
97.0
55.7
52.4
37.6
37.2
230 220 210 200 190 180 170 160 150 140 130 120 110 100 90 80 70 60 50 40 30 20 10 0 -10
f1 (ppm)

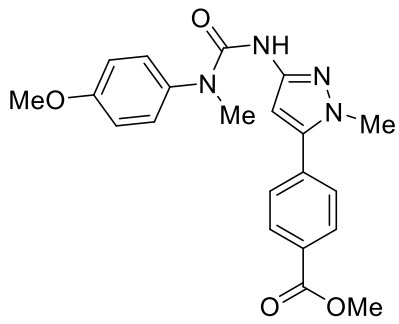
O
NH
N
MeO
N
Me
N
Me
O
OMe

398b

3.92
3.83
3.70
3.28
8.10
8.08
7.49
7.48
7.26 CDCl3
7.23
7.21
6.95
6.94
6.77
1.99
2.07
1.98
2.02
1.99
3.12
3.14
3.02
3.00
f1 (ppm)

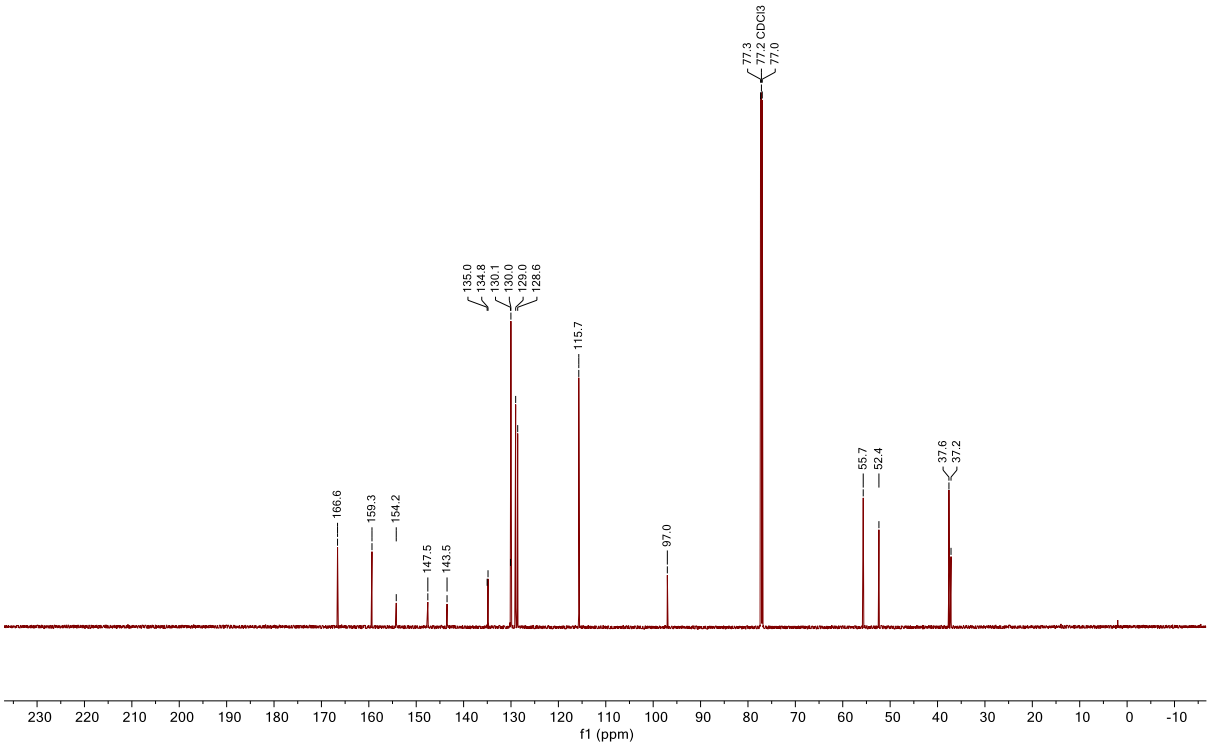
77.3
77.2 CDCl3
77.0
135.0
134.8
130.1
130.0
129.0
128.6
115.7
166.6
159.3
154.2
147.5
143.5
97.0
55.7
52.4
37.6
37.2
f1 (ppm)

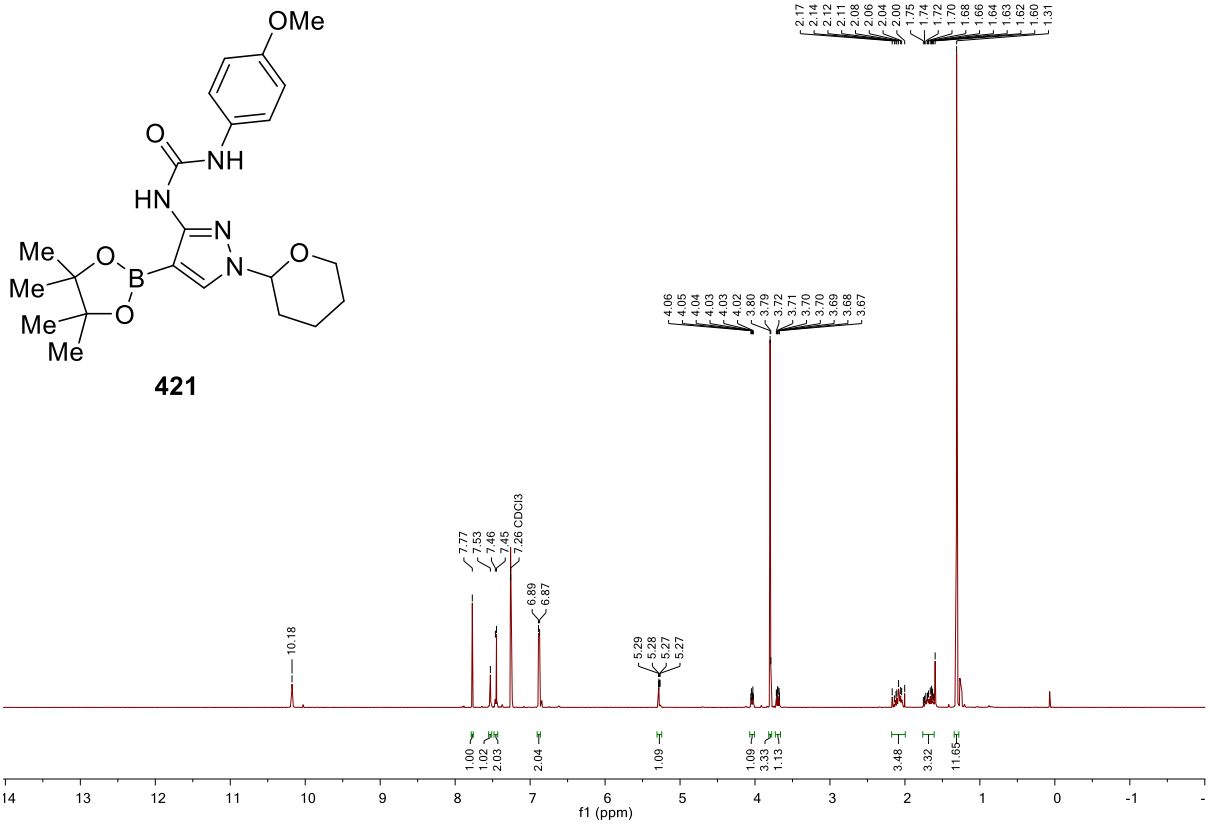
OMe
O
NH
HN
N
N
O
Me
Me
Me
Me
O
B
O
421
10.18
7.77
7.53
7.46
7.45
7.26 CDCl3
6.89
6.87
5.29
5.28
5.27
5.27
4.06
4.05
4.04
4.03
4.03
4.02
3.80
3.79
3.72
3.71
3.70
3.70
3.69
3.68
3.67
2.17
2.14
2.12
2.11
2.08
2.06
2.04
2.00
1.75
1.74
1.72
1.70
1.68
1.66
1.64
1.63
1.62
1.60
1.31
1.00
1.02
2.03
2.04
1.09
1.09
3.33
1.13
3.48
3.32
11.65
f1 (ppm)

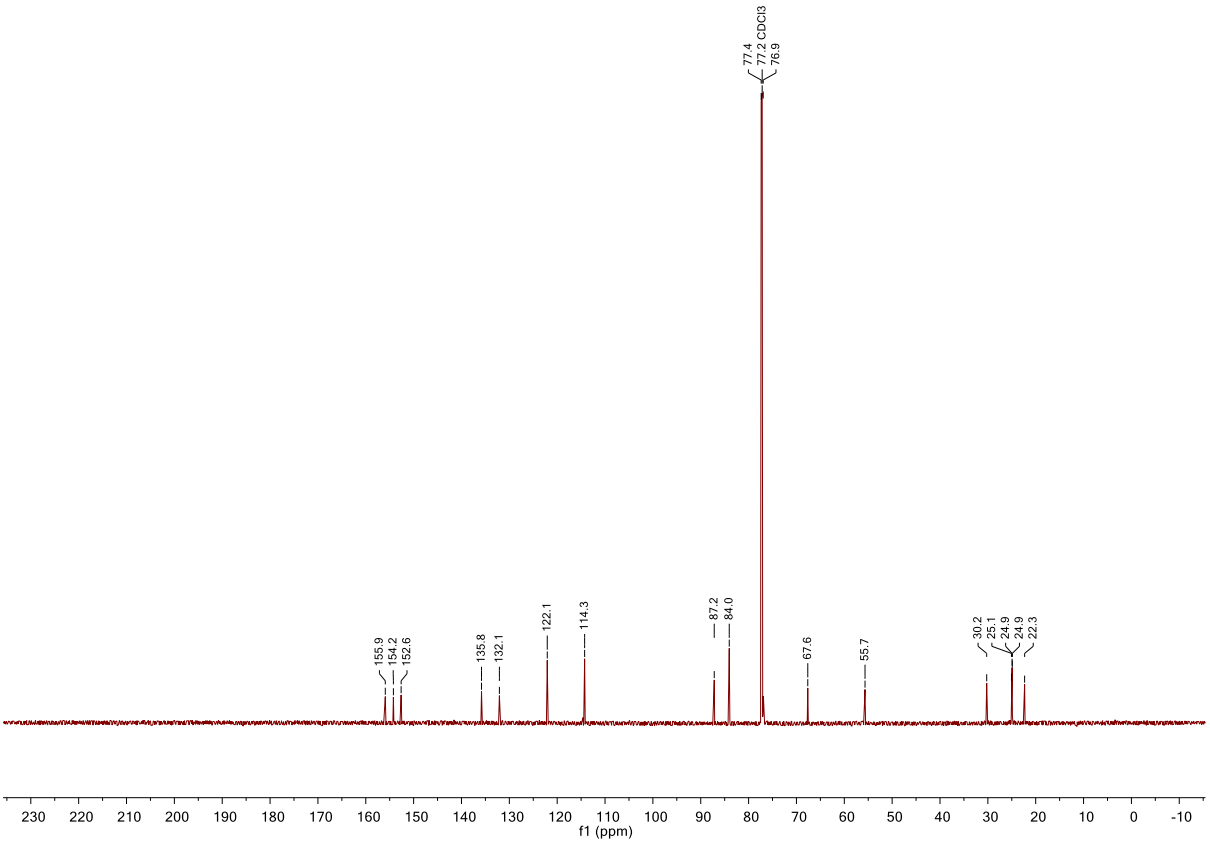
77.4
77.2 CDCl3
76.9
155.9
154.2
152.6
135.8
132.1
122.1
114.3
87.2
84.0
67.6
55.7
30.2
25.1
24.9
24.9
22.3
f1 (ppm)

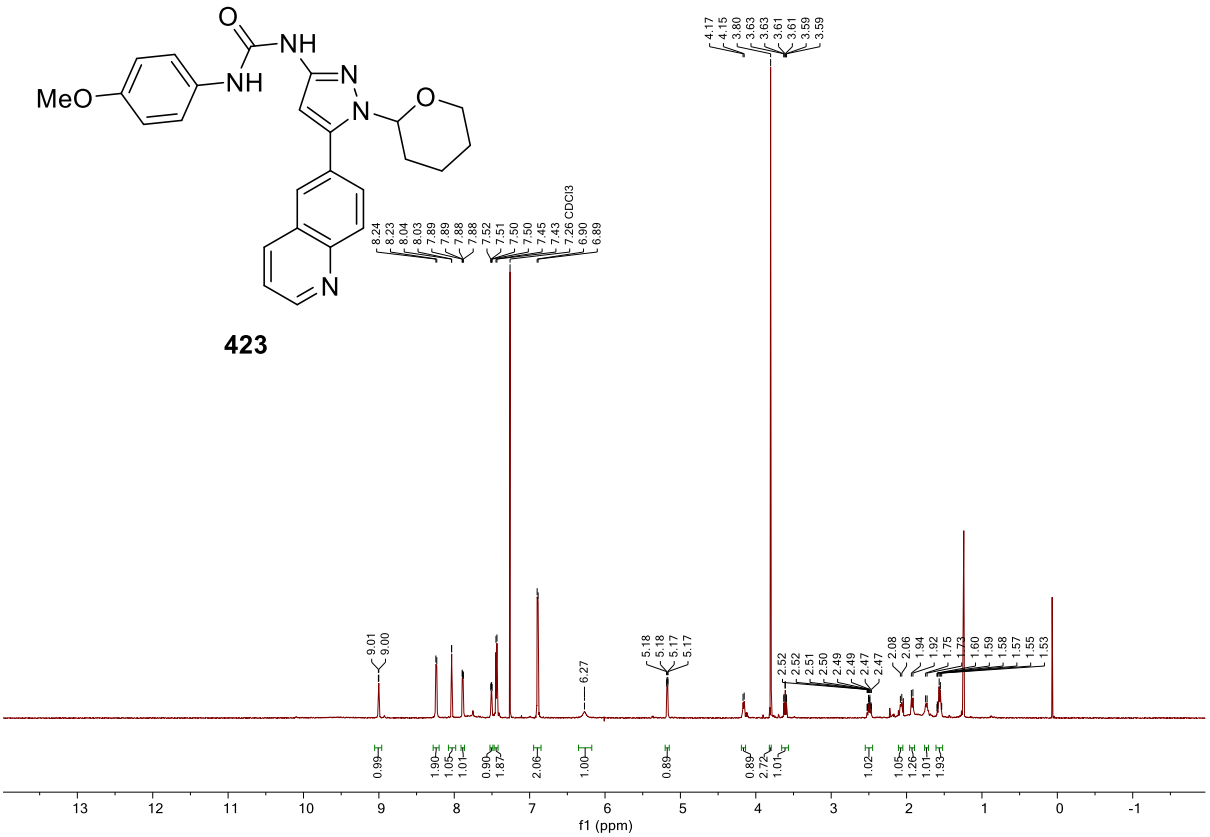
MeO
NH
NH
N
N
O
O
N
423
f1 (ppm)

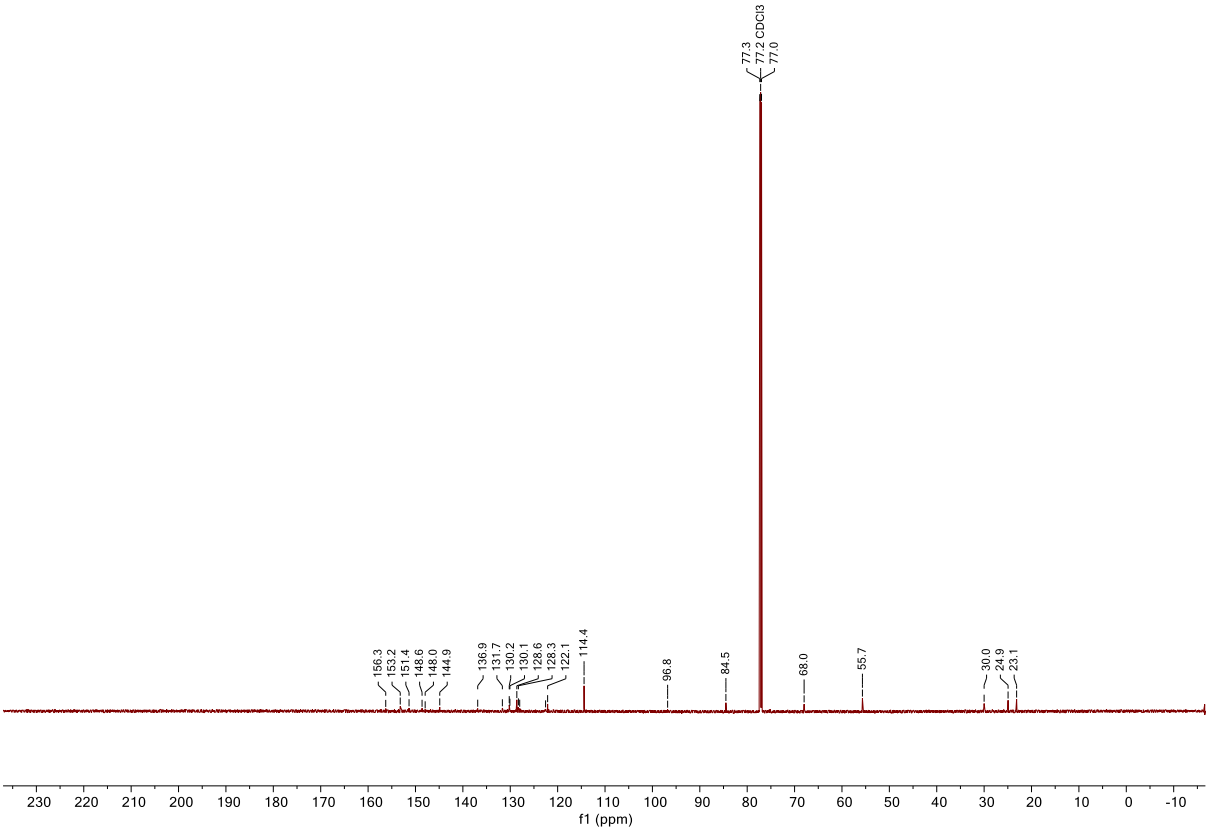
f1 (ppm)

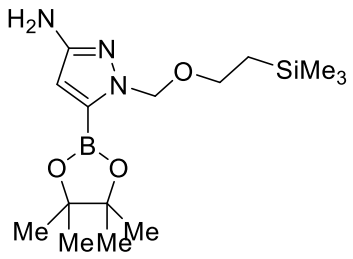
H2N
N
N
O
SiMe3
B
O
O
Me
Me
Me
Me

451

7.26 CDCl3
6.09
5.47
3.79
3.54
3.53
3.51
1.31
0.90
0.89
0.87
-0.05
1.00
1.94
2.33
2.23
12.35
2.07
9.07
f1 (ppm)

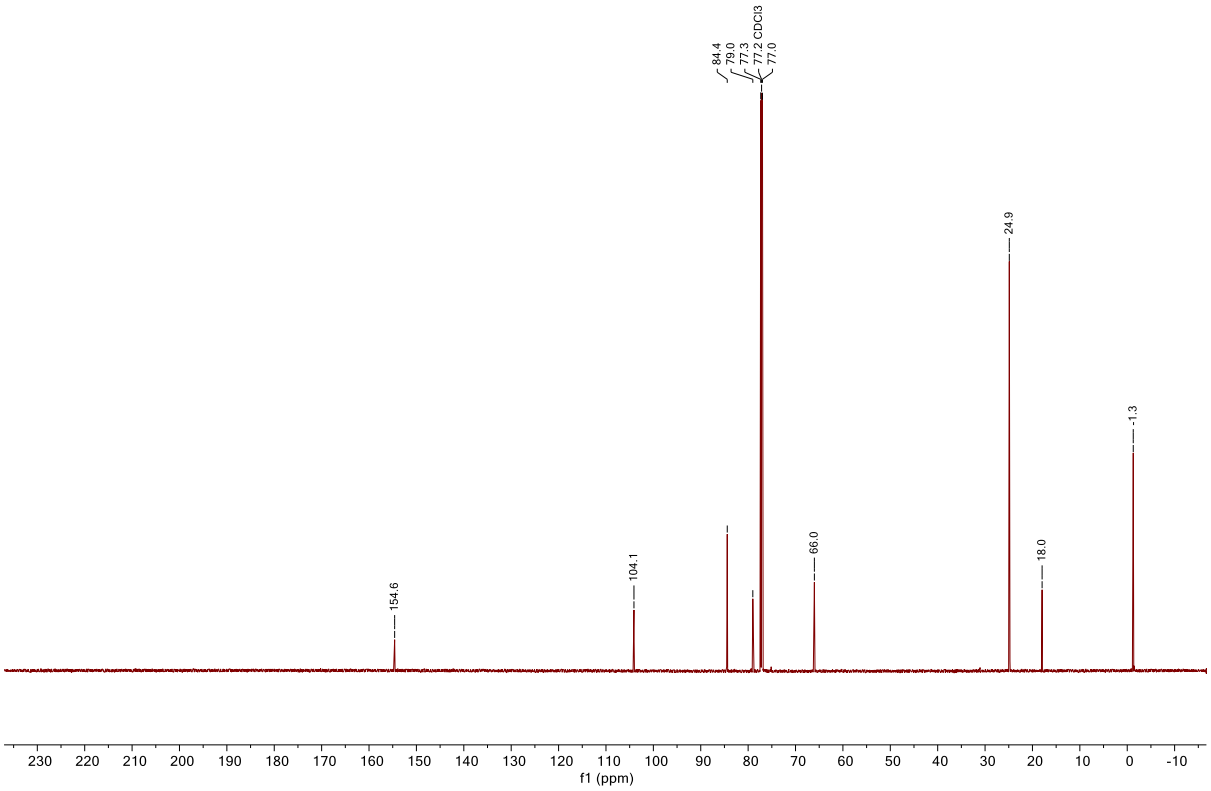
84.4
79.0
77.3
77.2 CDCl3
77.0
24.9
-1.3
154.6
104.1
66.0
18.0
f1 (ppm)

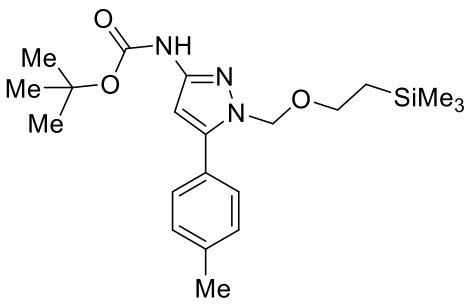
O
NH
Me
Me
O
Me
N
N
O
SiMe3
Me

454a

-0.04
1.52
2.39
5.32
7.82
7.52
7.51
7.26 CDCl3
7.25
7.23
6.69
3.69
3.68
3.67
0.93
0.92
0.91
0.99
1.87
1.81
1.05
1.95
2.11
2.88
8.81
2.08
9.00
f1 (ppm)

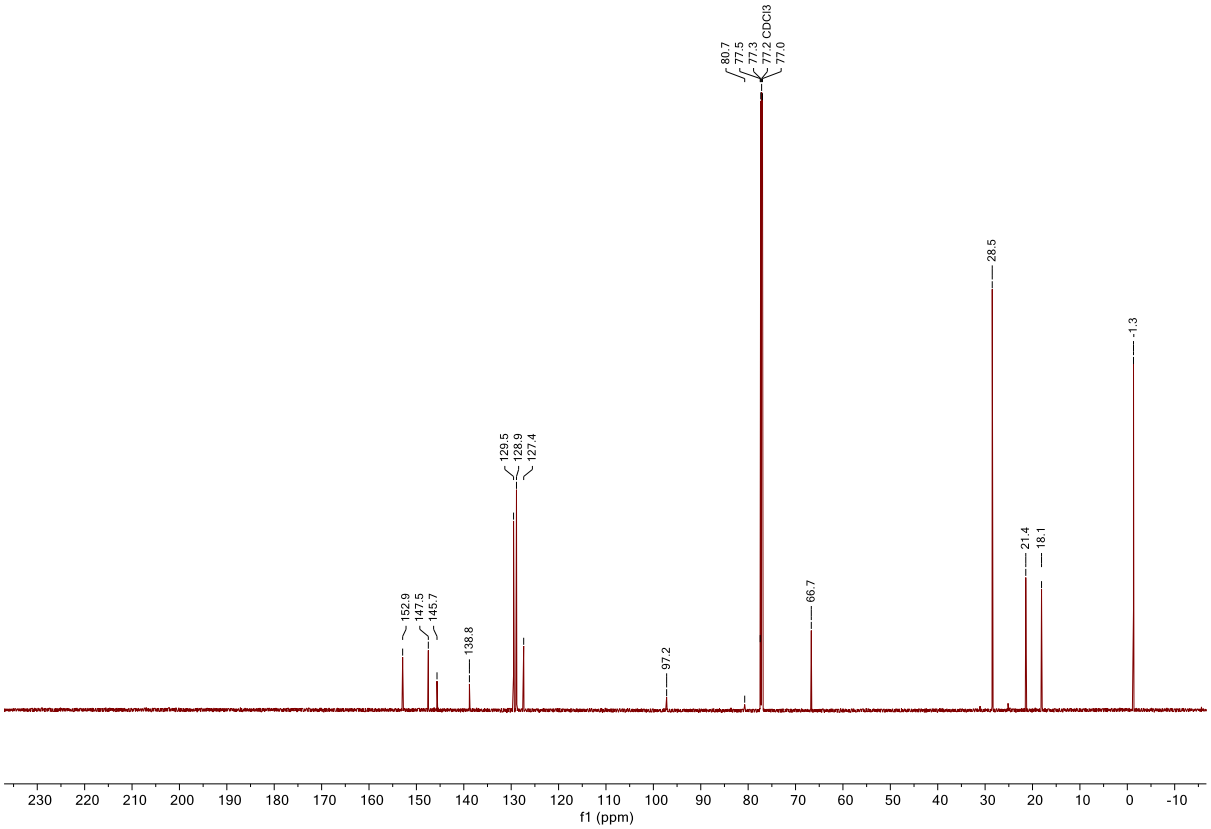
80.7
77.5
77.3
77.2 CDCl3
77.0
28.5
-1.3
129.5
128.9
127.4
152.9
147.5
145.7
138.8
97.2
66.7
21.4
18.1
f1 (ppm)

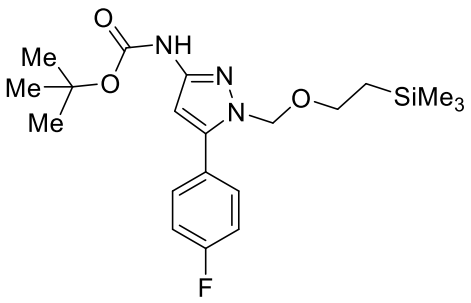
O
NH
Me
Me
O
Me
N
N
O
SiMe3
F

454b

7.94
7.63
7.62
7.62
7.61
7.26 CDCl3
7.14
7.13
7.11
6.71
5.31
3.72
3.70
3.69
1.53
0.94
0.93
0.91
-0.04
1.00
1.94
1.97
0.83
1.97
2.14
8.73
2.23
8.72
f1 (ppm)

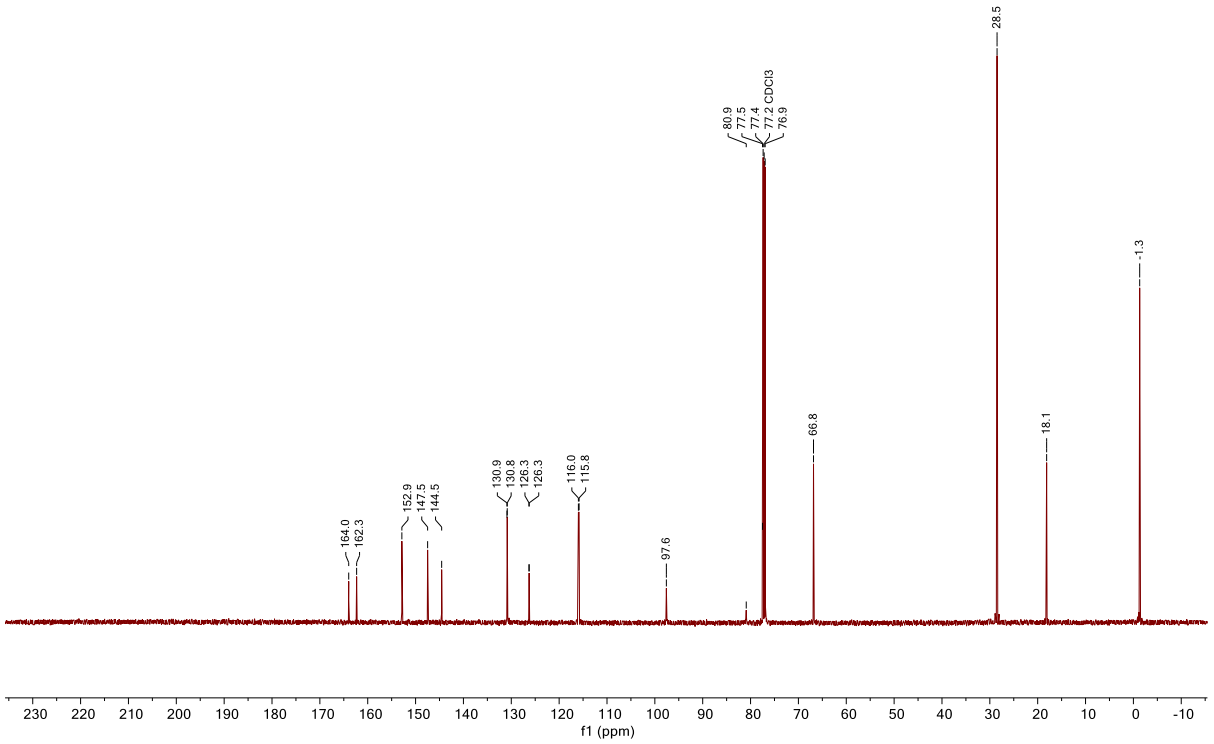
164.0
162.3
152.9
147.5
144.5
130.9
130.8
126.3
126.3
116.0
115.8
97.6
80.9
77.5
77.4
77.2 CDCl3
76.9
66.8
28.5
18.1
-1.3
f1 (ppm)

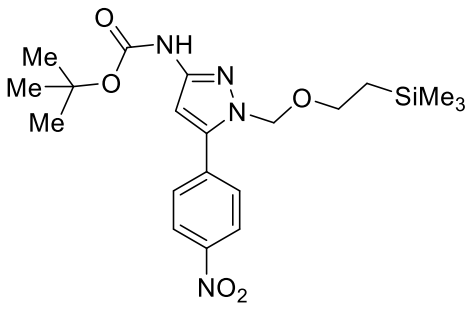
O
NH
Me
Me
O
Me
N
N
O
SiMe3
NO2

454c

8.30
8.29
7.87
7.86
7.26 CDCl3
6.88
5.36
3.76
3.75
3.74
1.53
0.96
0.95
0.94
0.03
2.05
3.00
1.05
2.12
2.09
9.17
2.16
9.45
13 12 11 10 9 8 7 6 5 4 3 2 1 0 -1
f1 (ppm)

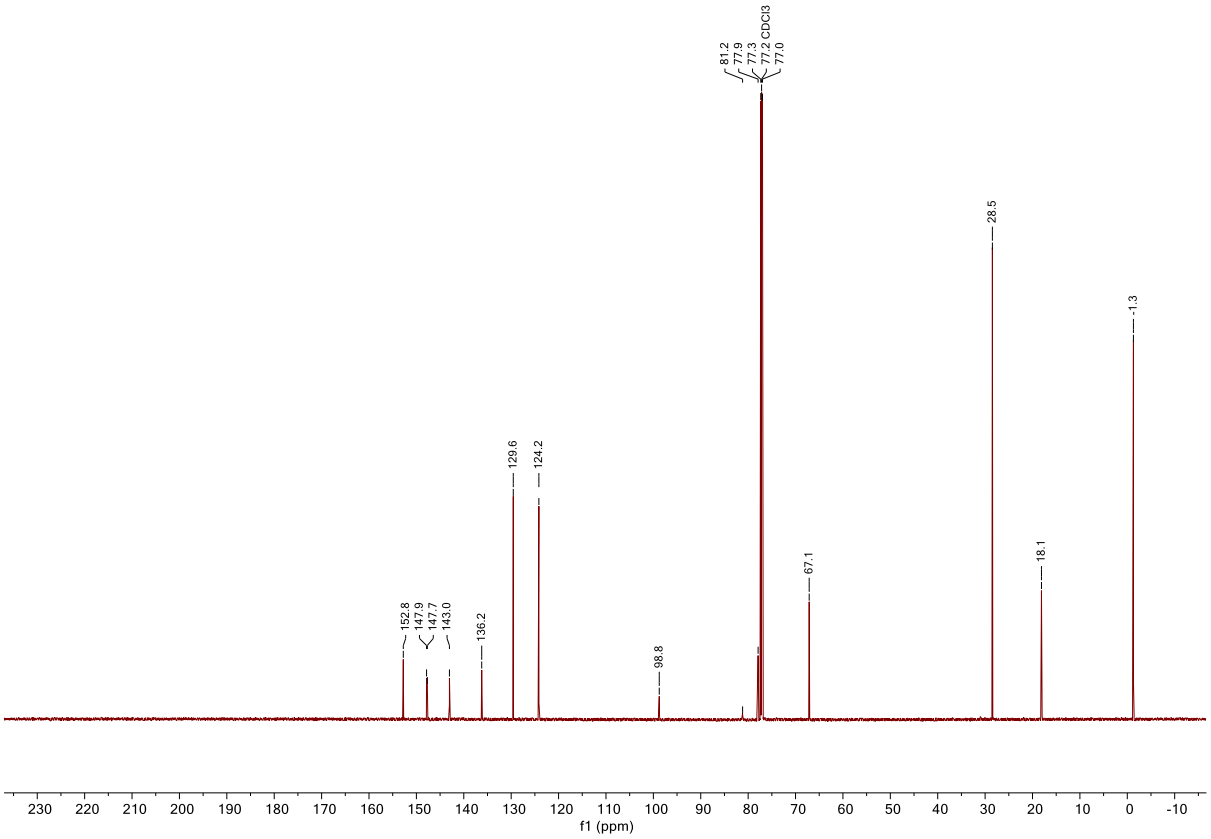
81.2
77.9
77.3
77.2 CDCl3
77.0
28.5
-1.3
129.6
124.2
67.1
18.1
152.8
147.9
147.7
143.0
136.2
98.8
230 220 210 200 190 180 170 160 150 140 130 120 110 100 90 80 70 60 50 40 30 20 10 0 -10
f1 (ppm)

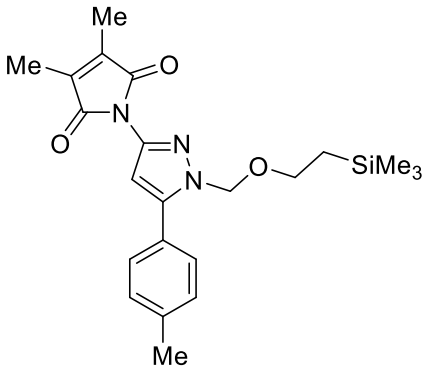
Me
Me
O
O
N
N
N
O
SiMe3
Me

479

-0.01
2.40
2.05
7.53
7.52
7.26 CDCl3
7.25
6.40
5.41
3.79
3.77
3.76
0.95
0.94
0.92
1.95
3.04
1.05
2.00
1.98
3.00
5.91
1.99
8.37
f1 (ppm)

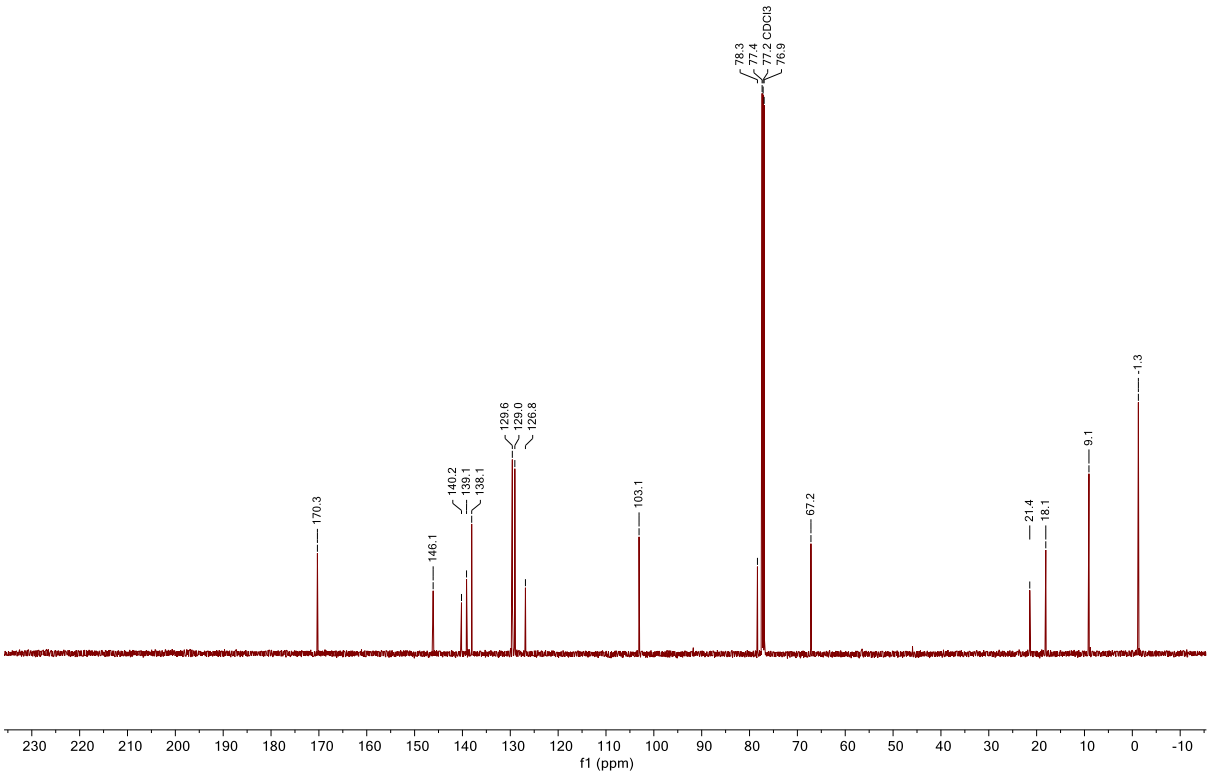
78.3
77.4
77.2 CDCl3
76.9
170.3
146.1
140.2
139.1
138.1
129.6
129.0
126.8
103.1
67.2
21.4
18.1
9.1
1.3
f1 (ppm)

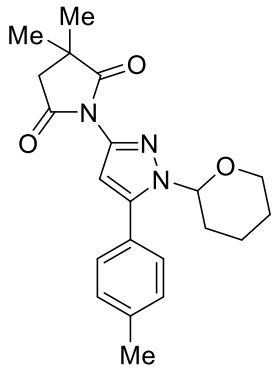

488a

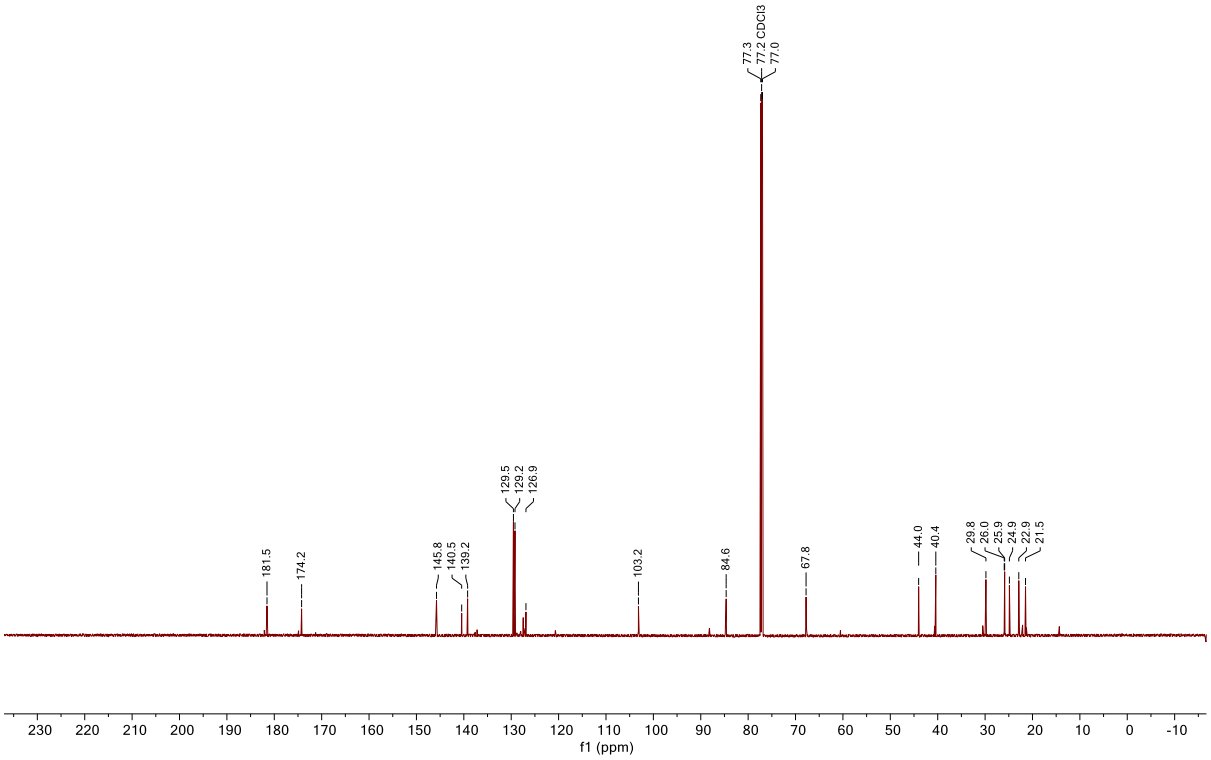

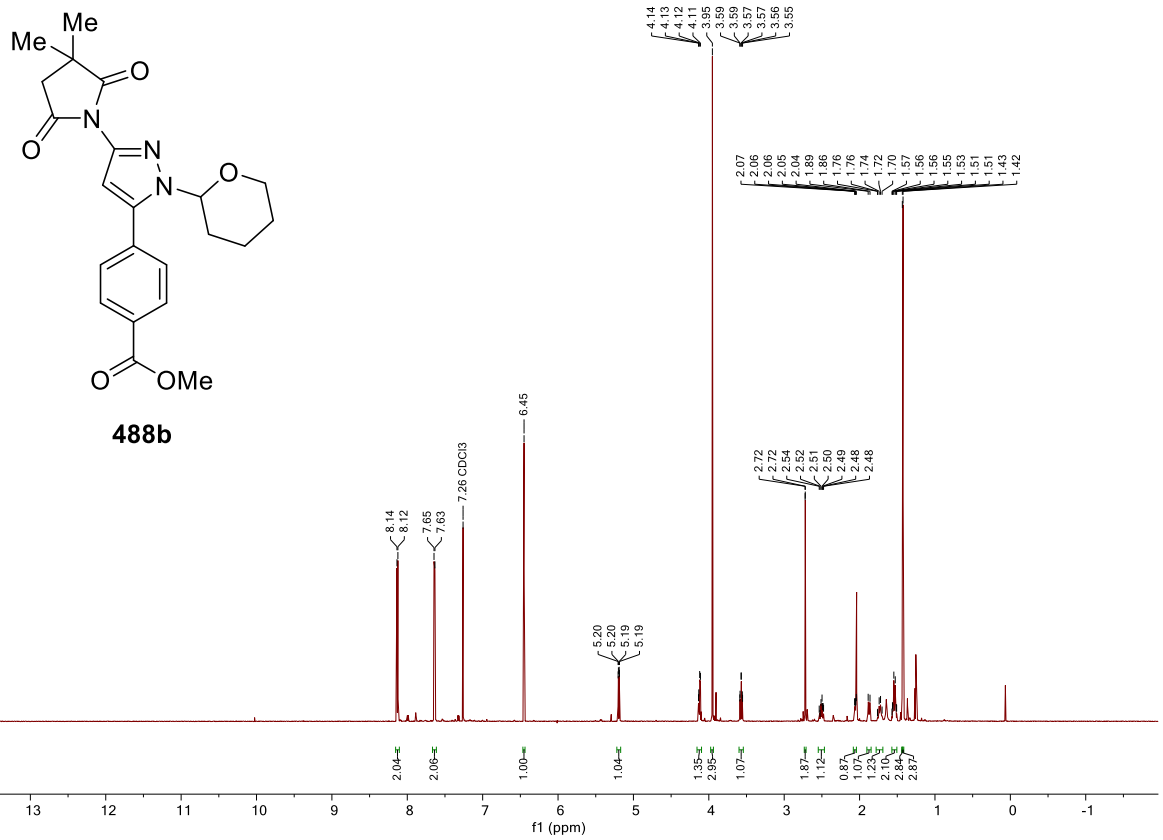
Me
Me
O
N
O
N
N
O
O
OMe
4.14
4.13
4.12
4.11
3.95
3.59
3.59
3.57
3.57
3.56
3.55
2.07
2.06
2.06
2.05
2.04
1.89
1.86
1.76
1.76
1.74
1.72
1.70
1.57
1.56
1.56
1.55
1.53
1.51
1.51
1.43
1.42
2.72
2.72
2.54
2.52
2.51
2.50
2.49
2.48
2.48
8.14
8.12
7.65
7.63
7.26 CDCl3
6.45
5.20
5.20
5.19
5.19
2.04
2.06
1.00
1.04
1.35
2.95
1.07
1.87
1.12
0.87
1.07
1.23
2.10
2.84
2.87
13 12 11 10 9 8 7 6 5 4 3 2 1 0 -1
f1 (ppm)

488b

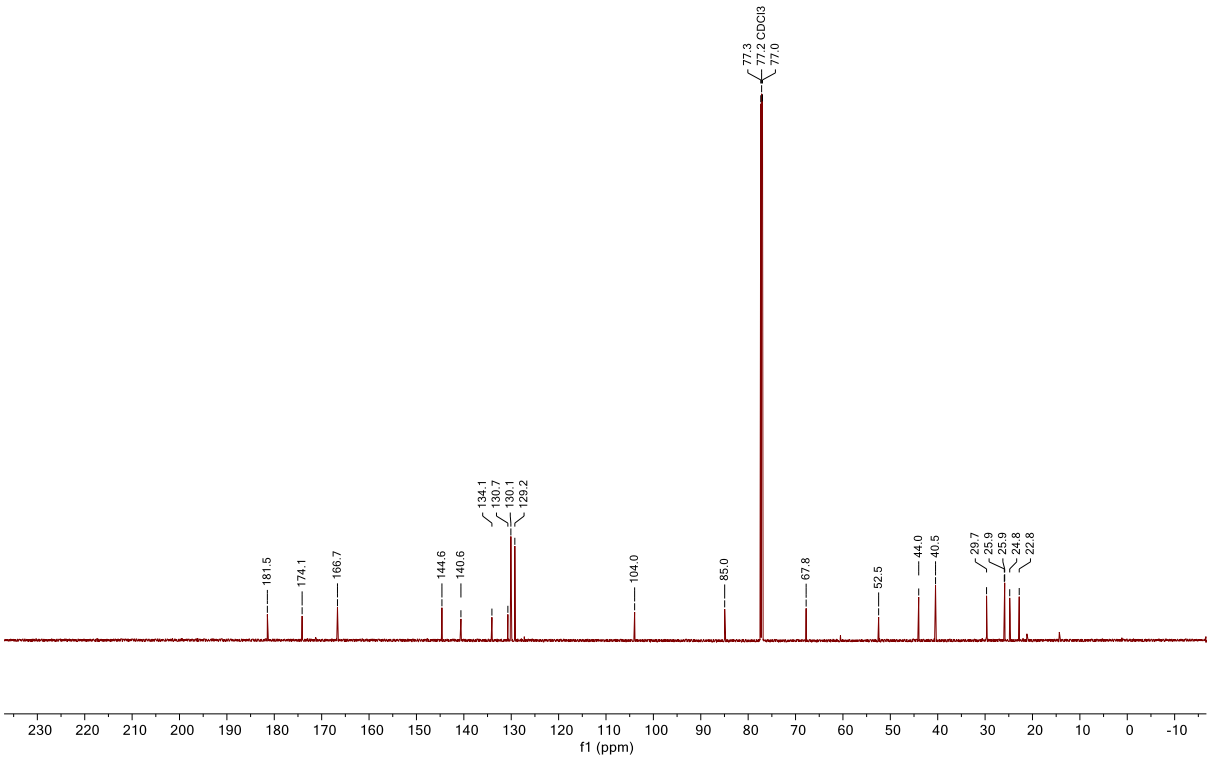
77.3
77.2 CDCl3
77.0
134.1
130.7
130.1
129.2
181.5
174.1
166.7
144.6
140.6
104.0
85.0
67.8
52.5
44.0
40.5
29.7
25.9
25.9
24.8
22.8
230 220 210 200 190 180 170 160 150 140 130 120 110 100 90 80 70 60 50 40 30 20 10 0 -10
f1 (ppm)

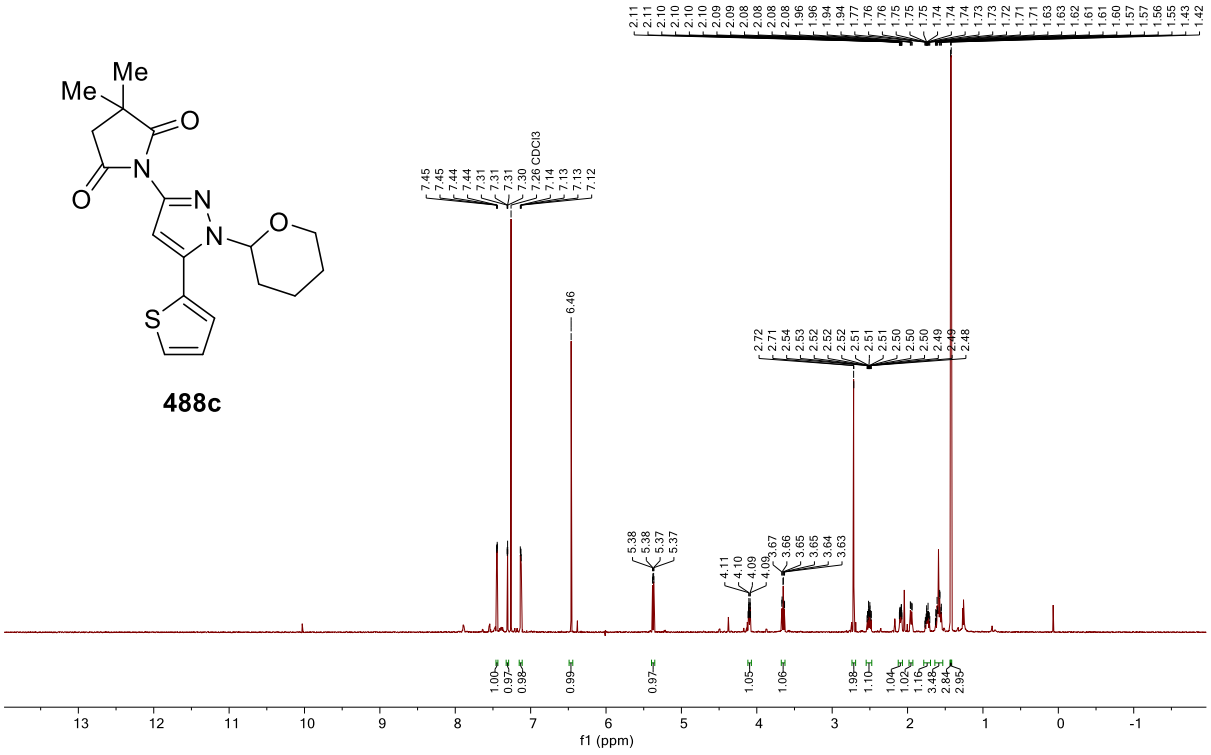
Me
Me
O
N
O
N
N
O
S
488c
f1 (ppm)

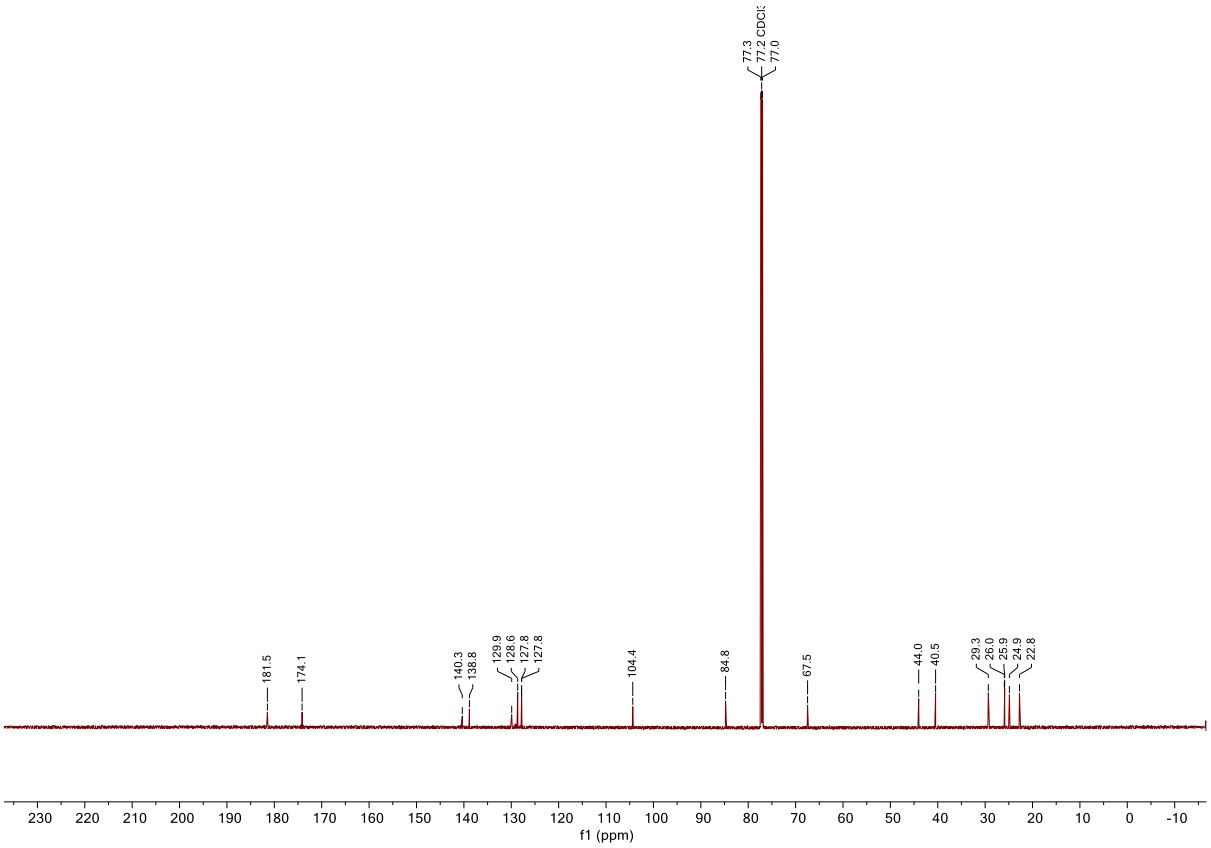
f1 (ppm)

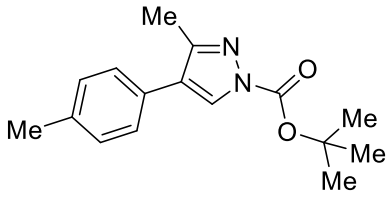
Me
N
N
O
O
Me
Me
Me
Me

494

1.65
2.43
2.37
8.05
7.30
7.29
7.26 CDCl3
7.22
7.20
1.01
1.97
2.12
2.98
3.00
9.08
f1 (ppm)

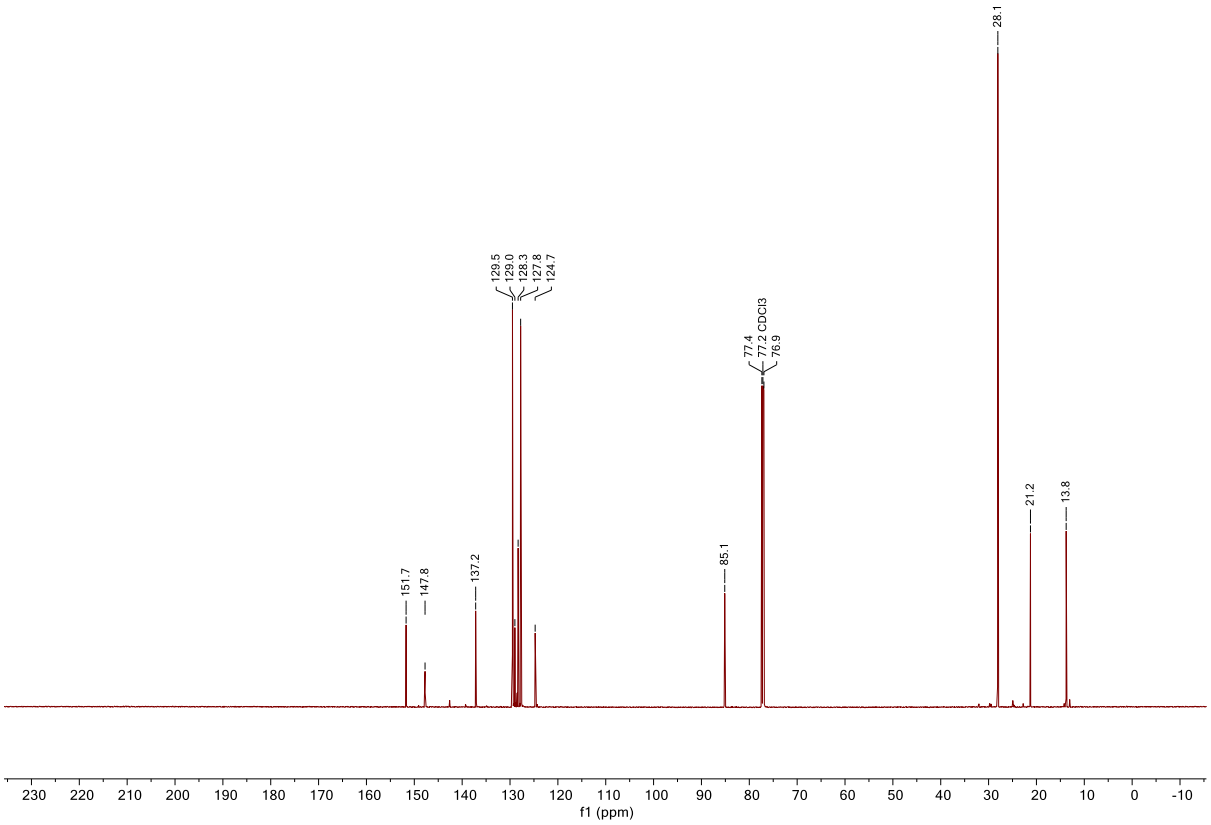
28.1
129.5
129.0
128.3
127.8
124.7
77.4
77.2 CDCl3
76.9
151.7
147.8
137.2
85.1
21.2
13.8
f1 (ppm)

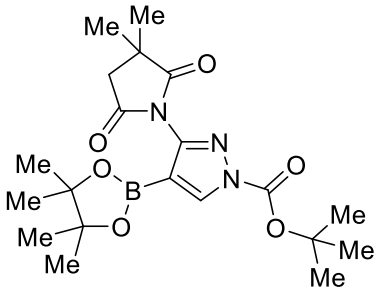

500

1.62
1.43
1.25
2.69
8.40
7.26 CDCl3
1.07
1.96
9.30
5.88
12.00
f1 (ppm)

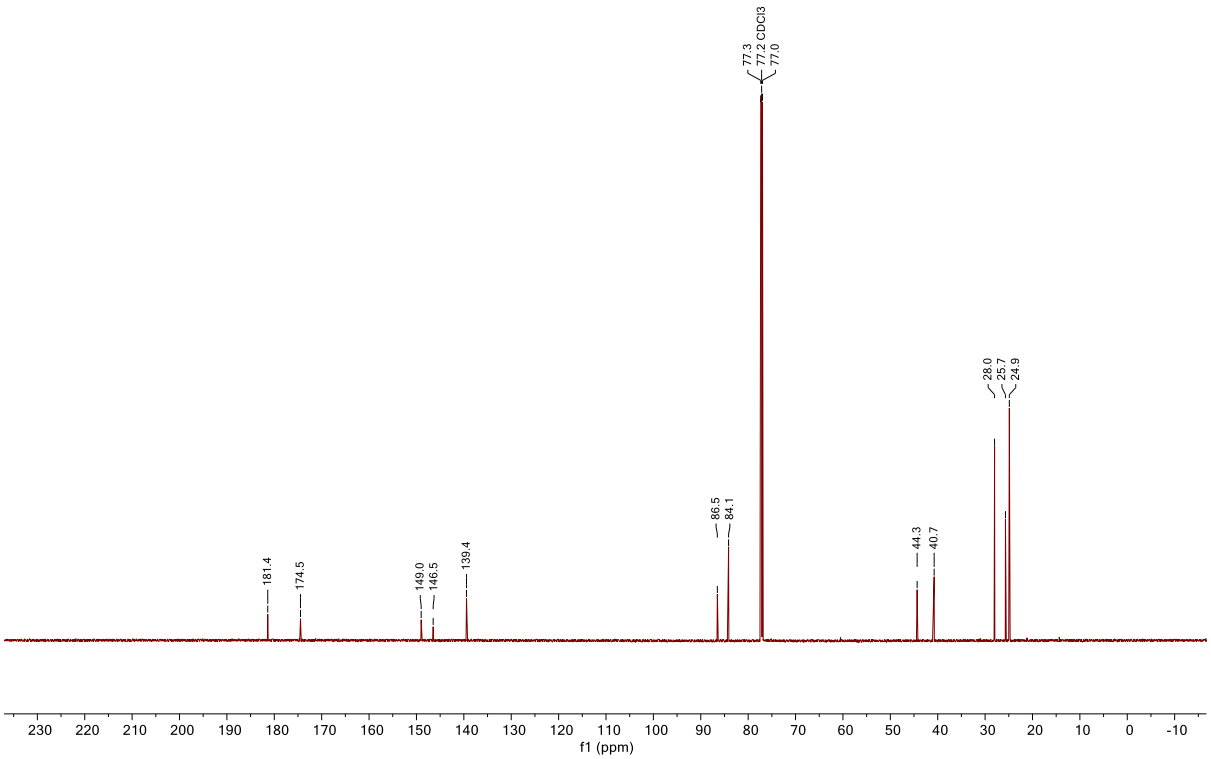
77.3
77.2 CDCl3
77.0
28.0
25.7
24.9
86.5
84.1
44.3
40.7
181.4
174.5
149.0
146.5
139.4
f1 (ppm)

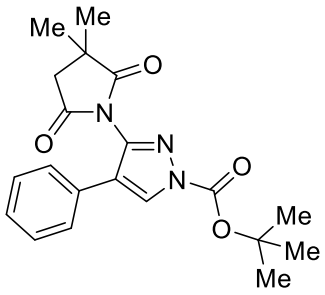

501a

1.66
1.33
8.22
7.37
7.35
7.35
7.34
7.34
7.33
7.33
7.32
7.28
7.28
7.27
7.26
7.26
7.26 CDCl3
2.67
1.07
3.11
1.95
2.32
9.00
6.21
f1 (ppm)

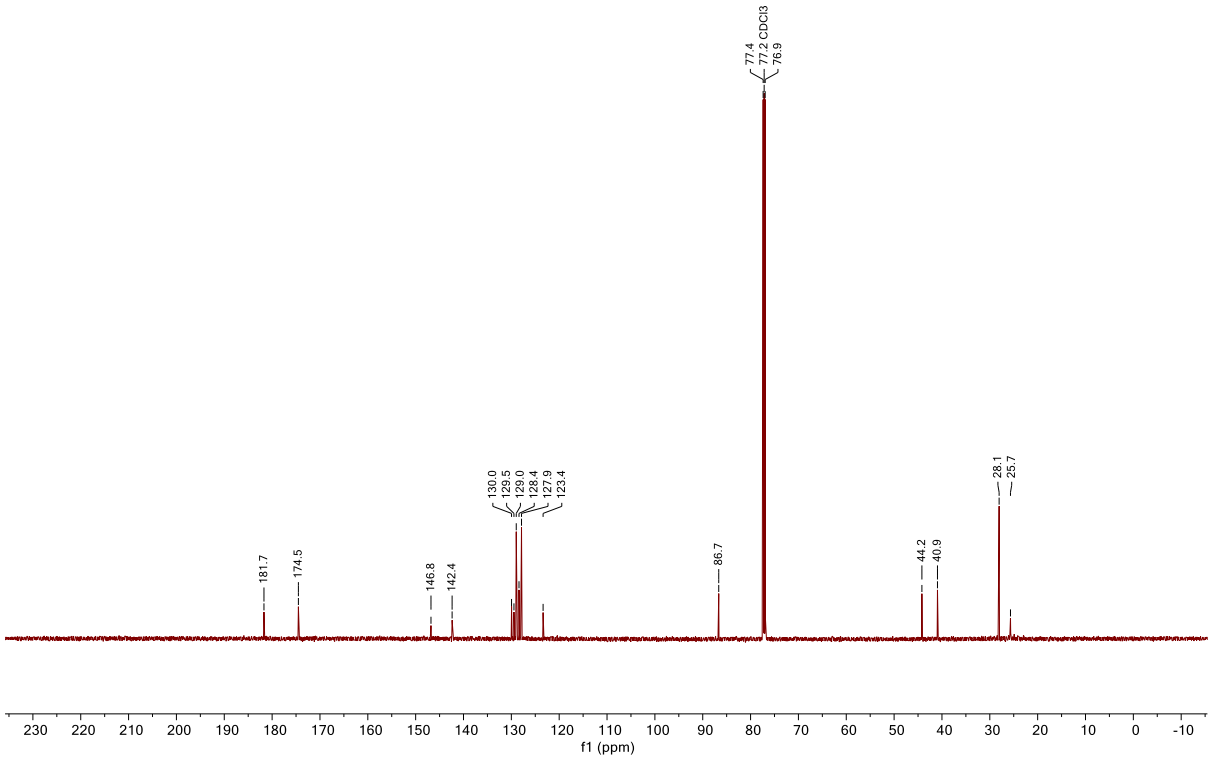
77.4
77.2 CDCl3
76.9
130.0
129.5
129.0
128.4
127.9
123.4
181.7
174.5
146.8
142.4
86.7
44.2
40.9
28.1
25.7
f1 (ppm)

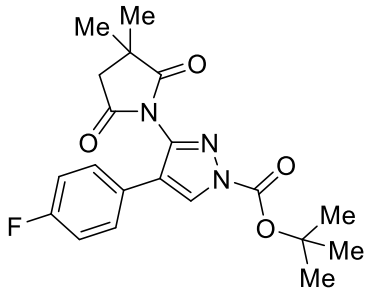
Me
Me
O
N
O
N
N
O
O
Me
Me
Me
F

501b

1.65
1.32
2.67
8.19
7.26 CDCl3
7.25
7.24
7.24
7.23
7.23
7.22
7.05
7.04
7.03
0.93
1.86
1.93
2.00
8.71
6.05
f1 (ppm)

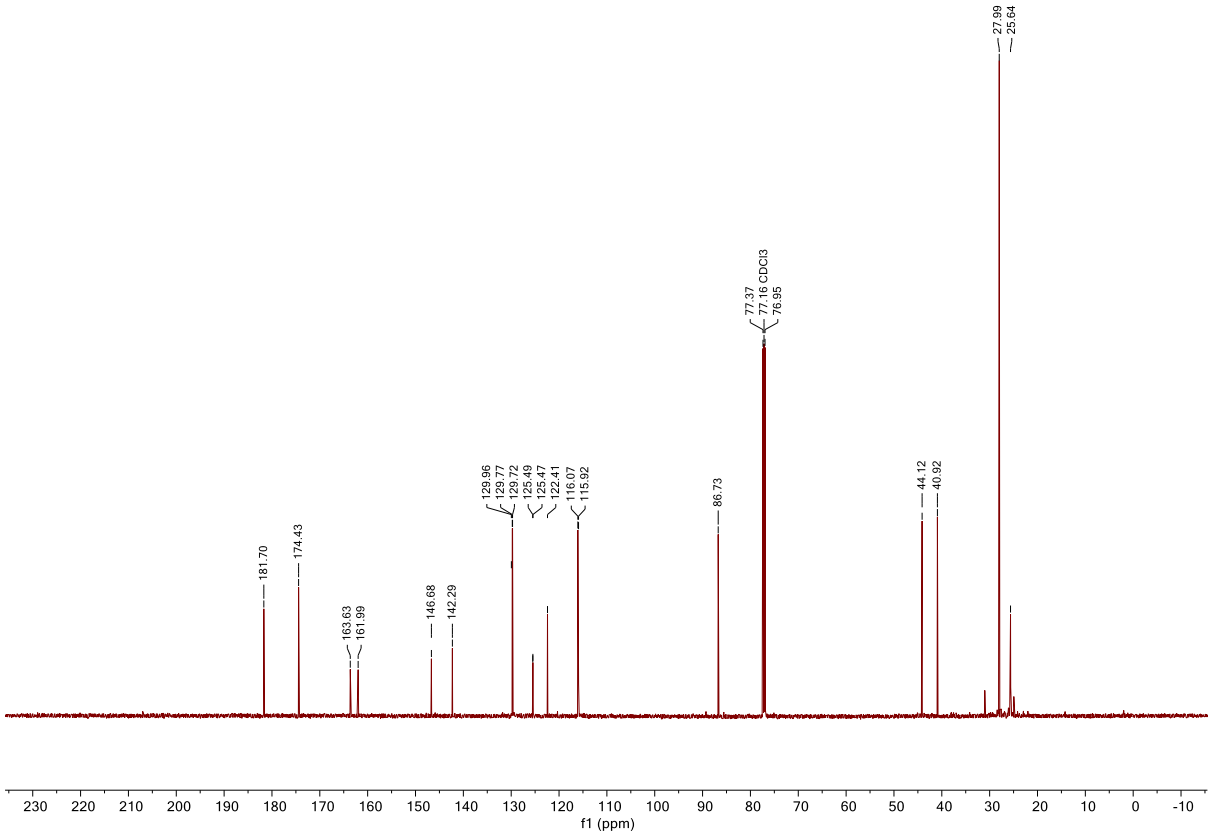
27.99
25.64
77.37
77.16 CDCl3
76.95
129.96
129.77
129.72
125.49
125.47
122.41
116.07
115.92
86.73
44.12
40.92
181.70
174.43
163.63
161.99
146.68
142.29
f1 (ppm)

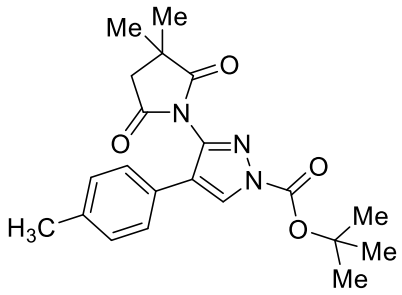
Me
Me
O
N
O
N
N
O
O
Me
Me
Me
H3C

501c

1.65
1.34
7.26 CDCl3
7.15
2.67
2.34
8.19
1.04
4.09
2.05
3.08
9.18
6.00
f1 (ppm)

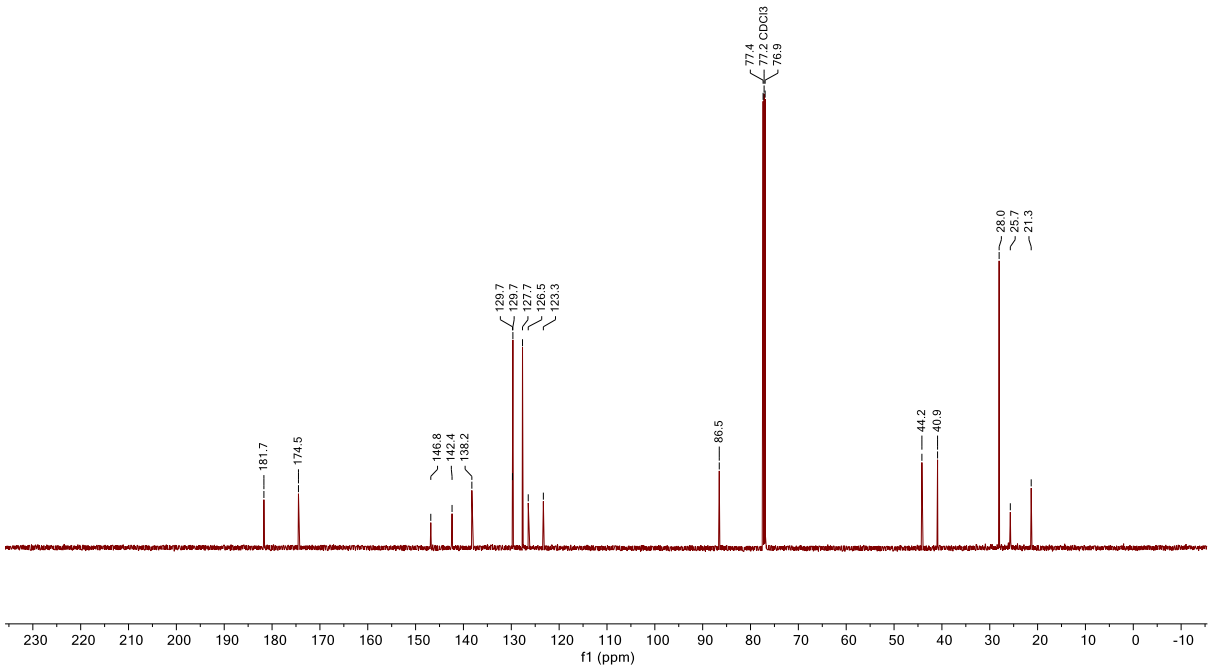
77.4
77.2 CDCl3
76.9
28.0
25.7
21.3
129.7
129.7
127.7
126.5
123.3
181.7
174.5
146.8
142.4
138.2
86.5
44.2
40.9
f1 (ppm)

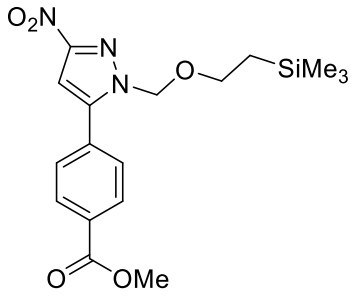
O2N
N
N
O
SiMe3
O
OMe

513

0.01
7.26 CDCl3
7.08
3.96
3.84
3.82
3.81
8.18
8.16
7.76
7.75
0.98
0.96
0.95
1.99
1.97
1.00
2.05
2.94
2.09
2.01
8.88
f1 (ppm)

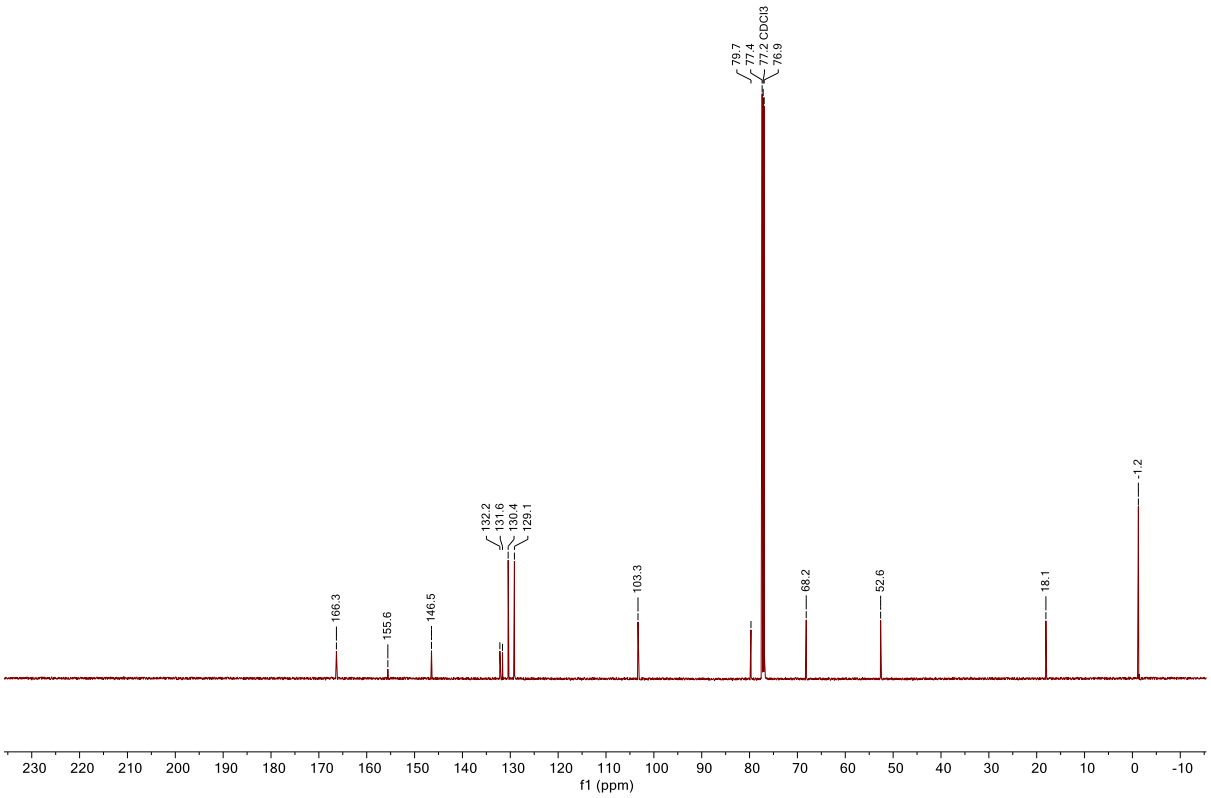
79.7
77.4
77.2 CDCl3
76.9
132.2
131.6
130.4
129.1
166.3
155.6
146.5
103.3
68.2
52.6
18.1
-1.2
f1 (ppm)

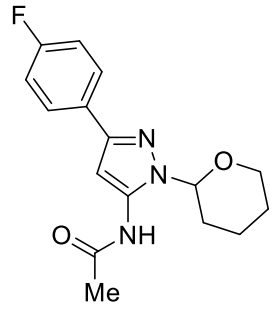
F
N
N
O
O
NH
Me

540

2.31
2.30
2.28
2.27
2.26
2.25
2.20
2.11
2.10
2.09
1.73
1.71
1.69
1.66
1.66
1.64
7.26 CDCl3
7.07
7.05
7.04
6.88
7.77
7.76
7.76
7.75
8.44
5.52
5.52
5.51
5.50
4.00
3.98
3.97
3.97
3.74
3.73
3.72
3.71
3.70
1.02
2.09
2.09
1.00
1.05
1.14
1.05
1.09
2.88
2.32
3.18
f1 (ppm)

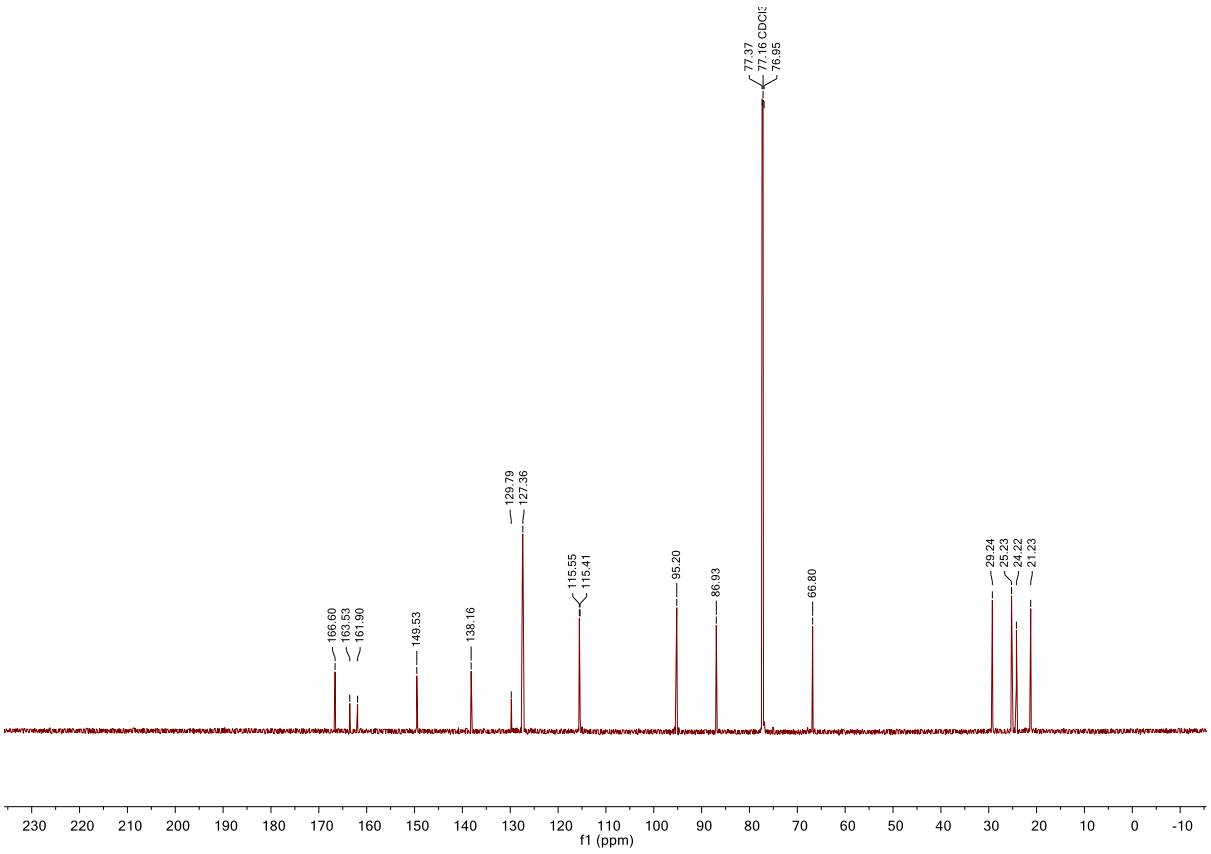
77.37
77.16 CDCl3
76.95
129.79
127.36
115.55
115.41
95.20
86.93
66.80
29.24
25.23
24.22
21.23
166.60
163.53
161.90
149.53
138.16
f1 (ppm)

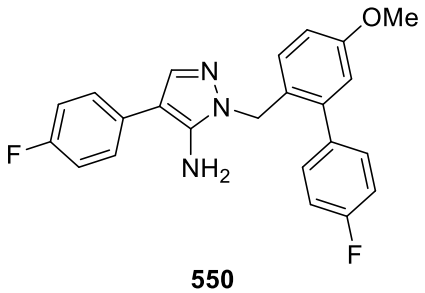
OMe
N
N
F
NH2
F

550

3.80
5.07
7.43
7.31
7.30
7.30
7.29
7.28
7.27
7.27
7.26
7.26 CDCl3
7.26
7.15
7.14
7.12
7.12
7.10
7.07
7.06
7.04
6.89
6.89
6.88
6.88
6.79
6.79
1.00
2.09
2.17
2.12
0.99
2.00
1.04
0.97
2.05
3.33
13 12 11 10 9 8 7 6 5 4 3 2 1 0 -1
f1 (ppm)

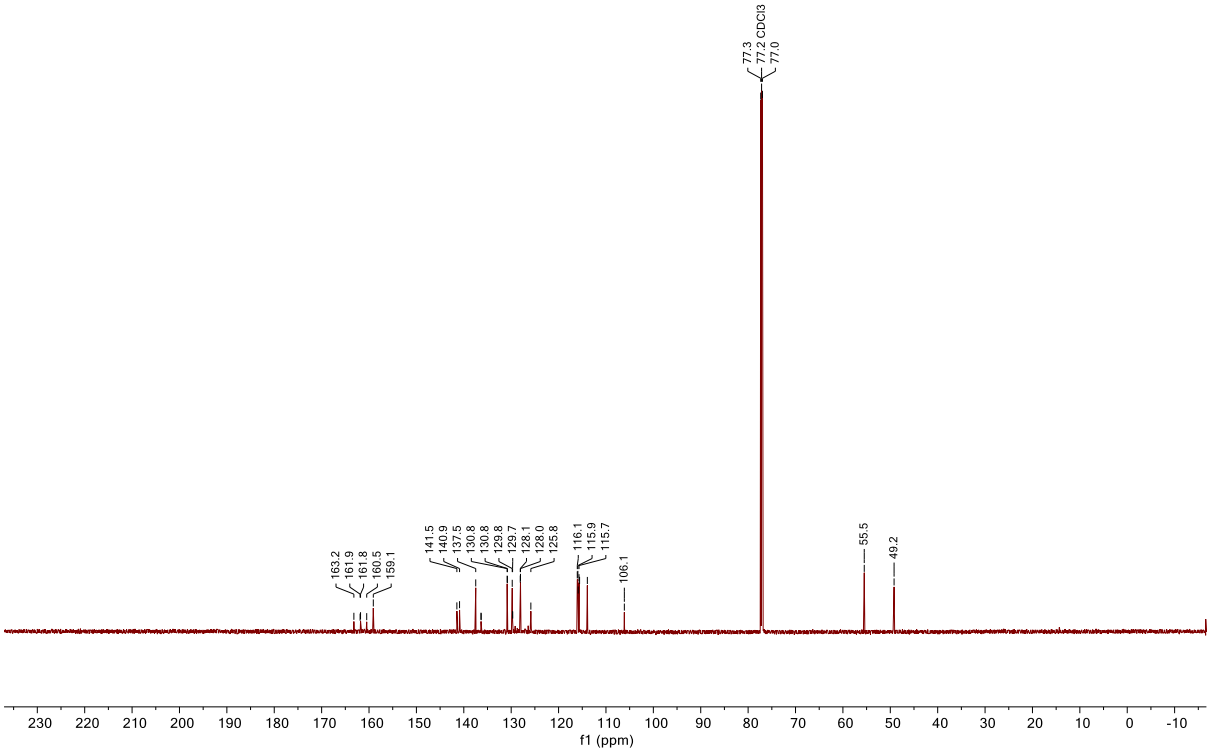
77.3
77.2 CDCl3
77.0
163.2
161.9
161.8
160.5
159.1
141.5
140.9
137.5
130.8
130.8
129.8
129.7
128.1
128.0
125.8
116.1
115.9
115.7
106.1
55.5
49.2
230 220 210 200 190 180 170 160 150 140 130 120 110 100 90 80 70 60 50 40 30 20 10 0 -10
f1 (ppm)

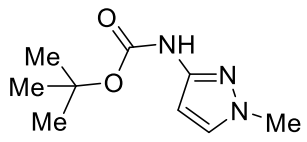
O
NH
Me
Me
O
N
Me
N
Me

376

3.80
1.49
7.26
7.19
8.55
8.39
6.45
0.30
0.74
1.00
1.02
3.04
8.73
13 12 11 10 9 8 7 6 5 4 3 2 1 0 -1
f1 (ppm)

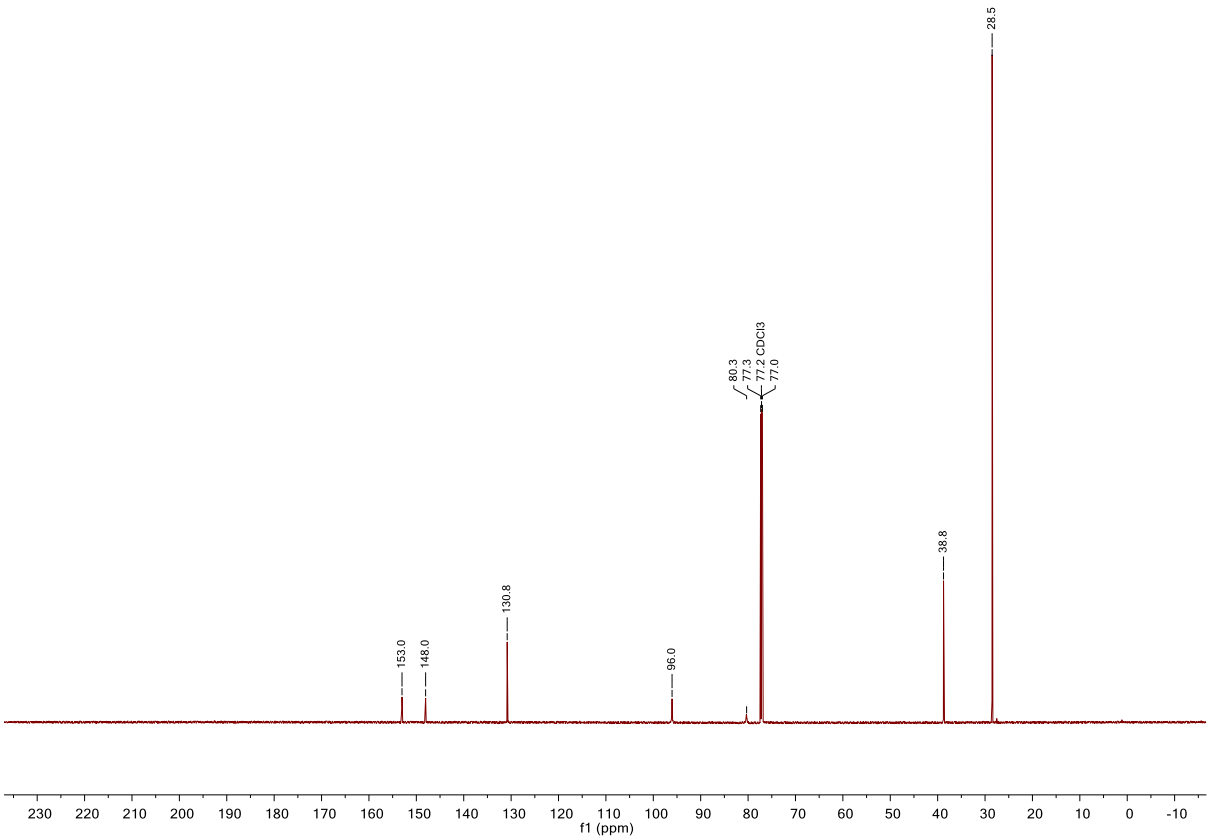
28.5
80.3
77.3
77.2 CDCl3
77.0
38.8
130.8
153.0
148.0
96.0
230 220 210 200 190 180 170 160 150 140 130 120 110 100 90 80 70 60 50 40 30 20 10 0 -10
f1 (ppm)

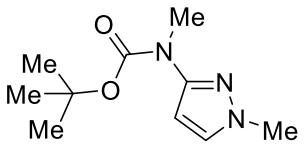
O
Me
N
Me
Me
O
N
Me
Me

376b

1.47
3.74
3.28
7.26 CDCl3
7.16
7.15
6.33
1.00
1.24
3.10
3.04
8.91
f1 (ppm)

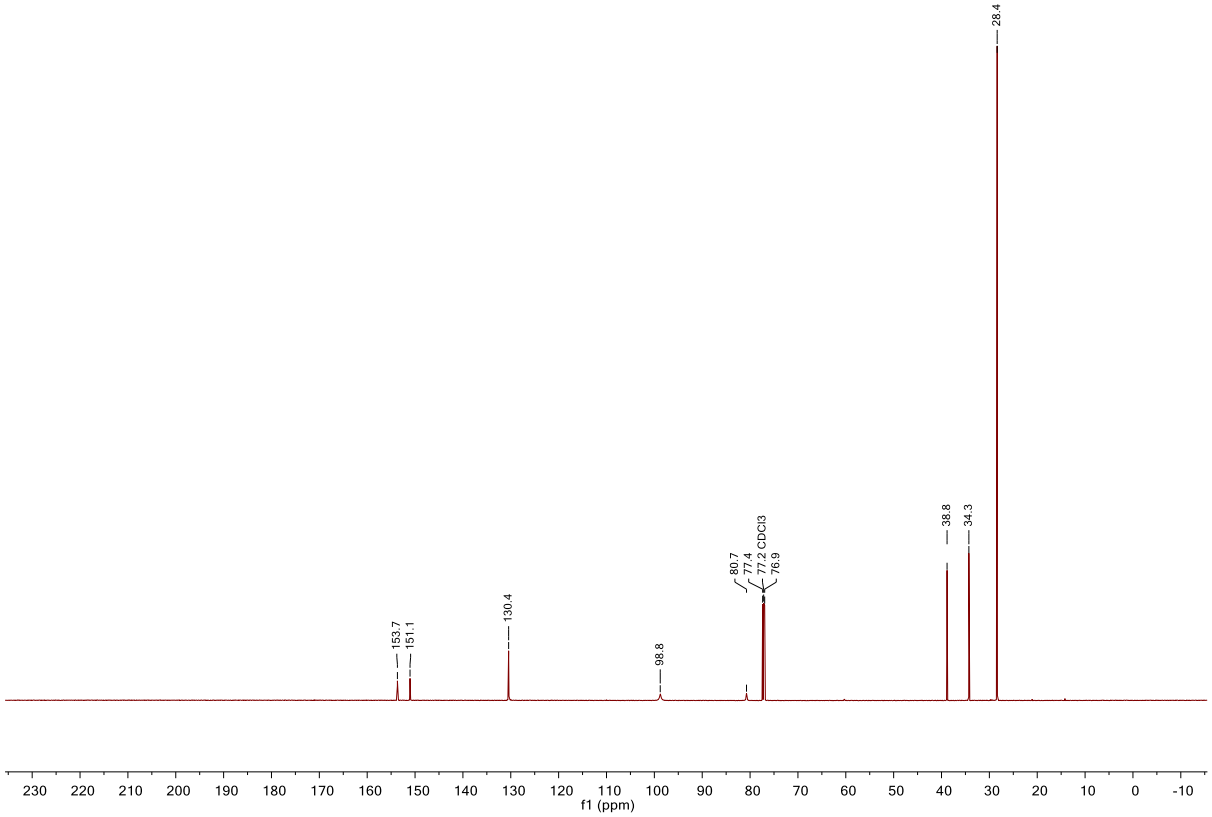
28.4
38.8
34.3
80.7
77.4
77.2 CDCl3
76.9
153.7
151.1
130.4
98.8
f1 (ppm)

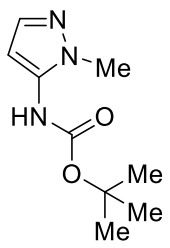
N
N
Me
HN
O
O
Me
Me
Me

383

1.47
3.70
7.34
7.34
7.26 CDCl3
6.87
6.09
1.03
1.00
1.06
3.13
9.00
13
12
11
10
9
8
7
6
5
4
3
2
1
0
-1
f1 (ppm)

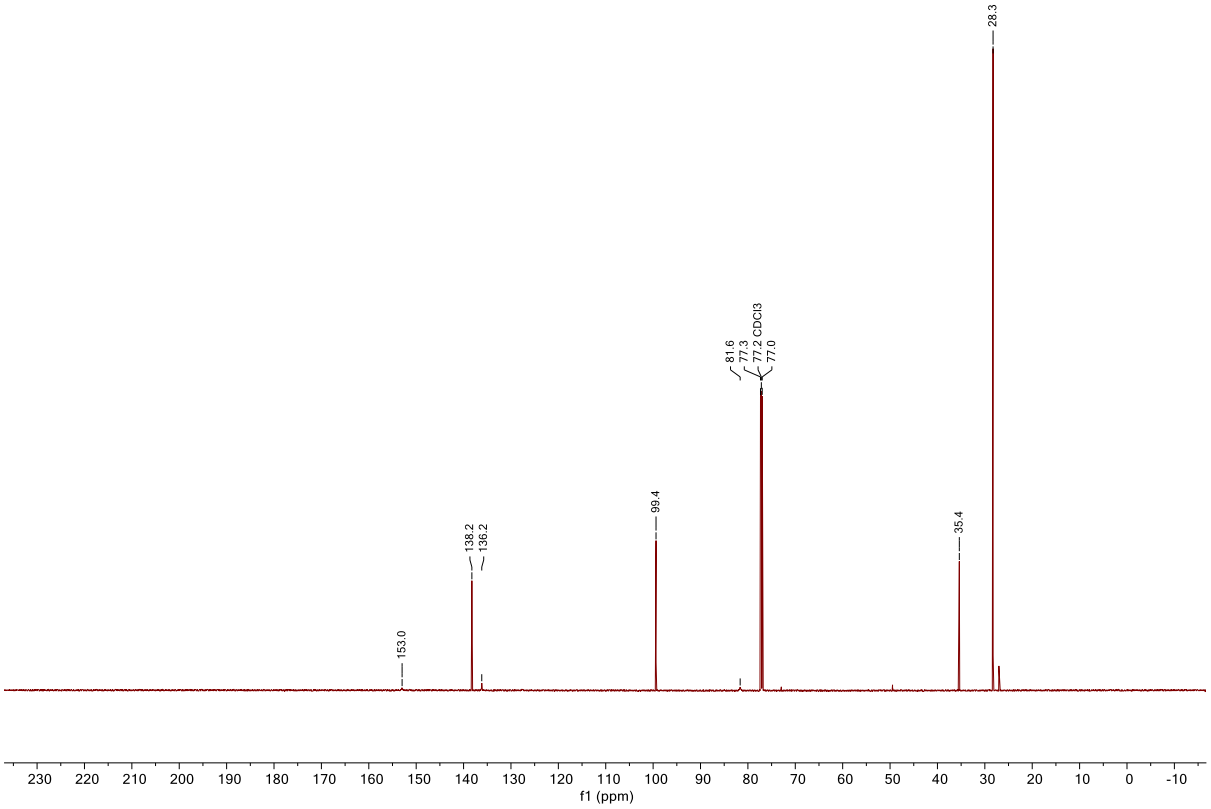
28.3
81.6
77.3
77.2 CDCl3
77.0
99.4
138.2
136.2
35.4
153.0
230
220
210
200
190
180
170
160
150
140
130
120
110
100
90
80
70
60
50
40
30
20
10
0
-10
f1 (ppm)

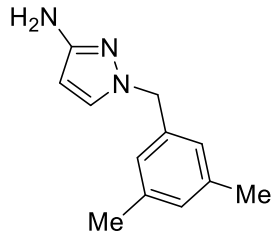
H2N
N
N
Me
Me

402

2.28
7.26 CDCl3
7.13
7.13
6.91
6.82
5.61
5.61
5.01
3.44
1.00
1.03
2.00
1.05
2.09
1.97
6.30
13 12 11 10 9 8 7 6 5 4 3 2 1 0 -1
f1 (ppm)

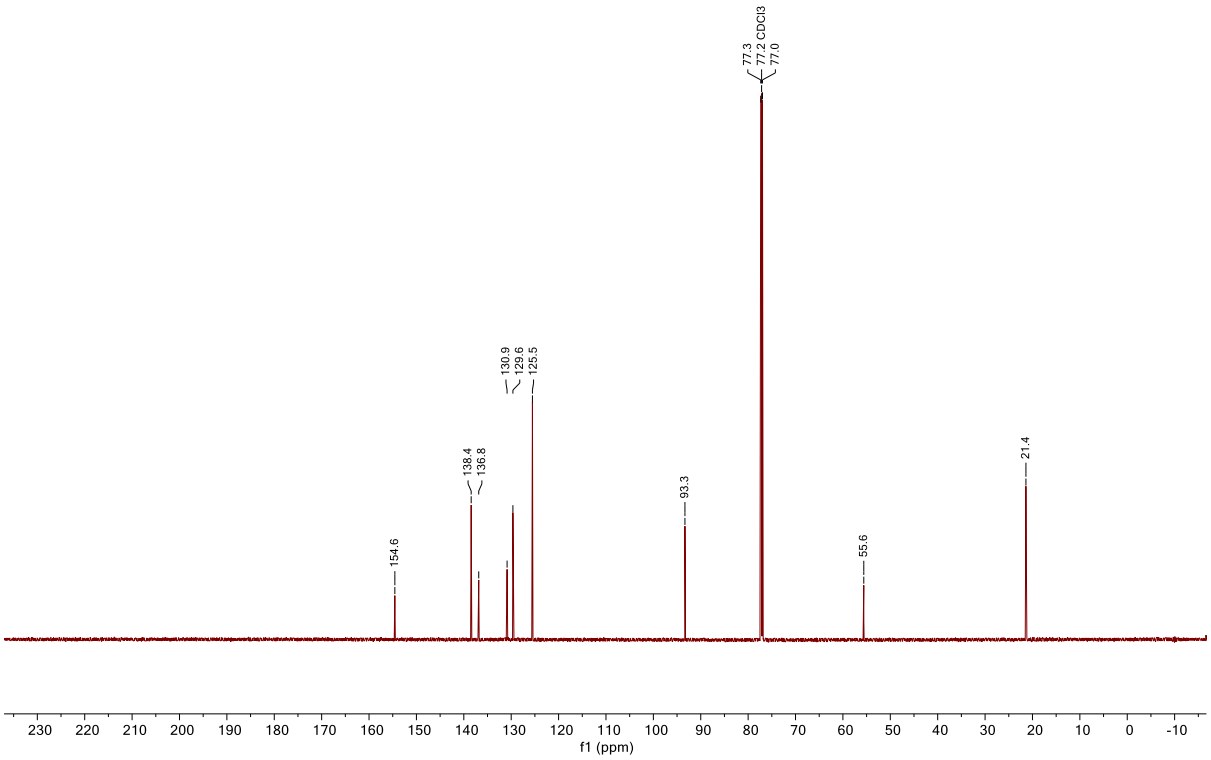
77.3
77.2 CDCl3
77.0
130.9
129.6
125.5
138.4
136.8
154.6
93.3
55.6
21.4
230 220 210 200 190 180 170 160 150 140 130 120 110 100 90 80 70 60 50 40 30 20 10 0 -10
f1 (ppm)

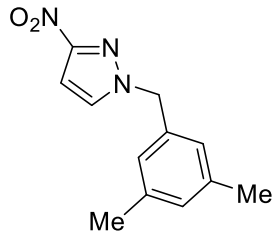
O2N
N
N
Me
Me

403

2.30
5.28
7.39
7.38
7.26 CDCl3
6.99
6.90
6.88
6.88
1.00
1.01
1.97
1.00
2.00
5.98
13 12 11 10 9 8 7 6 5 4 3 2 1 0 -1
f1 (ppm)

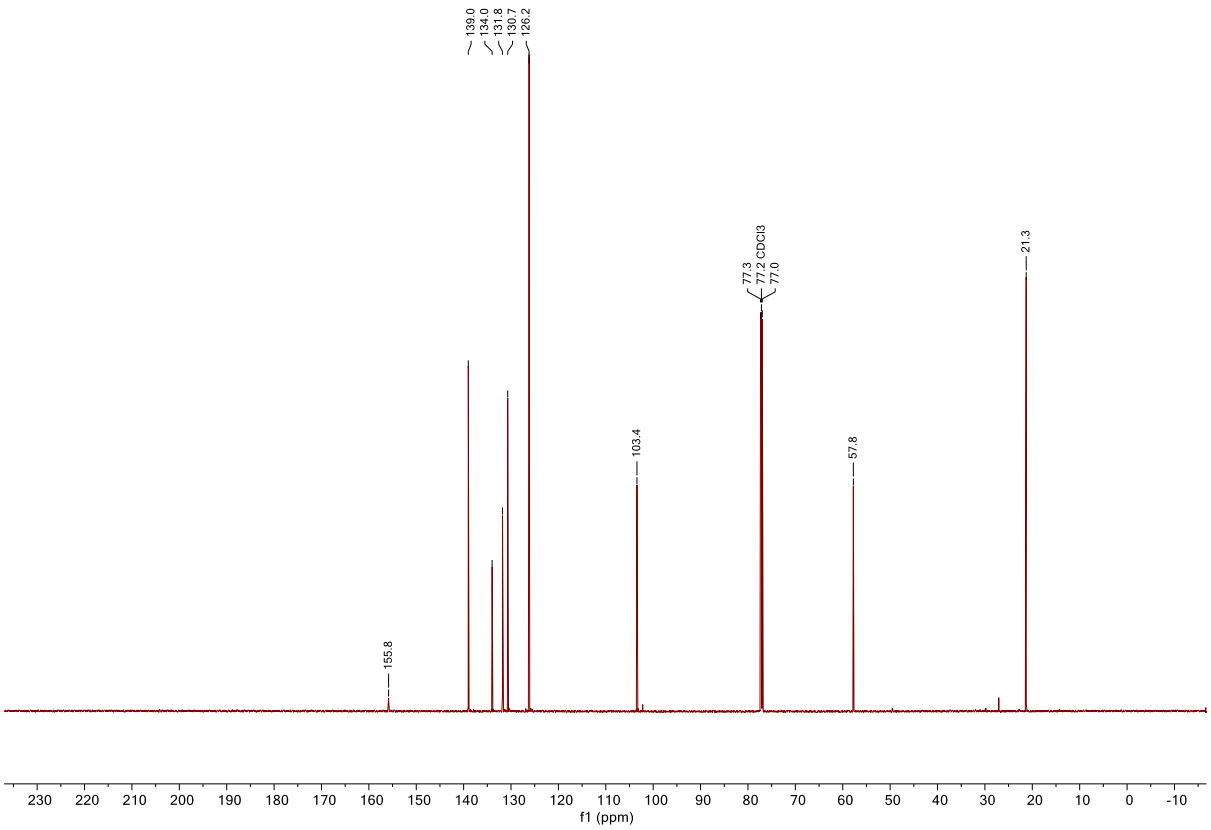
139.0
134.0
131.8
130.7
126.2
77.3
77.2 CDCl3
77.0
21.3
103.4
57.8
155.8
230 220 210 200 190 180 170 160 150 140 130 120 110 100 90 80 70 60 50 40 30 20 10 0 -10
f1 (ppm)

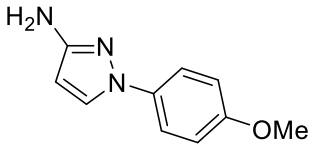
H2N
N
N
OMe

410

3.75
2.50 DMSO-d6
7.99
7.99
7.55
7.54
6.96
6.95
5.67
5.67
4.92
0.89
1.78
1.80
0.89
1.63
2.80
f1 (ppm)

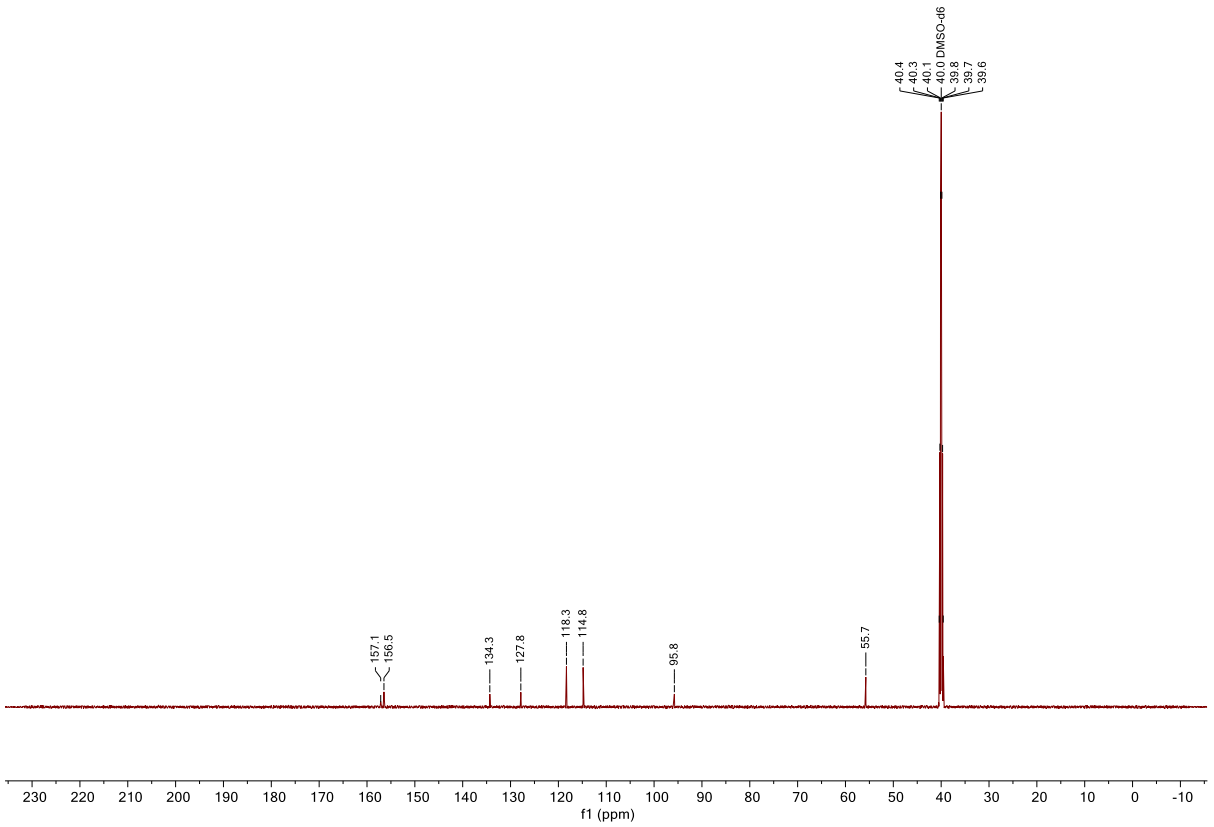
40.4
40.3
40.1
40.0 DMSO-d6
39.8
39.7
39.6
157.1
156.5
134.3
127.8
118.3
114.8
95.8
55.7
f1 (ppm)

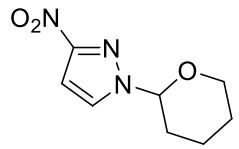
O2N
N
N
O

413

7.70
7.69
7.26 CDCl3
6.92
6.91
5.45
5.44
5.43
5.43
4.06
4.06
4.05
4.04
4.04
4.03
4.03
3.72
3.72
3.71
3.71
3.70
3.70
3.69
3.68
2.16
2.15
2.14
2.05
2.03
2.03
2.02
2.01
2.01
2.00
2.00
1.99
1.99
1.99
1.71
1.70
1.70
1.69
1.69
1.68
1.68
1.67
1.66
1.66
1.65
1.64
1.64
1.63
0.94
0.94
0.95
0.95
1.01
0.99
2.07
3.49
f1 (ppm)

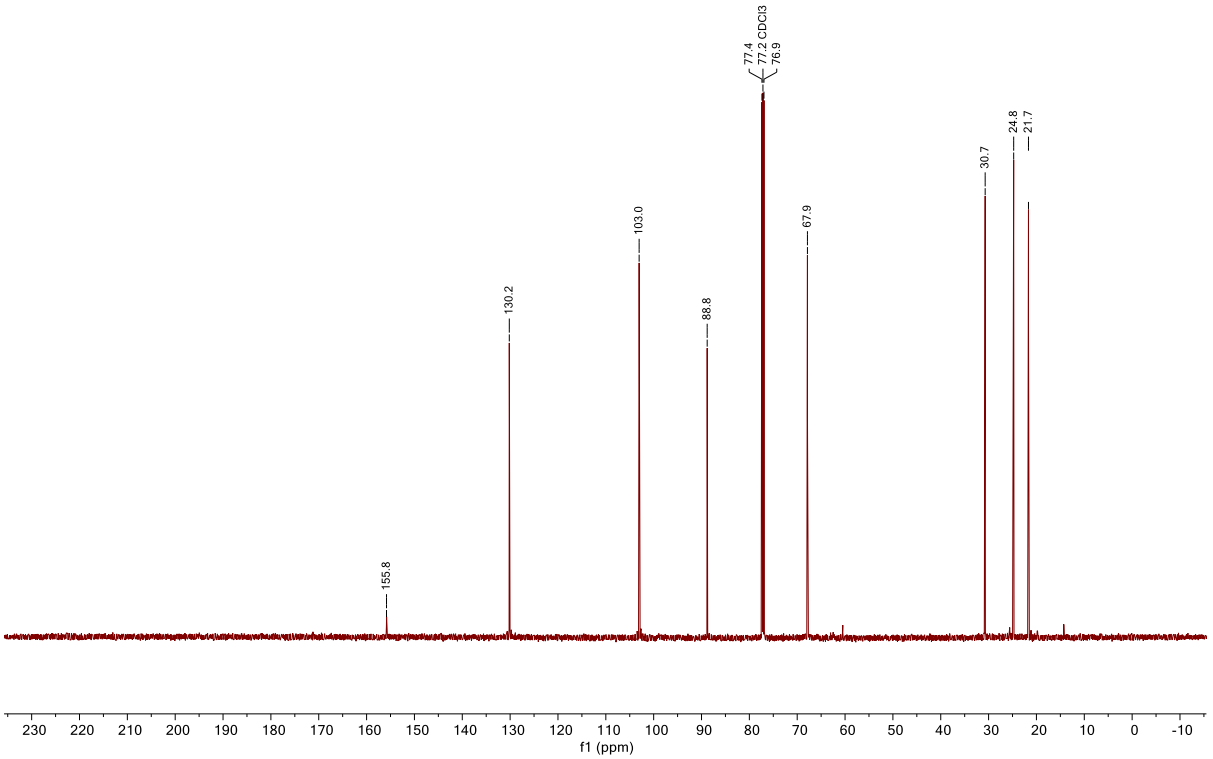
155.8
130.2
103.0
88.8
77.4
77.2 CDCl3
76.9
67.9
30.7
24.8
21.7
f1 (ppm)

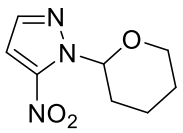

414

7.56
7.56
7.07
7.06
6.18
6.17
6.16
6.16
3.99
3.97
3.74
3.73
3.72
3.71
3.70
3.69
2.42
2.41
2.39
2.37
2.37
2.13
2.12
2.11
2.11
2.10
2.05
2.05
2.03
2.03
1.76
1.75
1.74
1.73
1.73
1.71
1.70
1.67
1.67
1.65
1.61
1.60
0.97
0.97
0.98
1.08
0.99
1.00
0.99
1.09
3.53
f1 (ppm)

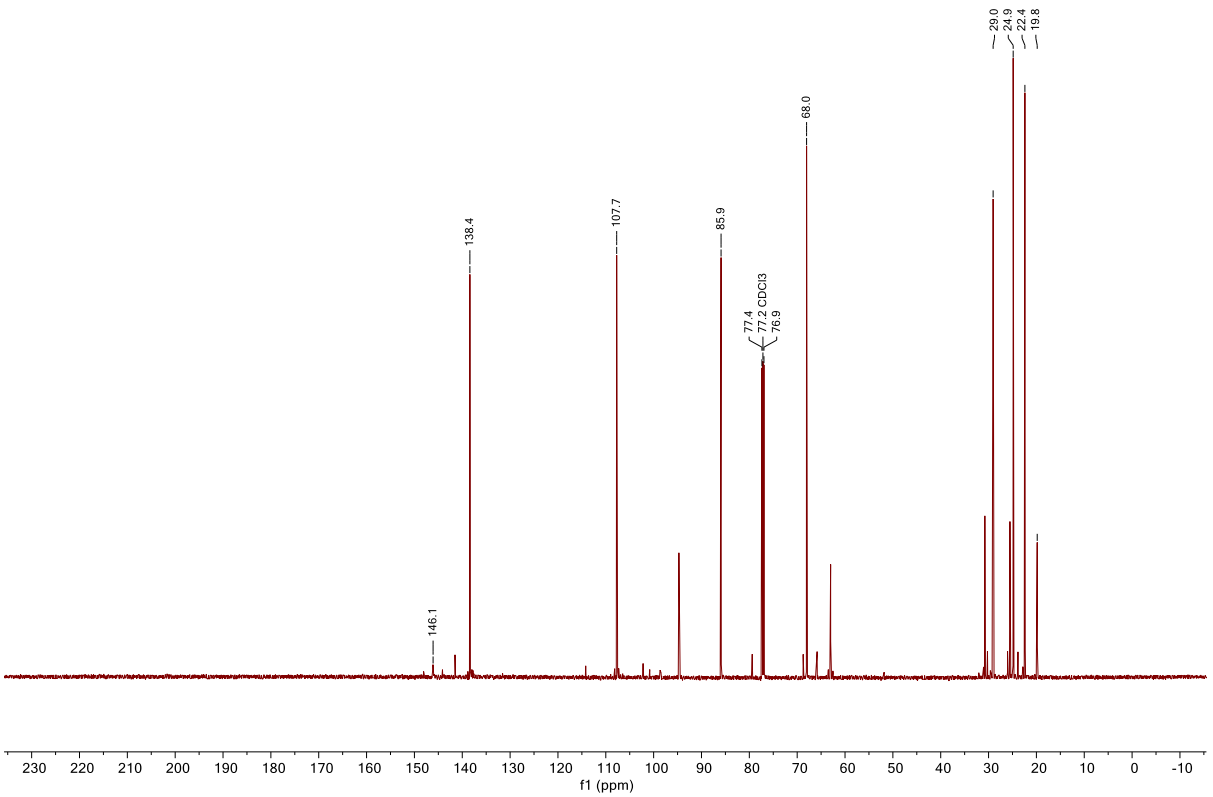
29.0
24.9
22.4
19.8
68.0
138.4
107.7
85.9
77.4
77.2 CDCl3
76.9
146.1
f1 (ppm)

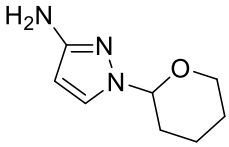

418

7.32
7.31
7.26 CDCl3
5.64
5.63
5.11
5.11
5.10
5.09
4.06
4.05
4.05
4.04
4.04
4.03
4.03
4.03
3.65
3.64
3.63
3.62
3.54
2.09
2.07
2.07
2.01
2.01
2.00
2.00
1.97
1.97
1.97
1.95
1.94
1.66
1.66
1.66
1.65
1.65
1.64
1.64
1.64
1.63
1.62
1.55
1.55
1.55
1.53
1.00
1.00
1.01
1.04
1.10
2.02
1.06
2.01
2.11
1.09
f1 (ppm)

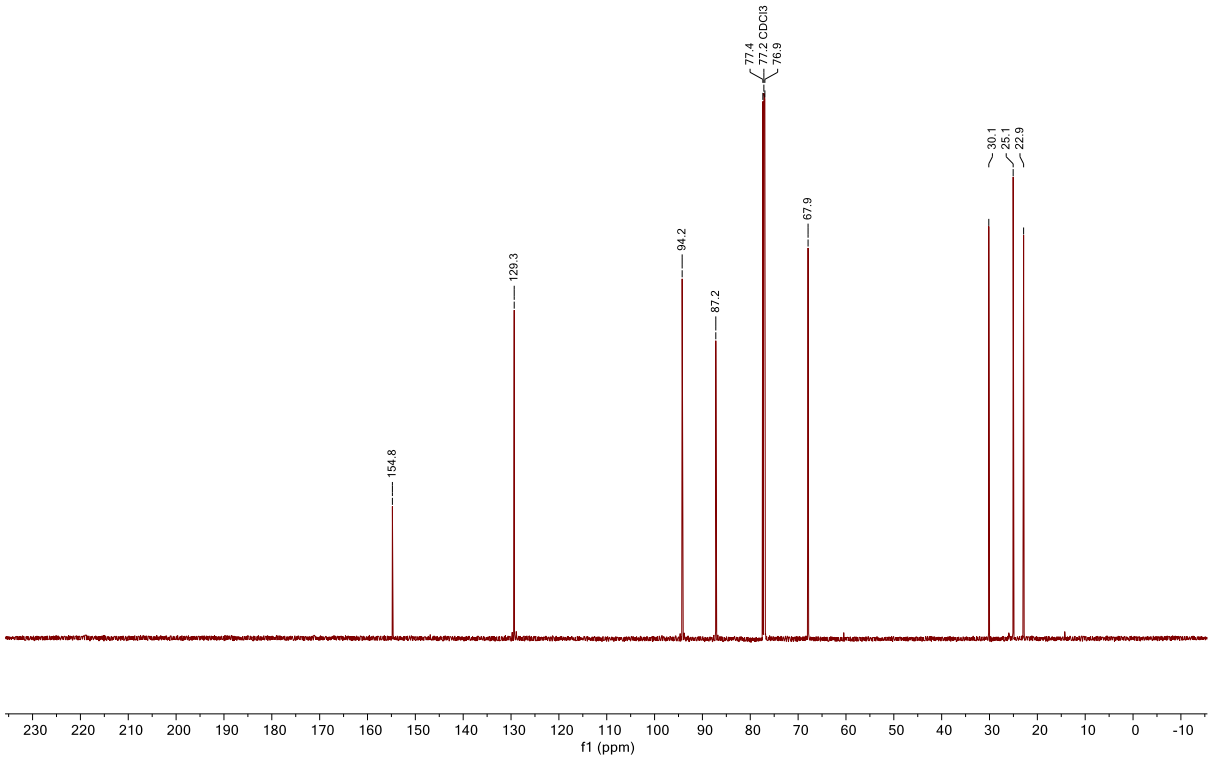
77.4
77.2 CDCl3
76.9
67.9
30.1
25.1
22.9
94.2
87.2
129.3
154.8
f1 (ppm)

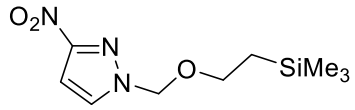
O2N
N
N
O
SiMe3

449

7.66
7.66
7.26 CDCl3
6.97
6.96
5.49
3.61
3.60
3.59
0.92
0.91
0.90
-0.03
1.00
1.00
2.00
2.01
8.90
f1 (ppm)

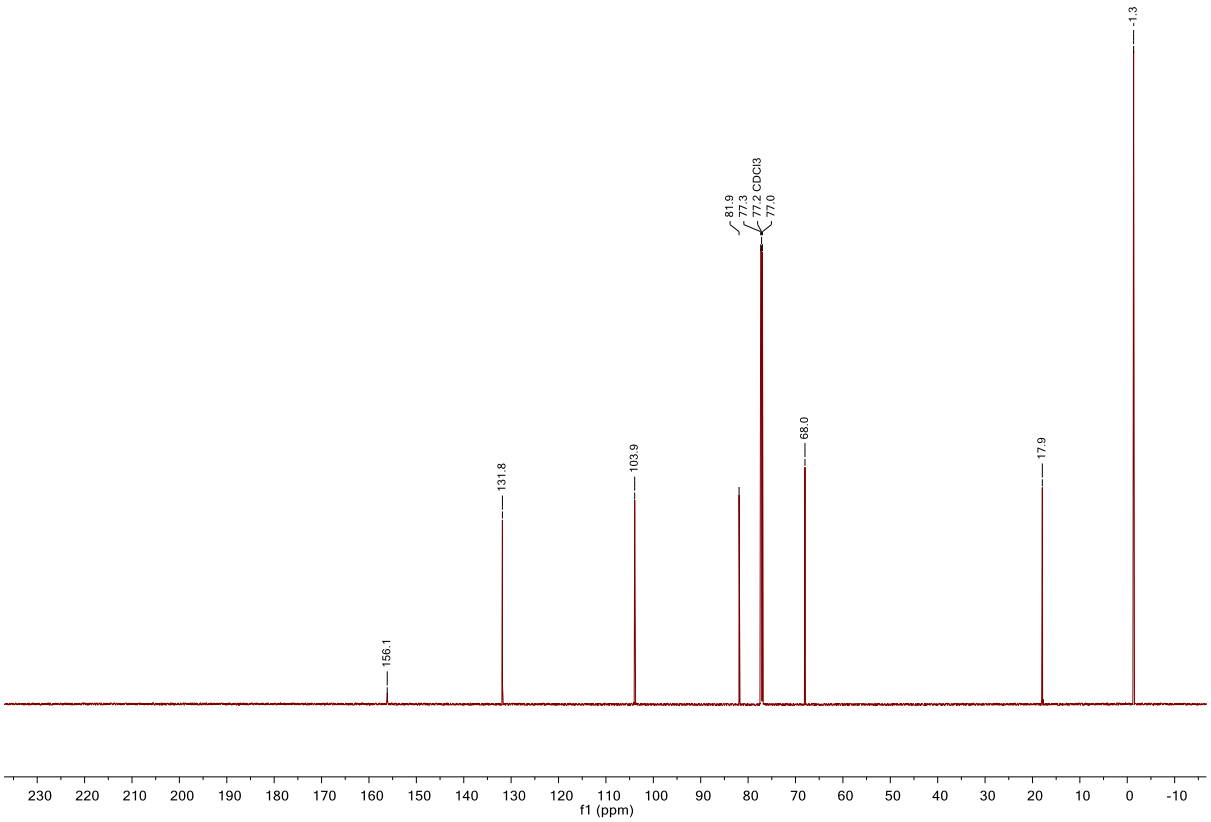
156.1
131.8
103.9
81.9
77.3
77.2 CDCl3
77.0
68.0
17.9
-1.3
f1 (ppm)

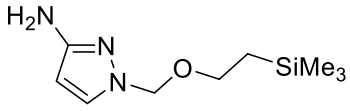
H2N
N
N
O
SiMe3

450

0.03
5.20
7.28
7.28
7.26 CDCl3
5.68
5.67
3.76
3.55
3.53
3.52
0.90
0.89
0.88
13 12 11 10 9 8 7 6 5 4 3 2 1 0 -1
f1 (ppm)

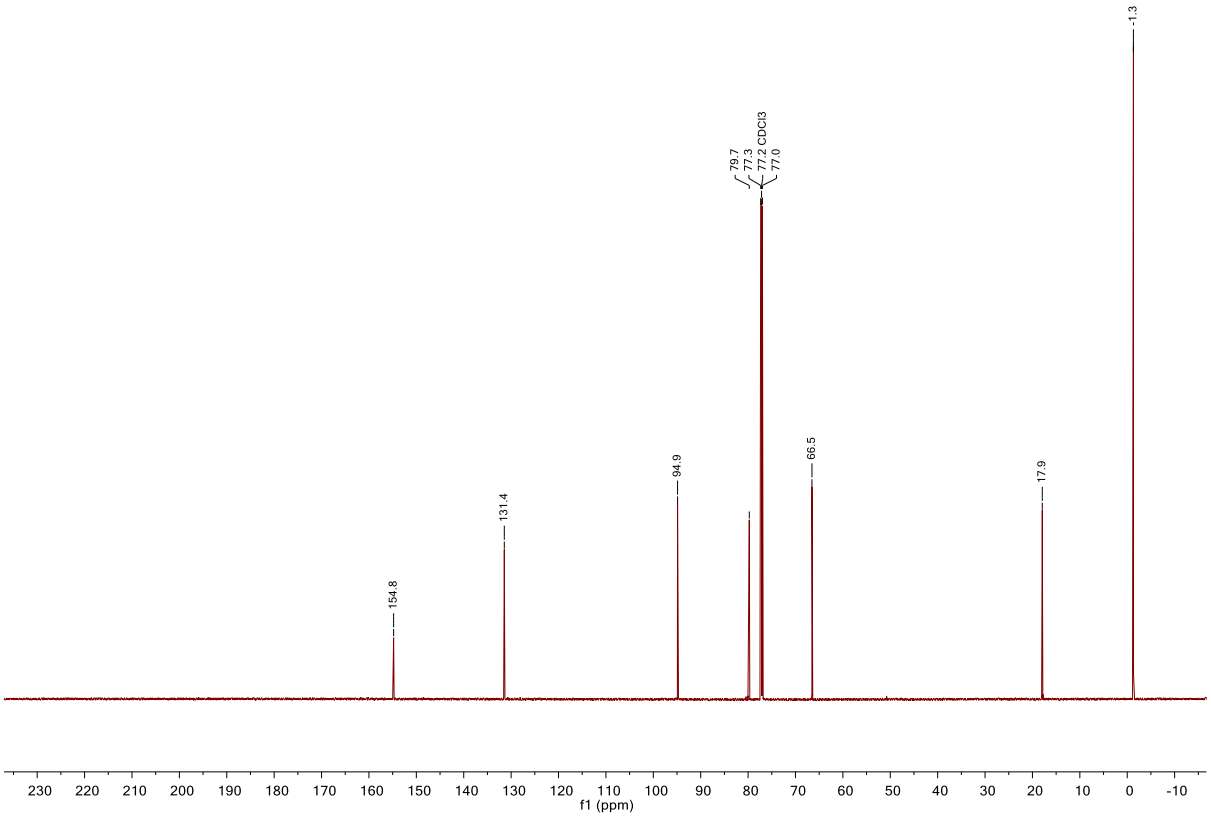
-1.3
79.7
77.3
77.2 CDCl3
77.0
66.5
94.9
131.4
154.8
17.9
230 220 210 200 190 180 170 160 150 140 130 120 110 100 90 80 70 60 50 40 30 20 10 0 -10
f1 (ppm)

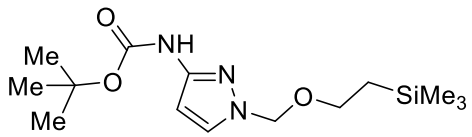
O
NH
Me
Me
Me
O
N
N
O
SiMe3

452

-0.04
1.51
5.29
7.49
7.41
7.40
7.26
6.56
3.54
3.52
3.50
0.91
0.89
0.87
1.00
1.02
0.95
2.37
2.28
9.72
9.52
f1 (ppm)

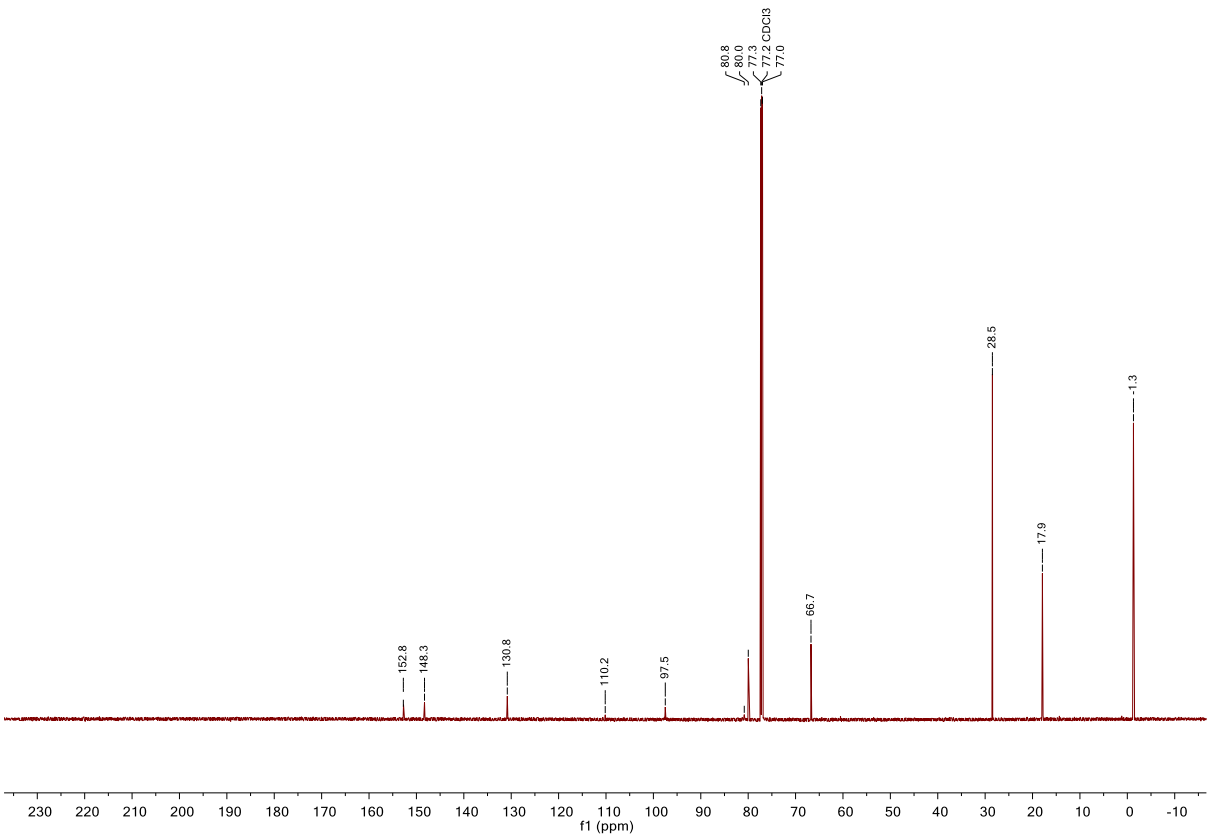
80.8
80.0
77.3
77.2 CDCl3
77.0
28.5
-1.3
17.9
66.7
152.8
148.3
130.8
110.2
97.5
f1 (ppm)

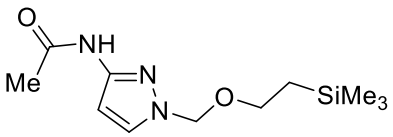
O
NH
Me
N
N
O
SiMe3

458

8.19
7.44
7.43
7.26 CDCl3
6.78
6.77
5.28
3.53
3.52
3.50
2.15
0.90
0.89
0.88
-0.03
0.94
1.00
1.00
2.06
1.97
2.96
2.00
8.64
f1 (ppm)

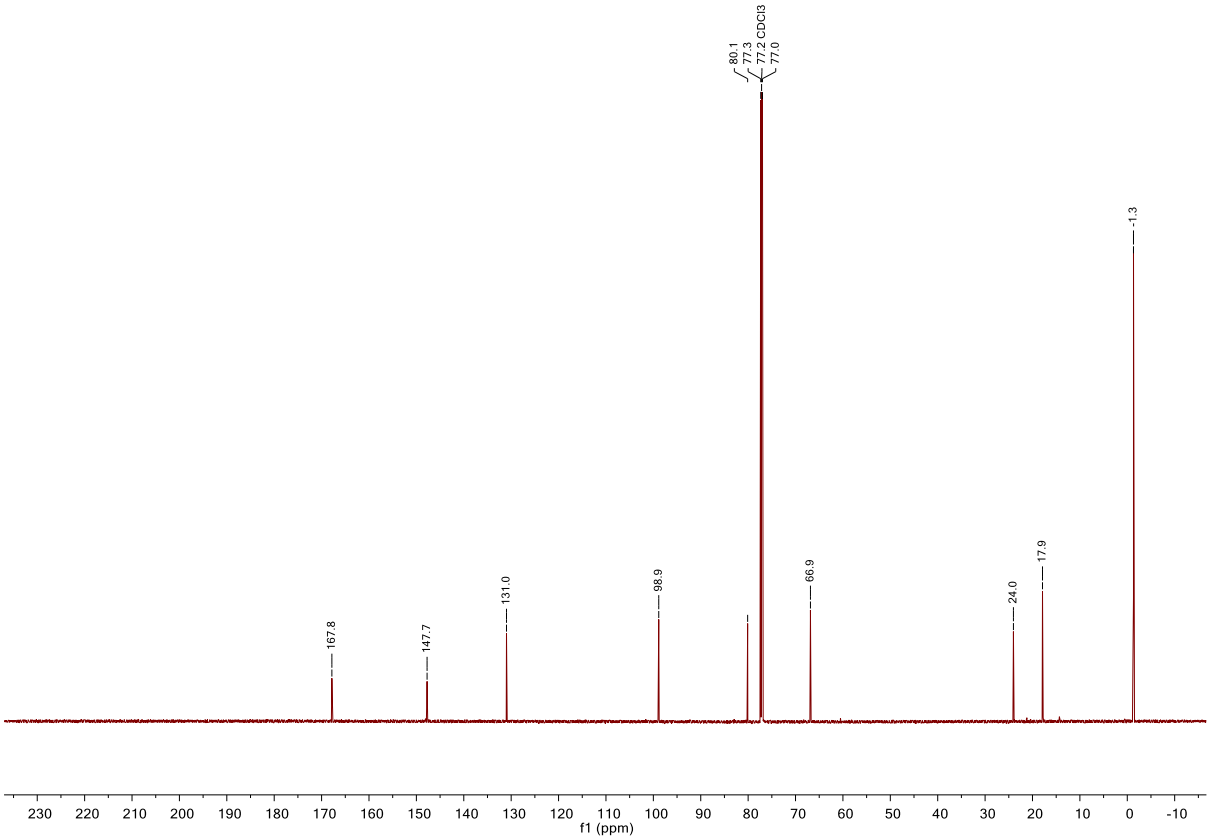
80.1
77.3
77.2 CDCl3
77.0
167.8
147.7
131.0
98.9
66.9
24.0
17.9
-1.3
f1 (ppm)

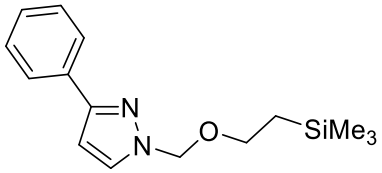
N
N
O
SiMe3

466a

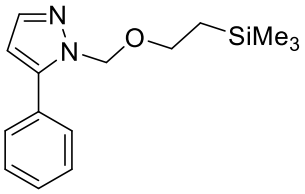
N
N
O
SiMe3

466b

0.00
-0.01
7.84
7.83
7.64
7.63
7.59
7.59
7.58
7.47
7.46
7.44
7.42
7.41
7.40
7.32
7.31
7.30
7.26 CDCl3
6.64
6.64
6.41
6.41
3.77
3.76
3.74
3.65
3.64
3.63
0.97
0.95
0.94
0.93
13
12
11
10
9
8
7
6
5
4
3
2
1
0
-1
f1 (ppm)

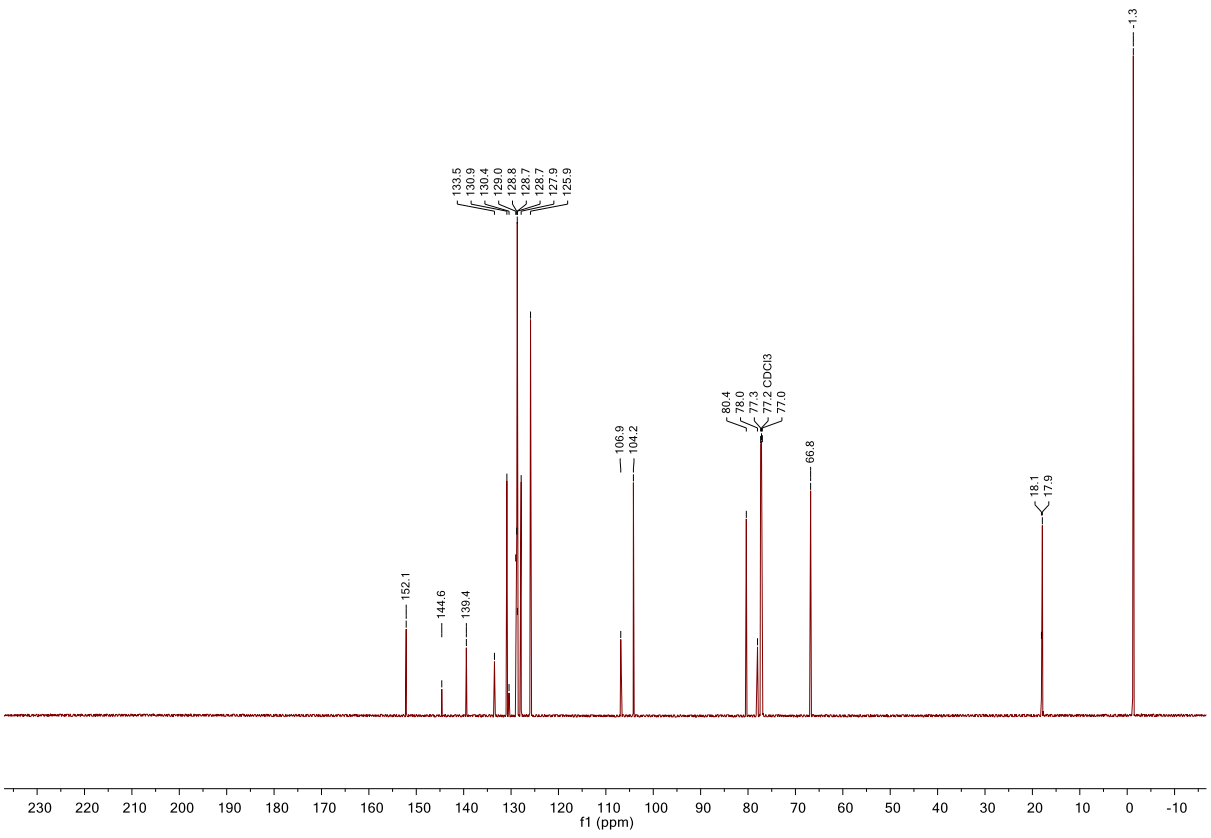
-1.3
133.5
130.9
130.4
129.0
128.8
128.7
127.9
125.9
106.9
104.2
80.4
78.0
77.3
77.2 CDCl3
77.0
66.8
18.1
17.9
152.1
144.6
139.4
230
220
210
200
190
180
170
160
150
140
130
120
110
100
90
80
70
60
50
40
30
20
10
0
-10
f1 (ppm)

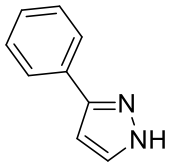
N
NH

467

7.76
7.76
7.62
7.43
7.42
7.41
7.35
7.34
7.33
7.26 CDCl3
6.62
1.94
1.00
1.96
1.00
0.98
13 12 11 10 9 8 7 6 5 4 3 2 1 0 -1
f1 (ppm)

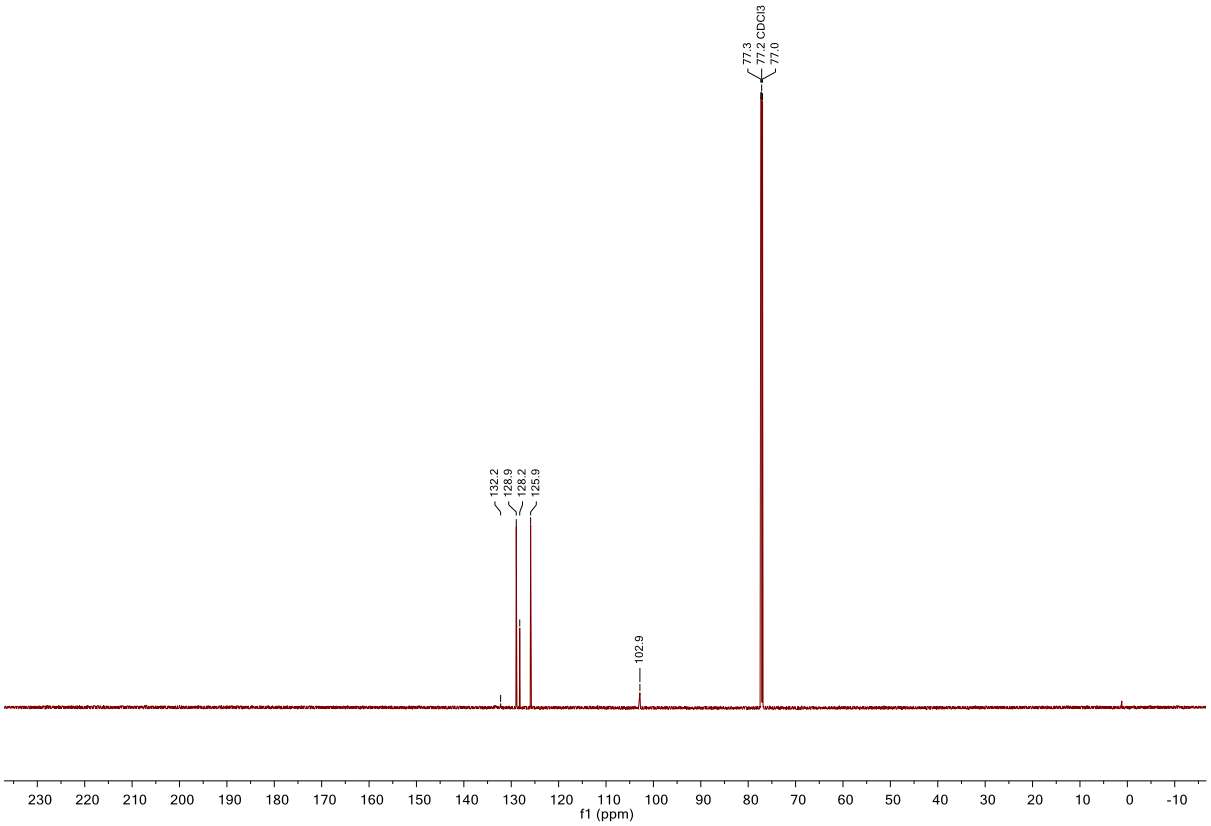
77.3
77.2 CDCl3
77.0
132.2
128.9
128.2
125.9
102.9
230 220 210 200 190 180 170 160 150 140 130 120 110 100 90 80 70 60 50 40 30 20 10 0 -10
f1 (ppm)

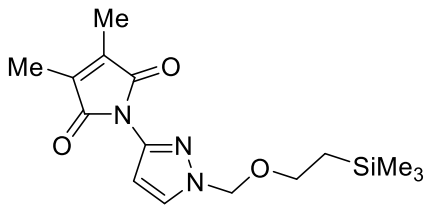
Me
Me
O
O
N
N
N
O
SiMe3

470

-0.04
2.02
5.41
7.59
7.59
7.26 CDCl3
6.37
6.37
3.60
3.59
3.57
0.90
0.89
0.88
1.00
1.03
1.93
1.97
5.83
2.01
8.54
f1 (ppm)

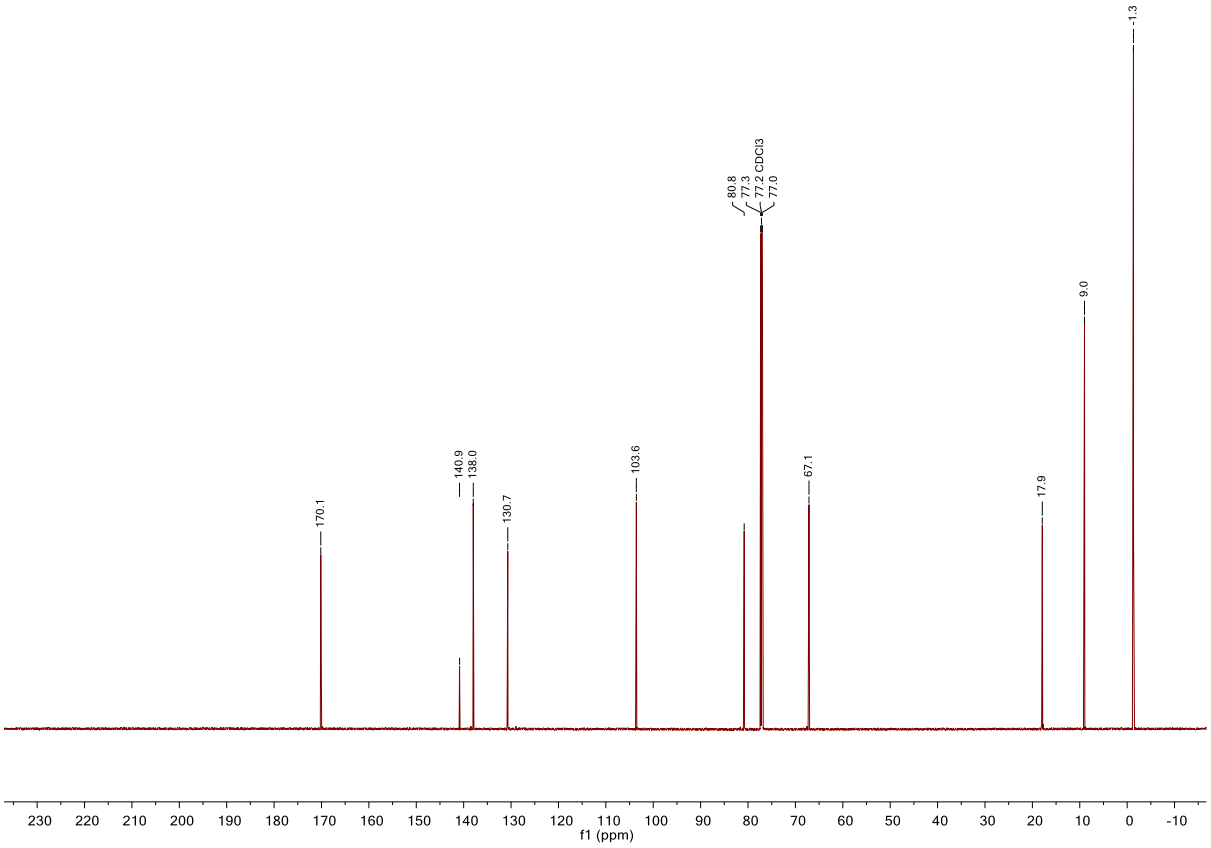
-1.3
80.8
77.3
77.2 CDCl3
77.0
9.0
140.9
138.0
103.6
67.1
170.1
130.7
17.9
f1 (ppm)

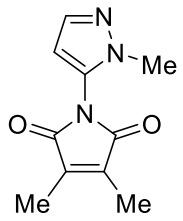
N
N
Me
N
O
O
Me
Me

471

2.08
3.71
7.54
7.53
7.26 CDCl3
6.19
6.19
13 12 11 10 9 8 7 6 5 4 3 2 1 0 -1
f1 (ppm)

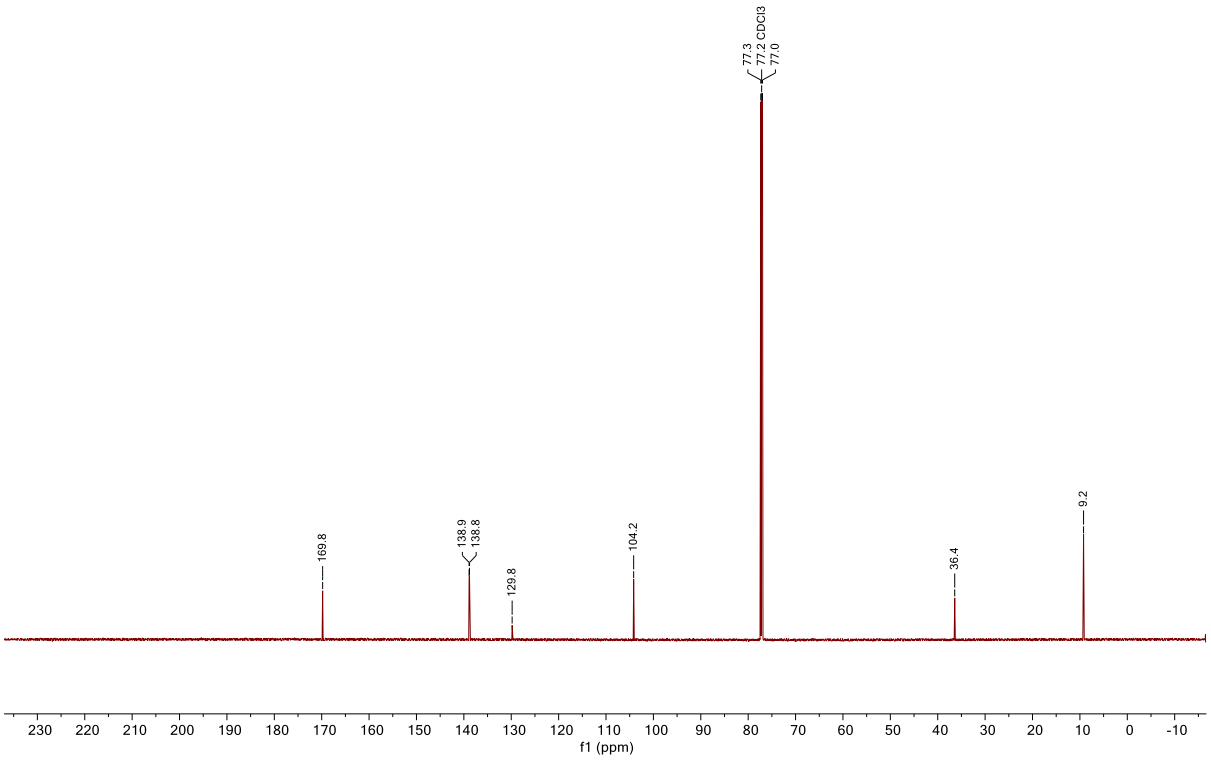
77.3
77.2 CDCl3
77.0
169.8
138.9
138.8
129.8
104.2
36.4
9.2
230 220 210 200 190 180 170 160 150 140 130 120 110 100 90 80 70 60 50 40 30 20 10 0 -10
f1 (ppm)

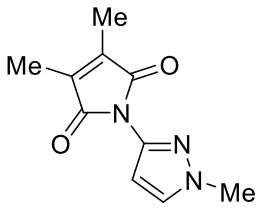
Me
Me
O
O
N
N
N
Me

471b

2.02
3.90
7.38
7.37
7.26 CDCl3
6.26
6.26
1.00
1.01
3.08
5.95
13 12 11 10 9 8 7 6 5 4 3 2 1 0 -1
f1 (ppm)

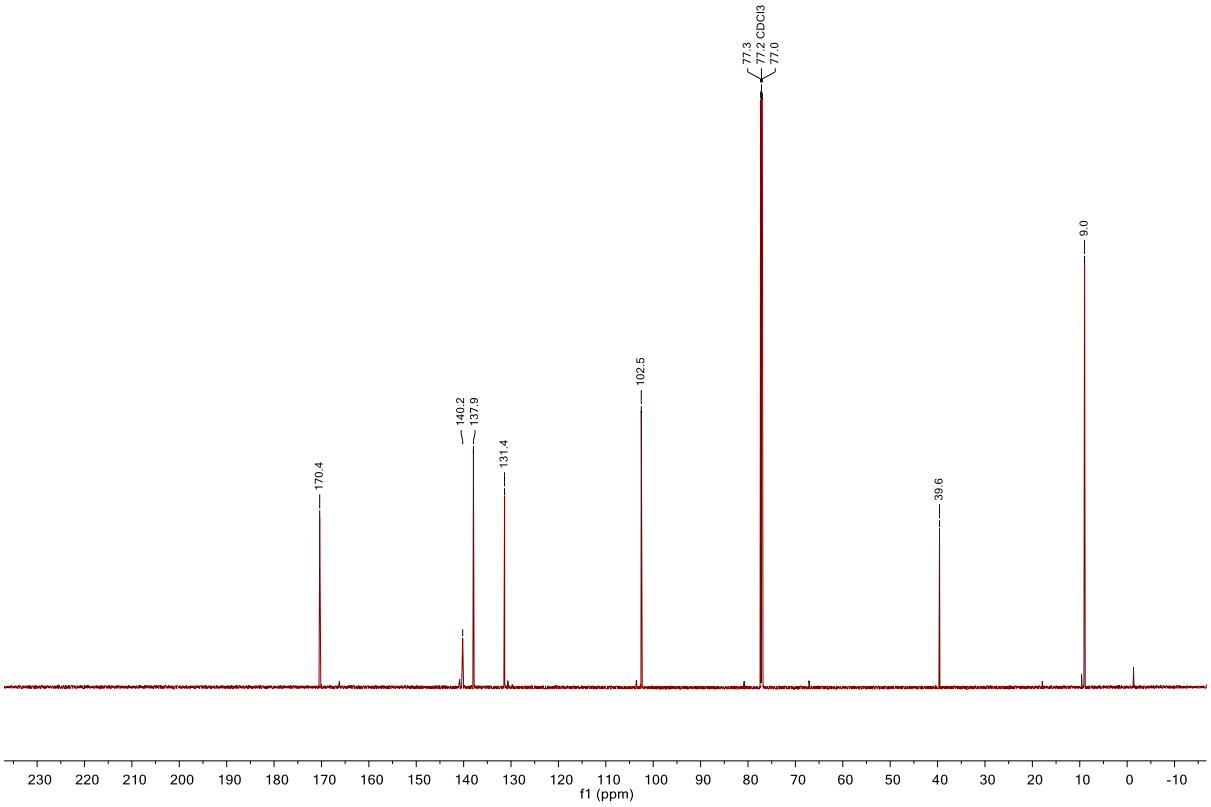
77.3
77.2 CDCl3
77.0
9.0
102.5
140.2
137.9
131.4
170.4
39.6
230 220 210 200 190 180 170 160 150 140 130 120 110 100 90 80 70 60 50 40 30 20 10 0 -10
f1 (ppm)

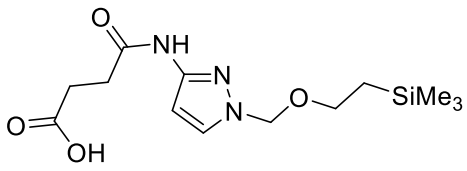
O
NH
N
N
O
SiMe3
O
OH

474

10.41
7.44
7.44
7.26 CDCl3
6.85
6.85
5.26
3.52
3.51
3.50
2.83
2.82
2.81
2.79
2.78
2.77
2.77
0.91
0.90
0.88
0.02
1.08
1.00
1.01
2.11
2.21
1.91
1.96
2.17
9.14
f1 (ppm)

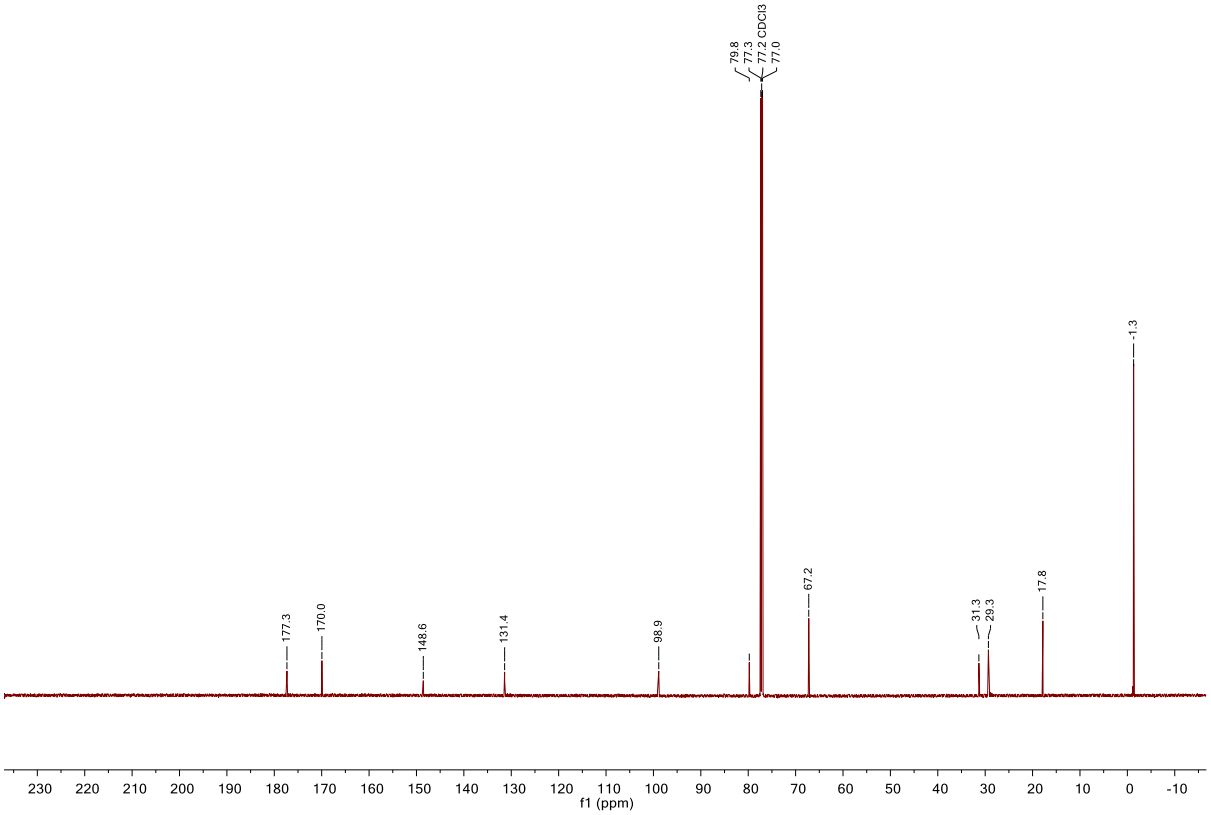
79.8
77.3
77.2 CDCl3
77.0
177.3
170.0
148.6
131.4
98.9
67.2
31.3
29.3
17.8
-1.3
f1 (ppm)

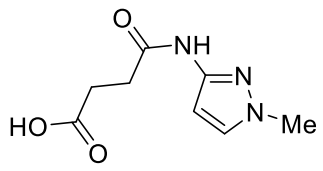
O
NH
N
N
Me
HO
O

475

12.14
9.93
7.30
7.29
6.14
6.14
3.63
2.60
2.59
2.58
2.53
2.52
2.51
2.51
2.50
2.50 DMSO-d6
2.50
2.49
0.98
0.95
1.00
1.01
2.86
1.74
1.71
f1 (ppm)

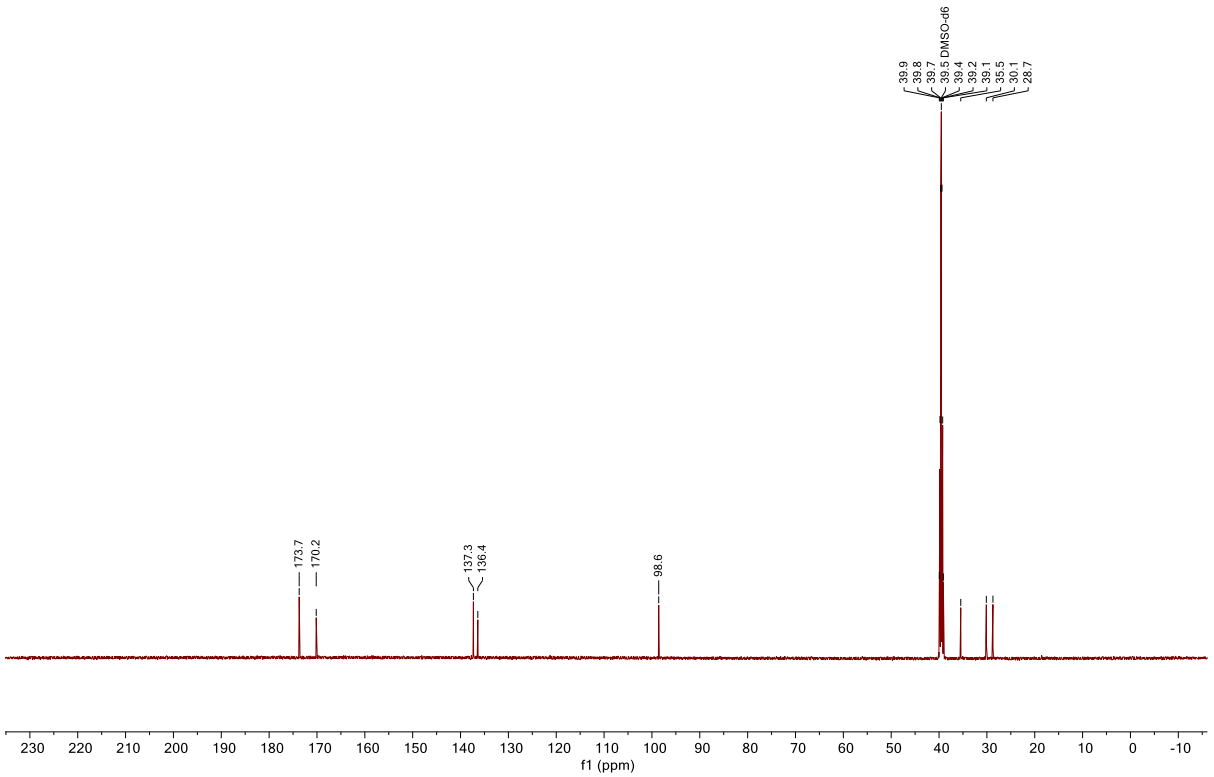
173.7
170.2
137.3
136.4
98.6
39.9
39.8
39.7
39.5 DMSO-d6
39.4
39.2
39.1
35.5
30.1
28.7
f1 (ppm)

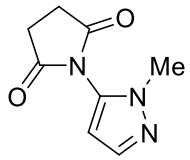
O
O
N
Me
N
N

476

3.60
2.82
2.48
2.48
2.47 DMSO-d6
2.47
2.47
7.49
7.48
6.20
6.19
1.00
1.00
2.98
3.94
f1 (ppm)

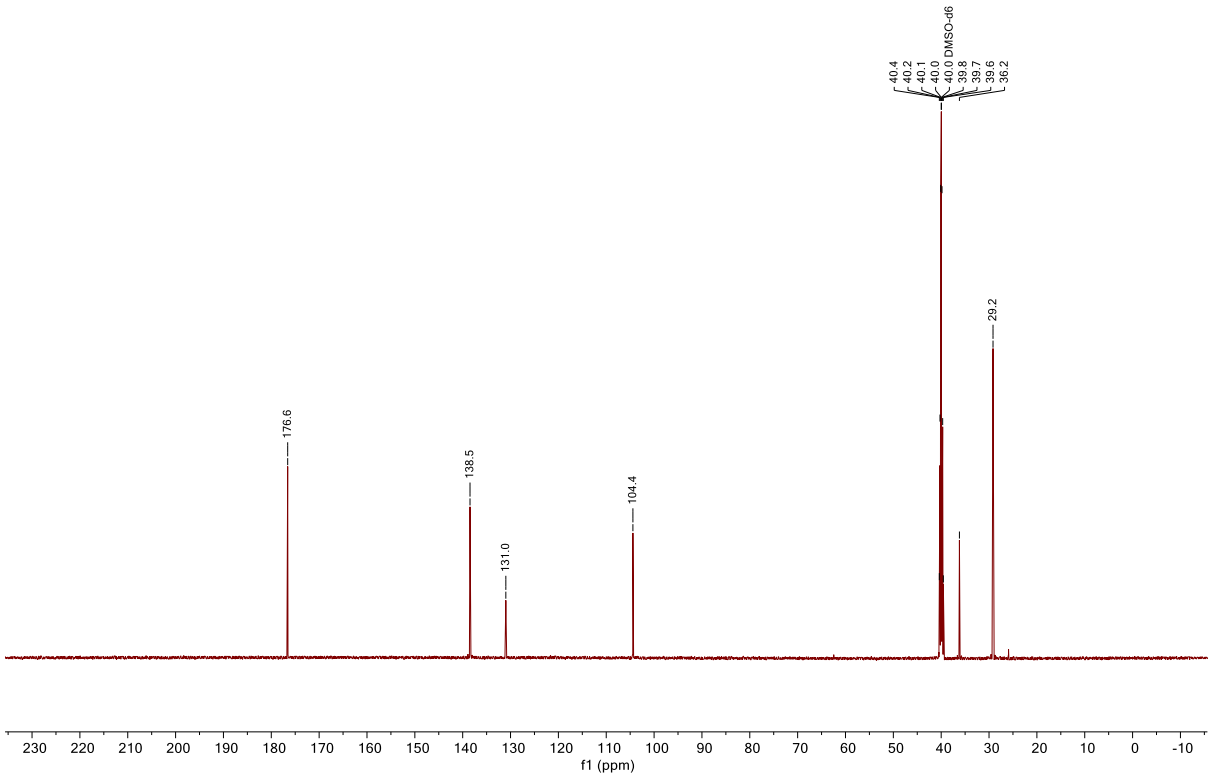
40.4
40.2
40.1
40.0
40.0 DMSO-d6
39.8
39.7
39.6
36.2
29.2
176.6
138.5
131.0
104.4
f1 (ppm)

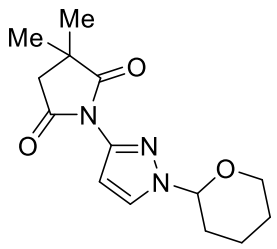
Me
Me
O
N
O
N
N
O

485

2.10 2.09 2.09 2.08 2.08 2.07 2.07 2.06 2.05 2.04 2.03 2.03 2.02 2.02 2.01 2.01 2.01 2.00 2.00 1.99 1.99 1.99 1.98 1.97 1.97 1.96 1.95 1.69 1.68 1.67 1.66 1.66 1.65 1.65 1.65 1.64 1.64 1.63 1.63 1.62 1.62 1.61 1.60 1.60 1.59 1.59 1.58 1.58 1.57 1.57 1.56 1.56 1.55 1.55 1.55 1.39
2.68
7.65
7.64
7.26 CDCl3
6.34
6.34
5.40
5.40
5.39
5.38
4.04
4.03
4.02
4.01
3.88
3.87
3.66
3.66
3.64
3.64
0.96
0.96
0.97
0.97
0.97
1.94
3.10
2.01
1.05
5.93
13 12 11 10 9 8 7 6 5 4 3 2 1 0 -1
f1 (ppm)

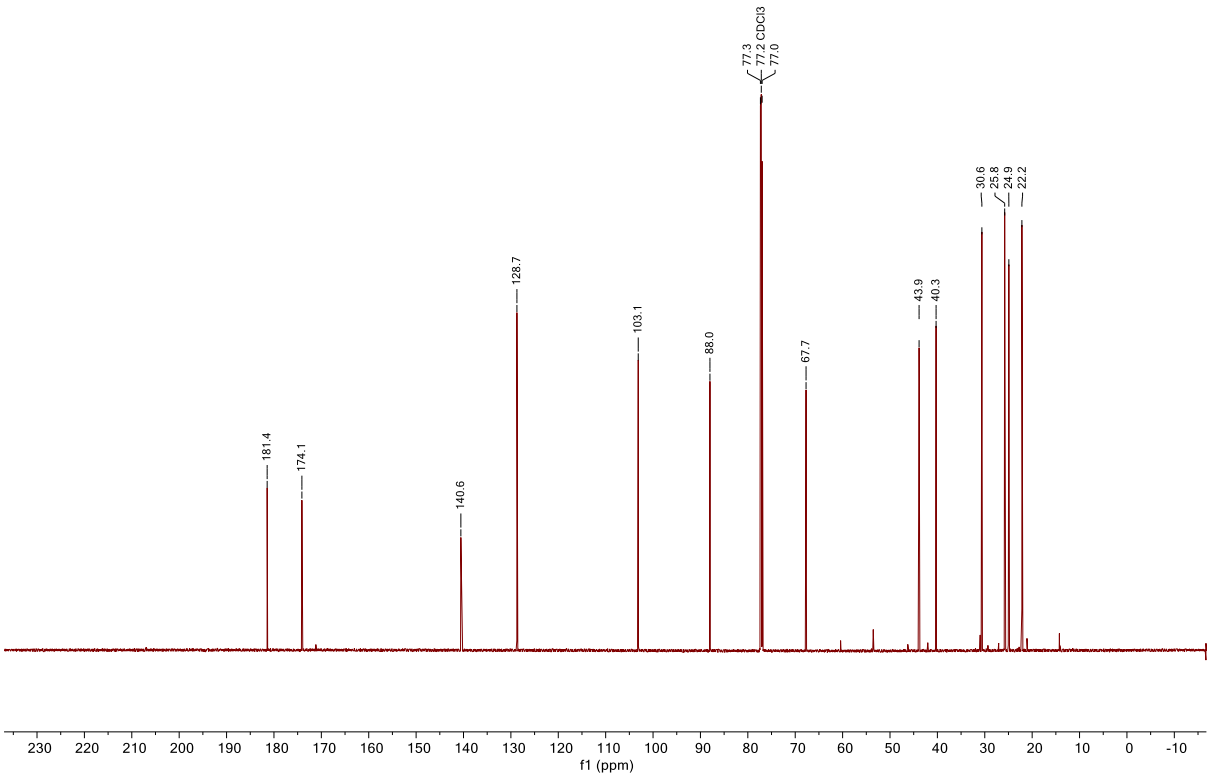
77.3
77.2 CDCl3
77.0
30.6
25.8
24.9
22.2
128.7
103.1
88.0
67.7
43.9
40.3
181.4
174.1
140.6
230 220 210 200 190 180 170 160 150 140 130 120 110 100 90 80 70 60 50 40 30 20 10 0 -10
f1 (ppm)

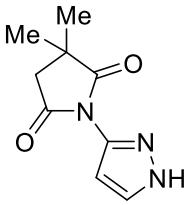
Me
Me
O
N
O
N
NH

486

12.22
7.65
7.65
7.26 CDCl3
6.45
6.44
2.71
1.39
1.00
1.06
1.06
2.00
5.72
13 12 11 10 9 8 7 6 5 4 3 2 1 0 -1
f1 (ppm)

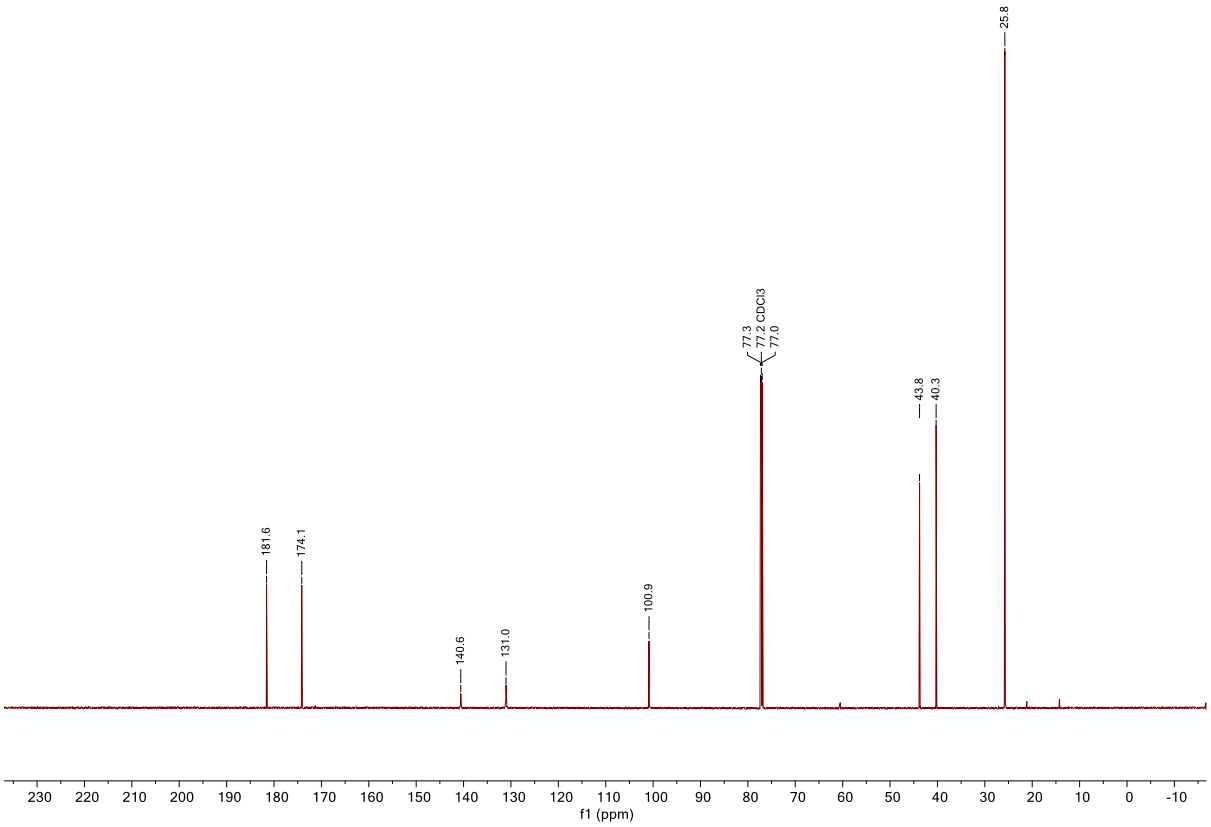
181.6
174.1
140.6
131.0
100.9
77.3
77.2 CDCl3
77.0
43.8
40.3
25.8
230 220 210 200 190 180 170 160 150 140 130 120 110 100 90 80 70 60 50 40 30 20 10 0 -10
f1 (ppm)

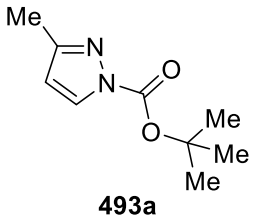
Me
N
N
O
O
Me
Me
Me

493a

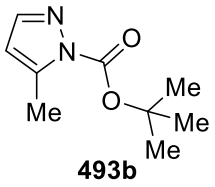
N
N
O
O
Me
Me
Me
Me

493b

1.64
1.62
2.52
2.32
7.95
7.54
7.26 CDCl3
6.16
6.10
1.00
0.12
1.02
0.11
0.23
2.95
0.76
8.38
0.26
f1 (ppm)

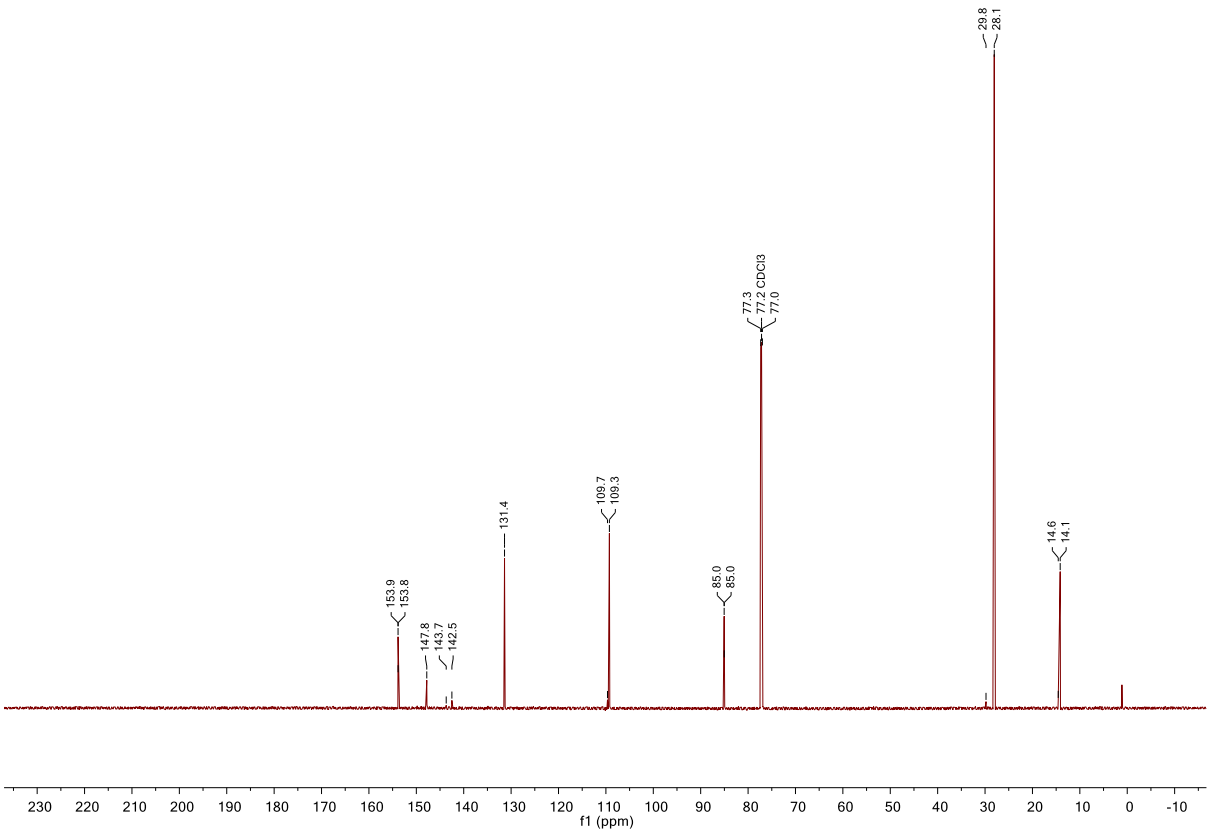
29.8
28.1
77.3
77.2 CDCl3
77.0
109.7
109.3
131.4
85.0
85.0
153.9
153.8
147.8
143.7
142.5
14.6
14.1
f1 (ppm)

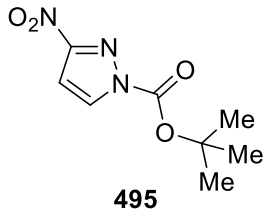
O2N
N
N
O
O
Me
Me
Me

495

1.68
8.18
8.18
7.26 CDCl3
6.98
6.98
14 13 12 11 10 9 8 7 6 5 4 3 2 1 0 -1
f1 (ppm)

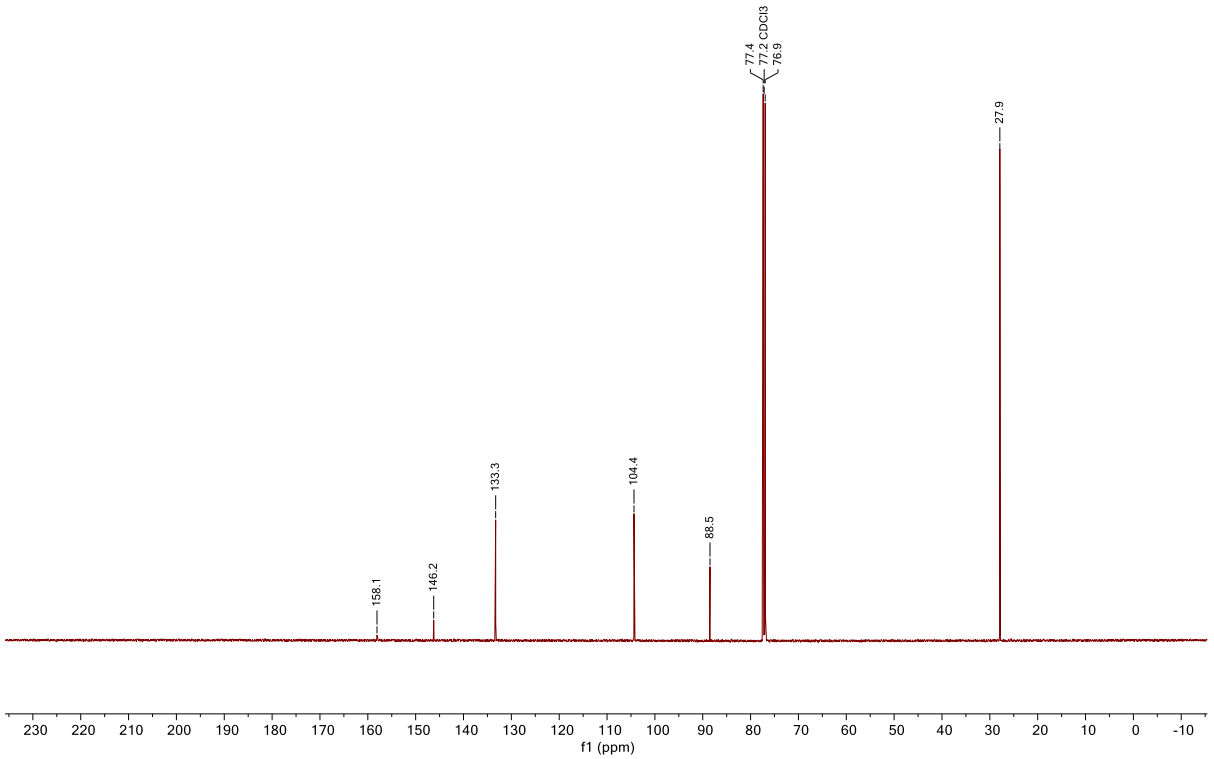
77.4
77.2 CDCl3
76.9
27.9
133.3
104.4
88.5
158.1
146.2
230 220 210 200 190 180 170 160 150 140 130 120 110 100 90 80 70 60 50 40 30 20 10 0 -10
f1 (ppm)

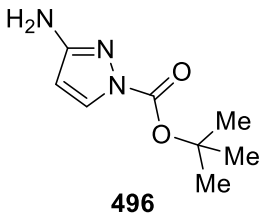
H2N
N
N
O
O
Me
Me
Me

496

1.60
7.82
7.82
7.26 CDCl3
5.81
5.80
3.89
13 12 11 10 9 8 7 6 5 4 3 2 1 0 -1
f1 (ppm)

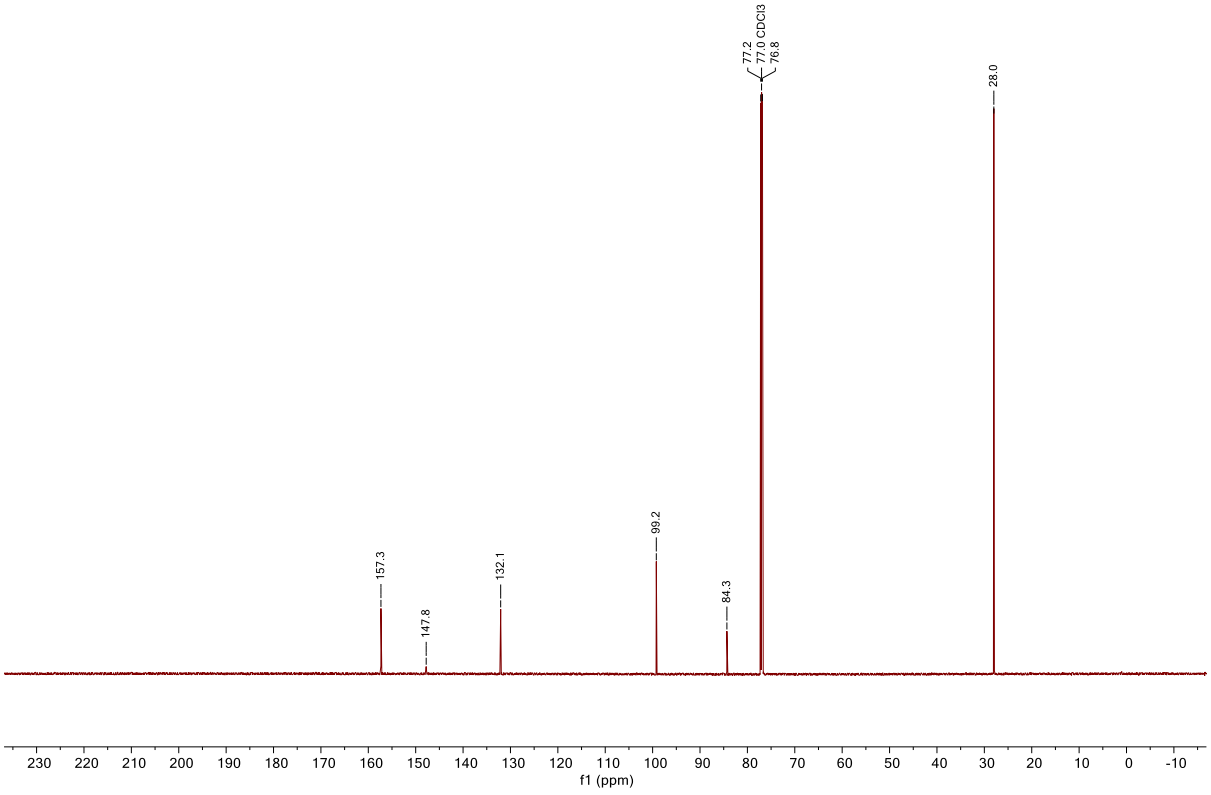
77.2
77.0 CDCl3
76.8
28.0
157.3
147.8
132.1
99.2
84.3
230 220 210 200 190 180 170 160 150 140 130 120 110 100 90 80 70 60 50 40 30 20 10 0 -10
f1 (ppm)

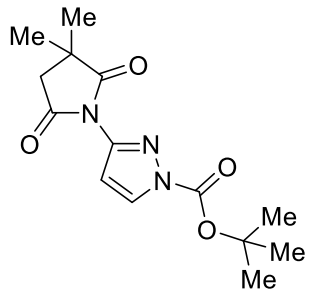
Me
Me
O
N
O
N
N
O
O
Me
Me
Me

498

1.63
1.40
2.70
8.12
8.12
7.26 CDCl3
6.48
6.47
1.03
1.01
2.00
9.00
6.19
13 12 11 10 9 8 7 6 5 4 3 2 1 0 -1
f1 (ppm)

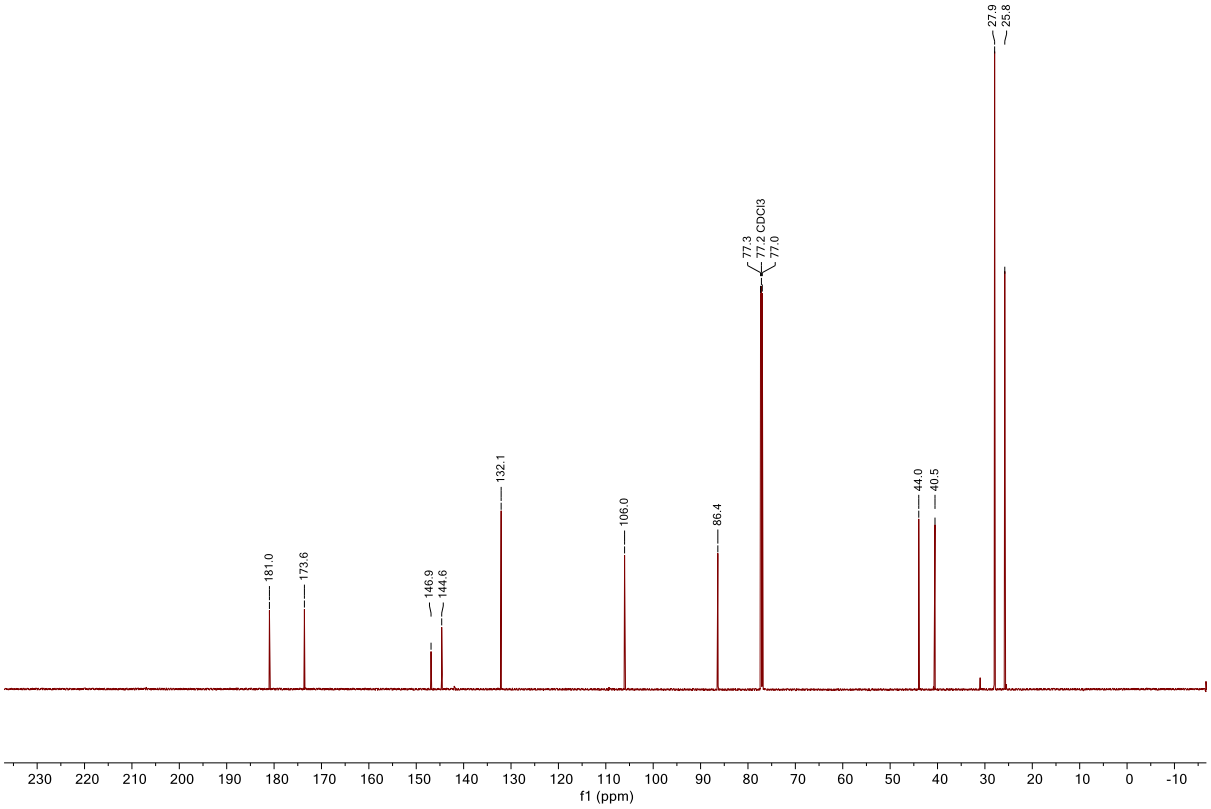
27.9
25.8
77.3
77.2 CDCl3
77.0
132.1
106.0
86.4
44.0
40.5
181.0
173.6
146.9
144.6
230 220 210 200 190 180 170 160 150 140 130 120 110 100 90 80 70 60 50 40 30 20 10 0 -10
f1 (ppm)

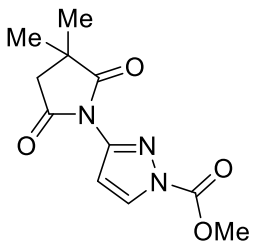
Me
Me
O
N
O
N
N
O
OMe

503

1.39
4.05
2.70
8.20
8.20
7.26 CDCl3
6.55
6.54
1.12
1.07
3.16
1.94
5.87
13 12 11 10 9 8 7 6 5 4 3 2 1 0 -1
f1 (ppm)

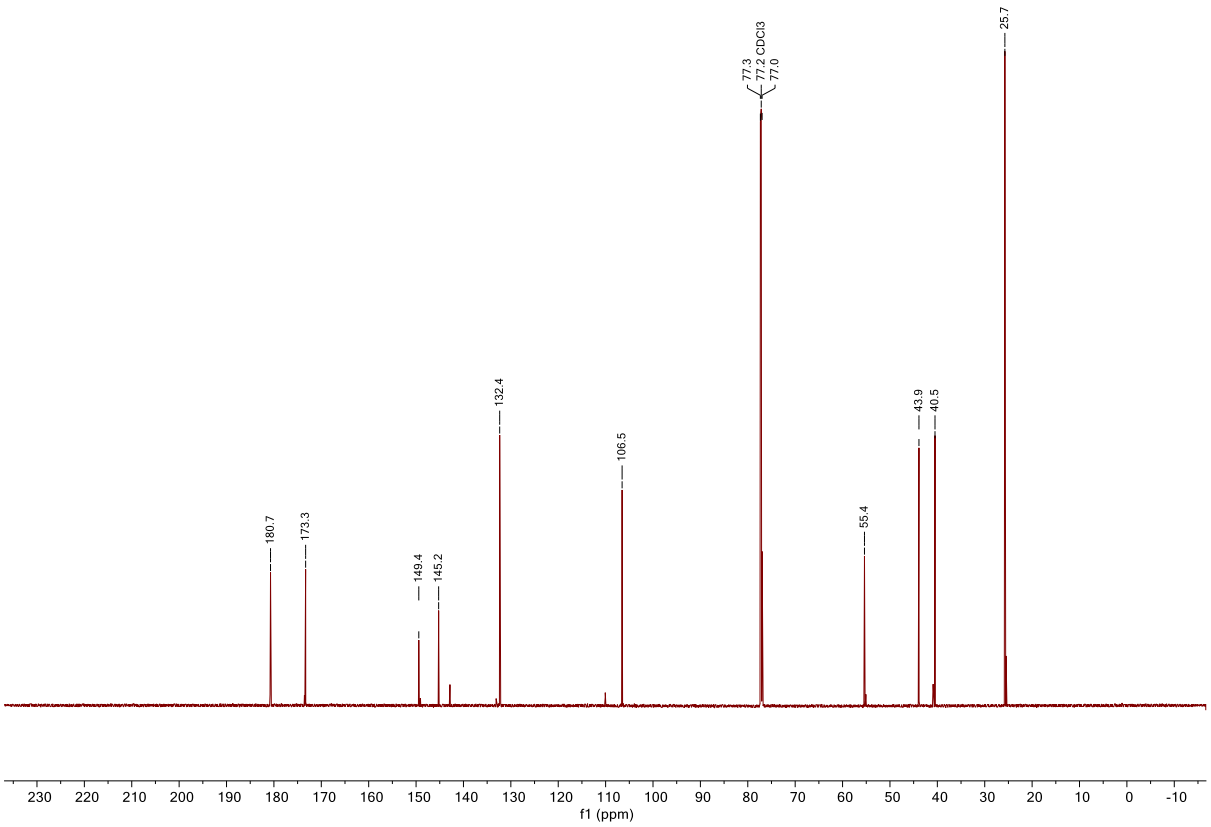
25.7
77.3
77.2 CDCl3
77.0
132.4
106.5
43.9
40.5
180.7
173.3
149.4
145.2
55.4
230 220 210 200 190 180 170 160 150 140 130 120 110 100 90 80 70 60 50 40 30 20 10 0 -10
f1 (ppm)

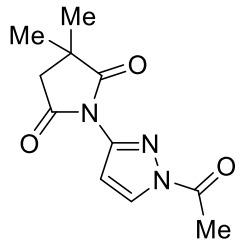
Me
Me
O
N
O
N
N
O
Me

505

8.29
8.28
7.26 CDCl3
6.57
6.56
2.74
2.70
1.43
1.15
1.08
1.82
2.73
6.00
13 12 11 10 9 8 7 6 5 4 3 2 1 0 -1
f1 (ppm)

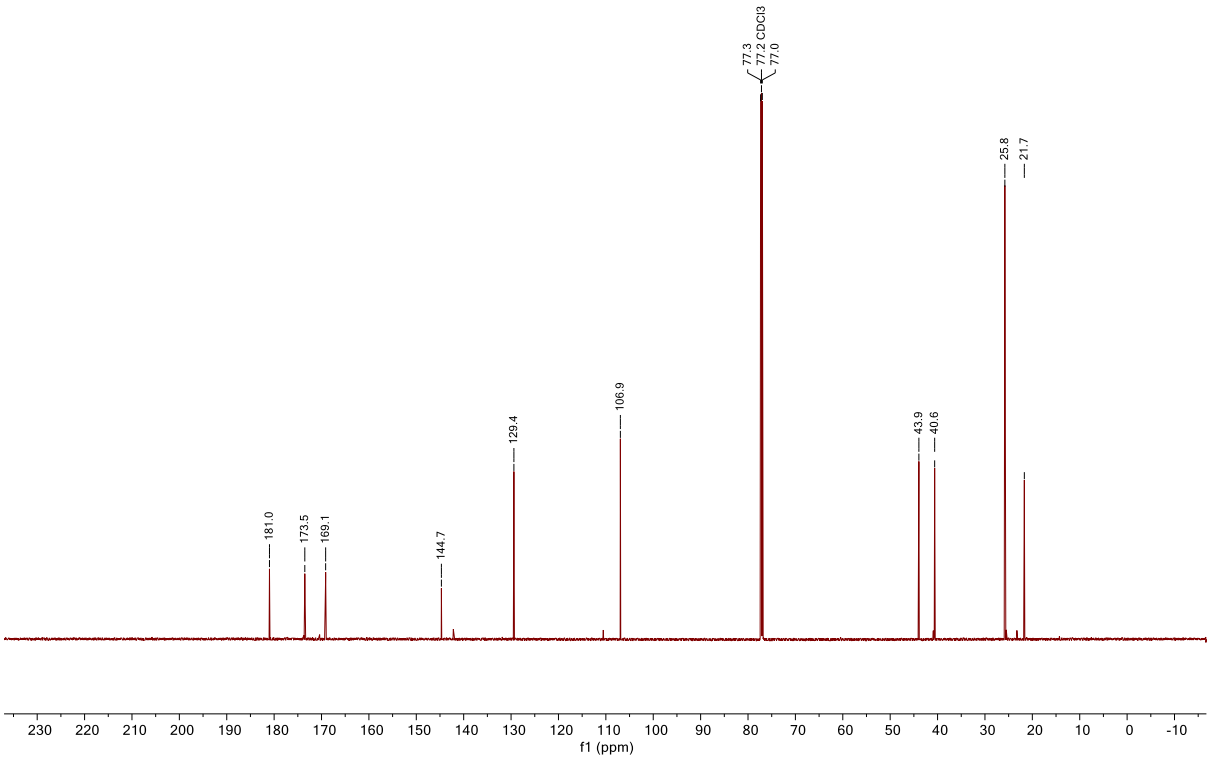
77.3
77.2 CDCl3
77.0
25.8
21.7
181.0
173.5
169.1
144.7
129.4
106.9
43.9
40.6
230 220 210 200 190 180 170 160 150 140 130 120 110 100 90 80 70 60 50 40 30 20 10 0 -10
f1 (ppm)

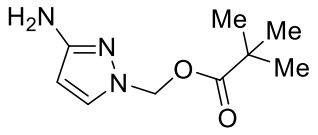
H2N
N
N
O
Me
Me
Me
O

514

1.13
7.34
7.25 CDCl3
5.77
5.63
3.59
1.00
2.00
1.02
2.21
9.26
13 12 11 10 9 8 7 6 5 4 3 2 1 0 -1
f1 (ppm)

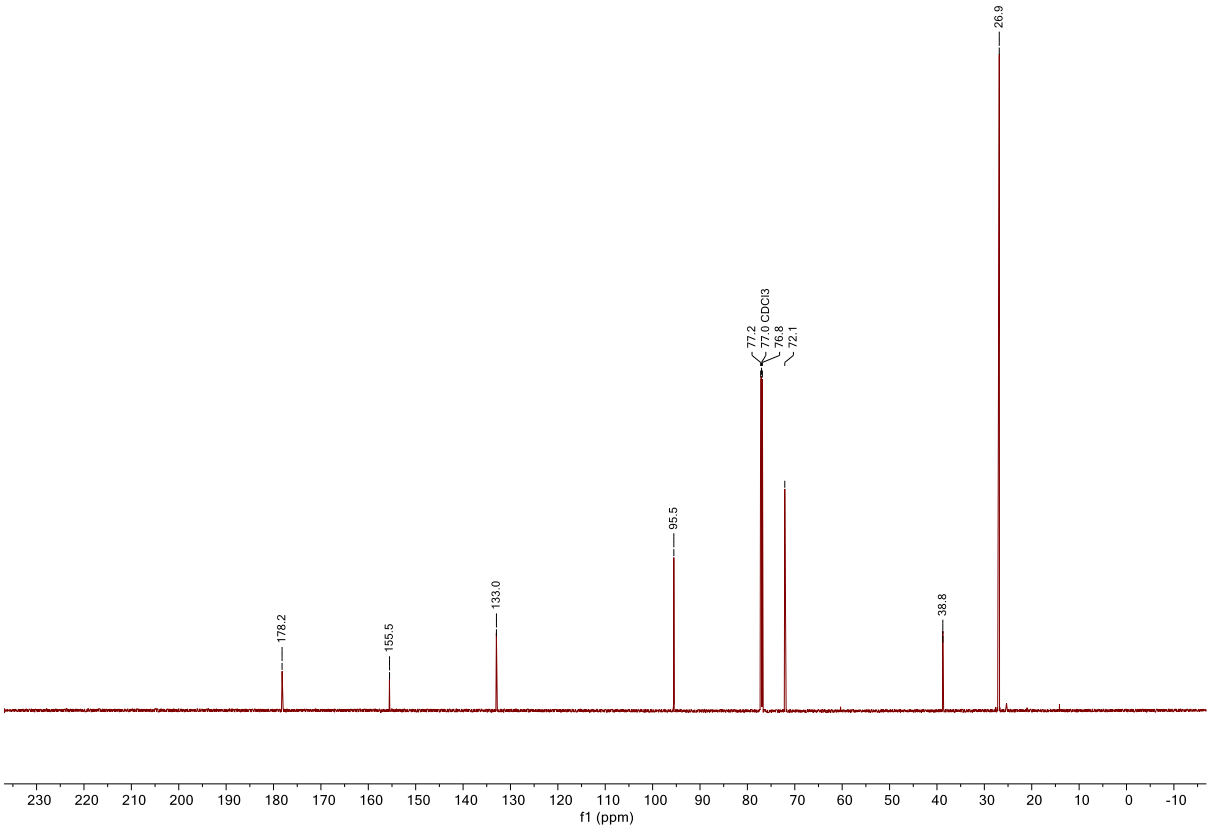
26.9
77.2
77.0 CDCl3
76.8
72.1
95.5
178.2
155.5
133.0
38.8
230 220 210 200 190 180 170 160 150 140 130 120 110 100 90 80 70 60 50 40 30 20 10 0 -10
f1 (ppm)

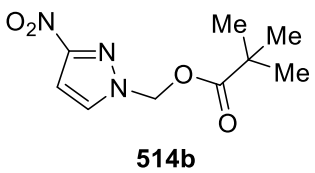
O2N
N
N
O
Me
Me
Me
O

514b

1.17
6.04
7.75
7.75
7.26 CDCl3
6.91
6.90
1.00
1.01
1.84
8.68
f1 (ppm)

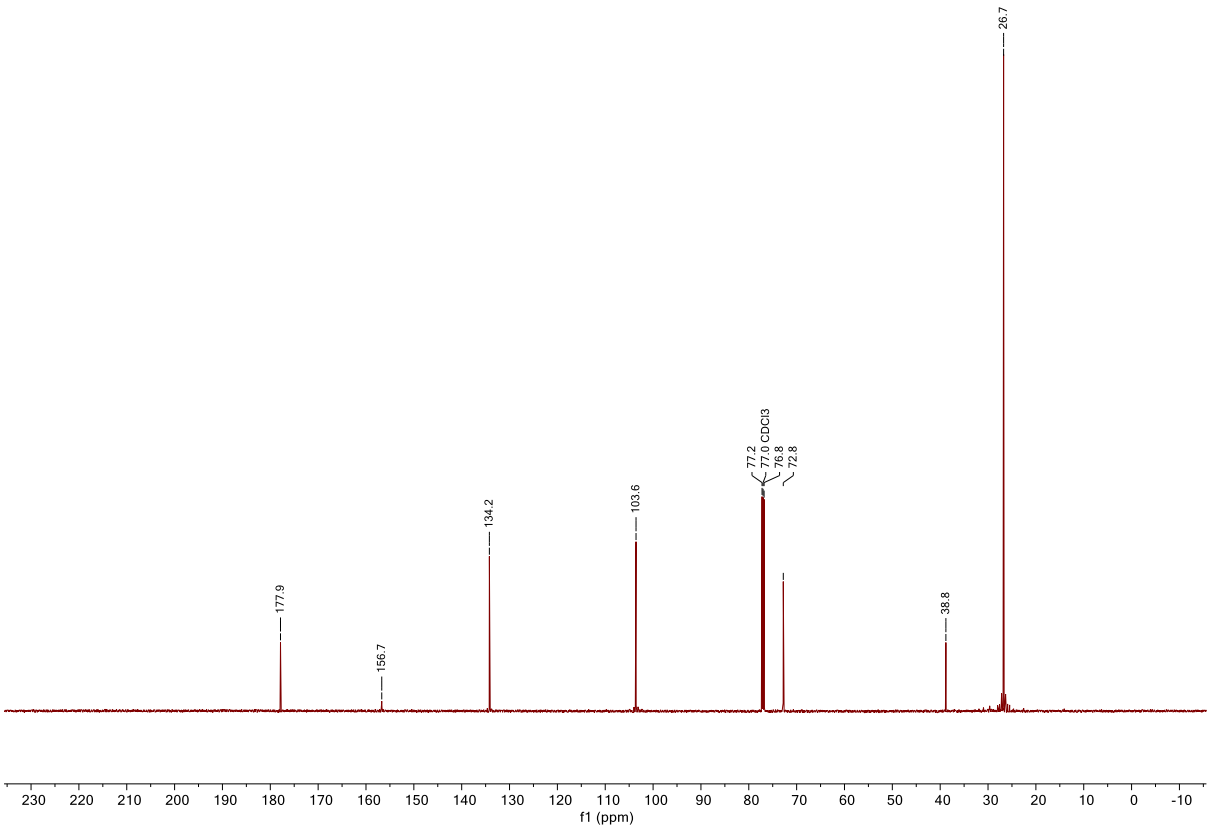
26.7
77.2
77.0 CDCl3
76.8
72.8
134.2
103.6
177.9
156.7
38.8
f1 (ppm)

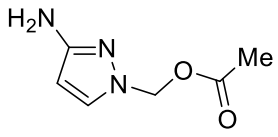
H2N
N
N
O
Me
O

515

2.06
5.79
5.66
5.66
7.37
7.37
7.26 CDCl3
3.73
1.00
1.94
0.99
2.06
2.92
f1 (ppm)

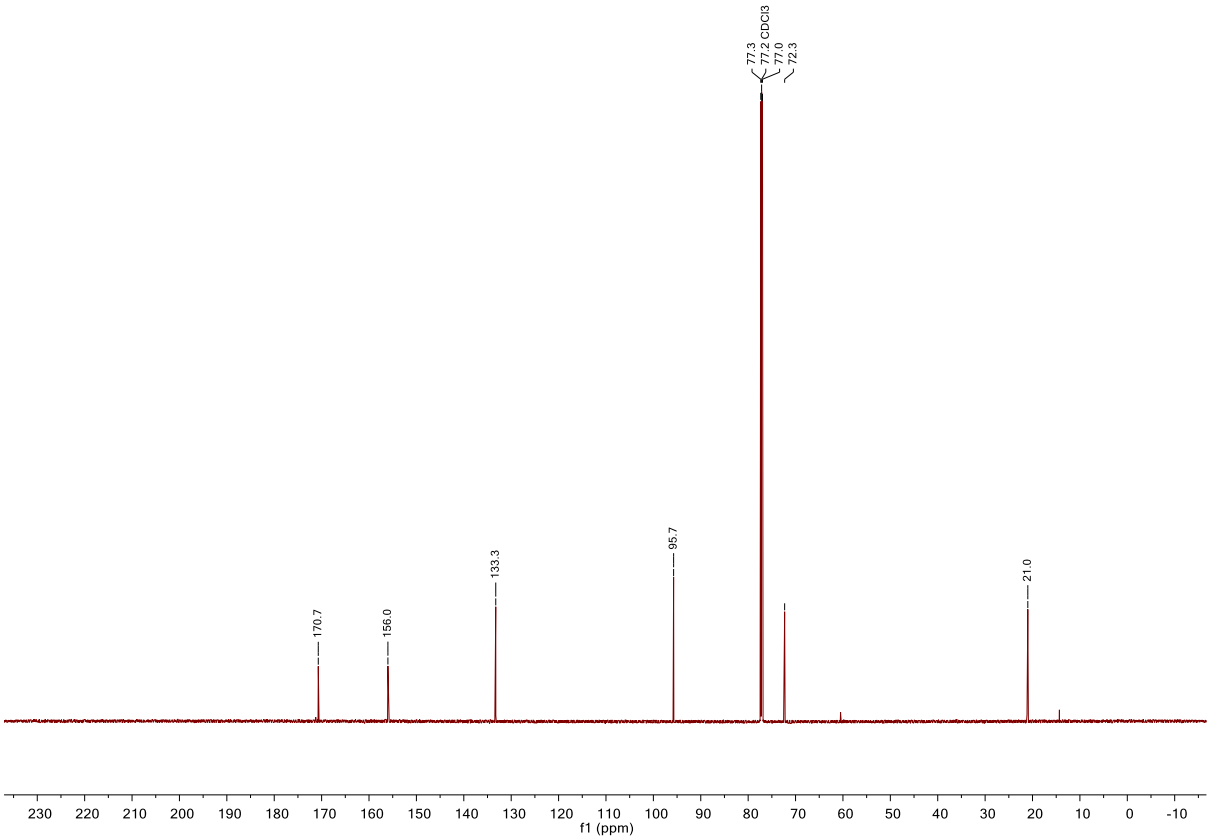
77.3
77.2 CDCl3
77.0
72.3
170.7
156.0
133.3
95.7
21.0
f1 (ppm)

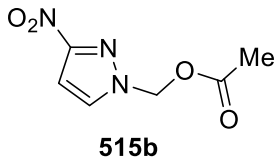
O2N
N
N
O
Me
O

515b

2.12
6.03
7.77
7.76
7.26 CDCl3
6.91
6.91
1.00
1.00
1.98
3.09
13 12 11 10 9 8 7 6 5 4 3 2 1 0 -1
f1 (ppm)

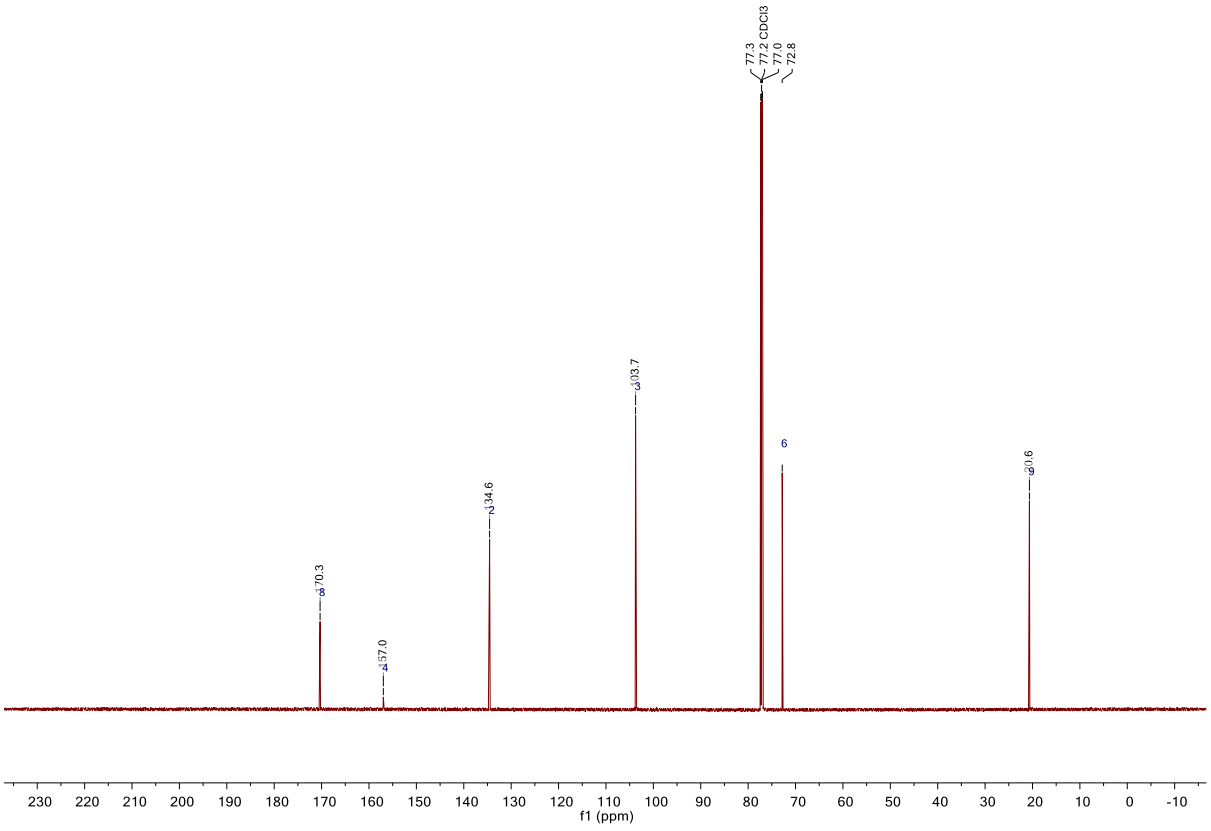
77.3
77.2 CDCl3
77.0
72.8
170.3
157.0
134.6
103.7
6
20.6
230 220 210 200 190 180 170 160 150 140 130 120 110 100 90 80 70 60 50 40 30 20 10 0 -10
f1 (ppm)

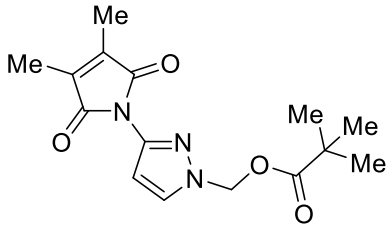
Me
Me
O
N
O
N
N
O
Me
Me
Me
O

515c

1.16
2.02
5.99
7.25 CDCl3
7.66
7.66
6.37
6.37
1.00
0.99
1.99
5.95
8.66
13 12 11 10 9 8 7 6 5 4 3 2 1 0 -1
f1 (ppm)

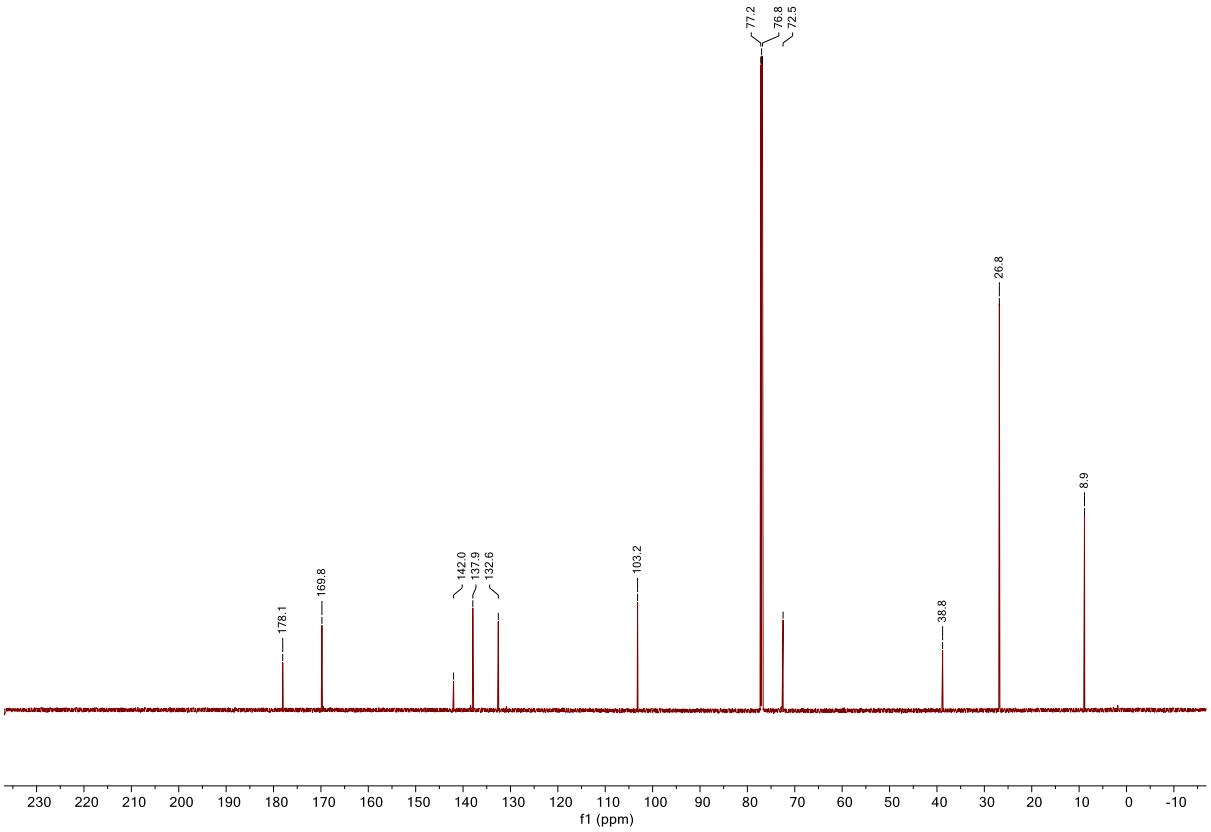
77.2
76.8
72.5
26.8
8.9
178.1
169.8
142.0
137.9
132.6
103.2
38.8
230 220 210 200 190 180 170 160 150 140 130 120 110 100 90 80 70 60 50 40 30 20 10 0 -10
f1 (ppm)

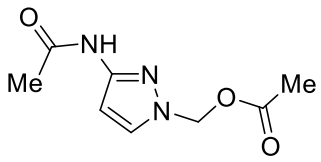
O
NH
Me
N
N
O
Me
O

515d

2.15
2.07
5.87
7.53
7.52
7.26 CDCl3
6.78
6.77
8.22
0.93
1.00
0.93
1.87
13 12 11 10 9 8 7 6 5 4 3 2 1 0 -1
f1 (ppm)

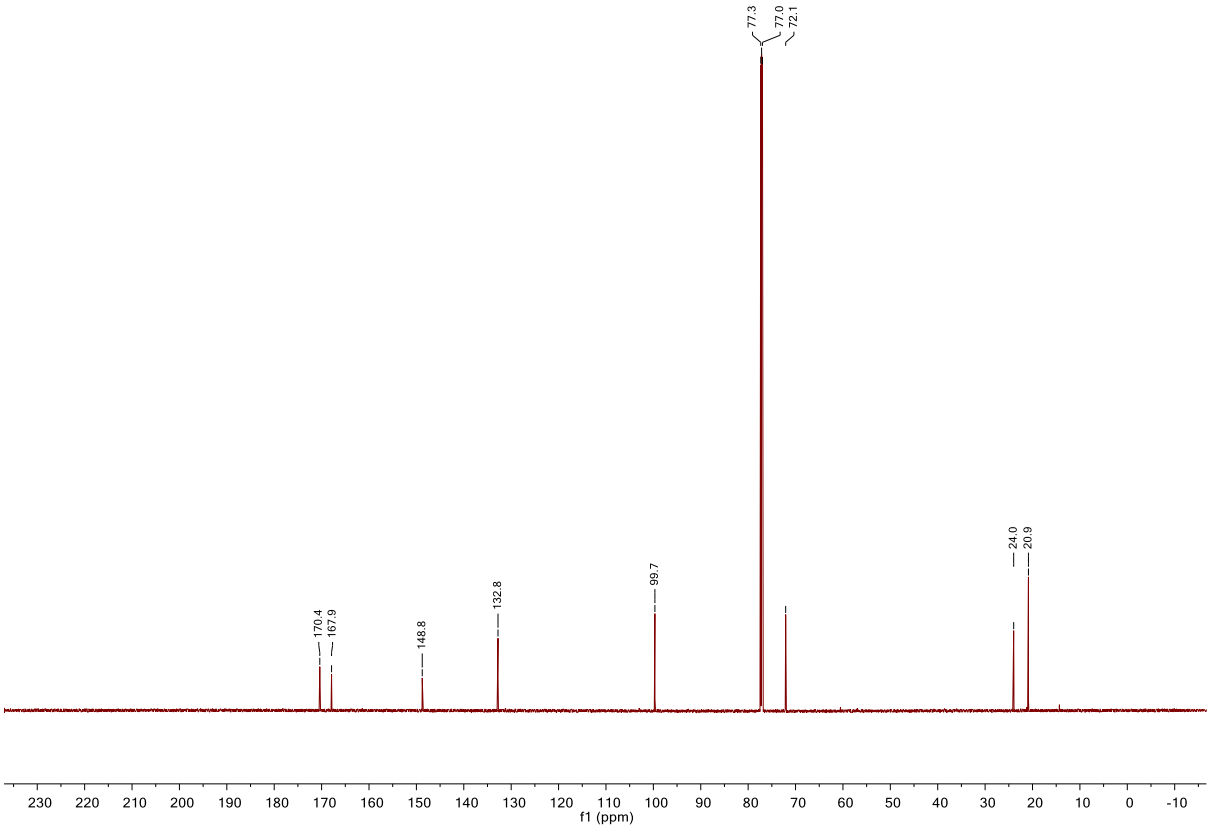
77.3
77.0
72.1
24.0
20.9
99.7
132.8
170.4
167.9
148.8
230 220 210 200 190 180 170 160 150 140 130 120 110 100 90 80 70 60 50 40 30 20 10 0 -10
f1 (ppm)

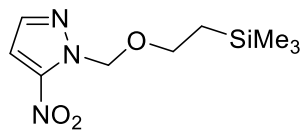
N
N
O
SiMe3
NO2

525

-0.04
5.88
7.57
7.57
7.26 CDCl3
7.11
7.11
3.61
3.59
3.58
0.90
0.89
0.88
0.95
0.97
2.00
1.96
1.99
8.29
f1 (ppm)

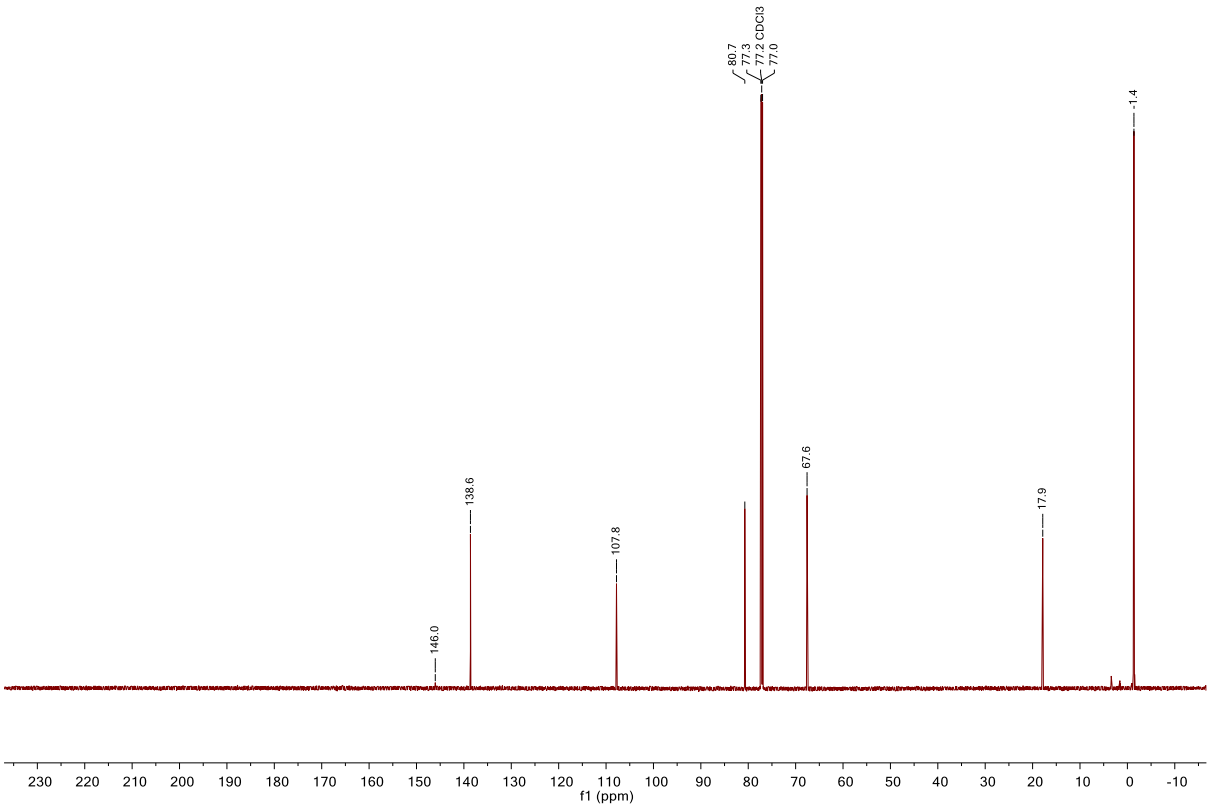
80.7
77.3
77.2 CDCl3
77.0
-1.4
67.6
138.6
107.8
17.9
146.0
f1 (ppm)

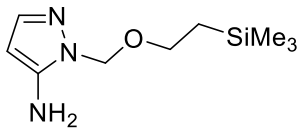
N
N
O
SiMe3
NH2

526

7.26 CDCl3
7.24
7.23
5.51
5.50
5.34
3.94
3.55
3.54
3.53
0.89
0.88
0.87
0.97
0.99
2.03
1.80
2.03
2.14
9.50
f1 (ppm)

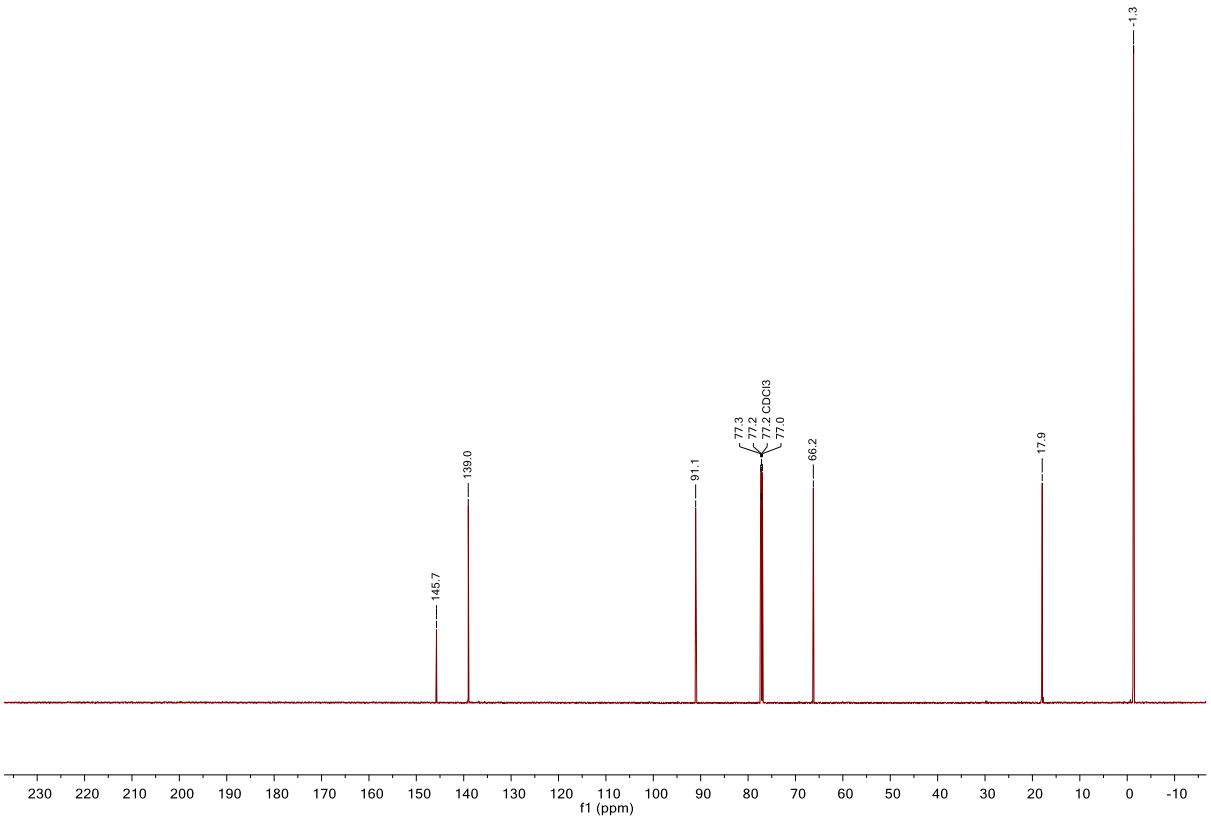
145.7
139.0
91.1
77.3
77.2
77.2 CDCl3
77.0
66.2
17.9
-1.3
f1 (ppm)

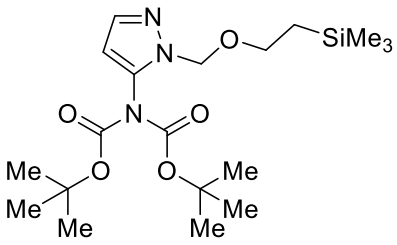
N
N
O
SiMe3
O
N
O
O
Me
O
O
Me
Me
Me
Me
Me

526b

1.42
-0.03
7.49
7.49
7.25 CDCl3
6.15
6.15
5.30
3.56
3.55
3.53
0.92
0.90
0.89
1.08
1.07
1.98
2.10
18.00
2.15
8.83
f1 (ppm)

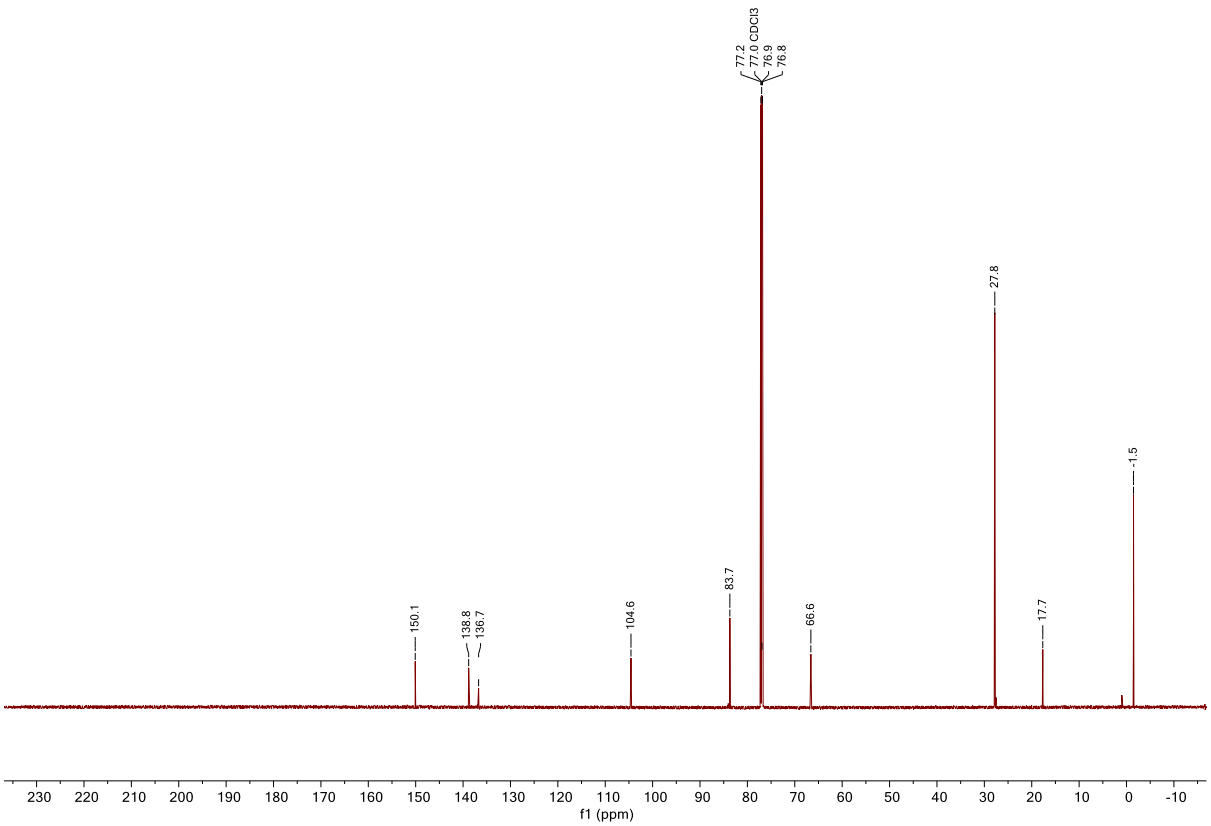
77.2
77.0 CDCl3
76.9
76.8
27.8
-1.5
150.1
138.8
136.7
104.6
83.7
66.6
17.7
f1 (ppm)

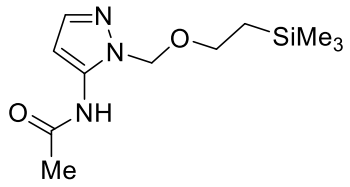
N
N
O
SiMe3
O
NH
Me

531

7.48
7.48
6.42
6.41
5.44
4.87 CD3OD
3.56
3.54
3.53
2.18
0.89
0.88
0.87
-0.01
1.00
1.01
2.02
1.99
3.03
2.00
8.87
f1 (ppm)

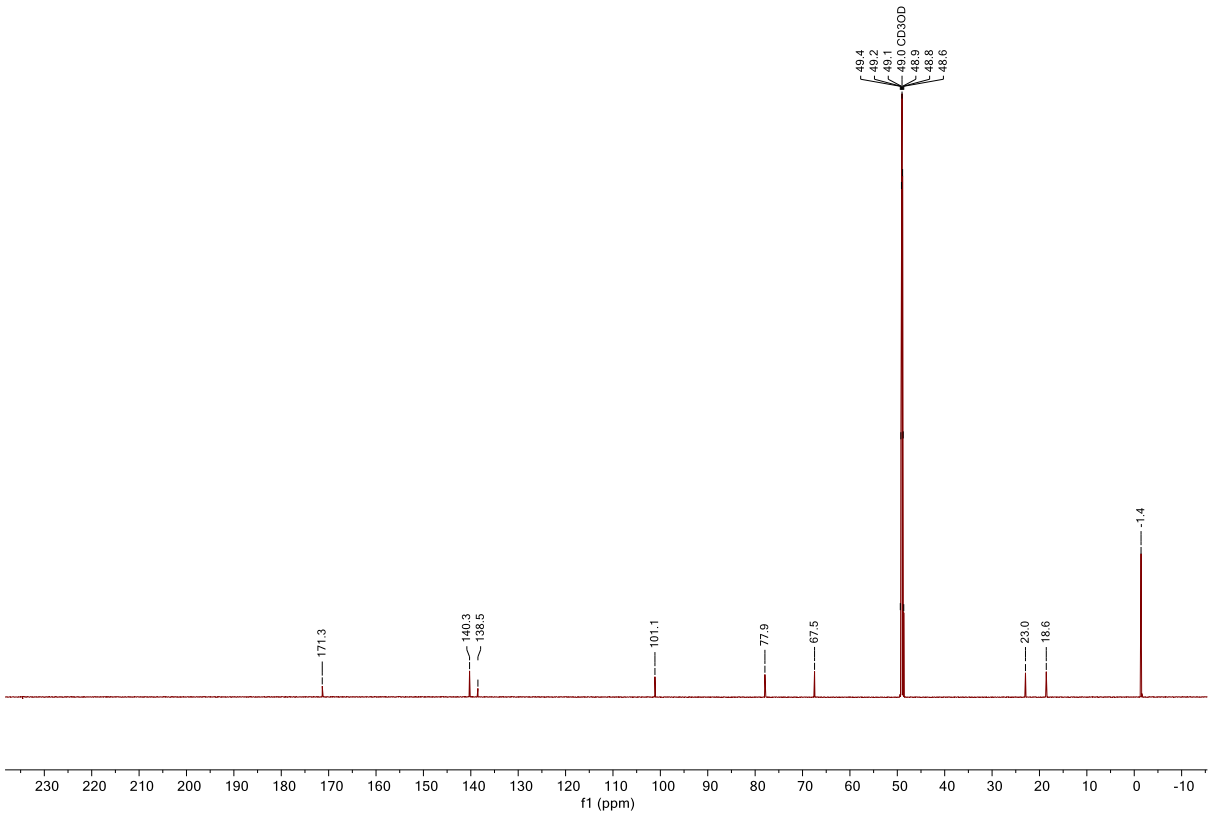
49.4
49.2
49.1
49.0 CD3OD
48.9
48.8
48.6
171.3
140.3
138.5
101.1
77.9
67.5
23.0
18.6
-1.4
f1 (ppm)

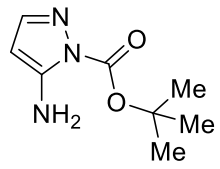
N
N
O
O
Me
Me
Me
NH2

534

1.64
4.87 CD3OD
7.36
7.35
5.41
5.41
1.00
1.00
9.00
f1 (ppm)

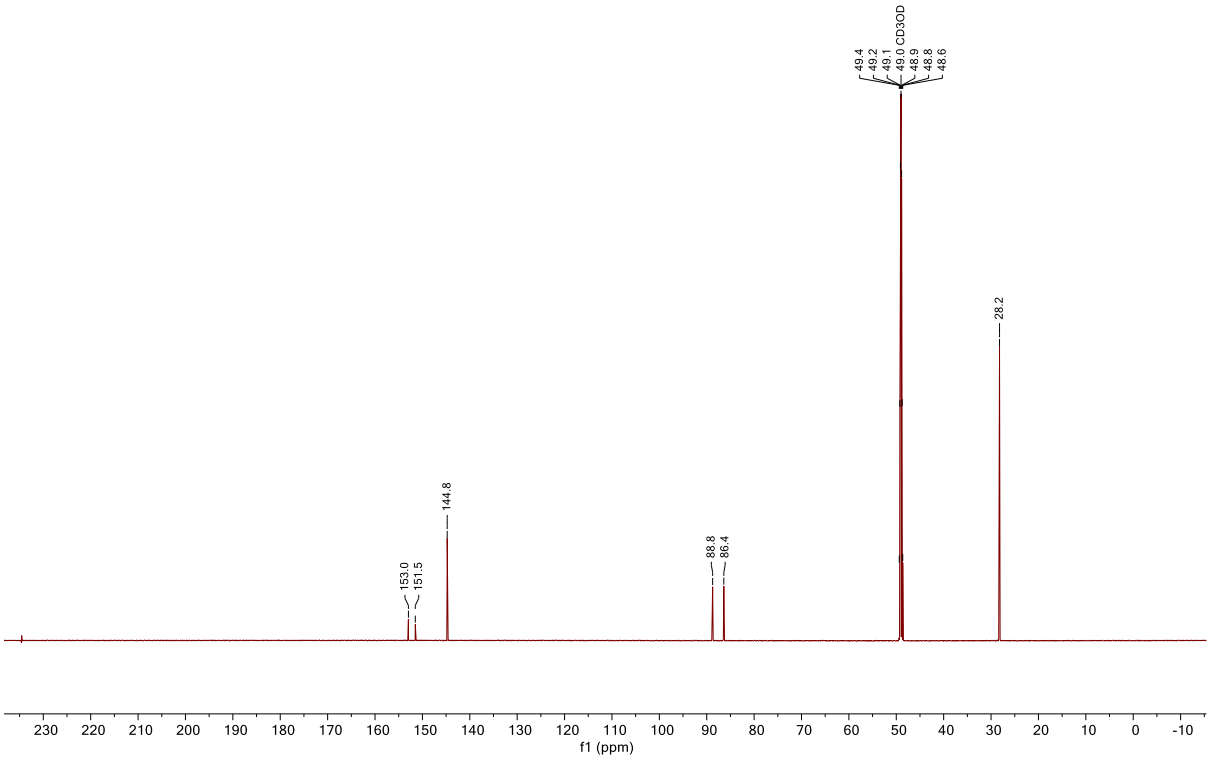
49.4
49.2
49.1
49.0 CD3OD
48.9
48.8
48.6
28.2
144.8
153.0
151.5
88.8
86.4
f1 (ppm)

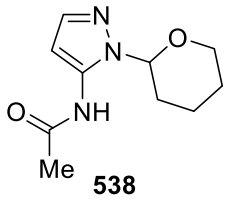
N
N
O
NH
O
Me

538

2.23
2.21
2.20
2.19
2.14
2.06
2.06
2.04
2.03
2.01
1.69
1.68
1.67
1.66
1.63
1.62
1.60
1.60
7.39
7.26 CDCl3
6.50
8.45
5.42
5.42
5.41
5.40
3.92
3.91
3.90
3.90
3.89
3.68
3.67
3.66
3.66
3.64
3.64
1.00
1.06
1.02
1.02
1.14
1.14
1.27
3.13
2.34
3.33
f1 (ppm)

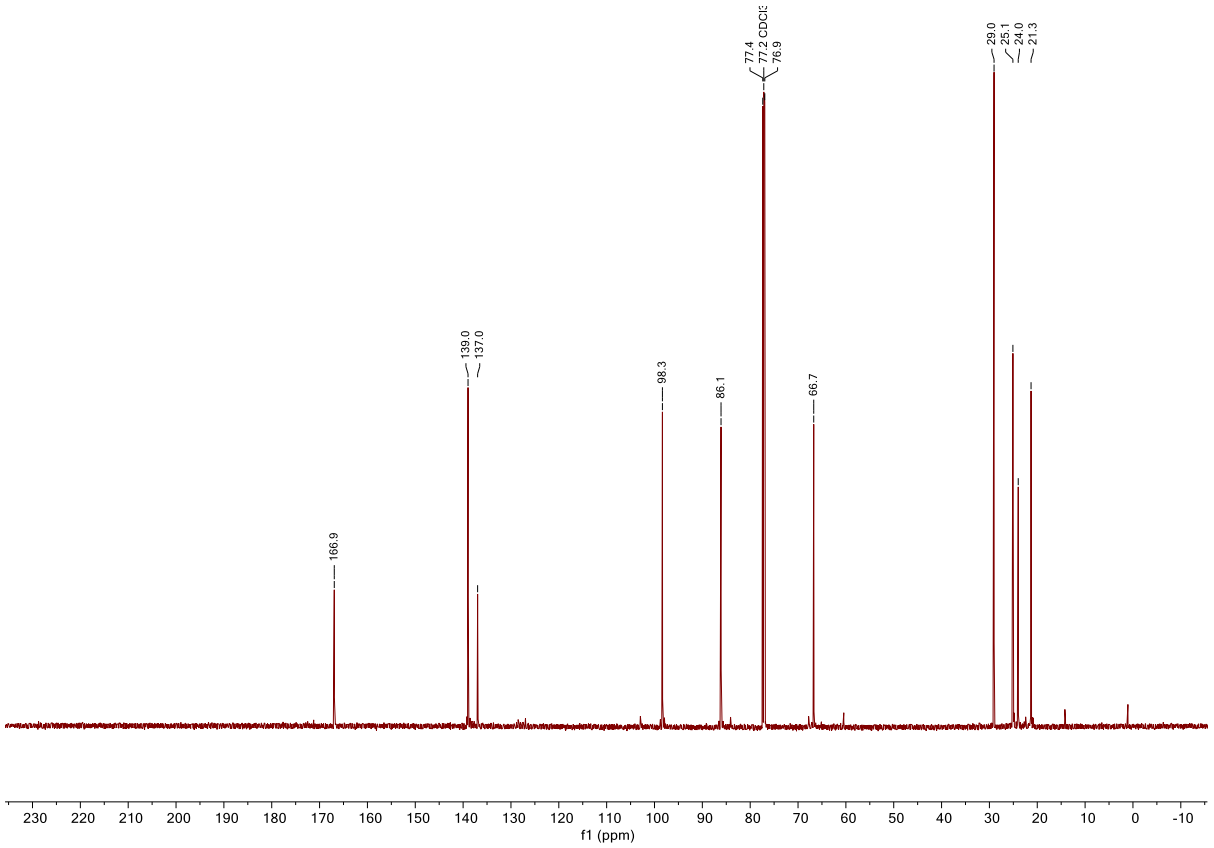
77.4
77.2 CDCl3
76.9
29.0
25.1
24.0
21.3
139.0
137.0
98.3
86.1
66.7
166.9
f1 (ppm)

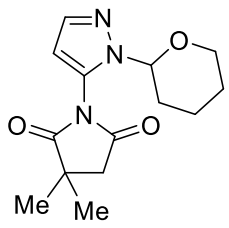
N
N
O
N
O
O
Me
Me

542

7.59
7.59
7.26 CDCl3
6.32
6.31
5.36
5.35
5.35
5.35
3.64
3.64
3.63
3.63
3.62
3.62
3.61
3.49
3.48
3.47
3.47
3.46
3.46
1.00
0.98
1.00
1.07
1.10
2.27
1.11
2.11
1.01
2.22
2.88
3.00
f1 (ppm)

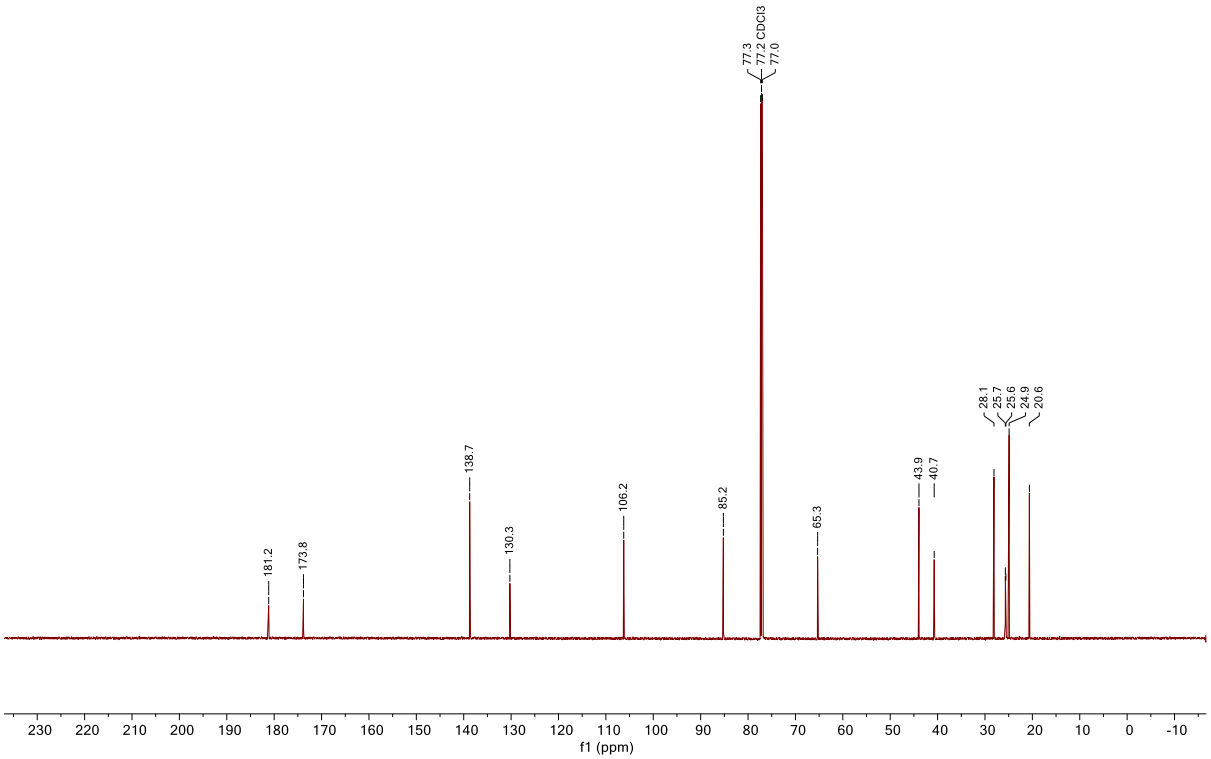
77.3
77.2 CDCl3
77.0
181.2
173.8
138.7
130.3
106.2
85.2
65.3
43.9
40.7
28.1
25.7
25.6
24.9
20.6
f1 (ppm)

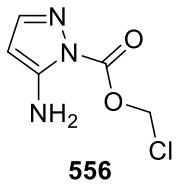

556

6.11
7.42
7.42
6.51
5.34
5.33
2.51
2.50
2.50 DMSO-d6
2.50
2.49
1.00
2.03
2.11
1.04
f1 (ppm)

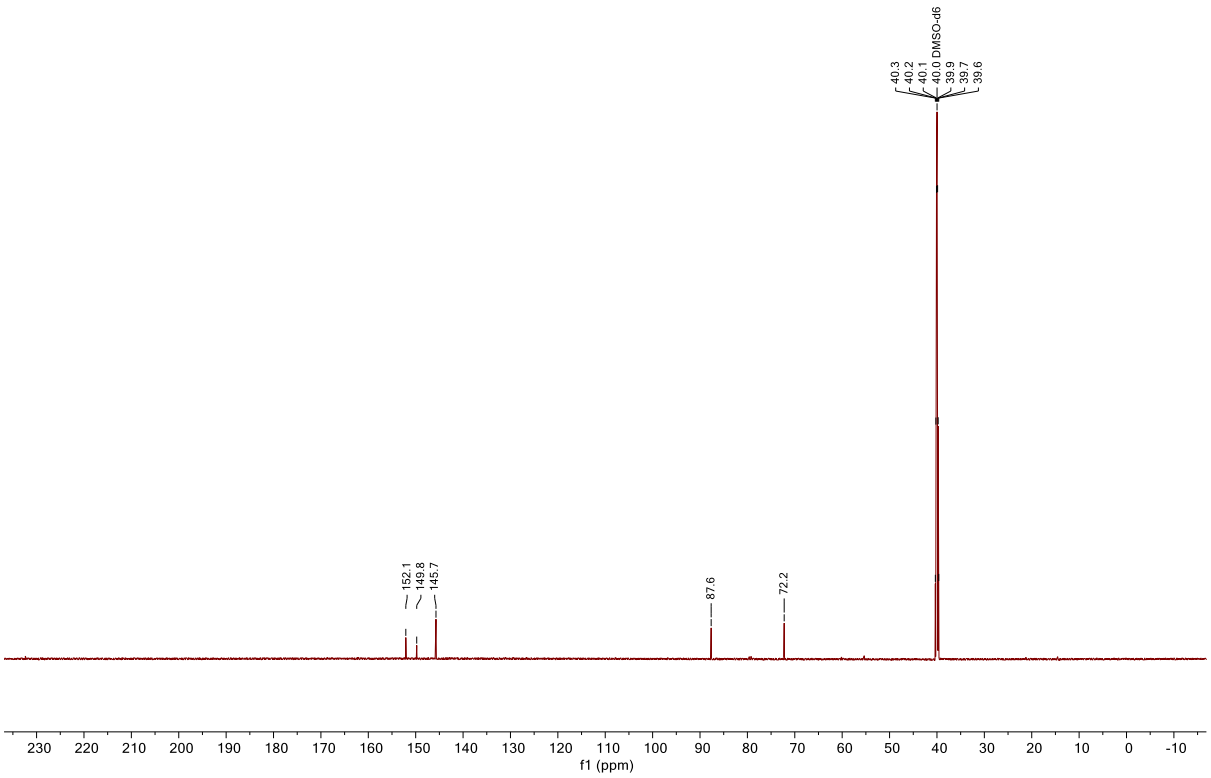
40.3
40.2
40.1
40.0 DMSO-d6
39.9
39.7
39.6
152.1
149.8
145.7
87.6
72.2
f1 (ppm)

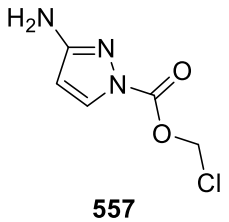
H2N
N
N
O
O
Cl

557

40.34
40.22
40.10
39.98 DMSO-d6
39.86
39.74
39.62
160.00
132.78
102.61
72.38
230 220 210 200 190 180 170 160 150 140 130 120 110 100 90 80 70 60 50 40 30 20 10 0 -10
f1 (ppm)

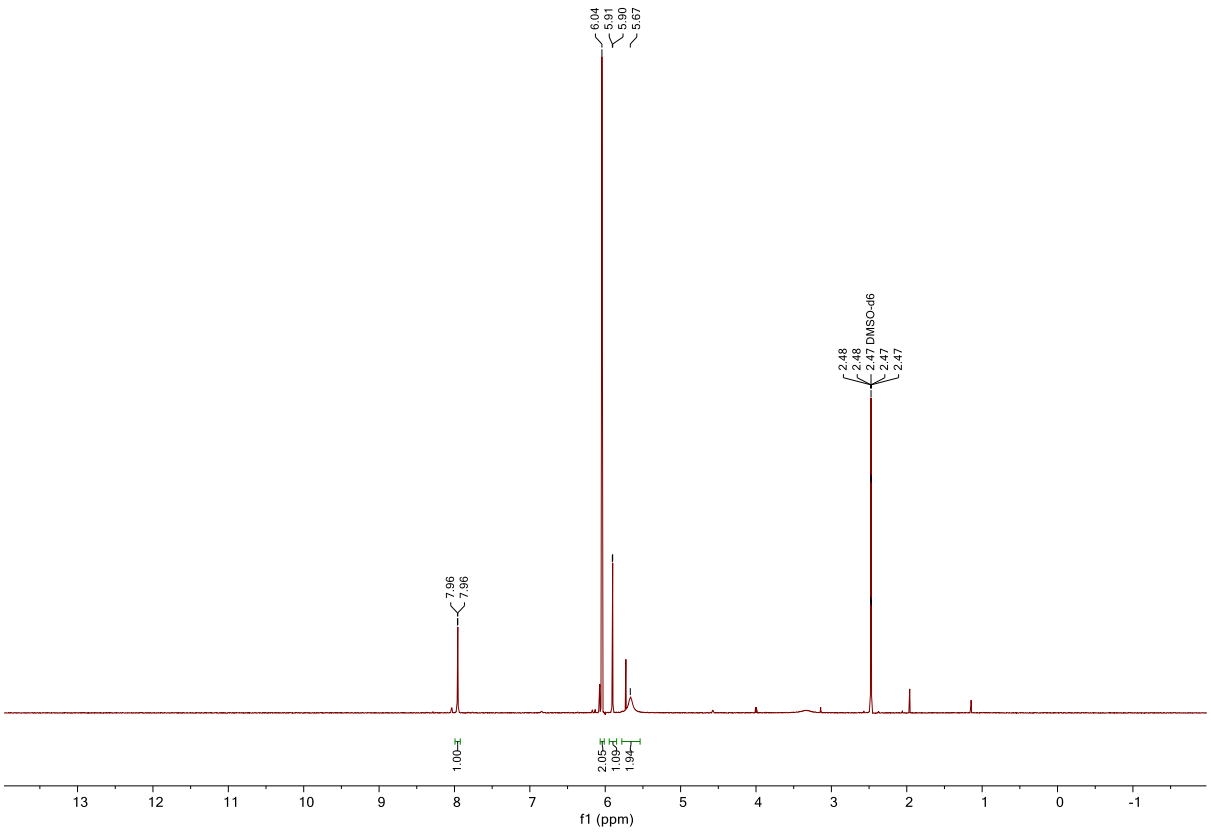
6.04
5.91
5.90
5.67
2.48
2.48
2.47 DMSO-d6
2.47
2.47
7.96
7.96
1.00
2.05
1.09
1.94
13 12 11 10 9 8 7 6 5 4 3 2 1 0 -1
f1 (ppm)

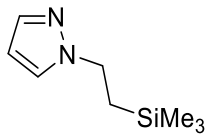
N
N
SiMe3

558

0.03
7.48
7.48
7.39
7.39
7.26 CDCl3
6.22
6.22
6.22
4.18
4.18
4.17
4.17
4.16
1.23
1.22
1.21
1.21
1.20
13 12 11 10 9 8 7 6 5 4 3 2 1 0 -1
f1 (ppm)

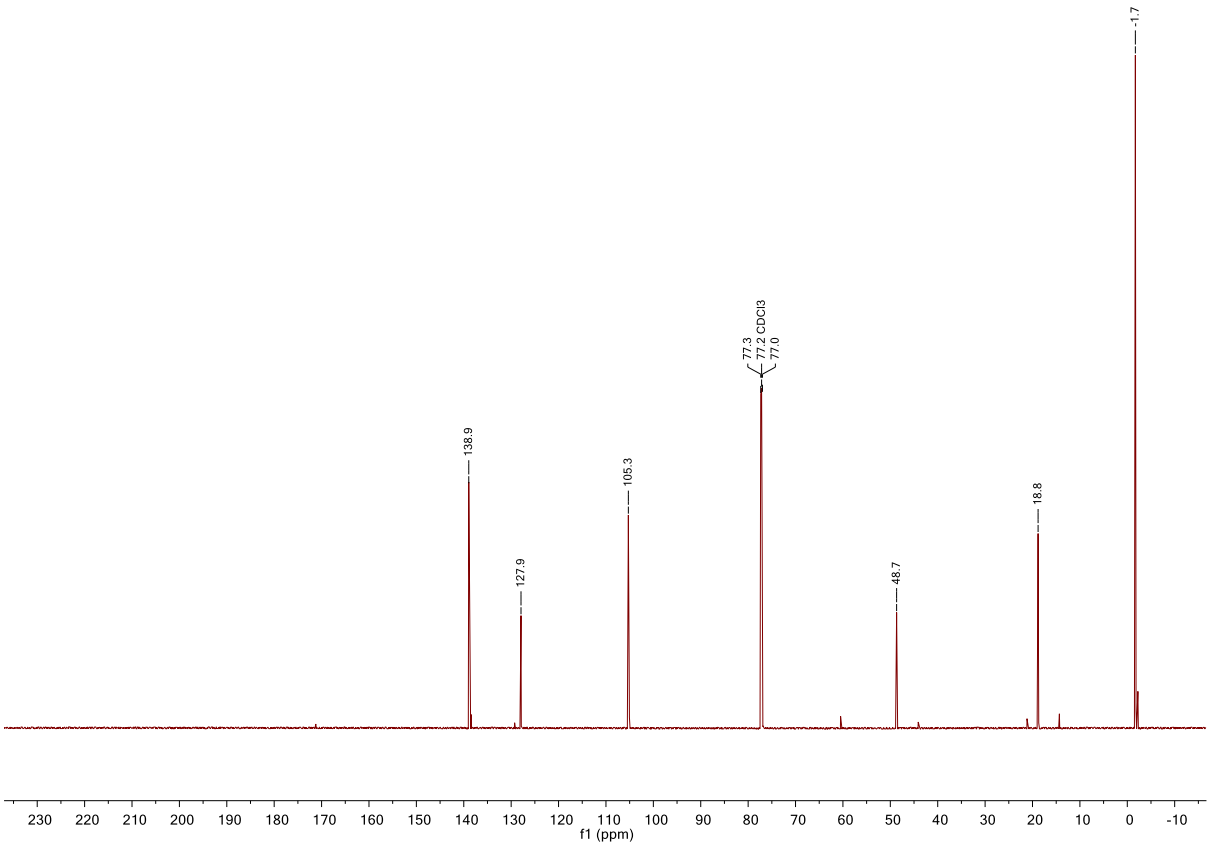
-1.7
77.3
77.2 CDCl3
77.0
138.9
127.9
105.3
48.7
18.8
230 220 210 200 190 180 170 160 150 140 130 120 110 100 90 80 70 60 50 40 30 20 10 0 -10
f1 (ppm)

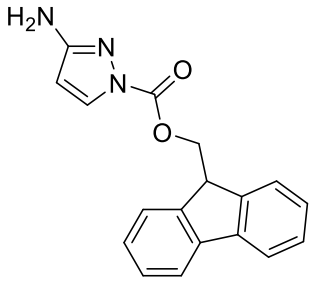

559

7.89
7.88
7.71
7.70
7.42
7.41
7.40
7.33
7.33
7.32
7.32
7.31
7.31
5.85
5.84
5.55
4.59
4.58
4.39
4.38
4.37
2.48
2.48
2.47 DMSO-d6
2.47
2.47
1.95
1.05
1.06
2.03
2.04
1.02
1.97
1.91
1.00
f1 (ppm)

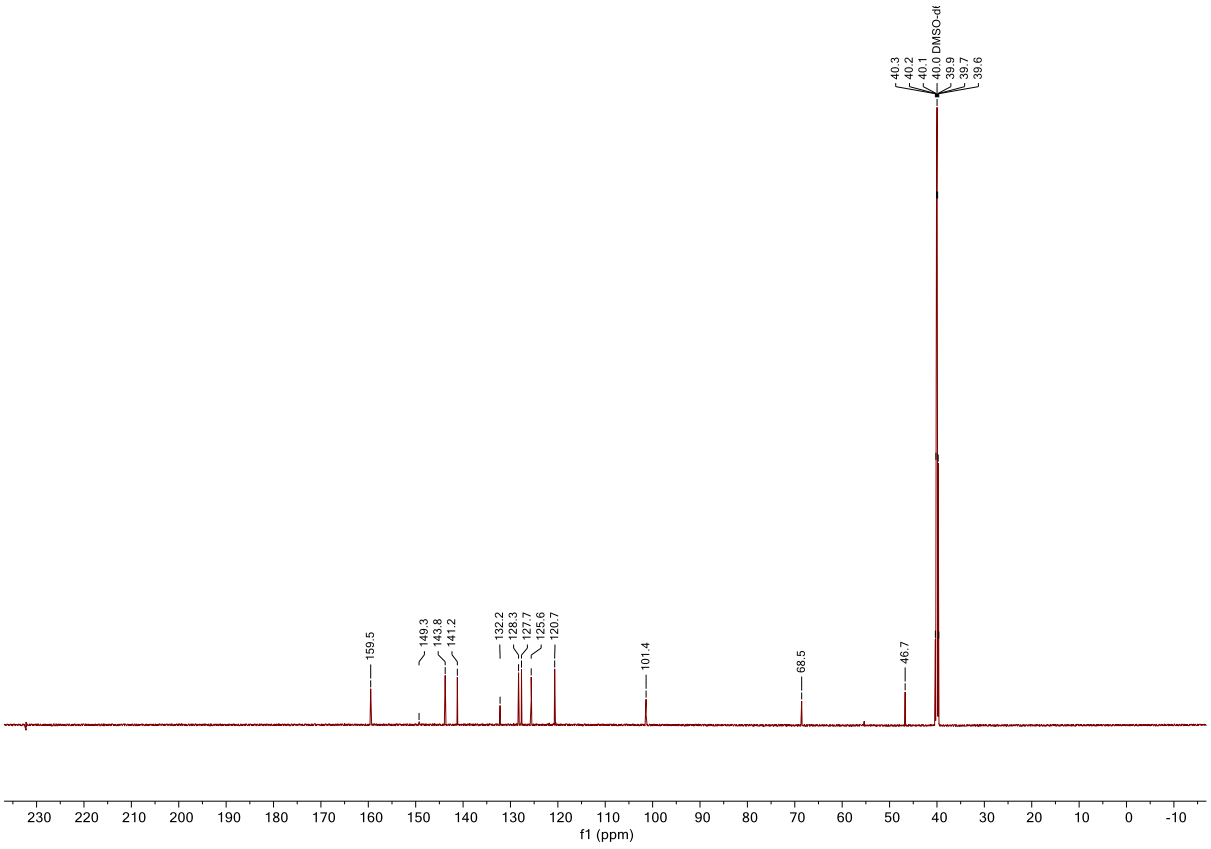
40.3
40.2
40.1
40.0 DMSO-d6
39.9
39.7
39.6
159.5
149.3
143.8
141.2
132.2
128.3
127.7
125.6
120.7
101.4
68.5
46.7
f1 (ppm)

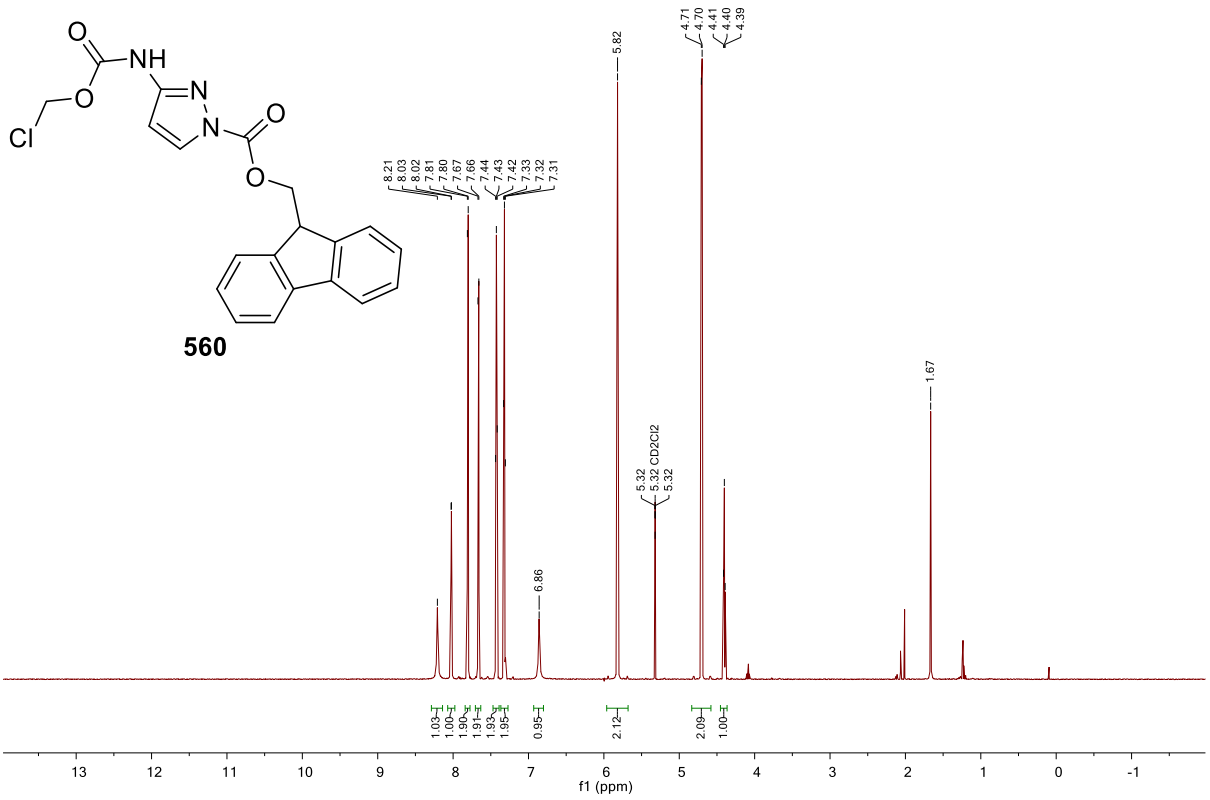
560
8.21
8.03
8.02
7.81
7.80
7.67
7.66
7.44
7.43
7.42
7.33
7.32
7.31
5.82
4.71
4.70
4.41
4.40
4.39
5.32
5.32 CD2Cl2
5.32
6.86
1.67
1.03
1.00
1.90
1.91
1.93
1.95
0.95
2.12
2.09
1.00
f1 (ppm)

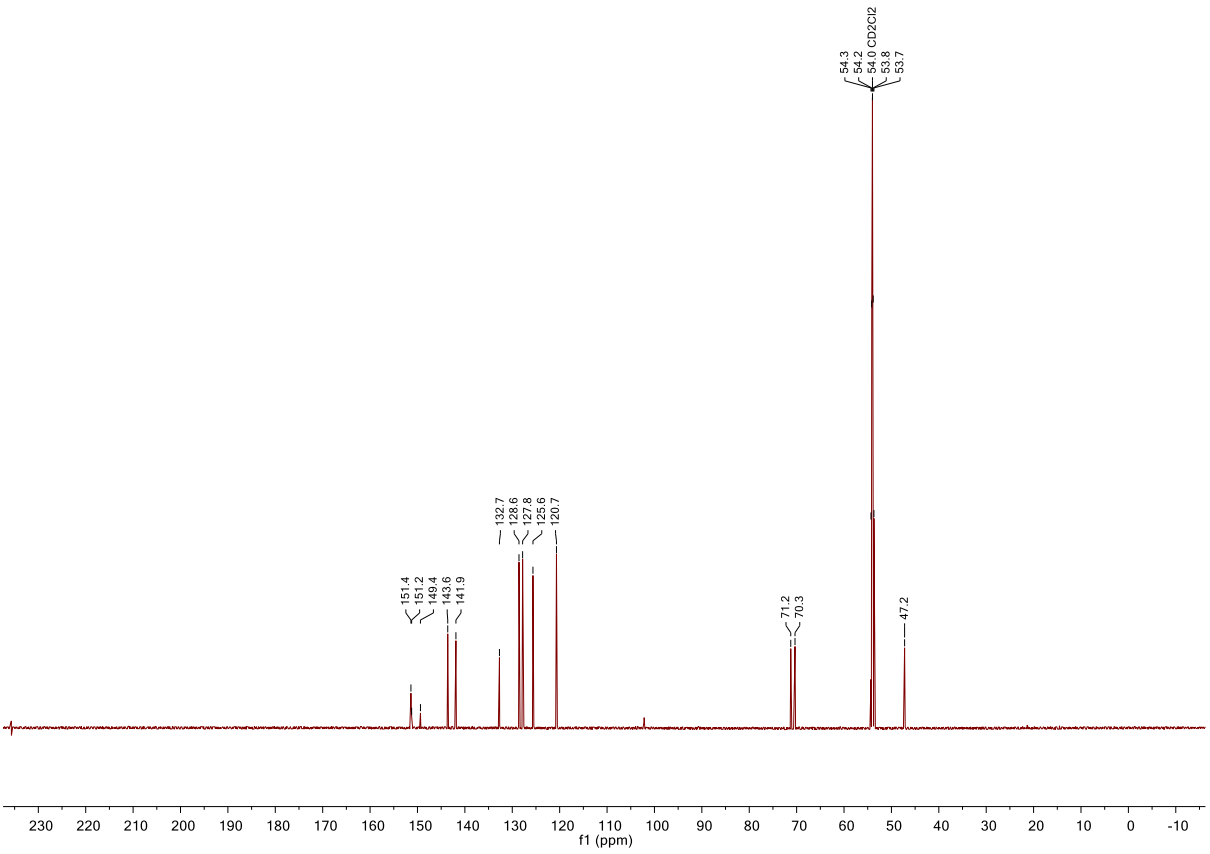
54.3
54.2
54.0 CD2Cl2
53.8
53.7
132.7
128.6
127.8
125.6
120.7
151.4
151.2
149.4
143.6
141.9
71.2
70.3
47.2
f1 (ppm)

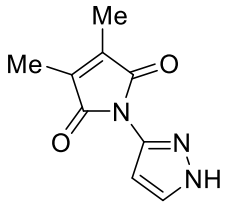
Me
Me
O
N
O
N
NH

561

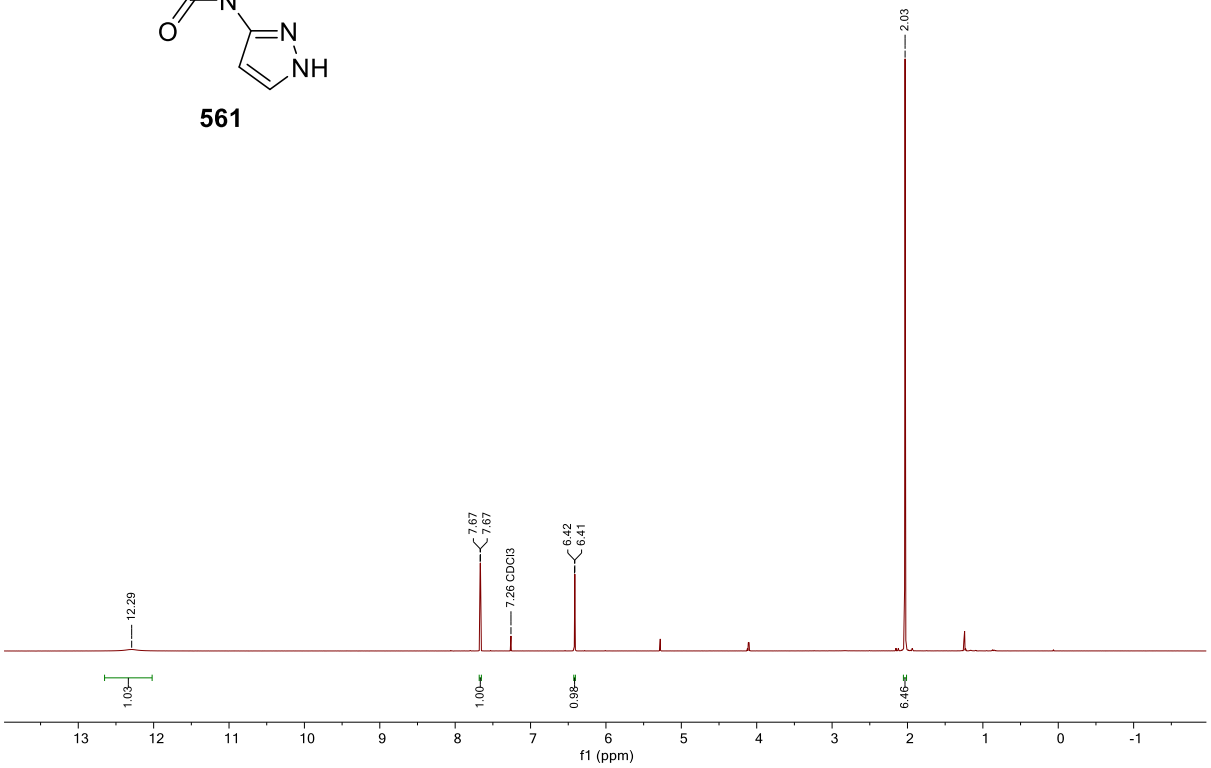
2.03
7.67
7.67
7.26 CDCl3
6.42
6.41
12.29
1.03
1.00
0.98
6.46
13 12 11 10 9 8 7 6 5 4 3 2 1 0 -1
f1 (ppm)

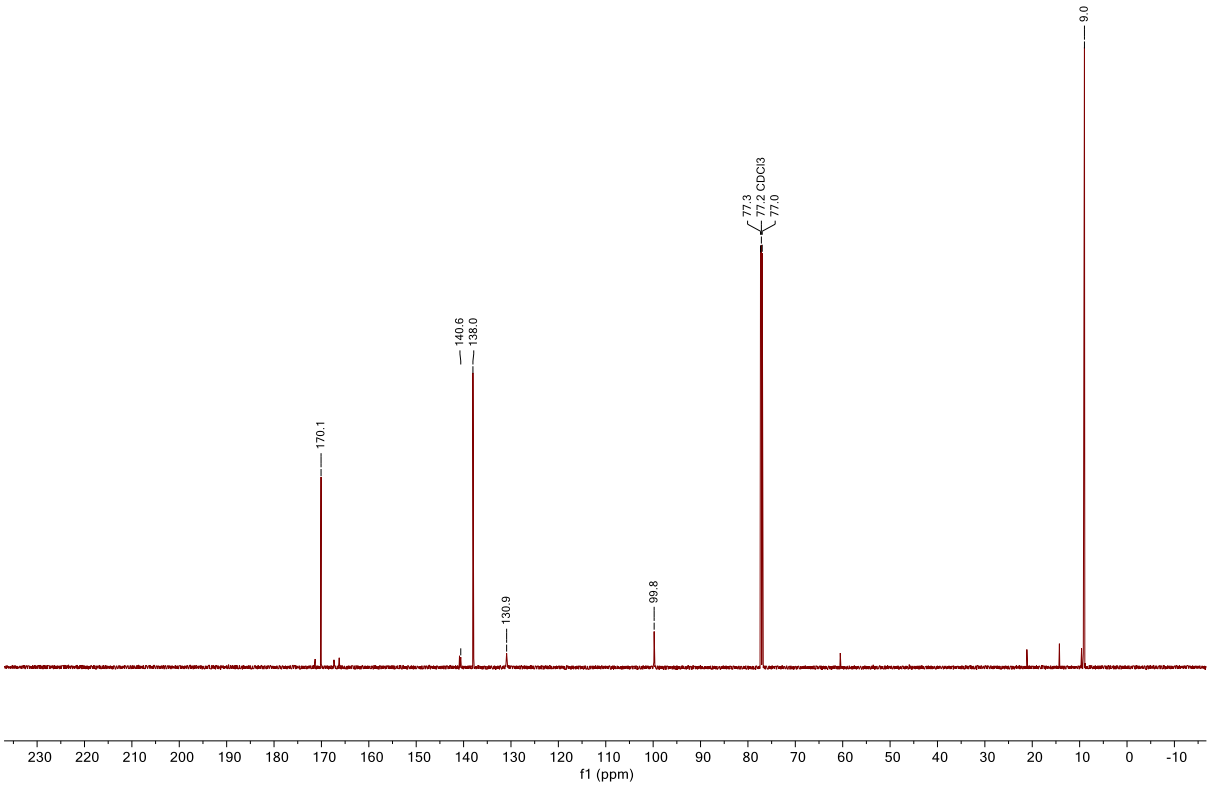
9.0
77.3
77.2 CDCl3
77.0
140.6
138.0
170.1
130.9
99.8
230 220 210 200 190 180 170 160 150 140 130 120 110 100 90 80 70 60 50 40 30 20 10 0 -10
f1 (ppm)

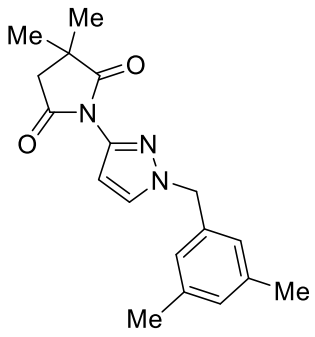
Me
Me
O
N
O
N
N
Me
Me

562

1.41
2.28
2.70
5.24
7.33
7.33
7.25 CDCl3
6.94
6.86
6.30
6.30
1.00
1.02
2.00
1.03
2.02
2.05
5.92
5.96
13 12 11 10 9 8 7 6 5 4 3 2 1 0 -1
f1 (ppm)

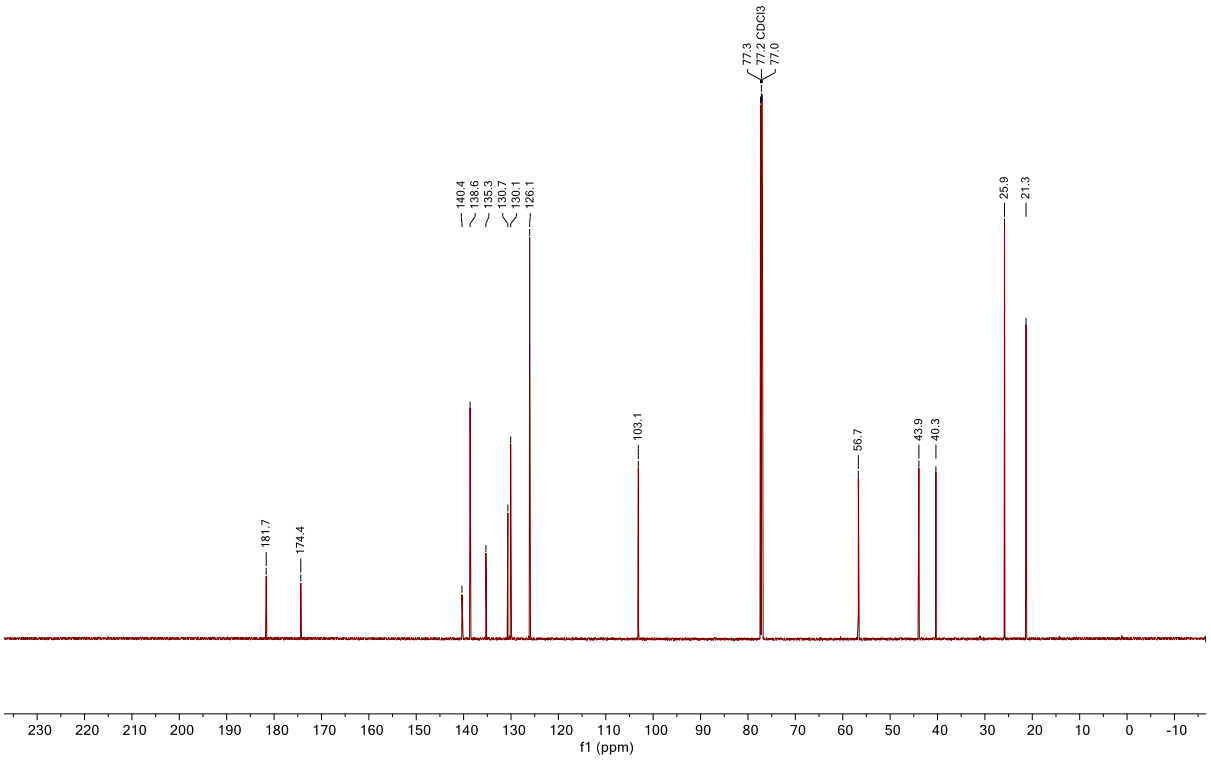
77.3
77.2 CDCl3
77.0
140.4
138.6
135.3
130.7
130.1
126.1
103.1
56.7
43.9
40.3
25.9
21.3
181.7
174.4
230 220 210 200 190 180 170 160 150 140 130 120 110 100 90 80 70 60 50 40 30 20 10 0 -10
f1 (ppm)

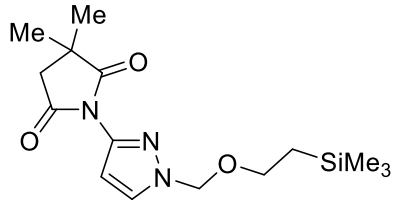
Me
Me
O
N
O
N
N
O
SiMe3

563

7.63
7.62
7.26 CDCl3
6.40
6.40
5.44
3.60
3.59
3.58
2.71
1.42
0.91
0.90
0.89
-0.02
1.00
0.97
2.21
1.92
2.19
5.98
2.02
8.85
f1 (ppm)

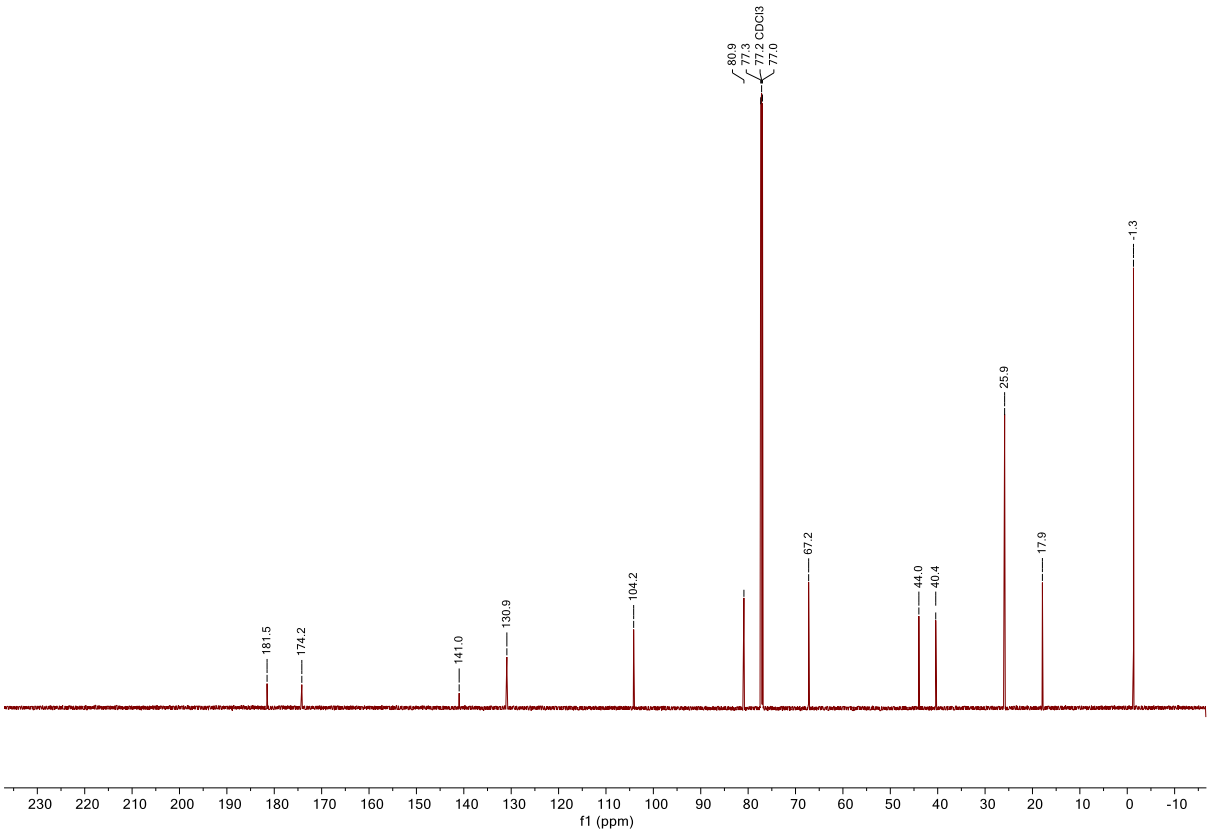
80.9
77.3
77.2 CDCl3
77.0
181.5
174.2
141.0
130.9
104.2
67.2
44.0
40.4
25.9
17.9
-1.3
f1 (ppm)

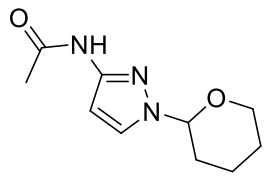
O
NH
N
N
O

564

2.11
2.08
2.06
2.06
2.04
2.03
2.01
2.01
2.00
1.98
1.96
1.96
1.93
1.70
1.69
1.67
1.65
1.64
1.62
1.61
1.60
1.58
1.56
7.47
7.46
7.26 CDCl3
6.73
6.73
5.20
5.20
5.19
5.18
4.04
4.02
3.66
3.66
3.65
3.64
3.63
3.62
8.21
1.00
0.97
0.99
0.98
1.06
1.10
2.91
3.36
2.05
1.12
f1 (ppm)

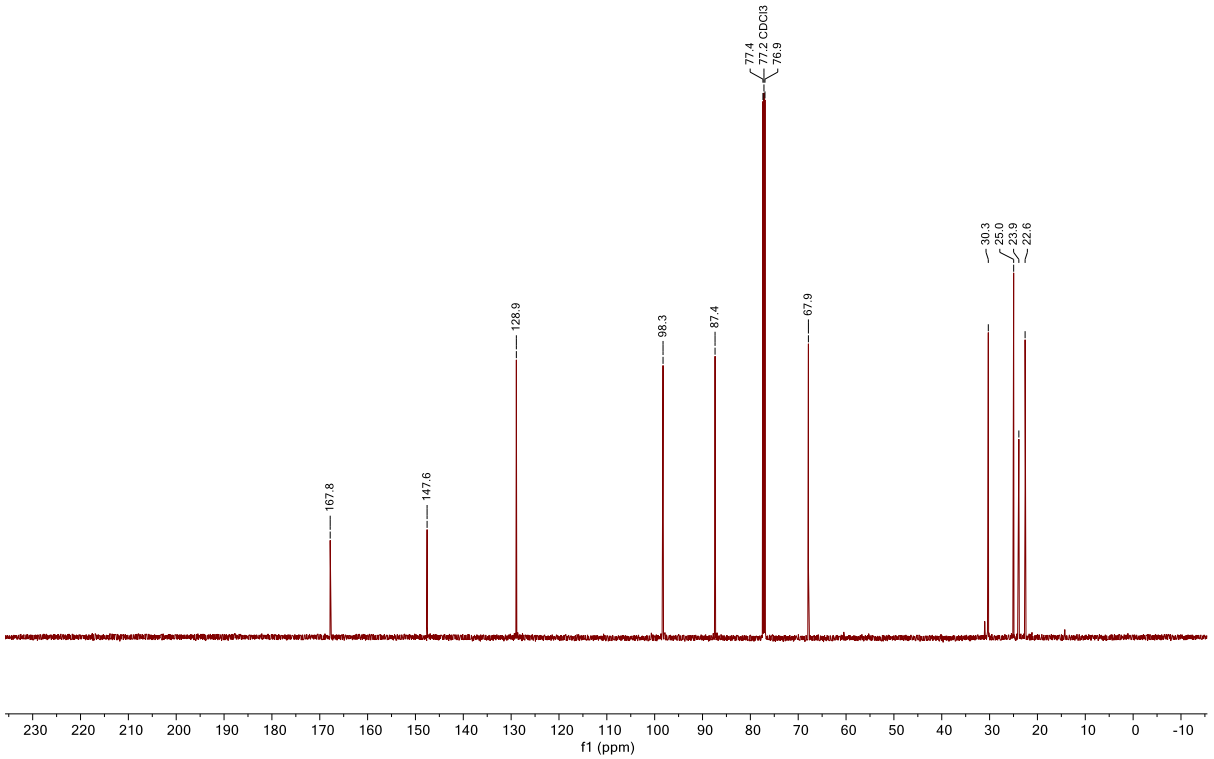
77.4
77.2 CDCl3
76.9
30.3
25.0
23.9
22.6
128.9
98.3
87.4
67.9
167.8
147.6
f1 (ppm)

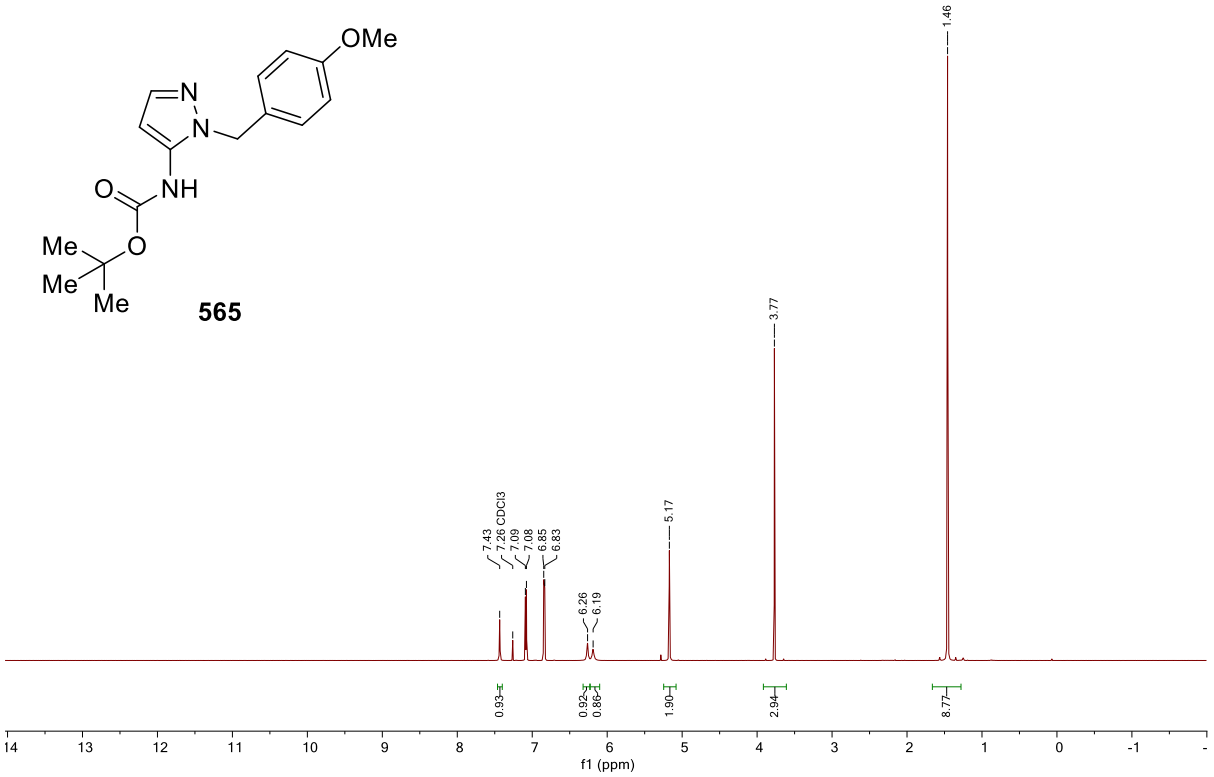
OMe
N
N
O
NH
Me
O
Me
Me
565
1.46
3.77
5.17
7.43
7.26 CDCl3
7.09
7.08
6.85
6.83
6.26
6.19
0.93
0.92
0.86
1.90
2.94
8.77
f1 (ppm)

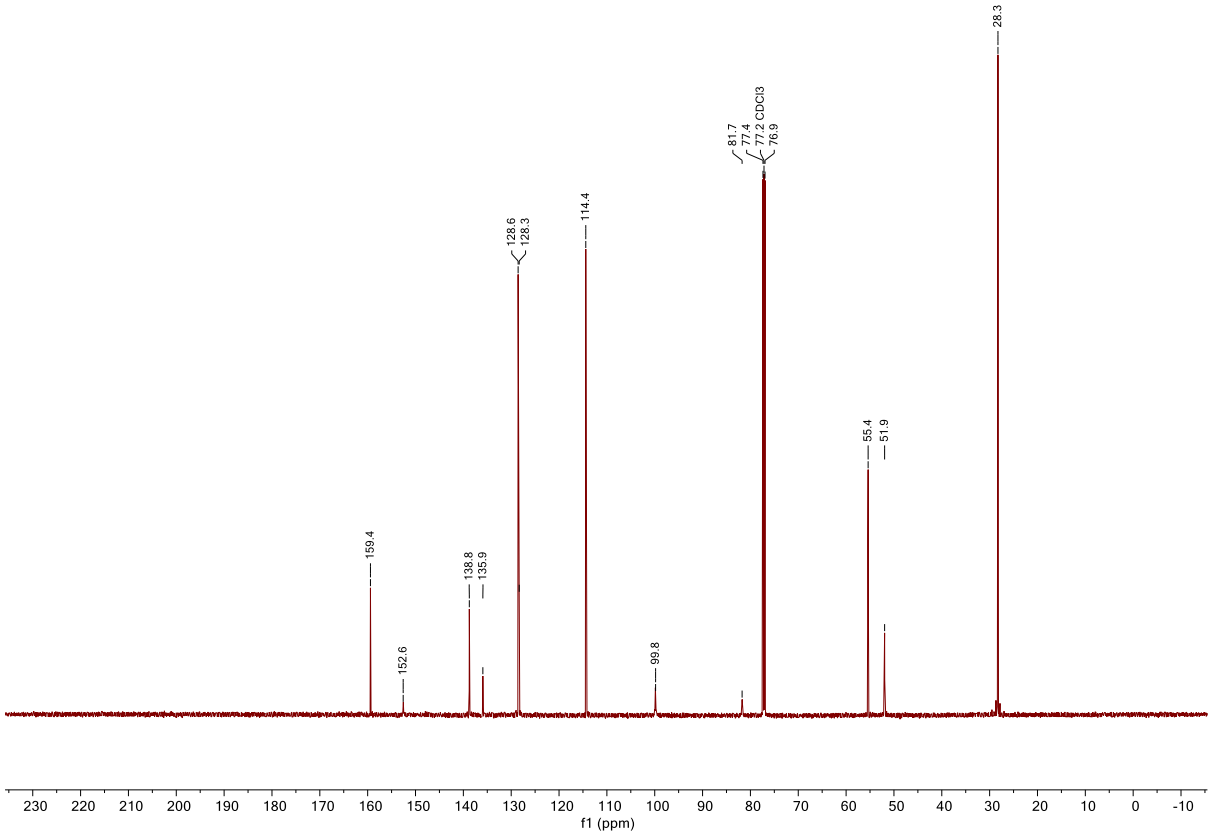
28.3
81.7
77.4
77.2 CDCl3
76.9
128.6
128.3
114.4
55.4
51.9
159.4
138.8
135.9
152.6
99.8
f1 (ppm)

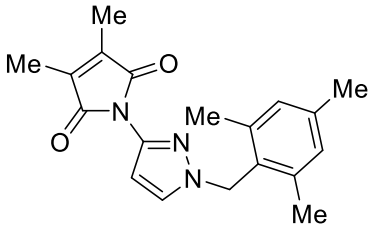
Me
Me
O
O
N
N
N
Me
Me
Me

566

2.29
2.28
2.03
7.26 CDCl3
6.96
6.96
6.91
6.21
6.20
5.34
1.00
2.00
1.00
2.01
3.07
5.92
6.11
13 12 11 10 9 8 7 6 5 4 3 2 1 0 -1
f1 (ppm)

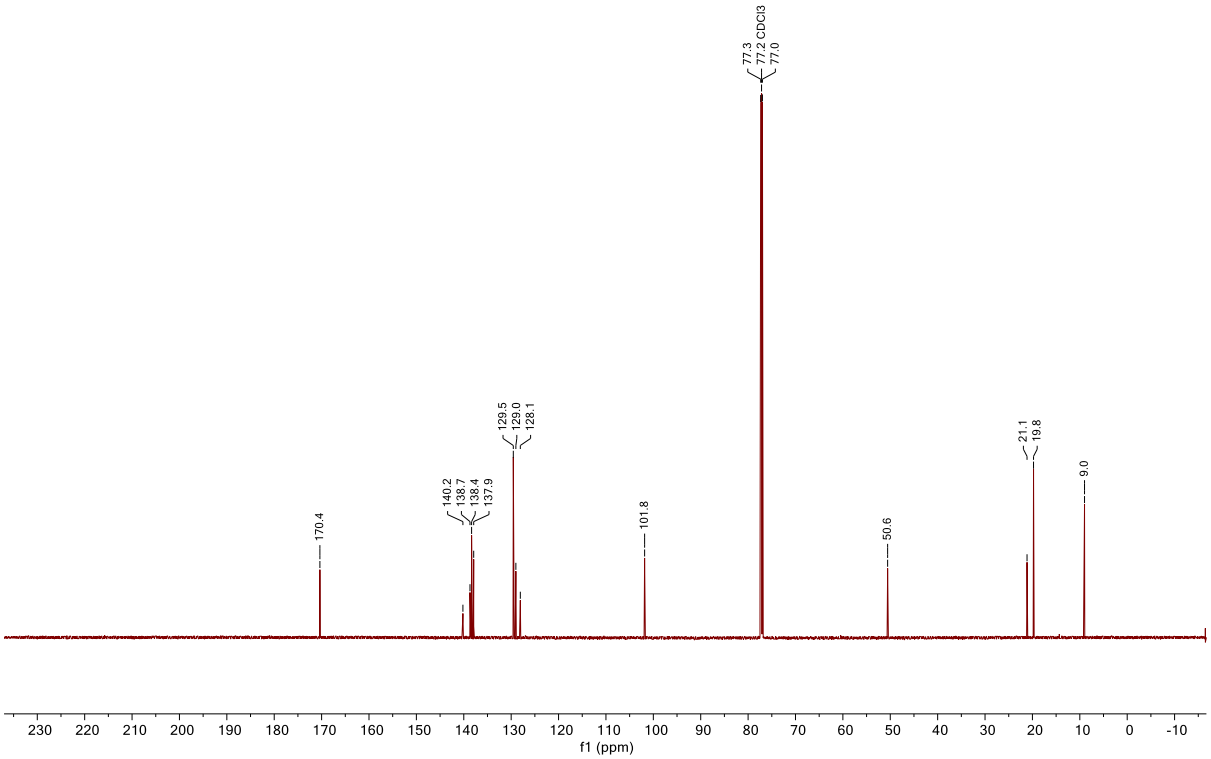
77.3
77.2 CDCl3
77.0
170.4
140.2
138.7
138.4
137.9
129.5
129.0
128.1
101.8
50.6
21.1
19.8
9.0
230 220 210 200 190 180 170 160 150 140 130 120 110 100 90 80 70 60 50 40 30 20 10 0 -10
f1 (ppm)

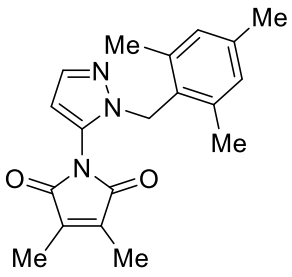
Me
Me
N
N
Me
N
O
O
Me
Me

567

2.22
2.10
1.93
7.55
7.55
7.26 CDCl3
6.78
6.19
6.19
5.24
1.00
1.92
0.99
1.91
2.94
5.78
5.72
13
12
11
10
9
8
7
6
5
4
3
2
1
0
-1
f1 (ppm)

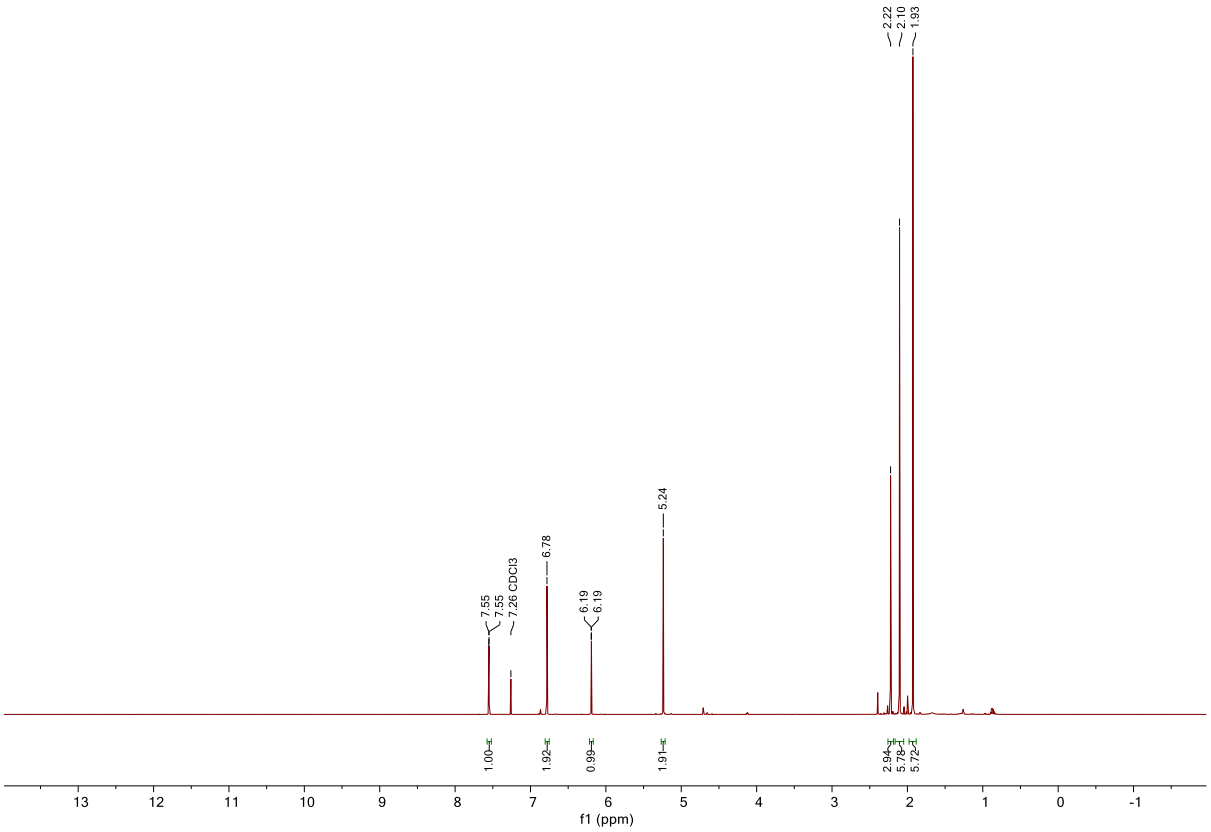
2.22
2.10
1.93
7.55
7.55
7.26 CDCl3
6.78
6.19
6.19
5.24
1.00
1.92
0.99
1.91
2.94
5.78
5.72
13
12
11
10
9
8
7
6
5
4
3
2
1
0
-1
f1 (ppm)

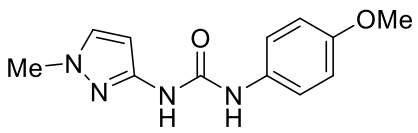
Me
N
N
O
N
H
N
H
OMe

391

3.80
3.79
7.42
7.41
7.26
7.20
7.19
6.86
6.85
9.58
8.51
5.93
1.16
1.07
1.98
1.03
2.01
1.00
2.93
2.95
f1 (ppm)

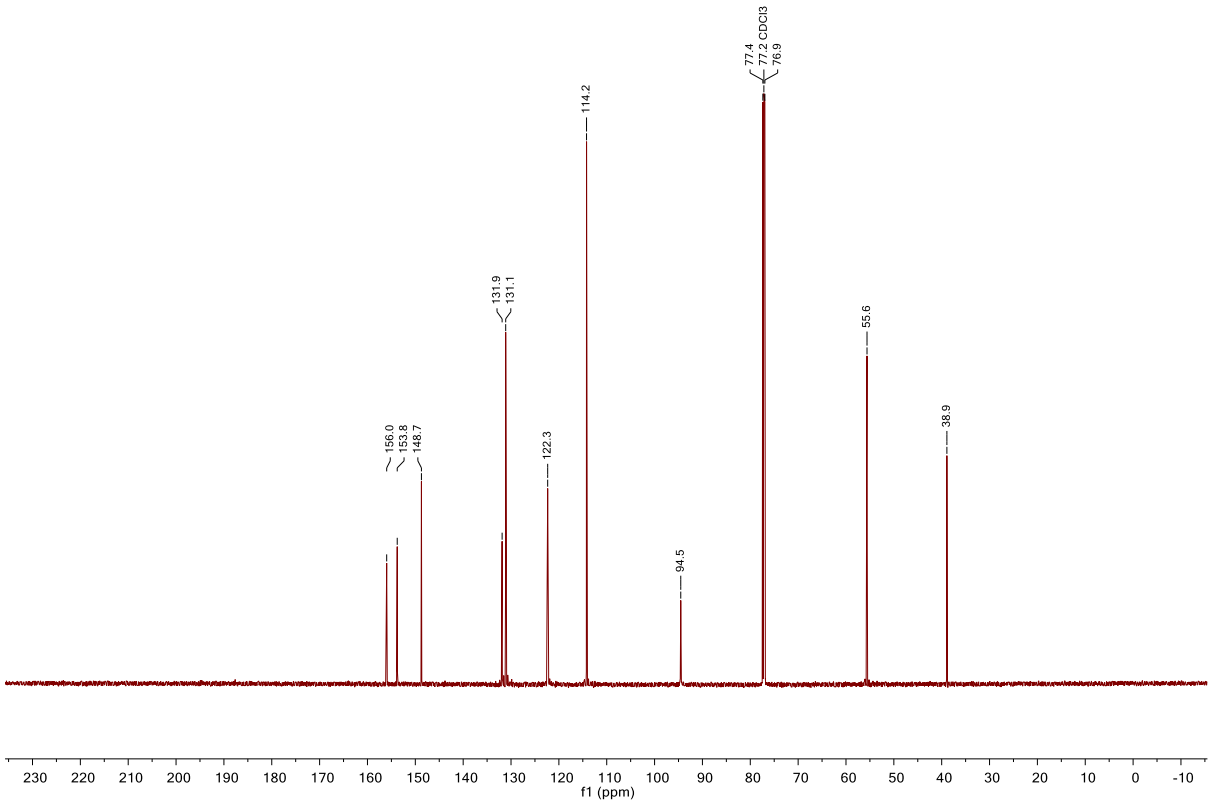
77.4
77.2 CDCl3
76.9
114.2
131.9
131.1
55.6
156.0
153.8
148.7
122.3
94.5
38.9
f1 (ppm)

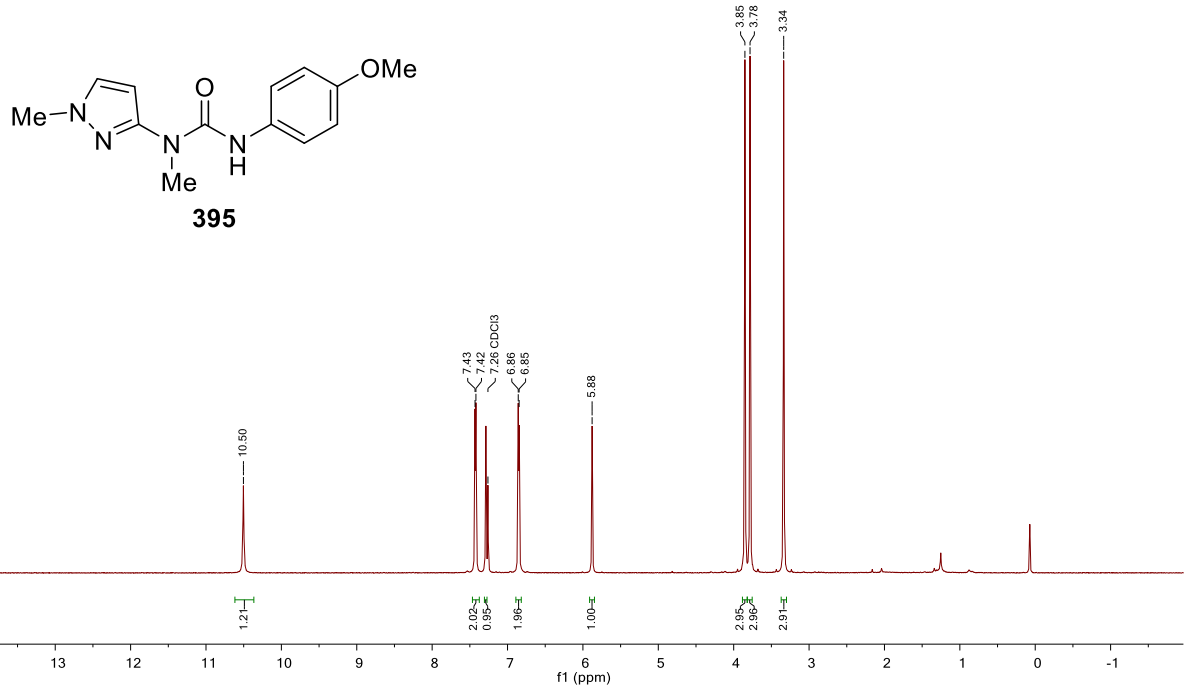
Me
N
N
O
N
Me
N
H
OMe
395
10.50
7.43
7.42
7.26 CDCl3
6.86
6.85
5.88
3.85
3.78
3.34
1.21
2.02
0.95
1.96
1.00
2.95
2.96
2.91
f1 (ppm)

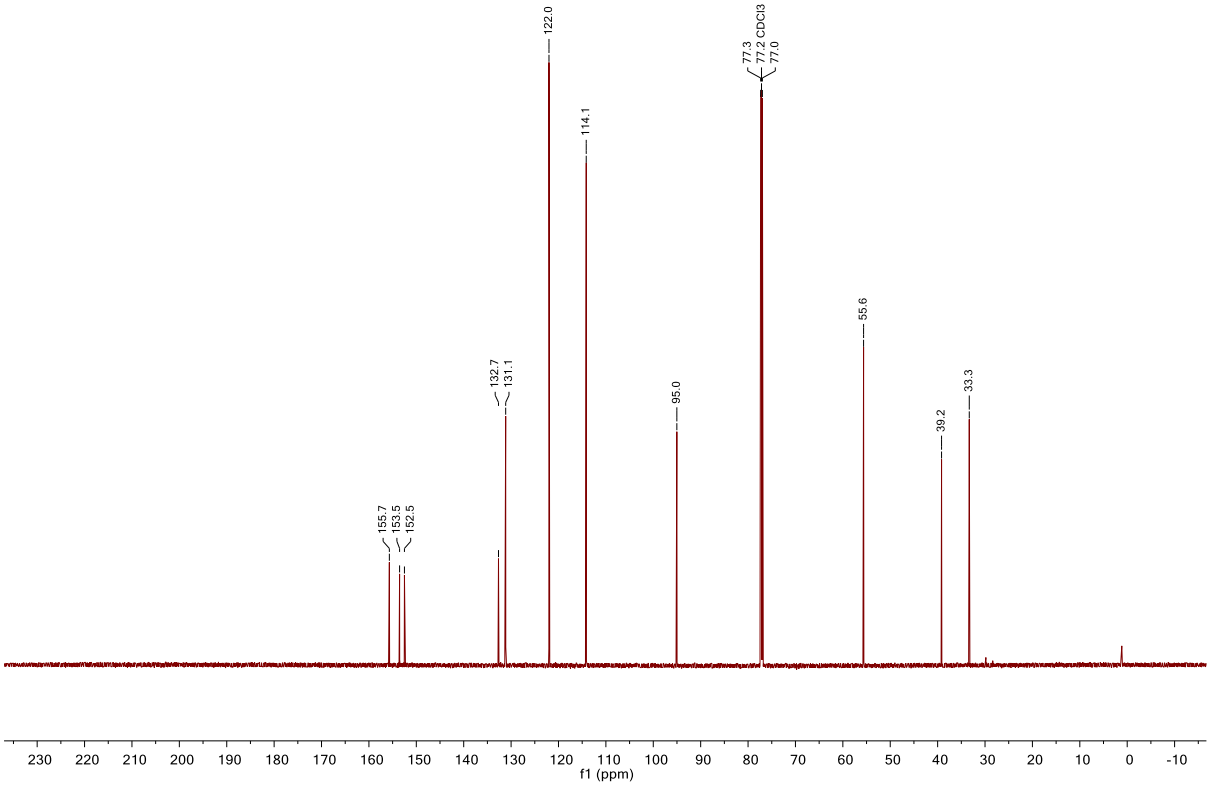
122.0
114.1
77.3
77.2 CDCl3
77.0
55.6
39.2
33.3
132.7
131.1
95.0
155.7
153.5
152.5
f1 (ppm)

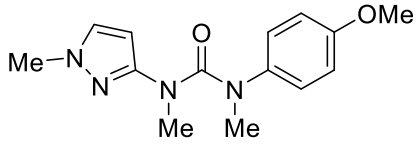
Me
N
N
O
N
Me
N
Me
OMe

396

3.72
3.64
3.18
3.05
7.26 CDCl3
7.00
6.99
6.89
6.87
6.70
6.69
5.91
1.00
2.03
2.02
0.95
3.16
3.08
3.04
3.08
f1 (ppm)

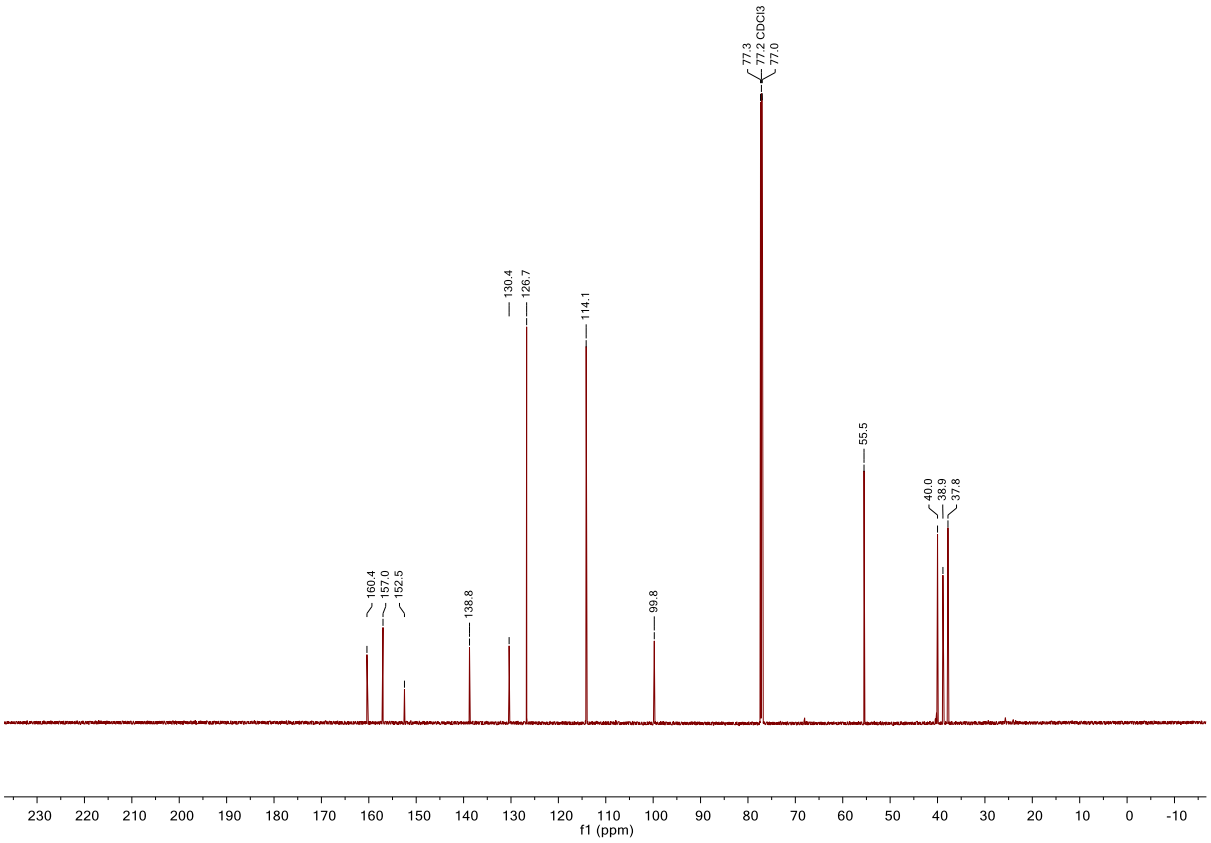
77.3
77.2 CDCl3
77.0
130.4
126.7
114.1
55.5
40.0
38.9
37.8
160.4
157.0
152.5
138.8
99.8
f1 (ppm)

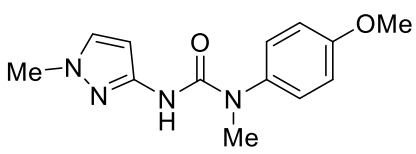
Me
N
N
O
N
H
N
Me
OMe

398

3.81
3.68
3.27
7.26 CDCl3
7.20
7.19
7.16
6.93
6.92
6.73
6.56
1.86
0.95
1.92
0.95
0.92
2.96
2.97
3.00
f1 (ppm)

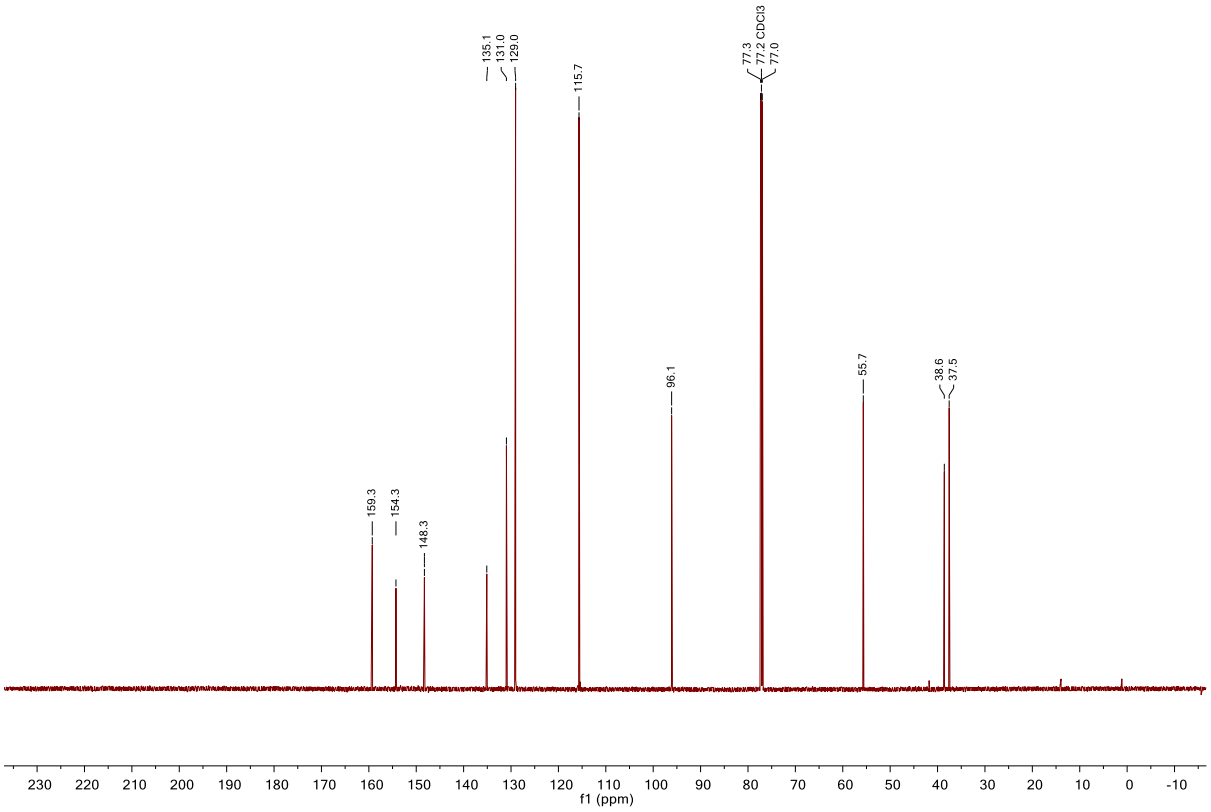
135.1
131.0
129.0
115.7
77.3
77.2 CDCl3
77.0
96.1
55.7
38.6
37.5
159.3
154.3
148.3
f1 (ppm)

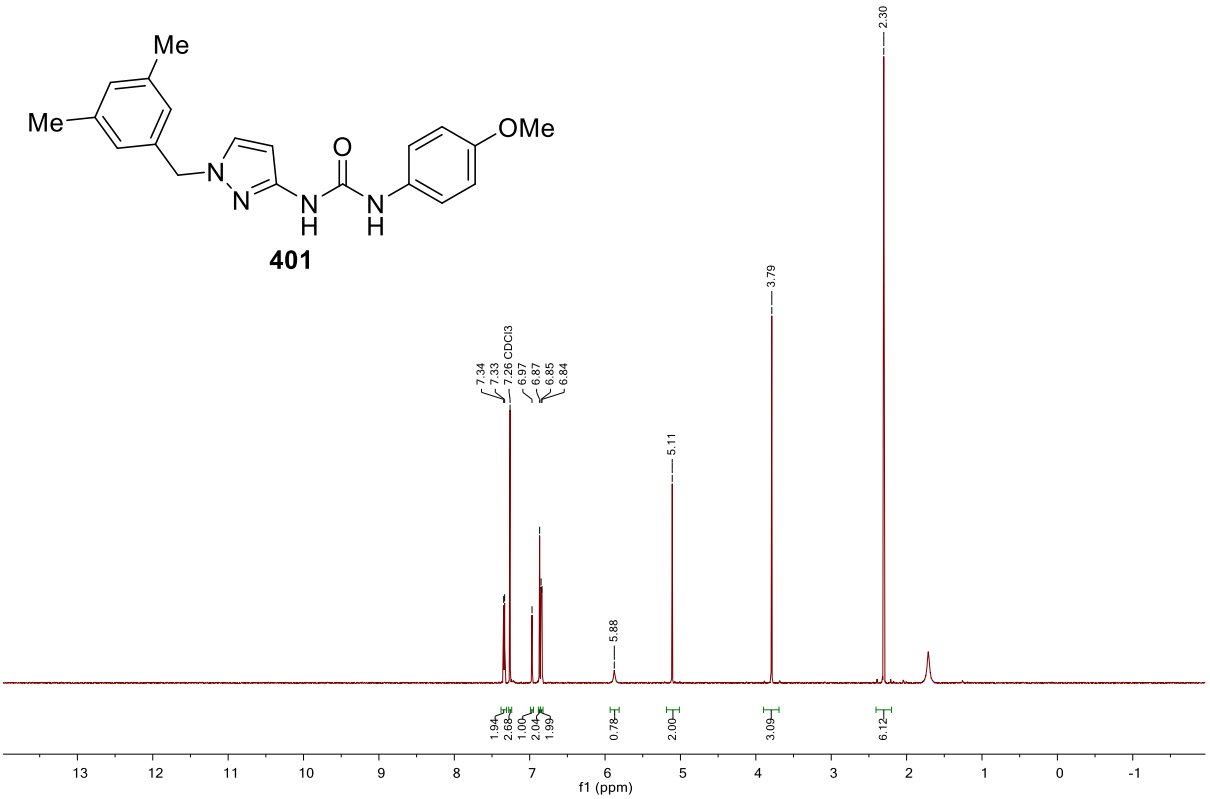
Me
Me
OMe
O
N
N
N
H
N
H
401
2.30
3.79
7.34
7.33
7.26 CDCl3
6.97
6.87
6.85
6.84
5.11
5.88
1.94
2.68
1.00
2.04
1.99
0.78
2.00
3.09
6.12
13 12 11 10 9 8 7 6 5 4 3 2 1 0 -1
f1 (ppm)

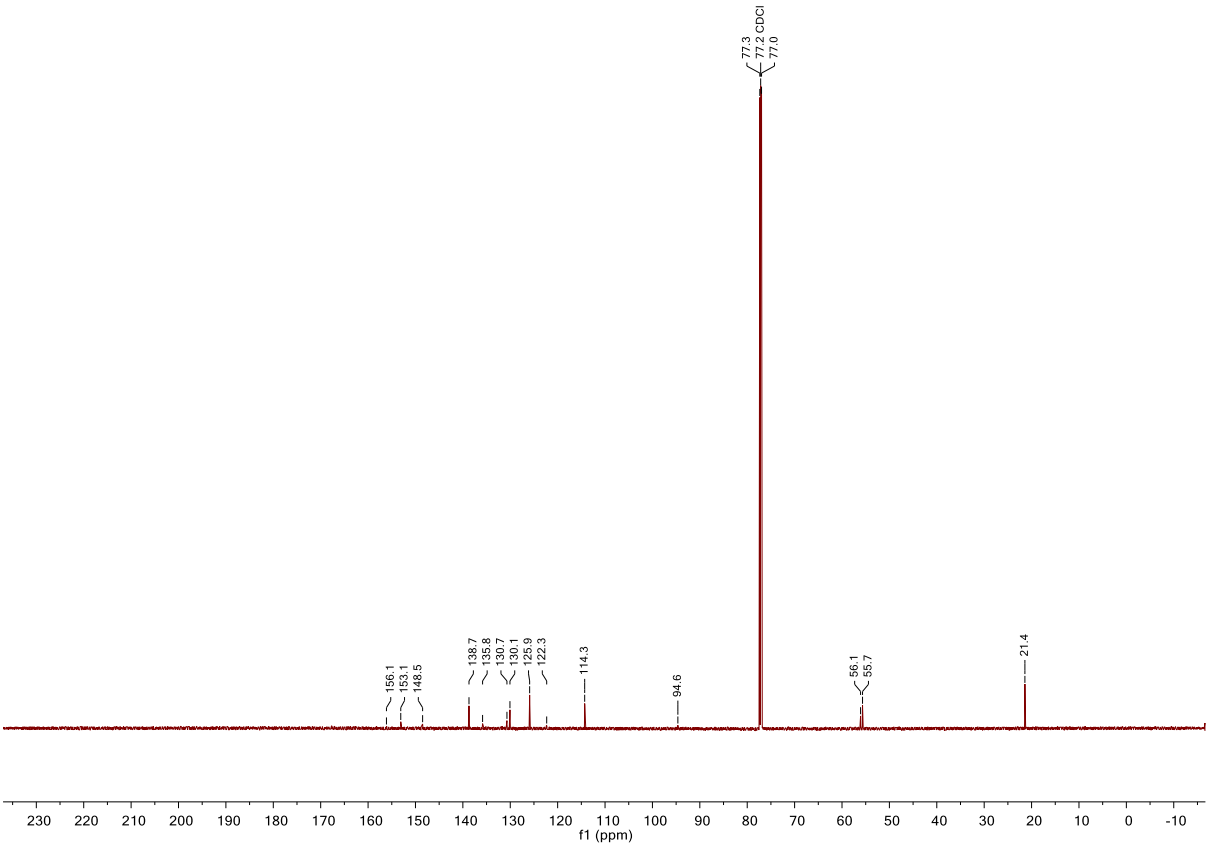
77.3
77.2 CDCl
77.0
156.1
153.1
148.5
138.7
135.8
130.7
130.1
125.9
122.3
114.3
94.6
56.1
55.7
21.4
230 220 210 200 190 180 170 160 150 140 130 120 110 100 90 80 70 60 50 40 30 20 10 0 -10
f1 (ppm)

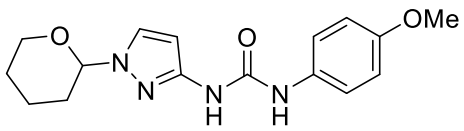
O
N
N
N
H
O
N
H
OMe

420

3.91
3.90
3.71
3.61
3.60
3.59
3.58
2.51
2.50
2.50 DMSO-d6
2.50
2.49
8.92
8.84
7.72
7.72
7.72
7.35
7.34
6.87
6.86
6.27
5.27
5.26
5.25
5.25
2.07
2.06
2.05
2.04
2.03
2.02
1.94
1.92
1.92
1.89
1.89
1.87
1.87
1.66
1.66
1.65
1.65
1.64
1.63
1.62
1.53
1.53
1.52
1.52
1.50
1.00
0.93
0.98
2.02
1.95
0.97
0.96
0.99
2.86
1.08
1.22
1.01
0.97
1.07
1.95
f1 (ppm)

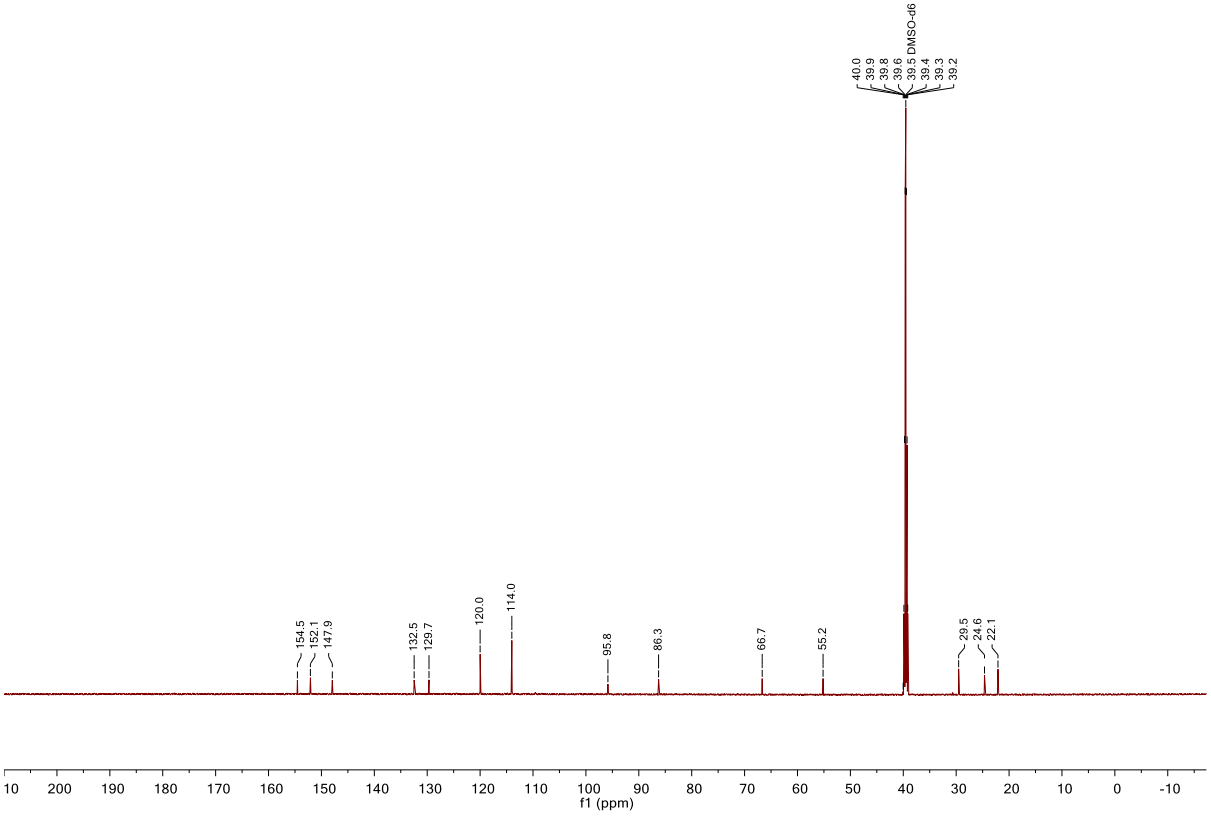
40.0
39.9
39.8
39.6
39.5 DMSO-d6
39.4
39.3
39.2
154.5
152.1
147.9
132.5
129.7
120.0
114.0
95.8
86.3
66.7
55.2
29.5
24.6
22.1
f1 (ppm)

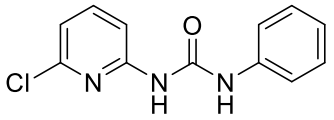
Cl
N
O
N
H
N
H

429a

2.50 DMSO-d6
7.81
7.79
7.78
7.76
7.75
7.47
7.46
7.33
7.31
7.30
7.10
7.09
7.04
7.02
7.01
9.54
9.33
0.99
0.98
0.98
0.97
1.96
1.98
0.97
1.00
14 13 12 11 10 9 8 7 6 5 4 3 2 1 0 -1
f1 (ppm)

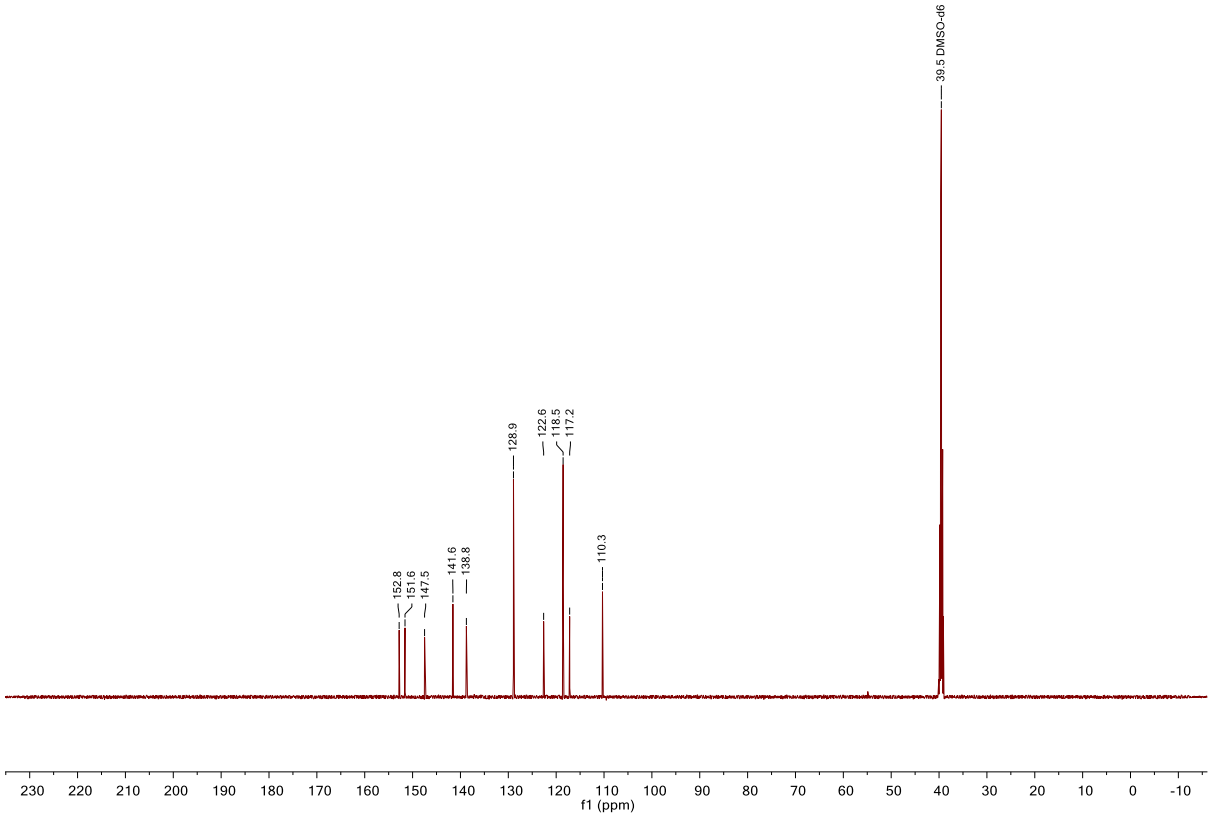
39.5 DMSO-d6
152.8
151.6
147.5
141.6
138.8
128.9
122.6
118.5
117.2
110.3
230 220 210 200 190 180 170 160 150 140 130 120 110 100 90 80 70 60 50 40 30 20 10 0 -10
f1 (ppm)

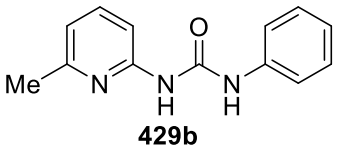
Me
N
O
N
H
N
H

429b

2.50
2.50 DMSO-d6
2.50
2.45
7.64
7.63
7.62
7.52
7.51
7.32
7.31
7.30
7.20
7.19
7.03
7.02
7.01
6.87
6.86
9.47
10.89
1.05
1.06
1.00
1.95
1.96
1.01
1.02
1.02
2.90
4
13
12
11
10
9
8
7
6
5
4
3
2
1
0
-1
f1 (ppm)

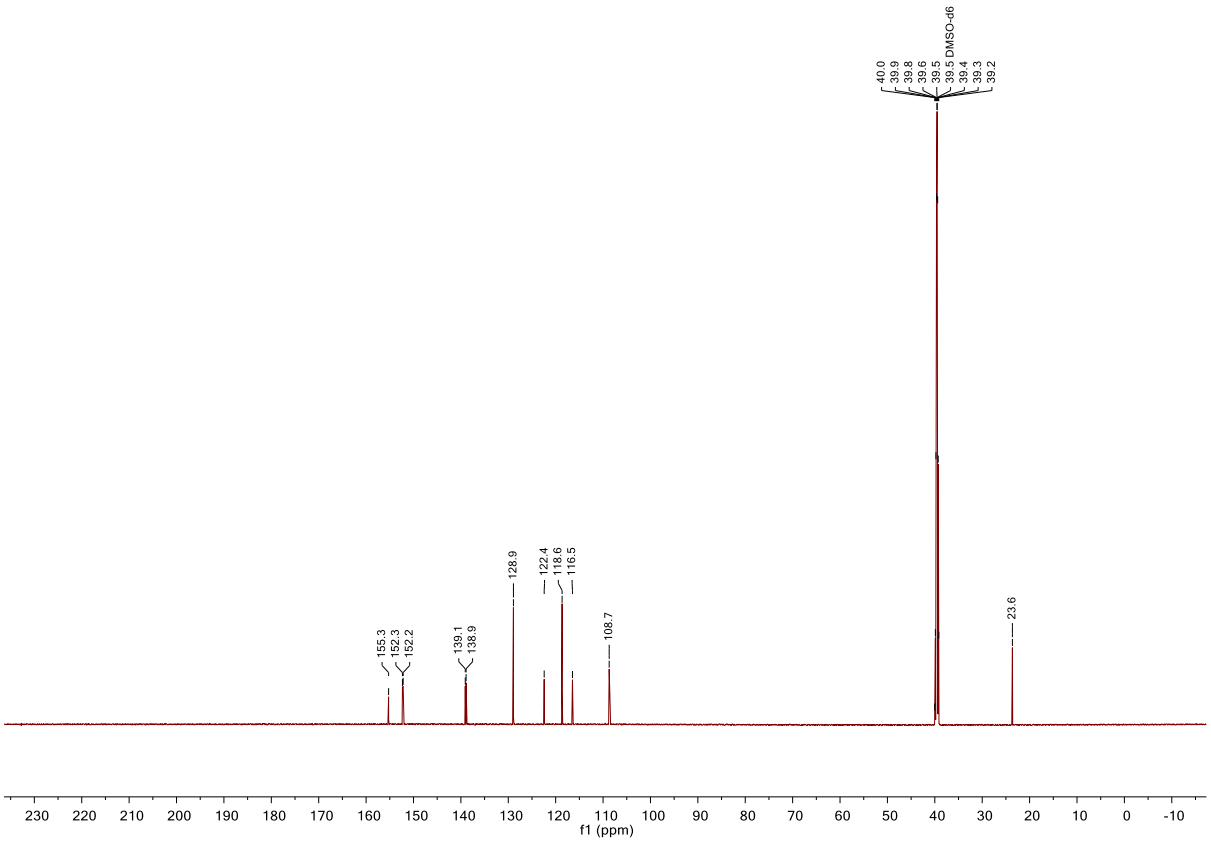
40.0
39.9
39.8
39.6
39.5
39.5 DMSO-d6
39.4
39.3
39.2
155.3
152.3
152.2
139.1
138.9
128.9
122.4
118.6
116.5
108.7
23.6
230
220
210
200
190
180
170
160
150
140
130
120
110
100
90
80
70
60
50
40
30
20
10
0
-10
f1 (ppm)

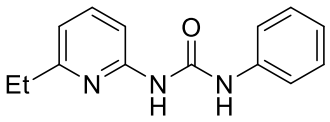
Et
N
O
N
H
N
H

429c

2.76
2.75
2.74
2.73
2.51
2.50
2.50 DMSO-d6
2.50
2.49
1.28
1.27
1.26
7.67
7.65
7.64
7.52
7.51
7.33
7.32
7.31
7.18
7.17
7.03
7.02
7.01
6.89
6.87
9.50
11.00
1.13
1.05
1.04
2.00
2.01
1.00
1.04
1.02
1.97
3.05
f1 (ppm)

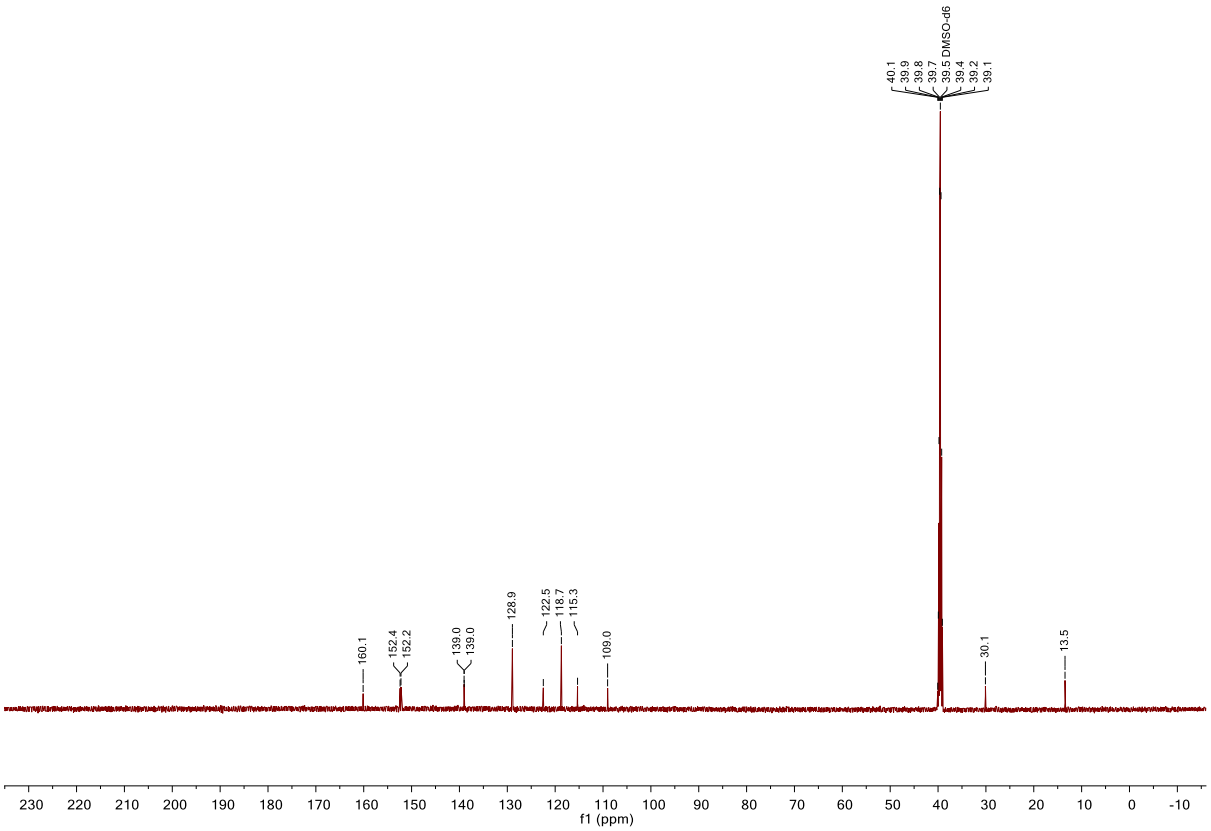
40.1
39.9
39.8
39.7
39.5 DMSO-d6
39.4
39.2
39.1
160.1
152.4
152.2
139.0
139.0
128.9
122.5
118.7
115.3
109.0
30.1
13.5
f1 (ppm)

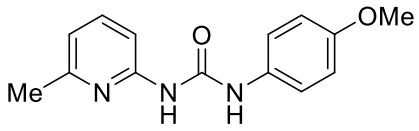
Me
N
O
N
H
N
H
OMe

429d

10.73
9.39
7.63
7.61
7.60
7.43
7.41
7.17
7.16
6.90
6.89
6.85
6.84
3.72
2.51
2.50
2.50 DMSO-d6
2.50
2.49
2.44
0.97
1.13
1.08
2.05
1.05
2.01
1.02
3.00
2.95
f1 (ppm)

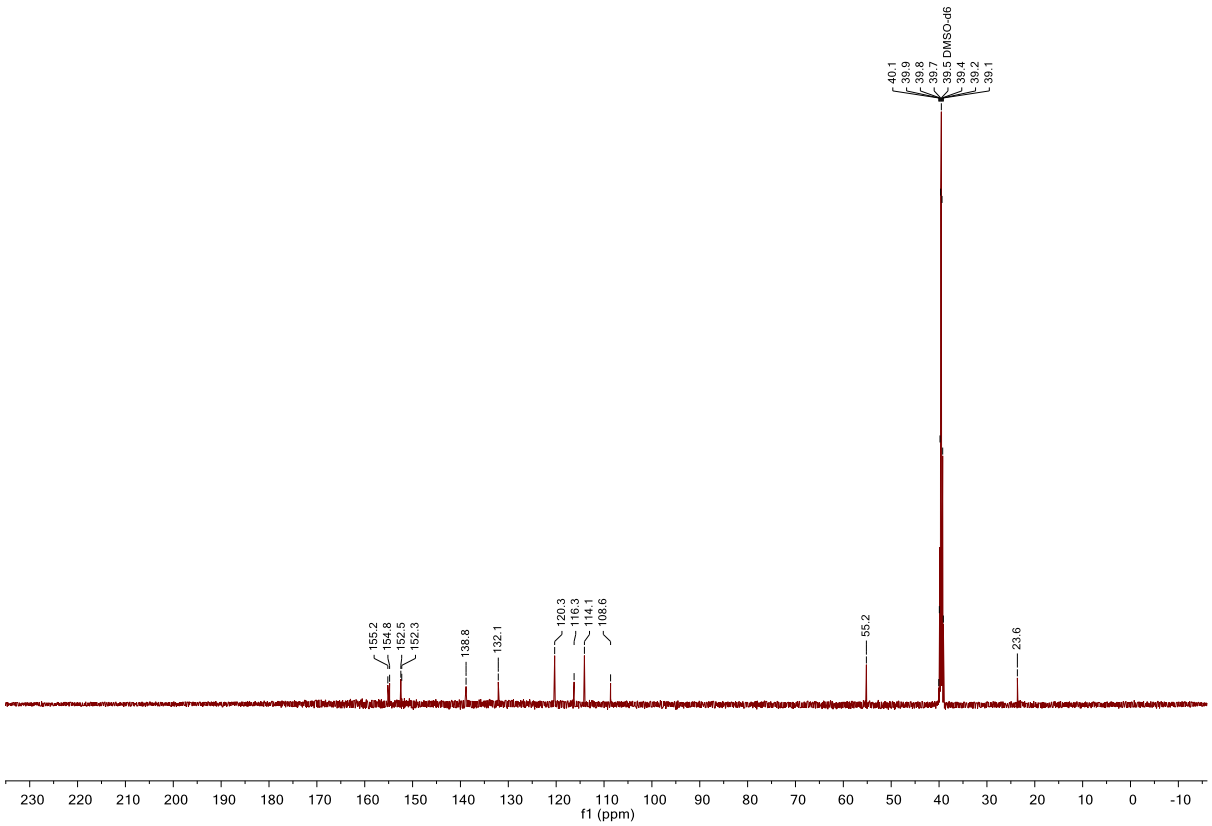
155.2
154.8
152.5
152.3
138.8
132.1
120.3
116.3
114.1
108.6
55.2
40.1
39.9
39.8
39.7
39.5 DMSO-d6
39.4
39.2
39.1
23.6
f1 (ppm)

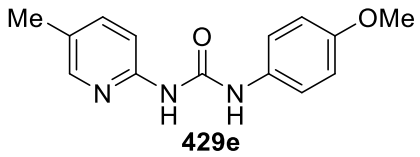
Me
OMe
O
N
N
H
N
H

429e

3.72
2.51
2.50
2.50 DMSO-d6
2.50
2.49
2.22
7.57
7.55
7.42
7.40
7.37
7.35
6.89
6.88
8.09
8.09
9.25
10.32
1.03
0.99
0.97
1.06
2.02
1.00
2.01
3.00
2.95
f1 (ppm)

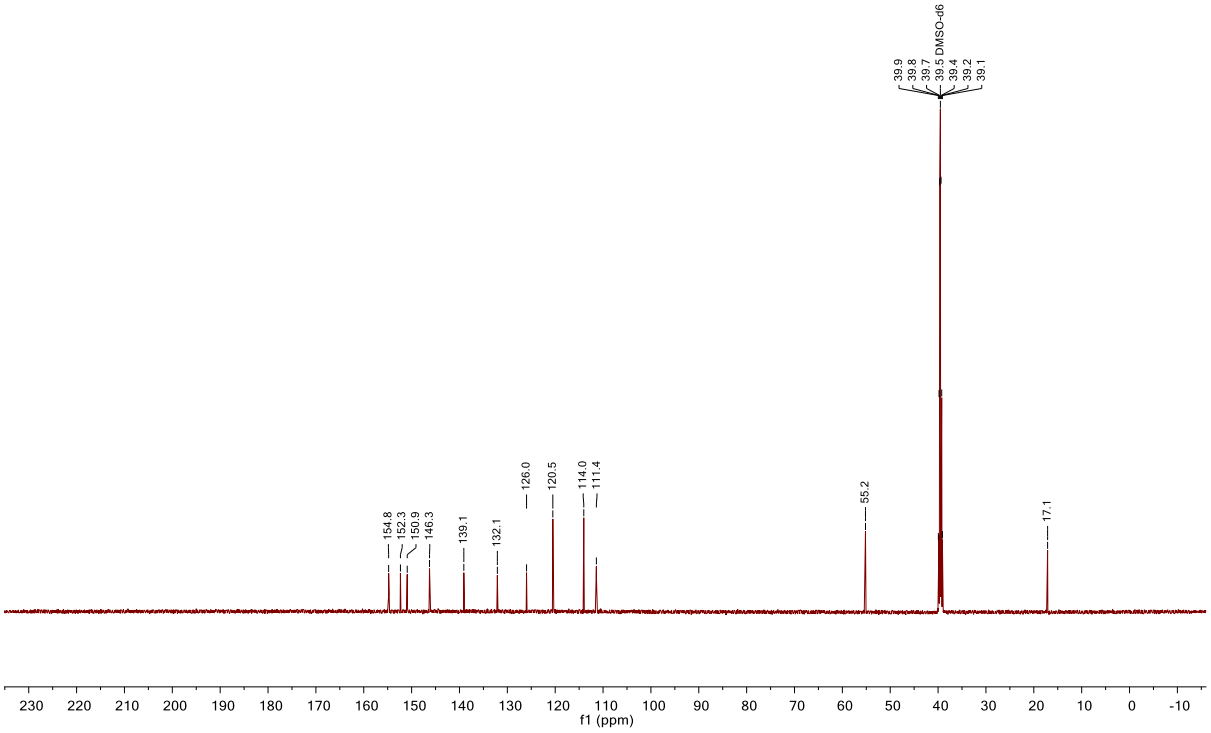
39.9
39.8
39.7
39.5 DMSO-d6
39.4
39.2
39.1
154.8
152.3
150.9
146.3
139.1
132.1
126.0
120.5
114.0
111.4
55.2
17.1
f1 (ppm)

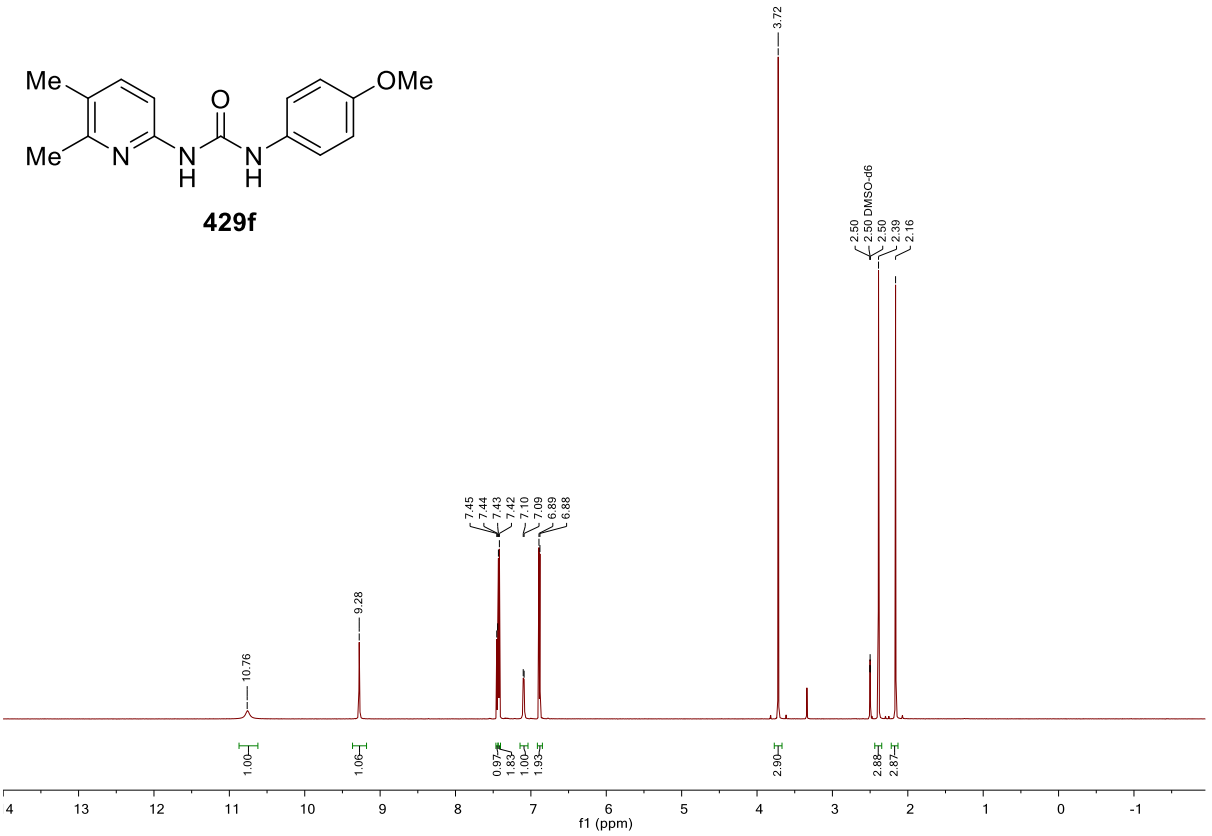
Me
Me
N
O
N
H
N
H
OMe
429f
3.72
2.50
2.50 DMSO-d6
2.50
2.39
2.16
7.45
7.44
7.43
7.42
7.10
7.09
6.89
6.88
9.28
10.76
1.00
1.06
0.97
1.83
1.00
1.93
2.90
2.88
2.87
f1 (ppm)

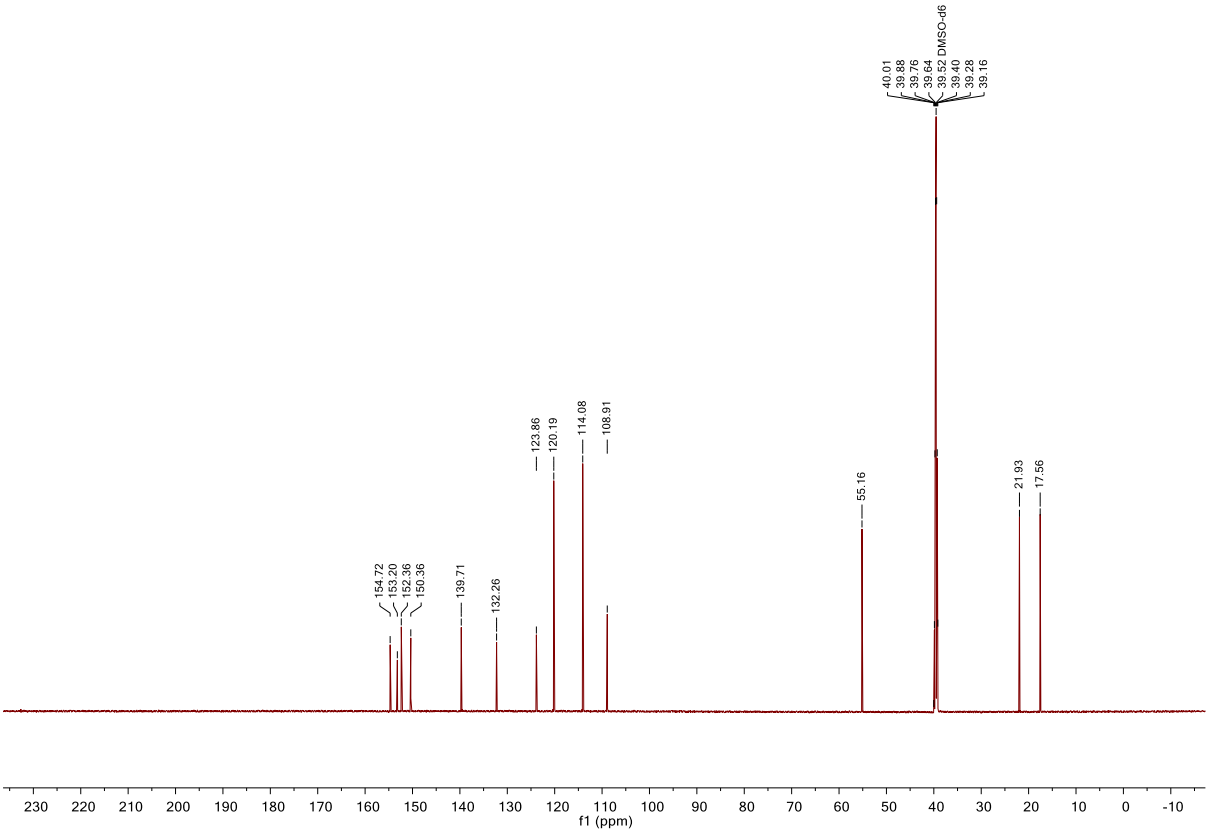
40.01
39.88
39.76
39.64
39.52 DMSO-d6
39.40
39.28
39.16
123.86
120.19
114.08
108.91
55.16
21.93
17.56
154.72
153.20
152.36
150.36
139.71
132.26
f1 (ppm)

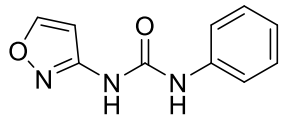

433a

2.50
2.50 DMSO-d6
2.50
9.57
8.81
8.74
7.45
7.30
7.02
6.84
1.00
0.95
0.96
1.94
1.94
0.97
0.97
14 13 12 11 10 9 8 7 6 5 4 3 2 1 0 -1
f1 (ppm)

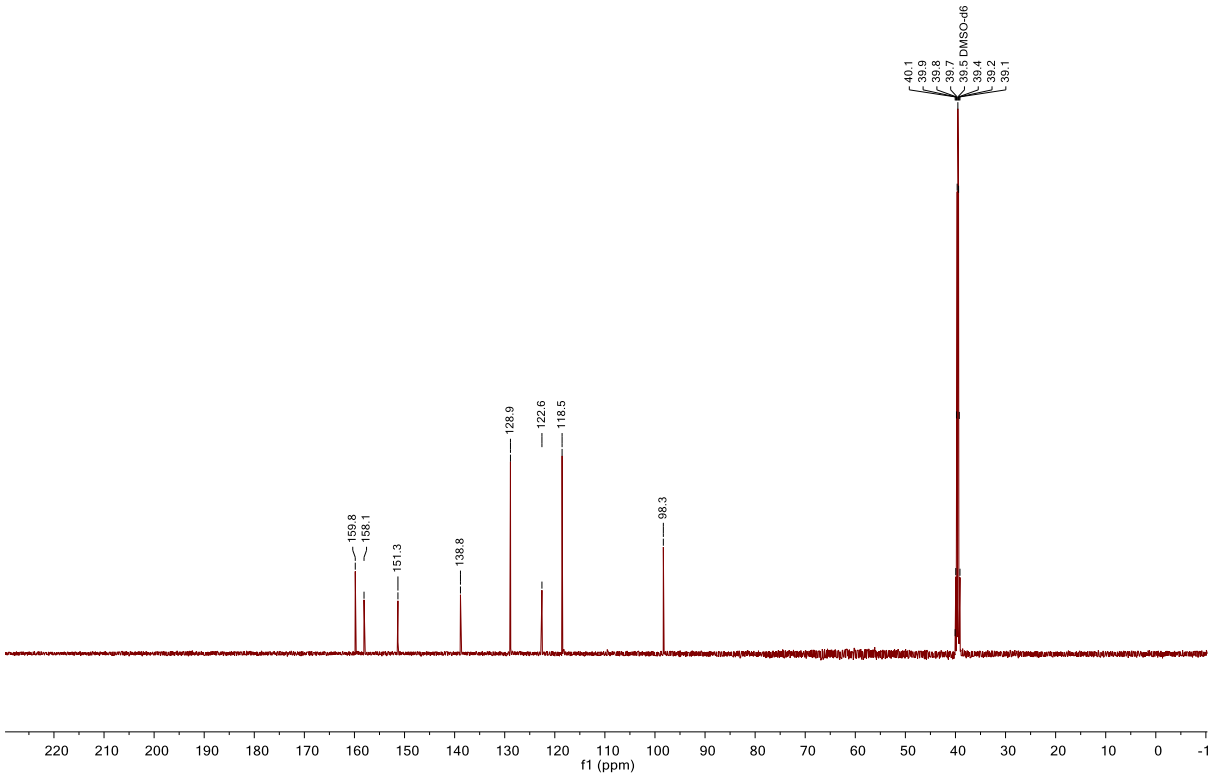
40.1
39.9
39.8
39.7
39.5 DMSO-d6
39.4
39.2
39.1
159.8
158.1
151.3
138.8
128.9
122.6
118.5
98.3
220 210 200 190 180 170 160 150 140 130 120 110 100 90 80 70 60 50 40 30 20 10 0 -1
f1 (ppm)

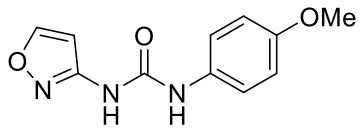
OMe
O
O
N
N
H
N
H

433b

9.50
8.72
8.71
8.64
7.36
7.34
6.89
6.87
6.82
6.82
3.72
2.50
2.50 DMSO-d6
2.50
1.10
1.01
1.00
2.02
2.03
1.02
3.01
f1 (ppm)

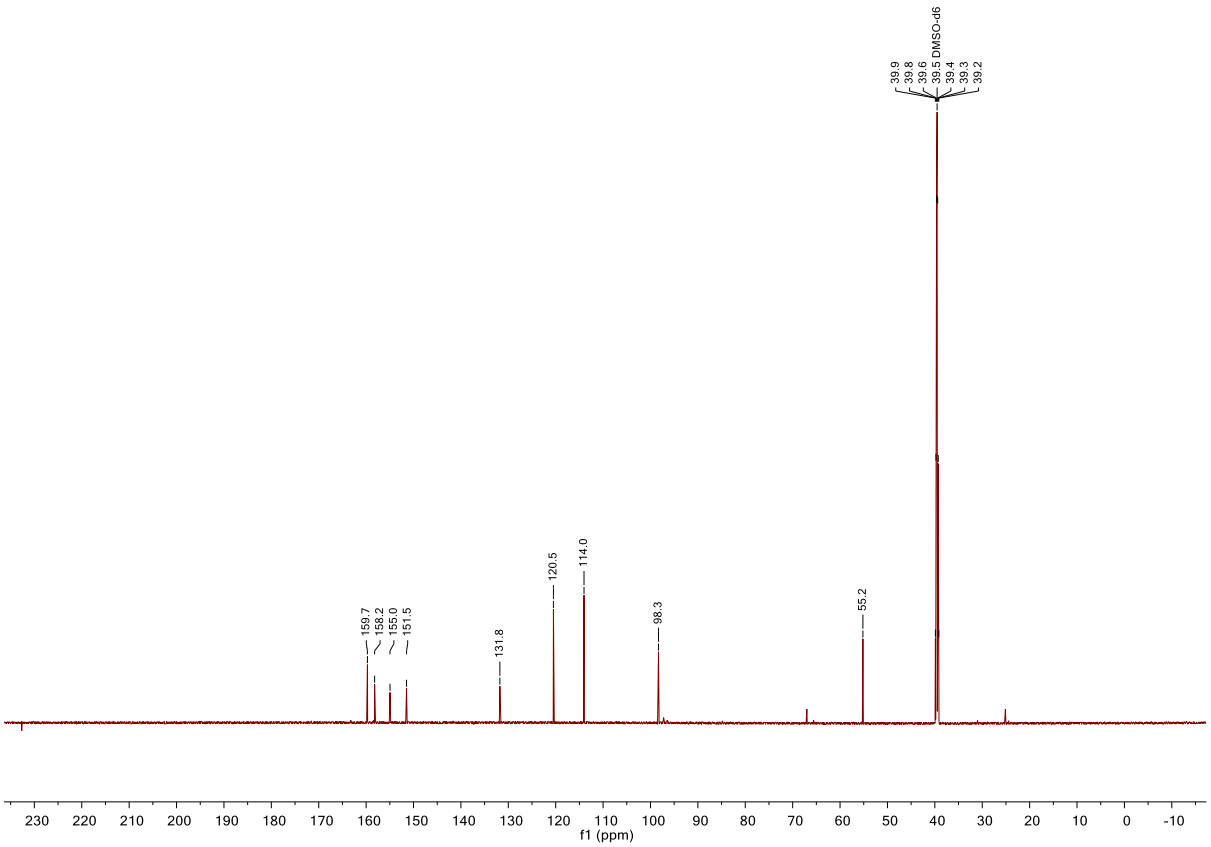
159.7
158.2
155.0
151.5
131.8
120.5
114.0
98.3
55.2
39.9
39.8
39.6
39.5 DMSO-d6
39.4
39.3
39.2
f1 (ppm)

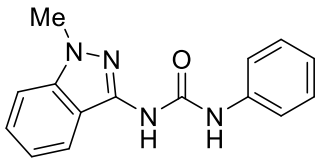
Me
N
N
O
N
H
N
H

433c

3.97
2.50
2.50
2.50 DMSO-d6
2.50
2.49
9.80
9.56
8.00
7.99
7.57
7.56
7.54
7.53
7.42
7.41
7.40
7.33
7.32
7.31
7.09
7.08
7.07
7.03
7.02
7.01
1.00
1.05
1.01
1.90
0.97
1.00
1.94
0.99
1.00
2.90
f1 (ppm)

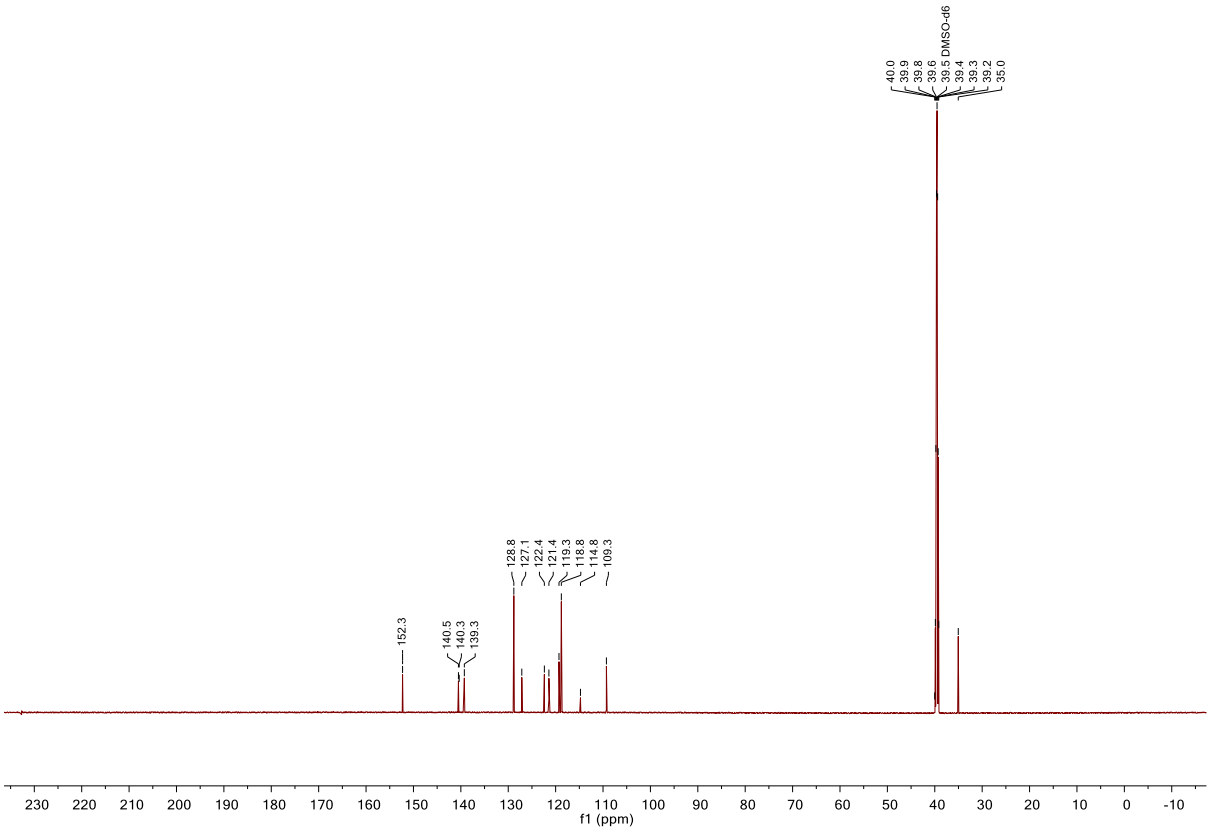
40.0
39.9
39.8
39.6
39.5 DMSO-d6
39.4
39.3
39.2
35.0
152.3
140.5
140.3
139.3
128.8
127.1
122.4
121.4
119.3
118.8
114.8
109.3
f1 (ppm)

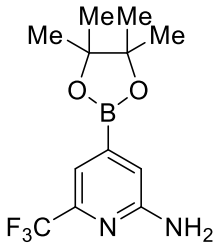
Me
Me
Me
O
B
O
F3C
N
NH2

425a

1.34
1.34
7.33
7.26 CDCl3
7.03
4.70
0.98
1.00
2.05
11.40
f1 (ppm)

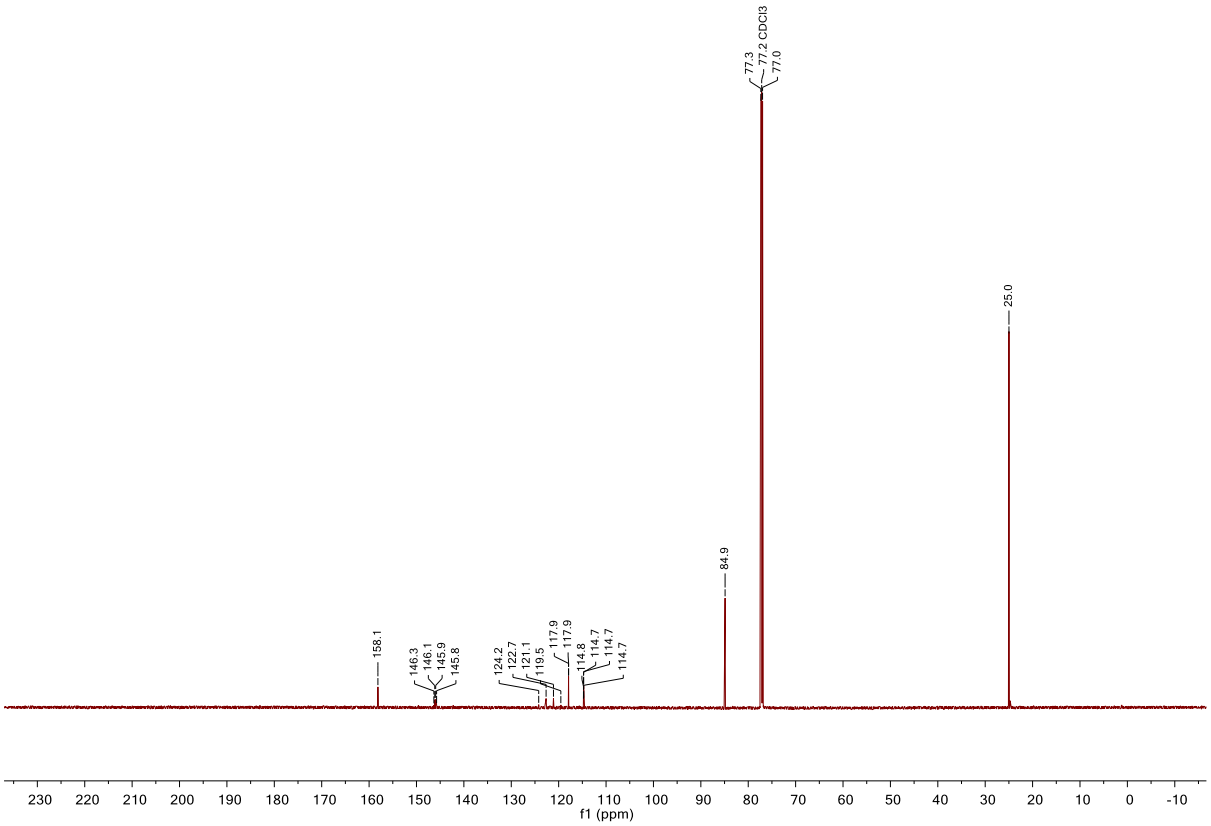
77.3
77.2 CDCl3
77.0
25.0
84.9
158.1
146.3
146.1
145.9
145.8
124.2
122.7
121.1
119.5
117.9
117.9
114.8
114.7
114.7
114.7
f1 (ppm)

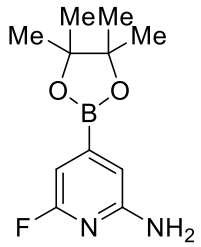
Me
Me
Me
O
O
B
F
N
NH2

425b

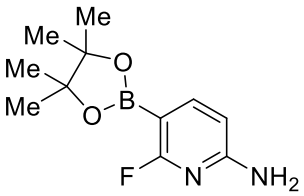
Me
Me
Me
O
O
B
F
N
NH2

425c

1.33
1.33
7.26 CDCl3
7.87
7.86
7.85
6.69
6.69
6.55
6.55
6.30
6.30
6.29
6.29
4.75
4.49
0.80
1.04
1.00
0.81
1.64
2.14
11.26
9.96
f1 (ppm)

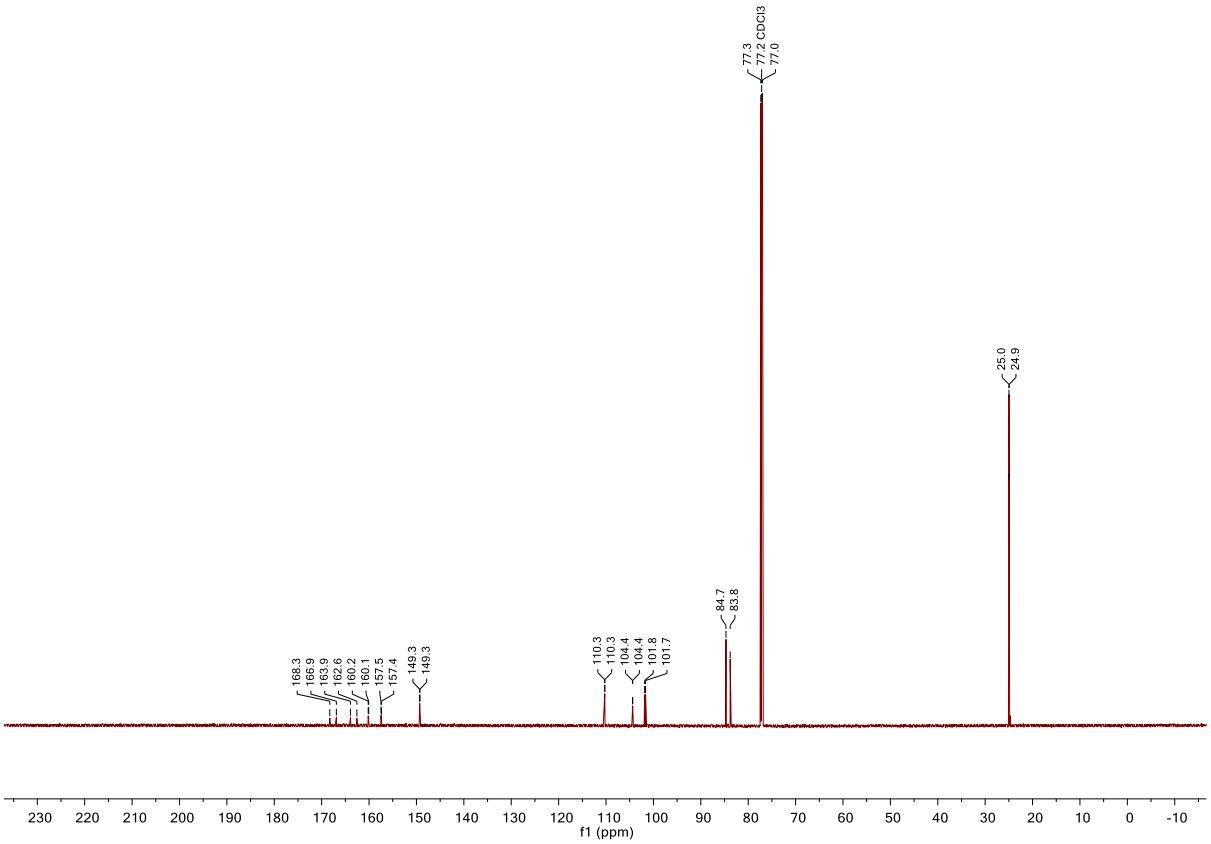
77.3
77.2 CDCl3
77.0
25.0
24.9
168.3
166.9
163.9
162.6
160.2
160.1
157.5
157.4
149.3
149.3
110.3
110.3
104.4
104.4
101.8
101.7
84.7
83.8
f1 (ppm)

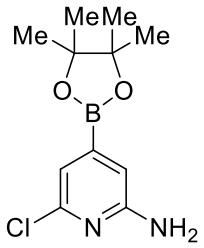
Me
Me
Me
O
O
B
Cl
N
NH2

425d

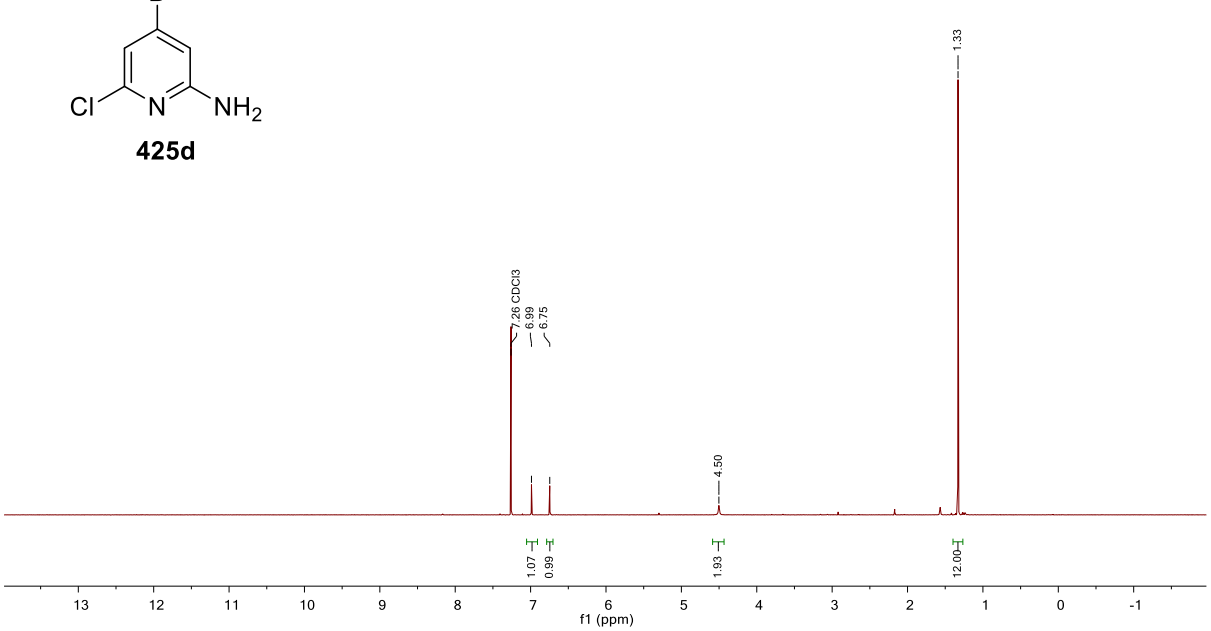
7.26 CDCl3
6.99
6.75
4.50
1.33
1.07
0.99
1.93
12.00
f1 (ppm)

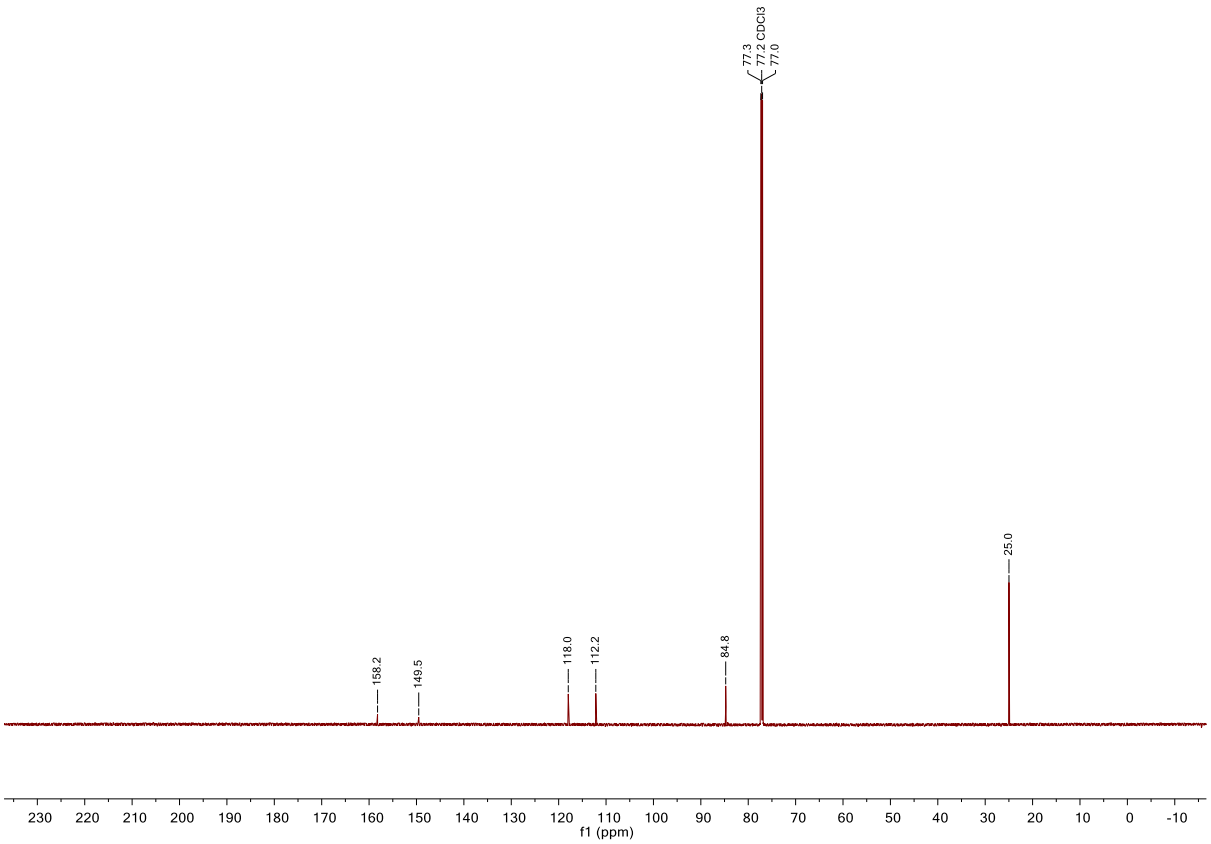
77.3
77.2 CDCl3
77.0
158.2
149.5
118.0
112.2
84.8
25.0
f1 (ppm)

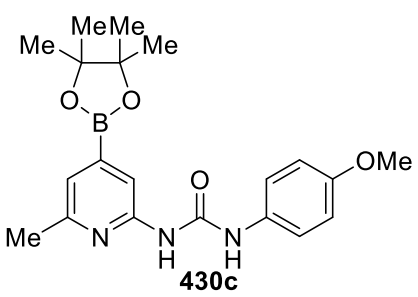
Me
Me
Me
Me
O
O
B
O
Me
N
N
H
O
N
H
OMe

430c

10.52
9.36
7.50
7.42
7.41
6.90
6.88
3.73
2.51
2.50
2.50 DMSO-d6
2.50
2.49
2.45
1.30
1.00
1.02
1.02
2.01
1.00
1.99
2.93
2.91
11.85
f1 (ppm)

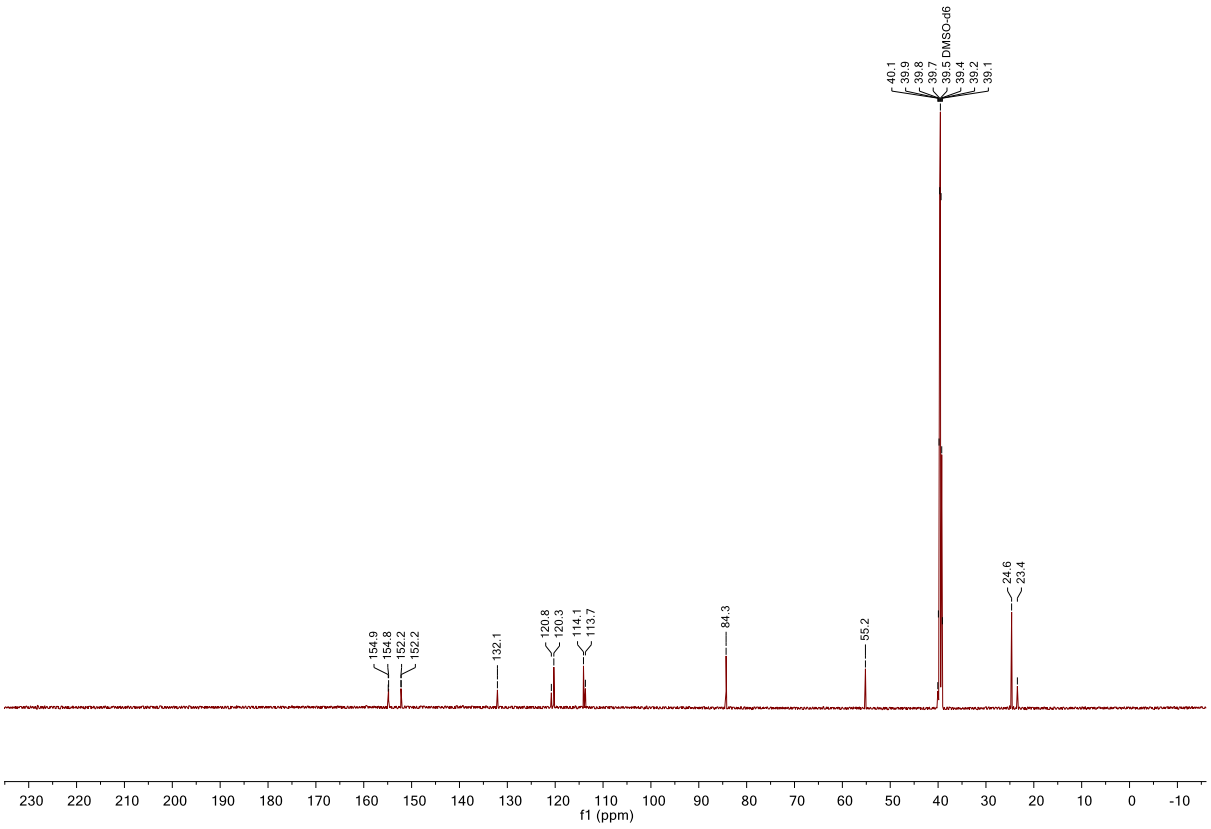
40.1
39.9
39.8
39.7
39.5 DMSO-d6
39.4
39.2
39.1
154.9
154.8
152.2
152.2
132.1
120.8
120.3
114.1
113.7
84.3
55.2
24.6
23.4
f1 (ppm)

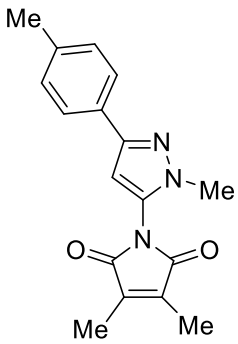
Me
N
N
Me
N
O
O
Me
Me

480

2.36
2.08
3.75
7.66
7.65
7.26 CDCl3
7.20
7.19
6.46
1.89
1.95
1.00
3.31
2.90
5.81
f1 (ppm)

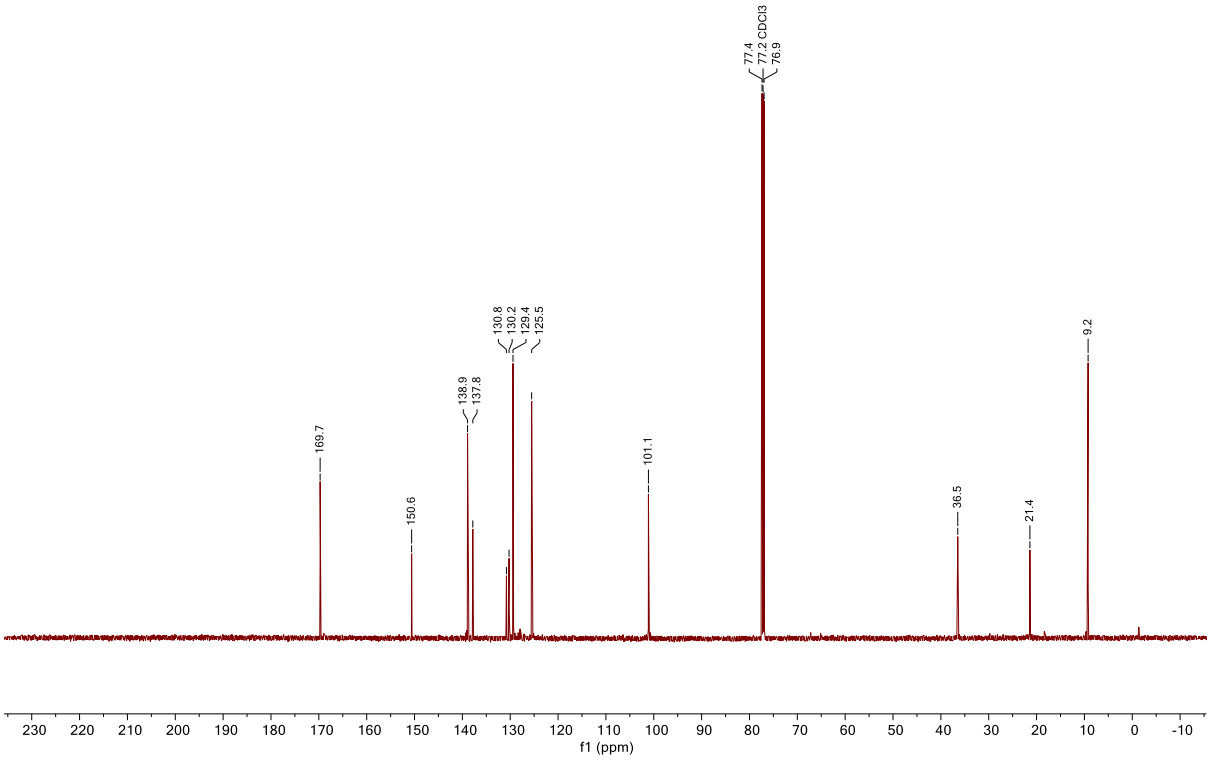
77.4
77.2 CDCl3
76.9
130.8
130.2
129.4
125.5
138.9
137.8
169.7
150.6
101.1
36.5
21.4
9.2
f1 (ppm)

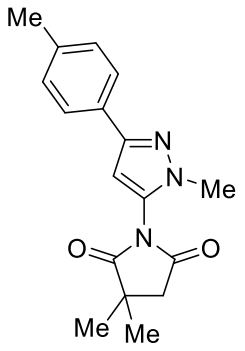
Me
N
N
Me
N
O
O
Me
Me

489

7.65
7.64
7.26 CDCl3
7.20
7.19
6.52
3.72
2.80
2.36
1.48
1.85
1.84
0.92
2.89
1.87
2.84
5.70
f1 (ppm)

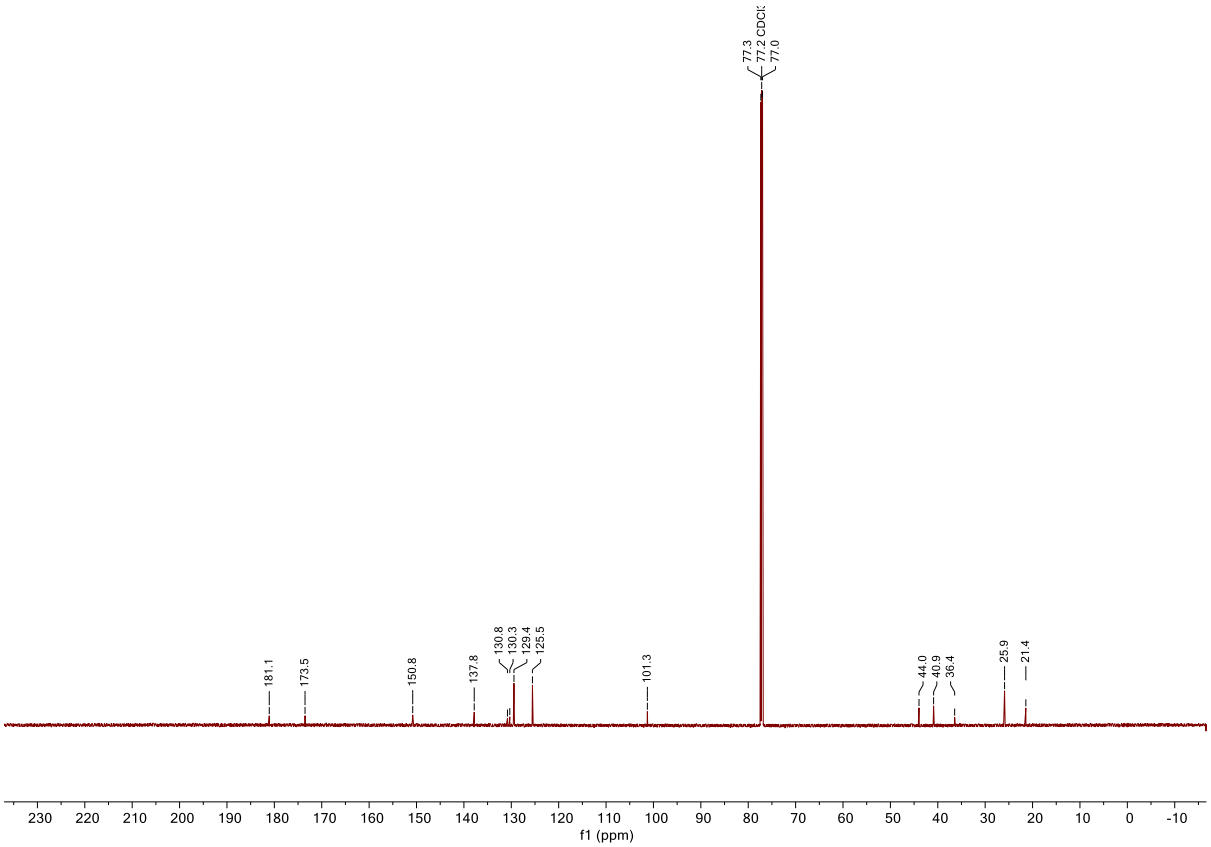
77.3
77.2 CDCl3
77.0
181.1
173.5
150.8
137.8
130.8
130.3
129.4
125.5
101.3
44.0
40.9
36.4
25.9
21.4
f1 (ppm)

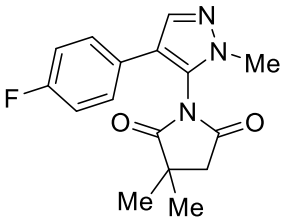
N
N
Me
F
O
N
O
Me
Me

502b

3.71
1.46
1.34
7.67
7.26 CDCl3
7.21
7.20
7.20
7.19
7.04
7.03
7.02
2.79
2.76
2.72
2.70
1.00
1.99
1.97
3.19
2.19
3.19
3.15
f1 (ppm)

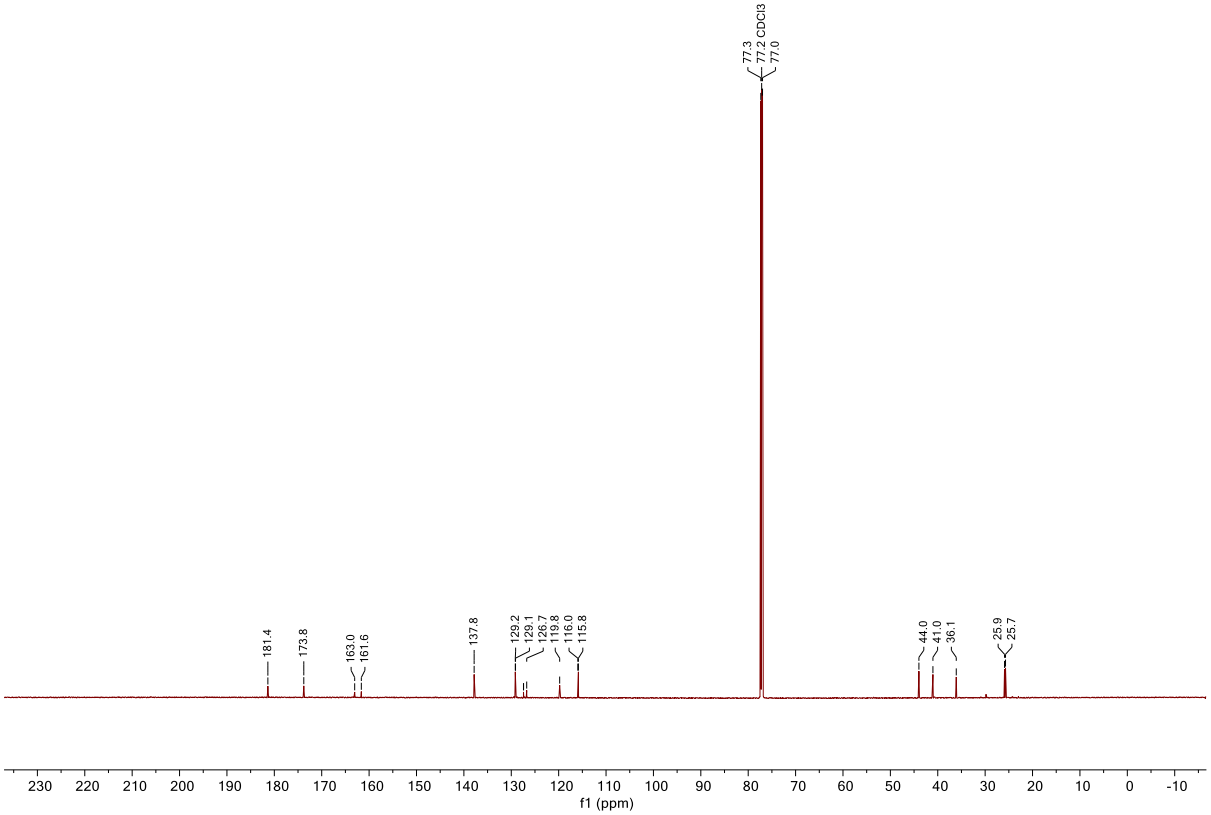
77.3
77.2 CDCl3
77.0
181.4
173.8
163.0
161.6
137.8
129.2
129.1
126.7
119.8
116.0
115.8
44.0
41.0
36.1
25.9
25.7
f1 (ppm)

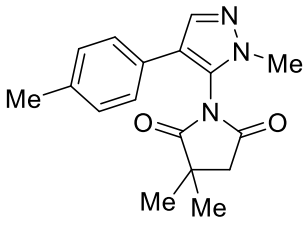
N
N
Me
Me
N
O
O
Me
Me

502c

3.71
2.33
1.46
1.36
7.26 CDCl3
7.15
7.14
7.13
7.13
7.12
7.12
7.12
7.12
7.69
2.78
2.76
2.73
2.70
0.93
3.95
3.00
2.19
3.16
3.17
3.32
f1 (ppm)

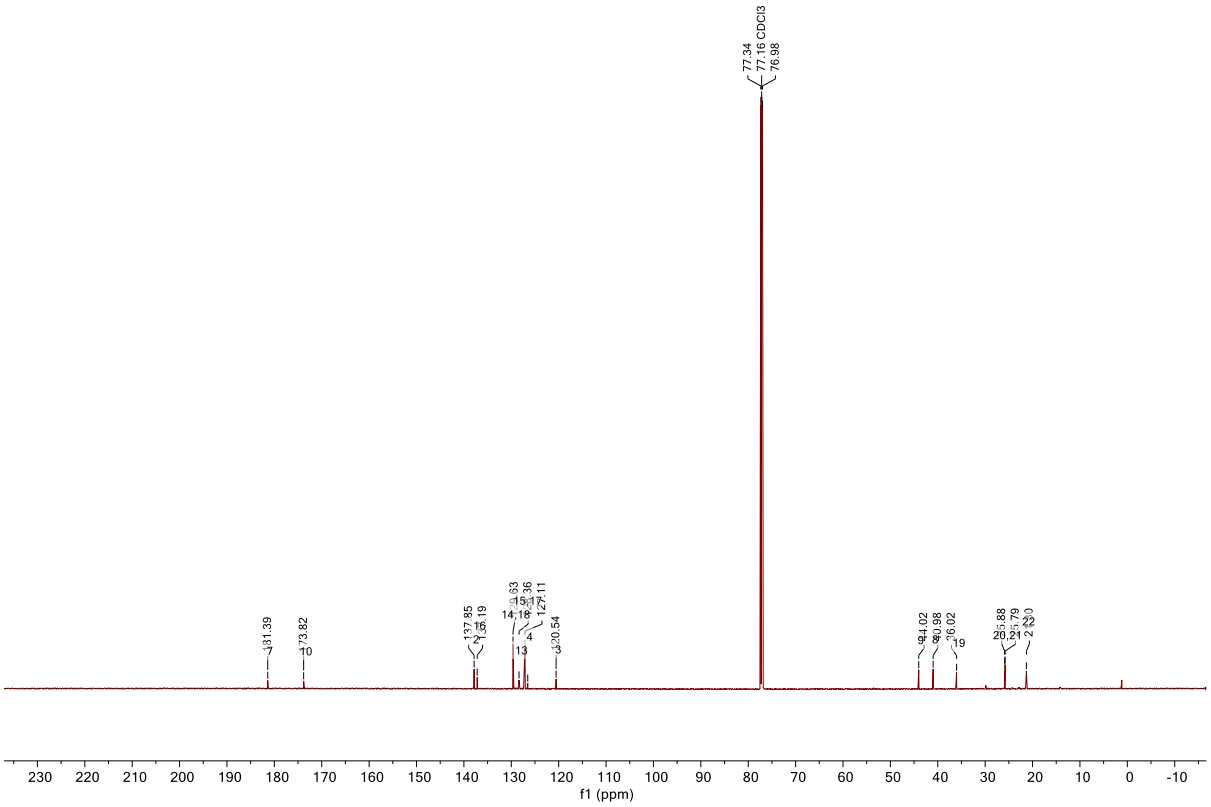
77.34
77.16 CDCl3
76.98
131.39
73.82
137.85
135.19
129.33
128.36
127.11
120.54
44.02
40.98
36.02
29.88
29.79
f1 (ppm)

5.2 X-Ray Crystallography Data*

3-Nitro-1-{[2'-(trimethylsilyl)ethoxy]methyl}-1H-pyrazole (**450**)

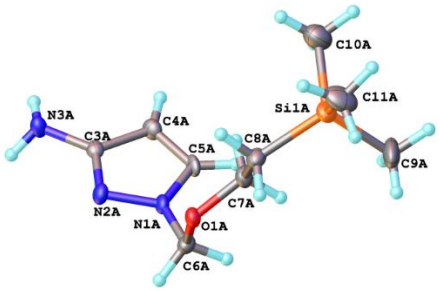

Empirical formula	$C_9H_{19}N_3OSi$
Formula weight	213.36
Temperature/K	120.0
Crystal system	triclinic
Space group	P-1
a/Å	7.7755(19)
b/Å	9.616(2)
c/Å	17.385(4)
α/°	93.324(9)
β/°	102.300(9)
γ/°	91.292(9)
Volume/Å^3	1267.1(5)
Z	4
ρ_{calc}g/cm^3	1.118
μ/mm^{-1}	0.163
F(000)	464.0
Crystal size/mm^3	0.36 × 0.18 × 0.05
Radiation	MoKα (λ = 0.71073)
2Θ range for data collection/°	4.246 to 54.998
Index ranges	-10 ≤ h ≤ 10, -12 ≤ k ≤ 12, -22 ≤ l ≤ 22
Reflections collected	20779
Independent reflections	5791 [R_{int} = 0.0738, R_{sigma} = 0.0934]
Data/restraints/parameters	5791/0/275
Goodness-of-fit on F^2	1.151
Final R indexes [I>=2σ (I)]	R_1 = 0.0980, wR_2 = 0.3227
Final R indexes [all data]	R_1 = 0.1466, wR_2 = 0.3477
Largest diff. peak/hole / e Å^{-3}	0.82/-0.63

* Analyses performed by Dr Dmitry Yufit and Dr Andrei Batsanov

Table 1: Crystal data and structure refinement for **450**

Atom	*x*	*y*	*z*	U(eq)
Si1	-244(2)	6281.5(19)	1442.7(9)	30.4(4)
O1	-535(5)	8227(4)	3592(2)	20.1(8)
N1	2424(6)	7631(4)	4145(2)	17.6(9)
N2	3452(5)	8847(4)	4268(2)	15.1(9)
N3	6269(6)	9484(5)	4075(3)	20.7(10)
C3	4906(7)	8498(5)	4016(3)	17.7(10)
C4	4801(7)	7092(5)	3719(3)	20.4(11)
C5	3206(7)	6590(5)	3808(3)	20.2(11)
C6	634(7)	7659(5)	4233(3)	19.4(11)
C7	-970(7)	7292(6)	2895(3)	22.6(11)
C8	102(7)	7630(6)	2284(3)	23.3(11)
C9	-2563(10)	6239(8)	879(4)	46.6(18)
C10	1276(11)	6718(10)	783(4)	59(2)
C11	256(10)	4542(7)	1844(4)	43.4(17)
Si1A	4584(2)	1341.3(18)	1396.0(9)	28.9(4)
O1A	4093(5)	3183(4)	3534(2)	19.8(8)
N1A	1637(6)	2639(4)	4097(2)	17.7(9)
N2A	801(6)	3840(4)	4251(3)	19.7(9)
N3A	-2144(7)	4460(5)	4077(3)	21.1(10)
C3A	-885(7)	3501(5)	4010(3)	17.5(10)
C4A	-1173(7)	2100(5)	3684(3)	21.2(11)
C5A	468(7)	1605(5)	3755(3)	19.7(11)
C6A	3515(7)	2665(6)	4184(3)	20.8(11)
C7A	3785(7)	2177(6)	2867(3)	22.5(11)
C8A	4719(8)	2667(6)	2239(3)	24.6(12)
C9A	5408(12)	-335(7)	1786(4)	50(2)
C10A	2257(9)	1073(8)	835(4)	45.3(17)
C11A	5988(10)	1984(9)	727(4)	48.1(19)

Table 2: Fractional Atomic Coordinates ($\times 10^4$) and Equivalent Isotropic Displacement Parameters ($Å^2 \times 10^3$) for **450**. U_{eq} is defined as 1/3 of of the trace of the orthogonalised U_{IJ} tensor

Atom	U_{11}	U_{22}	U_{33}	U_{23}	U_{13}	U_{12}
Si1	37.7(10)	31.9(9)	21.1(8)	-4.6(6)	6.3(7)	8.3(7)
O1	22.1(18)	15.2(18)	22.3(18)	-3.0(14)	4.1(14)	2.6(14)
N1	25(2)	6.5(19)	21(2)	0.4(16)	5.3(17)	0.3(16)
N2	21(2)	8.9(19)	15.0(19)	-1.3(15)	3.6(16)	0.1(16)
N3	21(2)	17(2)	26(2)	0.6(18)	7.2(18)	5.7(18)
C3	20(2)	14(2)	18(2)	1.4(19)	1.2(19)	3.4(19)
C4	26(3)	15(3)	21(2)	-0.6(19)	5(2)	7(2)
C5	28(3)	8(2)	22(2)	0.4(19)	2(2)	2(2)
C6	26(3)	17(3)	16(2)	0.9(19)	5(2)	1(2)
C7	22(3)	23(3)	22(3)	-1(2)	5(2)	0(2)
C8	31(3)	23(3)	18(2)	5(2)	8(2)	6(2)
C9	49(4)	48(4)	36(4)	-3(3)	-5(3)	11(3)
C10	66(5)	75(6)	37(4)	-26(4)	23(4)	-7(4)
C11	57(4)	22(3)	47(4)	-10(3)	3(3)	13(3)
Si1A	36.6(9)	31.6(9)	18.7(7)	-2.2(6)	6.2(6)	9.6(7)
O1A	22.6(18)	15.1(18)	21.5(18)	-2.8(14)	5.6(14)	2.5(14)
N1A	24(2)	10(2)	19(2)	0.9(16)	4.9(17)	3.7(17)
N2A	23(2)	13(2)	24(2)	1.9(17)	6.6(18)	3.7(17)
N3A	20(3)	17(2)	26(2)	-4.8(19)	5.2(19)	0.0(19)
C3A	23(3)	16(2)	14(2)	3.3(18)	5.1(19)	1(2)
C4A	25(3)	15(3)	23(3)	1(2)	5(2)	-3(2)
C5A	32(3)	7(2)	20(2)	-0.1(18)	8(2)	0(2)
C6A	23(3)	21(3)	19(2)	3(2)	4(2)	6(2)
C7A	25(3)	20(3)	23(3)	-2(2)	8(2)	3(2)
C8A	30(3)	24(3)	20(2)	4(2)	4(2)	8(2)
C9A	79(5)	30(4)	41(4)	-5(3)	12(4)	26(4)
C10A	44(4)	51(5)	36(4)	-8(3)	2(3)	2(3)
C11A	51(4)	69(5)	24(3)	-6(3)	11(3)	-2(4)

Table 3: Anisotropic Displacement Parameters ($Å^2 \times 10^3$) for 17srv285. The Anisotropic displacement factor exponent takes the form: $-2\pi^2[h^2a^{*2}U_{11}+2hka^*b^*U_{12}+\ldots]$

Atom	Atom	Length/Å	Atom	Atom	Length/Å
Si1	C8	1.868(6)	Si1A	C8A	1.870(6)
Si1	C9	1.858(7)	Si1A	C9A	1.859(7)
Si1	C10	1.871(8)	Si1A	C10A	1.868(7)
Si1	C11	1.867(7)	Si1A	C11A	1.876(7)
O1	C6	1.424(6)	O1A	C6A	1.412(6)
O1	C7	1.441(6)	O1A	C7A	1.443(6)
N1	N2	1.381(6)	N1A	N2A	1.378(6)
N1	C5	1.352(6)	N1A	C5A	1.353(7)
N1	C6	1.433(7)	N1A	C6A	1.435(7)
N2	C3	1.338(6)	N2A	C3A	1.316(7)
N3	C3	1.390(7)	N3A	C3A	1.378(7)
C3	C4	1.413(7)	C3A	C4A	1.424(7)
C4	C5	1.363(8)	C4A	C5A	1.356(8)
C7	C8	1.527(7)	C7A	C8A	1.523(7)

Table 4: Bond Lengths for **450**

Atom	Atom	Atom	Angle/˚	Atom	Atom	Atom	Angle/˚
C8	Si1	C10	108.4(3)	C8A	Si1A	C11A	108.6(3)
C9	Si1	C8	110.6(3)	C9A	Si1A	C8A	109.1(3)
C9	Si1	C10	109.8(4)	C9A	Si1A	C10A	109.4(4)
C9	Si1	C11	109.0(4)	C9A	Si1A	C11A	109.9(4)
C11	Si1	C8	108.7(3)	C10A	Si1A	C8A	110.3(3)
C11	Si1	C10	110.3(4)	C10A	Si1A	C11A	109.5(3)
C6	O1	C7	113.5(4)	C6A	O1A	C7A	111.8(4)
N2	N1	C6	119.9(4)	N2A	N1A	C6A	120.0(4)
C5	N1	N2	111.4(4)	C5A	N1A	N2A	111.5(4)
C5	N1	C6	127.5(4)	C5A	N1A	C6A	127.6(4)
C3	N2	N1	104.1(4)	C3A	N2A	N1A	104.1(4)
N2	C3	N3	119.6(4)	N2A	C3A	N3A	120.6(5)
N2	C3	C4	111.5(5)	N2A	C3A	C4A	112.2(4)
N3	C3	C4	128.8(5)	N3A	C3A	C4A	127.2(5)
C5	C4	C3	105.0(4)	C5A	C4A	C3A	104.3(5)
N1	C5	C4	107.9(4)	N1A	C5A	C4A	107.9(4)
O1	C6	N1	113.8(4)	O1A	C6A	N1A	113.7(4)
O1	C7	C8	112.4(4)	O1A	C7A	C8A	109.9(4)
C7	C8	Si1	112.2(4)	C7A	C8A	Si1A	112.8(4)

Table 5: Bond Angles for **450**

D	H	A	d(D-H)/Å	d(H-A)/Å	d(D-A)/Å	D-H-A/°
N3	H3A	O1[1]	0.89(6)	2.17(6)	3.041(6)	165(5)
N3	H3B	N2[2]	0.87(6)	2.31(6)	3.179(6)	176(5)
N3A	H3AA	N2A[3]	0.86(6)	2.36(7)	3.209(7)	171(5)
N3A	H3AB	O1A[4]	0.77(6)	2.33(6)	3.080(6)	165(6)

Table 6: Hydrogen Bonds for **450** ([1]1+X,+Y,+Z; [2]1-X,2-Y,1-Z; [3]-X,1-Y,1-Z; [4]-1+X,+Y,+Z)

A	B	C	D	Angle/˚		A	B	C	D	Angle/˚
O1	C7	C8	Si1	172.4(3)		O1A	C7A	C8A	Si1A	174.1(3)
N2	N1	C6	O1	75.7(5)		N2A	N1A	C6A	O1A	-80.5(5)
C5	N1	C6	O1	-90.7(6)		C5A	N1A	C6A	O1A	88.0(6)
C7	O1	C6	N1	75.4(5)		C7A	O1A	C6A	N1A	-75.3(5)
C7	C8	Si1	C9	64.5(5)		C7A	C8A	Si1A	C9A	-54.0(5)
C7	C8	Si1	C10	-175.0(5)		C7A	C8A	Si1A	C10A	66.2(5)
C7	C8	Si1	C11	-55.1(5)		C7A	C8A	Si1A	C11A	-173.7(4)
C8	C7	O1	C6	-99.9(5)		C8A	C7A	O1A	C6A	-169.7(4)

Table 7: Selected Torsion Angles for **450**

Atom	*x*	*y*	*z*	U(eq)
H4	5657	6603.24	3504.57	24
H5	2729.08	5671.61	3659.01	24
H6A	219.21	6695.99	4287.49	23
H6B	591.09	8215.27	4725.16	23
H7A	-2239.34	7347.3	2655.64	27
H7B	-751.61	6324.45	3046.51	27
H8A	1367.76	7700	2542.03	28
H8B	-237.08	8546.49	2078.83	28
H9A	-3351.99	5996.56	1225.43	70
H9B	-2713.36	5540.63	434.36	70
H9C	-2846.92	7157.82	680.26	70
H10A	1148.22	7694.19	653.66	88
H10B	982.91	6112.82	297.16	88
H10C	2494.73	6577.14	1053.83	88
H11A	1447.25	4577.02	2175.32	65
H11B	179.17	3837.07	1406.63	65
H11C	-596.93	4299.21	2160.54	65
H3A	7250(70)	9070(60)	4030(30)	12(9)
H3B	6400(70)	9930(60)	4540(30)	12(9)
H4A	-2266.5	1622.29	3466	25
H5A	748.06	691.91	3593.85	24
H6AA	4058.65	3251.31	4664.96	25
H6AB	3933.38	1707.66	4258.1	25
H7AA	2504.71	2059.03	2642.92	27
H7AB	4229.62	1263.33	3038.54	27
H8AA	5973.66	2885.48	2484.43	29
H8AB	4188.41	3534.66	2035.7	29
H9AA	6633.3	-198.41	2074.86	75
H9AB	5342.22	-1033.89	1346.41	75
H9AC	4681.84	-656.3	2141.94	75
H10D	1548.1	653.49	1170.48	68
H10E	2221.58	452.34	364.44	68
H10F	1780.93	1973.1	677.02	68
H11D	5734.22	2957.42	624.27	72
H11E	5728.07	1412.89	227.61	72
H11F	7233.65	1915.82	979.17	72
H3AA	-1880(80)	4980(60)	4510(40)	19(15)
H3AB	-3140(80)	4280(60)	3960(30)	11(14)

Table 8: Hydrogen Atom Coordinates (Å×10^4) and Isotropic Displacement Parameters (Å^2×10^3) for

450

tert-butyl 3-nitro-1H-pyrazole-1-carboxylate (**495**)

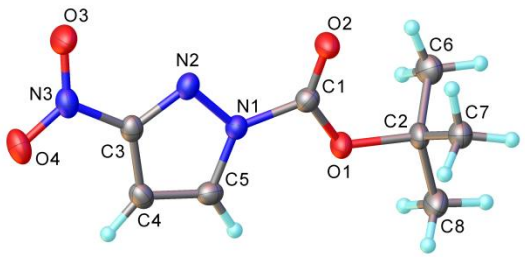

Empirical formula	$C_8H_{11}N_3O_4$
Formula weight	213.20
Temperature/K	120
Crystal system	monoclinic
Space group	$P2_1/n$
a/Å	5.8959(5)
b/Å	26.572(2)
c/Å	6.4821(6)
α/°	90
β/°	101.672(4)
γ/°	90
Volume/Å^3	994.53(15)
Z	4
ρ_{calc}g/cm^3	1.424
μ/mm^{-1}	0.116
F(000)	448.0
Crystal size/mm^3	0.337 × 0.266 × 0.102
Radiation	MoKα (λ = 0.71073)
2Θ range for data collection/°	6.132 to 50.082
Index ranges	-7 ≤ h ≤ 6, 0 ≤ k ≤ 31, 0 ≤ l ≤ 7
Reflections collected	3363
Independent reflections	3363 [R_{int} = ?, R_{sigma} = 0.0473]
Data/restraints/parameters	3363/0/144
Goodness-of-fit on F^2	1.038
Final R indexes [I>=2σ (I)]	R_1 = 0.0423, wR_2 = 0.0955
Final R indexes [all data]	R_1 = 0.0634, wR_2 = 0.1037
Largest diff. peak/hole / e Å^{-3}	0.17/-0.18

Table 9: Crystal data and structure refinement for **495**

Atom	x	y	z	U(eq)
O(1)	6572(2)	1316.0(5)	2761(2)	26.4(4)
O(2)	10357(2)	1542.1(5)	3118(2)	30.9(4)
O(3)	10429(2)	3460.6(5)	2560(2)	38.1(4)
O(4)	7248(2)	3758.0(5)	3263(2)	36.2(4)
N(1)	7440(3)	2127.1(5)	2933(2)	22.9(4)
N(2)	8889(3)	2520.0(5)	2871(2)	24.9(4)
N(3)	8479(3)	3409.8(6)	2925(2)	27.9(4)
C(1)	8342(3)	1626.3(7)	2953(3)	24.6(4)
C(2)	6944(3)	759.2(7)	2940(3)	25.9(5)
C(3)	7524(3)	2907.3(7)	2952(3)	23.5(4)
C(4)	5257(3)	2787.2(7)	3090(3)	25.8(5)
C(5)	5248(3)	2276.9(7)	3062(3)	25.6(4)
C(6)	7870(4)	578.4(7)	1062(3)	33.3(5)
C(7)	8502(3)	639.6(7)	5032(3)	29.4(5)
C(8)	4513(3)	569.5(7)	2870(4)	34.3(5)

Table 10: Fractional Atomic Coordinates ($\times 10^4$) and Equivalent Isotropic Displacement Parameters ($Å^2 \times 10^3$) for **495**. U_{eq} is defined as 1/3 of of the trace of the orthogonalised U_{IJ} tensor.

Atom	U_{11}	U_{22}	U_{33}	U_{23}	U_{13}	U_{12}
O(1)	25.5(7)	17.6(7)	36.5(8)	1.1(6)	7.4(6)	-0.4(5)
O(2)	24.7(8)	22.3(7)	47.2(9)	1.4(7)	10.5(7)	0.1(6)
O(3)	35.0(9)	24.3(8)	57.7(11)	1.9(7)	15.9(8)	-3.7(6)
O(4)	41.4(9)	21.7(8)	43.3(9)	-3.0(7)	3.6(7)	7.3(6)
N(1)	25.0(9)	18.6(8)	26.2(9)	1.1(7)	7.5(7)	-0.8(6)
N(2)	30.0(9)	20.0(8)	25.1(9)	1.2(7)	6.3(7)	-1.9(7)
N(3)	33.4(10)	21.2(9)	27.9(9)	0.6(7)	3.2(8)	3.4(8)
C(1)	26.0(11)	23.1(10)	25.5(10)	0.5(8)	7.2(8)	-1.4(8)
C(2)	27.3(11)	15.0(9)	36.2(12)	1.2(8)	8.3(9)	1.1(8)
C(3)	30.0(11)	20.4(10)	20(1)	0.4(8)	5.0(8)	1.6(8)
C(4)	29.3(11)	24.1(10)	24.8(10)	-0.9(9)	7.4(9)	5.5(8)
C(5)	23.4(10)	29.3(10)	25.1(10)	1.8(9)	7.1(8)	0.2(8)
C(6)	38.2(12)	25.3(11)	37.6(12)	-3.9(9)	10.5(10)	-0.6(9)
C(7)	31.6(11)	22.3(10)	35.4(12)	1.7(9)	9.4(9)	1.2(8)
C(8)	29.6(11)	23(1)	50.9(14)	3.4(10)	9.8(10)	-2.2(9)

Table 11: Anisotropic Displacement Parameters ($Å^2 \times 10^3$) for **495**. The Anisotropic displacement factor exponent takes the form: $-2\pi^2[h^2a^{*2}U_{11}+2hka^*b^*U_{12}+\ldots]$

Atom	Atom	Length/Å	Atom	Atom	Length/Å
O(1)	C(1)	1.316(2)	N(2)	C(3)	1.314(2)
O(1)	C(2)	1.497(2)	N(3)	C(3)	1.451(2)
O(2)	C(1)	1.192(2)	C(2)	C(6)	1.510(3)
O(3)	N(3)	1.228(2)	C(2)	C(7)	1.510(3)
O(4)	N(3)	1.223(2)	C(2)	C(8)	1.512(3)
N(1)	N(2)	1.355(2)	C(3)	C(4)	1.395(3)
N(1)	C(1)	1.432(2)	C(4)	C(5)	1.356(3)
N(1)	C(5)	1.371(2)			

Table 12: Bond Lengths for **495**

Atom	Atom	Atom	Angle/˚	Atom	Atom	Atom	Angle/˚
C(1)	O(1)	C(2)	120.73(14)	O(1)	C(2)	C(6)	108.88(15)
N(2)	N(1)	C(1)	118.78(15)	O(1)	C(2)	C(7)	109.29(15)
N(2)	N(1)	C(5)	112.71(15)	O(1)	C(2)	C(8)	101.77(14)
C(5)	N(1)	C(1)	128.45(16)	C(6)	C(2)	C(7)	113.81(16)
C(3)	N(2)	N(1)	101.96(15)	C(6)	C(2)	C(8)	111.43(17)
O(3)	N(3)	C(3)	118.98(15)	C(7)	C(2)	C(8)	110.94(17)
O(4)	N(3)	O(3)	124.38(16)	N(2)	C(3)	N(3)	118.55(16)
O(4)	N(3)	C(3)	116.64(16)	N(2)	C(3)	C(4)	115.23(16)
O(1)	C(1)	N(1)	107.21(15)	C(4)	C(3)	N(3)	126.21(16)
O(2)	C(1)	O(1)	130.35(17)	C(5)	C(4)	C(3)	103.25(17)
O(2)	C(1)	N(1)	122.44(17)	C(4)	C(5)	N(1)	106.85(17)

Table 13: Bond Angles for **495**

Atom	*x*	*y*	*z*	U(eq)
H(4)	4018.36	3009.17	3182.35	31
H(5)	3967.92	2063.99	3120.72	31
H(6A)	6759.14	660.03	-235.5	42(4)
H(6B)	8102.47	213.28	1156.01	42(4)
H(6C)	9350.57	744.59	1045.68	42(4)
H(7A)	10091.23	742.46	5001.38	36(3)
H(7B)	8464.78	276.91	5297.19	36(3)
H(7C)	7961.76	821.81	6155.94	36(3)
H(8A)	3951.4	697.95	4093.21	41(4)
H(8B)	4517.77	200.79	2898.53	41(4)
H(8C)	3492.61	686.93	1574.45	41(4)

Table 14: Hydrogen Atom Coordinates (Å×10^4) and Isotropic Displacement Parameters (Å^2×10^3) for 18srv048.

tert-butyl 5-amino-1H-pyrazole-1-carboxylate (534)

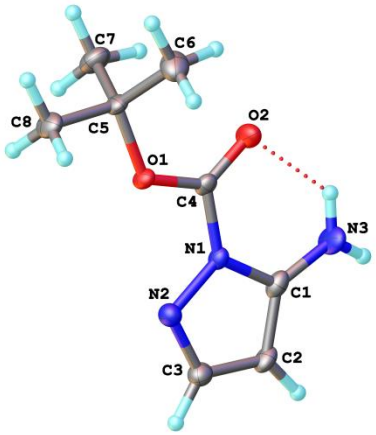

Empirical formula	$C_8H_{13}N_3O_2$
Formula weight	183.21
Temperature/K	120.0
Crystal system	monoclinic
Space group	$P2_1/c$
a/Å	9.9588(6)
b/Å	8.3675(5)
c/Å	12.2360(7)
α/°	90
β/°	108.404(3)
γ/°	90
Volume/Å^3	967.48(10)
Z	4
ρ_{calc}g/cm^3	1.258
μ/mm^{-1}	0.093
F(000)	392.0
Crystal size/mm^3	0.29 × 0.17 × 0.04
Radiation	MoKα (λ = 0.71073)
2Θ range for data collection/°	6.002 to 55.986
Index ranges	-13 ≤ h ≤ 12, 0 ≤ k ≤ 11, 0 ≤ l ≤ 16
Reflections collected	2318
Independent reflections	2318 [R_{int} = 0.0660, R_{sigma} = 0.0395]
Data/restraints/parameters	2318/0/137
Goodness-of-fit on F^2	1.054
Final R indexes [I>=2σ (I)]	R_1 = 0.0492, wR_2 = 0.1142
Final R indexes [all data]	R_1 = 0.0694, wR_2 = 0.1249
Largest diff. peak/hole / e Å^{-3}	0.31/-0.29

Table 15: Crystal data and structure refinement for **534**

Atom	*x*	*y*	*z*	U(eq)
O1	7603.3(11)	4971.8(13)	6447.4(9)	18.2(3)
O2	8281.9(13)	4673.0(14)	8386.1(10)	26.6(3)
N1	6814.7(14)	6693.7(15)	7501.4(11)	16.2(3)
N2	6083.4(16)	7482.6(15)	6488.0(13)	20.6(3)
N3	7185(2)	6854(2)	9533.8(14)	32.2(4)
C1	6578.7(19)	7387.8(19)	8457.9(16)	20.8(4)
C2	5673.2(18)	8643(2)	8035.8(16)	22.3(4)
C3	5415.9(17)	8637(2)	6847.3(16)	22.3(4)
C4	7642.4(16)	5342.0(17)	7503.4(13)	16.7(3)
C5	8343.6(17)	3516.1(19)	6227.2(15)	19.4(4)
C6	9905.8(19)	3593(2)	6898.1(17)	33.8(5)
C7	7609(2)	2057(2)	6505.9(18)	31.3(4)
C8	8114(2)	3650(2)	4946.2(15)	28.3(4)

Table 16: Fractional Atomic Coordinates ($\times 10^4$) and Equivalent Isotropic Displacement Parameters ($Å^2 \times 10^3$) for **534**. U_{eq} is defined as 1/3 of of the trace of the orthogonalised U_{IJ} tensor

Atom	U_{11}	U_{22}	U_{33}	U_{23}	U_{13}	U_{12}
O1	25.3(6)	16.4(5)	15.0(6)	-1.1(4)	9.2(5)	4.4(4)
O2	40.8(7)	22.8(6)	16.1(6)	2.7(5)	8.7(5)	6.5(5)
N1	21.4(7)	16.0(7)	13.2(7)	-0.9(5)	8.5(5)	-0.7(5)
N2	24.0(7)	21.2(7)	16.7(8)	1.2(5)	6.7(7)	2.4(5)
N3	52.4(11)	32.0(9)	16.5(8)	-1.7(7)	17.0(8)	10.6(8)
C1	24.5(8)	20.3(8)	21.6(10)	-6.2(6)	13.3(7)	-5.7(6)
C2	22.2(8)	23.0(8)	24.4(9)	-9.3(7)	11.2(7)	0.1(7)
C3	21.0(8)	22.6(8)	23.5(9)	-1.9(7)	7.4(7)	2.6(7)
C4	21.4(7)	12.7(7)	17.9(8)	-1.1(6)	9.0(6)	-2.6(6)
C5	23.7(8)	16.8(8)	18.6(8)	-3.2(7)	8.1(7)	5.3(6)
C6	25.1(9)	42.9(11)	32.8(11)	-7.1(9)	8.1(8)	8.3(8)
C7	44.9(11)	17.7(8)	34.0(11)	-2.2(8)	16.3(10)	-0.4(8)
C8	39.4(10)	27.6(9)	20.6(9)	-3.9(7)	13.4(8)	8.9(8)

Table 17: Anisotropic Displacement Parameters ($Å^2 \times 10^3$) for **534**. The Anisotropic displacement factor exponent takes the form: $-2\pi^2[h^2a^{*2}U_{11}+2hka^*b^*U_{12}+\ldots]$

Atom	Atom	Length/Å	Atom	Atom	Length/Å
O1	C4	1.3173(18)	N3	C1	1.340(3)
O1	C5	1.4916(18)	C1	C2	1.374(2)
O2	C4	1.2047(18)	C2	C3	1.395(3)
N1	N2	1.391(2)	C5	C6	1.514(2)
N1	C1	1.392(2)	C5	C7	1.517(3)
N1	C4	1.399(2)	C5	C8	1.515(2)
N2	C3	1.324(2)			

Table 18: Bond Lengths for **534**

Atom	Atom	Atom	Angle/˚	Atom	Atom	Atom	Angle/˚
C4	O1	C5	120.39(12)	O1	C4	N1	110.70(13)
N2	N1	C1	111.83(13)	O2	C4	O1	127.86(14)
N2	N1	C4	121.86(13)	O2	C4	N1	121.44(14)
C1	N1	C4	126.29(14)	O1	C5	C6	110.44(13)
C3	N2	N1	103.11(14)	O1	C5	C7	108.42(14)
N3	C1	N1	122.95(16)	O1	C5	C8	101.79(12)
N3	C1	C2	131.50(17)	C6	C5	C7	113.48(15)
C2	C1	N1	105.54(16)	C6	C5	C8	110.59(15)
C1	C2	C3	105.77(15)	C8	C5	C7	111.48(15)
N2	C3	C2	113.75(16)				

Table 19: Bond Angles for **534**

D	H	A	d(D-H)/Å	d(H-A)/Å	d(D-A)/Å	D-H-A/°
N3	H3A	O2	0.87(2)	2.12(2)	2.732(2)	126.9(18)
N3	H3B	$N2^{1}$	0.83(3)	2.17(3)	2.981(2)	165(2)

Table 20: Hydrogen Bonds for **534** (1+X,3/2-Y,1/2+Z)

A	B	C	D	Angle/˚	A	B	C	D	Angle/˚
N2	N1	C4	O1	-0.25(19)	C5	O1	C4	N1	-176.60(12)
N2	N1	C4	O2	179.39(15)	C6	C5	O1	C4	-58.23(19)
C1	N1	C4	O1	177.88(14)	C7	C5	O1	C4	66.67(18)
C1	N1	C4	O2	-2.5(2)	C8	C5	O1	C4	-175.69(14)
C5	O1	C4	O2	3.8(2)					

Table 21: Selected Torsion Angles for **534**

Atom	*x*	*y*	*z*	U(eq)
H6A	10040.89	3406.9	7716.6	51
H6B	10275.32	4650.43	6799.77	51
H6C	10412.42	2772.22	6612.13	51
H7A	6601.37	2089.84	6058.82	47
H7B	7715.23	2049.3	7329.86	47
H7C	8035.83	1087.99	6309	47
H8A	8501.47	4666.8	4784.03	42
H8B	7097.7	3607.55	4526.5	42
H8C	8592.65	2763.56	4699.46	42
H2	5319(19)	9350(20)	8508(16)	22(5)
H3	4830(20)	9400(20)	6269(18)	40(6)
H3A	7720(20)	6010(30)	9648(18)	39(6)
H3B	6940(30)	7210(30)	10070(20)	37(6)

Table 22: Hydrogen Atom Coordinates (Å×10^4) and Isotropic Displacement Parameters (Å^2×10^3) for

534

5.3 Additional Metal Complexes and Ligands

5.3.1 Structures of Metal Complexes

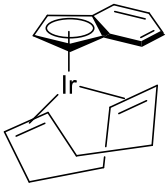

(Ind)Ir(cod)

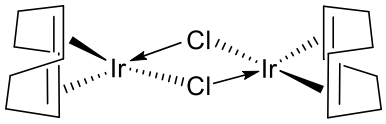

$[Ir(cod)(Cl)]_2$

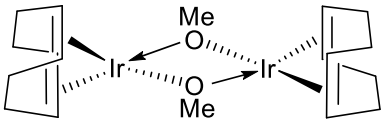

$[Ir(cod)(OMe)]_2$

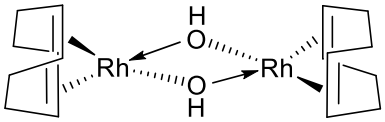

$[Rh(cod)(OH)]_2$

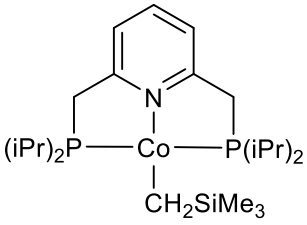

MC1

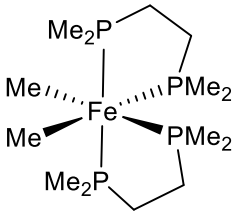

MC2

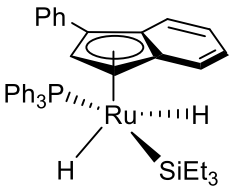

MC3

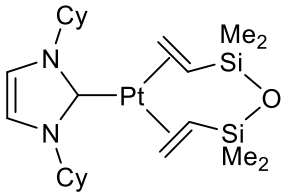

MC4

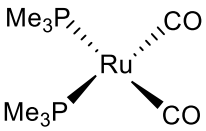

MC5

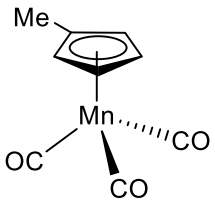

MC6

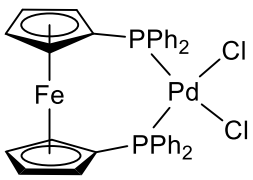

$Pd(dppf)Cl_2$

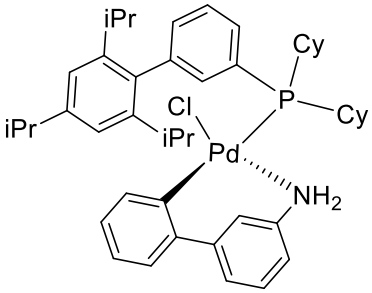

XPhos Pd G2

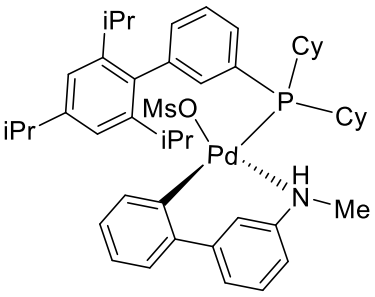

XPhos Pd G4

5.3.2 Strucutures of Ligands

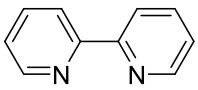

bpy

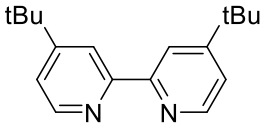

dtbpy

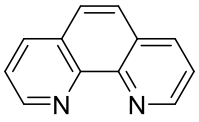

phen

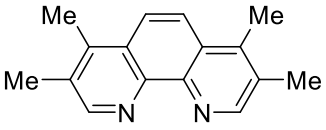

tmphen

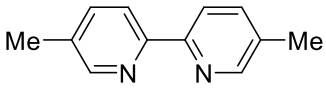

dmbpy

Indenyl

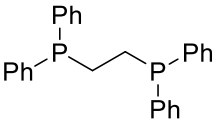

dppp

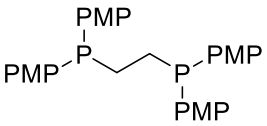

(*p*-MeO)dppp

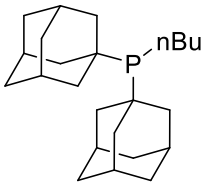

P(nBu)Ad$_2$

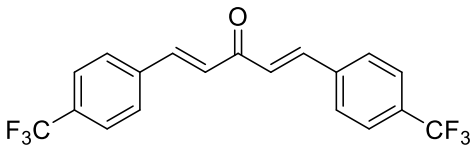

(*p*-CF$_3$)dba

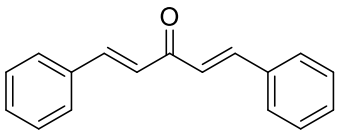

dba

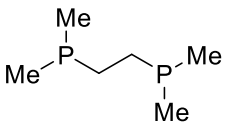

dmpe

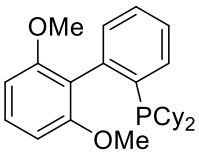

SPhos

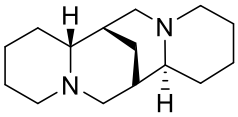

sparteine

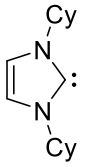

ICy